JOHANNES GUTENBERG UNIVERSITÄT MAINZ

Material-efficient dual role of supporting electrolytes for electro-organic sulfonylation and oxo-functionalization reactions

Dissertation for achieving the academic degree of

"Doctor rerum naturalium" (Dr. rer. nat.) in Chemistry

at the Faculty 09: Chemistry, Pharmaceutical sciences, Geography and Geosciences,

Department of Chemistry

submitted by

JOACHIM NIKL

born in Simmerath, Germany

Mainz, September 2023

Dean: [redacted]

First reviewer: [redacted]

Second reviewer: [redacted]

Chair of the audit: [redacted]

Date of oral exam: 14.06.2024

Meiner Familie

Declaration

The experimental and written part of this dissertation has been carried out from October 2018 until September 2023 at the Department of Chemistry, Johannes Gutenberg University Mainz, Germany, under the supervision of [redacted].

I, Joachim Nikl, declare that I have written this thesis independently and without any unauthorized assistance. I have indicated any written or electronic sources or other aids appropriately and referenced all textual passages, figures, schemes, and information taken verbatim or paraphrased from other written or oral sources.

Mainz, _____ _____

Joachim Nikl, M.Sc.

Acknowledgements

An dieser Stelle möchte ich die Gelegenheit zu einer längeren Danksagung nutzen. Zunächst möchte ich mich bei meinem Doktorvater [redacted] für die Betreuung während meiner Promotionsarbeit und die Vergabe spannender und zukunftsrelevanter Themen bedanken. In Deinem Arbeitskreis hatte ich die Möglichkeit mich sowohl fachlich als auch persönlich weiterzuentwickeln, Kontakte zu Industriepartnern zu knüpfen und meinen Forschungsinteressen nachzugehen.

[redacted] und [redacted] danke ich für die freundliche Übernahme des Zweitgutachtens und des Prüfungsvorsitzes.

Als nächstes möchte ich dem „Büro“ und insbesondere [redacted] herzlich danken. Wann immer ich ein Anliegen hatte, seien es Vertragsfragen, oder organisatorische und sonstige Hilfestellungen hattet Ihr immer ein offenes Ohr.

Bei den Kollegen möchte ich als Exilant zweiter Generation zunächst bei den Alt-Exilanten beginnen. Ich danke [redacted] für die anfängliche Betreuung und dafür, dass ich das Sulfonylierungs-Thema übernehmen durfte, was mir eine komfortable Ausgangssituation zu Beginn meiner Promotion verschaffte. Dieses Glück ist nicht selbstverständlich, sodass ich es sehr zu schätzen weiß. Danke an [redacted] für viele hilfreiche und gute Gespräche, und für die Bereitstellung einiger Substrate. Danke an [redacted] für viele lustige Momente, u.a. beim Dart-Spielen mit den „Röschis“ und beim Drohnenfliegen. Gastforscher [redacted] danke ich für die tatkräftige Unterstützung bei den Sulfonylierungsreaktionen. Selbstverständlich gilt nun ein besonderer Dank der zweiten Exilgeneration: [redacted], Freudens- und Leidensgenosse erster Stunde, danke ich für die schöne gemeinsame Zeit. Du bist ein toller Kollege, stets hilfsbereit und freundlich. Besonders das Frisbee-Spielen und Drohnenfliegen werden mir in Erinnerung bleiben. [redacted] danke ich sehr für viele hilfreiche Gespräche und lustige Momente, wie etwa bei Feierabendrunden und Grillevents, aber auch einfach im Laboralltag. Als Snowboard-Lehrer hättest Du stets ein zweites Standbein (nicht, dass Du das bräuchtest). Die Letzte und für mich wichtigste Person der 2. Generation findet sich am Ende der Danksagung wieder!

Unserem Predoc-Postdoc [redacted] danke ich herzlich für viele lustige und unterhaltsame Momente dies- und abseits des Labors und für die tatkräftige Unterstützung, sowohl bei den

Oxo-Funktionalisierungsreaktionen, als auch einfach beim Brainstorming. Ein Dank gilt auch seiner Familie. Ich bin froh, dass sich aus einer Bekanntschaft eine Freundschaft entwickelt hat.

Von den (ehemaligen) Kollegen im „Hauptgebäude“ möchte ich insbesondere [redacted], [redacted], [redacted] und [redacted] danken. Die netten gemeinsamen, nicht arbeitsbezogenen, Gespräche und Hut-Bastel-Aktionen machten mir immer viel Spaß. Vielen Dank auch an [redacted] und [redacted] für viele tolle Gespräche, Hilfestellungen und lustige Momente. [redacted] danke ich für die tolle Unterstützung bzgl. der Installation der Gaseinleitungsapparatur und -steuersoftware im Exil. Allen anderen AK Mitgliedern danke ich ebenfalls für die angenehme Atmosphäre und gute Zusammenarbeit und wünsche Allen viel Erfolg für Eure beruflichen und privaten Vorhaben.

Bezüglich der AK-Externen beginne ich bei den ehemaligen Mitgliedern der Gruppe [redacted] und danke für eine angenehme Labornachbarschaft in einem Gebäude, bei dem selbst die Poster tragend sind (Zitat [redacted]). Vor allem danke ich meinen langjährigen Studienkollegen und letzten „Röschi“ [redacted] für eine tolle gemeinsame Zeit.

Für ihre Unterstützung bei meiner Forschung danke ich herzlich meinen Studenten [redacted], [redacted], [redacted] und [redacted]. Ich wünsche Euch alles Gute für Euren weiteren Weg! Des Weiteren danke ich unseren Kooperationspartnern von [redacted], insbesondere [redacted] und [redacted] für eine großartige Zusammenarbeit und viele interessante und hilfreiche Fachgespräche, die mich in meiner Forschung weitergebracht haben. Im Rahmen des ELOXYCHEM-Projektentwurfs danke ich des Weiteren [redacted] und [redacted], und [redacted] für den engen Informationsaustausch.

Nun möchte ich einigen Personen abseits des alltäglichen Arbeitsbereiches danken. Zunächst zu langjährigen Studienfreunden: Danke an [redacted] und [redacted] für eine tolle gemeinsame Studienzeit vom ersten Semester an, mit vielen lustigen Momenten. Ich wünsche euch und Euren Familien alles Gute! Selbstverständlich danke ich auch meiner Familie: Meinen Eltern und deren Lebenspartnern, meinen Großeltern, meinem Onkel und meinen Tanten, sowie meiner Schwester und ihrem Ehemann. Danke für Eure stetige Unterstützung in allen Belangen. Ich weiß jeder von Euch hat in den vergangenen Jahren viel Turbulentes

durchgemacht und doch habt Ihr alle Situationen gemeistert. Ich bin stolz auf euch!
Auch danken möchte ich der Familie [redacted], ihren Partnern und Verstorbenen, für Eure Herzlichkeit, Freundschaft und langjährige Unterstützung. Ich werde es nicht vergessen!
Außerdem danke ich meinen langjährigen Freunden: [redacted] und [redacted] und natürlich deren Partnerinnen und Familien. Auch wenn der Kontakt zueinander manchmal abgebrochen war und jeder seine eigenen beruflichen und privaten Wege geht, fühlt man sich gegenseitig nie fremd.
Ebenfalls danke ich [redacted], einen meiner langjährigsten Freunde, für alljährliche Besuche aus Berlin, den Erfahrungsaustausch bezüglich unserer Doktorandenzeit, nostalgisches PS2 Zocken und ein unvergleichliches „Durchhalte"-Paket.

Zuletzt bedanke ich mich bei meiner Partnerin [redacted]. Selten habe ich einen Menschen zuvor getroffen, der so stark und selbstbestimmt ist und gleichzeitig ein so großes Herz und Verständnis für andere hat. Du hast es geschafft mir, trotz aller eigenen Schwierigkeiten während der Promotion, Kraft und Inspiration für die Meine zu geben. Ich weiß, ich konnte und kann mich stets auf Deine Unterstützung verlassen. Köszönök mindent! Tudom, hogy veled az oldalamon minden jól fog alakulni.

"*It is our responsibilities, not ourselves, that we should take seriously*."

– Peter Ustinov

Abstract

Transforming conventional chemical processes into more sustainable methods, such as replacing chemical reducing and oxidizing agents, is an attractive target in modern synthetic organic chemistry. Therefore, electro-organic synthesis is taking over an increasingly important aspect of chemical process design. However, many of these processes use indispensable supporting electrolytes merely as charge carriers for electrolyte conductivity. A simultaneous dual role of these as a nucleophilic/electrophilic reagent or an electrochemical mediator increases cost- and material efficiencies and, therefore, represents a resource-saving approach. This dissertation focuses on sustainable reaction development studies using supporting electrolyte salts as a nucleophilic reagent and an electrochemical mediator in a dual role. For instance, sodium sulfinate salts were successfully applied in electrochemical sulfonylation reactions with electron-rich aromatic compounds to form sulfones. Furthermore, nitrate salts were discovered and investigated as electrochemical mediators for oxo-functionalization reactions of cyclic alkanes and alkenes. Demonstrating two different aspects of the supporting electrolyte's dual role as a reagent or mediator is intended to illustrate the great possibilities of broad application areas, which may be of fundamental interest for future electro-organic reaction control.

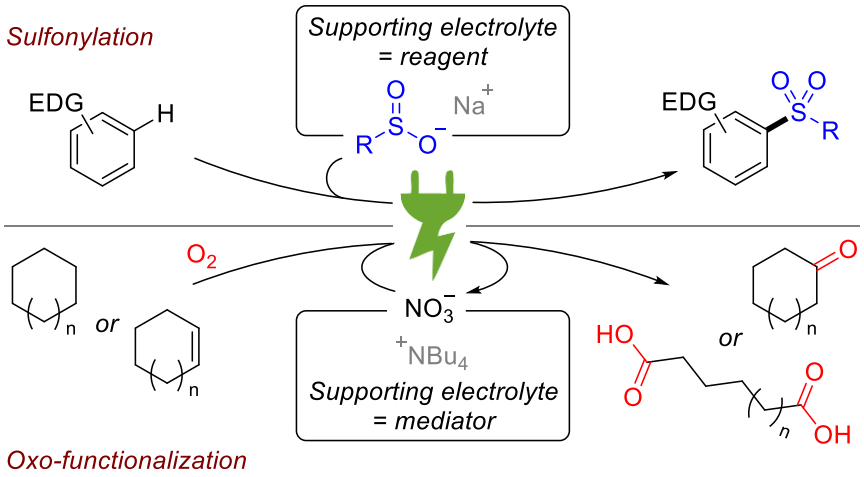

Kurzzusammenfassung

Die Umwandlung konventioneller chemischer Prozesse in nachhaltigere Methoden, wie z.B. durch den Ersatz chemischer Reduktions- und Oxidationsmittel, ist ein attraktives Ziel der modernen, präparativen, organischen Chemie. Daher spielt die elektroorganische Synthese eine immer wichtigere Rolle bei der Gestaltung chemischer Prozesse. Viele dieser Verfahren basieren jedoch auf der Verwendung unverzichtbarer Leitsalze lediglich als Ladungsträger zur Elektrolytleitfähigkeit. Eine gleichzeitige Doppelnutzung dieser als nukleophile/elektrophile Reaktanten oder als elektrochemische Mediatoren ermöglicht eine höhere Kosten- und Materialeffizienz und stellt somit einen ressourcenschonenden Ansatz dar. Diese Dissertation befasst sich mit Studien zur nachhaltigen Reaktionsentwicklung durch den dualen Einsatz von Leitsalzen, als nukleophile Reaktanden und als elektrochemische Mediatoren. So wurden beispielsweise Natriumsulfinat-Salze erfolgreich in elektrochemischen Sulfonylierungs-reaktionen mit elektronenreichen, aromatischen Verbindungen zur Bildung von Sulfonen eingesetzt. Des Weiteren wurden Nitrat-Salze als elektrochemische Mediatoren für Oxo-Funktionalisierungsreaktionen von cyclischen Alkanen und Alkenen entdeckt und untersucht. Die Demonstration zweier unterschiedlicher Rollen in der Doppelnutzung von Leitsalzen als Reaktant bzw. Mediator soll die Möglichkeiten breiter Anwendungsbereiche verdeutlichen, die für die zukünftige elektroorganische Reaktionsführung von grundlegendem Interesse sein können.

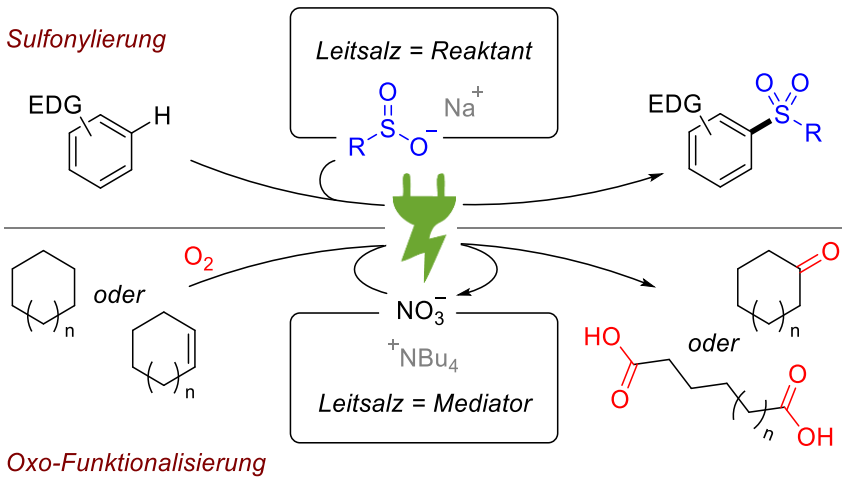

Contents

1 Motivation

In its 2012 report, the United Nations Environment Program (UNEP) lists 21 emerging environmental challenges for the 21st century, with the transition of human capabilities toward a green economy in second place.[1] It is stated: "Adapting to global change and attaining a green economy will require a variety of new capabilities, in particular [...] research efforts. Action is needed to [...] encourage research to address the sustainability challenge."[1] Climate change and resource depletion due to dependence on fossil fuels are just some of the increasing challenges for the energy industry.[2] The need for renewable energy sources for power generation and the electrification of economic processes becomes evident here.[3] These considerations have led to the development of a so-called "Power-to-X" model in recent years.[4] Here, intermittent electrical power is converted into different energy sources and thereby, or directly, made available for various applications (see Figure 1).[4b] The Power-to-Chemicals approach refers to the production of commodity chemicals for large-scale industry, which is classically done via the Power-to-Gas route,[5] in which syngas (a mixture of hydrogen and carbon monoxide) is produced electrochemically.[6] Instead, the beneficial approach of using the generated electricity directly for organic chemical synthesis develops into a research area of high interest. The scarcity of minerals and the environmental impact of excessive waste, contributed by chemical processes, can be reduced by electrochemical methods,[7] making them imperative as a 21st-century technology.[8]

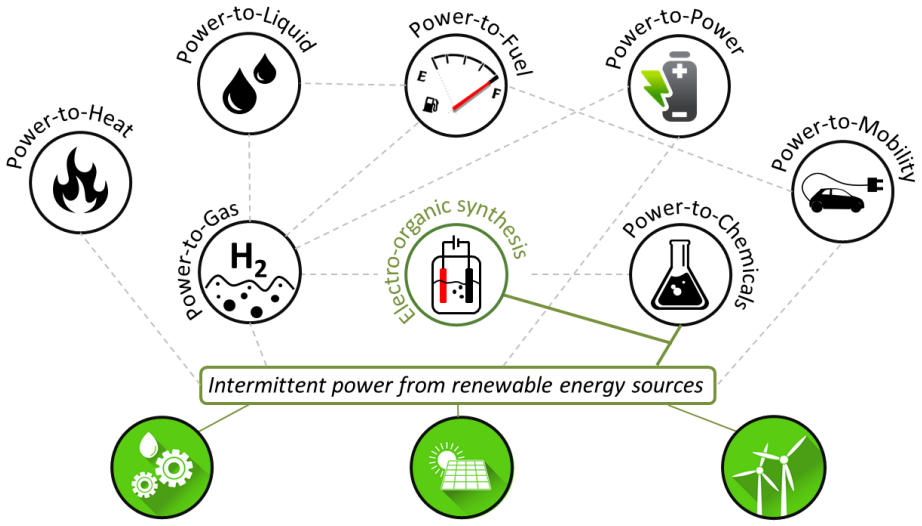

Figure 1: Electro-organic synthesis in the context of the "Power-to-X" model.[9]

2 Introduction

Electrochemistry as a manufacturing method for organic compounds has been known for centuries but has experienced a renaissance in recent years due to its sustainable aspects.[10] The demand for electro-organic processes can be observed in the increasing interest of the chemical industry to implement such synthesis routes.[11] The advantage of this methodology over classical chemical reactions lies in substituting partially harmful reducing and oxidizing agents, often used stoichiometrically.[12] Instead, electric current as an inherently "clean reagent" is employed, consisting of electrons (Figure 2). The reagent waste otherwise produced can thus be effectively reduced or even avoided. In addition, the reaction process can be easily controlled by interrupting the electrolysis by switching the control unit on or off, which makes the methodology safe. These examples are just a few that indicate the consensus of organic electrosynthesis with the rules of green chemistry.[13] Meanwhile, protocols have been reported in which electrochemical synthesis steps are crucial, e.g., to shorten extensive synthesis routes elegantly.[14] Thus, additional advantages of the methodology come to the fore, significantly improving the economics of the processes under consideration. Since electrons serve as the "reagent," electrochemical reactions are radical or radical-induced reactions running via a single electron transfer (SET) process.[15] Due to the high reactivity of the thereby formed organic radicals, it is challenging to promote targeted conversions. Nevertheless, in order to force selectivity, additives or certain environment-impacting solvents are often used to stabilize radical intermediates.[16] A practical approach to improve the economic efficiency as well as the sustainability of electrochemical processes is pursued in this dissertation. In order to perform electrolysis, an electrolyte, as an electric current conducting medium, is required. Therefore, the following chapters deal with general aspects of organic electrolysis and show possibilities for combining the roles of electrolyte components in a material-efficient manner.

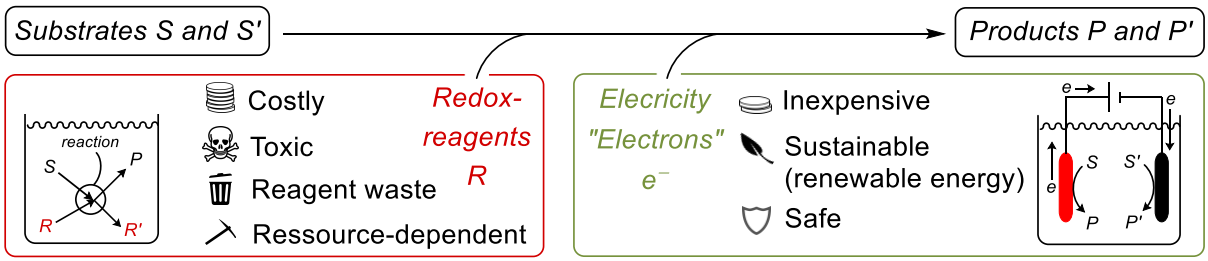

Figure 2: Selected advantages of electricity as a chemical “reagent” compared to classical redox reagents.

2.1 General aspects about electro-organic chemistry

Electrolysis is carried out in an electrolysis cell with two or three electrodes contacted with an electrically conducting medium. The number of electrodes varies depending on the mode of operation. While in constant current electrolysis (CCE), the potential adjusts to the species with the lowest redox potential within the electrolysis time, in constant potential electrolysis (CPE), the potential is maintained, resulting in a current adjustment (Figure 3a).[17] A working electrode WE and a counter electrode CE are used in constant current electrolysis, whereas a reference electrode RE is employed additionally in constant potential electrolysis. The working electrode is usually the electrode at which the chemical target reaction occurs or is initiated. It can be used as the electrochemical cell's anode (+, positive terminal, ▬) or cathode (–, negative terminal, ▬). To ensure electroneutrality, a counter-reaction occurs at the counter electrode, which has the opposite polarity to the working electrode. The International Electrotechnical Commission (IEC) defines *oxidation reactions* as occurring at the anode[18] and *reduction reactions* at the cathode.[19] A common advantage of constant current electrolysis is the more straightforward cell construction and the associated possibilities for scale-up reactions, making this method attractive for preparative chemistry.[8] On the other hand, the constant potential mode of operation is increasingly used in analytical chemistry, like in cyclic voltammetry, since specific components in the reaction solution can be electrochemically investigated in a targeted manner. In addition to these working methods, cell design can be distinguished by two processes. Electrochemical reactions can be carried out in a conventional batch-wise or a continuous process. The second one is also called flow electrolysis, which can be operated in a single-pass or multiple-pass manner (Figure 3b).[20] Several parameters and other variables must be considered when performing and optimizing electrochemical reactions. Those and some important equations in routine practice are listed in Figure 3c.[21] For this work, pictograms were used to illustrate the type of electrochemical cell applied in the respective reactions (Figure 3d). The pictograms are above the reaction arrow in the corresponding reaction schemes. The choice of the electrode material is dependent on the target reaction, as well as the electrolysis conditions. Different materials have different overpotentials towards the same electrochemical reaction, for example, the hydrogen evolution reaction (HER) shown in Figure 4a, which is a meaningful cathodic counter-reaction in protic media.[22] Traditionally, metal electrodes are used. Among

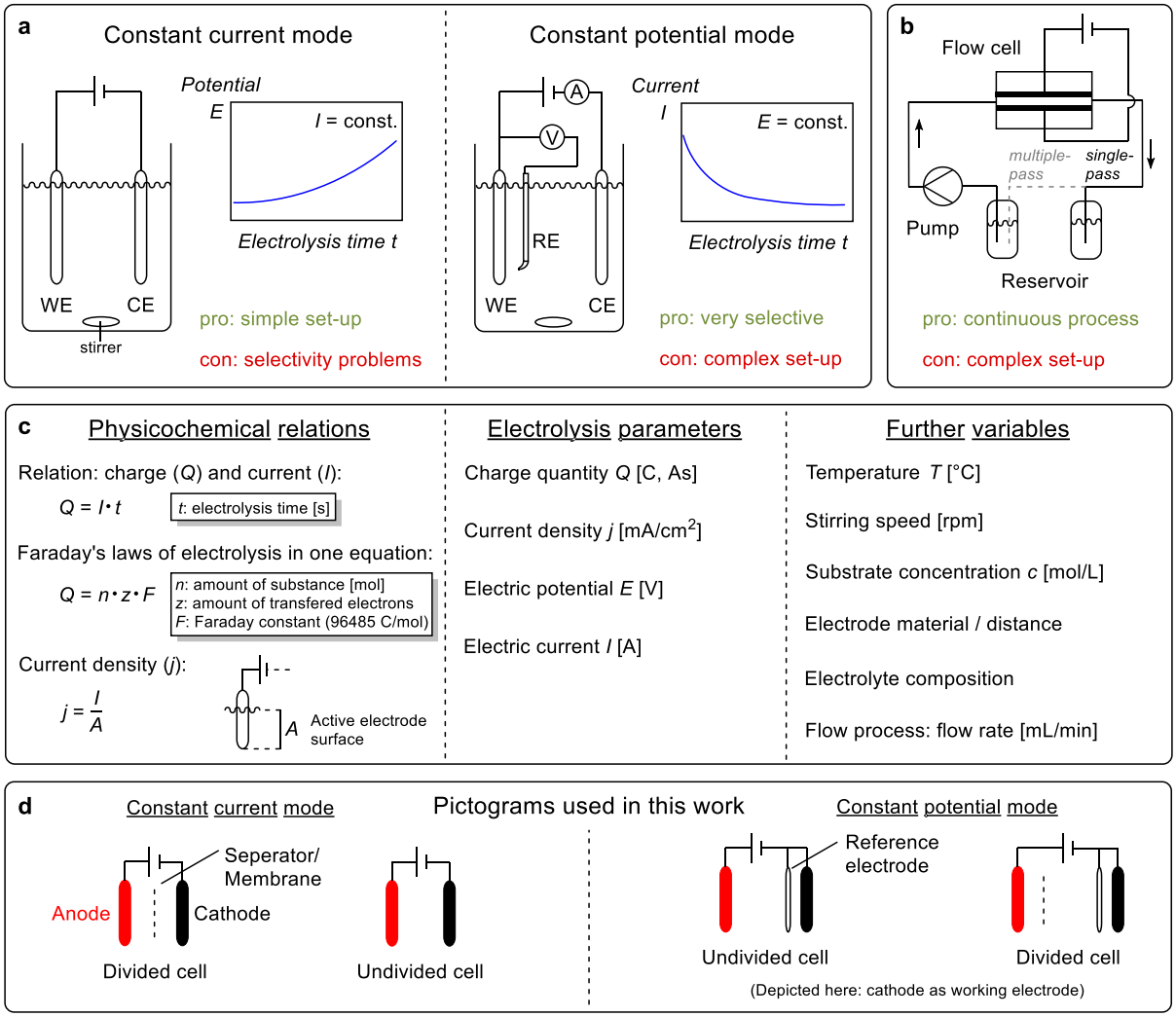

Figure 3: a Electrolytic cell set-ups for constant current and constant potential modes of batch-wise operation in beaker-type cells, WE: working electrode, CE: counter electrode, RE: reference electrode.[17] **b** Set-up for flow electrolysis processes. **c** Main equations, parameters, and variables to be considered in electro-organic reactions.[21,22a] **d** Meaning of cell illustrations (pictograms) used in this work.

them, the noble metal platinum is strongly represented, but also other metals like mercury, nickel, copper, lead, and iron are used commonly, the latter often as stainless steel (Figure 4c).[23] Apart from the excellent properties of metals for electrical conductivity, they have disadvantages. For example, the formation of passivation layers (electrode fouling) or electrode corrosion in general within electrochemical reactions.[24] Apart from that, metals like mercury and lead are known to show toxic properties,[25] causing less frequent use of them nowadays. In addition, noble metals such as platinum, rhodium, and palladium remain expensive due to their low abundance and high demand in different sectors.[26] Therefore, the trend in using electrode materials in electro-organic synthesis is increasingly moving toward metal-free electrodes, like carbon-based ones.[23,27] Here, the most important

representatives are graphite, glassy carbon, and boron-doped diamond (BDD), which are suitable as both anode and cathode materials.[22b,28] The electrical conductivity of graphite and glassy carbon is based on their sp^2-hydridized graphene-carbon skeleton, which ensures π-orbital interactions (glassy carbon structure: graphitic ribbons cross-linked by sp^3-bonded atoms).[29] For BDD, the boron-doping of electrically non-conductive diamond causes the material to be undersupplied with electrons, making it a p-type semiconductor.[28] Graphite is inexpensive and, therefore, interesting for industrial applications. However, graphite's low mechanical stability and low durability are disadvantages.[23] In contrast, glassy carbon has better chemical and mechanical stability but is more difficult to process and expensive.[30] It is one of the most commonly used carbon-based electrode materials.[23] BDD is a highly robust and inert material that has unique electrochemical properties. It has a wide potential window in various electrolytes and promotes the formation of radicals.[28] A disadvantage is its high price, comparable to platinum foil (Figure 4b). For comparison, electrode prices of the same electrode dimension from the same supplier are shown in Figure 4b.[30a] Bulk material prices can differ from the ones shown.

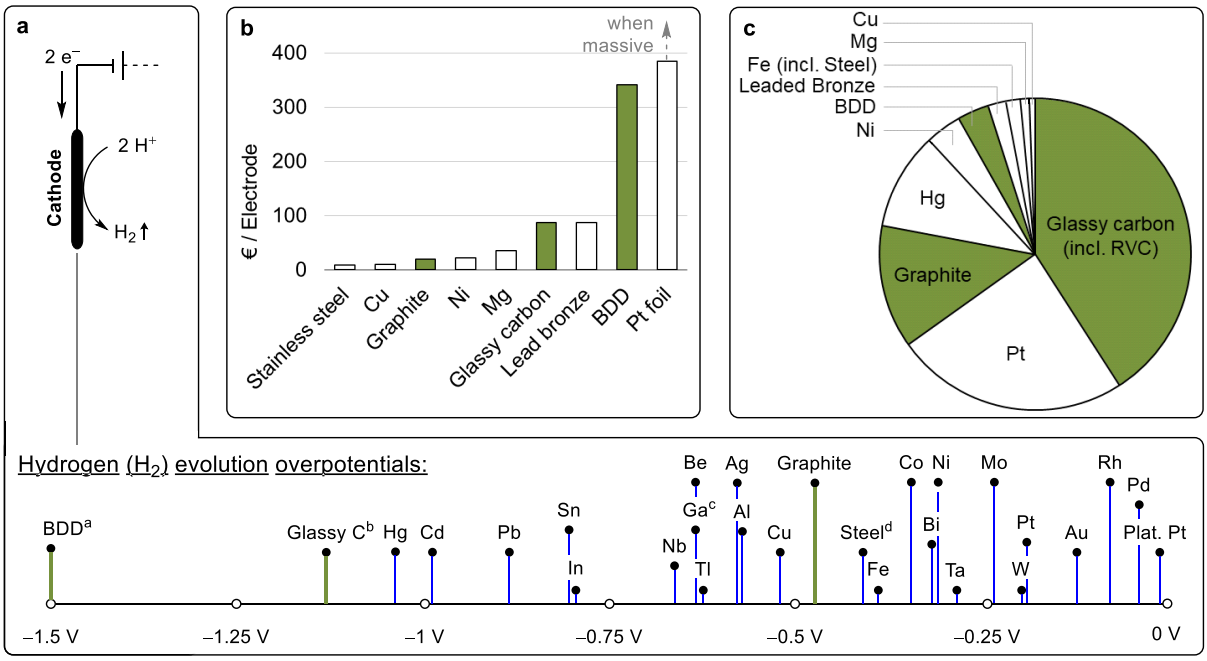

Figure 4: a Cathodic hydrogen evolution reaction (HER) and overpotentials for selected electrode materials; conditions: 1 mA/cm², 25 °C, 1 M HCl (or H_2SO_4) in H_2O. [a] 0.5 M H_2SO_4. [b] pH 3.4. [c] 0.2 mA/cm². [d] 1 M KOH.[23] **b** Price comparison of different electrode materials from the same supplier; dimension: 5.25 x 0.8 x 0.2 cm (IKA®-Werke GmbH & CO. KG).[30a] **c** Occurrence of electrode materials (anode or cathode) in a survey of 915 synthetic electrochemical protocols published between 2000–2017.[23] The graphics shown in **4a** and **4c** were taken from the cited literature and adapted in consideration of the CC BY 4.0 license terms.[23,31]

A conducting medium is essential to ensure a current flow in the electrolytic cell, which thus induces an electrical contact between the electrodes. This medium is called an *electrolyte* and consists primarily of a solvent and an electrical charge-carrying compound. In 1903, Svante A. Arrhenius was awarded the Nobel Prize in Chemistry for his "Theory of Electrolytic Dissociation," in which he described the electrical conductivity of an electrolyte resulting from the dissociation of a salt into solvated anions and cations.[32] This charge-carrying dissociating compound is commonly referred to as a *supporting electrolyte* and has the following definition according to IUPAC (1985):

> *"An electrolyte solution, whose constituents are not electroactive in the range of applied potentials being studied, and whose ionic strength (and, therefore, contribution to the conductivity) is usually much larger than the concentration of an electroactive substance to be dissolved in it."*[33]

So the most influential role of a supporting electrolyte is to enable electrical conductivity to a liquid medium, mainly a solvent, that has barely any conductivity by itself.[34] A prominent quantity in electrodynamics to describe the polarisability of a solvent is its relative permittivity (or dielectric constant) ε.[22b] The higher the permittivity, the more likely solvent molecules reorientate their electric dipoles along an applied electric field and foster dissociation of supporting electrolyte ions. Both increase the electrolyte conductivity and reduce the ohmic resistance of the medium.[22b] Examples are shown in Figure 5a. Popular solvents in electro-organic chemistry can be categorized into protic and aprotic ones. Protic solvents like water or short-chained alcohols are preferably used when cathodic hydrogen evolution is desired.[35] One of the most commonly used solvents is acetonitrile (MeCN) which combines all the necessary properties of an excellent solvent for electro-organic synthesis.[22b] It has great electrochemical stability, dissolves many ionic supporting electrolytes and nonpolar substrates, and has a high relative permittivity.[22b] Another less common but great-featured solvent is 1,1,1,3,3,3-hexafluoro-2-propanol (HFIP, **1**), known for its excellent radical stabilizing abilities.[36] A combination of BDD electrodes and HFIP-based electrolytes is well studied and often applied in electrochemical homo- and cross-coupling reactions.[28,37]

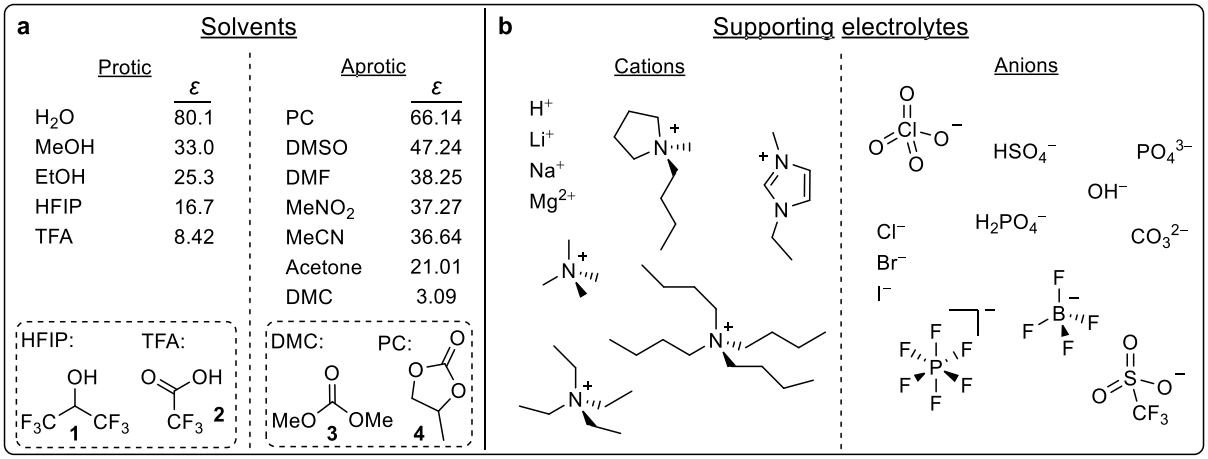

Figure 5: a Examples of commonly used solvents in electro-organic synthesis, categorized by protic and aprotic properties. Values of the relative permittivity (ε) are given.[38] **b** Examples of commonly used supporting electrolytes in electro-organic synthesis, categorized by cations and anions.[22b,39] As a salt, a supporting electrolyte always consists of a combination of cations and anions, so charge neutrality is ensured.

Applying an electric potential in an electrolyte solution leads to the migration of dissociated cations and anions to the oppositely charged electrode, forming an electrical double layer at the electrode's surface, which was first described in theory by H. Helmholtz in 1853.[40] This double-layer model was modified several times, resulting in an inner Helmholtz plane (IHP), an outer Helmholtz plane (OHP), and a diffuse layer (DL) defined by D. C. Grahame in 1947 (Figure 6a).[41] The IHP consists of molecules specifically adsorbed on the electrode surface, e.g., solvent molecules, ions, or other electrolyte constituents.[42] The OHP is defined by the nearest layer of non-adsorbed solvated ions that are attracted due to electrostatic forces.[42] The DL, introduced by L. G. Guoy and D. L. Chapman in the 1910s,[43] hosts mainly solvated anions and cations diffusing into the OHP and back, maintaining charge neutrality and causing the exponential profile of the electrode potential with increasing distance to the electrodes' surface (Figure 6a).[42]

The abovementioned IUPAC definition of supporting electrolytes indicates an important feature: they must remain stable within the applied voltage range. Supporting electrolyte ions should not undergo a decomposition (oxidative for anions on the anode/reductive for cations on the cathode) but retain their chemical structure.[17] Instead, the definition indicates another electrolyte component, the *electroactive substance*. This species does not correspond to the supporting electrolyte. The electroactive substance is ultimately the component in the electrolyte which is electrochemically transformed and whose electronic

structure is modified. In order to better understand this process, two basic types of electrolysis are discussed, direct electrolysis and indirect (or mediated) electrolysis.

In direct electrolysis, the electroactive substance is the substrate S, converted directly at the working electrode (e.g., at the anode by oxidation - transfer of an electron from the substrate to the anode). This step occurs at a particular oxidation potential E_{ox}(S) at which the substrate is oxidized. Subsequently, reactions occur, converting the oxidized species $S^{\bullet+}$ to a stable product P (Figure 6b). If the cathode is considered the working electrode, the target reaction is a reduction (transfer of an electron from the cathode to the substrate). In the case of a mediated electrolysis, the electroactive substance is a mediator M, which is subject to the electrochemical reaction at the respective electrode, e.g., the anode. As a requirement, the oxidation potential of the mediator E_{ox}(M) has to be lower than that of the substrates E_{ox}(S). Otherwise, the substrate is getting oxidized prior to the mediator.[17]

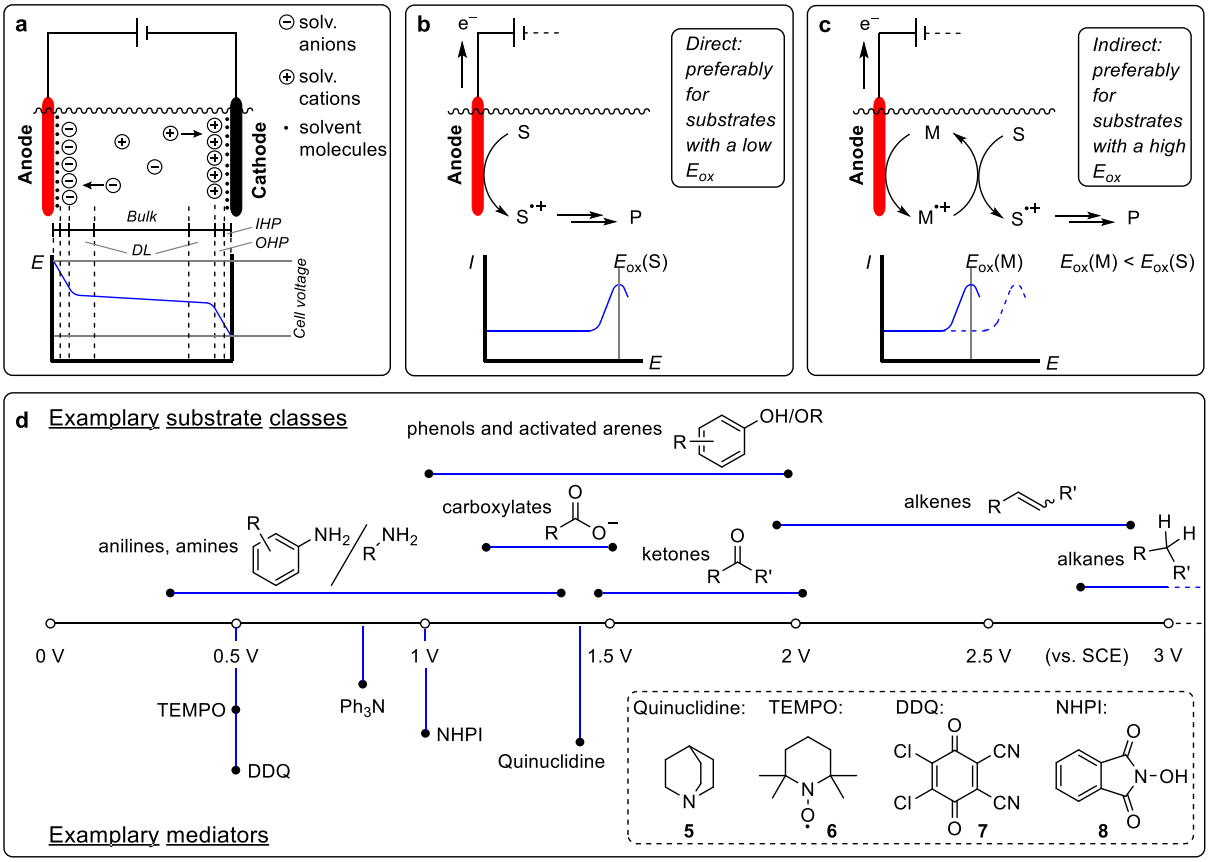

Figure 6: a Ion migration to the oppositely charged electrode in an electric field and influence of the electrical double-layer and electrode distance onto the cell voltage. IHP: inner Helmholtz plane, OHP: outer Helmholtz plane, DL: diffuse layer.[42,44] **b** Schematic model of direct electrochemical oxidation of a substrate S.[17] **c** Schematic model of an indirect (mediated) electrochemical oxidation of a substrate S via a mediator M.[17,45] **d** Different oxidation potentials range from several substrate classes and common mediators. Potentials are given against SCE (saturated calomel electrode).[45,46]

Subsequently, the activated species $M^{\cdot+}$ can oxidize the substrate S and is reduced back to the initial mediator M (Figure 6c). Examples of the oxidation potential range from different substrate classes and common organic mediators are depicted in Figure 6d. Mediated electrolysis has some advantages over direct electrolysis. For example, they can help overcome kinetic inhibitions regarding the direct conversion of substrates at the electrode, induce specific selectivities and reactivities, and allow the target reaction to occur at lower potentials (milder conditions).[45] Certainly, the use of additional substances as mediators are connected with additional costs and a more complex workup and recovery procedure, which could lead to additional waste. Therefore, using substances as electrochemical mediators already present in the electrolyte would be beneficial. The electron transfer process from an electrode to an electroactive substance and vice versa follows the principles of an "outer-sphere electron transfer."[47] In that respect, R. A. Marcus was awarded 1992 the Nobel Prize in Chemistry for describing this type of electron transfer on a classical model.[48] From an energetic point of view, an electron transfer is thermodynamically favored when the electroactive substance's corresponding electronic energy levels (molecular orbitals, MOs) are above or below the so-called Fermi level (limit of occupied energy levels in a solid material) of the respective electrode.[17] If the HOMO (highest occupied molecular orbital) of the electroactive substance is above the Fermi level of the anode, an oxidative electron transfer takes place.

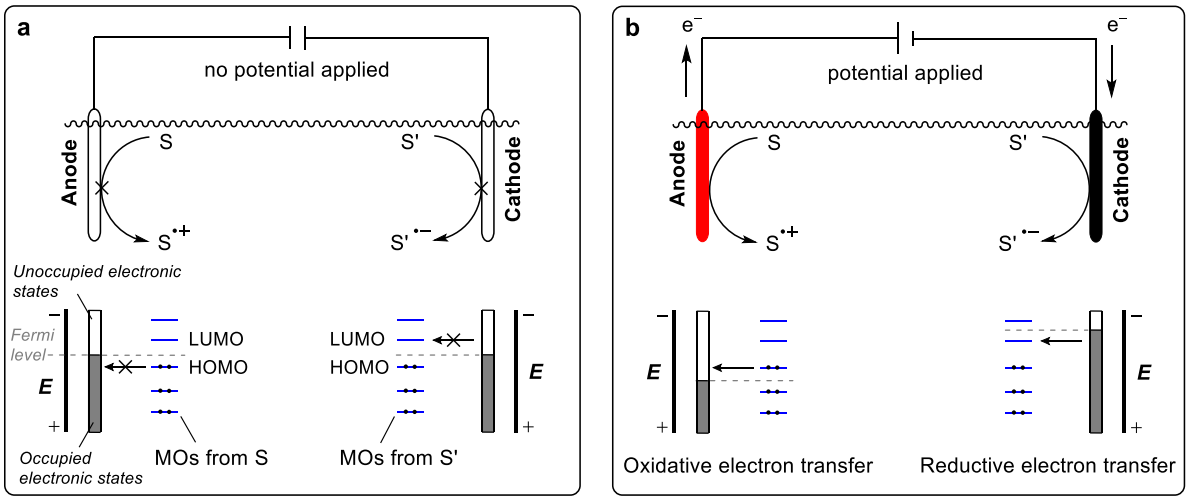

Figure 7: Simplified illustration of an electrolytically forced electron transfer between electrodes and substrates S and S'. **a** Without any applied electronic potential, no electrochemical reaction takes place when the energetic state of the substrates' HOMO is below, or the substrates' LUMO is above the electrodes Fermi level.[17] **b** After applying an electronic potential at the electrodes, their Fermi levels are shifted towards a positive potential (anode, electron deficiency) and a negative potential (cathode, electron excess), inducing an electron transfer with the electroactive species at both electrodes and an external current flow.[17]

If the Fermi level of the cathode is above the LUMO (lowest unoccupied molecular orbital) of the electroactive substance, a reductive electron transfer occurs (Figure 7b). The shifting of the Fermi levels within the electrodes is accomplished by applying an electrical potential.[17] In order to bring the subject of sustainability and resource efficiency to the fore, it is desirable to combine the role of the supporting electrolyte as a charge carrier and an electroactive substance. Therefore, the following two chapters describe existing synthesis protocols, demonstrating examples of dual roles.

2.2 Additional role of the supporting electrolyte: *reagent*

One possibility for a dual role of the supporting electrolyte is as a reagent, a substance that causes a chemical reaction and is consumed in the reaction process.[49] For that, different theoretical examples are shown in Figure 8. For electrochemical oxidation, the supporting electrolyte anion can serve as a nucleophile to scavenge an electrochemically oxidized substrate (Figure 8a) or get oxidized itself prior to the substrate (Figure 8b). An electrochemical reduction will likely reduce a substrate before the supporting electrolyte cation, whereby the latter can act as a scavenger (Figure 8c). The last case depicted (Figure 8d) is more hypothetical since no literature reports could be found that would cover the approach of a preferred reduction of a supporting electrolyte cation towards a substrate. Nevertheless, the existence of methods and reports covering this approach is not excluded. In all depicted cases, the electrochemically converted substance gets consumed via a covalent bond formation. In the following, only a few example protocols from the literature are described that have implemented these presented theoretical approaches in practice.

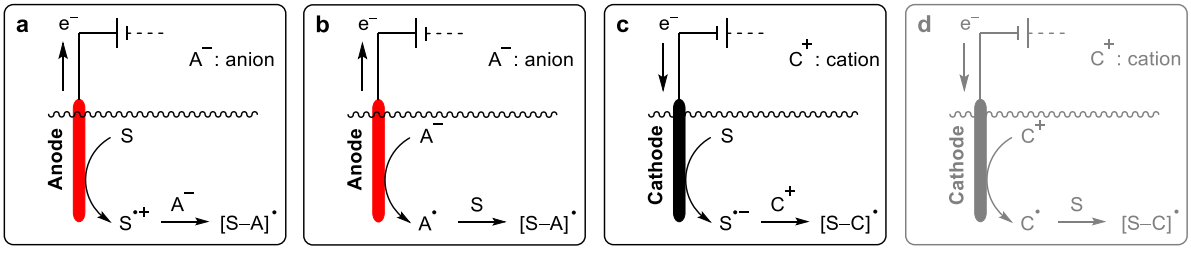

Figure 8: Different theoretical examples for the dual function of supporting electrolyte constituents as reagents. **a** Electrochemical oxidation of the substrate S and subsequent bond formation with the anion A^-. **b** Electrochemical oxidation of the anion A^- and subsequent bond formation with the substrate S. **c** Electrochemical reduction of the substrate S and subsequent bond formation with the cation C^+. **d** Hypothetical electrochemical reduction of the cation C^+ and subsequent bond formation with the substrate S. No literature-reported procedure has been found for this case.

Recent approaches to drive electrochemical procedures to more sustainability are based on the in-situ formation of the supporting electrolyte by combining non-ionic, acidic, and alkaline starting materials. Exemplarily, an electrochemical procedure for a multicomponent sulfur dioxide (SO_2) incorporation was published by Waldvogel et al. The procedure allows the synthesis of sulfonamides[50] and alkyl arylsulfonates[51] via an SO_2 stock solution. The supporting electrolyte is elegantly formed in situ using SO_2, *N*,*N*-diisopropylethylamine (DIPEA, **9**), and a nucleophile (amine or alcohol). At the same time, the anion acts as a reagent to scavenge the electrochemically oxidized substrate (Scheme 1a). Other approaches combine HFIP/amine mixtures to form ionic species.[52] Here, the deprotonated HFIP anion can serve as a nucleophile to form HFIP ethers, which can be further converted in a second step with various nucleophiles for cyanation[53] and C–C cross-coupling reactions[54] (Scheme 1b). Besides the context of in situ formed supporting electrolytes, Waldvogel et al. demonstrated the first electrochemical nitration protocol for electron-rich arenes with nitrite anions from a tetra-butylammonium nitrite supporting electrolyte.[55] The reaction was performed in a divided cell with inexpensive graphite electrodes using an acetonitrile/HFIP solvent mixture (Scheme 1c). A frequently encountered method is the electrochemical halo-functionalization of double and triple bonds.[56] With this, two halide anions serve as electroactive substances and get oxidized to a halogen molecule that adds to the multiple bonds. In particular, many electrochemical bromination reactions using bromide-based supporting electrolytes are reported.[57] Exemplarily, Waldvogel et at. presented lately a method for a selective bromination of terpene double bonds, whereby bench-stable sodium bromide is used as a supporting electrolyte (Scheme 1d).[58] A comparable method was shown by Hilt et al. with the addition that the cathodic counter reaction (oxygen reduction to hydrogen peroxide) is used to oxidize bromide to bromine, providing two pathways at once for the double bond bromination.[59] Among electrochemical reduction reactions, hydrogenation of multiple bonds is prominent. Exemplarily a reduced substrate molecule can form bonds with protons (H^+). The supporting electrolyte usually consists of an aqueous or alcoholic solution of a Brønsted-Lowry acid.[60] Estrada and Rieker showed an example of 2-nitrobenzonitrile (**10**) hydrogenation using a sulfuric acid solution in different alcohols as an electrolyte (Scheme 1e).[61] The nitro group gets reduced to hydroxylamine that reacts further with electrochemically generated aldehyde compounds from the solvent to form

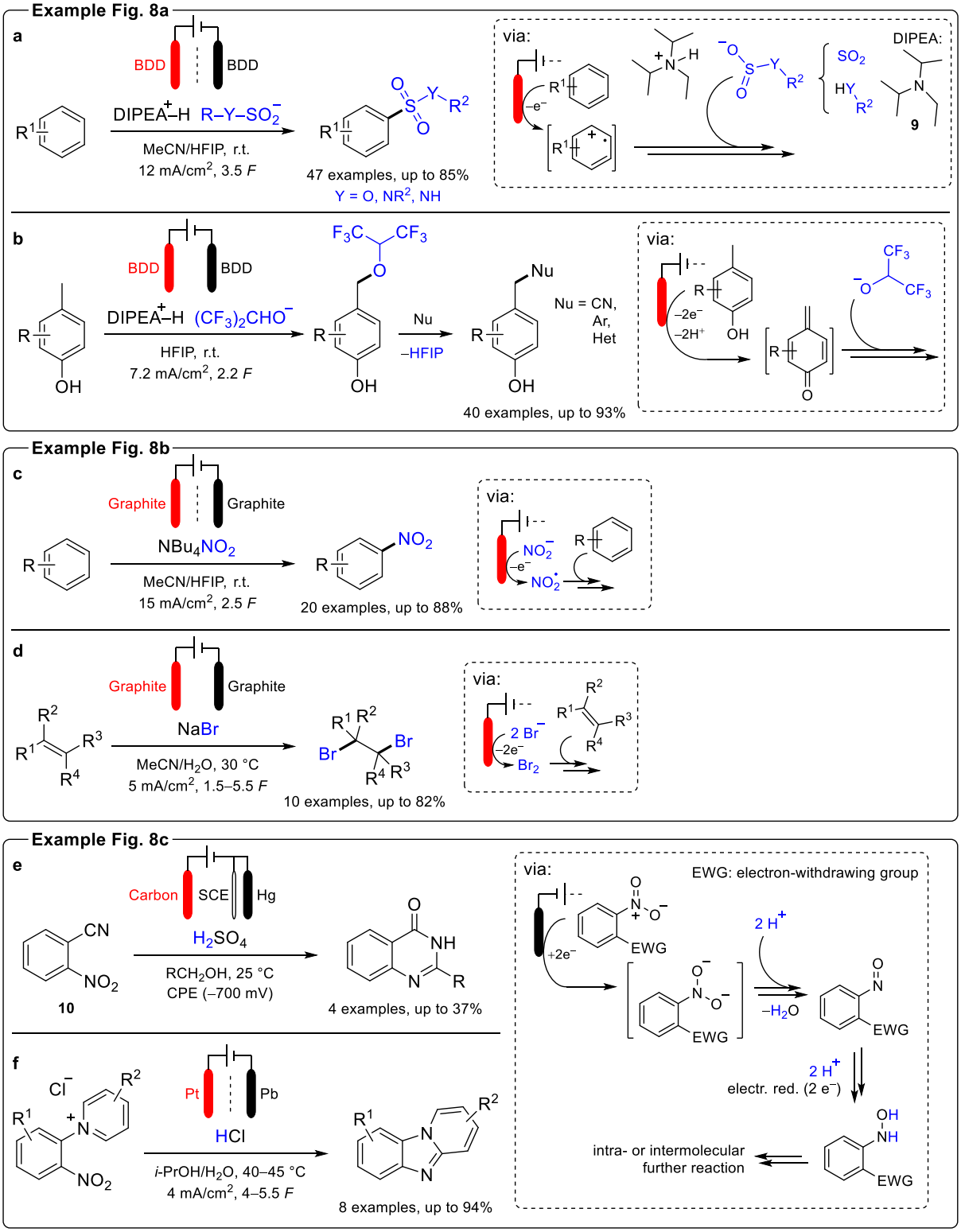

Scheme 1: Different literature examples regarding the approaches in Figure 8. **a** Electrochemical C–S coupling of electron-rich arenes with in situ formed amidosulfinates/mono alkyl sulfites as supporting electrolytes.[50,51] **b** Electrochemical benzylic HFIP ether formation with phenols and subsequent nucleophilic further functionalization.[53,54] Nu: nucleophile. **c** Electrochemical nitration of electron-rich arenes with NBu_4NO_2 supporting electrolyte.[55] **d** Electrochemical bromination of terpene double bonds with NaBr supporting electrolyte.[58] **e and f** Electrochemical hydrogenation of nitroarenes with Brønsted-Lowry acids as supporting electrolytes.[61,62] CPE: constant potential electrolysis.

2-alkyl-4(3H)-quinazolinones. Gultyai et al. demonstrated a similar approach in an example to form pyrido[1,2-a]benzimidazoles from *N*-aryl pyridinium chloride salts (Scheme 1f).[62] Besides the ionic substrate, hydrochloric acid is a supporting electrolyte and hydrogen supplier for the hydrogenation reaction. In both cases, the strategy of using cathode materials, here: Hg and Pb, with high overpotentials towards hydrogen evolution (compare Figure 4a), is applied to primarily foster substrate reduction.

2.3 Additional role of the supporting electrolyte: *mediator*

Another approach to effectively use the supporting electrolyte in a dual function is as an electrochemical mediator. For that, different examples are shown in Figure 9. Besides a classical single electron transfer (SET) reaction depicted in Figure 9a, a different pathway proceeds via a hydrogen abstraction (hydrogen atom transfer, HAT), as shown in Figure 9b. As a particular case of a mediatory system within bond formation reactions, halogen molecules can be formed oxidatively from halide anions and initiate nucleophilic-type reactions, whereby the halide, as a leaving group, is regenerated (Figure 9c). After subsequent reaction steps, the halide anions are formed back, serving again as the supporting electrolyte. Regarding a cathodic mediation, the supporting electrolyte cation can be a reducing agent after electrochemical reduction by transferring electrons to a substrate (Figure 9d).

Figure 9a schematically shows a typical single electron transfer from the oxidized anion of the supporting electrolyte to a substrate. Hardly any synthesis protocols with such characteristics were found during the literature search for this work. For example, a protocol by Zeng et al. can be demonstrated using a dual redox catalyst system with bromide and tetrachloro-

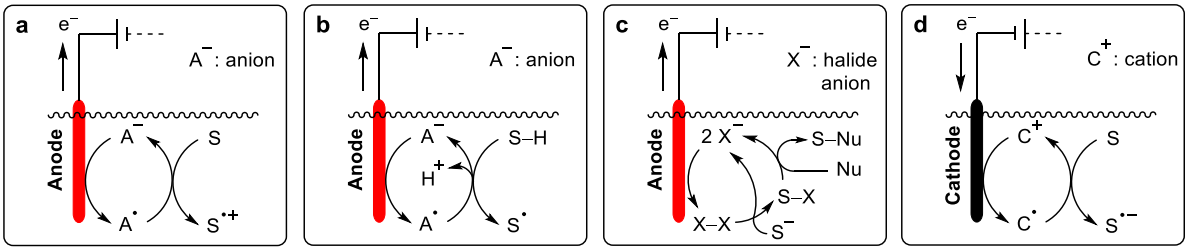

Figure 9: Different theoretical examples for the dual function of supporting electrolyte constituents as mediators. **a** Electrochemical oxidation of the anion A^- and subsequent electron transfer from the substrate S. **b** Electrochemical oxidation of the anion A^- and subsequent hydrogen abstraction reaction from the substrate S. **c** Electrochemical oxidation of halide anions X^- to form a halogen molecule. Nucleophilic attack by the substrate S and an additional nucleophile regenerate the supporting electrolyte anion. **d** Electrochemical reduction of the cation C^+ and subsequent electron transfer to the substrate S.

hydroquinone (TCHQ, **11**).[63] Here, the anion is electrochemically oxidized to bromine (Br_2), which oxidizes the hydroquinone to the corresponding quinone via an outer-sphere electron transfer.[63,64] The actual substrate is then further oxidized by the quinone (Scheme 2a). An exemplary hydrogen abstraction reaction, as shown in Figure 9b, has been demonstrated by Baran et al. for the fluorination of $C(sp^3)$–H bonds.[65] As part of the supporting electrolyte, nitrate anions serve as electrochemical mediators to generate carbon radicals that react with Selectfluor (**12**), a fluorination reagent (Scheme 2b). Selectfluor, as an ionic species, is also part of the electrolyte system. Indirect electro-organic synthesis accommodates many protocols that involve inorganic anions as redox catalysts, particularly halide anions.[64,66] In some of these protocols, these catalysts are also used as supporting electrolytes. Torii et al. demonstrated a protocol for a bromide-mediated sulfenylation of a penicillin derivative **13**, amongst other substrates (Scheme 2c).[67] Here magnesium bromide is a supporting electrolyte in a two-phase system of water and dichloromethane. Furthermore, similar to the before-mentioned multicomponent SO_2 incorporation reactions, Waldvogel et al. investigated using iodide as an electrochemical mediator to form symmetric sulfamides (Scheme 2d).[68] With this method, unprotected aniline substrates can be converted selectively, which is challenging since anilines readily undergo an electrochemical over-oxidation to polyaniline species (so-called aniline black).[69] Dehalogenation reactions are often accomplished via electrochemical reductions.[70] A protocol from Pletcher et al. shows a zinc(II) chloride supporting electrolyte as an electro-reductive mediator (Scheme 2e).[71] The reduced zinc particles appear in the catholyte as an emulsion. 1,1,2-trichloroethane (**14**) is reduced to gaseous vinyl chloride (**15**) and condensed in cold traps.[71] Another example of an electro-reductive mediation technique was provided by Tomat and Rigo, who published a series of electro-Fenton reactions.[72] The Fenton's reagent was discovered by H. J. H. Fenton in 1894 and consists of hydrogen peroxide (H_2O_2) and iron(II) sulfate, resulting in a strong oxidant for various applications due to the formation of hydroxyl radicals.[73] Tomat and Rigo reduced molecular oxygen cathodically to hydrogen peroxide and used iron(II)/iron(III) as a redox couple. Hence, for example, the oxidation of toluene (**16**) to benzaldehyde (**17**) could be accomplished (Scheme 2f).[72c] Iron(III) sulfate is a supporting electrolyte constituent and a redox mediator.

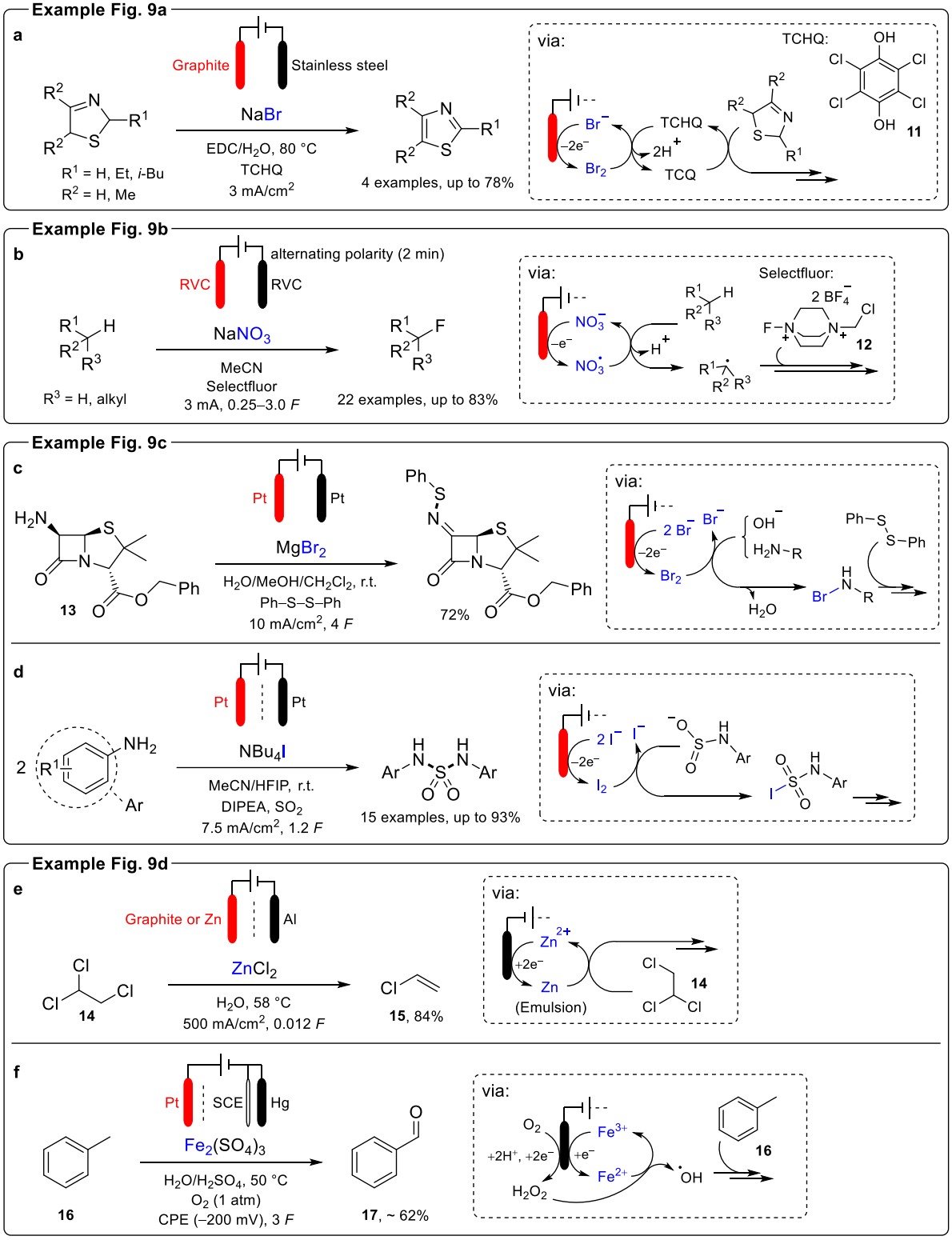

Scheme 2: Different literature examples regarding the approaches in Figure 9. **a** Electrochemical synthesis of thiazoles via bromide/TCHQ dual mediation with NaBr as supporting electrolyte; EDC: 1,2-dichloroethane.[63] **b** Electrochemical fluorination of C(sp^3)–H bonds via nitrate mediation with $NaNO_3$ as supporting electrolyte constituent.[65] **c** Electrochemical sulfenylation of penicillin derivatives via bromide-mediated steps with $MgBr_2$ supporting electrolyte.[67] **d** Electrochemical sulfamide synthesis via iodide-mediated steps with NBu_4I supporting electrolyte.[68] **e** Electrochemical dehalogenation of alkylhalogenides via $ZnCl_2$ as supporting electrolyte.[71] **f** Electrochemical benzylic oxidation via Fe(II)/Fe(III) mediation with $Fe_2(SO_4)_3$ as supporting electrolyte constituent.[72c]

2.4 Sulfones and sulfonylation reactions

Sulfones are a class of substances structurally characterized by a sulfonyl group, in which the sulfur atom carries two double-bonded oxygen atoms and two single-bonded hydrocarbon moieties. In this constitution, sulfur has an oxidation state of +II (Figure 10a). Because of the double-bonded oxygen atoms attached to the sulfur atom, sulfones are bioisostere to ketones (Figure 10b),[74] which means that both classes share similar biological activities based on their molecular structure.[74] The general reactivities of sulfonyl groups are also comparable to the ones of carbonyl groups. Due to the high electronegativity of the double-bonded oxygen atoms, the sulfonyl group undergoes nucleophilic attacks at the sulfur atom. It also induces a C–H acidity in the α-position (Figure 10b).[75] Furthermore, the electron-withdrawing effect of sulfonyl groups causes a negative mesomeric effect (–M effect) onto aromatic substituents (Figure 10b), which decreases the nucleophilicity of the ring and directs electrophiles into *meta*-position during an electrophilic aromatic substitution.[76]

The structural motive of the sulfonyl group can be found in various active substances and functional materials (Figure 10c). Besides sulfonic acid amides, which are structurally related, sulfones play a valuable role in medicine as pharmaceutical agents,[77] especially for treating leprosy.[78] The most prominent representative therein is Dapsone (**18**).[79] Other examples include Vismodegib (**19**), a cytostatic drug used for basal cell carcinoma treatment,[80] and Bicalutamide (**20**), used against prostate cancer.[81] Ceritinib (**21**) against non-small cell lung carcinoma (NSCLC)[82] and Eletriptan (**22**) as an antimigraine agent[83] are also of pharmaceutical relevance. In addition to their role as medicinal agents, sulfones are also used as herbicides like Mesotrione (**23**),[84] as heat-resistant thermoplastics like the Polysulfon PSF[85] (**24**), or as membranes in fuel cells.[86] Apart from material sciences, sulfone-containing molecules can function as reagents and building blocks in organic synthesis,[87] as shown in the Julia olefination reaction. This reaction was reported by Marc Julia and Jean-Marc Paris in 1973 and represents an important pathway to synthesize alkenes, starting from sulfone derivatives.[88] After metalation of the sulfone in α-position and adding a carbonyl compound, a reductive elimination leads to the alkene and sodium benzenesulfinate (**25**) as a by-product (Figure 10d).[89]

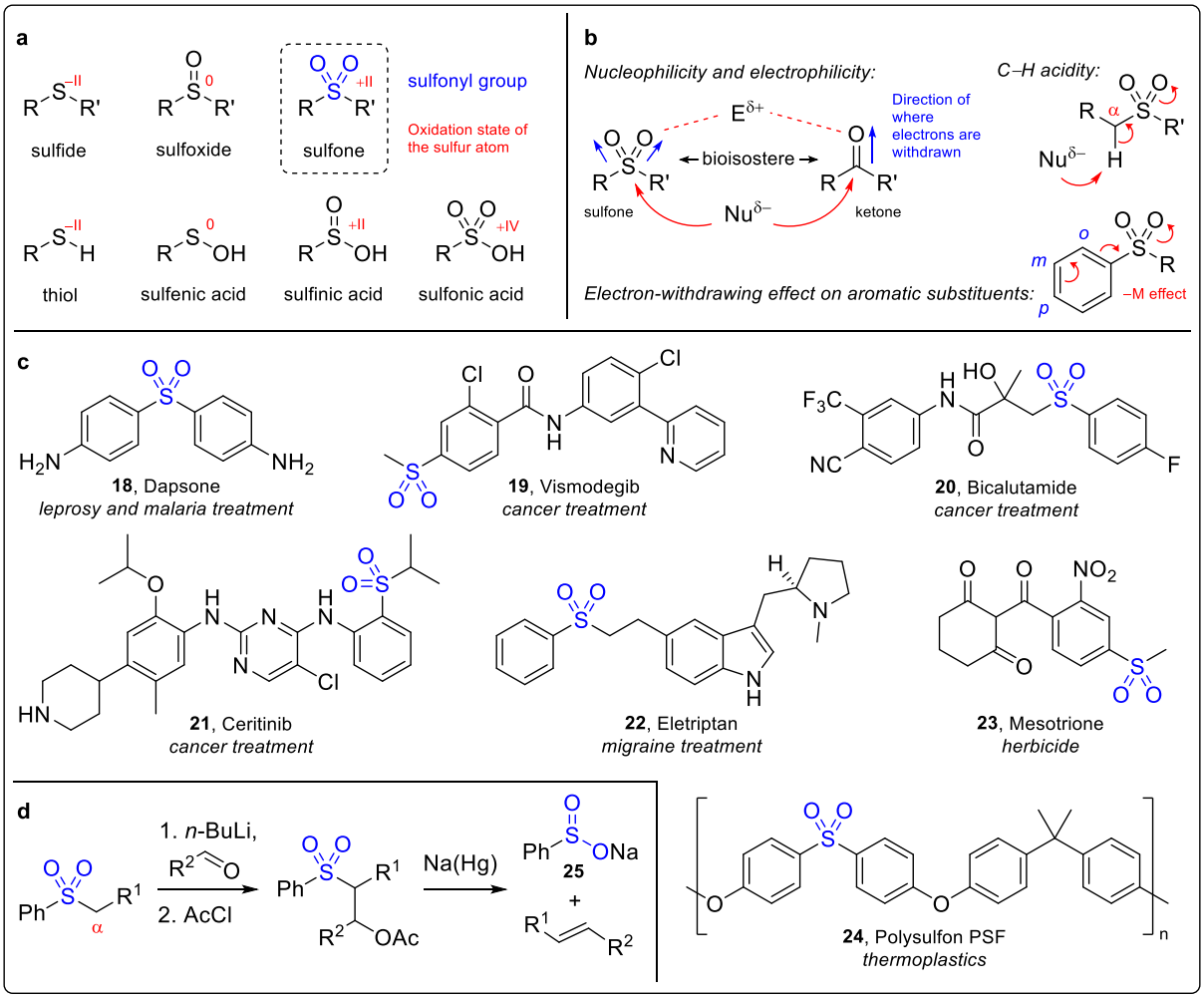

Figure 10: a Different sulfur-containing substance classes, including oxidation states of the respective sulfur atom. **b** Reactivity examples of sulfones. The sulfonyl group reactivity's driving force is the sulfur atom's positive polarization, induced by the electronegativity of the oxygen atoms. **c** Examples of sulfonyl group containing active substances and materials. **d** Scheme of the Julia reaction for synthesizing alkenes.[89]

Over decades several advances in the synthesis of sulfones have been investigated.[90] Classical synthesis pathways are the oxidation of sulfides with various oxidizing agents (Scheme 3a),[91] Friedel-Crafts-type reactions with sulfonyl halides and arenes (Scheme 3b),[92] alkylation and arylation of sulfinate salts with organohalides (Scheme 3c)[93] and radical addition reactions with alkenes and alkynes (Scheme 3d).[94] Using sodium sulfinate salts for synthesizing sulfones and other organosulfur compounds is very popular and has led to various synthesis protocols.[95] Coupling reactions of sulfinate salts with arenes are predominantly transition metal-catalyzed. Generally, for these reactions, the arenes require substituents as leaving groups (Scheme 3e). Common protocols describe using copper[96] or palladium[97] transition metals as catalysts. Common leaving groups on the arenes are tosylate,[96a] chloride,[96c] bromide,[97] iodide,[97] triflate,[97] boronic acid,[96b] and nitrogen from

diazonium salts.[96d] The overall great regioselectivity of these reactions contrasts with their disadvantages. Depleting reserves of transition metals,[98] their environmental and social problems linked to their extractive exploitation,[99] and a necessary multi-step pre-functionalization of the arene substrates cast a shadow over these procedures regarding resource-efficient processes. Other protocols provide conditions where transition metals as catalysts are not necessarily required. In those C–H functionalization reactions, unfunctionalized arenes can get coupled with sulfinate salts with specific oxidizing agents (Scheme 3f). Here, protocols often still use transition metals like manganese(III),[100] copper(II)[101] and silver(I),[102] but also metal-free alternatives like phenyliodine(III) diacetate (PIDA),[103] iodine[104] or peroxides like *tert*-butyl peroxybenzoate.[104b,105] The great advantage of these methods is that unfunctionalized arene substrates can be applied, which saves the necessary preparatory work of multi-step synthesis to build up the pre-functionalization. However, a disadvantage of these methods is the accumulation of reagent waste from oxidizing agents after the reaction.

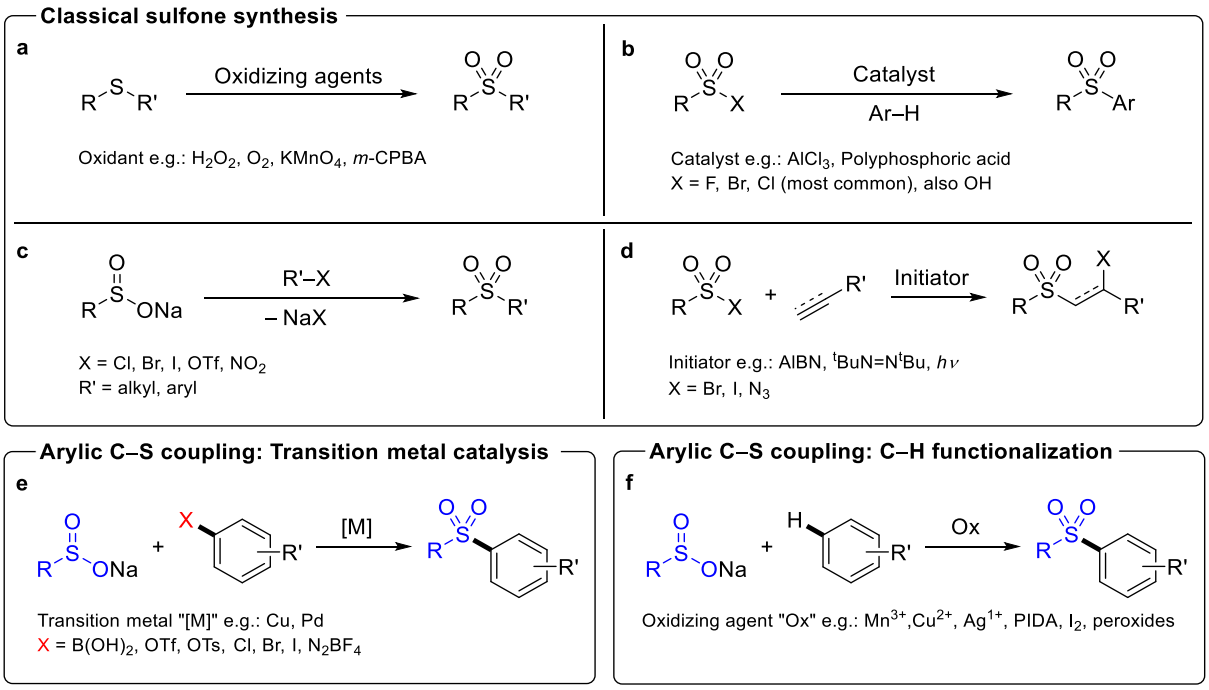

Scheme 3: Overview of classical, non-electrochemical sulfone synthesis strategies. **a** Oxidation of sulfides to sulfones with oxidizing, O-transferring agents. **b** Friedel-Crafts-type reaction with sulfonic acid (-halides) and arenes catalyzed by Lewis acidic catalysts. **c** Nucleophilic substitution reactions between sulfinic acid sodium salts and organohalides or derivatives. **d** Radical addition reaction of sulfonic acid halides or derivatives with alkenes or alkynes and an initiator. **e** General scheme of transition metal-catalyzed arylic C–S coupling reactions between sodium sulfinates and pre-functionalized arenes. **f** Arylic C–S coupling reactions between sodium sulfinates and unfunctionalized arenes via oxidizing agents.

Electrochemical protocols can overcome these disadvantages by applying electricity as a "clean" reagent. Oxidizing agents, pre-functionalized substrates, and transition metal-containing catalysts can be avoided. In 2020, Röschenthaler and Han et al. published an extensive review of sulfinate salts for electrochemical sulfonylation reactions, illustrating the high research interest in that field.[106] Exemplarily, different application procedures are shown in Scheme 4. Wang et al. reported an electrochemical decarboxylative coupling reaction of cinnamic acids with sodium sulfinates to form α,β-unsaturated sulfones (Scheme 4a).[107] In this protocol, tetra-butylammonium perchlorate serves as an additional supporting electrolyte. Comparable to this, Chen et al. published a procedure for a decarboxylative sulfonylation of arylacetylenic acids, while tetra-butylammonium hexafluorophosphate is the supporting electrolyte (Scheme 4a).[108] Another procedure for alkene sulfonylation is presented by Yuan et al. Styrene derivatives are sulfonylated here, while sodium iodide is the supporting electrolyte (Scheme 4b).[109] The iodide anion serves simultaneously as an anodic mediator (compare Figure 9c). Chang et al. also used styrene substrates to functionalize them into β-hydroxysulfones, whereby the reaction is iodide mediated and operated via constant potential electrolysis (CPE) (Scheme 4c).[110] Another functionalization of styrene double bonds where shown by Li et al. in terms of a 1,2-aminosulfonylation (Scheme 4d).[111] Tetra-butylammonium hexafluorophosphate is used here as a supporting electrolyte. A deoxygenating method for a sulfonylation of quinoline *N*-oxides has been demonstrated by Lei et al. to form quinoline sulfones (Scheme 4e).[112] Tetra-butylammonium tetrafluoroborate functions as an additional supporting electrolyte. With the sulfonylation of indoles, Yu et al. demonstrated a different method to synthesize *N*-heteroaromatic sulfones (Scheme 4f).[113] The reaction is also mediated via a supporting electrolyte iodide anion. Parallel to the timeframe of the electrochemical sulfonylation research on electron-rich aromatics presented in this thesis, Li et al.[114] and Lei et al.[115] published in 2019 very similar procedures for a sulfonylation of *N*,*N*-disubstituted anilines with sodium sulfinates (Scheme 4g and 4h). Both methods include the use of tetra-butylammonium tetrafluoroborate as an additional supporting electrolyte. In 2013, Zeng et al. reported a sulfonylation of *ortho*- or *para*-aminophenols with a sodium acetate buffer as a supporting electrolyte (Scheme 4j).[116] The authors postulated a benzoquinone-like intermediate and an ionic reaction pathway. Similarly, Alizadeh et al. published a procedure to sulfonylate caffeic acid derivatives electro-

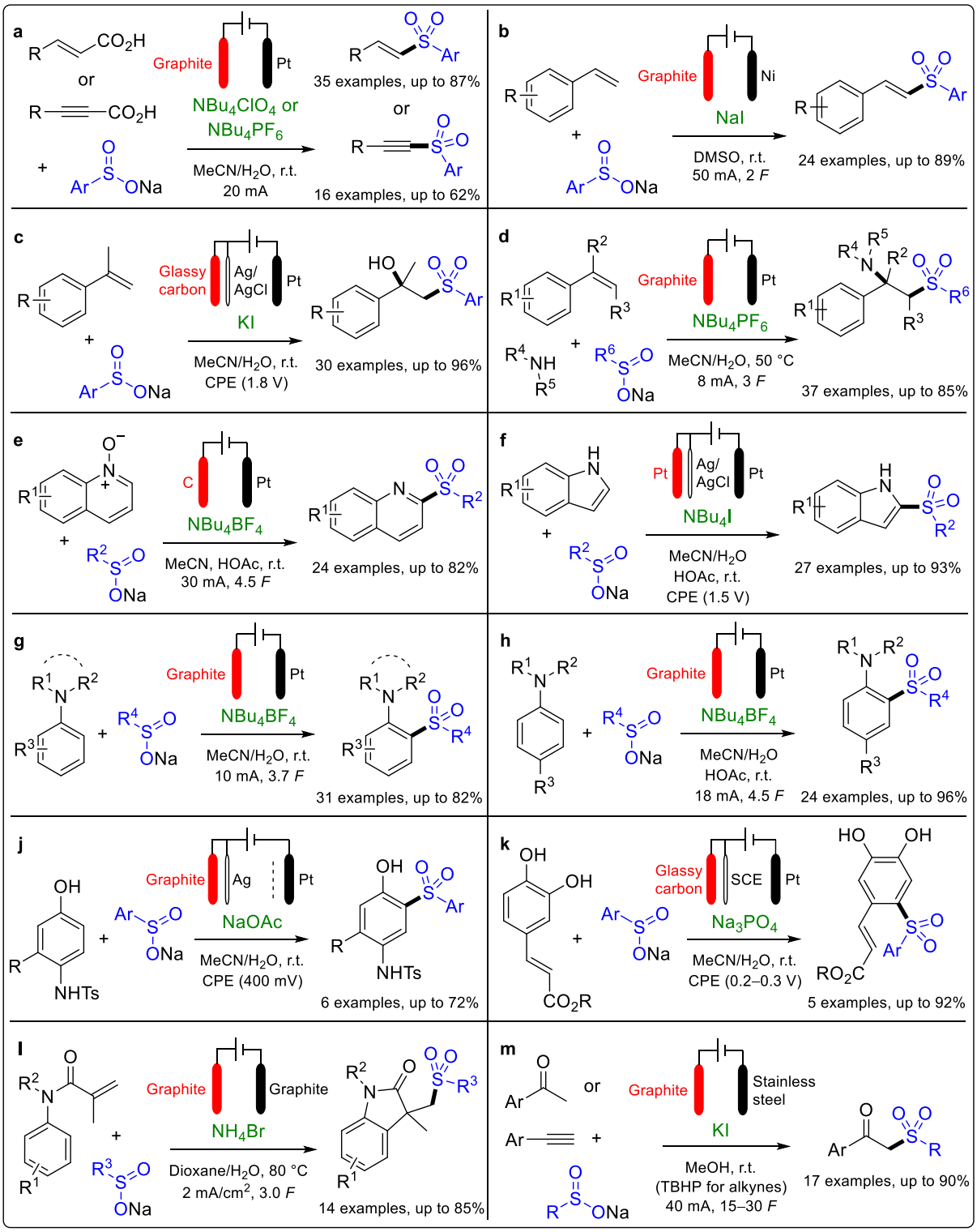

Scheme 4: a Decarboxylative sulfonylation of cinnamic- and arylacetylenic acids.[107,108] **b** Iodide mediated sulfonylation of styrene derivatives.[109] **c** Iodide mediated hydroxy- and alkoxysulfonalytaion of styrene derivatives.[110] **d** 1,2-Aminosulfonylation of styrene derivatives.[111] **e** Deoxygenative sulfonylation of quinoline *N*-oxides.[112] **f** Dehydrogenative sulfonylation of indoles.[113] **g and h** Sulfonylation of *N,N*-disubstituted anilines.[114,115] **j** Sulfonylation of *ortho*- and *para*-aminophenols.[116] **k** Sulfonylation of caffeic acid derivatives.[117] **l** Radical induced sulfonylation and cyclisation of acrylamides to oxindoles.[118] **m** Sulfonylation to β-ketosulfones from different starting materials.[119]

chemically (Scheme 4k).[117] The authors postulated an ionic thia-Michael reaction pathway, including an *ortho*-benzoquinone intermediate. Reactions involving intramolecular cyclization steps are also known. An example from Zeng and Sun et al. shows a way of forming sulfonylated oxindoles from acrylamides via an electrochemical bromide mediation (Scheme 4l).[118] A method that provides identical products from different starting material classes was demonstrated by Yavari et al.[119] The synthesis of β-ketosulfones can be conducted using acetophenone derivatives or terminal alkynes, where *tert*-butyl hydroperoxide (TBHP) as an additional oxidant is used for the alkyne conversion (Scheme 4m). Iodide, as a supporting electrolyte anion, acts as a mediator.

By taking a closer look at the single reaction conditions in Scheme 4a–m, one recognizes that apart from the sulfinate salts in every reaction procedure, an additional supporting electrolyte is introduced. Partially these serve as electroactive mediators (halide anions, Scheme 4b, 4c, 4f, 4l, 4m). The advantages of using the sulfinate salts in a dual role as charge carriers and reagents are based on resource-efficiency and sustainability aspects. A reaction protocol from Gao et al. published in 2018 follows that example. As the only charge carrier, sulfinate salts are used as reagents to sulfonylate an alkene double-bond, after which an alkyne or alkene moiety migration happens (Scheme 5a).[120] A different protocol from Han et al. is similar to Scheme 4c and describes the synthesis of β-alkoxysulfones (Scheme 5b).[121] Here, sodium sulfinates are the charge-carrying supporting electrolyte and the electroactive reagent when methanol is used as a solvent. Additionally, *p*-toluenesulfonic acid (TsOH) is a proton provider for the cathodic counter-reaction.

The idea of sulfinate salts as reagents and supporting electrolytes in a dual function for sulfonylation reactions has been taken up in single methods as described (Scheme 5). In order to expand the scope of such material-efficient, electrochemical syntheses, it makes sense to

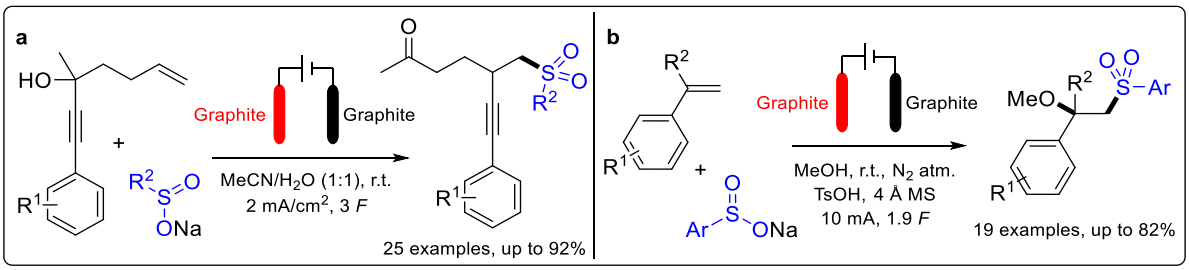

Scheme 5: Electrochemical sulfonylation with sodium sulfinates as supporting electrolytes and reagents. **a** Addition onto a double-bond with subsequent alkyne migration.[120] **b** Addition onto a double-bond with the subsequent addition of the alcoholic solvent.[121]

develop complementary methods for the sulfonylation of aromatic compounds. The Waldvogel group has become known for its wide-ranging, pioneering phenol coupling reactions,[16a] so a focus on electron-rich aromatics was set for this dissertation.

2.5 Oxo-functionalization of cyclic alkanes and alkenes

The term “oxo-functionalization” (or oxygenation) has no fixed definition. However, it is generally understood as an oxidation reaction, in which an implementation of at least one oxygen atom into the hydrocarbon scaffold of the substrate molecule occurs. The scope of possible products is broad and not further defined. Nevertheless, all products are connected via a common feature: from a synthetic point of view, they are valorized regarding their substrates, especially when they arrive from unfunctionalized alkanes. Modification of unreactive C(sp^3)–H bonds is still one of the greatest challenges in organic chemistry[122] due to its relatively high bond dissociation energy of 99 kcal/mol (Figure 11a),[123] which is even higher than for stabile C(sp^3)–C(sp^3) bonds with 90 kcal/mol.[123] Stabile vinylic C(sp^2)–H bonds also have high dissociation energies of 111 kcal/mol but are still lower than the high energetic C(sp^2)=C(sp^2) double bond of alkenes with 174 kcal/mol.[123] The C–H bond values for cyclic alkanes and alkenes are comparable.[124] For oxo-functionalization, these C–H or C–C bonds are cleaved, and C–O bonds are formed, resulting in molecules of different substrate classes like alcohols, aldehydes, ketones, and carboxylic acids (Figure 11c). Mostly reactive oxygen-transferring agents are used for these reactions, as described below. However, molecular oxygen can serve as a reactive oxidizing agent as well.[125] Defined by Hund's rule and the Pauli exclusion principle, the multiplicity *M* of molecular oxygen (in this work referred to as $^3O_2$ or just O_2) is 3 (triplet) in the ground state, caused by the two unpaired electrons in the π^*_{2p} molecular orbitals with a parallel electron spin of ½ (Figure 11b).[126] Therefore, the total electronic spin is $S = ½ + ½ = 1$ and the multiplicity $M = 2S + 1 = 3$. In 1931, Pauling and Linnett described for molecular oxygen in the triplet state a 2-fold two-center three-electron (2c-3e) bonding,[127] that covers the π-character of the bond (short atom distance, 121 pm) and the paramagnetic properties of the molecule.[126] By applying the so-called exchange energy, a spin flip of one electron into an anti-parallel configuration occurs.[126] This state is highly unstable with an increased energy of +1.63 eV (158 kJ/mol), compared to the triplet ground state,[128] and has a general lifetime of nanoseconds.[129] Via

an electron pairing into one orbital, the energy is decreased to +0.98 eV (95 kJ/mol)[128] with an increased lifetime of microseconds to milliseconds.[129] This state has a multiplicity of 1 (singlet) and is, in this work, referred to as $^1O_2$ (Figure 11b).[128a] Despite the diradical property of triplet oxygen, singlet oxygen is more reactive, which is caused by its both filled and emptied π^*_{2p} orbitals, leading to concerted addition reactions,[130] like [4+2]- and [2+2]-cycloadditions and Alder-ene reactions.[131] The kinetic barrier for triplet oxygen to perform concerted reactions is too high as it faces a spin restriction,[130] which is why radical-based reaction pathways, like free radical autoxidations, are favored.[132] A one-electron reduction of oxygen leads to the formation of a superoxide species in the form of a radical anion (Figure 11b).[130] Preferably, superoxide disproportionates into hydrogen peroxide and oxygen in the presence of protons in an aqueous environment.[130] However, in aprotic solvents and the absence of protons, it is quite stable, especially in the form of ionic alkylammonium complexes $R_4N^+ O_2^-$.[133] Furthermore, in aprotic media, superoxide acts as a strong base (pK_a of $HO_2^{\cdot}$ radical ≈ 12 in DMF).[134] The electrochemical reduction of molecular oxygen to super-

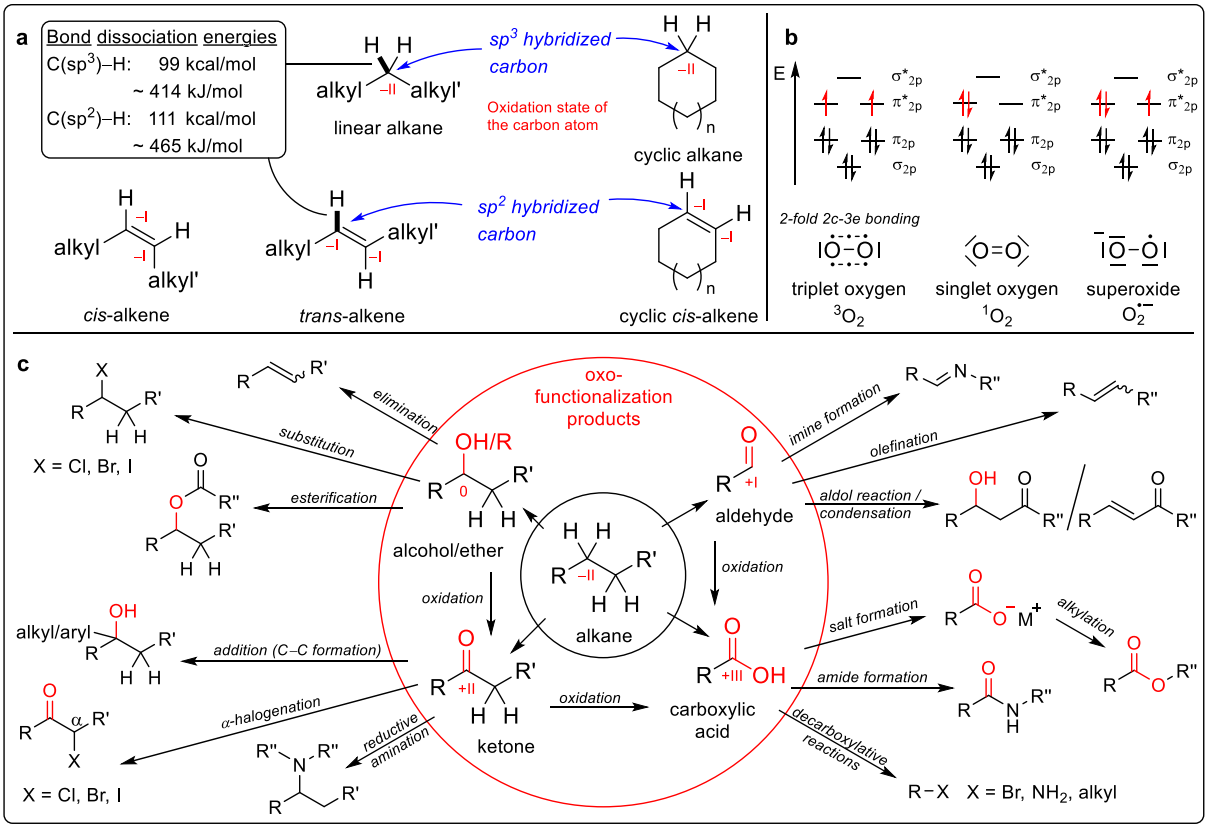

Figure 11: a Alkane and alkene structures in linear and cyclic form, with associated bond dissociation energies for C(sp^3)–H and C(sp^2)–H bonds.[123] **b** Schematic representation of molecular orbitals (MOs) and their electronic occupation of triplet oxygen, singlet oxygen, and superoxide.[125] **c** Overview of oxo-functionalization products from alkanes and their various chemical modification options.

oxide and its stabilization in aprotic media opens great possibilities for organic oxo-functionalization reactions, starting from simple oxygen.[135] Figure 11c illustrates an exemplary range of oxo-functionalization products and their various applications as building blocks or starting materials in organic synthesis. The carbonyl group (included in ketones and aldehydes), in particular, plays an outstanding role in organic synthesis, as it can be easily chemically modified and used for C–C bond formation reactions.[136] Due to the broad research field of classical and electrochemical oxo-functionalization reactions, this work focuses on cycloalkane oxidations and oxidative cycloalkene double-bond cleavage.

The two most important unsubstituted monocyclic alkanes are cyclohexane (**27**) and cyclododecane (**30**) (Figure 12a) since both compounds serve as starting materials for the industrial synthesis of adipic acid (**41**) and 1,12-dodecanedioic acid (**51**).[137] Both dicarboxylic acids are essential for PA 6.6, PA 12.12, and PA 6.12 polyamide production.[138] In 2020, polyamides covered about 7% of synthetic fiber's world production, with an increasing tendency due to a greater demand for textile and industrial yarns.[139] Industrial production processes for **27** and **30** are shown in Figure 12a. While **27** is formed by hydrogenation of benzene (**26**) using a nickel catalyst,[137] **30** is produced over two steps, including trimerization of butadiene (**28**) to cyclododeca-1,5,9-triene (**29**) and subsequent hydrogenation.[137]

Monocyclic alkanes can be classified by their ring sizes into small (3- and 4-membered), common (5- to 7-membered), medium (8- to 11-membered), and large (from 12-membered on) (Figure 12b).[140] The ring strain energy is exceptionally high in the 3- and 4-membered rings since their conformation does not allow low-energetic, stabile tetrahedral angles between the C–C bonds. Instead, the bonds are bent outwards with a decreased overlap of the binding sp^3-hybridized carbon orbitals. In these cases, the ring strain contribution constitutes angle strain, the so-called Baeyer strain,[141] and the torsional strain, the so-called Pitzer strain.[142] The larger the rings, the lower becomes the strain energy until it peaks again at the 9-membered ring. The transannular Prelog strain causes this increase by the repulsive interaction of hydrogen atoms in spatial proximity.[143] This effect declines with increasing ring sizes, resulting in lower strain energies. Values are given to the corresponding rings in Figure 12b.[144]

Several non-electrochemical strategies have been developed for the oxo-functionalization of monocyclic alkanes. In the following, exemplary synthesis methods are listed for transition

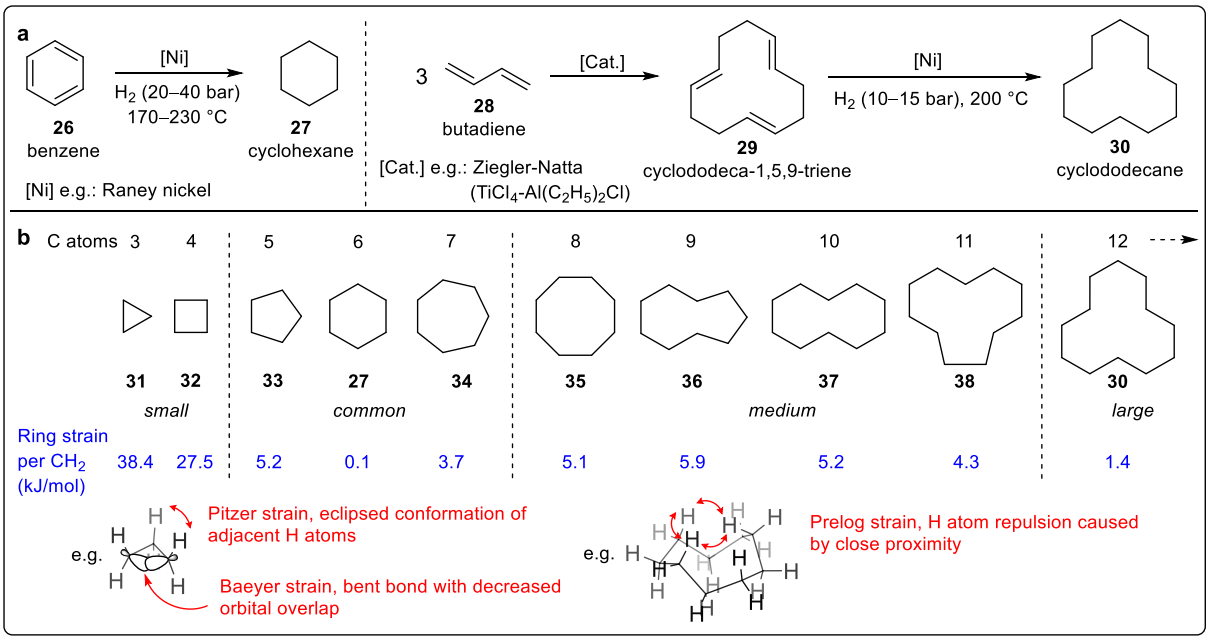

Figure 12: a Industrial production processes of cyclohexane and cyclododecane.[137] **b** Classification of monocyclic alkanes regarding their ring sizes and ring strain energies per CH_2 group.[140,144] Different ring strain contributions are depicted exemplarily on spatial structures of cyclopropane (**31**, left) and cyclononane (**36**, right).[143]

metal-free and transition metal-catalyzed procedures. Biotechnological oxidations of cycloalkanes in multiple steps via the cyclic ketone to the dicarboxylic acid have already been investigated.[145] In the case of cyclohexane, *Xanthobacter* sp.,[146] and the case of cyclododecane, *Rhodococcus ruber* CD4[147] have been identified for these reaction pathways (Scheme 6a). Specific enzymes are needed for each step, performing the reactions under a cofactor (usually NADPH) and oxygen consumption. Notably, the active catalytic site of the enzymes contains transition metals (usually iron), even though the method is categorized here under metal-free oxygenation reactions. Curci et al. show that a chemical, transition metal-free method for oxidizing cycloalkanes can be performed using dioxiranes.[148] Here, methyl(trifluoromethyl)dioxirane (**39**) was used to convert cyclohexane (**27**) into cyclohexanone (**40**) in a very selective manner (Scheme 6b). Even though dioxiranes are selective oxygen-transferring reagents, they can only be stored and used at low temperatures due to their high reactivity. A protocol at ambient temperature and pressure was provided by Onomura et al.[149] Using catalytic amounts of NHPI in nitric acid (HNO_3, 70%), direct oxidation of cycloalkanes to their dicarboxylic acids was achieved (Scheme 6c). Industrially, the first step of cycloalkane oxidation is performed by the Bashkirov oxidation,[137] where boric acid (H_3BO_3) and air oxygen are used at elevated temperatures to convert the cycloalkanes into

KA oil (KA = ketone/alcohol) (Scheme 6d). Further treatment of this mixture with nitric acid leads to dicarboxylic acid formation[137] while ozone-depleting nitrous oxide gas (N_2O) is produced.[150]

Many processes are known for the transition metal-catalyzed oxygenation of cycloalkanes, so only examples with the most frequently used metals are specified hereafter. Iron-catalyzed oxygenation reactions of hydrocarbons are important, as iron is the most abounded metal on earth.[151] In the past, unique systems, like the Gif system, were developed for this purpose. It was derived by modification of the Fenton system introduced in Chapter 2.3.[152] The Gif system, developed by Barton et al. in Gif-sur-Yvette, France, has been modified several times since initial studies in the early 1980s.[153] Within the Gif^{IV} system, a mixed-valence iron(II,III) acetate complex is combined with oxygen and zinc in pyridine/acetic acid as solvent. Thus, cycloalkanes can be selectively converted into the ketone species (Scheme 6e).[154] A similar protocol, including iron(II) perchlorate and hydrogen peroxide, was presented by Bolm et al.[155] Cyclohexane (**27**) and -octane (**35**) were converted into their ketones and alcohols, respectively, in yields up to 44% (Scheme 6f). Chromium(VI) derivatives are common oxidants in organic synthesis. Fuchs et al. demonstrated both one stoichiometric and one catalytic system based on chromium(IV) and periodate reagents, enabling oxygenation of **27** to cyclohexanone (**40**) (Scheme 6g).[156] Also, manganese complexes in combination with peroxides are reported for oxidation of cycloalkanes to the alcohol or ketone in different selectivities. Ganeshpure et al. reported about a Mn(II)(salen) complex (salen = *N*,*N*′-ethylene bis(salicylideneaminato)), which provides in combination with *tert*-butyl hydroperoxide (TBHP) alcohols and ketones in a ratio of 1:2.5 (Scheme 6h).[157] In a different protocol, Ogawa et al. presented a macrocyclic manganese(III) complex that provides a higher selectivity towards the alcohol, using hydrogen peroxide (Scheme 6h).[158] Besides the Bashkirov oxidation mentioned above, cycloalkanes are industrially oxidized using cobalt(III) salts as catalysts, e.g., cobalt acetate or naphthenate.[137] The reaction conditions are rather harsh and lead to by-products, so the process is run at a conversion of 10–12% of the starting material (Scheme 6j).[137] Ishii et al. improved the methodology by using a combination of a cobalt(II) acetylacetonate complex and NHPI as an organo-catalyst under an oxygen atmosphere (1 atm) to convert a variety of cycloalkanes to the corresponding ketones and dicarboxylic acids (Scheme 6k).[159]

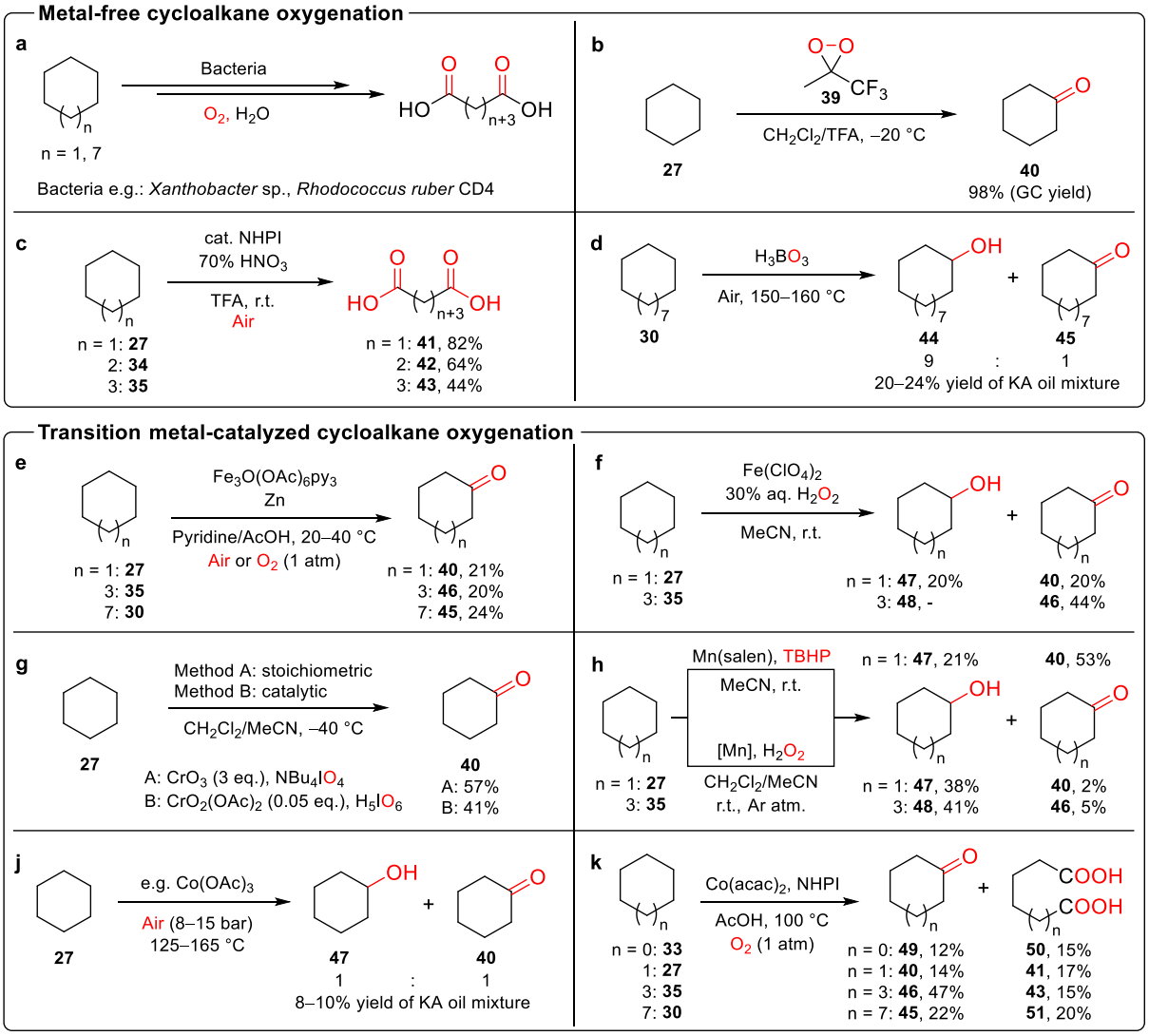

Scheme 6: a Biotechnological approach to convert cycloalkanes to dicarboxylic acids.[146,147] **b** Oxygenation with dioxiranes as organic oxidants.[148] **c** Organo-catalyzed approach using NHPI and nitric acid for dicarboxylic acid formation out of cycloalkanes.[149] **d** Industrial approach of oxidizing cycloalkanes to KA oil via Bashkirov oxidation.[137] **e** Gif^{IV} system applied to cycloalkenes for the synthesis of ketones.[154] **f** Iron(II) catalyzed oxygenation using hydrogen peroxide as an oxidant.[155] **g** Chromium(IV) based reactions, including periodate oxidants.[156] **h** Manganese (II) and (II) catalyzed approaches in combination with peroxides.[157,158] **j** Industrial approach of oxidizing cycloalkanes to KA oil via Co(III) catalysts.[137] **k** Cobalt(II) and NHPI catalyzed oxidation to ketones and dicarboxylic acids.[159]

Apart from the mentioned transition metals, also ruthenium-based reactions of cycloalkanes to ketones are known, e.g., by using in situ formed ruthenium tetroxide (RuO_4)[160] or water-soluble Ru-catalysts in combination with TBHP.[161] Electrochemical methods for the oxo-functionalization of cycloalkanes are limited nowadays. Examples are given hereafter. In a collaboration between the groups of D. H. R. Barton, from Gif-sur-Yvette, and G. Balavoine, from the Université de Paris-Sud in Orsay, an electrochemical variant of the Gif system, the Gif-Orsay system was developed.[162] Here, a mixed-valence iron(II,III) acetate complex is used

as an electrochemical mediator, and zinc is replaced by a cathodic reduction, where superoxide is formed out of oxygen in pyridine/trifluoroacetic acid (TFA). By this, cycloalkanes could be converted into their ketones (Scheme 7a).[163] Elegantly, the electrolyte conductivity is already provided by forming pyridinium trifluoroacetate from the solvents. Yamanaka et al. used a membrane reactor with iridium(III) acetylacetonate-supported carbon fiber anode to oxygenate cyclohexane (**27**) into cyclohexanone (**40**) (Scheme 7b).[164] Water is the oxygen source, while sulfuric acid is the supporting electrolyte. The authors highlight the electrocatalytic role of iridium in this protocol. Baran et al. demonstrated in 2017 an oxo-functionalization protocol for C–H bonds using quinuclidine as an electro-organic mediator and tetramethylammonium tetrafluoroborate as a supporting electrolyte (Scheme 7c).[165] Despite the large substrate scope, no unsubstituted monocyclic alkanes were tested within this protocol. All the mentioned protocols do not use the supporting electrolyte in a dual role as an electrochemical mediator.

Methods for oxo-functionalizing cycloalkanes usually differ from those for cycloalkenes, as the unsaturated C=C double bond features a different reactivity than saturated C–C single bonds. Here, the focus is set on forming carboxylic acids since these products are of high industrial interest, as stated before. Regarding a non-double bond cleaving alkene conversion, the hydrocarboxylation of ethene to propionic acid under Reppe conditions (named after W. J. Reppe) is of industrial relevance.[137] Another approach of synthesizing carboxylic acids from alkenes leads via an oxidative cleavage of the C=C double bond. Therefore, exemplary procedures are given to provide first an overview of transition metal-free and transition

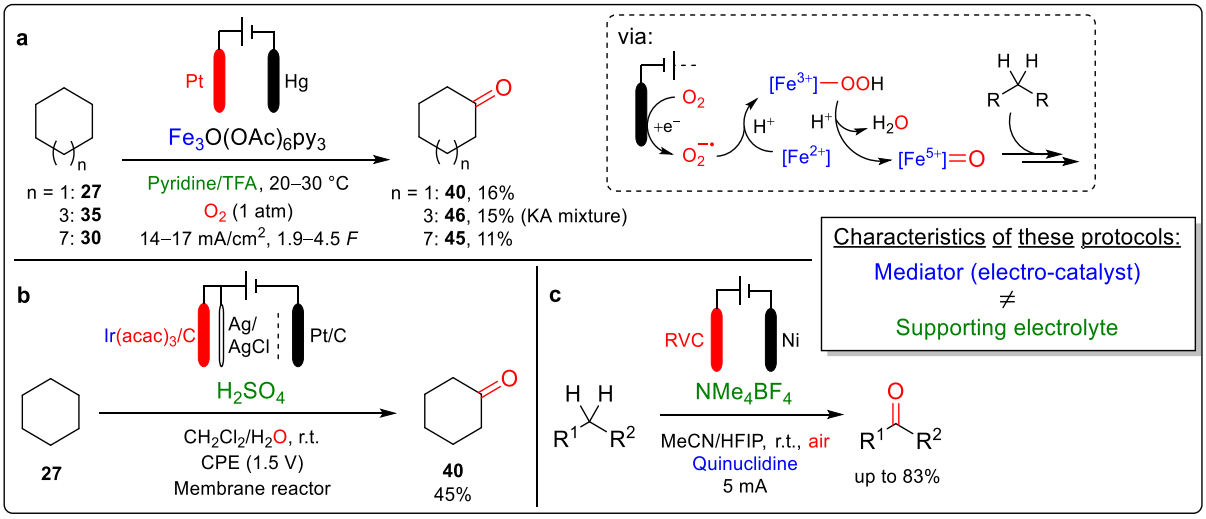

Scheme 7: a Electrochemical Gif-Orsay reaction for cycloalkane oxidation to ketones.[163] **b** Iridium supported anode as electro-catalyst.[164] **c** Quinuclidine mediated C–H activation and oxidation with air oxygen.[165]

metal-catalyzed procedures. A few methodologies are known for a transition metal-free cleavage of C=C double bonds to carboxylic acids. Ozonolysis plays the most significant role, as Unilever Emery also uses it to produce pelargonic acid (**54**) and azelaic acid (**53**) out of oleic acid (**52**) on a commercial scale (Scheme 8a).[137] Apart from that, academic research has been conducted, e.g., by Klein Gebbink et al., by using oxone ($2KHSO_5 \cdot KHSO_4 \cdot K_2SO_4$) and periodate (here sodium metaperiodate, $NaIO_4$) (Scheme 8b).[166] Although the method was able to convert cyclohexene (**55**) to adipic acid (**41**), for cyclooctene (**57**), just its epoxide derivative was observed. The authors assume that the oxygen source is derived from oxone and water, while the metaperiodate causes the C–C bond cleavage. A similar protocol from Vinod et al. demonstrates the conversion of cyclododecene (**56**) to 1,12-dodecanedioic acid (**51**) in the presence of oxone and an in situ generated iodonium species from iodobenzene (C_6H_5I) (Scheme 8b).[167] Several protocols are known for oxidative C=C double bond cleavage using transition metal catalysts.[168] The most important ones are ruthenium, tungsten, osmium, and indium, of which examples are given in Scheme 8. Sharpless et al. presented in 1981 a ruthenium-catalyzed reaction using sodium metaperiodate as oxidant and ruthenium(III) chloride as catalyst (Scheme 8c).[169] In situ formed ruthenium tetroxide (RuO_4) is the active

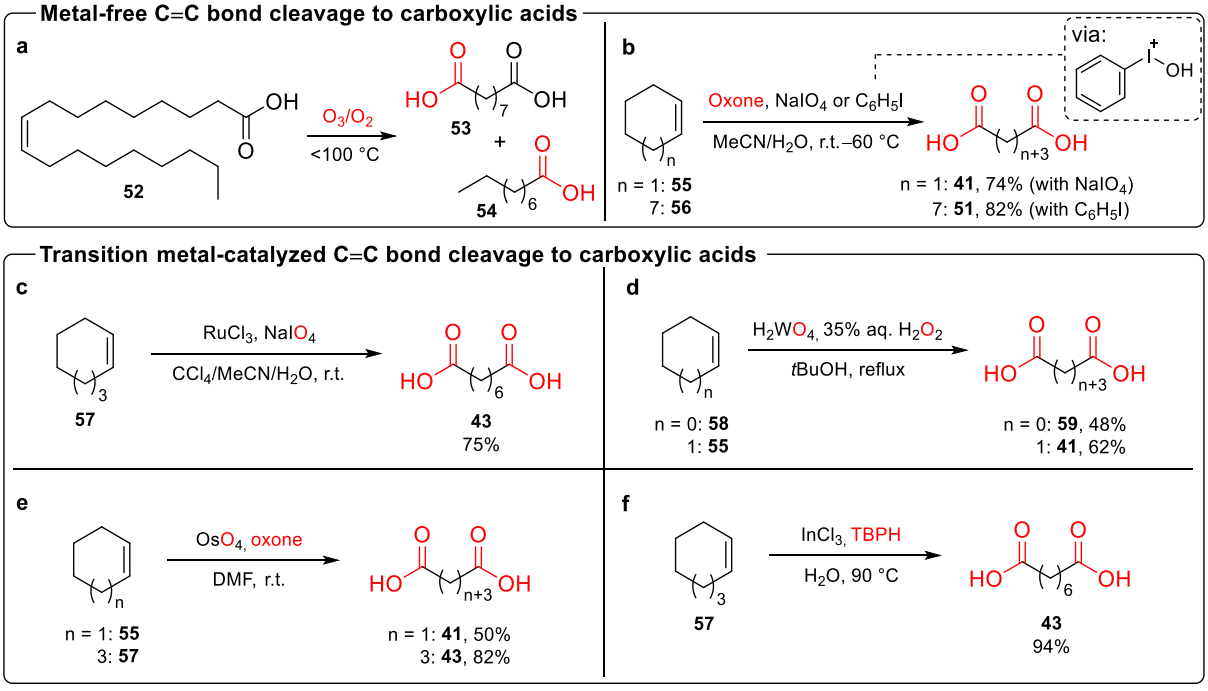

Scheme 8: a Ozonolysis reaction of oleic acid to pelargonic acid and azelaic acid.[137] **b** Oxidation of cyclic alkenes to dicarboxylic acids using oxone.[166,167] **c** Ruthenium-catalyzed procedure with RuO_4 in situ formed as active species.[169] **d** Tungstic acid-catalyzed alkene cleavage with hydrogen peroxide.[170] **e** Osmium-catalyzed reaction with oxone.[171] **f** Indium-catalyzed reaction with TBHP.[172]

species and is reduced to ruthenium(IV) oxide (RuO_2) after reaction with the double bond. Reoxidation to RuO_4 completes the catalytic cycle. Subsequently, this Sharpless system has been further developed by other groups.[168] In the case of tungsten, its metal oxide tungstic acid (H_2WO_4) can cleave C=C double bonds in combination with peroxides, as shown by Ishii et al. (Scheme 8d).[170] Other prominent forms are based on tungstophosphoric acid ($H_3PW_{12}O_{40}$) and peroxo species thereof.[173] Similar to its ruthenium analog, also osmium is used in alkene cleavage reactions in the form of osmium tetroxide (OsO_4) as active species. Since OsO_4 is primarily known for the dihydroxylation of double bonds to 1,2-diols, an additional oxidant, e.g., oxone, can be used for the C–C bond cleavage as shown by Borhan et al. (Scheme 8e).[171] An indium-catalyzed reaction with the aid of TBHP was shown by Ranu et al. to form suberic acid (**43**) out of cyclooctene (**57**) in high yields (Scheme 8f).[172]

Electrochemically known procedures for a C=C double bond cleavage of cyclic alkanes into dicarboxylic acids are barely described, despite many electrochemical protocols for C–C bond functionalization.[174] Preliminary work was achieved by Bäumer and Schäfer in the early 2000s, adopting the Sharpless conditions for oxidative alkene cleavage. The super-stoichiometric amounts of sodium periodate used in the conventional reaction were lowered due to its electrochemical regeneration (Scheme 9a).[175] The same authors provided a protocol for electrochemical ozonolysis by anodic water oxidation to ozone (O_3) (Scheme 9b).

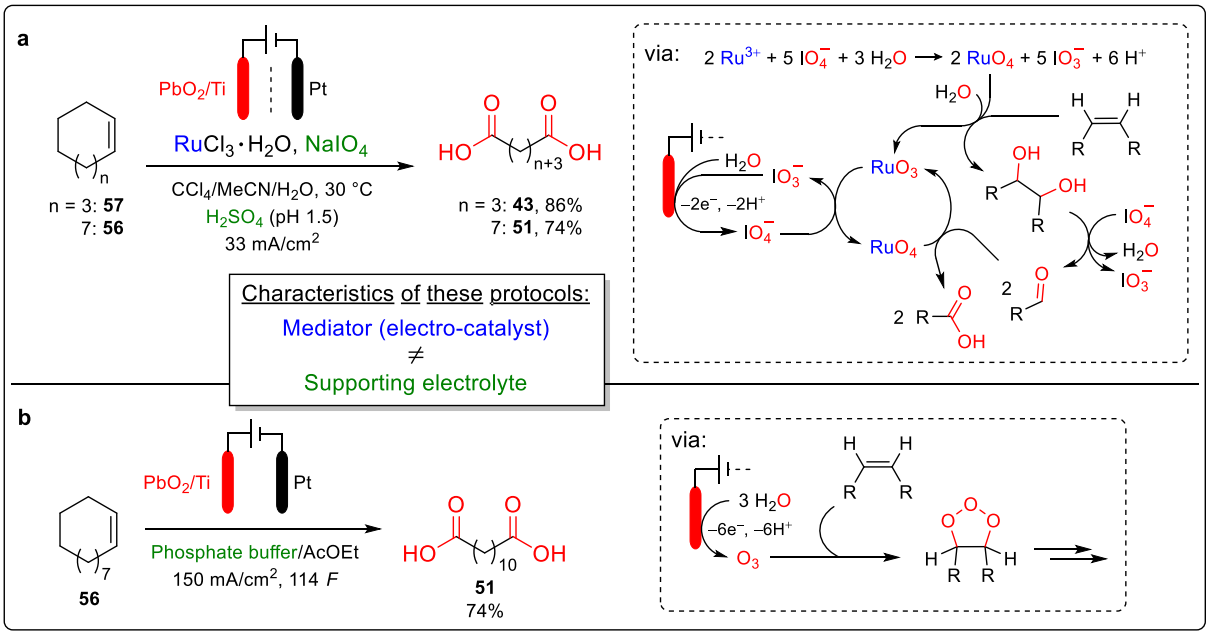

Scheme 9: a Ruthenium tetroxide- and sodium periodate-mediated cleavage of alkene double bonds to dicarboxylic acids. Yields refer to dimethyl ester products after workup.[175] **b** Electrochemical ozonolysis for dicarboxylic acid formation. Yield refers to the dimethyl ester product after workup.[176]

Remarkably, no electrochemical mediator is used in this protocol, but the current yield is only 4% due to the high charge amount applied.[176] Like in the case of the before mentioned alkane oxidation, both electrochemical procedures do not use the supporting electrolyte in an additional role as an electrochemical mediator. Since the reaction conditions regarding the oxo-functionalization of alkanes and alkenes differ due to their different reactivities, it would be advantageous to implement one electrochemical method to convert both substrate classes into value-added products.

2.6 Use of nitrate as an electrochemical mediator

Studies on the electrolysis of nitrate salts in organic solvents such as acetonitrile were already carried out in the 1950s.[177] Schimdt and Stange provided hints that a nitrate radical ($NO_3^{\cdot}$) is formed as an intermediate after anodic oxidation. In 1970, Rao et al. determined the voltammetric peak potential for the irreversible oxidation of the nitrate ion (from tetra-butylammonium nitrate) to the nitrate radical with +1.76 V on a platinum anode in acetonitrile against an $Ag/AgNO_3$ reference electrode.[178] The use of nitrate anions as electrochemical mediators has been subsequently described for several chemical conversions. Leonard et al. used the electrolytically formed nitrate radical to oxidize secondary alcohols to ketones (Scheme 10a).[179] In contrast, Christopher et al. oxidized benzyl alcohol (**62**) to benzaldehyde (**17**) in a two-phase system with chloroform and water (Scheme 10b).[180] Shono et al. reported two reaction pathways promoted by nitrate radicals. Intermediately formed acyl radicals from aldehyde starting materials could recombine to yield 1,2-diketones or add to an activated olefine double bond to yield 1,4-diketones (Scheme 10c).[181] Apart from the protocols shown here, an article published by Baran et al. for an electrochemical fluorination procedure using nitrate as a mediator has already been presented in Chapter 2.3 (Scheme 2b).[65] Partially, nitrate salts were used both as a mediator and as sole supporting electrolytes (Scheme 10a and 10c), whereby no oxo-functionalization of alkenes and alkanes has been demonstrated yet.

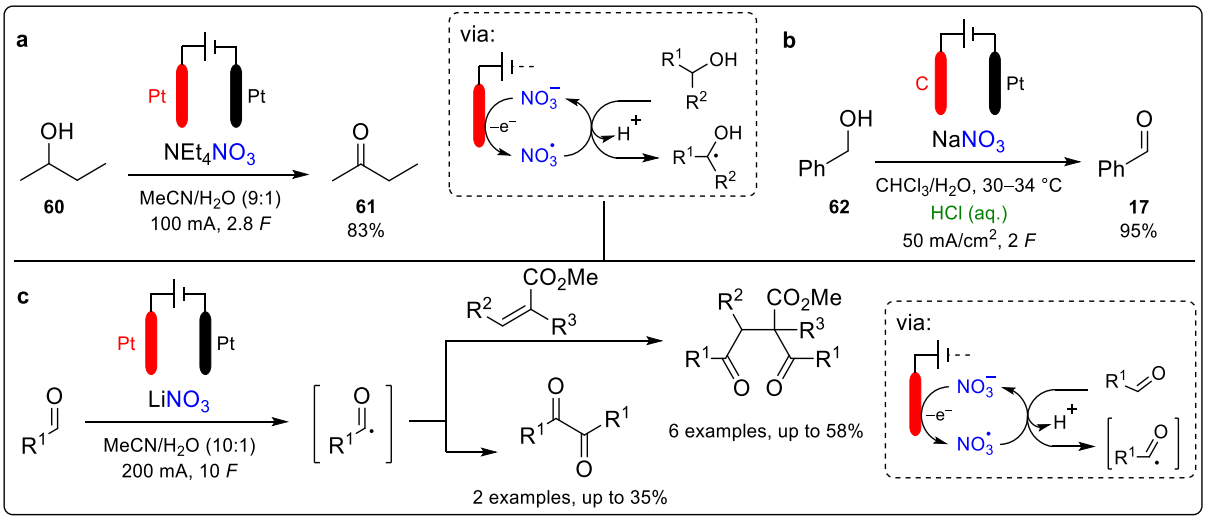

Scheme 10: a Oxidation of secondary alcohols using nitrate as an anodic mediator.[179] **b** Oxidation of benzyl alcohol (**62**) to benzaldehyde (**17**), using nitrate as an anodic mediator.[180] **c** Nitrate-promoted diacylation starting from aldehydes.[181]

3 Objectives

In order to lead the electrochemical methodology for organic synthesis in a more material-efficient and resource-saving direction, approaches to the use of supporting electrolyte components in a dual role as ionic charge carriers and chemical reagents or electrochemical mediators are pursued in this dissertation.

In terms of a dual role as a reagent, this work aims to extend the existing repertoire of electrochemical sulfonylation reactions to electron-rich aromatic compounds using sulfinate salts. The sulfinate salts should serve as a supporting electrolyte and sulfonylation reagent without further additives. The protocols of the anodic phenol coupling reactions, extensively studied in the Waldvogel group, serve as template methods.

Regarding the dual role as a mediator, a methodology for the oxo-functionalization of cyclic alkanes and alkenes should be established in this work. Here, the supporting electrolyte catalyzes the reaction as an electroactive mediator. Inspired by existing electrochemical protocols for C–H activation reactions, the focus should be on using nitrate salts. One method should be implemented to foster the conversion of both substrate classes.

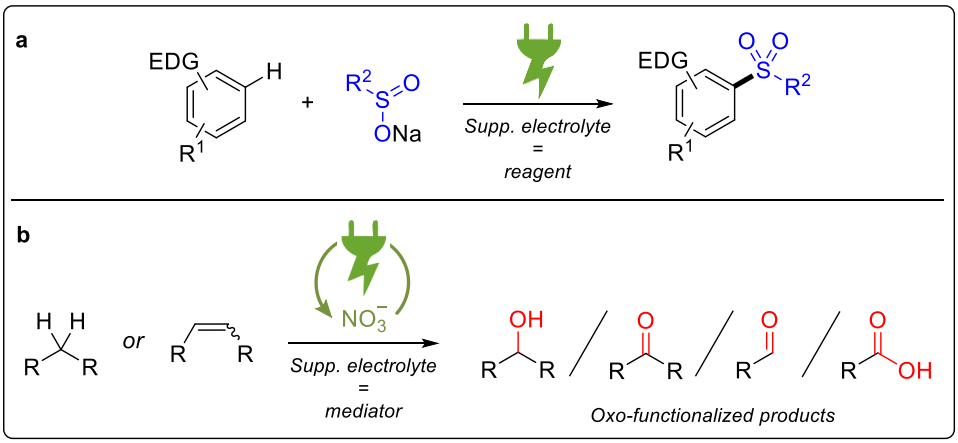

Scheme 11: Objectives of this dissertation. **a** Electrochemical sulfonylation of electron-rich aromatics with sodium sulfinates in a dual role as supporting electrolyte and reagent. EDG: electron-donating group. **b** Electrochemical oxo-functionalization of alkanes and alkenes with nitrate salts as supporting electrolytes and mediators.

4 Results and Discussion

4.1 Electrochemical sulfonylation of electron-rich aromatic compounds with sodium sulfinates

Two manuscripts were published for this chapter:

J. Nikl, S. Lips, D. Schollmeyer, R. Franke, S. R. Waldvogel, *Direct Metal- and Reagent-Free Sulfonylation of Phenols with Sodium Sulfinates by Electrosynthesis, Chem. Eur. J.* **2019**, *25*, 6891–6895.

DOI: 10.1002/chem.201900850

Contribution:

S. R. Waldvogel, S. Lips and **I** conceived this work and designed the experiments. **I** conducted the experiments and analysed related data. D. Schollmeyer conducted crystallographic experiments and provided data thereof. S. R. Waldvogel and **I** wrote the manuscript and the supporting information. R. Franke and S. Lips revised the manuscript.

J. Nikl, D. Ravelli, D. Schollmeyer, S. R. Waldvogel, *Straightforward Electrochemical Sulfonylation of Arenes and Aniline Derivatives using Sodium Sulfinates, ChemElectroChem* **2019**, *6*, 4450–4455.

DOI: 10.1002/celc.201901212

Contribution:

S. R. Waldvogel and **I** conceived this work and designed the experiments. D. Ravelli and **I** conducted the experiments and **I** analysed related data. D. Schollmeyer conducted crystallographic experiments and provided data thereof. S. R. Waldvogel and **I** wrote the manuscript and the supporting information. D. Ravelli revised the manuscript.

Motivation

Extensive research about electrochemical sulfonylation of electron-rich hydroquinone- and catechol-like structures has been carried out by Nematollahi.[182] Within that research, mostly arylsulfinic acids are used as sulfonylation reagents. The electrolyte usually consists of an acidic aqueous buffer solution, including acetate or phosphate salts, adjusted to a pH of 2–5. The proposed reaction mechanism in all cases consists of an electrochemical oxidation of the substrates, followed by a subsequent 1,4-nucleophilic addition (Figure 13).

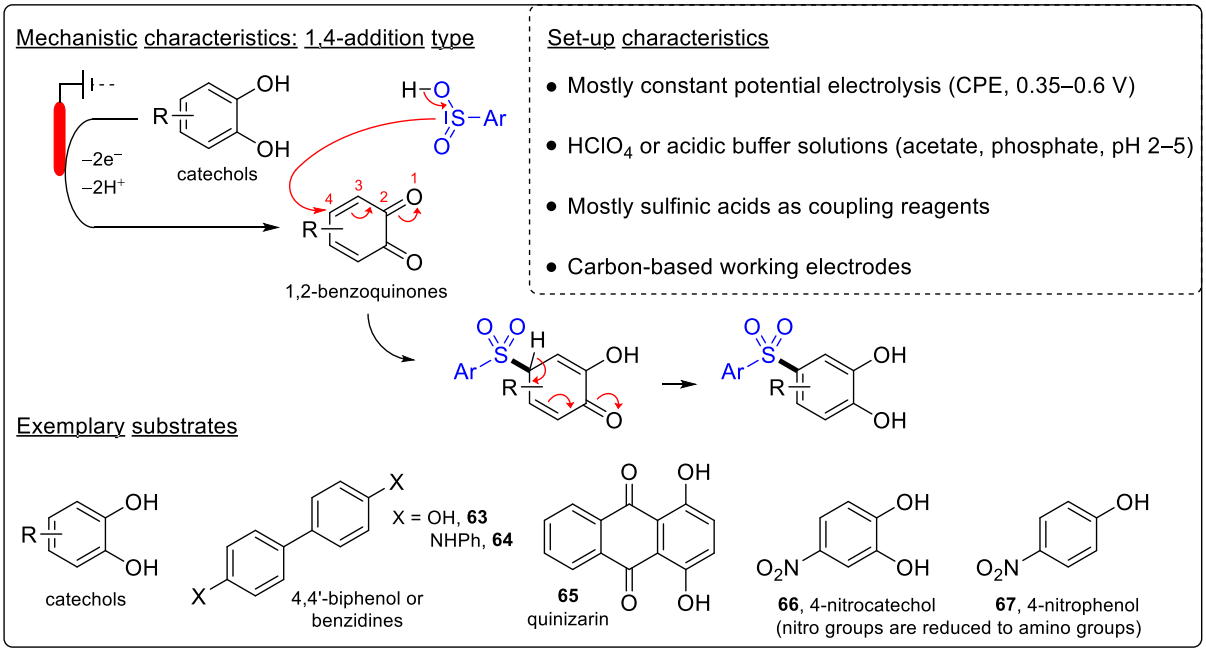

Figure 13: The general mechanistic proposal regarding Nematollahi's research on electrochemical sulfonylation consists of a twofold oxidation of the substrates to quinone-like structures. The sulfonylation takes place via a nucleophilic conjugate addition. Characteristically, the reactions occur at constant potential and in aqueous buffer solutions.

In distinction to this methodology, this dissertation's research provides a pathway not limited to hydroquinone- or catechol-like substrates. Furthermore, instead of sulfinic acids, the corresponding sodium salts were used in a dual role as supporting electrolyte and sulfonylation reagent to establish a more material-efficient synthesis protocol. Additives to adjust the pH value and ensure ion conductivity in the electrolyte are therefore avoided.

In his dissertation, S. Lips has already presented preliminary experiments on the sulfonylation of phenols.[183] The following insights have been reported (Scheme 12). Different phenols containing alkyl and methoxy substituents have been converted with sodium benzenesulfinate (**25**) to corresponding sulfones at BDD electrodes in HFIP. The screening reactions were carried out in undivided 5 mL PTFE cells. Application of methyltributylammonium methylsulfate (MTBS, **68**) as a supporting electrolyte, which is commonly used in phenol coupling reactions in combination with HFIP,[16a] showed no or even a decreasing effect for the sulfonylation reaction, compared to its omission (Scheme 12a). Scale-up experiments without an additional supporting electrolyte in 25 mL beaker-type glass cells led to isolated yields of 15–35% of sulfone product **70**, depending on the water content in the electrolyte (Scheme 12b). S. Lips concluded that the reaction could be optimized by adjusting the water content in the electrolyte.

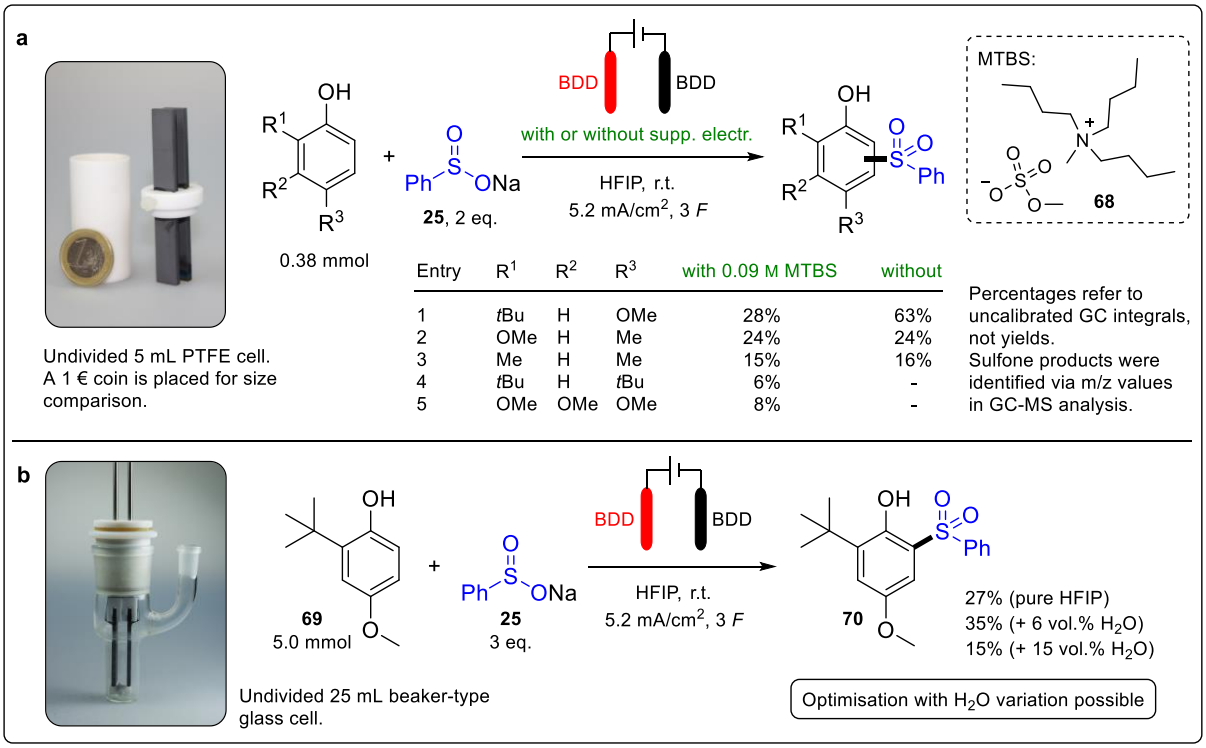

Scheme 12: a Preliminary screening experiments in undivided 5 mL PTFE cells, using different substrates with and without MTBS as supporting electrolyte, conducted by S. Lips.[183] **b** Preliminary experiments in undivided 25 mL beaker-type glass cells, using different water contents, conducted by S. Lips.[183]

Summary of the results

Based on the results of S. Lips, the research was initially focused on the sulfonylation of phenols and the composition of the electrolyte. Different solvents mixtures were tested as varying electrolyte water contents influenced the reaction outcome.[184] It was found that the water content had the most significant influence on the reaction, with an optimum being achieved in the range of 15 vol.% while applying 12 mA/cm^2 and 1.3 mol-equivalents of sulfinate salt **25**. The optimized reaction conditions can be found in Scheme 13a. Under these conditions, sulfone **70** was obtained with a yield of 53%. A test reaction using a combination of HFIP and MTBS without the presence of water resulted in a low yield of 9% of sulfone **70**. Several challenges had to be considered for the reaction, which could be controlled using specific solvents. For example, phenols as electron-rich and easily oxidizable substrates tend to over-oxidize to form oligomeric by-products and homo-coupling products.[185] HFIP is not only known to stabilize radicals and cations,[16b] it also forms microstructural domains due to its hydrophilic and hydrophobic nature,[186] which allows solvation of both charged (like sulfinate anions or radical-cations) and uncharged substrate molecules. Thus, a reaction control towards the cross-coupling product is promoted, and a phenol-phenol homo-coupling could be suppressed. As a comparison, a test reaction with acetonitrile instead of HFIP was performed under the optimized conditions with 15 vol.% water.[184] The yield of **70** dropped to 17%, which supports this argumentation. As another challenge, aryl sulfones tend to undergo electrochemical reduction and decomposition to sulfinates and arenes.[187] Advantageously, adding water to the HFIP solvent not only improved the solubility of the sulfinate salt and enabled its dual role but also promoted a hydrogen evolution as a cathodic counter-reaction since water is reduced in the same potential range as the sulfone products.[187] Sulfone decomposition can be therefore diminished.

Besides the water influence, it was ascertained that only equimolar amounts of sulfinate salts are needed for the reaction, and no yield improvement of sulfones was obtained with higher equivalents.[184] The reaction is temperature independent within a moderate range of 23 °C to 50 °C.[184] Other carbon-based electrodes (glassy carbon and graphite) proved to be comparably suitable for the reaction.[184] Nevertheless, BDD was mainly applied due to its higher stability towards electrochemical conversions in an aqueous media. The scope of sulfonylated phenols is presented in Scheme 13a. As demonstrated, aryl sulfinates, with or

without halogen-substituents, and alkyl sulfinates are applicable for the reaction.[184] Due to the simple set-up of an undivided cell and a constant current mode of operation, a straightforward 8-fold scale-up synthesis of **70** could be demonstrated, furnishing a comparable yield of 47%.

After establishing this methodology for phenols, a subsequent research target was to enlarge the scope of possible substrates to provide one method for the general sulfonylation of different electron-rich aromatic substrate classes. Therefore, the focus was set to electron-rich arenes and aniline derivatives. Starting from the same reaction conditions used for the phenol-coupling, 15 vol.% water in the electrolyte also proved to deliver the best yields.[188] The electrolysis time could be reduced from 3 h to 1.5 h due to the possibility of applying higher current densities of 26 mA/cm^2. As with the conversion of the phenols, for the arene reactions, it was possible to use 0.5 *F* as a low charge amount excess (2.5 *F* in total, as 2.0 *F* is the theoretical charge amount) and only a low mol-equivalent excess of sulfinate salt (1.3 eq.). By testing inexpensive graphite electrodes, the yield of **82** dropped slightly from 67% (with BDD) to 60%. The conditions for the anilide reactions were adjusted to 3.5 *F*, 12 mA/cm^2, and 1.5 eq. of sulfinate. Applying glassy carbon electrodes showed comparable but slightly decreased yields than BDD electrodes. Generally, the yields of anilides were decreased than for the dimethyl anilines. This observation was explained by a partial deprotection of the anilides, with a subsequent over-oxidation of the electron-rich anilines, which causes the formation of polyaniline.[189] Furthermore, sterical effects of the sulfonylated products were discussed based on molecular structure analysis, which could explain further electrochemical degradation of the sulfonylated anilides.[188] The scope also represents toleration of halogen-containing sulfinates and arenes and non-methoxy substituted arenes (Scheme 13a). An 8-fold scale-up reaction was demonstrated for **82**.[188]

Mechanistically, CV studies revealed the initial electrochemical step as to arise from the oxidation of the electron-rich substrates **I** (Scheme 13c), followed by a nucleophilic attack from the sulfinate species **III**. As a counter-reaction, water reduction to hydrogen was determined (Scheme 13b).

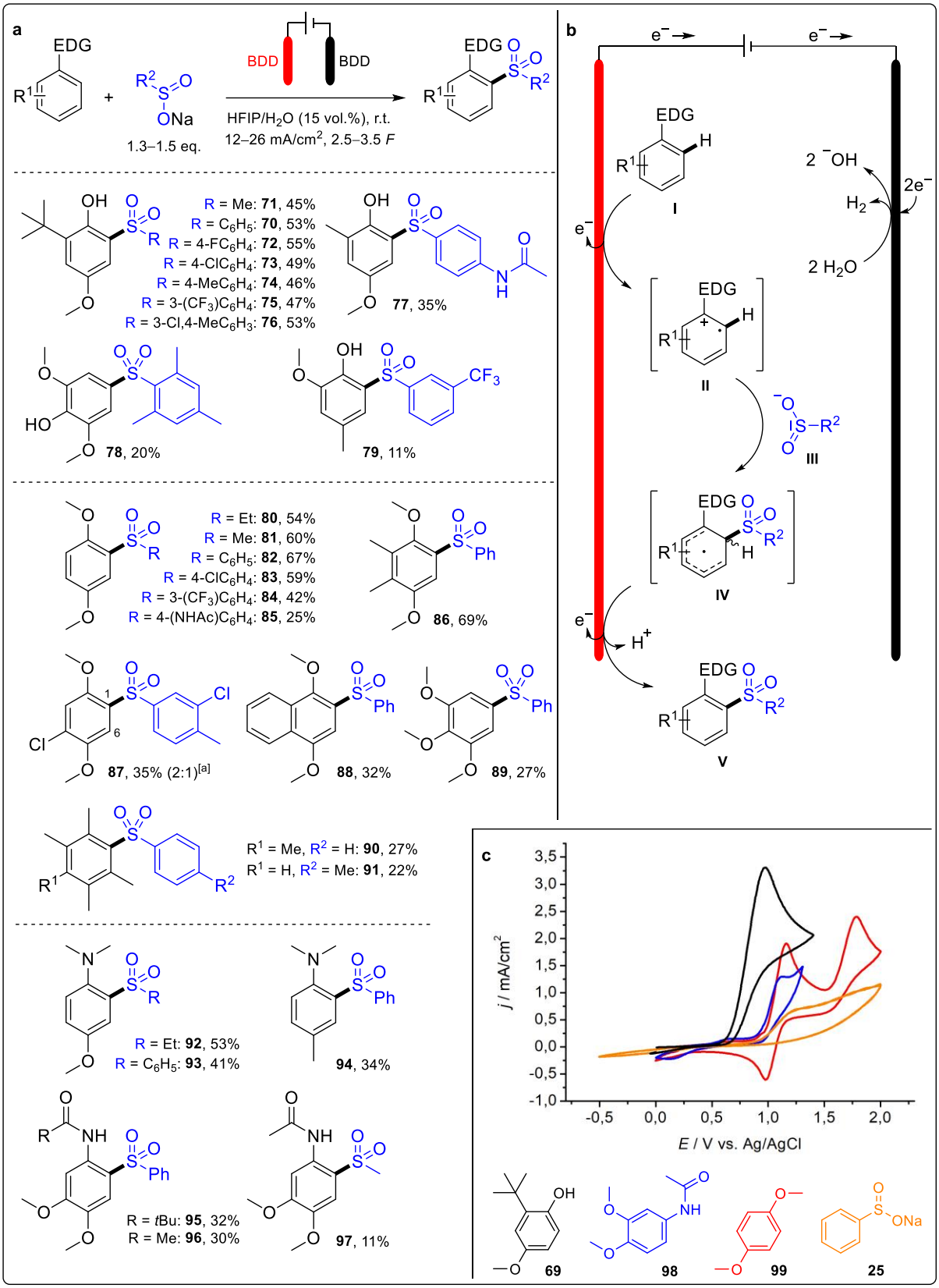

Scheme 13: a General reaction scheme and scope of sulfonylated electron-rich aromatic compounds. [a] Yield ratio between regio isomers (C1:C6 coupling).[184,188] **b** Proposed reaction mechanism based on CV study findings.[184,188] **c** Exemplary cyclic voltammograms of 2-(1,1-dimethylethyl)-4-methoxyphenol (**69**, black), 3,4-dimethoxyacetanilide (**98**, blue), 1,4-dimethoxybenzene (**99**, red) and sodium benzenesulfinate (**25**, orange).[184,188]

Conclusion

A unifying method for a material-efficient electrochemical sulfonylation of electron-rich aromatic compounds was successfully established. The conditions apply to phenols, arenes, and aniline derivatives, including alkyl, methoxy, and halogen substituents. The mild reaction conditions allow moderate to good yields within short reaction times. Aryl and alkyl sodium sulfinates were applied in a dual role as supporting electrolytes and nucleophilic reagents after the model of Figure 8a (Chapter 2.2), illustrating the material-saving approach of this work. The solvent HFIP can be easily distilled and purified after the electrolysis for reuse. This presented method is a valuable contribution to existing electrochemical sulfonylation approaches, where the focus was set on alternative, less material-encompassing conditions.

The results of the electrochemical sulfonylation of phenols have been published in *Chem. Eur. J.*[184] Detailed information about experimental data can be found in the manuscript (pp. 41–45) and in the supporting information (pp. 46–72), which are included immediately after this section. The results of the electrochemical sulfonylation of arenes and aniline derivatives have been published in *ChemElectroChem*.[188] Detailed information about experimental data can be found in the manuscript (pp. 73–78) and in the supporting information (pp. 79–114), which are included immediately after this section.

ChemPubSoc Europe

DOI: 10.1002/chem.201900850

CHEMISTRY A European Journal Communication

Sustainable Chemistry |*Hot Paper*|

Direct Metal- and Reagent-Free Sulfonylation of Phenols with Sodium Sulfinates by Electrosynthesis

Joachim Nikl,[a] Sebastian Lips,[a] Dieter Schollmeyer,[a] Robert Franke,[b, c] and Siegfried R. Waldvogel*[a]

Abstract: A novel electrochemical strategy for the synthesis of aryl sulfones by direct sulfonylation of phenols with sodium sulfinates has been developed. The C,S-coupling products are of particular interest for chemical synthesis, material sciences and pharmaceutical sciences. By using this metal- and reagent-free electrochemical method, aryl and diaryl sulfones can be obtained directly in good yields. The established one-step protocol is easy to perform, scalable, inherently safe, and enables a broad scope, which is not limited by quinoid-forming substrates.

Aryl sulfones are used in many different areas, especially in pharmaceutical sciences.[1] In active pharmaceutical ingredients the sulfone group represents an important structural motif.[2] Significant representatives among them are the antibiotic dapsone (**1**),[3] which is used for the treatment of leprosy and malaria. Examples for cytostatics are Vismodegib (**2**),[4] a basal cell carcinoma treatment agent, and Bicalutamide (**3**) against prostate cancer (Scheme 1).[5] In addition, many others are reported illustrating the bioactive features of the sulfone group.[6]

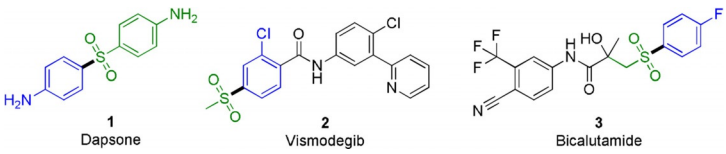

Scheme 1. Examples of active ingredients involving a sulfone moiety.[3–5]

Apart from the development of active substances, sulfones are used in material sciences as polysulfones in fuel cell membranes.[7] Many protocols for the synthesis of sulfonylated aromatic structures have already been reported, which underlines the high research interest.[8] Most of the reported syntheses consist of classical coupling reactions in which mainly transition metals and oxidative coupling reagents are employed.[9] Generation of the cross-coupling product from phenol and benzenesulfinic acid has been reported by Ullmann et al. in 1901.[10] This elaborative multistep reaction resulted in moderate yields of 47% (Scheme 2). In addition to the high reagent waste, the harsh reaction conditions are disadvantageous as well. A versatile method for coupling aryliodides with sulfinic acids has been developed by Manolikakes et al.[11] Here the sulfones are obtained via a photocatalytic reaction. However, the assistance of harmful transition metals as catalysts and intermediate oxidizing agents provides additional reagent waste. The coupling also requires a preliminary synthesis of the starting materials and it is only one phenol-sulfinate coupling product described by this method.

In contrast to conventional coupling reactions, electrochemical methods are highly advantageous since utilization of harmful transition metals and drastic reaction conditions are avoided. A safe experimental execution and precise control is guaranteed by the simple switching on and off of the electric current.[12] By using electrons as reagents a direct C–H activation is possible, which makes the presence of functional groups at the coupling positions superfluous. This leads to a prevention of any reagent waste and the associated significant costs.[12] Therefore the electrochemical mode of operation provides a safe and sustainable manner of organic synthesis in general, and also especially for producing aryl sulfones.[13] A recent example was presented by Feng et al.[13a] By an iodide-mediated potentiostatic electrolysis, a sulfonylation of 1*H*-indoles with sodium sulfinates was performed. In this conversion, the use of tetrabutylammonium iodide as a redox mediator is indispensable, which leads to additional reagent waste. In particular, the group of Nematollahi et al. has conducted extensive research in electrochemical sulfonylation.[14] But a central aspect of these conversions described is a postulated 1,4-addition mechanism of the sulfinate anion to quinoid-forming substrates. For electrochemical sulfonylation, a reaction between anodically formed amino-*ortho*-quinones and sulfinic acid sodium salts by a 1,4-addition mechanism is anticipated.[14a] This involves working with medi-

[a] *J. Nikl, S. Lips, Dr. D. Schollmeyer, Prof. Dr. S. R. Waldvogel*
Institut für Organische Chemie, Johannes Gutenberg-Universität Mainz
Duesbergweg 10–14, 55128 Mainz (Germany)
E-mail: waldvogel@uni-mainz.de
Homepage: http//www.chemie.uni-mainz.de/OC/AK-Waldvogel/

[b] *Prof. Dr. R. Franke*
Evonik Performance Materials GmbH
Paul-Baumann-Straße 1, 45772 Marl (Germany)

[c] *Prof. Dr. R. Franke*
Lehrstuhl für Theoretische Chemie, Ruhr-Universität Bochum
44780 Bochum (Germany)

Supporting information and the ORCID identification number(s) for the author(s) of this article can be found under:
https://doi.org/10.1002/chem.201900850.

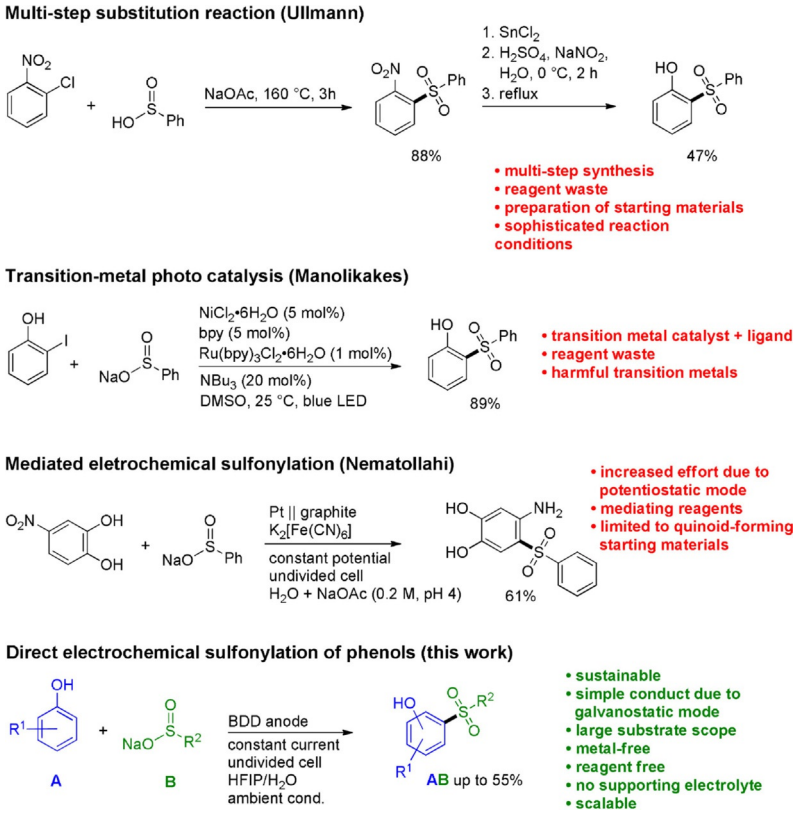

Scheme 2. Strategies to generate cross-coupling products of phenols with sulfinic acids and concept of this work.[10,11,14a]

ating reagents in potentiostatic mode, which results in increased effort, hardly scalable conditions and additional waste.

Herein, we present a sustainable, waste-preventing method by a direct electrochemical coupling of phenols with sodium sulfinates. Furthermore, the use of additional supporting electrolytes is not necessary as the sulfinates are acting as both, reagent and electrolyte. A simple galvanostatic mode of operation in an undivided electrolysis cell ensures scalability and an easy, rapid performance. These characteristics, supplemented by the use of water in the solvent, provides this protocol the attributes of green chemistry.[15,16]

Anodic coupling reactions are an important and sustainable alternative to conventional methods, as numerous publications have already shown.[17–25] The coupling reactions of phenols are particularly noteworthy. Various successfully homo- and cross-coupling reactions of phenols have been carried out so far like the synthesis of symmetric and nonsymmetric biphenols,[17] phenol-arenes,[18] *meta*-terphenyl-2,2″-diols,[19] 2-hydroxy-*para*-terphenyls,[20] phenol-thiophenes,[21] phenol-benzofurans,[22] phenol-naphthylamines,[23] and phenol-benzo[*b*]thiophenes.[24] In all of such electrochemical coupling reactions, one particular challenge is to avoid byproducts resulting from homocoupling and over-oxidation reactions to poly- and oligomeric products.[26] This challenging task also had to be mastered in this protocol as well. A key role in accomplishing that is a solvent-controlled reaction process using 1,1,1,3,3,3-hexafluoroisopropanol (HFIP).[27] As a strong hydrogen-bridge donor, HFIP is able to stabilize radical and cationic intermediates by solvation.[28] In addition, HFIP is a low-electron compound and is characterized by the fact that substances with an increased electron density are more strongly solvated, whereby a decoupling of oxidation potential and nucleophilicity can be ensured.[15,27] These advantages lead to supply selective coupling products for anodic conversions.[29] Moreover, several studies have shown that sulfones are subject to electrochemical reduction and decomposition,[30] which makes galvanostatic electrolysis in an undivided cell challenging. We succeeded in solving this difficulty by adjusting the reaction conditions and the electrolysis parameters to enable a direct electrochemical sulfonylation of phenols. By adding water to the solvent, decomposition of the generated sulfones can be diminished, since their redox potentials are mostly located in the same range as those of protons and water,[31] with the consequence that hydrogen is preferably generated at the cathode. Due to the aqueous media, the additional possibility to use the sulfinates as a supporting electrolyte is created, ensuring their dual function as electrolyte and coupling component. Therefore, additional reagent waste is prevented efficiently. Upon intensive optimization of electrolysis conditions with the test substrates 2-(1,1-dimethylethyl)-4-methoxyphenol (**4**) and sodium benzenesulfinate (**5**) by means of an electrosynthetic screening setup,[32] the best ones were figured out and are displayed in Scheme 3.

The amount of water in the solvent has a major impact on the conversion (Table 1). Carrying out the reaction in HFIP and 0.09 M methyltributylammonium methyl sulfate (MTBS) led to a

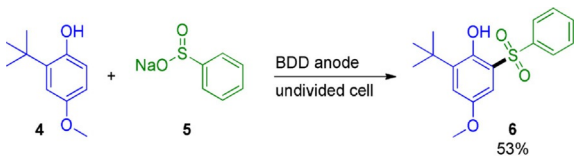

Scheme 3. Test reaction under optimized conditions for electroorganic synthesis of 2-(1,1-dimethylethyl)-4-methoxy-6-(phenylsulfonyl)phenol (**6**). Conditions: BDD anode and cathode, 15 vol.% water in HFIP, rt, $j = 12$ mA cm^{-2}, $Q = 2.5$ F (ref. **4**), **4**/**5** = 1:1.3.

Table 1. Influence of the water onto the yield of **6**.[a]

Entry	Water content in HFIP [vol.%]	Yield [%][b]
1[c]	0	9
2	6	35
3	10	51
4	15	52
5	20	49
6	25	37
7	35	40
8	45	38

[a] BDD anode and cathode, $j = 7.2$ mA cm^{-2}, $Q = 2.5$ F (ref. **4**), **4**/**5** = 1:3. [b] Isolated yield. [c] Electrolyte: MTBS (0.09 M) in HFIP.

nonselective conversion to 2-(1,1-dimethylethyl)-4-methoxy-6-(phenylsulfonyl)phenol (**6**) with a yield of 9% (Table 1, entry 1). Instead, a water content of 15 vol.% was found to be optimal for the reaction. Consequently, further investigation were carried out with this electrolyte system. Varying the current density and the charge quantity clarified an influence on conversion (Table 2), whereas increasing the reaction temperature showed no effect (Table 3). The highest isolated yield of **6** was achieved by applying 2.5 F referring to **4** at BDD electrodes in a HFIP/water mixture with 15 vol.% water. Best conversion to the cross-coupling product was observed with 12 mA cm^{-2}. At first,

Table 2. Influence of the current density and the charge quantity onto the yield of **6**.[a]

Entry	j [mA cm^{-2}]	Q [F (ref. **4**)]	Yield [%][b]
1	7.2	2.5	47
2	12.0	2.5	53
3	12.0	3.0	42

[a] j: current density, Q: charge quantity. BDD anode and cathode, 15 vol.% water in HFIP, **4**/**5** = 1:1.3. [b] Isolated yield.

Table 3. Influence of the temperature onto the yield of **6**.[a]

Entry	Electrolysis T [°C]	Yield [%][b]
1	23	53
2	35	50
3	50	50

[a] BDD anode and cathode, 15 vol.% water in HFIP, $j = 12$ mA cm^{-2}, $Q = 2.5$ F (ref. **4**), **4**/**5** = 1:1.3. [b] Isolated yield.

a large excess of sulfinate with three equivalents were tested, to ensure conductivity (Table 1). But since the ratio of phenol to sulfinate needs to be 1 to 1.3, there is just a small excess of component **B** necessary, which reveals a very good atom economy in this conversion (Tables 2 and 3). This fact can be explained by the ambivalent solubility properties of HFIP. Due to its polar hydroxy group and the nonpolar fluorinated carbon chain, microheterogeneous domains are formed.[33] Polar and nonpolar reagents can thus be separated, which is assumed to be the reason for the low sulfinate excess required. At a phenol to sulfinate ratio of 1 to 3, compound **6** was obtained in a comparable yield of 52% (Table 1, entry 4), which is considered as an indication for this hypothesis. To underline the influence of HFIP on the conversion, the test reaction was performed with acetonitrile/water (15 vol.% H_2O) under the given conditions and parameters, whereby compound **6** was obtained with a yield of 17%. A further advantage of HFIP is its low boiling point, which allows it to be easily recovered by distillation after electrolysis.[34]

The outstanding properties of boron-doped diamond electrodes (BDD) in electro-organic synthesis have been studied extensively.[35] The high robustness and chemical inertness of diamond, supplemented by the conductivity due to doping, also delivered the best results in this coupling reaction. For comparison, a reaction was performed on graphite electrodes under the conditions displayed in Scheme 3, giving **6** in an isolated yield of 41%, whereas the use of glassy carbon electrodes delivered a yield of 49%. The better results of BDD are explained by its higher robustness and ability to form highly reactive radicals in a wider electrochemical window. The combination of HFIP and BDD electrodes has proven itself in various anodic coupling reactions,[35] and thus delivered the best results also for this protocol. By applying the conditions shown in Scheme 3, a collection of sulfonylated phenols were isolated (Scheme 4). As indicated, the established protocol allows several cross-coupling products with a phenol moiety in good isolated yields up to 55% by a simple and fast implementation. Functional groups like halogen substituents are tolerated, which is illustrated by the examples of **7**, **8**, and **9**. By using aryl sulfinates, diaryl sulfones are obtained as coupling products. Not only aryl sulfinates but also aliphatic ones are suitable which is demonstrated by example **12**. Therefore both, diaryl and aryl sulfones, are accessible. In general, the decrease in yield is mainly due to the formation of over-oxidation products, since just small amounts of starting material were recovered after workup. Differences in yields occur when the phenol component is varied. For example also *meta*-substituted methoxyphenols were tested, showing a significantly lower conversion to the sulfonylation product, which was verified by GCMS analytics. The better yields of *ortho*-coupling can be explained by a directing effect of the hydroxy group to the sulfinic acid group. This is illustrated by the stabilizing hydrogen bond in example **6** (Figure 1). Furthermore, the molecular structure of **14** is displayed, which demonstrates that methoxy groups at the 2-position can also form hydrogen bonds, neutralizing a directing effect. This might explain the lower yields of **14** and **15**.

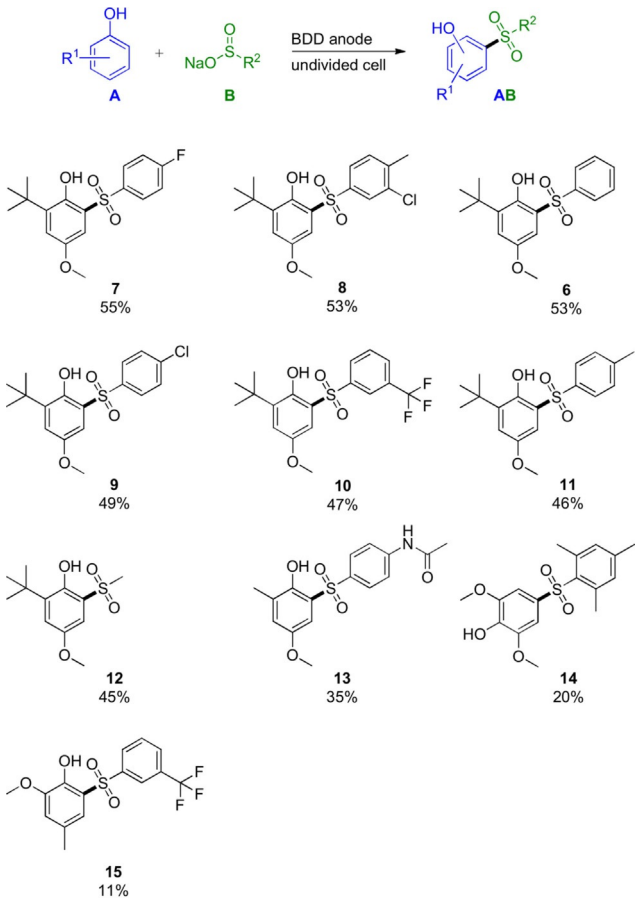

Scheme 4. Scope of hydroxyarylsulfones. Conditions: BDD anode and cathode, 15 vol.% water in HFIP, rt, $j = 12$ mA cm^{-2}, $Q = 2.5$ F (ref. **A**), **A**/**B** = 1:1.3.

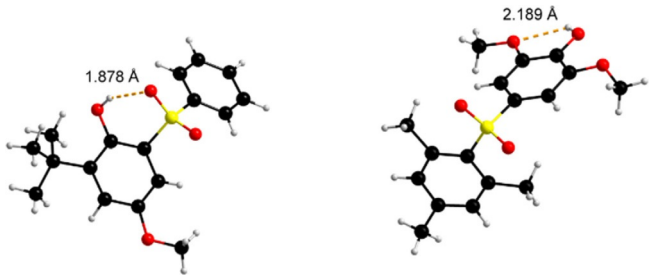

Figure 1. Molecular structures by X-ray analysis of **6** and **14** with indicated hydrogen bonds.

When using low-substituted phenols, the reaction is less selective. At unsubstituted 4- and 6-positions, product mixtures are partially obtained, which is attributed to the radical stabilization at these positions.

To demonstrate the scalability and robustness of this electro-organic reaction, a scale-up from a 25 mL beaker-type electrolysis cell (5.00 mmol of **4**) to a 200 mL beaker-type cell (40.0 mmol of **4**) was performed. Application of this electrolytic protocol gives **6** in almost the same yield of 47% (6.06 g). More detailed information can be found within the Supporting Information.

With regard to the mechanism, a prior oxidation of the phenol component **A** is assumed. Afterwards a phenoxyl radical is formed, which is conserved by the radical-stabilizing properties of HFIP. For C–S bond formation, a nucleophilic attack from the sulfinate **B** on the radical takes place. After a further anodic oxidation step, the arylsulfone **AB** is formed. The assumption of this mechanism is supported by oxidation potential determinations, revealing the lower oxidation potentials of the phenol components. Thus the preferred oxidation of the phenols can be confirmed, which confers with the frequently described mechanism describing anodic C,C-cross-coupling reactions (Supporting Information).[17]

In conclusion, we have established a safe and sustainable approach for the direct coupling of phenols with sulfinates, which provides aryl and diaryl sulfones in acceptable yields. In this electrochemical method, the sulfinates are used both as supporting electrolytes and coupling components, leading to a prevention of further additives and reagent waste. This process uses constant current in an undivided cell with a two-electrode arrangement and is, therefore, scalable and easy to perform. Overall, this anodic oxidation protocol represents a metal- and reagent-free alternative and complies with basic requirements of the green chemistry concept.

Experimental Section

Detailed information on general procedures, electrolytic conversions and product characterization can be found in the Supporting Information.

Acknowledgements

S.R.W. thanks the DFG (Wa1276/15-1) for financial support. S.L. and S.R.W. acknowledge the Carl-Zeiss Foundation for granting a fellowship and the research network ELYSION, respectively.

Conflict of interest

The authors declare no conflict of interest.

Keywords: C–H activation · cross-coupling · electrochemistry · oxidation · sustainable chemistry

[1] a) M. Feng, B. Tang, S. H. Liang, X. Jiang, *Curr. Top. Med. Chem.* **2016**, *16*, 1200 – 1216; b) D. C. Meadows, J. Gervay-Hague, *Med. Res. Rev.* **2006**, *26*, 793 – 814.
[2] K. Hofman, N.-W. Liu, G. Manolikakes, *Chem. Eur. J.* **2018**, *24*, 11852 – 11863.
[3] A. C. McDougall, *Clin. Exp. Dermatol.* **1979**, *4*, 139 – 142.
[4] J. T. Lear, *N. Engl. J. Med.* **2012**, *366*, 2225 – 2226.
[5] I. D. Cockshott, *Clin. Pharmacokinet.* **2004**, *43*, 855 – 878.
[6] a) M. Artico, R. Silvestri, S. Massa, A. G. Loi, S. Corrias, G. Piras, P. La Colla, *J. Med. Chem.* **1996**, *39*, 522 – 530; b) T. M. Williams, T. M. Ciccarone, S. C. MacTough, C. S. Rooney, S. K. Balani, J. H. Condra, E. A. Emini, M. E. Goldman, W. J. Greenlee, L. R. Kauffman, J. A. O'Brien, V. V. Sardana, W. A. Schleif, A. D. Theoharides, P. S. Anderson, *J. Med. Chem.* **1993**, *36*, 1291 – 1294.

[7] J. K. Fink, *High Performance Polymers*, William Andrew, Norwich, **2008**; R. Padmavathi, R. Karthikumar, D. Sangeetha, *Electrochim. Acta* **2012**, *71*, 283 – 293.
[8] a) K. P. Borujeni, B. Tamami, *Catal. Commun.* **2007**, *8*, 1191 – 1196; b) K. P. Boroujeni, *Bull. Korean Chem. Soc.* **2010**, *31*, 1887 – 1890; c) H. Sharghi, Z. Shahsavari-Fard, *Helv. Chim. Acta* **2005**, *88*, 42 – 52; d) B. F. Mirjalili, M. A. Zolfigol, A. Bamoniri, L. Khazdooz, *Bull. Korean Chem. Soc.* **2003**, *24*, 1009 – 1010; e) A. R. Hajipour, A. Zarei, L. Khazdooz, S. A. Pourmousavi, *Phosphorus Sulfur Silicon Relat. Elem.* **2005**, *180*, 2029 – 2034; f) N. Umierski, G. Manolikakes, *Org. Lett.* **2013**, *15*, 188 – 191; g) N. Umierski, G. Manolikakes, *Org. Lett.* **2013**, *15*, 4972 – 4975; h) A. Hossan, *Chem. Heterocycl. Compd.* **2016**, *52*, 570 – 573; i) A. Ahmad, A. K. Chauhan, S. Javed, A. Kumar, *Biotechnol. Lett.* **2014**, *36*, 2209 – 2214.
[9] a) B. P. Bandgar, S. V. Bettigeri, J. Phopase, *Org. Lett.* **2004**, *6*, 2105 – 2108; b) C. Wang, H. Zhang, Z. Li, Z. Wang, *J. Chem. Res.* **2014**, *38*, 639 – 642; c) D. H. Kim, J. Lee, A. Lee, *Org. Lett.* **2018**, *20*, 764 – 767; d) J. Marquié, A. Laporterie, J. Dubac, N. Roques, J.-R. Desmurs, *J. Org. Chem.* **2001**, *66*, 421 – 425; e) C. G. Frost, J. P. Hartley, A. J. Whittle, *Synlett* **2001**, 0830 – 0832; f) S. Répichet, C. Le Roux, P. Hernandez, J. Dubac, J.-R. Desmurs, *J. Org. Chem.* **1999**, *64*, 6479 – 6482; g) H. Yue, C. Zhu, M. Rueping, *Angew. Chem. Int. Ed.* **2018**, *57*, 1371 – 1375; *Angew. Chem.* **2018**, *130*, 1385 – 1389.
[10] F. Ullmann, Q. Pasdermadjian, *Ber. Dtsch. Chem. Ges.* **1901**, *34*, 1150 – 1157.
[11] N.-W. Liu, K. Hofman, A. Herbert, G. Manolikakes, *Org. Lett.* **2018**, *20*, 760 – 763.
[12] a) A. Wiebe, T. Gieshoff, S. Möhle, E. Rodrigo, M. Zirbes, S. R. Waldvogel, *Angew. Chem. Int. Ed.* **2018**, *57*, 5594 – 5619; *Angew. Chem.* **2018**, *130*, 5694 – 5721; b) S. Möhle, M. Zirbes, E. Rodrigo, T. Gieshoff, A. Wiebe, S. R. Waldvogel, *Angew. Chem. Int. Ed.* **2018**, *57*, 6018 – 6041; *Angew. Chem.* **2018**, *130*, 6124 – 6149.
[13] a) M.-L. Feng, L.-Y. Xi, S.-Y. Chen, X.-Q. Yu, *Eur. J. Org. Chem.* **2017**, 2746 – 2750; b) Y.-C. Luo, X.-J. Pan, G.-Q. Yuan, *Tetrahedron* **2015**, *71*, 2119 – 2123.
[14] a) D. Nematollahi, F. Varmaghani, *Electrochim. Acta* **2008**, *53*, 3350 – 3355; b) D. Nematollahi, M. Baniardalan, S. Khazalpour, M. R. Pajohi-Alamoti, *Electrochim. Acta* **2016**, *191*, 98 – 105; c) D. Nematollahi, M. Malakzadeh, *J. Electroanal. Chem.* **2003**, *547*, 191 – 195; d) D. Nematollahi, R. A. Rahchamani, *J. Electroanal. Chem.* **2002**, *520*, 145 – 149; e) D. Nematollahi, R. Esmaili, *Tetrahedron Lett.* **2010**, *51*, 4862 – 4865; f) H. Beiginejad, D. Nematollahi, F. Varmaghani, M. Bayat, H. Salehzadeh, *J. Electrochem. Soc.* **2013**, *160*, G3001 – G3007; g) D. Nematollahi, D. Habibi, A. Alizadeh, *Phosphorus Sulfur Silicon Relat. Elem.* **2006**, *181*, 1391 – 1396.
[15] S. R. Waldvogel, S. Lips, M. Selt, B. Riehl, C. J. Kampf, *Chem. Rev.* **2018**, *118*, 6706 – 6765.
[16] B. A. Frontana-Uribe, R. D. Little, J. G. Ibanez, A. Palma, R. Vasquez-Medrano, *Green Chem.* **2010**, *12*, 2099 – 2119.
[17] a) B. Riehl, K. Dyballa, R. Franke, S. Waldvogel, *Synthesis* **2017**, *49*, 252 – 259; b) A. Wiebe, D. Schollmeyer, K. M. Dyballa, R. Franke, S. R. Waldvogel, *Angew. Chem. Int. Ed.* **2016**, *55*, 11801 – 11805; *Angew. Chem.* **2016**, *128*, 11979 – 11983; c) B. Elsler, D. Schollmeyer, K. M. Dyballa, R. Franke, S. R. Waldvogel, *Angew. Chem. Int. Ed.* **2014**, *53*, 4979; *Angew. Chem.* **2014**, *126*, 5311 – 5314.
[18] a) A. Kirste, G. Schnakenburg, F. Stecker, A. Fischer, S. R. Waldvogel, *Angew. Chem. Int. Ed.* **2010**, *49*, 971 – 975; *Angew. Chem.* **2010**, *122*, 983 – 987; b) A. Kirste, B. Elsler, G. Schnakenburg, S. R. Waldvogel, *J. Am. Chem. Soc.* **2012**, *134*, 3571 – 3576.
[19] S. Lips, A. Wiebe, B. Elsler, D. Schollmeyer, K. M. Dyballa, R. Franke, S. R. Waldvogel, *Angew. Chem. Int. Ed.* **2016**, *55*, 10872 – 10876; *Angew. Chem.* **2016**, *128*, 11031 – 11035.
[20] S. Lips, R. Franke, S. R. Waldvogel, *Synlett* **2019**, DOI https://doi.org/10.1055/s-0037-1611942.
[21] A. Wiebe, S. Lips, D. Schollmeyer, R. Franke, S. R. Waldvogel, *Angew. Chem. Int. Ed.* **2017**, *56*, 14727 – 14731; *Angew. Chem.* **2017**, *129*, 14920 – 14925.
[22] S. Lips, B. A. Frontana-Uribe, M. Dörr, D. Schollmeyer, R. Franke, S. R. Waldvogel, *Chem. Eur. J.* **2018**, *24*, 6057 – 6061.
[23] B. Dahms, R. Franke, S. R. Waldvogel, *ChemElectroChem* **2018**, *5*, 1249 – 1252.
[24] S. Lips, D. Schollmeyer, R. Franke, S. R. Waldvogel, *Angew. Chem. Int. Ed.* **2018**, *57*, 13325 – 13329; *Angew. Chem.* **2018**, *130*, 13509 – 13513.
[25] L. Schulz, M. Enders, B. Elsler, D. Schollmeyer, K. M. Dyballa, R. Franke, S. R. Waldvogel, *Angew. Chem. Int. Ed.* **2017**, *56*, 4877 – 4881; *Angew. Chem.* **2017**, *129*, 4955 – 4959.
[26] a) X. Yang, J. Kirsch, J. Fergus, A. Simonian, *Electrochim. Acta* **2013**, *94*, 259 – 268; b) J. Iniesta, P. A. Michaud, M. Panizza, G. Cerisola, A. Aldaz, C. Comninellis, *Electrochim. Acta* **2001**, *46*, 3573 – 3578; c) M. A. Rodrigo, P. A. Michaud, I. Duo, M. Panizza, G. Cerisola, C. Comninellis, *J. Electrochem. Soc.* **2001**, *148*, D60 – D64.
[27] B. Elsler, A. Wiebe, D. Schollmeyer, K. M. Dyballa, R. Franke, S. R. Waldvogel, *Chem. Eur. J.* **2015**, *21*, 12321 – 12325.
[28] a) L. Eberson, M. P. Hartshorn, O. Persson, *J. Chem. Soc. Perkin Trans. 2* **1995**, 1735 – 1744; b) S. R. Waldvogel, S. Mentizi, A. Kirste, *Top. Curr. Chem.* **2012**, *320*, 1 – 31.
[29] L. Schulz, S. R. Waldvogel, *Synlett* **2019**, *30*, 275 – 286.
[30] a) J. Delaunay, G. Mabon, M. Chaquiq El Badre, A. Orliac, J. Simonet, *Tetrahedron Lett.* **1992**, *33*, 2149 – 2150; b) S. Prigent, P. Cauliez, J. Simonet, D. G. Peters, *Acta Chem. Scand.* **1999**, *53*, 892 – 900; c) J.-F. Bergamini, P. Hapiot, C. Lagrost, L. Preda, J. Simonet, E. Volanschi, *Phys. Chem. Chem. Phys.* **2003**, *5*, 4846 – 4850.
[31] J. Simonet, *Phosphorus Sulfur Silicon Relat. Elem.* **1993**, *74*, 93 – 112.
[32] C. Gütz, B. Klöckner, S. R. Waldvogel, *Org. Process Res. Dev.* **2016**, *20*, 26 – 32.
[33] O. Hollóczki, A. Berkessel, J. Mars, M. Mezger, A. Wiebe, S. R. Waldvogel, B. Kirchner, *ACS Catal.* **2017**, *7*, 1846 – 1852.
[34] I. Colomer, A. E. R. Chamberlain, M. B. Haughey, T. J. Donohoe, *Nat. Chem. Rev.* **2017**, *1*, 88.
[35] S. Lips, S. R. Waldvogel, *ChemElectroChem* **2019**, *6*, 1649 – 1660.

Manuscript received: February 24, 2019
Accepted manuscript online: March 12, 2019
Version of record online: April 8, 2019

CHEMISTRY
A European Journal

Supporting Information

Direct Metal- and Reagent-Free Sulfonylation of Phenols with Sodium Sulfinates by Electrosynthesis

Joachim Nikl,[a] Sebastian Lips,[a] Dieter Schollmeyer,[a] Robert Franke,[b, c] and Siegfried R. Waldvogel*[a]

chem_201900850_sm_miscellaneous_information.pdf

Contents

1. General information

All reagents were used in analytical grades and were obtained from standard providers like ABCR, TCI, Aldrich, Fluka and Acros. Solvents were purified by standard methods.[1] Electrochemical reactions were carried out at boron-doped diamond (BDD) electrodes. BDD electrodes were obtained as DIACHEM™ quality from CONDIAS GmbH, Itzehoe, Germany. BDD (15 µm diamond layer) was used on silicon support.

Column Chromatography was performed on silica gel 60 M (0.040–0.063 mm, Macherey-Nagel GmbH & Co, Düren, Germany). Therefore, a preparative chromatography system (Büchi, Flawil, Switzerland) was used with a Büchi Control Unit C-620, an UV detector Büchi UV photometer C-635, a Büchi fraction collector C-660 and two Pump Modules C-605 for adjusting the solvent mixtures. As eluent, mixtures of cyclohexane and ethyl acetate were used. Silica gel 60 sheets on aluminium (F254, Merck KGaA, Darmstadt, Germany) were used for thin layer chromatography.

Gas chromatography was performed on a Shimadzu GC-2025 (Shimadzu, Japan) using a ZB-5MSi column (Phenomenex Inc., Torrance, California; length: 30 m, inner diameter: 0.25 mm, film: 0.25 µm, carrier gas: hydrogen). GC-MS measurements were carried out on a Shimadzu GC-2010 (Shimadzu, Japan) using a HP-1 column (Agilent Technologies, Santa Clara, California; length: 30 m, inner diameter: 0.25 mm, film: 0.25 µm, carrier gas: helium). The chromatograph was coupled to a mass spectrometer Shimadzu GC-MS-QP2010.

Melting points were determined with a Melting Point Apparatus B-565 (Büchi, Flawil, Switzerland) and are uncorrected. Heating rate: 1 °C/min.

NMR Spectroscopy of ^{1}H, ^{13}C and ^{19}F spectra were recorded at 25 °C, using a Bruker Avance II 400 (400 MHz, 5 mm BBFO-SmartProbe with z gradient and ATM, SampleXPress 60 sample changer, Analytische Messtechnik, Karlsruhe, Germany). Chemical shifts (δ) are reported in parts per million (ppm) relative to traces of $CHCl_3$ or DMSO-d_5 in the corresponding deuterated solvent. For ^{19}F spectra $CFCl_3$ serves as reference compound.[2]

High-resolution mass spectra were obtained by using an Agilent 6545 QTOF-MS (Agilent Technologies, Santa Clara, California) apparatus employing ESI^+ and $APCI^+$.

Cyclic voltammetry was performed in a 10 mL snap-cap vial equipped with an Autolab PGSTAT101 potentiostat (Metrohm AG, Herisau, Switzerland). *WE*: BDD electrode tip, 2 mm diameter; *CE*: glassy carbon rod; *RE*: Ag/AgCl in saturated LiCl/EtOH. Solvent: HFIP+15 vol.% H_2O. v = 100 mV/s, T = 20 °C, c = 0.01 M, supporting electrolyte: $_n$Bu$_4$NPF$_6$, c ($_n$Bu$_4$NPF$_6$) = 0.1 M.

X-ray analysis data were collected on a STOE IPDS-2T diffractometer (STOE & Cie GmbH, Darmstadt, Germany) using graphite monochromated Mo-*K*α radiation (λ = 0.71073 Å). Intensities were measured using fine-slicing ω and ϕ-scans and corrected for background, polarization and Lorentz effects. The structures were solved by direct methods and refined anisotropically by the least-squares procedure implemented in the SHELX program system.[3]

The supplementary crystallographic data for this paper can be obtained free of charge from the Cambridge Crystallographic Data Center via www.ccdc.cam.ac.uk/data_request/cif. Deposition numbers and further details are given with the individual characterization data.

2. Set-up and general protocol for electrolytic cross-coupling

The used beaker-type glass cells are homemade by the university's own mechanical shop. The undivided beaker-type cells are only briefly described here, whereby more detailed information has already been reported.[4] The cells are operated with boron-doped diamond electrodes (BDD).

GP 1: Beaker-type cell (25 mL)

The reactions were performed in a 25 mL beaker-type glass cell, which consists of a simple glass beaker with or without cooling jacket and is closed by a Teflon plug, which allows a precise arrangement of the BDD electrodes. Dimension of the BDD electrodes are 7 cm x 2 cm x 0.3 cm.

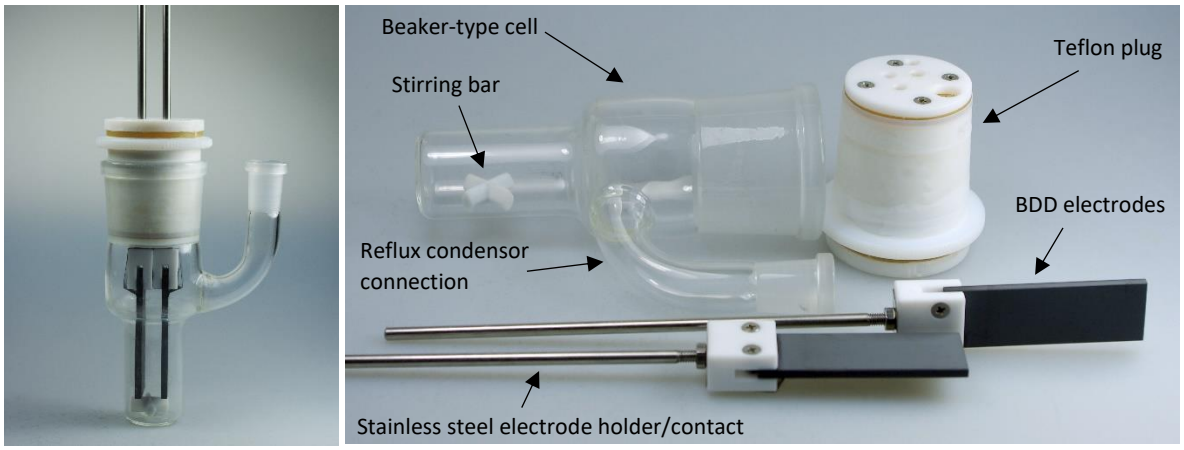

Figure 1: Beaker-type cell; left: assembled; right: individual parts.

The phenolic compound **A** (5 mmol) and the sulfinate **B** (6.5 mmol) are transferred into the undivided beaker-type electrolysis cell and are solved by 25 mL of a solvent mixture constituted of HFIP (21.25 mL) and deionized water (3.75 mL, 15 vol. %). The cell is equipped with a BDD anode and a BDD cathode, which has a distance of 1.1 cm to each other. The operable anode surface is about 9 cm^2. A constant current electrolysis with a current density of 12 mA/cm^2 has performed at 23 °C.

After application of 1206 C (2.5 F per phenol **A**) the HFIP is recaptured by distillation *in vacuo* (50 °C, 200–90 mbar). The crude product is solved by dichloromethane (50 mL) and deionized water (50 mL) and is transferred into a separatory funnel. After phase separation the aqueous layer is extracted with dichloromethane (2 x 50 mL). The combined organic fractions are washed with deionized water (2 x 50 mL) and dried with magnesium sulfate. Afterwards purification is carried out via column chromatography (SiO_2, cyclohexane/ethyl acetate).

GP 2: Cyclic voltammetry protocol

A 10 mM solution of the substrate in a HFIP-H_2O-mixture (2.5 mL, 15 vol.% H_2O) containing 0.1 M *N*,*N*,*N*,*N*-tetrabutylammonium hexafluorophosphate (nBu_4NPF_6) was placed in a 10 mL snap-cap vial. Degassing of the solution was carried out by bubbling argon through the solution for 5 minutes. Cyclic voltammetry was performed with a 0.1 V/s scan rate using a BDD working electrode (tip, 2 mm diameter), a glassy carbon rod as counter electrode and an Ag/AgCl reference electrode in saturated LiCl/EtOH.

GP 3: Beaker-type cell (200 mL)

The reactions were performed in a 200 mL beaker-type glass cell, which consists of a simple glass beaker with a glass adapter and is closed by a Teflon plug, which allows a precise arrangement of the BDD electrodes. Dimension of the BDD electrodes are 14 cm x 3.5 cm x 0.3 cm.

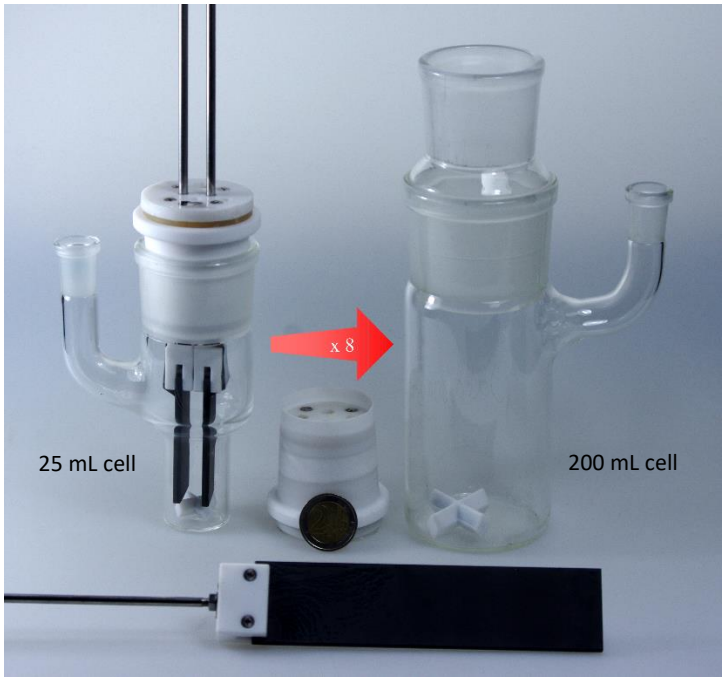

Figure 2: Size comparison of a 25 mL beaker-type cell (left) and a 200 mL beaker-type cell (right). One 2 € coin (diameter 25.75 mm ≈ 1.01 inches) is placed in front of the teflon plug.

The phenolic compound **A** (40 mmol) and the sulfinate **B** (60 mmol) are transferred into the undivided beaker-type electrolysis cell and are solved by 200 mL of a solvent mixture constituted of HFIP (170 mL) and deionized water (30 mL, 15 vol. %). The cell is equipped with a BDD anode and a BDD cathode, which has a distance of 1.7 cm to each other. The operable anode surface is about 21 cm^2. A constant current electrolysis with a current density of 12 mA/cm^2 has performed at 23 °C.

After application of 9649 C (2.5 F per phenol **A**) the HFIP is recovered by distillation *in vacuo* (50 °C, 200–90 mbar). The crude product is solved by dichloromethane (100 mL) and deionized water (100 mL) and is transferred into a separatory funnel. After phase separation the aqueous layer is extracted with dichloromethane (3 x 50 mL). The combined organic fractions are washed with deionized water (2 x 50 mL) and dried with magnesium sulfate. Afterwards purification is carried out via column chromatography (SiO_2, cyclohexane/ethyl acetate).

3. Mechanistic proposal and cyclic voltammetry data

Based on the already published postulated mechanism for anodic cross-coupling, a mechanism is described here which has a comparable course and provides an explanation for the resulting substitution patterns of the cross-coupling products.[5]

Initially, the phenolic component **A** is electrochemically oxidized to a phenoxyl radical **I**. Species **I** is trapped by a nucleophilic attack from the sulfinate anion **B**, which leads to a C–S bond formation. In a second oxidation step, the radical anion **V**/**VI** is oxidatively converted to the cross-coupling product **AB**.

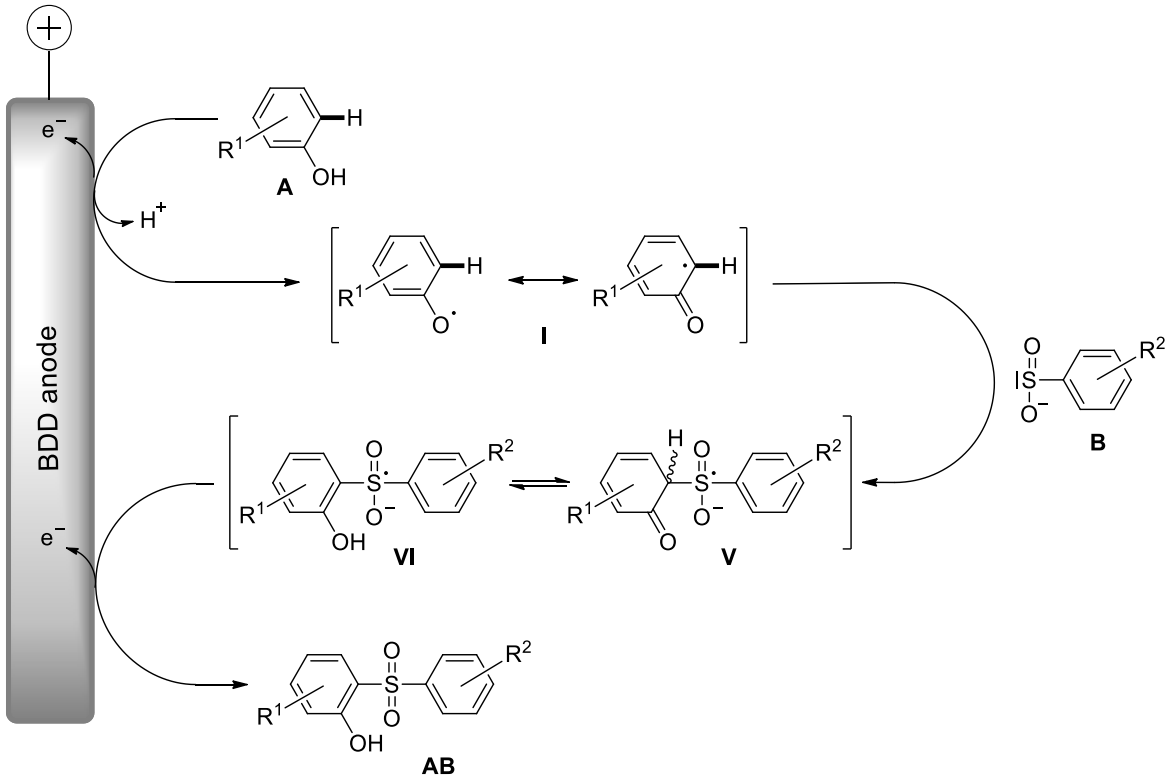

Scheme 1: Postulated mechanism for the anodic phenol-sulfinate cross-coupling.

The initial oxidation step is confirmed by cyclic voltammetry measurements. Figure 2 depicts, that the phenolic components 2-(1,1-dimethylethyl)-4-methoxyphenol (0.97 V) and 2,6-dimethoxyphenol (1.15 V) have lower oxidation potentials than the sulfinates sodium methanesulfinate (1.29 V) and sodium benzenesulfinate (1.27 V). This clearly reveals, that an initial oxidation of the phenolic components can be assumed.

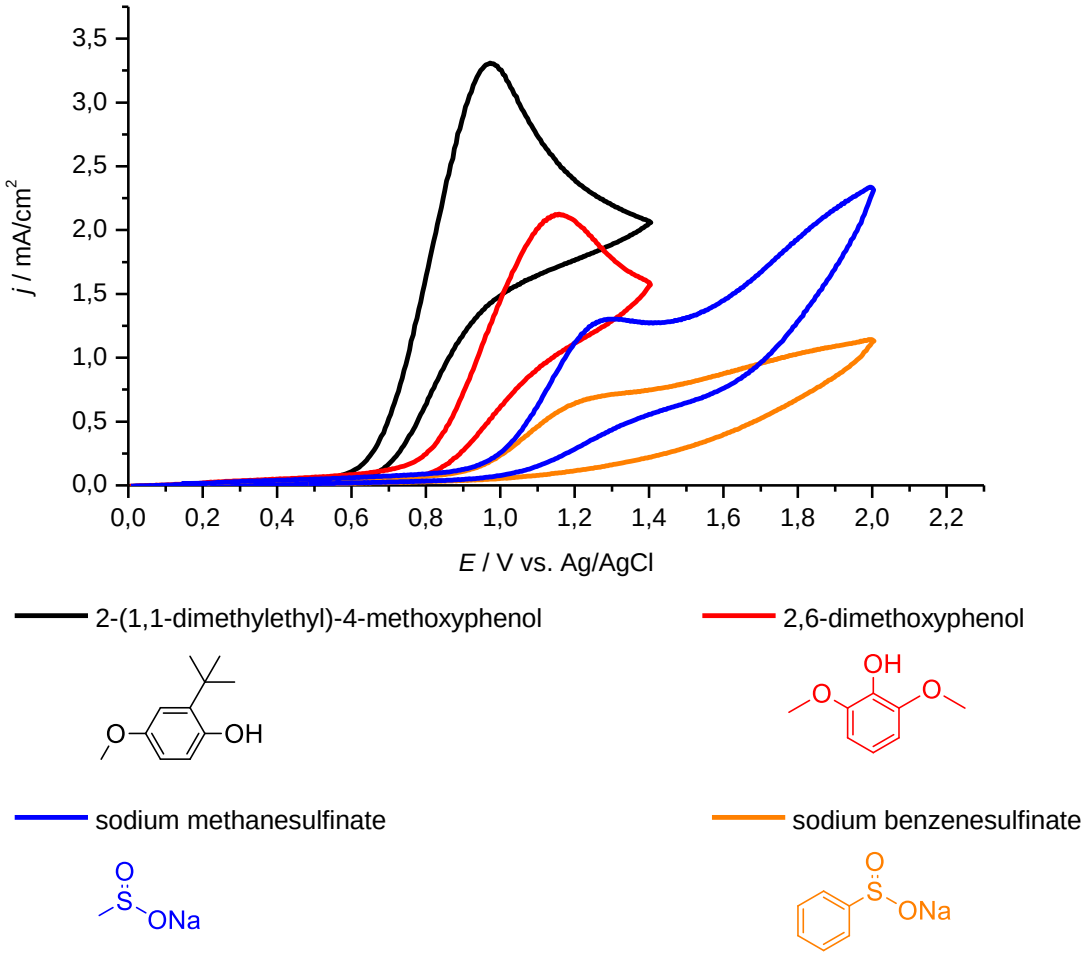

Figure 3: Cyclic voltammetric data of 2-(1,1-dimethylethyl)-4-methoxyphenol (black), 2,6-dimethoxyphenol (red), sodium methanesulfinate (blue) and sodium benzenesulfinate (orange). The measurements were carried out according to the general protocol **GP 2**.

4. Data of cross-coupling products

4.1 2-(1,1-Dimethylethyl)-6-(4-fluorophenylsulfonyl)-4-methoxyphenol (**7**)

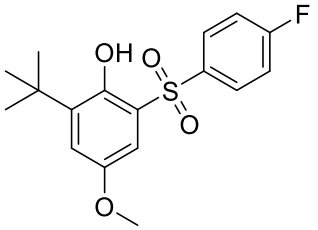

According to the general protocol (**GP 1**) 2-(1,1-dimethylethyl)-4-methoxyphenol (0.90 g, 5.00 mmol, 1.0 eq.) and 4-fluorobenzenesulfinic acid sodium salt (1.18 g, 6.50 mmol, 1.3 eq.) are solved in HFIP + 15 vol.% water (25 mL). After constant current electrolysis and workup, the residue is purified by column chromatography (cyclohexane/ethyl acetate = 100:0 → 98:2) to yield the product as a yellow-colored solid (yield: 55%, 0.93 g, 2.74 mmol).

m_R: 98–100 °C; R_f (cyclohexane/ethyl acetate = 9:1): 0.30; ^{1}H NMR (400 MHz, $CDCl_3$) δ [ppm] = 9.16 (s, 1H), 7.98–7.93 (m, 2H), 7.23–7.17 (m, 2H), 7.09 (d, *J* = 3.1 Hz, 1H), 6.98 (d, *J* = 3.1 Hz, 1H), 3.74 (s, 3H), 1.37 (s, 9H); ^{13}C NMR (101 MHz, $CDCl_3$) δ [ppm] = 165.8 (d, *J* = 257.0 Hz), 152.5, 149.5, 141.8, 138.1 (d, *J* = 3.0 Hz), 129.7 (d, *J* = 9.8 Hz), 123.0, 122.8, 116.9 (d, *J* = 22.8 Hz), 108.0, 56.0, 35.7, 29.4; ^{19}F NMR (282 MHz, $CDCl_3$) δ [ppm] = −104.57; HRMS for $C_{17}H_{19}FO_4S$ (APCI+) $[M]^{\bullet+}$: calc.: 338.0983, found: 338.0976.

4.2 6-(3-Chloro-4-methylphenylsulfonyl)-2-(1,1-dimethylethyl)-4-methoxyphenol (**8**)

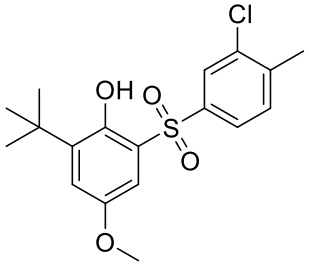

According to the general protocol (**GP 1**) 2-(1,1-dimethylethyl)-4-methoxyphenol (0.90 g, 5.00 mmol, 1.0 eq.) and 3-chloro-4-methylbenzenesulfinic acid sodium salt (1.38 g, 6.50 mmol, 1.3 eq.) are solved in HFIP + 15 vol.% water (25 mL). After constant current electrolysis and workup, the residue is purified by column chromatography (cyclohexane/ethyl acetate = 100:0 → 98:2) to yield the product as a yellow-colored solid (yield: 53%, 0.97 g, 2.64 mmol).

m_R: 69–72 °C; R_f (cyclohexane/ethyl acetate = 9:1): 0.43; ^{1}H NMR (400 MHz, $CDCl_3$) δ [ppm] = 9.15 (s, 1H), 7.90 (d, *J* = 1.9 Hz, 1H), 7.71 (dd, *J* = 8.1 Hz, *J* = 1.9 Hz, 1H), 7.38 (d, *J* = 8.1 Hz, 1H), 7.09 (d, *J* = 3.0 Hz, 1H), 6.98 (d, *J* = 3.0 Hz, 1H), 3.75 (s, 3H), 2.42 (s, 3H), 1.37 (s, 9H); ^{13}C NMR (101 MHz, $CDCl_3$) δ [ppm] = 152.4, 149.6, 142.9, 141.7, 140.8, 135.7, 131.9, 127.3, 124.9, 122.8, 122.8, 107.9, 56.0, 35.7, 29.4, 20.5; HRMS for $C_{18}H_{22}{}^{35}ClO_4S$ (ESI+) $[M+H]^+$: calc.: 369.0922, found: 369.0917.

4.3 2-(1,1-Dimethylethyl)-4-methoxy-6-(phenylsulfonyl)phenol (**6**)

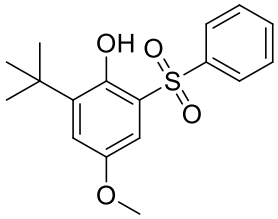

25 mL undivided beaker-type cell

According to the general protocol (**GP 1**) 2-(1,1-dimethylethyl)-4-methoxyphenol (0.90 g, 5.00 mmol, 1.0 eq.) and benzenesulfinic acid sodium salt (1.07 g, 6.50 mmol, 1.3 eq.) are solved in HFIP + 15 vol.% water (25 mL). After constant current electrolysis and workup, the crude product is purified by column chromatography (cyclohexane/ethyl acetate = 100:0 → 98:2) to yield the product as a beige-colored solid (yield: 53%, 0.84 g, 2.62 mmol).

Scale-up in 200 mL undivided beaker-type cell

According to the general protocol (**GP 3**) 2-(1,1-dimethylethyl)-4-methoxyphenol (7.21 g, 40 mmol, 1.0 eq.) and benzenesulfinic acid sodium salt (9.85 g, 60 mmol, 1.5 eq.) are solved in HFIP + 15 vol.% water (200 mL). After constant current electrolysis and workup, the crude product is purified by column chromatography (cyclohexane/ethyl acetate = 100:0 → 98:2) to yield the product as a beige-colored solid (yield: 47%, 6.06 g, 18.90 mmol).

m_R: 116–119 °C; R_f (cyclohexane/ethyl acetate = 9:1): 0.36; ^{1}H NMR (400 MHz, $CDCl_3$) δ [ppm] = 9.27 (s, 1H), 7.95–7.92 (m, 2H), 7.62–7.58 (m, 1H), 7.55–7.55 (m, 1H), 7.08 (d, *J* = 3.1 Hz, 1H), 7.00 (d, *J* = 3.1 Hz, 1H), 3.74 (s, 3H), 1.37 (s, 9H); ^{13}C NMR (101 MHz, $CDCl_3$) δ [ppm] = 152.3, 149.7, 142.0, 141.6, 133.7, 129.5, 126.8, 123.0, 122.6, 108.1, 56.0, 35.7, 29.4; HRMS for $C_{17}H_{20}O_4SNa$ (ESI+) $[M+Na]^+$: calc.: 343.0975, found: 343.0976; Elemental anal. for $C_{17}H_{20}O_4S$: calc.: C: 63.73%, H: 6.29%, found: C: 63.63%, H: 6.29%.

Crystallization was performed by dissolving **6** (50 mg) in dichloromethane (ca. 0.8 mL) and slow diffusion of over layered *n*-heptane (ca. 4 mL) into the solution at 23 °C.

Crystal structure determination of **6**: $C_{17}H_{20}O_4S$, M_r = 320.4; colorless block-like crystals (0.22 x 0.72 x 0.72 mm³), T = 213 K, λ (Mo-$K\alpha$) = 0.71073 Å, monoklin space group $P\,2_1/c$, a = 11.2852(8) Å, b = 13.0143(7) Å, ß = 114.712(5)°, c = 12.1128(8) Å, V = 1616.07(18) Å^3, Z = 4, ρ_{calcd} = 1.317 g/cm^3, $2\theta_{max}$ = 56°, μ = 0.22 mm^{-1}, F(000) = 680, 10365 reflections, 3910 unique reflections (R_{int} = 0.0781), $w = 1/[\sigma^2(F_0^2)+(0.0831*P)^2+0.51*P]$ while $P = (Max(F_0^2,0)+2*F_c^2)/3$, R_1 = 0.0531 [$I > 2\sigma(I)$], R_1 = 0.0673 [all data], wR_2 = 0.1494, CCDC-1891217.

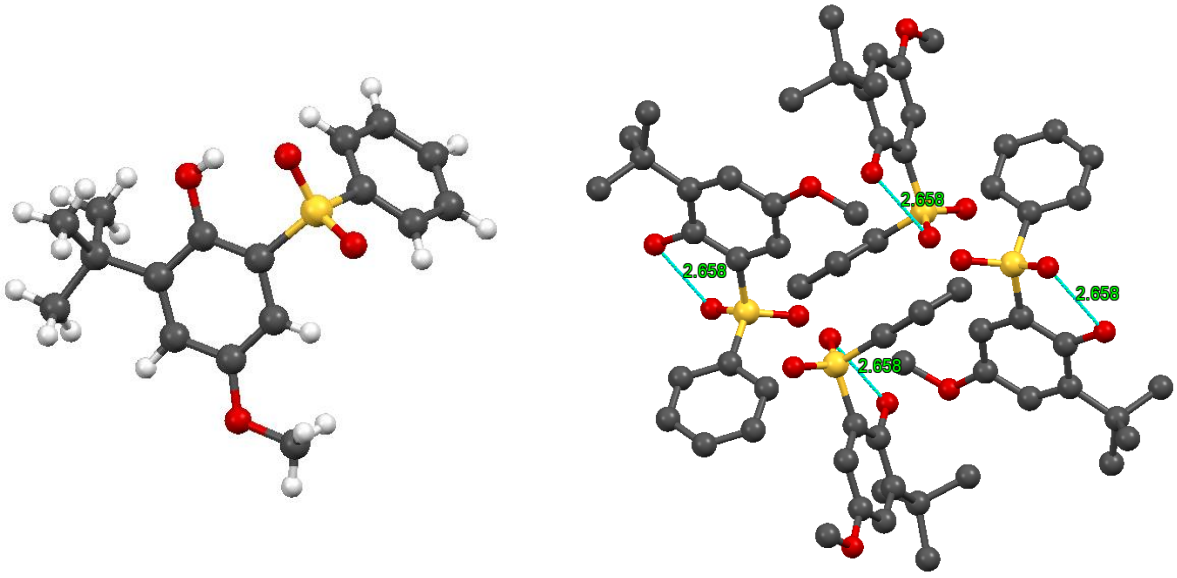

Figure 4: Molecular structure (left) and packing (right) of **6**. Hydrogen atoms are omitted for clarity. Intramolecular hydrogen bonding is indicated in blue with lenghs of 2.658 Å.

4.4 6-(4-Chlorophenylsulfonyl)-2-(1,1-dimethylethyl)-4-methoxyphenol (**9**)

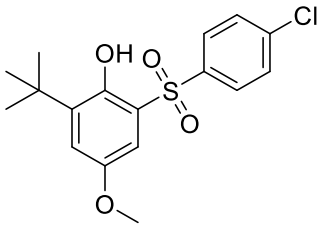

According to the general protocol (**GP 1**) 2-(1,1-dimethylethyl)-4-methoxyphenol (0.90 g, 5.00 mmol, 1.0 eq.) and 4-chlorobenzenesulfinic acid sodium salt (1.29 g, 6.50 mmol, 1.3 eq.) are solved in HFIP + 15 vol.% water (25 mL). After constant current electrolysis and workup, the residue is purified by column chromatography (cyclohexane/ethyl acetate = 100:0 → 98:2) to yield the product as a yellow-colored solid (yield: 49%, 0.87 g, 2.44 mmol).

m_R: 85–89 °C; R_f (cyclohexane/ethyl acetate = 9:1): 0.46; ^{1}H NMR (400 MHz, $CDCl_3$) δ [ppm] = 9.14 (s, 1H), 7.88–7.85 (m, 2H), 7.51–7.48 (m, 2H), 7.09 (d, *J* = 3.1 Hz, 1H), 6.97 (d, *J* = 3.1 Hz, 1H), 3.74 (s, 3H), 1.37 (s, 9H); ^{13}C NMR (101 MHz, $CDCl_3$) δ [ppm] = 152.5, 149.6, 141.8, 140.5, 140.5, 129.9, 128.3, 122.9, 122.8, 107.9, 56.0, 35.7, 29.4; HRMS for $C_{17}H_{19}{}^{35}ClO_4SNa$ (ESI+) $[M+Na]^+$: calc.: 377.0585, found: 377.0579. Elemental anal. for $C_{17}H_{19}ClO_4S$: calc.: C: 57.54%, H: 5.40%, found: C: 57.63%, H: 5.52%.

4.5 2-(1,1-Dimethylethyl)-4-methoxy-6-(3-(trifluoromethyl)phenylsulfonyl)phenol (**10**)

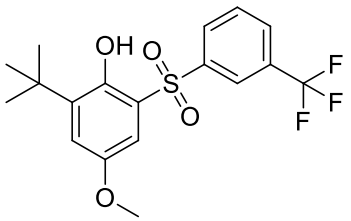

According to the general protocol (**GP 1**) 2-(1,1-dimethylethyl)-4-methoxyphenol (0.90 g, 5.00 mmol, 1.0 eq.) and 3-(trifluoromethyl)benzenesulfinic acid sodium salt (1.51 g, 6.50 mmol, 1.3 eq.) are solved

in HFIP + 15 vol.% water (25 mL). After constant current electrolysis and workup, the residue is purified by column chromatography (cyclohexane/ethyl acetate = 100:0 → 98:2) to yield the product as a beige-colored solid (yield: 47%, 0.92 g, 2.37 mmol).

m_R: 81–83 °C; R_f (cyclohexane/ethyl acetate = 9:1): 0.42; ^{1}H NMR (400 MHz, $CDCl_3$) δ [ppm] = 9.12 (s, 1H), 8.20 (s, 1H), 8.11 (d, *J* = 7.8 Hz, 1H), 7.86 (d, *J* = 7.8 Hz, 1H), 7.68 (t, *J* = 7.8 Hz, 1H), 7.12 (d, *J* = 3.1 Hz, 1H), 7.00 (d, *J* = 3.1 Hz, 1H), 3.75 (s, 3H), 1.38 (s, 9H); ^{13}C NMR (101 MHz, $CDCl_3$) δ [ppm] = 152.6, 149.8, 143.2, 142.1, 132.2 (d, *J* = 34.0 Hz), 130.5–130.4 (m), 130.4, 130.0, 123.9–123.7 (m), 123.3, 123.2 (d, *J* = 272.7 Hz), 122.2, 107.9, 56.0, 35.8, 29.4; ^{19}F NMR (282 MHz, $CDCl_3$) δ [ppm] = −64.09; HRMS for $C_{18}H_{19}F_3O_4S$ (APCI+) $[M]^{\bullet+}$: calc.: 388.0951, found: 388.0954.

4.6 2-(1,1-Dimethylethyl)-4-methoxy-6-(4-methylphenylsulfonyl)phenol (**11**)

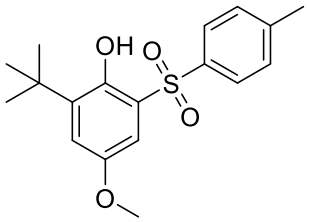

According to the general protocol (**GP 1**) 2-(1,1-dimethylethyl)-4-methoxyphenol (0.90 g, 5.00 mmol, 1.0 eq.) and 4-methylbenzenesulfinic acid sodium salt (1.16 g, 6.50 mmol, 1.3 eq.) are solved in HFIP + 15 vol.% water (25 mL). After constant current electrolysis and workup, the residue is purified by column chromatography (cyclohexane/ethyl acetate = 100:0 → 98:2) to yield the product as a beige-colored solid (yield: 46%, 0.77 g, 2.31 mmol).

m_R: 101–106 °C; R_f (cyclohexane/ethyl acetate = 9:1): 0.38; ^{1}H NMR (400 MHz, $CDCl_3$) δ [ppm] = 9.27 (s, 1H), 7.83–7.80 (m, 2H), 7.33–7.30 (m, 2H), 7.06 (d, *J* = 3.1 Hz, 1H), 6.99 (d, *J* = 3.1 Hz, 1H), 3.74 (s, 3H), 2.41 (s, 3H), 1.37 (s, 9H); ^{13}C NMR (101 MHz, $CDCl_3$) δ [ppm] = 152.3, 149.6, 144.8, 141.5, 139.1, 130.2, 126.8, 123.4, 122.4, 108.0, 56.0, 35.7, 29.4, 21.8; HRMS for $C_{18}H_{23}O_4S$ (ESI+) $[M+H]^+$: calc.: 335.1312, found: 335.1310.

4.7 2-(1,1-Dimethylethyl)-4-methoxy-6-(methylsulfonyl)phenol (**12**)

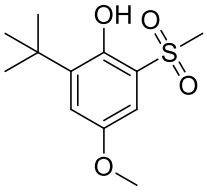

According to the general protocol (**GP 1**) 2-(1,1-dimethylethyl)-4-methoxyphenol (0.90 g, 5.00 mmol, 1.0 eq.) and methanesulfinic acid sodium salt (0.66 g, 6.50 mmol, 1.3 eq.) are solved in HFIP + 15 vol.% water (25 mL). After constant current electrolysis and workup, the residue is purified by column chromatography (cyclohexane/ethyl acetate = 100:0 → 92:8) to yield the product as a beige-colored solid (yield: 45%, 0.58 g, 2.26 mmol).

m_R: 65–69 °C; R_f (cyclohexane/ethyl acetate = 9:1): 0.23; ^{1}H NMR (400 MHz, $CDCl_3$) δ [ppm] = 8.73 (s, 1H), 7.15 (d, *J* = 3.2 Hz, 1H), 7.02 (d, *J* = 3.2 Hz, 1H), 3.79 (s, 3H), 3.12 (s, 3H), 1.39 (s, 9H); ^{13}C NMR (101 MHz, $CDCl_3$) δ [ppm] = 152.5, 149.3, 141.8, 122.9, 122.8, 107.5, 56.0, 44.8, 35.7, 29.4; HRMS for $C_{12}H_{18}O_4S$ (APCI+) $[M]^{\bullet+}$: calc.: 258.0920, found: 258.0920.

4.8 4-(2-Hydroxy-5-methoxy-3-methylphenylsulfonyl)acetanilid (**13**)

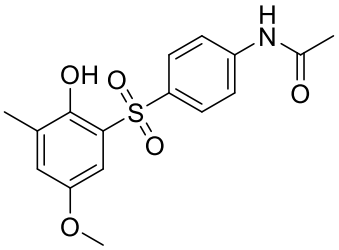

According to the general protocol (**GP 1**) 4-methoxy-2-methylphenol (0.69 g, 5.00 mmol, 1.0 eq.) and 4-acetamidobenzenesulfinic acid sodium salt (1.44 g, 6.50 mmol, 1.3 eq.) are solved in HFIP + 15 vol.% water (25 mL). After constant current electrolysis and workup, the residue is purified by column chromatography (cyclohexane/ethyl acetate = 9:1 → 4:6) to yield the product as a colorless solid (yield: 35%, 0.61 g, 1.82 mmol).

m_R: 159–162 °C; R_f (cyclohexane/ethyl acetate = 1:1): 0.19; ^{1}H NMR (400 MHz, $CDCl_3$) δ [ppm] = 10.34 (s, 1H), 9.08 (s, 1H), 7.87–7.84 (m, 2H), 7.76–7.73 (m, 2H), 7.24 (d, *J* = 3.2 Hz, 1H), 7.04 (d, *J* = 3.2 Hz, 1H), 3.75 (s, 3H), 2.12 (s, 3H), 2.07 (s, 3H); ^{13}C NMR (101 MHz, $CDCl_3$) δ [ppm] = 169.1, 151.7, 147.0, 143.5, 134.7, 129.5, 129.1, 128.3, 123.0, 118.4, 109.5, 55.6, 24.2, 16.4; HRMS for $C_{16}H_{18}NO_5S$ (ESI+) $[M+H]^+$: calc.: 336.0900, found: 336.0902. Elemental anal. for $C_{16}H_{17}NO_5S$: calc.: C: 57.30%, H: 5.11%, N: 4.18%, found: C: 56.15%, H: 5.17%, N: 4.01%.

4.9 2,6-Dimethoxy-4-(2,4,6-trimethylphenylsulfonyl)phenol (**14**)

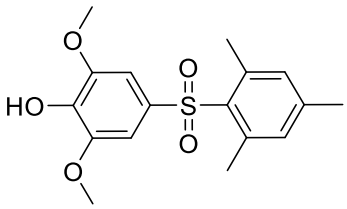

According to the general protocol (**GP 1**) 2,6-dimethoxyphenol (0.77 g, 5.00 mmol, 1.0 eq.) and 2,4,6-trimethylbenzenesulfinic acid sodium salt (1.34 g, 6.50 mmol, 1.3 eq.) are solved in HFIP + 15 vol.% water (25 mL). After constant current electrolysis and workup, the residue is purified by column chromatography (cyclohexane/ethyl acetate = 10:0 → 6:4) to yield the product as a colorless solid (yield: 20%, 0.33 g, 0.98 mmol).

m_R: 122–124 °C; R_f (cyclohexane/ethyl acetate = 4:1): 0.16; ^{1}H NMR (400 MHz, $CDCl_3$) δ [ppm] = 7.03 (s, 2H), 6.94 (s, 2H), 5.89 (s, 1H), 3.88 (s, 6H), 2.61 (s, 6H), 2.29 (s, 3H); ^{13}C NMR (101 MHz, $CDCl_3$) δ [ppm] = 146.9, 143.3, 139.9, 138.7, 134.4, 134.3, 132.4, 103.9, 56.7, 23.1, 21.1; HRMS for $C_{17}H_{20}O_5SNa$ (ESI+) $[M+Na]^+$: calc.: 359.0924, found: 359.0922.

Crystallization was performed by dissolving **14** (50 mg) in dichloromethane (ca. 0.8 mL) and slow diffusion of over layered *n*-heptane (ca. 4 mL) into the solution at 23 °C.

Crystal structure determination of **14**: $C_{17}H_{20}O_5S$, M_r = 336.4; colorless disk-like crystals (0.1 x 0.28 x 0.39 mm³), T = 213 K, λ (Mo-$K\alpha$) = 0.71073 Å, monoklin space group $P\,2_1/c$, a = 8.0625(3) Å, b = 13.1567(4) Å, ß = 91.789(3)°, c = 30.4378(13) Å, V = 3227.2(2) Å^3, Z = 8, ρ_{calcd} = 1.385 g/cm^3, $2\theta_{max}$ = 56°, μ = 0.22 mm^{-1}, F(000) = 1424, 17984 reflections, 8116 unique reflections (R_{int} = 0.032), $w = 1/[\sigma^2(F_o^2)+(0.0615*P)^2+1.34*P]$ while $P = (Max(F_o^2,0)+2*F_c^2)/3$, R_1 = 0.0504 [$I > 2\sigma(I)$], R_1 = 0.0914 [all data], wR_2 = 0.1366, CCDC-1891216.

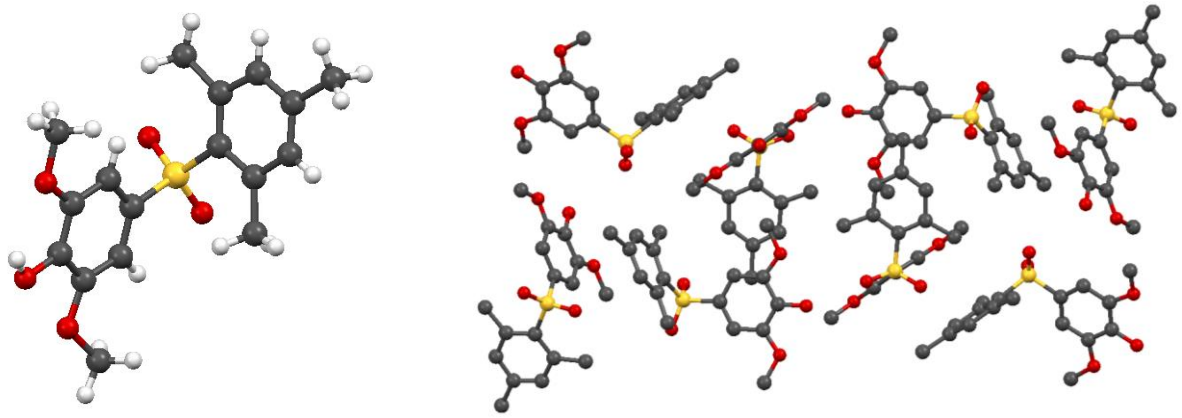

Figure 5: Molecular structure (left) and packing (right) of **14**. Hydrogen atoms are omitted for clarity.

4.10 2-Methoxy-4-methyl-6-(3-(trifluormethyl)phenylsulfonyl)phenol (**15**)

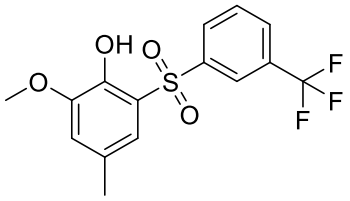

According to the general protocol (**GP 1**) 2-methoxy-4-methylphenol (0.69 g, 5.00 mmol, 1.0 eq.) and 3-(trifluoromethyl)benzenesulfinic acid sodium salt (1.51 g, 6.50 mmol, 1.3 eq.) are solved in HFIP + 15 vol.% water (25 mL). After constant current electrolysis and workup, the residue is purified by column chromatography (cyclohexane/ethyl acetate = 9:1 → 6:4) to yield the product as a colorless solid (yield: 11%, 0.19 g, 0.55 mmol).

m_R: 138–144 °C; R_f (cyclohexane/ethyl acetate = 4:1): 0.11; ^{1}H NMR (400 MHz, $CDCl_3$) δ [ppm] = 8.28 (s, 1H), 8.18 (d, *J* = 7.9 Hz, 1H), 7.83 (d, *J* = 7.8 Hz, 1H), 7.65 (dd, *J* = 7.9 Hz, *J* = 7.8 Hz, 1H), 7.38 (bs, 1H), 7.28–7.27 (m, 1H), 6.87 (d, *J* = 1.7 Hz, 1H), 3.87 (s, 3H), 2.33 (s, 3H); ^{13}C NMR (101 MHz, $CDCl_3$) δ [ppm] = 148.0, 143.1, 142.8, 131.76 (d, *J* = 33.7 Hz), 131.2, 130.4, 130.2–130.1 (m), 129.9, 125.1–125.0 (m), 123.9, 123.3 (d, *J* = 272.9 Hz), 119.9, 117.8, 56.6, 21.2; ^{19}F NMR (282 MHz, $CDCl_3$) δ [ppm] = –63.93; HRMS for $C_{15}H_{14}F_3O_4S$ (ESI+) $[M+H]^+$: calc.: 347.0559, found: 347.0563.

5. NMR spectra of novel compounds

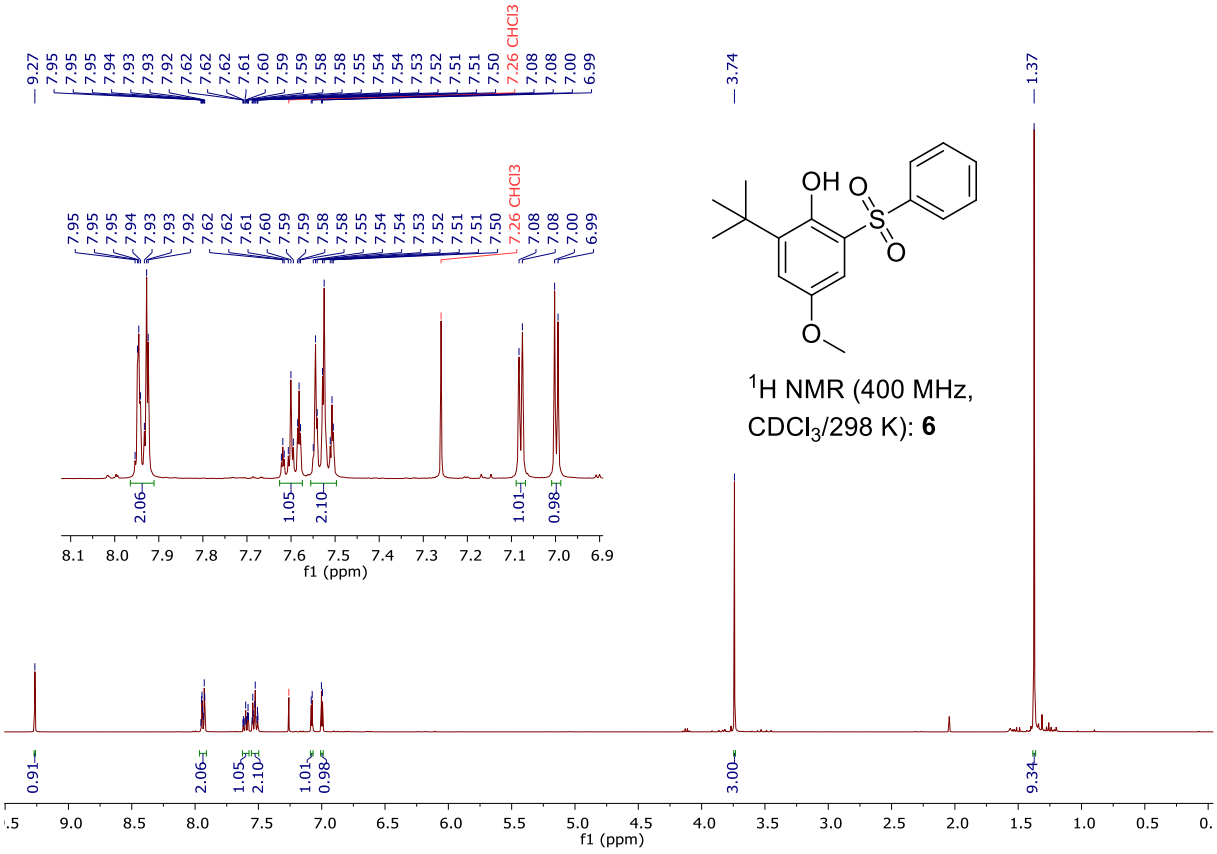

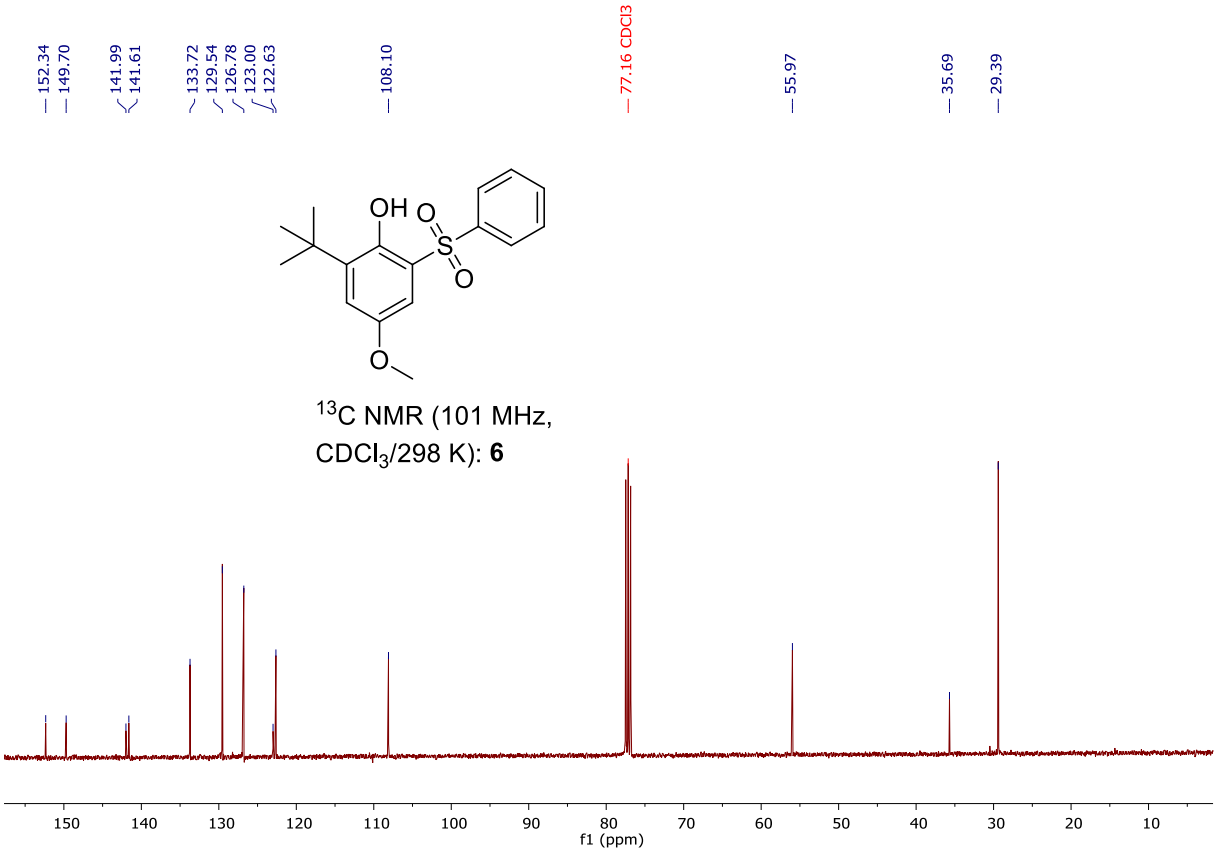

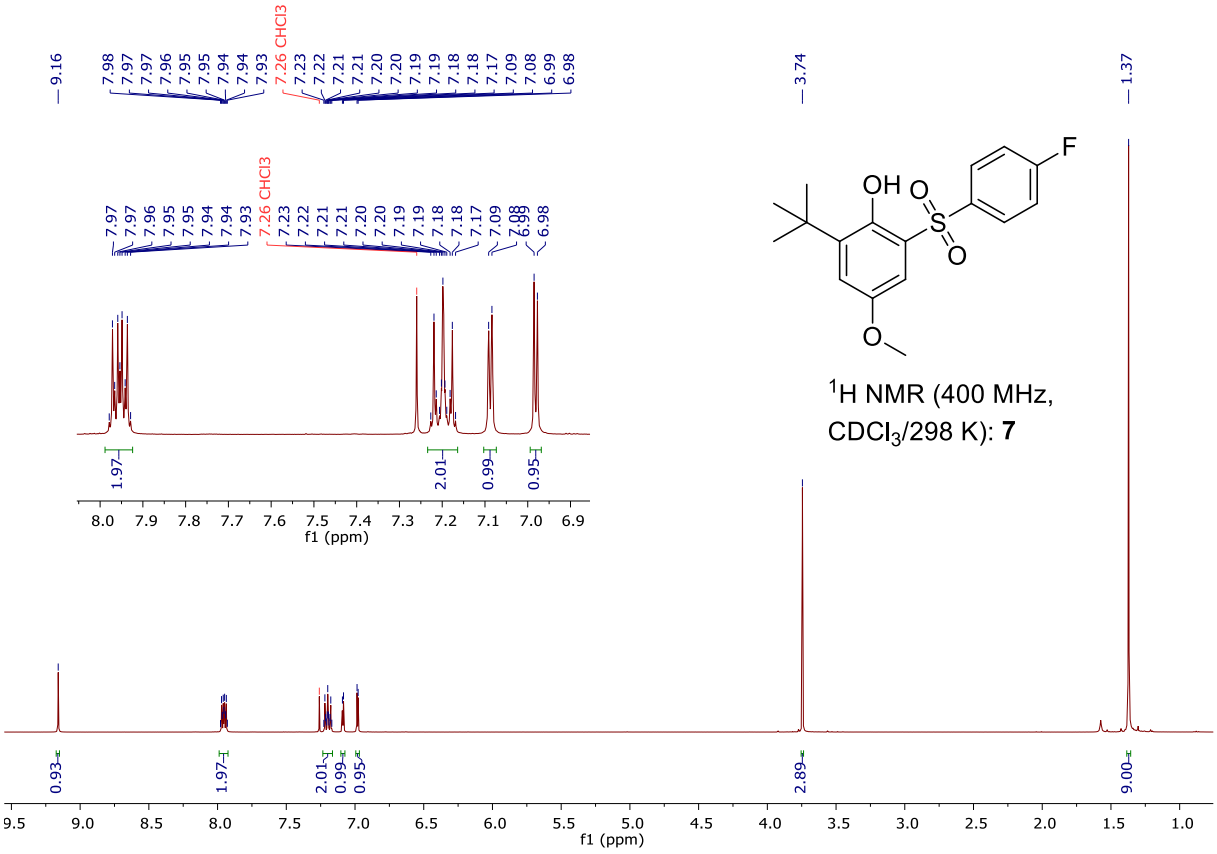

^{1}H NMR (400 MHz, $CDCl_3$/298 K): **7**

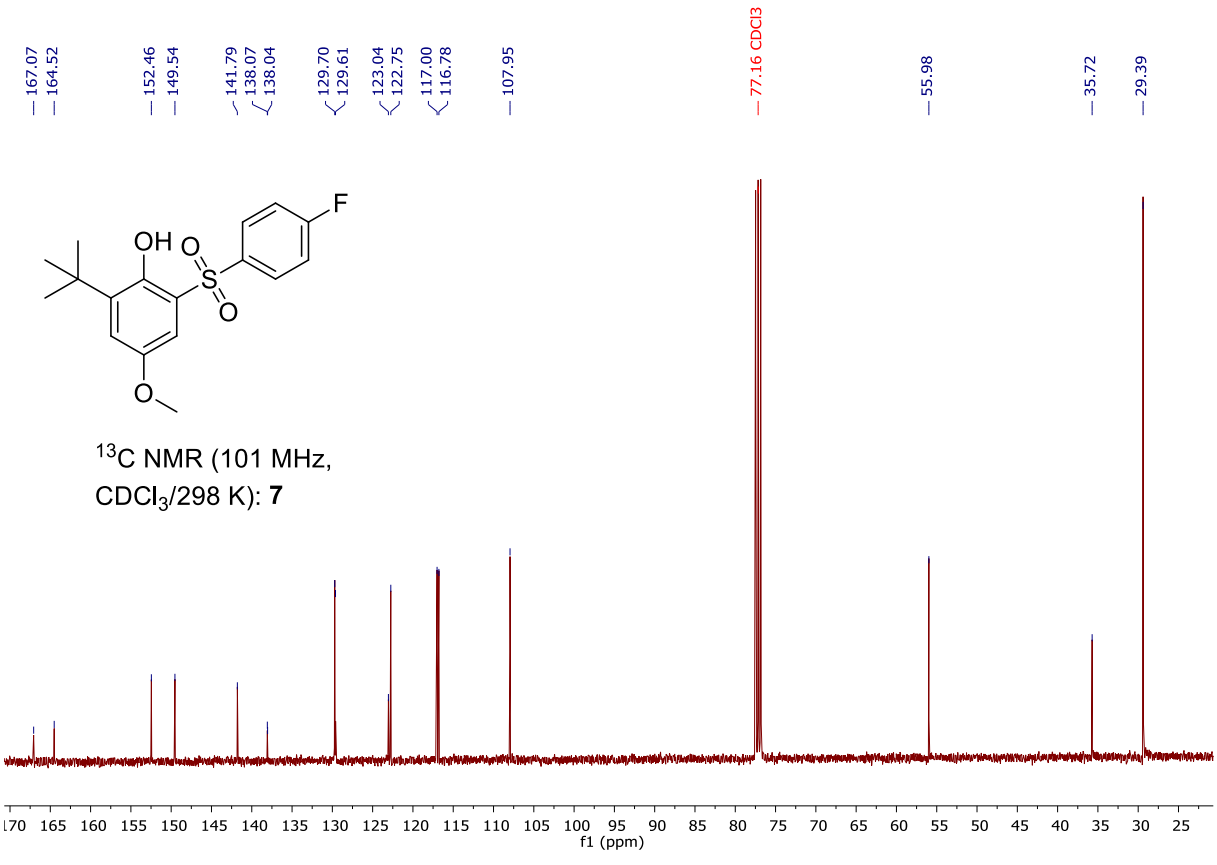

^{13}C NMR (101 MHz, $CDCl_3$/298 K): **7**

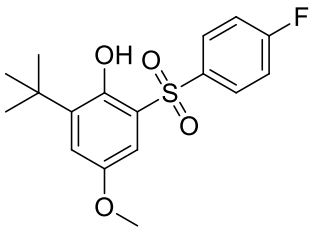

^{19}F NMR (282 MHz, $CDCl_3$/298 K): **7**

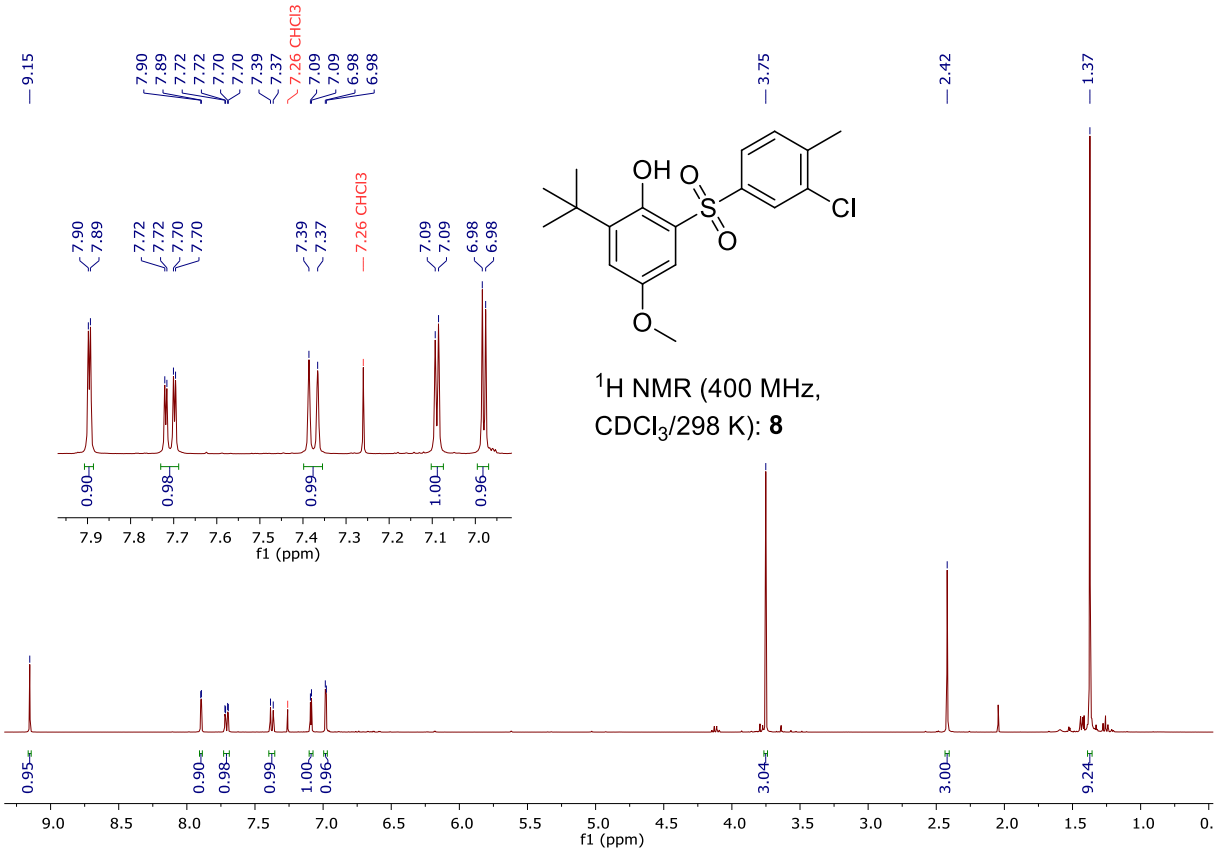

^{1}H NMR (400 MHz, $CDCl_3$/298 K): **8**

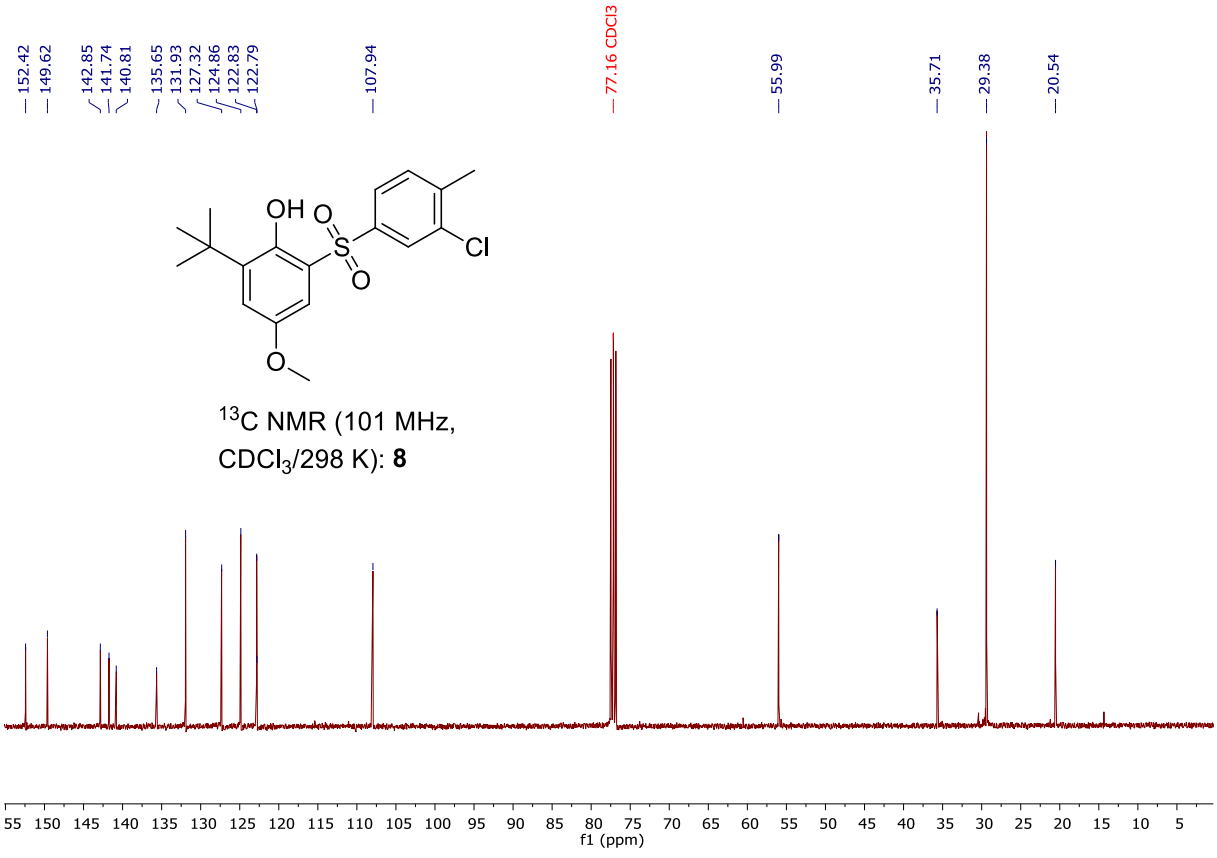

^{13}C NMR (101 MHz, $CDCl_3$/298 K): **8**

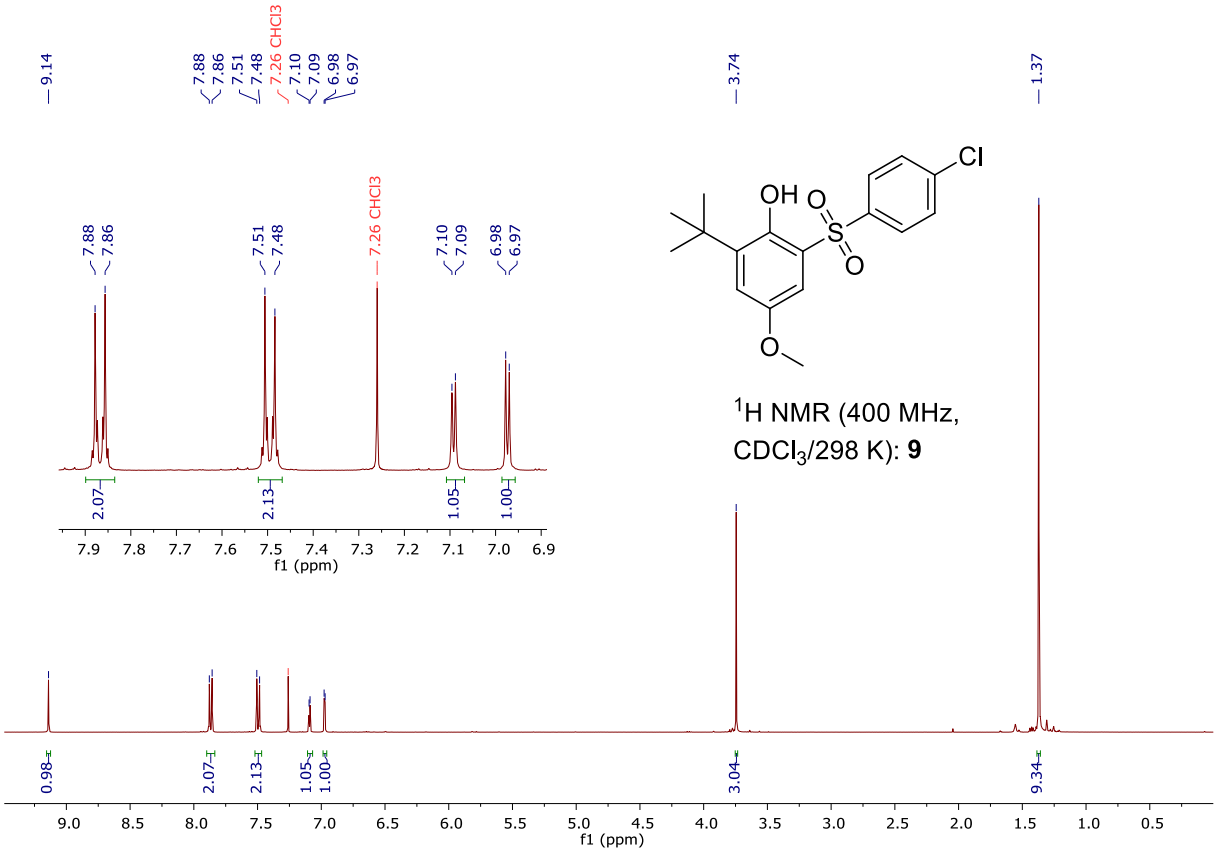

^{1}H NMR (400 MHz, $CDCl_3$/298 K): **9**

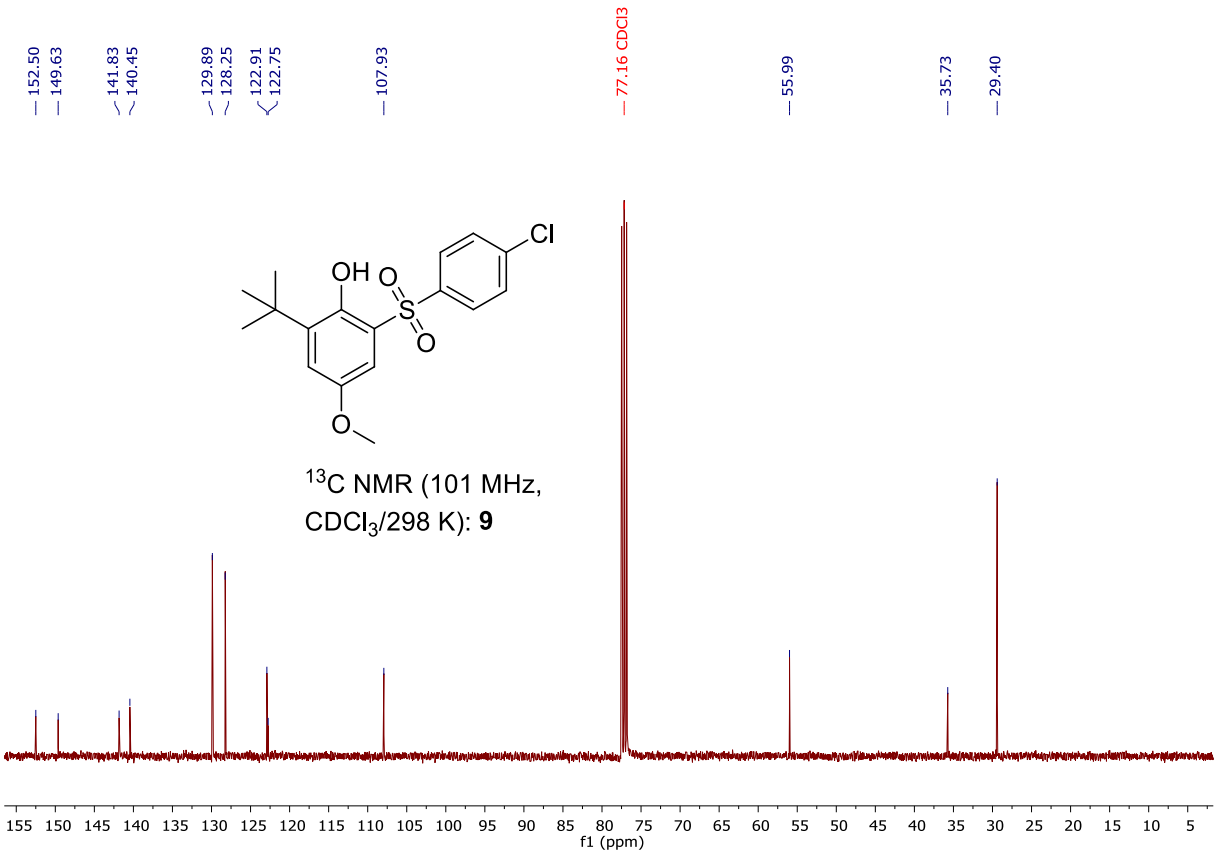

^{13}C NMR (101 MHz, $CDCl_3$/298 K): **9**

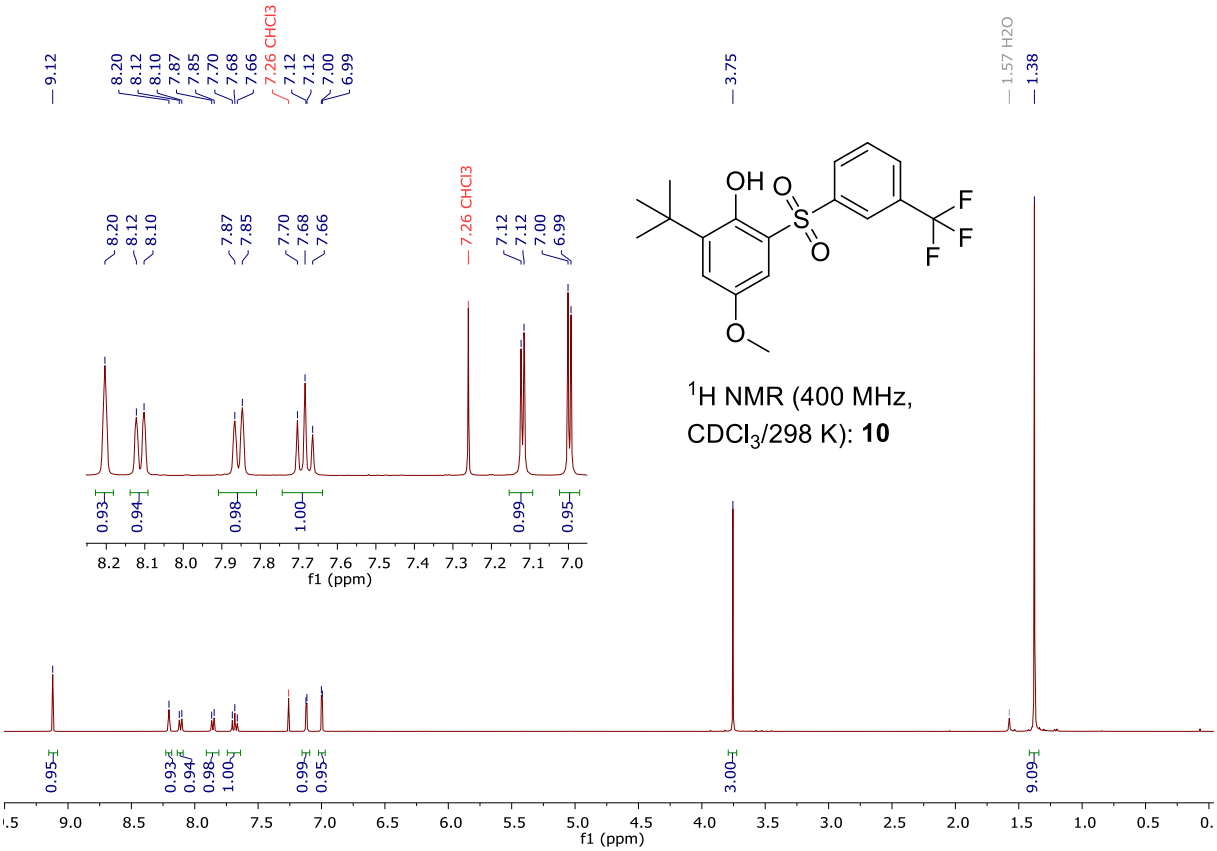

^{1}H NMR (400 MHz, $CDCl_3$/298 K): **10**

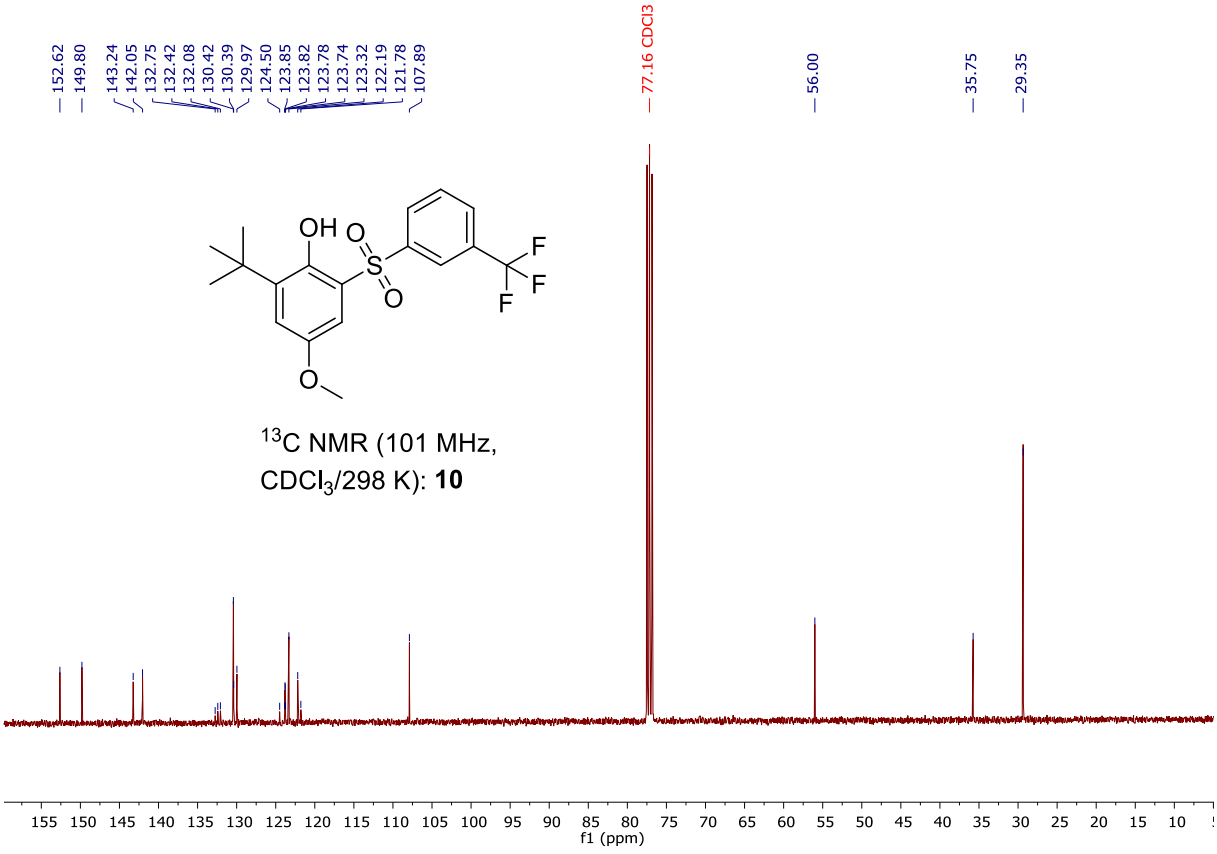

^{13}C NMR (101 MHz, $CDCl_3$/298 K): **10**

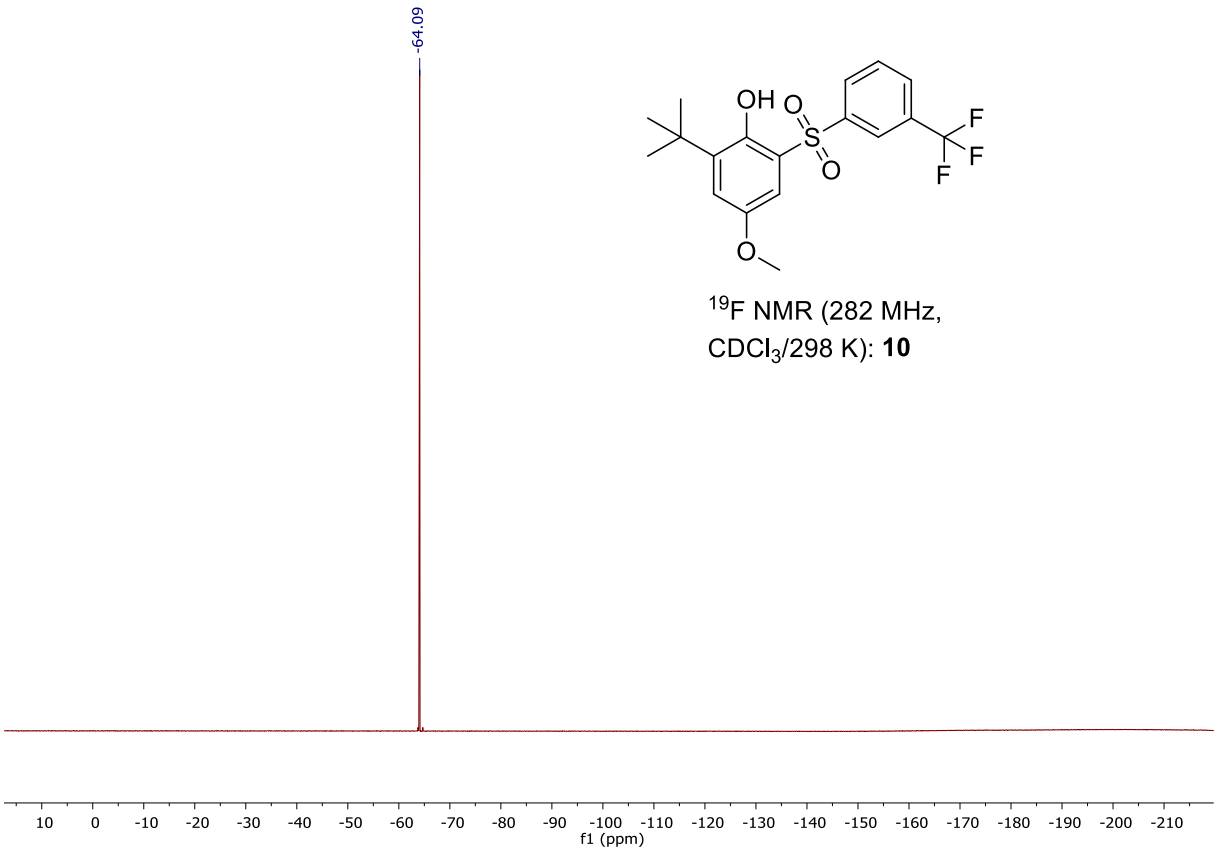

^{19}F NMR (282 MHz, $CDCl_3$/298 K): **10**

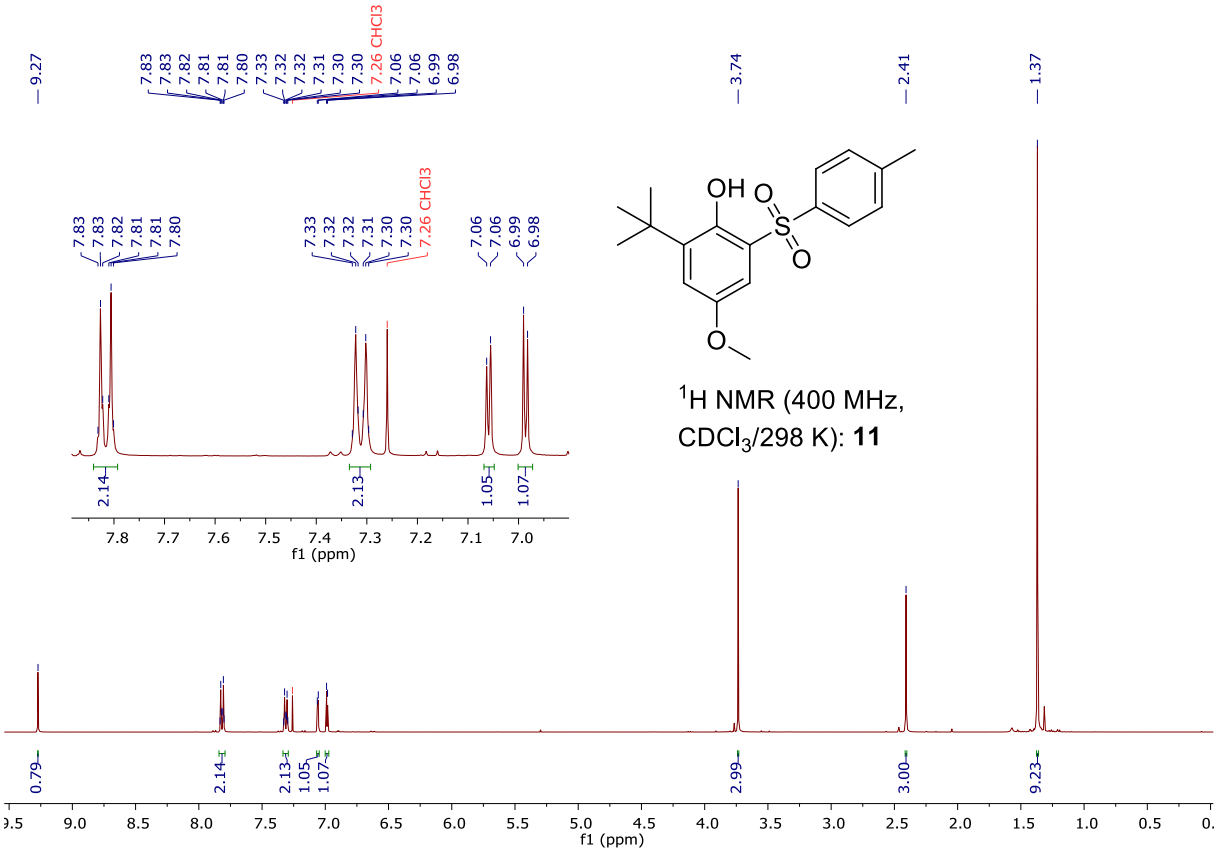

^{1}H NMR (400 MHz, $CDCl_3$/298 K): **11**

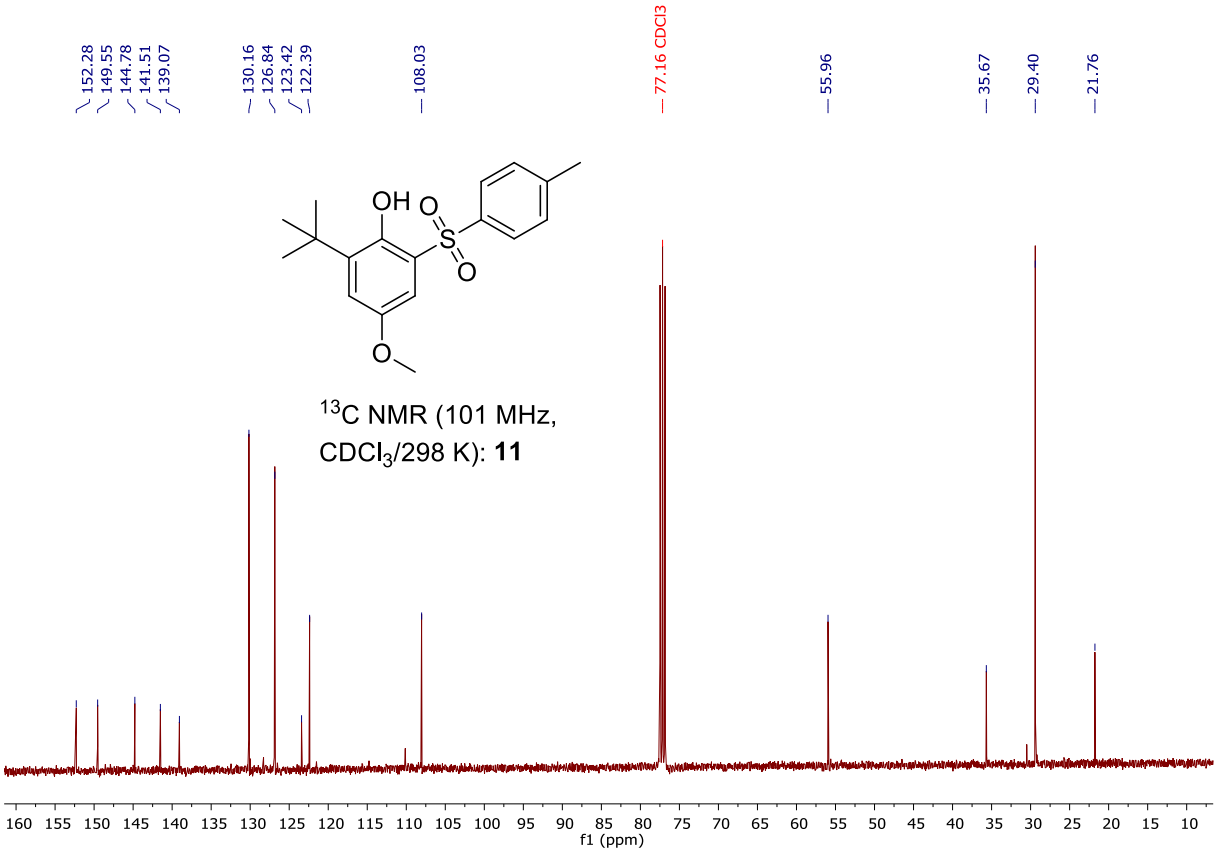

^{13}C NMR (101 MHz, $CDCl_3$/298 K): **11**

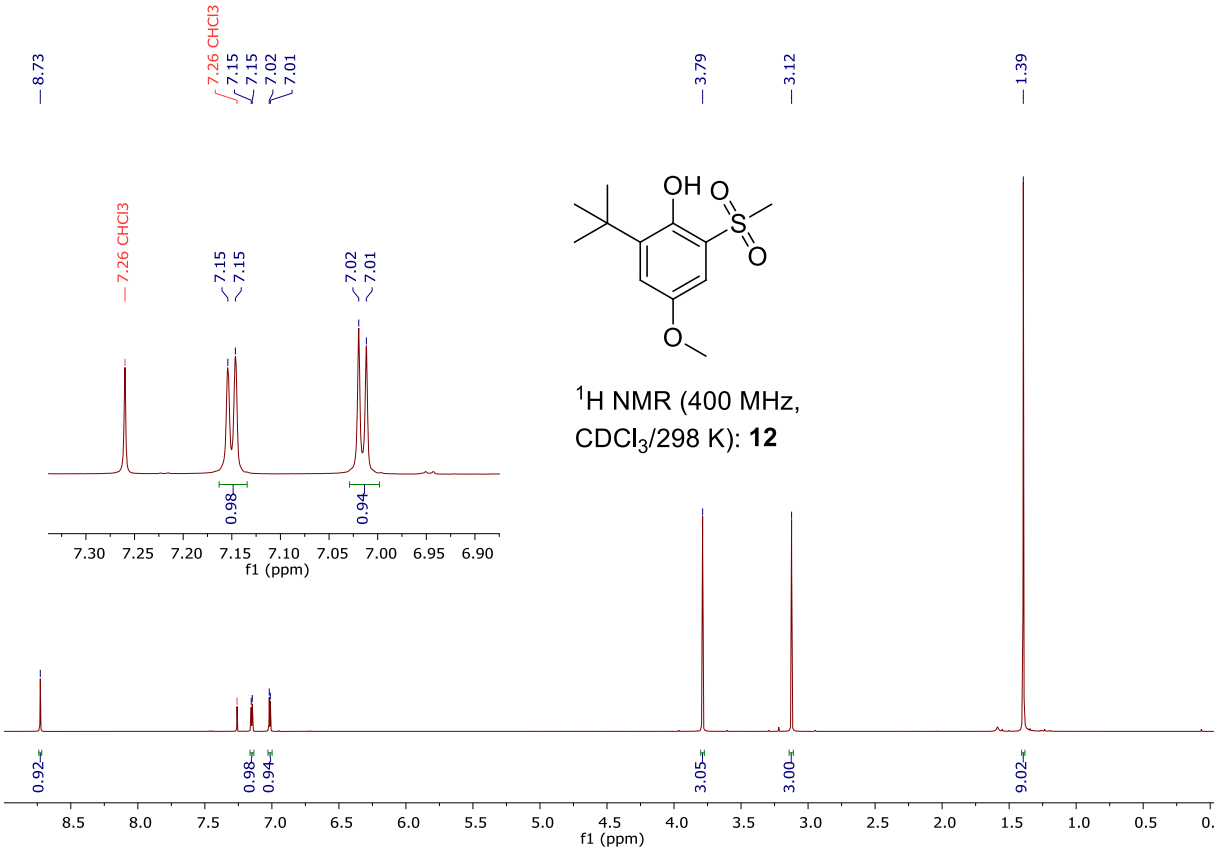

^{1}H NMR (400 MHz, $CDCl_3$/298 K): **12**

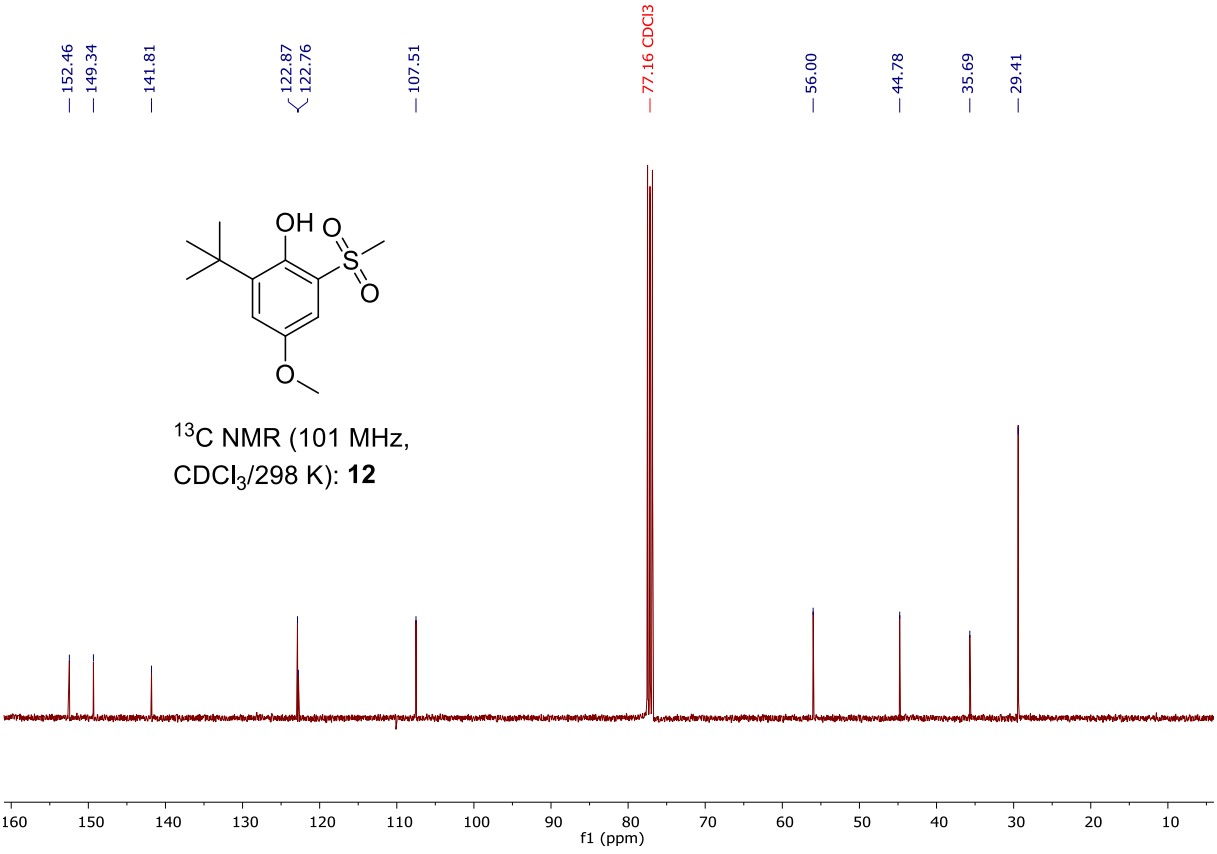

^{13}C NMR (101 MHz, $CDCl_3$/298 K): **12**

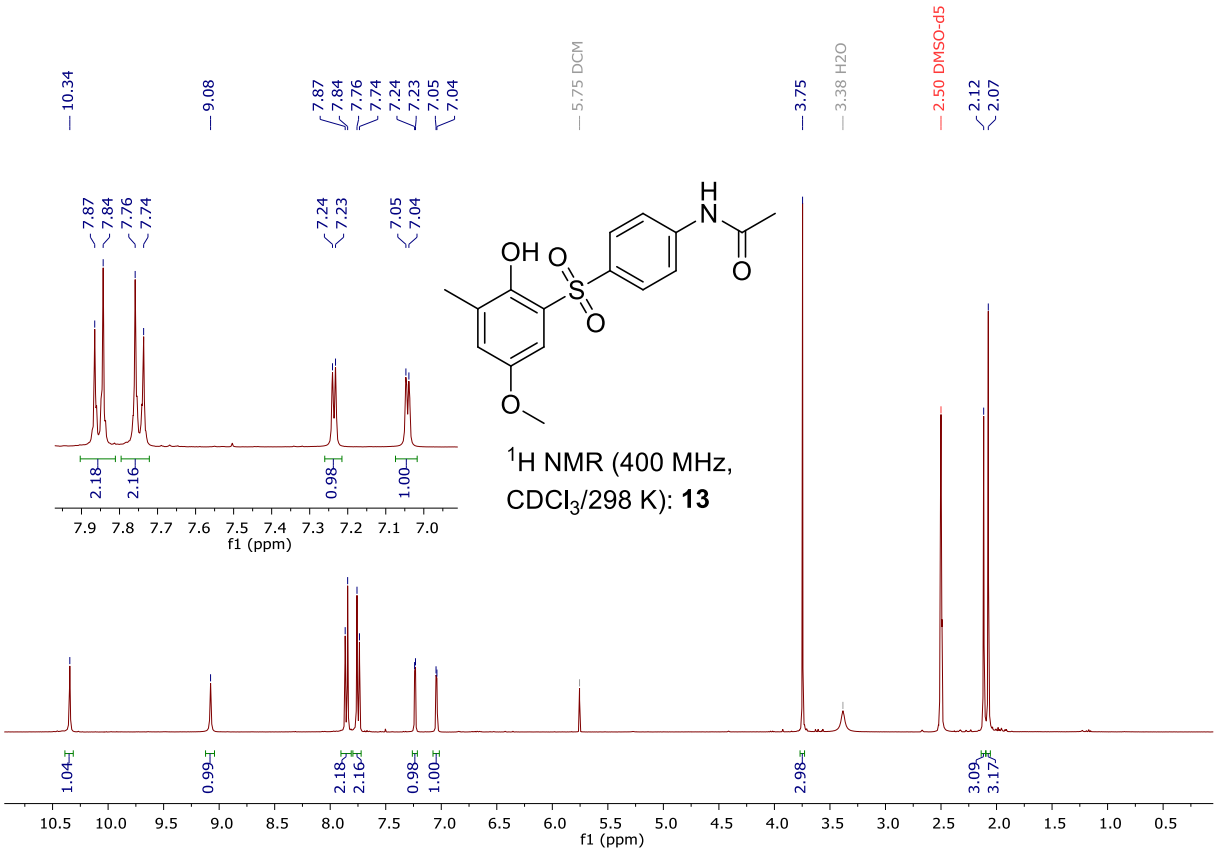

^{1}H NMR (400 MHz, $CDCl_3$/298 K): **13**

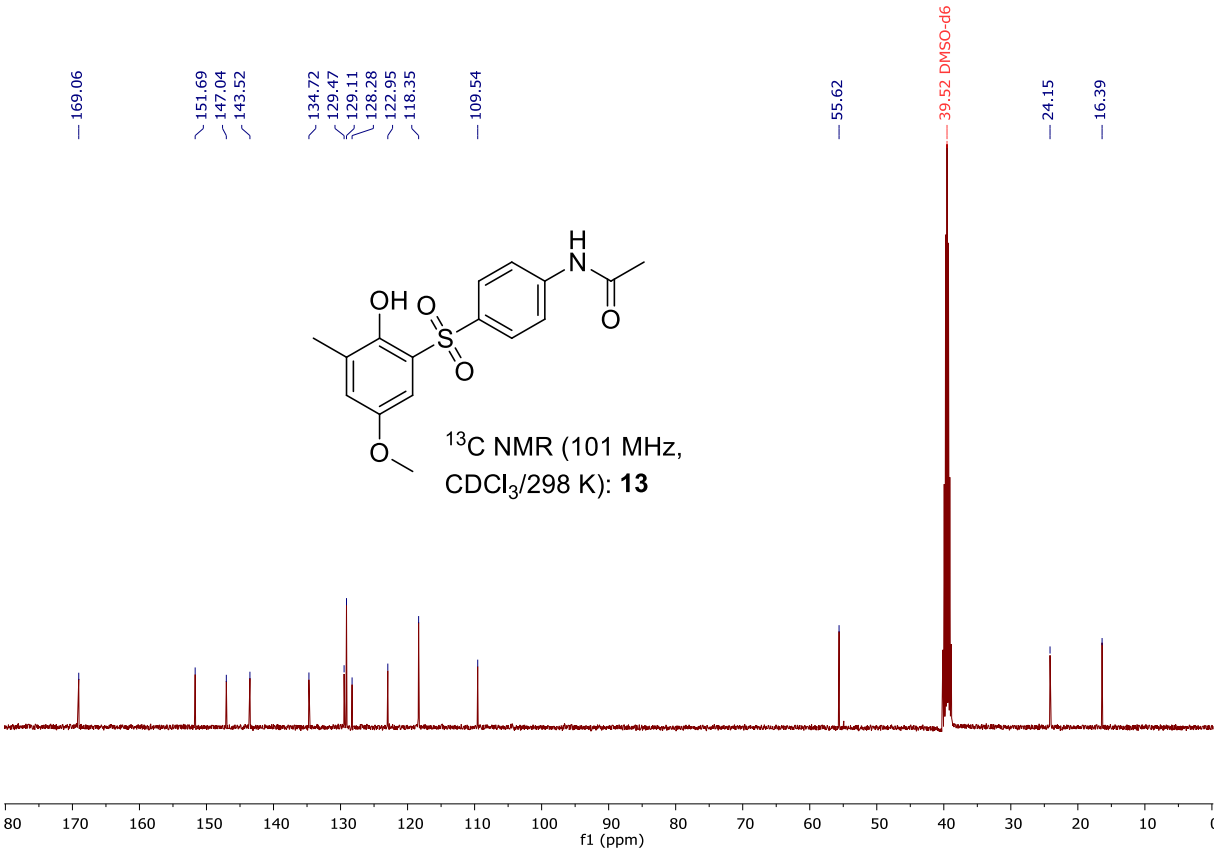

^{13}C NMR (101 MHz, $CDCl_3$/298 K): **13**

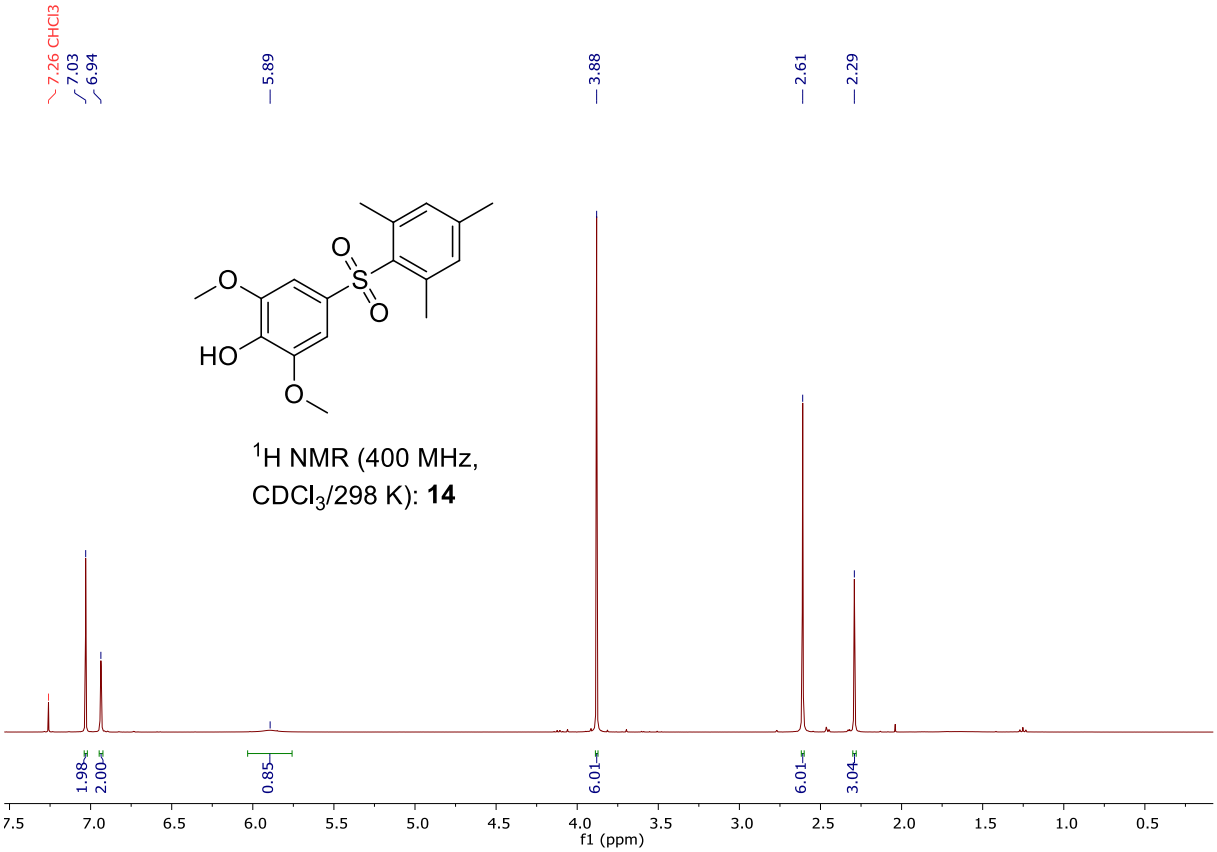
7.26 CHCl3
7.03
6.94
5.89
3.88
2.61
2.29
O
S
O
O
HO
O
1H NMR (400 MHz,
CDCl3/298 K): 14
1.98
2.00
0.85
6.01
6.01
3.04
7.5
7.0
6.5
6.0
5.5
5.0
4.5
4.0
3.5
3.0
2.5
2.0
1.5
1.0
0.5
f1 (ppm)

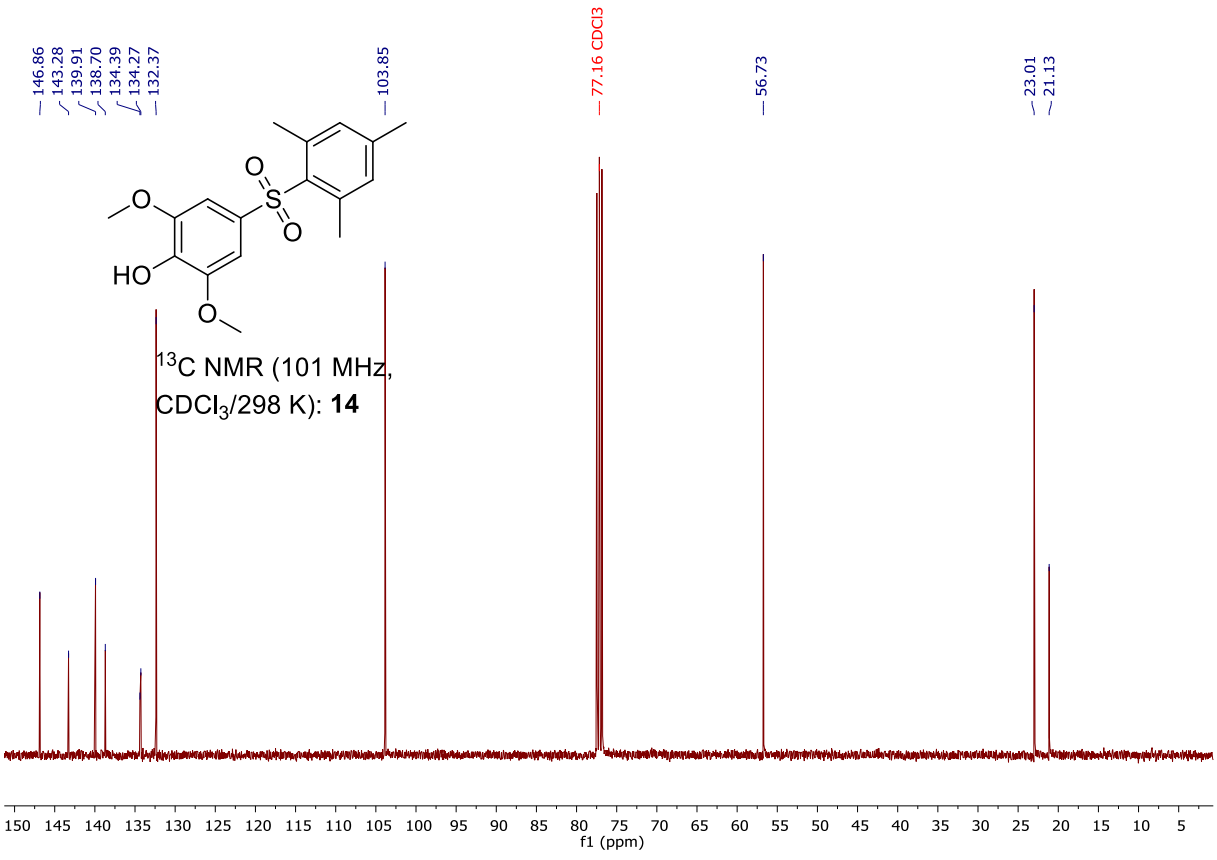
146.86
143.28
139.91
138.70
134.39
134.27
132.37
103.85
77.16 CDCl3
56.73
23.01
21.13
O
S
O
O
HO
O
13C NMR (101 MHz,
CDCl3/298 K): 14
150
145
140
135
130
125
120
115
110
105
100
95
90
85
80
75
70
65
60
55
50
45
40
35
30
25
20
15
10
5
f1 (ppm)

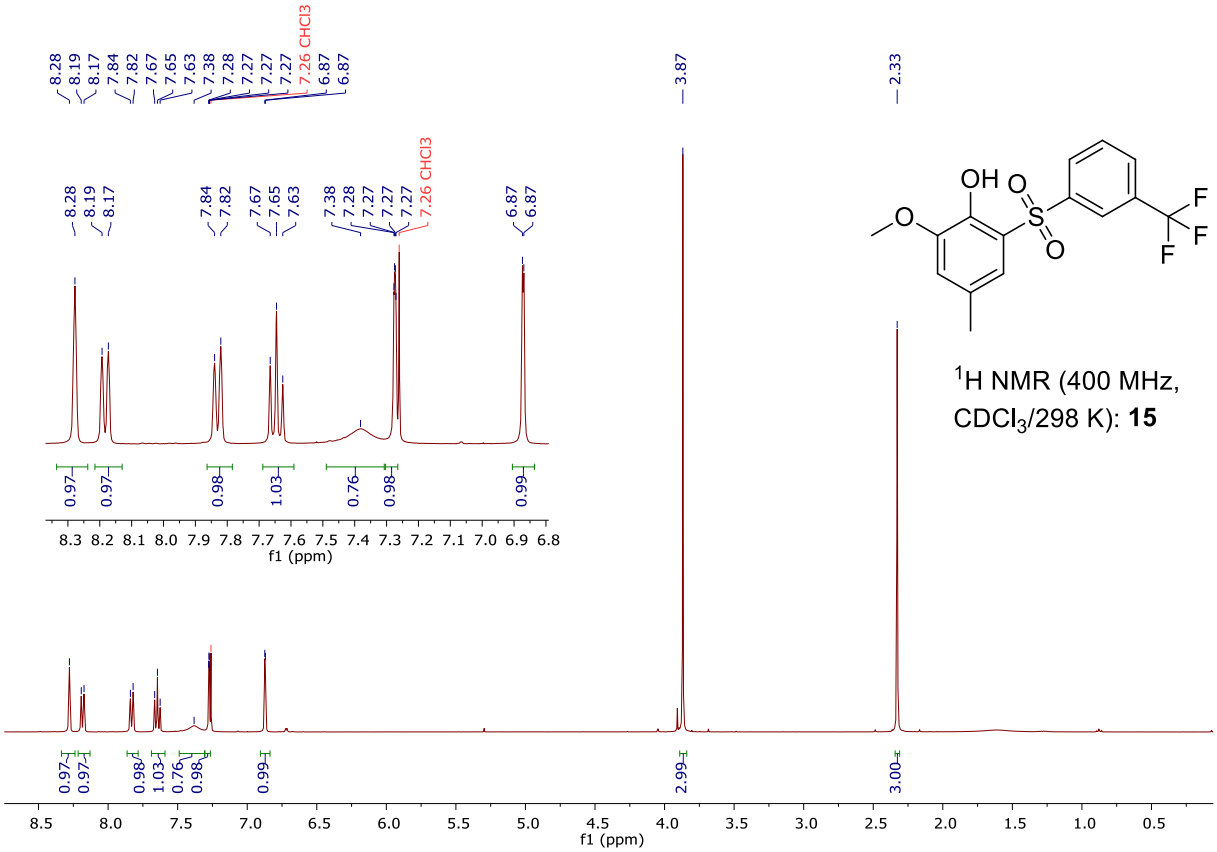

^{1}H NMR (400 MHz, $CDCl_3$/298 K): **15**

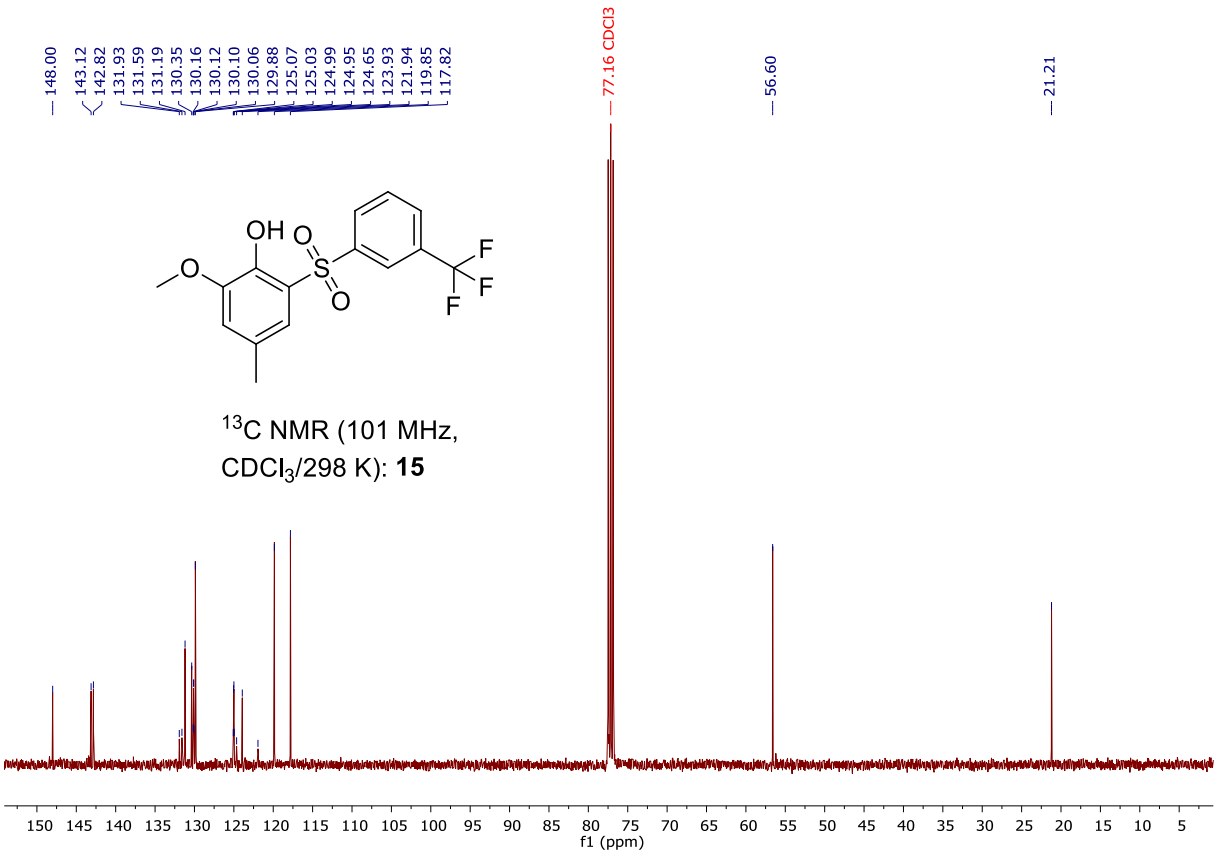

^{13}C NMR (101 MHz, $CDCl_3$/298 K): **15**

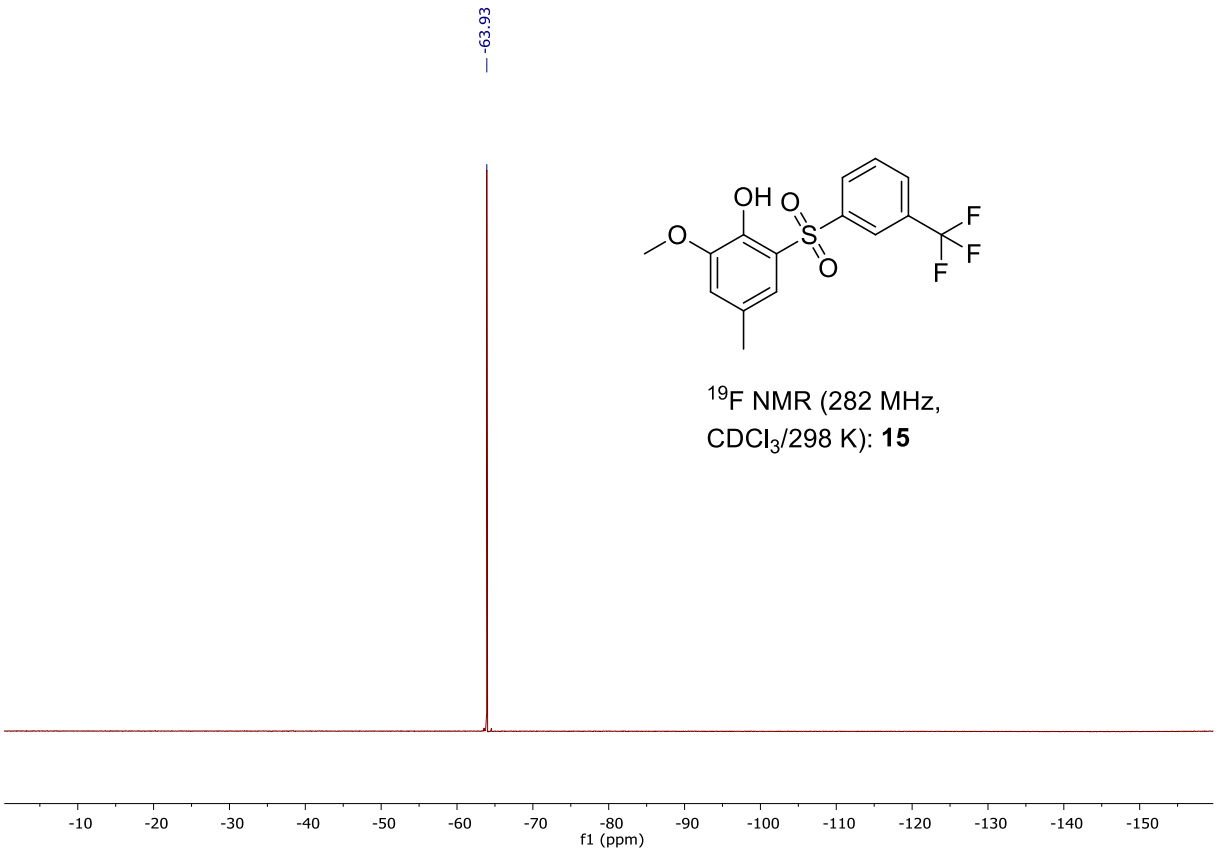

^{19}F NMR (282 MHz, $CDCl_3$/298 K): **15**

6. References

[1] W. L. F. Armarego, C. L. L. Chai, *Purification of Laboratory Chemicals*, Elsevier Ltd., Oxford, **2012**.

[2] R. K. Harris, E. D. Becker, S. M. Cabral de Menezes, R. Goodfellow, P. Granger, *Pure Appl. Chem.* **2001**, *73*, 1795–1818.

[3] Sheldrick, G.M. SHELXS97 and SHELXL97: *Programm for the Refinement of Crystal Structures*; Dept. of Structural Chemistry, University of Göttingen: Germany, **1997**

[4] a) C. Gütz, B. Klöckner, S. R. Waldvogel, *Org. Process Res. Dev.* **2016**, *20*, 26–32; b) A. Kirste, G. Schnakenburg, F. Stecker, A. Fischer, S. R. Waldvogel, *Angew. Chem. Int. Ed.* **2010**, *49*, 971-975; *Angew. Chem.* **2010**, *122*, 983-987. (see SI thereof).

[5] a) B. Riehl, K. M. Dyballa, R. Franke, S. R. Waldvogel, *Synthesis* **2017**, *49*, 252–259; b) A. Kirste, G. Schnakenburg, F. Stecker, A. Fischer, S. R. Waldvogel, *Angew. Chem. Int. Ed.* **2010**, *49*, 971–975; *Angew. Chem.* **2010**, *122*, 983–987; c) B. Elsler, A. Wiebe, D. Schollmeyer, K. M. Dyballa, R. Franke, S. R. Waldvogel, *Chem. Eur. J.* **2015**, *21*, 12321–12325.

ChemPubSoc Europe

DOI: 10.1002/celc.201901212

CHEMELECTROCHEM Communications

Straightforward Electrochemical Sulfonylation of Arenes and Aniline Derivatives using Sodium Sulfinates

Joachim Nikl,[a] Davide Ravelli,[a, b] Dieter Schollmeyer,[a] and Siegfried R. Waldvogel*[a]

We present a general electrochemical synthesis of sulfones from arenes and aniline derivatives with sodium sulfinates. A wide range of C–S cross-coupling products is available by this oxidant- and transition metal-free method. Both aryl and diaryl sulfones can be readily obtained, using this scalable and inherently safe one-step protocol. Since the synthesis excludes the need for additional supporting electrolyte and occurs in an aqueous electrolyte system that is easily recovered and recycled, this strategy represents a sustainable and green alternative to existing sulfonylation reactions.

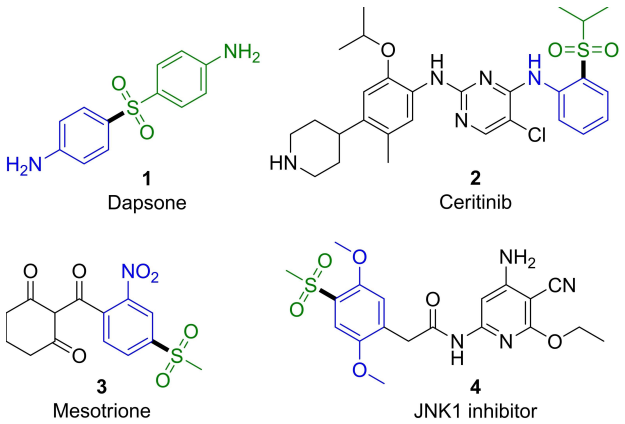

Scheme 1. Sulfone containing examples of bioactive ingredients and technically relevant compounds.

Sulfonylated aromatics are widely applicable biologically active substances, for example in medicine and agriculture (Scheme 1).[1] In particular, sulfones are the most important drugs used in the treatment of leprosy.[2] The most prominent example is Dapsone (**1**), which is also used as a malaria treatment agent.[3] An example of a sulfonylated *N*-functionalized aniline derivative is the prescription-only drug Ceritinib (**2**), which is used to treat non-small cell lung carcinoma (NSCLC).[4] Mesotrione (**3**) is a herbicide, belonging to the class of 4-hydroxyphenylpyruvate dioxygenase (HPPD) inhibitors and is especially used for maize cultivation.[5] A further derivative showing biological activity is the c-Jun N-terminal kinase 1 (JNK1) inhibitor **4**, whereby these kinases are associated with a number of different diseases such as asthma, Alzheimer and type 2 diabetes mellitus.[6]

In addition, sulfones are commonly used as reagents in organic synthesis,[7] as well as for high temperature plastics and fuel cell membranes.[8] Over the past years, the synthesis of sulfonyl containing architectures has increasingly attracted interest, as demonstrated by the numerous reports in the field.[9]

Overcoming the conventional Friedel-Crafts reactions or the employment of transition metal-catalysts,[12] the use of sulfinates as direct C–S bond coupling components experienced significant interest.[13] For example, the group of Willis described a direct photoinduced sulfonylation of *N*-alkylated anilines using an iridium catalyst (Scheme 2).[10] This procedure allows to obtain good overall yields. However, harmful and expensive transition metals, ligands and mediators are needed. Manolikakes and co-workers reported the first example of a purely manganese-promoted coupling of sulfinates (Scheme 2) in 1,1,1,3,3,3-hexafluoropropan-2-ol (HFIP).[11] While the reaction tolerates various functional groups and provides a broad scope, over-stoichiometric amounts of transition metals are utilized, resulting in additional reagent waste. Nevertheless, the fundamental role of HFIP was outlined in this synthesis, describing a radical stabilizing effect. Furthermore, a metal-free preparation of sulfonylated *N*,*N*-dimethylanilines has been recently reported.[14] The process makes use of DABCO·$(SO_2)_2$ and arenediazonium salts, albeit it only works at high temperatures and under inert gas atmosphere, leading to further disadvantages.

At variance with existing conventional reactions, electroorganic synthesis offers safer, sustainable and precisely controlled methods for direct C–H activation processes.[15,16] Since, electrons are used as reagents, pre-functionalized substrates and oxidizing agents can be avoided.[16]

So far, only a few precedents describing the electrochemical sulfonylation of arenes are present in the literature. Only 5 examples were reported in up to 59% yield and, importantly, the preparation of sulfonyl hydrazide reagents is essential, also requiring the use of an additional supporting electrolyte.[17]

[a] J. Nikl, Dr. D. Ravelli, Dr. D. Schollmeyer, Prof. Dr. S. R. Waldvogel
Institut für Organische Chemie
Johannes Gutenberg-Universität Mainz
Duesbergweg 10–14, 55128 Mainz (Germany)
E-mail: waldvogel@uni-mainz.de
Homepage: http://www.chemie.uni-mainz.de/OC/AK-Waldvogel/
[b] Dr. D. Ravelli
PhotoGreen Lab, Department of Chemistry
Viale Taramelli 12, 27100 Pavia (Italy)

Supporting information for this article is available on the WWW under https://doi.org/10.1002/celc.201901212

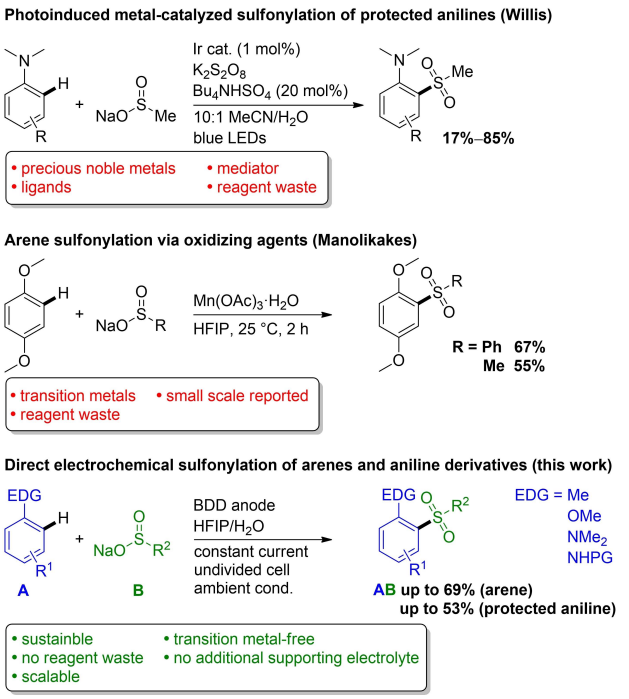

Scheme 2. Reported strategies for sulfinate-arene/aniline cross-coupling reactions and combining concept of this work.[10,11]

Recently, an elegant method for the anodic sulfonylation of *N,N*-disubstituted anilines was reported by Li and co-workers.[18] In this case, $^nBu_4NBF_4$ had to be used as supporting electrolyte and the reaction was only described for *N,N*-disubstituted anilines. In contrast to that, sulfonylation of *N,N*-dimethylanilines and anilides are performed and compared in this work.

Previously, we reported a direct method for the electrochemical sulfonylation of phenols by using sodium sulfinates.[19] In this work, an extension to arene and aniline derivative sulfonylation is described, applying an undivided electrolysis cell by using a constant current mode of operation, ensuring scalability and an easy implementation.[20] The utilization of additional supporting electrolyte is redundant, since the sulfinates act both as the coupling substrate and the supporting electrolyte. The use of an aqueous solvent system and the efficient depletion of chemicals guarantees this protocol with attributes coinciding with a green chemistry methodology.[20,21] Previously, the direct electrochemical, oxidative coupling of aromatic systems involving phenols,[22] anilides,[23] and arenes[24] has been successfully established. The resulting products are of particular interest, since they offer access to unique substitution patterns,[25] and can be used for example as ligand systems.[26] A general challenge in these reactions is to minimize formation of poly- and oligomeric substances via over-oxidation in which aniline derivatives are particularly at risk.[27] A central part in solving this shortcoming is provided by the utilization of 1,1,1,3,3,3-hexafluoropropan-2-ol (HFIP), enabling a solvent-controlled reaction process.[28] Due to its remarkable solvation abilities, HFIP is able to stabilize radical and cationic intermediates by forming strong hydrogen bonds,[29] and can lead to the decoupling of oxidation potential and nucleophilicity, triggering distinctive cross-coupling reactions.[21,28,30] Furthermore, sulfones are susceptible to electrochemical reduction,[31] which makes constant current electrolysis under simple, scalable conditions particularly difficult. We have overcome these challenges by adapting the electrolysis conditions and reaction parameters reported in the past.[19] A key concept is the addition of water to the solvent system enabling the use of sodium sulfinates as supporting electrolyte, due to improved solubility.[19,32] By intensive optimization through an electrochemical screening set-up (see Supporting Information),[33] electrolysis parameters were determined and applied in scale-up experiments, whereby the respective product was isolated (Scheme 3 and Table 1). For

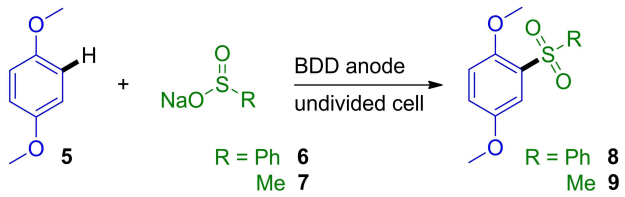

Scheme 3. Test reaction under optimized conditions for electro-organic synthesis of 2,5-dimethoxydiphenylsulfone (**8**) and 2,5-dimethoxyphenylmethylsulfone (**9**).

Table 1. Influence of water amount and current density onto the test reaction (Scheme 3).[a]

Entry	R	H_2O in HFIP [vol.%]	j [mA cm^{-2}]	Yield[b] [%]
1	Ph	15	18	60
2	Ph	30	18	53
3	Ph	15	26	67
4	Ph	15	52	51
5[c]	Me	15	12	40
6	Me	15	26	60
7[d]	Ph	15	26	60

[a] BDD electrodes, r.t., $Q = 2.5$ F (ref. **5**), **5**/**6** and **5**/**7** = 1:1.3. [b] Isolated yield. [c] $Q = 5.0$ F (ref. **5**), **5**/**7** = 1:1.5. [d] Graphite electrodes.

validating the optimization, both sodium benzenesulfinate **6** and sodium methanesulfinate **7** were used to investigate whether the conditions identified as optimal were equally valid for both substrates.

In analogy to the sulfonylation of phenols,[19] the best results for arene sulfonylation were consistently obtained with a water content of 15 vol.%. For the conversion of both reagents, high current densities of 26 mA cm^{-2} were yield promoting, which considerably shortens the electrolysis time from approximately 3 h (for 12 mA cm^{-2}) to 1.5 h. The highest conversions referring to arene sulfonylation were achieved by applying 2.5 F at boron-doped diamond electrodes (BDD) with a HFIP-water mixture of 15 vol.% and a current density of 26 mA cm^{-2} (Table 1, entries 3 and 6). Due to the small sulfinate excess of only 1.3 equivalents, this protocol also prevents the formation of significant amounts of waste. This advantage is attributed to the ambivalent solvent properties of HFIP. Due to its polar (hydroxyl) and non-polar (fluorinated) groups, microheteroge-

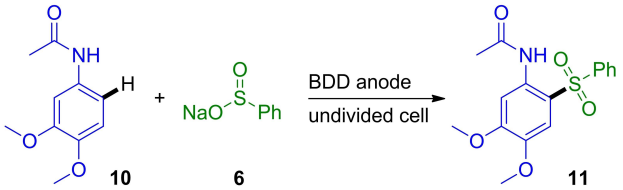

Scheme 4. Test reaction under optimized conditions for electro-organic synthesis of 2-acetamido-4,5-dimethoxydiphenylsulfone (**11**).

Table 2. Influence of charge quantity and current density onto the test reaction (Scheme 4).[a]

Entry	*Q* [F ref. **10**]	*j* [mA cm^{-2}]	Yield[b] [%]
1	3.5	12	30
2	2.5	6	24
3	3.5	26	18
4[c]	3.5	12	27

[a] BDD electrodes, r.t., 15 vol.% water in HFIP, **10**/**6** = 1 : 1.5. [b] Isolated yield. [c] Glassy carbon electrodes.

neous domains are formed, which allow polar and non-polar reagents to be separated from each other,[34] explaining the non-necessity of a high sulfinate excess. Another advantage of HFIP as a solvent is its low boiling point, which makes the complete recovery easy upon electrolysis.[35] A variation of the electrode material does not lead to any yield improvement. Boron-doped diamond electrodes (BDD) have proven to be unsurpassed for these sulfonylation processes. Thus, when the reaction was carried out on graphite electrodes under optimized reaction conditions, **8** was obtained in 60% isolated yield (Table 1, entry 7). The results obtained by using BDD can be explained by its high robustness in electrochemical reactions.[36] The extraordinary properties of BDD as an electrode material for electro-organic synthesis have already been manifold described, as well as the superior combination of BDD electrodes and HFIP in anodic coupling reactions.[37] Besides arene sulfonylation, the protocol was also extended to anilides and *N*,*N*-dimethylanilines to demonstrate the great diversity of tolerable substrates for this approach. Therefore, the test substrate **10** was converted to the sulfonylated anilide **11** in the presence of sulfinate **6** (Scheme 4).

Screening results revealed different optimal parameter values, as opposed to the arene coupling. Lowering the current density from 26 mA cm^{-2} resulted in increasing conversions (Table 2, entry 3). Best results were obtained with the application of 3.5 F on BDD electrodes in a HFIP-water mixture of 15 vol.% and a current density of 12 mA cm^{-2} (Table 2, entry 1). However, during the optimization it was observed that the sulfonylation of substrate **10** leads to lower yields than in case of substrate **5**. Cyclic voltammetry measurements show a similar oxidation potential for both substrates (see Supporting Information). Therefore, it is assumed that a partial decomposition of the starting material takes place in the case of **10**, possibly leading to unprotected anilines and to easily occurring over-oxidation, which makes the anilide coupling in general challenging. Referring to the previously reported anodic anilide

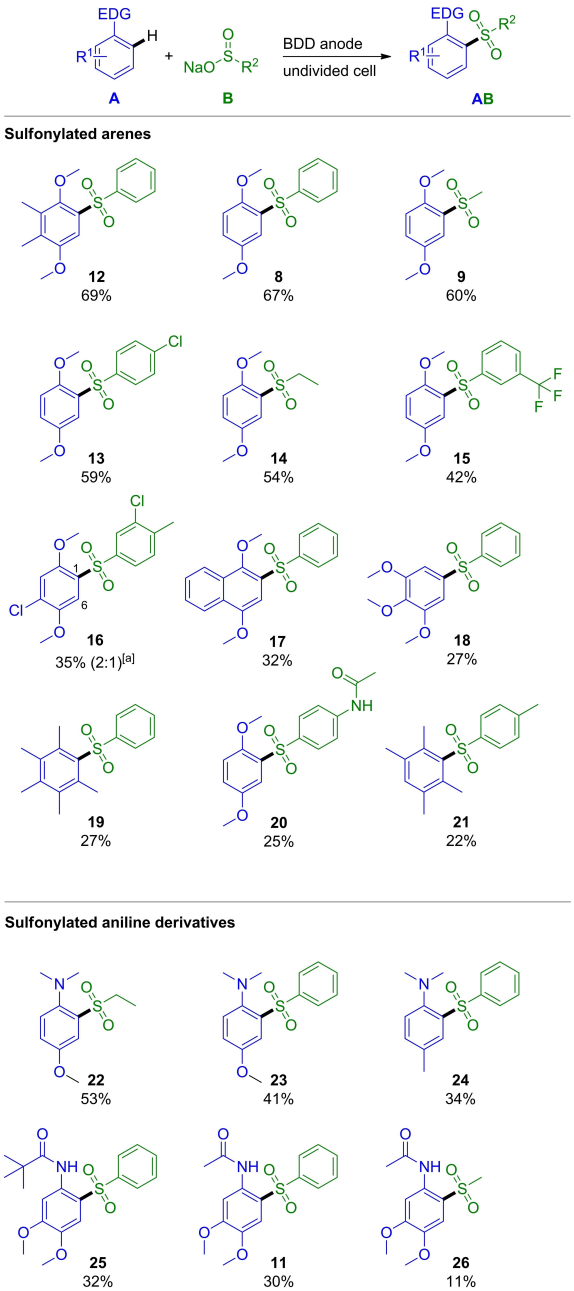

Scheme 5. Scope of aryl sulfones. Conditions for arene sulfonylation: BDD electrodes, r.t., 15 vol.% water in HFIP, j = 26 mA cm^{-2}, Q = 2.5 F (ref. **A**), **A**/**B** = 1 : 1.3. Conditions for aniline sulfonylation: BDD electrodes, r.t., 15 vol.% water in HFIP, j = 12 mA cm^{-2}, Q = 3.5 F (ref. **A**), **A**/**B** = 1 : 1.5. [a] yield ratio between regioisomers **16a** (C1-coupling) and **16b** (C6-coupling).

coupling,[23] also glassy carbon electrodes were tested (Table 2, entry 4). Here, a minor decreasing effect was observed, delivering **11** in 27% yield.

By applying the optimized conditions for arene sulfonylation (Table 1, entry 3 and 6), a collection of examples was produced (Scheme 5). The described protocol allows the conversion of different substituted arenes with a variety of functionalized sulfinates resulting in isolated yields up to 69%. As demonstrated by the examples **13**, **15** and **16**, halogen-containing sulfinates and arenes are tolerated as well as non-

methoxy-substituted arenes (e.g. **19**, **21**). Due to the variation of component **B**, monoarylsulfones (e.g. **9**, **14**) or diarylsulfones can be synthesized, opening a large accessible product scope. In order to demonstrate the broad applicability of this protocol, anilides and *N*,*N*-dimethylanilines were utilized as well. Overall, the isolated yields of the dimethylanilines **22**, **23** and **24** are higher than for the anilides **11**, **25** and **26**, after application of the same electrochemical protocol. This fact can be explained by two major assumptions. First, the amino moiety induces selectivity via the initial oxidation of the dimethylanilines prior to the sulfinates, due to their fundamentally lower oxidation potentials (see Supporting Information).

Second, after generation of the sulfones, a hydrogen bond between the sulfinate oxygen and the amide hydrogen can be formed, keeping the nitrogen lone pair in π-contact with the aromatic ring (Figure 1). Due to the persistent higher electron

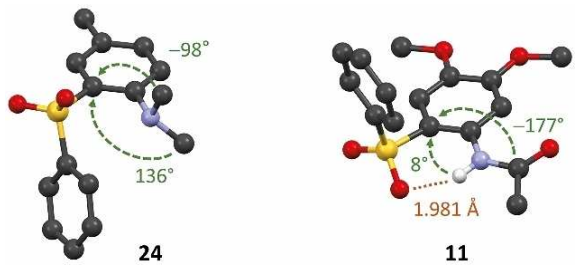

Figure 1. Molecular structures by X-ray analysis of **11** and **24** with indicated hydrogen bond for **11** (1.981 Å, dotted orange line). The remaining hydrogen atoms are omitted for clarity. Torsion angles for **11** are 8° and −177°, and for **24**, 136° and −98° (dashed green arrows).

density the products are prone to over-oxidation. As opposed to this, the sulfonylated *N*,*N*-dimethylanilines presumed to have a twist in the amino N–Ar bond due to the steric hindrance with the sulfone moiety, causing diminished conjugation of the nitrogen lone pair with the π-system of the aromatic ring (Figure 1). Therefore, less over-oxidation of these products is concluded.[22b]

In general, diversification of the substrates was turned out to be challenging for the sulfonylation of aniline derivatives. By using the most promising reaction conditions, a few examples could be isolated, demonstrating concurrently the first electrochemically generated sulfonylation products of anilides (Scheme 5). As a general remark due to anodic oxidation reactions, a great decrease of yield is attributed to the formation of over-oxidation products, which remain on the silica as a dark residue during column chromatographic purification. In cases of the anilide conversions certain amounts of starting material were recovered after work-up, confirming a possible competing effect due to the oxidation of the sulfinates. To demonstrate the high scalability of this protocol, the reaction shown in Scheme 3 was performed in a 8-times magnified approach (Figure 2). The scale-up was performed from a 5 mmol batch scale (ref. **5**, 25 mL electrolysis cell) to a 40 mmol batch scale (ref. **5**, 200 mL electrolysis cell). Here **8** was obtained in a comparable yield of 55% (6.10 g). Further

Figure 2. Scale-up from a 5 mmol to a 40 mmol batch. For size comparison of the beaker-type cells a 2 € coin is placed in front (diameter 25.75 mm ≈ 1.01 in).

experimental details can be obtained in the Supporting Information.

For mechanistic considerations regarding the reaction, cyclic voltammetry measurements of the substrates were performed (see Supporting Information). The postulated sulfinate oxidation by Li and co-workers, which leads to sulfone formation,[18] cannot be completely excluded. However, for both cases (arenes and aniline derivatives), it is apparent that an initial oxidation step of the **A** component is likely, due to the lower oxidation potentials. Stabilization of the positive charge is obtained through the electron donating properties of the functionalities. The following C–S bond formation occurs via a nucleophilic attack of the sulfinate to the formed radical cation **I**. Finally, a second oxidation step of the HFIP-stabilized intermediate **II** to the sulfone **AB** is assumed (Scheme 6). These results also refer to the previously described mechanism for the oxidative phenol sulfonylation[19] and the anodic C,C cross-coupling reactions.[22a–c] As counter reaction, an electro-reduction of water leading to hydrogen evolution is probable, since a visible gas evolution at the cathode surface occurs. A pH value determination via universal indicator paper before and after electrolysis shows an increase from a pH of 3–4 to 9–10, revealing a consumption of the co-solvent H_2O.

In conclusion, a unifying, direct, safe, and sustainable method for the electrochemical sulfonylation of arenes and aniline derivatives has been established. The presented protocol takes inspiration from the previously reported sulfonylation of phenols and leads to the preparation of aryl and diaryl sulfones in good yields, up to 69%. The use of the sulfinates as coupling component and supporting electrolyte prevents additional

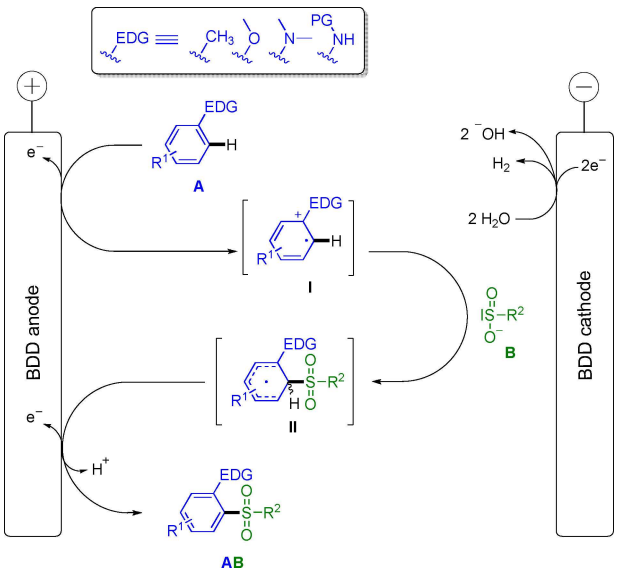

Scheme 6. Postulated mechanism for the anodic arene/aniline sulfonylation. The functionalities are depicted as EDG (Electron Donating Group).

additives and reagent waste. This transition-metal- and oxidant-free protocol is based on a constant current electrolysis in an undivided cell, whereby an easy performance, a high scalability and an efficient utilization of starting materials under green chemistry attributes is ensured.

Experimental Section

Detailed information on general procedures, electrolytic conversions and product characterization can be found in the Supporting Information.

Acknowledgements

S.R.W. thanks the DFG (Wa1276/17-1) for financial support. D.R. acknowledges Fondazione CARIPLO (grant n. 2018-2627) and the University of Pavia (InROAd project "ElectroLight") for financial support.

Conflict of Interest

The authors declare no conflict of interest.

Keywords: C–H activation · cross-coupling · electrochemistry · oxidation · sustainable chemistry

[1] a) M. Feng, B. Tang, S. H. Liang, X. Jiang, *Curr. Top. Med. Chem.* **2016**, *16*, 1200–1216; b) D. C. Meadows, J. Gervay-Hague, *Med. Res. Rev.* **2006**, *26*, 793–814; c) L. Garuti, M. Roberti, D. Pizzirani, G. Poggi, *Curr. Med. Chem.* **2005**, *4*, 167–183; d) J. Balzarini, M. Stevens, E. de Clercq, D. Schols, C. Pannecouque, *J. Antimicrob. Chemother.* **2005**, *55*, 135–138; e) P. Devendar, G.-F. Yang, *Top. Curr. Chem.* **2017**, *375*, 1–44.

[2] G. L. Patrick, *An Introduction to Medicinal Chemistry*; Oxford University Press, Oxford, **2013**.

[3] A. C. McDougall, *Clin. Exp. Dermatol.* **1979**, *4*, 139–142.

[4] S. Khozin, G. M. Blumenthal, L. Zhang, S. Tang, M. Brower, E. Fox, W. Helms, R. Leong, P. Song, Y. Pan, Q. Liu, P. Zhao, H. Zhao, D. Lu, Z. Tang, A. Al Hakim, K. Boyd, P. Keegan, R. Justice, R. Pazdur, *Clin. Cancer Res.* **2015**, *21*, 2436–2439.

[5] R. Beaudegnies, A. J. F. Edmunds, T. E. M. Fraser, R. G. Hall, T. R. Hawkes, G. Mitchell, J. Schaetzer, S. Wendeborn, J. Wibley, *Bioorg. Med. Chem.* **2009**, *17*, 4134–4152.

[6] B. G. Szczepankiewicz, C. Kosogof, L. T. J. Nelson, G. Liu, B. Liu, H. Zhao, M. D. Serby, Z. Xin, M. Liu, R. J. Gum, D. L. Haasch, S. Wang, J. E. Clampit, E. F. Johnson, T. H. Lubben, M. A. Stashko, E. T. Olejniczak, C. Sun, S. A. Dorwin, K. Haskins, C. Abad-Zapatero, E. H. Fry, C. W. Hutchins, H. L. Sham, C. M. Rondinone, J. M. Trevillyan, *J. Med. Chem.* **2006**, *49*, 3563–3580.

[7] a) R. J. K. Taylor, G. Casy, *Org. React.* **2003**, *62*, 357–475; b) M. Nielsen, C. B. Jacobsen, N. Holub, M. W. Paixão, K. A. Jørgensen, *Angew. Chem. Int. Ed.* **2010**, *49*, 2668–2679; *Angew. Chem.* **2010**, *122*, 2726–2738; c) M. Julia, J.-M. Paris, *Tetrahedron Lett.* **1973**, *14*, 4833–4836; d) M. Trost, *Bull. Chem. Soc. Jpn.* **1988**, *61*, 107–124.

[8] a) R. Nolte, K. Ledjeff, M. Bauer, R. Mülhaupt, *J. Membr. Sci.* **1993**, *83*, 211–220; b) G. Chang, X. Luo, Y. Xu, H. Hu, L. Wei, L. Zhang, R. Lin, *Polym. Bull.* **2012**, *68*, 95–111; c) J. B. Rose, *Polymer* **1974**, *15*, 456–465.

[9] a) S. Shaaban, S. Liang, N.-W. Liu, G. Manolikakes, *Org. Biomol. Chem.* **2017**, *15*, 1947–1955; b) A. Hossan, *Chem. Heterocycl. Compd.* **2016**, *52*, 570–573; c) A. Ahmad, A. K. Chauhan, S. Javed, A. Kumar, *Biotechnol. Lett.* **2014**, *36*, 2209–2214; d) N. Umierski, G. Manolikakes, *Org. Lett.* **2013**, *15*, 4972–4975; e) N. Umierski, G. Manolikakes, *Org. Lett.* **2013**, *15*, 188–191; f) K. P. Boroujeni, *Bull. Korean Chem. Soc.* **2010**, *31*, 1887–1890; g) H. Sharghi, Z. Shahsavari-Fard, *Helv. Chim. Acta.* **2005**, *88*, 42–52; h) A. R. Hajipour, A. Zarei, L. Khazdooz, S. A. Pourmousavi, Phosphorus, *Sulfur Silicon Relat. Elem.* **2005**, *180*, 2029–2034; i) B. F. Mirjalili, M. A. Zolfigol, A. Bamoniri, L. Khazdooz, *Bull. Korean Chem. Soc.* **2003**, *24*, 1009–1010.

[10] T. C. Johnson, B. L. Elbert, A. J. M. Farley, T. W. Gorman, C. Genicot, B. Lallemand, P. Pasau, J. Flasz, J. L. Castro, M. MacCoss, D. J. Dixon, R. S. Paton, C. J. Schofield, M. D. Smith, M. C. Willis, *Chem. Sci.* **2018**, *9*, 629–633.

[11] S. Liang, Y. Ren, G. Manolikakes, *Eur. J. Org. Chem.* **2017**, 4117–4120.

[12] a) K. P. Borujeni, B. Tamami, *Catal. Commun.* **2007**, *8*, 1191–1196; b) S. J. Nara, J. R. Harjani, M. M. Salunkhe, *J. Org. Chem.* **2001**, *66*, 8616–8620; c) R. P. Singh, R. M. Kamble, K. L. Chandra, P. Saravanan, V. K. Singh, *Tetrahedron* **2001**, *57*, 241–247; d) J. Marquié, A. Laporterie, J. Dubac, N. Roques, J.-R. Desmurs, *J. Org. Chem.* **2001**, *66*, 421–425. e) J. Liu, L. Zheng, *Adv. Synth. Catal.* **2019**, *361*, 1710–1732; f) D. H. Kim, J. Lee, A. Lee, *Org. Lett.* **2018**, *20*, 764–767; g) D. O. Jang, K. S. Moon, D. H. Cho, J.-G. Kim, *Tetrahedron Lett.* **2006**, *47*, 6063–6066; h) C. G. Frost, J. P. Hartley, A. J. Whittle, *Synlett* **2001**, 830–832; i) B. P. Bandgar, S. V. Bettigeri, J. Phopase, *Org. Lett.* **2004**, *6*, 2105–2108.

[13] a) H. Yue, C. Zhu, M. Rueping, *Angew. Chem. Int. Ed.* **2018**, *57*, 1371–1375; *Angew. Chem.* **2018**, *130*, 1385–1389; b) C. Wang, H. Zhang, Z. Li, Z. Wang, *J. Chem. Res.* **2014**, *38*, 639–642; c) J. Aziz, S. Messaoudi, M. Alami, A. Hamze, *Org. Biomol. Chem.* **2014**, *12*, 9743–9759; d) A. Kar, I. A. Sayyed, W. F. Lo, H. M. Kaiser, M. Beller, M. K. Tse, *Org. Lett.* **2007**, *9*, 3405–3408.; e) W. Zhu, D. Ma, *J. Org. Chem.* **2005**, *70*, 2696–2700; f) S. Cacchi, G. Fabrizi, A. Goggiamani, L. M. Parisi, R. Bernini, *J. Org. Chem.* **2004**, *69*, 5608–5614.

[14] K. Zhou, J. Zhang, L. Lai, J. Cheng, J. Sun, J. Wu, *Chem. Commun.* **2018**, *54*, 7459–7462.

[15] H. J. Schäfer, *C. R. Chim.* **2011**, *14*, 745–765.

[16] a) A. Wiebe, T. Gieshoff, S. Möhle, E. Rodrigo, M. Zirbes, S. R. Waldvogel, *Angew. Chem. Int. Ed.* **2018**, *57*, 5594–5619; *Angew. Chem.* **2018**, *130*, 5694–5721; b) S. Möhle, M. Zirbes, E. Rodrigo, T. Gieshoff, A. Wiebe, S. R. Waldvogel, *Angew. Chem. Int. Ed.* **2018**, *57*, 6018–6041; *Angew. Chem.* **2018**, *130*, 6124–6149.

[17] Y. Yuan, Y. Yu, J. Qiao, P. Liu, B. Yu, W. Zhang, H. Liu, M. He, Z. Huang, A. Lei, *Chem. Commun.* **2018**, *54*, 11471–11474.

[18] Y.-C. Wu, S.-S. Jiang, S.-Z. Luo, R.-J. Song, J.-H. Li, *Chem. Commun.* **2019**, *55*, 8995–8998.

[19] J. Nikl, S. Lips, D. Schollmeyer, R. Franke, S. R. Waldvogel, *Chem. Eur. J.* **2019**, *25*, 6891–6895.

[20] S. R. Waldvogel, S. Lips, M. Selt, B. Riehl, C. J. Kampf, *Chem. Rev.* **2018**, *118*, 6706–6765.
[21] B. A. Frontana-Uribe, R. D. Little, J. G. Ibanez, A. Palma, R. Vasquez-Medrano, *Green Chem.* **2010**, *12*, 2099–2119.
[22] a) B. Riehl, K. Dyballa, R. Franke, S. Waldvogel, *Synthesis* **2017**, *49*, 252–259; b) A. Wiebe, D. Schollmeyer, K. M. Dyballa, R. Franke, S. R. Waldvogel, *Angew. Chem. Int. Ed.* **2016**, *55*, 11801–11805; *Angew. Chem.* **2016**, *128*, 11979–11983; c) B. Elsler, D. Schollmeyer, K. M. Dyballa, R. Franke, S. R. Waldvogel, *Angew. Chem. Int. Ed.* **2014**, *53*, 5210–5213; *Angew. Chem.* **2014**, *126*, 5311–5314; d) A. Kirste, G. Schnakenburg, F. Stecker, A. Fischer, S. R. Waldvogel, *Angew. Chem. Int. Ed.* **2010**, *49*, 971–975; *Angew. Chem.* **2010**, *122*, 983–987; e) A. Kirste, B. Elsler, G. Schnakenburg, S. R. Waldvogel, *J. Am. Chem. Soc.* **2012**, *134*, 3571–3576; f) S. Lips, R. Franke, S. R. Waldvogel, *Synlett* **2019**, *30*, 1174–1177; g) B. Dahms, R. Franke, S. R. Waldvogel, *ChemElectroChem* **2018**, *5*, 1249–1252; h) S. Lips, D. Schollmeyer, R. Franke, S. R. Waldvogel, *Angew. Chem. Int. Ed.* **2018**, *57*, 13325–13329; *Angew. Chem.* **2018**, *130*, 13509–13513.
[23] a) L. Schulz, M. Enders, B. Elsler, D. Schollmeyer, K. M. Dyballa, R. Franke, S. R. Waldvogel, *Angew. Chem. Int. Ed.* **2017**, *56*, 4877–4881; *Angew. Chem.* **2017**, *129*, 4955–4959; b) L. Schulz, R. Franke, S. R. Waldvogel, *ChemElectroChem* **2018**, *5*, 2069–2072.
[24] S. B. Beil, P. Franzmann, T. Müller, M. M. Hielscher, T. Prenzel, D. Pollok, N. Beiser, D. Schollmeyer, S. R. Waldvogel, *Electrochim. Acta* **2019**, *302*, 310–315.
[25] a) S. Lips, B. A. Frontana-Uribe, M. Dörr, D. Schollmeyer, R. Franke, S. R. Waldvogel, *Chem. Eur. J.* **2018**, *24*, 6057–6061; b) M. Dörr, S. Lips, C. A. Martínez-Huitle, D. Schollmeyer, R. Franke, S. R. Waldvogel, *Chem. Eur. J.* **2019**, *25*, 7835–7838.
[26] a) S. Lips, A. Wiebe, B. Elsler, D. Schollmeyer, K. M. Dyballa, R. Franke, S. R. Waldvogel, *Angew. Chem. Int. Ed.* **2016**, *55*, 10872–10876; *Angew. Chem.* **2016**, *128*, 11031–11035; b) A. Wiebe, S. Lips, D. Schollmeyer, R. Franke, S. R. Waldvogel, *Angew. Chem. Int. Ed.* **2017**, *56*, 14727–14731; *Angew. Chem.* **2017**, *129*, 14920–14925.
[27] a) X. Yang, J. Kirsch, J. Fergus, A. Simonian, *Electrochim. Acta* **2013**, *94*, 259–268; b) J. Iniesta, P. A. Michaud, M. Panizza, G. Cerisola, A. Aldaz, C. Comninellis, *Electrochim. Acta* **2001**, *46*, 3573–3578; c) M. A. Rodrigo, P. A. Michaud, I. Duo, M. Panizza, G. Cerisola, C. Comninellis, *J. Electrochem. Soc.* **2001**, 148, D60–D64; d) H. Letheby, *J. Chem. Soc.* **1862**, *15*, 161–163; e) N. Gospodinova, L. Terlemezyan, *Prog. Polym. Sci.* **1998**, *23*, 1443–1484.
[28] B. Elsler, A. Wiebe, D. Schollmeyer, K. M. Dyballa, R. Franke, S. R. Waldvogel, *Chem. Eur. J.* **2015**, *21*, 12321–12325.
[29] a) L. Eberson, M. P. Hartshorn, O. Persson, *J. Chem. Soc. Perkin Trans. 2* **1995**, 1735–1744; b) S. R. Waldvogel, S. Mentizi, A. Kirste, *Top. Curr. Chem.* **2012**, *320*, 1–31.
[30] L. Schulz, S. R. Waldvogel, *Synlett* **2019**, *30*, 275–286.
[31] a) J. Delaunay, G. Mabon, M. Chaquiq El Badre, A. Orliac, J. Simonet, *Tetrahedron Lett.* **1992**, *33*, 2149–2150; b) S. Prigent, P. Cauliez, J. Simonet, D. G. Peters, *Acta Chem. Scand.* **1999**, *53*, 892–900; c) J.-F. Bergamini, P. Hapiot, C. Lagrost, L. Preda, J. Simonet, E. Volanschi, *Phys. Chem. Chem. Phys.* **2003**, *5*, 4846–4850.
[32] J. Simonet, *Phosphorus Sulfur Silicon Relat. Elem.* **1993**, *74*, 93–112.
[33] C. Gütz, B. Klöckner, S. R. Waldvogel, *Org. Process Res. Dev.* **2016**, *20*, 26–32.
[34] O. Hollóczki, A. Berkessel, J. Mars, M. Mezger, A. Wiebe, S. R. Waldvogel, B. Kirchner, *ACS Catal.* **2017**, *7*, 1846–1852.
[35] I. Colomer, A. E. R. Chamberlain, M. B. Haughey, T. J. Donohoe, *Nat. Rev. Chem.* **2017**, *1*, 88.
[36] S. R. Waldvogel, B. Elsler, *Electrochim. Acta* **2012**, *82*, 434–443.
[37] S. Lips, S. R. Waldvogel, *ChemElectroChem* **2019**, *6*, 1649–1660.

Manuscript received: July 21, 2019
Revised manuscript received: August 5, 2019
Accepted manuscript online: August 6, 2019

CHEMELECTROCHEM

Supporting Information

Straightforward Electrochemical Sulfonylation of Arenes and Aniline Derivatives using Sodium Sulfinates

Joachim Nikl, Davide Ravelli, Dieter Schollmeyer, and Siegfried R. Waldvogel*

Contents

1. General information

All reagents were of analytical grade and were obtained from common chemical providers such as ABCR, TCI, Aldrich, Fluka, and Acros. Solvents were purified by standard methods.[1] Electrochemical reactions were carried out at boron-doped diamond (BDD) electrodes. BDD electrodes were obtained as DIACHEM™ quality from CONDIAS GmbH, Itzehoe, Germany. BDD (15 µm diamond layer) was used on silicon as support.

Column Chromatography was performed on silica gel 60 M (0.040–0.063 mm, Macherey-Nagel GmbH & Co, Düren, Germany). Therefore, a preparative chromatography system (Büchi, Flawil, Switzerland) was used with a Büchi Control Unit C-620, an UV detector Büchi UV photometer C-635, a Büchi fraction collector C-660 and two Pump Modules C-605 for adjusting the solvent mixtures. As eluent, mixtures of cyclohexane and ethyl acetate were used. Silica gel 60 sheets on aluminium (F254, Merck KGaA, Darmstadt, Germany) were employed for thin layer chromatography.

Gas chromatography was performed on a Shimadzu GC-2025 (Shimadzu, Japan) using a HP-5 column (Agilent Technologies, Santa Clara, California; length: 30 m, inner diameter: 0.25 mm, film: 0.25 µm, carrier gas: hydrogen). GC-MS measurements were carried out on a Shimadzu GC-2010 (Shimadzu, Japan) using a HP-1 column (Agilent Technologies, Santa Clara, California; length: 30 m, inner diameter: 0.25 mm, film: 0.25 µm, carrier gas: helium). The chromatograph was coupled to a mass spectrometer Shimadzu GC-MS-QP2010.

Melting points were determined with a Melting Point Apparatus B-565 (Büchi, Flawil, Switzerland) and are uncorrected. Heating rate: 1 °C/min.

NMR Spectroscopy of ^{1}H, ^{13}C and ^{19}F spectra were recorded at 25 °C, using a Bruker Avance II 400 (400 MHz, 5 mm BBFO-SmartProbe with z gradient and ATM, SampleXPress 60 sample changer, Analytische Messtechnik, Karlsruhe, Germany). Chemical shifts (δ) are reported in parts per million (ppm) relative to traces of $CHCl_3$ or DMSO-d_5 in the corresponding deuterated solvent. For ^{19}F spectra $CFCl_3$ serves as reference compound.[2]

High-resolution mass spectra were obtained by using an Agilent 6545 QTOF-MS (Agilent Technologies, Santa Clara, California) apparatus employing ESI^+ and $APCI^+$.

Cyclic voltammetry was performed in a 10 mL snap-cap vial equipped with an Autolab PGSTAT101 potentiostat (Metrohm AG, Herisau, Switzerland). *WE*: BDD electrode tip, 2 mm diameter; *CE*: glassy carbon rod; *RE*: Ag/AgCl in saturated LiCl/EtOH. Solvent: HFIP+15 vol.% H_2O. v = 100 mV/s, T = 28 °C, c = 0.01 M, supporting electrolyte: $^{n}Bu_4NPF_6$, c ($^{n}Bu_4NPF_6$) = 0.1 M.

Elemental analysis was carried out with a vario EL Cube (Elementar Analysensysteme GmbH, Langenselbold, Germany).

X-ray analysis data were collected on a STOE IPDS-2T diffractometer (STOE & Cie GmbH, Darmstadt, Germany) using graphite monochromated Mo-Kα radiation (λ = 0.71073 Å). Intensities were measured using fine-slicing ω and ϕ-scans and corrected for background, polarization and Lorentz effects. The structures were solved by direct methods and refined anisotropically by the least-squares procedure implemented in the SHELX program system.[3]

The supplementary crystallographic data for this paper can be obtained free of charge from the Cambridge Crystallographic Data Center via www.ccdc.cam.ac.uk/data_request/cif. Deposition numbers and further details are given with the individual characterization data.

2. Set-up and general protocols for electrolytic cross-coupling (GP 1/GP 2/GP 3)

The undivided PTFE cells used are homemade by the university's own mechanical shop, which are described in literature.[4] The complete setup of these cells with screening block is also commercially available as IKA Screening System, IKE-Werke GmbH & Co. KG, Staufen, Germany. The used beaker-type glass cells are homemade by the university's own mechanical shop. The undivided beaker-type cells are only briefly described here, whereby more detailed information has already been reported.[4] The cells are operated with boron-doped diamond electrodes (BDD).

GP 1: PTFE cell (5 mL)

Screening reactions were performed in an undivided 5 mL PTFE cell. Dimensions of the BDD electrodes are 7 cm x 1 cm x 0.3 cm.

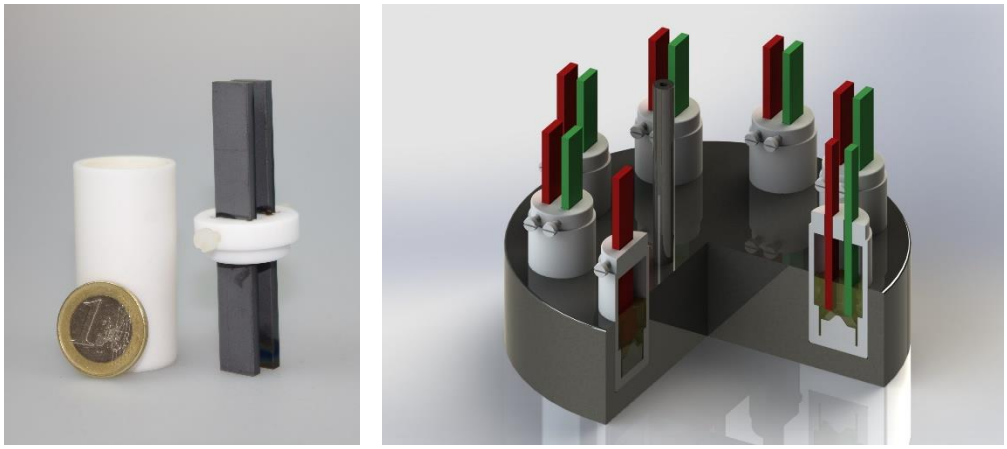

Figure 1: 5 mL PTFE cell; left: with one euro coin for size comparison; right: schematic visualization of 5 mL PTFE cells in a screening block.

The arene/aniline compound **A** (0.76 mmol) and varied amounts of the sulfinate **B** (from 1 eq. to 3 eq.) are transferred into the undivided PTFE electrolysis cell and are solved by 5 mL of a solvent mixture constituted of HFIP and deionized water in different volume percentages (from 0 vol% to 30 vol.%). The cell is equipped with a BDD anode and a BDD cathode, with a distance of 0.5 cm between each other. The electrodes are 1.8 cm^2 immersed. After fixing the cell in a stainless steel block, a constant current electrolysis with different current densities (from 2 mA/cm^2 to 28 mA/cm^2) has been performed at 23 °C.

After application of different charge quantities (from 2 F to 5 F per arene or aniline **A**) an aliquant of approx. 60 µL is taken from the reaction solution and filtered via approx. 330 mg silica gel 60M, whereby 2.4 mL ethyl acetate is used as eluent. The filtrate is examined via GC and GC-MS analysis. The resulting relative GC integrals of the product signals were used to evaluate the quality of the reaction.

GP 2: Beaker-type cell (25 mL)

The reactions were performed in a 25 mL beaker-type glass cell, which consists of a simple glass beaker with or without cooling jacket and is closed by a Teflon plug, which allows a precise arrangement of the BDD electrodes. Dimensions of the BDD electrodes are 7 cm x 2 cm x 0.3 cm.

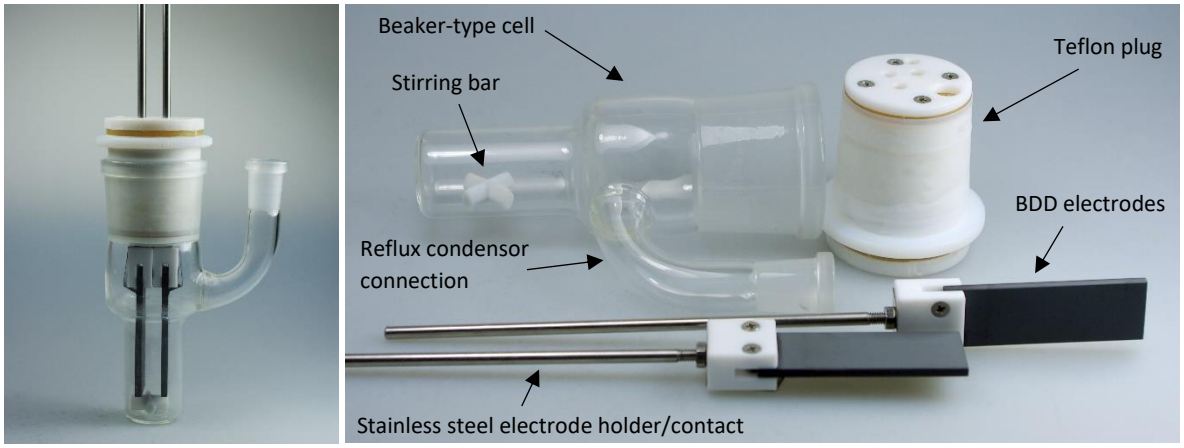

Figure 2: 25 mL beaker-type cell; left: assembled; right: individual parts.

The arene or aniline compound **A** (5 mmol) and the sulfinate **B** (6.5 mmol or 7.5 mmol) are transferred into the undivided beaker-type electrolysis cell and are solved by 25 mL of a solvent mixture constituted of HFIP (21.25 mL) and deionized water (3.75 mL, 15 vol.%). The cell is equipped with a BDD anode and a BDD cathode, with a distance of 1.1 cm between each other. The electrodes are 4.5 cm^2 immersed. A constant current electrolysis with a current density of 26 mA/cm^2 or 12 mA/cm^2 has been performed at 23 °C.

After application of 1206 C or 1688 C (2.5 F or 3.5 F per arene or aniline **A**) the HFIP is recovered by distillation *in vacuo* (50 °C, 200–90 mbar). The crude product is dissolved in a mixture of dichloromethane (50 mL) / deionized water (50 mL) and is then transferred into a separatory funnel. After phase separation the aqueous fraction is extracted with dichloromethane (2 x 50 mL). The combined organic fractions are washed with deionized water (2 x 50 mL) and dried with magnesium sulfate. Afterwards purification is carried out via column chromatography (SiO_2, cyclohexane/ethyl acetate).

GP 3: Beaker-type cell (200 mL)

The reactions were performed in a 200 mL beaker-type glass cell, which consists of a simple glass beaker with a glass adapter and is closed by a Teflon plug, which allows a precise arrangement of the BDD electrodes. Dimensions of the BDD electrodes are 14 cm x 3.5 cm x 0.3 cm.

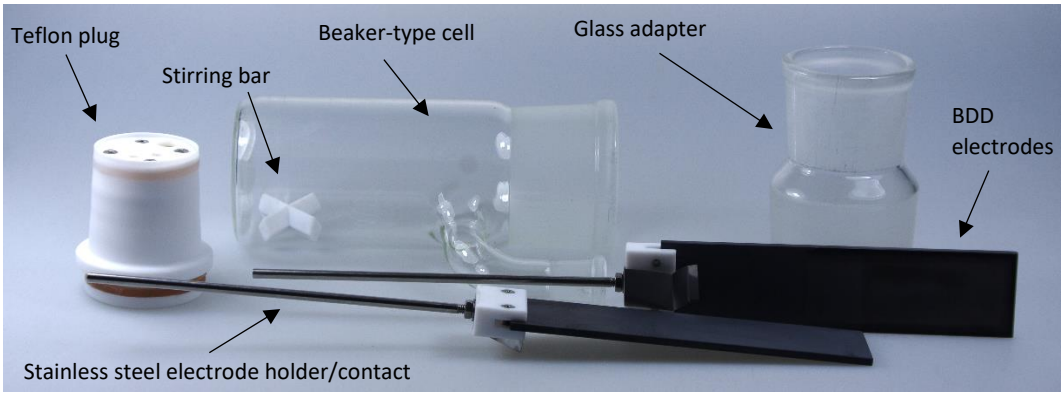

Figure 3: 200 mL beaker-type cell shown disassembled in individual parts.

The arene compound **A** (40 mmol) and the sulfinate **B** (52 mmol) are transferred into the undivided beaker-type electrolysis cell and are dissolved by 200 mL of a solvent mixture constituted of HFIP (170 mL) and deionized water (30 mL, 15 vol. %). The cell is equipped with BDD electrodes, which have a distance of 1.7 cm between each other. The electrodes are 7.1 cm^2 immersed. A constant current electrolysis with a current density of 26 mA/cm^2 has been performed at 27 °C.

After application of 11578 C (3.0 F per arene **A**) the HFIP is recovered by distillation *in vacuo* (50 °C, 200–90 mbar). The crude product is dissolved in a mixture of dichloromethane (100 mL) / deionized water (100 mL) and is then transferred into a separatory funnel. After phase separation the aqueous fraction is extracted with dichloromethane (2 x 50 mL). The combined organic fractions are washed with deionized water (2 x 50 mL) and dried with magnesium sulfate. Afterwards purification is carried out via column chromatography (SiO_2, cyclohexane/ethyl acetate).

3. General cyclic voltammetry protocol (GP 4)

A 10 mM solution of the substrate in a HFIP/H_2O mixture (5 mL, 15 vol.% H_2O) containing 0.1 M *N*,*N*,*N*,*N*-tetrabutylammonium hexafluorophosphate ($^nBu_4NPF_6$) was placed in a 10 mL snap-cap vial. Degassing of the solution was carried out by bubbling argon through for 5 minutes. Cyclic voltammetry was performed with a 0.1 V/s scan rate using a BDD working electrode (tip, 2 mm diameter), a glassy carbon rod as counter electrode and an Ag/AgCl reference electrode in saturated LiCl/EtOH. Ferrocene/Ferrocenium (FcH/FcH^+) was used as internal reference (half-wave potential 0.13 V versus Ag/AgCl).

4. Results of the electrochemical screening reactions

The electrochemical screening reactions were carried out via **GP 1**. Evaluation of the conversion was carried out on the basis of relative GC integrals (GC-int.).

4.1 Optimization of arene-sulfinate coupling

As model system, the reaction between 1,4-dimethoxybenzene **5** and sodium benzenesulfinate **6** was used, as shown in Scheme 1. The screening reactions were sorted by descending order of the GC integrals (Table 1).

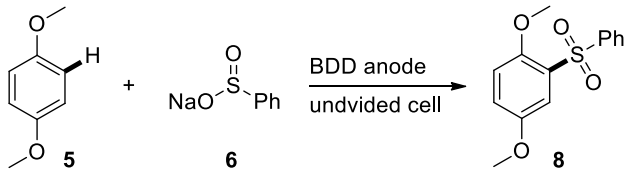

Scheme 1: Test reaction for parameter screening of the arene coupling.

Table 1: Parameter screening for the arene-sulfinate coupling reaction.

Entry	*j* [mA cm^{-2}]	*Q* [F ref. **5**]	H_2O in HFIP [vol.%]	Ratio **5**:**6**	GC-int. **8** [%]
1	26	2,5	15	1:1.3	74
2	24	2,5	15	1:1.3	73
3	28	2,5	15	1:1.3	73
4	18	2,5	10	1:1.3	73
5	22	2,5	15	1:1.3	72
6	18	2,5	15	1:1.5	70
7	20	2,5	15	1:1.3	69
8	18	5.0	15	1:2	68
9	18	2,5	15	1:1	68
10	18	3.0	15	1:1.3	67
11	15	2,5	15	1:1.3	66
12	26	3.0	15	1:1.3	66
13	18	2,5	30	1:1.3	65
14	12	2,5	15	1:1.3	64
15	18	2,5	0	1:1.3	51
16	6	2,5	15	1:1.3	48
17	18	2,5	15	1:2	48
18	9	2,5	15	1:1.3	47
19	2	2,5	15	1:1.3	43
20	18	2,5	15	1:3	42

j: current density. *Q*: charge quantity.

4.2 Optimization of anilide-sulfinate coupling

As model system, the reaction between 3,4-dimethoxyacetanilide **10** and sodium benzenesulfinate **6** was used, as shown in Scheme 2. The screening reactions were sorted by descending order of the GC integrals (Table 2).

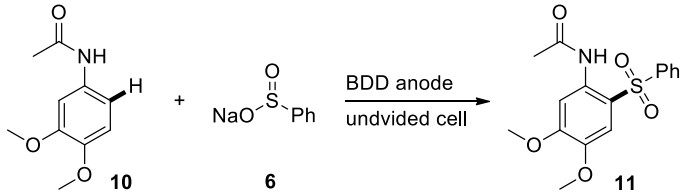

Scheme 2: Test reaction for parameter screening of the anilide coupling.

Table 2: Parameter screening for the anilide-sulfinate coupling reaction.

Entry	*j* [mA cm^{-2}]	*Q* [F ref. **5**]	H_2O in HFIP [vol.%]	Ratio **10**:**6**	GC-int. **11** [%]
1	6	2.5	15	1:1.5	67
2	6	2.5	15	1:1.3	63
3	6	2.5	15	1:2	60
4	12	3.5	15	1:1.5	55
5	9	2.5	15	1:1.5	52
6	12	2.5	15	1:1.5	52
7	12	3.0	15	1:1.5	50
8	12	2.5	15	1:1.5	49
9	15	2.5	15	1:1.5	49
10	12	2.0	15	1:1.5	49
11	12	4.0	15	1:1.5	49
12	26	3.5	15	1:1.5	49
13	26	2.5	15	1:1.5	46
14	18	2.5	15	1:1.5	45
15	21	2.5	15	1:1.5	44
16	12	3.5	25	1:1.5	43
17	12	3.5	5	1:1.5	39
18	3	2.5	15	1:1.5	36
19	24	2.5	15	1:1.5	25

j: current density. *Q*: charge quantity.

4.3 Screening of different substrate combinations

To extend the scope of the electrochemical sulfonylation reaction, different arenes and aniline derivatives were tested under the optimized conditions. Conversion data of starting material **A** and coupling product **AB** are given in Table 2 below.

Table 2: Substrate screening for the electrochemical sulfonylation reaction.[a]

Entry	**A**	**B**	**AB**	GC-int. **A** [%]	GC-int. **AB** [%]
1	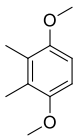	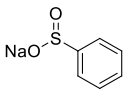	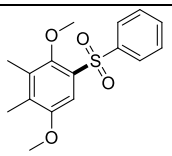	6	87
2	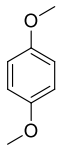	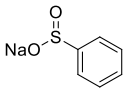	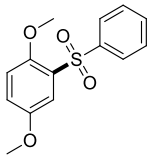	14	74
3	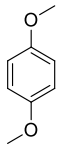		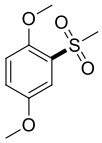	25	74
4	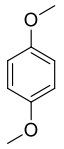	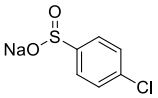	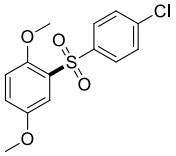	16	80
5	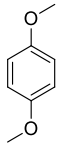	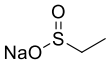	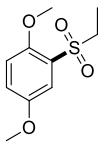	29	66
6	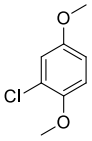	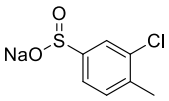	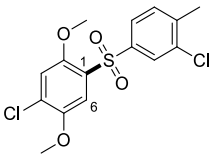	31	33 (C1) 16 (C6)
7	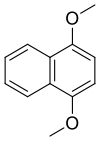	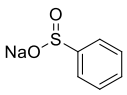	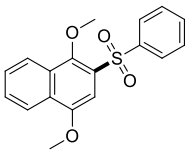	12	42
8	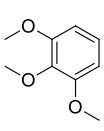	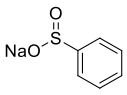	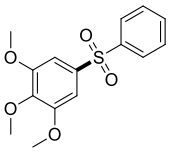	37	47
9	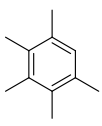	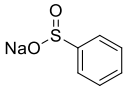	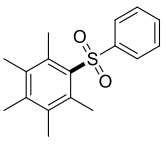	37	53

10	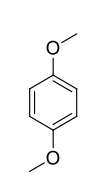	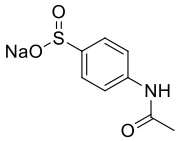	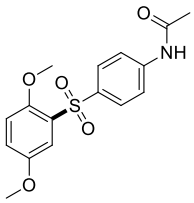	40	57
11	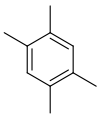	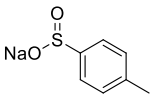	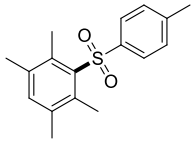	50	23
12[b]	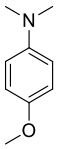	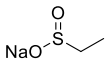	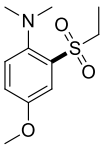	0	76
13[b]	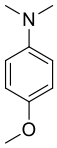	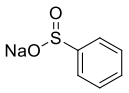	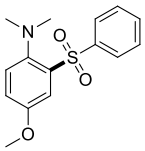	0	81
14[b]	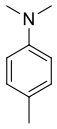	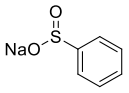	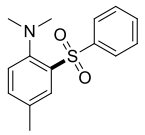	0	52
15[b]	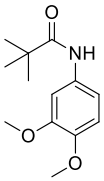	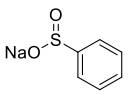	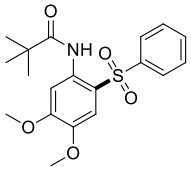	20	53
16[b]	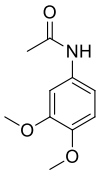	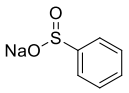	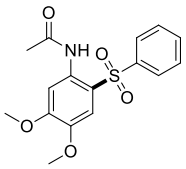	19	71
17[b]	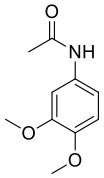		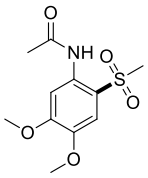	12	65

[a] BDD electrodes, r.t., 15 vol.% water in HFIP, **A**/**B** = 1:1.3, *Q* = 2.5 F (ref. **A**), *j* = 26 mA cm^{-2}.
[b] **A**/**B** = 1:1.5, *Q* = 3.5 F (ref. **A**), *j* = 12 mA cm^{-2}.

5. Cyclic voltammetry data

Based on the reported and postulated mechanism for anodic cross-coupling, a mechanism is proposed which has a comparable course and provides an rationale for the resulting substitution patterns of the cross-coupling products.[5] Here, the supporting cyclic voltammetric data are depicted.

The initial oxidation step is confirmed by cyclic voltammetry measurements. Figure 3 depicts that, for arenes and aniline derivatives, the oxidation potentials are generally below those of sodium sulfinates. This indicates that an initial oxidation of the arene or the protected aniline component can be assumed.

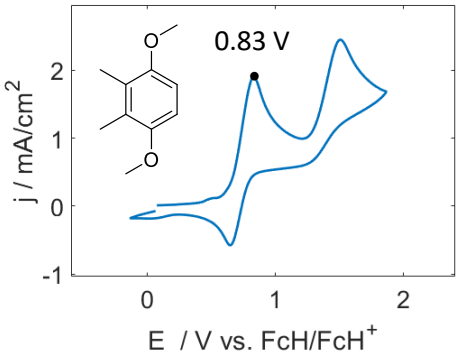

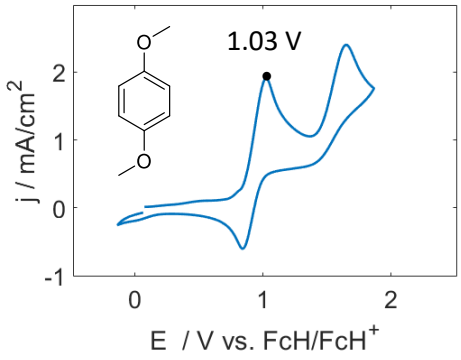

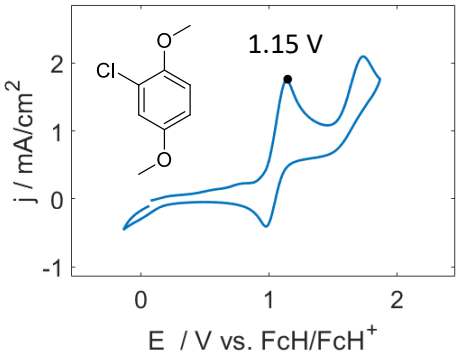

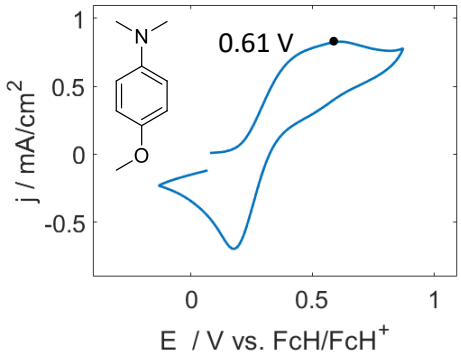

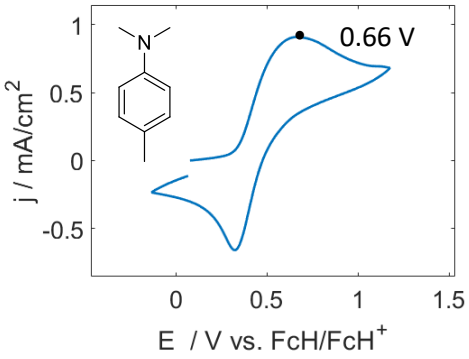

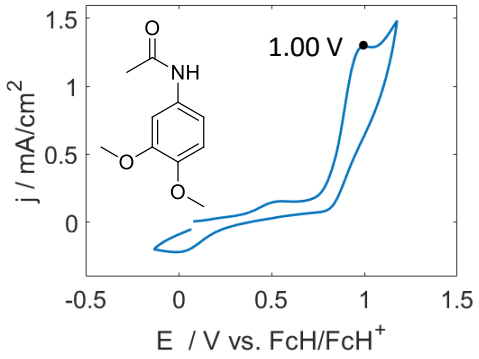

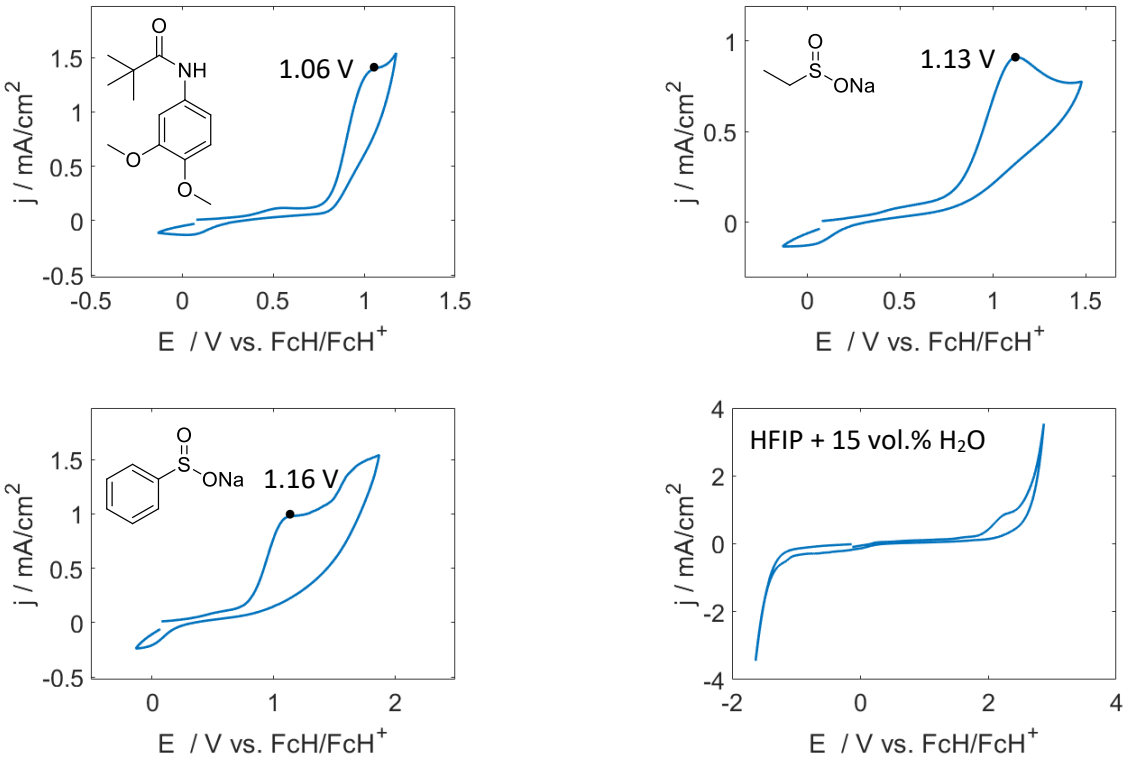

Figure 4: Cyclic voltammograms and oxidative peak potentials of some arenes, protected anilines and sodium sulfinates. The measurements were determined according to the general protocol **GP 4**.

6. Characterization of arene cross-coupling products

6.1 2,5-Dimethoxy-3,4-dimethyldiphenylsulfone (12)

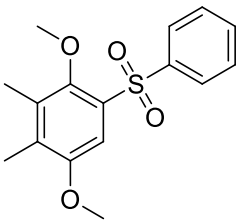

According to the general protocol (**GP 2**) 1,4-dimethoxy-2,3-dimethylbenzene (0.83 g, 5.00 mmol, 1.0 eq.) and sodium benzenesulfinate (1.07 g, 6.50 mmol, 1.3 eq.) are dissolved in HFIP + 15 vol.% water (25 mL). After constant current electrolysis and workup, the residue is purified by column chromatography (cyclohexane/ethyl acetate = 10:0 → 6:4) to yield the product as a colorless solid (yield: 69%, 1.06 g, 3.46 mmol).

m_R: 168–170 °C; R_f (cyclohexane/ethyl acetate = 9:1): 0.36; ^{1}H NMR (400 MHz, $CDCl_3$) δ [ppm] = 7.97–7.94 (m, 2H), 7.57–7.53 (m, 1H), 7.50–7.45 (m, 3H), 3.90 (s, 3H), 3.77 (s, 3H), 2.16 (s, 3H), 2.13 (s, 3H); ^{13}C NMR (101 MHz, $CDCl_3$) δ [ppm] = 153.6, 150.3, 142.4, 134.2, 133.4, 133.0, 131.6, 128.8, 127.9, 107.8, 62.4, 56.2, 13.1, 12.9; HRMS for $C_{16}H_{18}O_4SNa$ (ESI+) $[M+Na]^+$: calc.: 329.0818, found: 329.0823; Elemental anal. for $C_{16}H_{18}O_4S$: calc.: C: 62.73%, H: 5.92%, found: C: 62.59%, H: 5.56%.

6.2 2,5-Dimethoxydiphenylsulfone (8)

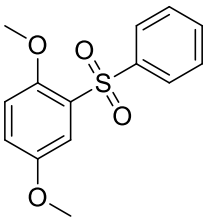

25 mL undivided beaker-type cell

According to the general protocol (**GP 2**) 1,4-dimethoxybenzene (0.69 g, 5.00 mmol, 1.0 eq.) and sodium benzenesulfinate (1.07 g, 6.50 mmol, 1.3 eq.) are dissolved in HFIP + 15 vol.% water (25 mL). After constant current electrolysis and workup, the residue is purified by column chromatography (cyclohexane/ethyl acetate = 10:0 → 0:10) to yield the product as an off-white solid (yield: 67%, 0.93 g, 3.33 mmol).

Scale-up in 200 mL undivided beaker-type cell

According to the general protocol (**GP 3**) 1,4-dimethoxybenzene (5.53 g, 40 mmol, 1.0 eq.) and benzenesulfinic acid sodium salt (8.54 g, 52 mmol, 1.3 eq.) are solved in HFIP + 15 vol.% water (200 mL). After constant current electrolysis and workup, the crude product is purified by column chromatography (cyclohexane/ethyl acetate = 0:10) to yield the product as a beige-colored solid (yield: 55%, 6.10 g, 21.92 mmol).

m_R: 117–119 °C; R_f (cyclohexane/ethyl acetate = 7:3): 0.36; ^{1}H NMR (400 MHz, $CDCl_3$) δ [ppm] = 7.98–7.95 (m, 2H), 7.69 (d, *J* = 3.2 Hz, 1H), 7.59–7.54 (m, 1H), 7.50–7.46 (m, 2H), 7.07 (dd, *J* = 9.0 Hz, *J* = 3.2 Hz, 1H), 6.84 (d, *J* = 9.0 Hz, 1H), 3.84 (s, 3H), 3.68 (s, 3H); ^{13}C NMR (101 MHz, $CDCl_3$) δ [ppm] = 153.4, 151.3, 141.5, 133.1, 129.6, 128.6, 128.5, 121.9, 114.4, 113.9, 56.6, 56.2; HRMS for $C_{14}H_{15}O_4S$ (ESI+) $[M+H]^+$: calc.: 279.0686, found: 279.0689.

All analytical data match to the reported data.[6]

6.3 2,5-Dimethoxyphenyl-methylsulfone (9)

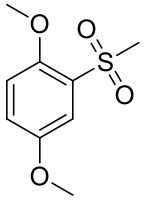

According to the general protocol (**GP 2**) 1,4-dimethoxybenzene (0.69 g, 5.00 mmol, 1.0 eq.) and sodium methanesulfinate (0.66 g, 6.50 mmol, 1.3 eq.) are dissolved in HFIP + 15 vol.% water (25 mL). After constant current electrolysis and workup, the crude product is purified by column chromatography (cyclohexane/ethyl acetate = 8:2 → 4:6) to yield the product as a colorless solid (yield: 60%, 0.65 g, 2.99 mmol).

m_R: 73–76 °C; R_f (cyclohexane/ethyl acetate = 7:3): 0.19; ^{1}H NMR (400 MHz, $CDCl_3$) δ [ppm] = 7.50 (d, *J* = 3.2 Hz, 1H), 7.12 (dd, *J* = 9.0 Hz, *J* = 3.2 Hz, 1H), 6.99 (d, *J* = 9.0 Hz, 1H), 3.94 (s, 3H), 3.81 (s, 3H), 3.22 (s, 3H); ^{13}C NMR (101 MHz, $CDCl_3$) δ [ppm] = 153.5, 151.3, 128.9, 121.9, 114.2, 113.6, 57.0, 56.2, 43.0; HRMS for $C_9H_{16}O_4SN$ (ESI+) $[M+NH_4]^+$: calc.: 234.0795, found: 234.0797.

All analytical data match to the reported data.[7]

6.4 4‘-Chloro-2,5-dimethoxydiphenylsulfone (13)

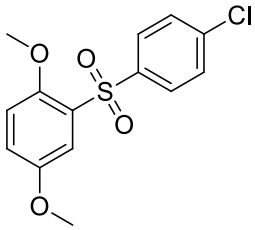

According to the general protocol (**GP 2**) 1,4-dimethoxybenzene (0.69 g, 5.00 mmol, 1.0 eq.) and sodium 4-chlorobenzenesulfinate (1.29 g, 6.50 mmol, 1.3 eq.) are dissolved in HFIP + 15 vol.% water (25 mL). After constant current electrolysis and workup, the residue is purified by column chromatography (cyclohexane/ethyl acetate = 0:10) to yield the product as an off-white solid (yield: 59%, 0.92 g, 2.94 mmol).

m_R: 109–111 °C; R_f (cyclohexane/ethyl acetate = 7:3): 0.41; ^{1}H NMR (400 MHz, $CDCl_3$) δ [ppm] = 7.92–7.89 (m, 2H), 7.67 (d, *J* = 3.2 Hz, 1H), 7.47–7.44 (m, 2H), 7.09 (dd, *J* = 9.0 Hz, *J* = 3.2 Hz, 1H), 6.85 (d, *J* = 9.0 Hz, 1H), 3.84 (s, 3H), 3.72 (s, 3H); ^{13}C NMR (101 MHz, $CDCl_3$) δ [ppm] = 153.5, 151.2, 140.0, 139.7, 130.1, 129.1, 128.9, 122.1, 114.3, 113.8, 56.6, 56.3; HRMS for $C_{14}H_{17}{}^{35}ClO_4SN$ (ESI+) $[M+NH_4]^+$: calc.: 330.0561, found: 330.0564.

All analytical data match to the reported data.[7]

6.5 2,5-Dimethoxyphenyl-ethylsulfone (14)

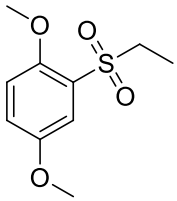

According to the general protocol (**GP 2**) 1,4-dimethoxybenzene (0.69 g, 5.00 mmol, 1.0 eq.) and sodium ethanesulfinate (0.76 g, 6.50 mmol, 1.3 eq.) are dissolved in HFIP + 15 vol.% water (25 mL). After constant current electrolysis and workup, the crude product is purified by column chromatography (cyclohexane/ethyl acetate = 9:1 → 6:4) to yield the product as a colorless solid (yield: 54%, 0.62 g, 2.69 mmol).

m_R: 70–72 °C; R_f (cyclohexane/ethyl acetate = 7:3): 0.26; ^{1}H NMR (300 MHz, $CDCl_3$) δ [ppm] = 7.48 (d, *J* = 3.2 Hz, 1H), 7.12 (dd, *J* = 9.0 Hz, *J* = 3.2 Hz, 1H), 6.98 (d, *J* = 9.0 Hz, 1H), 3.92 (s, 3H), 3.81 (s, 3H), 3.38 (q, *J* = 7.5 Hz, 2H), 1.24 (t, *J* = 7.5 Hz, 3H); ^{13}C NMR (101 MHz, $CDCl_3$) δ [ppm] = 153.5, 151.5, 126.9, 121.8, 114.7, 114.1, 57.0, 56.2, 48.8, 7.3; HRMS for $C_{10}H_{15}O_4S$ (ESI+) $[M+H]^+$: calc.: 231.0686, found: 231.0691.

6.6 2,5-Dimethoxy-3‘-trifluoromethyldiphenylsulfone (15)

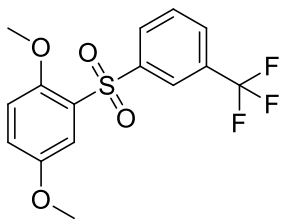

According to the general protocol (**GP 2**) 1,4-dimethoxybenzene (0.28 g, 2.00 mmol, 1.0 eq.) and sodium 3-(trifluoromethyl)benzenesulfinate (0.61 g, 2.60 mmol, 1.3 eq.) are dissolved in HFIP + 15 vol.% water (25 mL). After constant current electrolysis by applying 482 C (2.5 F) and workup, the residue is purified by column chromatography (cyclohexane/ethyl acetate = 8:2 → 7:3) to yield the product as a colorless solid (yield: 42%, 0.29 g, 0.83 mmol).

m_R: 106–108 °C; R_f (cyclohexane/ethyl acetate = 7:3): 0.39; ^{1}H NMR (400 MHz, $CDCl_3$) δ [ppm] = 8.32 (s, 1H), 8.14 (d, *J* = 8.0 Hz, 1H), 7.83 (d, *J* = 8.0 Hz, 1H), 7.68 (d, *J* = 3.2 Hz, 1H), 7.63 (t, *J* = 7.8 Hz, 1H), 7.11 (dd, *J* = 9.0 Hz, *J* = 3.2 Hz, 1H), 6.86 (d, *J* = 9.0 Hz, 1H), 3.85 (s, 3H), 3.72 (s, 3H); ^{13}C NMR (101 MHz, $CDCl_3$) δ [ppm] = 153.5, 151.2, 142.5, 131.8, 131.3 (d, *J* = 33.4 Hz), 129.8–129.7 (m), 129.4, 128.6, 126.2–126.1 (m), 123.4 (d, *J* = 272.7 Hz), 122.4, 114.2, 113.8, 56.4, 56.3; ^{19}F NMR (282 MHz, $CDCl_3$) δ [ppm] = −63.90; HRMS for $C_{15}H_{14}F_3O_4S$ (APCI+) $[M+H]^+$: calc.: 347.0560, found: 347.0564; Elemental anal. for $C_{15}H_{13}F_3O_4S$: calc.: C: 52.02%, H: 3.78%, found: C: 51.45%, H: 3.79%.

6.7 3‘,4-Dichloro-2,5-dimethoxy-4‘-methyldiphenylsulfone (16a)

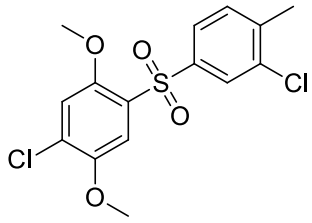

According to the general protocol (**GP 2**) 2-chloro-1,4-dimethoxybenzene (0.86 g, 5.00 mmol, 1.0 eq.) and sodium 3-chloro-4-methylbenzenesulfinate (1.38 g, 6.50 mmol, 1.3 eq.) are dissolved in HFIP + 15 vol.% water (25 mL). After constant current electrolysis and workup, the residue is purified by column chromatography (cyclohexane/ethyl acetate = 10:0 → 9:1) to yield the product as an off-white solid (yield: 22%, 0.40 g, 1.11 mmol).

m_R: 152–153 °C; R_f (cyclohexane/ethyl acetate =9:1): 0.19; ^{1}H NMR (400 MHz, $CDCl_3$) δ [ppm] = 7.93 (d, *J* = 1.9 Hz, 1H), 7.73 (dd, *J* = 8.0 Hz, *J* = 1.9 Hz, 1H), 7.69 (s, 1H), 7.35 (d, *J* = 8.0 Hz, 1H), 6.97 (s, 1H), 3.96 (s, 3H), 3.74 (s, 3H), 2.43 (s, 3H); ^{13}C NMR (101 MHz, $CDCl_3$) δ [ppm] = 151.0, 149.2, 142.3, 140.0, 134.8, 131.1, 129.9, 129.2, 127.6, 126.6, 115.6, 112.8, 57.1, 56.9, 20.5; HRMS for $C_{15}H_{14}{}^{35}Cl_2O_4SNa$ (ESI+) $[M+Na]^+$: calc.: 382.9882, found: 382.9886; Elemental anal. for $C_{15}H_{14}Cl_2O_4S$: calc.: C: 49.88%, H: 3.91%, found: C: 49.86%, H: 3.90%.

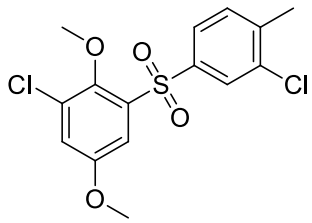

As side product the isomeric 3‘,3-dichloro-2,5-dimethoxy-4‘-methyldiphenylsulfone (**16b**) was obtained applying the same protocol to yield an off-white solid (yield: 13%, 0.23 g, 0.63 mmol).

m_R: 129–131 °C; R_f (cyclohexane/ethyl acetate = 9:1): 0.35; ^{1}H NMR (400 MHz, $CDCl_3$) δ [ppm] = 7.90 (d, *J* = 1.9 Hz, 1H), 7.74 (dd, *J* = 8.0 Hz, *J* = 1.9 Hz, 1H), 7.54 (d, *J* = 3.1 Hz, 1H), 7.35 (d, *J* = 8.0 Hz, 1H), 7.14 (d, *J* = 3.1 Hz, 1H), 3.95 (s, 3H), 3.85 (s, 3H), 2.42 (s, 3H); ^{13}C NMR (101 MHz, $CDCl_3$) δ [ppm] = 155.7, 147.8, 142.6, 140.0, 136.6, 135.0, 131.4, 130.4, 128.8, 126.4, 122.3, 112.7, 62.5, 56.4, 20.6; HRMS for $C_{15}H_{14}{}^{35}Cl_2O_4SNa$ (ESI+) $[M+Na]^+$: calc.: 382.9882, found: 382.9885.

6.8 1,4-Dimethoxynaphth-2-yl-phenylsulfone (17)

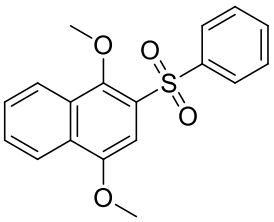

According to the general protocol (**GP 2**) 1,4-dimethoxynaphthalene (0.94 g, 5.00 mmol, 1.0 eq.) and sodium benzenesulfinate (1.07 g, 6.50 mmol, 1.3 eq.) are dissolved in HFIP + 15 vol.% water (25 mL). After constant current electrolysis and workup, the residue is purified by column chromatography (cyclohexane/ethyl acetate = 10:0 → 9:1) to yield the product as a brown-colored solid (yield: 32%, 0.53 g, 1.61 mmol).

m_R: 134–136 °C; R_f (cyclohexane/ethyl acetate = 9:1): 0.28; ^{1}H NMR (400 MHz, $CDCl_3$) δ [ppm] = 8.30–8.27 (m, 1H), 8.05–8.01 (m, 3H), 7.62–7.54 (m, 3H), 7.51–7.47 (m, 2H), 7.44 (s, 1H), 4.09 (s, 3H), 4.08 (s, 3H); ^{13}C NMR (101 MHz, $CDCl_3$) δ [ppm] = 152.2, 149.9, 142.4, 133.2, 130.0, 129.6, 128.8, 128.5, 127.9, 127.6, 123.3, 123.0, 101.2, 64.5, 56.3; HRMS for $C_{18}H_{17}O_4S$ (ESI+) $[M+H]^+$: calc.: 329.0842, found: 329.0845.

6.9 3,4,5-Trimethoxydiphenylsulfone (18)

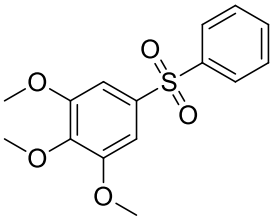

According to the general protocol (**GP 2**) 1,2,3-trimethoxybenzene (0.84 g, 5.00 mmol, 1.0 eq.) and sodium benzenesulfinate (1.07 g, 6.50 mmol, 1.3 eq.) are dissolved in HFIP + 15 vol.% water (25 mL). After constant current electrolysis and workup, the residue is purified by column chromatography (cyclohexane/ethyl acetate = 8:2 → 7:3) to yield the product as a colorless solid (yield: 27%, 0.42 g, 1.35 mmol).

m_R: 154–155 °C; R_f (cyclohexane/ethyl acetate = 7:3): 0.38; ^{1}H NMR (400 MHz, $CDCl_3$) δ [ppm] = 7.95–7.92 (m, 2H), 7.59–7.55 (m, 1H), 7.53–7.49 (m, 2H), 7.16 (s, 2H), 3.89 (s, 6H), 3.86 (s, 3H); ^{13}C NMR (101 MHz, $CDCl_3$) δ [ppm] = 153.6, 142.2, 141.9, 136.1, 133.2, 129.4, 127.5, 105.1, 61.1, 56.6; HRMS for $C_{15}H_{16}O_5SNa$ (ESI+) $[M+Na]^+$: calc.: 331.0610, found: 331.0612.

6.10 2,3,4,5,6-Pentamethyldiphenylsulfone (19)

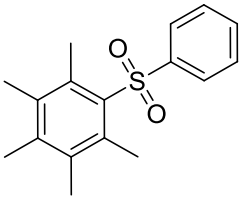

According to the general protocol (**GP 2**) pentamethylbenzene (0.74 g, 5.00 mmol, 1.0 eq.) and sodium benzenesulfinate (1.07 g, 6.50 mmol, 1.3 eq.) are dissolved in HFIP + 15 vol.% water (25 mL). After constant current electrolysis and workup, the residue is purified by column chromatography (cyclohexane/ethyl acetate = 100:0 → 95:5) to yield the product as a colorless solid (yield: 27%, 0.39 g, 1.34 mmol).

m_R: 159–161 °C; R_f (cyclohexane/ethyl acetate = 9:1): 0.40; ^{1}H NMR (400 MHz, $CDCl_3$) δ [ppm] = 7.79–7.76 (m, 2H), 7.55–7.51 (m, 1H), 7.49–7.44 (m, 2H), 2.50 (s, 6H), 2.29 (s, 3H), 2.22 (s, 6H); ^{13}C NMR (101 MHz, $CDCl_3$) δ [ppm] = 144.9, 140.9, 135.7, 135.5, 135.2, 132.3, 129.1, 125.8, 19.1, 18.0, 17.0; HRMS for $C_{17}H_{21}O_2S$ (ESI+) $[M+H]^+$: calc.: 289.1257, found: 289.1259; Elemental anal. for $C_{17}H_{20}O_2S$: calc.: C: 70.80%, H: 6.99%, found: C: 70.80%, H: 6.88%.

6.11 4‘-Acetamido-2,5-dimethoxydiphenylsulfone (20)

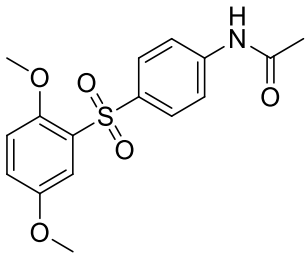

According to the general protocol (**GP 2**) 1,4-dimethoxybenzene (0.28 g, 2.00 mmol, 1.0 eq.) and sodium 4-acetamidobenzenesulfinate (1.44 g, 6.50 mmol, 1.3 eq.) are dissolved in HFIP + 15 vol.% water (25 mL). After constant current electrolysis and workup, the residue is purified by column chromatography (cyclohexane/ethyl acetate = 8:2 → 0:10) to yield the product as an off-white solid (yield: 25%, 0.42 g, 1.25 mmol).

m_R: 186–187 °C; R_f (cyclohexane/ethyl acetate = 1:1): 0.10; ^{1}H NMR (400 MHz, DMSO-d_6) δ [ppm] = 10.37 (s, 1H), 7.83 (d, *J* = 8.9 Hz, 2H), 7.76 (d, *J* = 8.9 Hz, 2H), 7.47 (d, *J* = 3.1 Hz, 1H), 7.23 (dd, *J* = 9.0 Hz, *J* = 3.1 Hz, 1H), 7.10 (d, *J* = 9.0 Hz, 1H), 3.79 (s, 3H), 3.66 (s, 3H), 2.07 (s, 3H); ^{13}C NMR (101 MHz, DMSO-d_6) δ [ppm] = 169.1, 152.6, 150.6, 143.7, 134.1, 129.4, 129.3, 121.1, 118.2, 115.0, 113.2, 56.4, 55.9, 24.2; HRMS for $C_{16}H_{18}NO_5S$ (ESI+) $[M+H]^+$: calc.: 336.0900, found: 336.0906.

6.12 2,3,4‘,5,6-Pentamethyldiphenylsulfone (21)

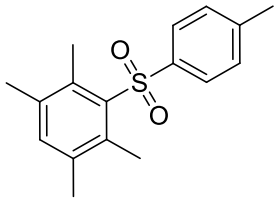

According to the general protocol (**GP 2**) 1,2,4,5-tetramethylbenzene (0.67 g, 5.00 mmol, 1.0 eq.) and sodium 4-methylbenzenesulfinate (1.16 g, 6.50 mmol, 1.3 eq.) are dissolved in HFIP + 15 vol.% water (25 mL). After constant current electrolysis and workup, the residue is purified by column chromatography (cyclohexane/ethyl acetate = 10:0 → 9:1) to yield the product as an off-white solid (yield: 22%, 0.31 g, 1.08 mmol).

m_R: 94–96 °C; R_f (cyclohexane/ethyl acetate = 9:1): 0.39; ^{1}H NMR (400 MHz, $CDCl_3$) δ [ppm] = 7.67–7.64 (m, 2H), 7.27–7.25 (m, 2H), 7.18 (s, 1H), 2.48 (s, 6H), 2.40 (s, 3H), 2.24 (s, 6H); ^{13}C NMR (101 MHz, $CDCl_3$) δ [ppm] = 143.3, 141.6, 137.9, 136.6, 136.3, 136.2, 129.6, 126.0, 21.7, 21.0, 18.0; HRMS for $C_{17}H_{21}O_2S$ (ESI+) $[M+H]^+$: calc.: 289.1257, found: 289.1257.

7. Characterization of aniline cross-coupling products

7.1 2-(*N*,*N*-Dimethylamino)-5-methoxyphenyl-ethylsulfone (22)

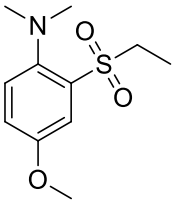

According to the general protocol (**GP 2**) *N*,*N*-dimethyl-4-methoxyaniline (0.76 g, 5.00 mmol, 1.0 eq.) and sodium ethanesulfinate (0.87 g, 7.50 mmol, 1.5 eq.) are dissolved in HFIP + 15 vol.% water (25 mL). After constant current electrolysis and workup, the residue is purified by column chromatography (cyclohexane/ethyl acetate = 8:2) to yield the product as a colorless viscous liquid (yield: 53%, 0.65 g, 2.65 mmol).

R_f (cyclohexane/ethyl acetate = 7:3): 0.50; ^{1}H NMR (400 MHz, $CDCl_3$) δ [ppm] = 7.50 (d, *J* = 3.1 Hz, 1H), 7.34 (d, *J* = 8.8 Hz, 1H), 7.09 (dd, *J* = 8.8 Hz, *J* = 3.1 Hz, 1H), 3.80 (s, 3H), 3.54 (q, *J* = 7.5 Hz, 2H), 2.67 (s, 6H), 1.17 (t, *J* = 7.5 Hz, 3H); ^{13}C NMR (101 MHz, $CDCl_3$) δ [ppm] = 156.8, 146.8, 135.6, 124.8, 121.0, 114.1, 55.9, 48.4, 46.4, 7.4; HRMS for $C_{11}H_{17}NO_3SNa$ (ESI+) $[M+Na]^+$: calc.: 266.0821, found: 266.0824.

7.2 2-(*N*,*N*-Dimethylamino)-5-methoxydiphenylsulfone (23)

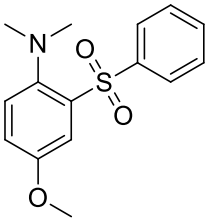

According to the general protocol (**GP 2**) *N*,*N*-dimethyl-4-methoxyaniline (0.76 g, 5.00 mmol, 1.0 eq.) and sodium benzenesulfinate (1.23 g, 7.50 mmol, 1.5 eq.) are dissolved in HFIP + 15 vol.% water (25 mL). After constant current electrolysis and workup, the residue is purified by column chromatography (cyclohexane/ethyl acetate = 9:1 → 8:2) to yield the product as a colorless solid (yield: 41%, 0.59 g, 2.02 mmol).

m_R: 146–147 °C; R_f (cyclohexane/ethyl acetate = 7:3): 0.63; ^{1}H NMR (400 MHz, $CDCl_3$) δ [ppm] = 7.91–7.88 (m, 2H), 7.76 (d, *J* = 3.0 Hz, 1H), 7.54–7.49 (m, 1H), 7.46–7.42 (m, 2H), 7.20 (d, *J* = 8.8 Hz, 1H), 7.09 (dd, *J* = 8.8 Hz, *J* = 3.0 Hz, 1H), 3.88 (s, 3H), 2.29 (s, 6H); ^{13}C NMR (101 MHz, $CDCl_3$) δ [ppm] = 157.0, 146.5, 142.4, 139.3, 132.5, 128.3, 128.1, 126.0, 121.6, 113.1, 56.1, 45.4; HRMS for $C_{15}H_{18}NO_3S$ (ESI+) $[M+H]^+$: calc.: 292.1002, found: 292.1004.

All analytical data match to the reported data.[8]

7.3 2-(*N*,*N*-Dimethylamino)-5-methyldiphenylsulfone (24)

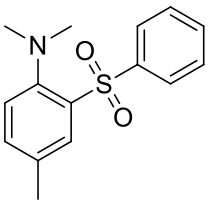

According to the general protocol (**GP 2**) *N*,*N*,4-trimethylaniline (0.68 g, 5.00 mmol, 1.0 eq.) and sodium benzenesulfinate (1.23 g, 7.50 mmol, 1.5 eq.) are dissolved in HFIP + 15 vol.% water (25 mL). After constant current electrolysis and workup, the residue is purified by column chromatography (cyclohexane/ethyl acetate = 10:0 → 7:3) to yield the product as an off-white solid (yield: 34%, 0.47 g, 1.72 mmol).

m_R: 95–98 °C; R_f (cyclohexane/ethyl acetate = 9:1): 0.40; ^{1}H NMR (400 MHz, $CDCl_3$) δ [ppm] = 8.06 (d, *J* = 1.6 Hz, 1H), 7.90–7.87 (m, 2H), 7.53–7.49 (m, 1H), 7.45–7.41 (m, 2H), 7.36 (dd, *J* = 8.1 Hz, *J* = 1.6 Hz, 1H), 7.16 (d, *J* = 8.1 Hz, 1H), 2.41 (s, 3H), 2.34 (s, 6H); ^{13}C NMR (101 MHz, $CDCl_3$) δ [ppm] = 151.3, 142.6, 137.8, 135.6, 135.5, 132.4, 129.9, 128.2, 128.1, 124.5, 45.4, 21.1; HRMS for $C_{15}H_{18}NO_2S$ (ESI+) $[M+H]^+$: calc.: 276.1053, found: 276.1050.

All analytical data match to the reported data.[9]

Crystallization was performed by dissolving **24** (50 mg) in dichloromethane (ca. 0.8 mL) and slow diffusion of over layered *n*-pentane (ca. 4 mL) into the solution at 23 °C.

Crystal structure determination of **24**: $C_{15}H_{17}NO_2S$, M_r = 275.35; colorless block (0.31 x 0.45 x 0.95 mm³), T = 120 K, λ (Mo-$K\alpha$) = 0.71073 Å, monoclinic space group $P\,2_1/n$, a = 6.0714(4) Å, b = 15.6163(8) Å, β = 93.504(6)°, c = 14.7969(11) Å, V = 1400.31(16) Å^3, Z = 4, ρ_{calcd} = 1.306 g/cm^3, $2\theta_{max}$ = 56°, μ = 0.228 mm^{-1}, F(000) = 584, 7185 reflections, 3313 unique reflections (R_{int} = 0.0201), $w = 1/[\sigma^2(F_0^2)+(0.0548*P)^2+0.52*P]$ while $P = (Max(F_0^2,0)+2*F_c^2)/3$, R_1 = 0.0348 [$I > 2\sigma(I)$], R_1 = 0.038 [all data], wR_2 = 0.0961, CCDC-1945340.

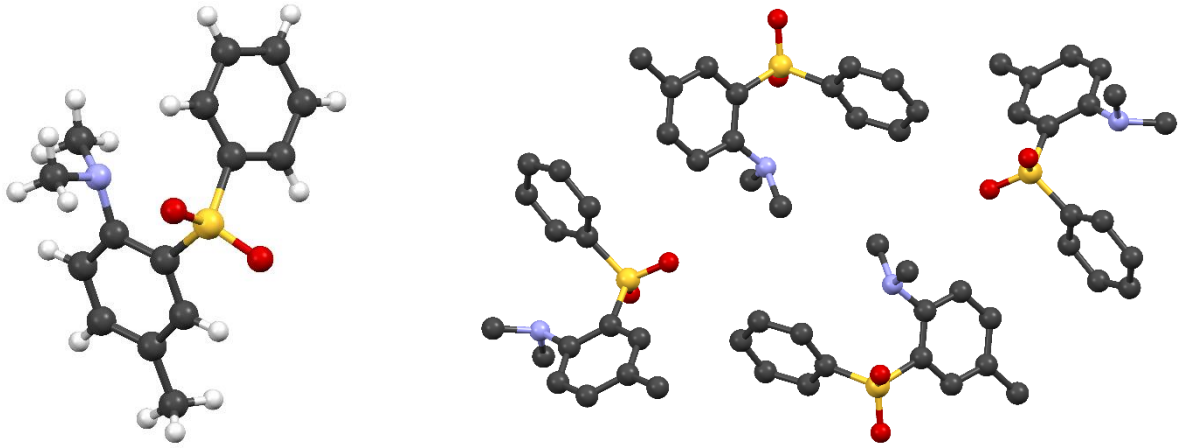

Figure 2: Molecular structure (left) and packing (right) of **24**. Hydrogen atoms are omitted for clarity.

7.4 4,5-Dimethoxy-2-pivaloylamidodiphenylsulfone (25)

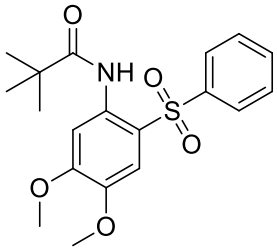

According to the general protocol (**GP 2**) 3,4-dimethoxypivaloylanilide (1.19 g, 5.00 mmol, 1.0 eq.) and sodium benzenesulfinate (1.23 g, 7.50 mmol, 1.5 eq.) are dissolved in HFIP + 15 vol.% water (25 mL). After constant current electrolysis and workup, the residue is purified by column chromatography (cyclohexane/ethyl acetate = 8:2 → 7:3) to yield the product as a colorless viscous liquid (yield: 32%, 0.60 g, 1.60 mmol).

R_f (cyclohexane/ethyl acetate = 7:3): 0.40; ^{1}H NMR (400 MHz, $CDCl_3$) δ [ppm] = 9.88 (s, 1H), 8.26 (s, 1H), 7.79–7.77 (m, 2H), 7.57–7.53 (m, 1H), 7.49–7.45 (m, 2H), 7.41 (s, 1H), 3.93 (s, 3H), 3.90 (s, 3H), 1.29 (s, 9H); ^{13}C NMR (101 MHz, $CDCl_3$) δ [ppm] = 177.5, 154.2, 145.0, 142.1, 133.4, 133.4, 129.4, 126.3, 117.1, 111.5, 105.4, 56.5, 56.5, 40.3, 27.5; HRMS for $C_{19}H_{24}NO_5S$ (ESI+) $[M+H]^+$: calc.: 378.1370, found: 378.1367.

7.5 2-Acetamido-4,5-dimethoxydiphenylsulfone (11)

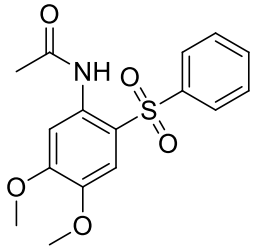

According to the general protocol (**GP 2**) 3,4-dimethoxyacetanilide (0.98 g, 5.00 mmol, 1.0 eq.) and sodium benzenesulfinate (1.23 g, 7.50 mmol, 1.5 eq.) are dissolved in HFIP + 15 vol.% water (25 mL). After constant current electrolysis and workup, the residue is purified by column chromatography (cyclohexane/ethyl acetate = 70:30 → 35:65) to yield the product as a brown-colored solid (yield: 30%, 0.50 g, 1.49 mmol).

m_R: 143–149 °C; R_f (cyclohexane/ethyl acetate = 1:1): 0.34; ^{1}H NMR (400 MHz, $CDCl_3$) δ [ppm] = 9.46 (s, 1H), 8.02 (s, 1H), 7.83–7.80 (m, 2H), 7.60–7.55 (m, 1H), 7.52–7.48 (m, 2H), 7.42 (s, 1H), 3.91 (s, 6H), 2.19 (s, 3H); ^{13}C NMR (101 MHz, $CDCl_3$) δ [ppm] = 168.4, 154.1, 145.3, 141.7, 133.6, 132.5, 129.5, 126.6, 118.3, 111.0, 106.0, 56.6, 56.5, 25.2; HRMS for $C_{16}H_{17}NO_5SNa$ (ESI+) $[M+Na]^+$: calc.: 358.0720, found: 358.0719.

Crystallization was performed by dissolving **11** (50 mg) in dichloromethane (ca. 0.8 mL) and slow diffusion of over layered *n*-pentane (ca. 4 mL) into the solution at 23 °C.

Crystal structure determination of **11**: $C_{16}H_{17}NO_5S$, M_r = 350.36; colorless needles (0.08 x 0.15 x 0.50 mm³), T = 213 K, λ (Mo-$K\alpha$) = 0.71073 Å, triclinic space group P -1, a = 7.5763(9) Å, α = 92.016(9)°, b = 9.9578(11) Å, β = 97.642(9)°, c = 10.7248(11) Å, γ = 100.635(9)°, V = 786.68(15) Å^3, Z = 2, ρ_{calcd} = 1.416 g/cm^3, $2\theta_{max}$ = 56°, μ = 0.23 mm^{-1}, F(000) = 352, 7005 reflections, 3854 unique reflections (R_{int} = 0.0235), $w = 1/[\sigma^2(F_0^2)+(0.0437*P)^2+0.56*P]$ while $P = (Max(F_0^2,0)+2*F_c^2)/3$, R_1 = 0.0426 [$I > 2\sigma(I)$], R_1 = 0.0562 [all data], wR_2 = 0.1139, CCDC-1945339.

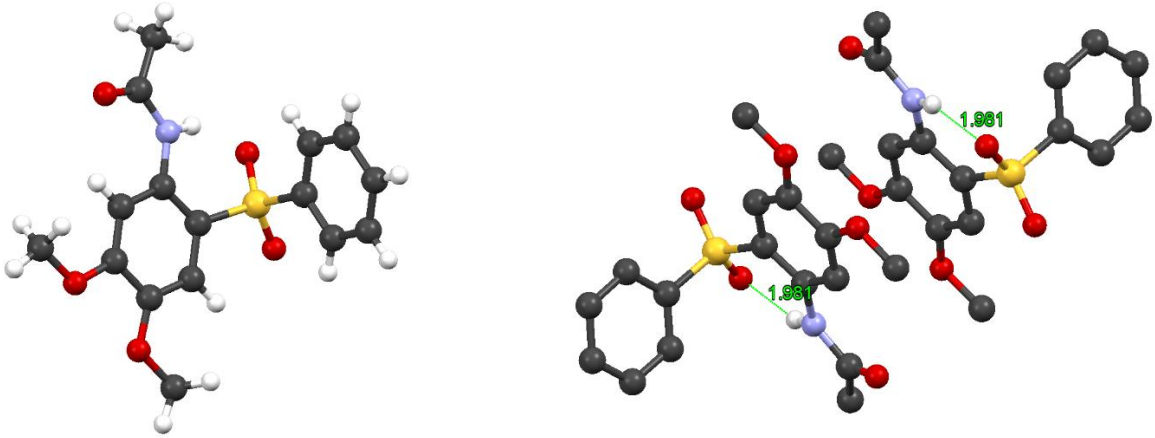

Figure 3: Molecular structure (left) and packing (right) of **11**. Hydrogen atoms are omitted for clarity. Intramolecular hydrogen bonding is indicated in green with lenghs of 1.981 Å.

7.6 2-Acetamido-4,5-dimethoxyphenyl-methylsulfone (26)

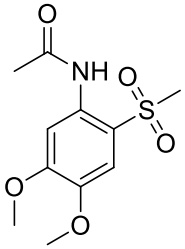

According to the general protocol (**GP 2**) 3,4-dimethoxyacetanilide (0.49 g, 2.50 mmol, 1.0 eq.) and sodium methanesulfinate (0.38 g, 3.75 mmol, 1.5 eq.) are dissolved in HFIP + 15 vol.% water (25 mL). After constant current electrolysis and workup, the residue is purified by column chromatography (cyclohexane/ethyl acetate = 8:2 → 7:3) to yield the product as a colorless solid (yield: 11%, 0.15 g, 0.55 mmol).

m_R: 182–183 °C; R_f (cyclohexane/ethyl acetate = 1:1): 0.18; ^{1}H NMR (400 MHz, $CDCl_3$) δ [ppm] = 9.36 (s, 1H), 8.06 (s, 1H), 7.26 (s, 1H), 3.92 (s, 3H), 3.87 (s, 3H), 3.02 (s, 3H), 2.20 (s, 3H); ^{13}C NMR (101 MHz, $CDCl_3$) δ [ppm] = 168.7, 154.1, 145.3, 132.2, 118.0, 110.5, 106.0, 56.5, 56.4, 44.5, 25.2; HRMS for $C_{11}H_{15}NO_5SNa$ (ESI+) $[M+Na]^+$: calc.: 296.0563, found: 296.0572.

8. NMR spectra of novel compounds

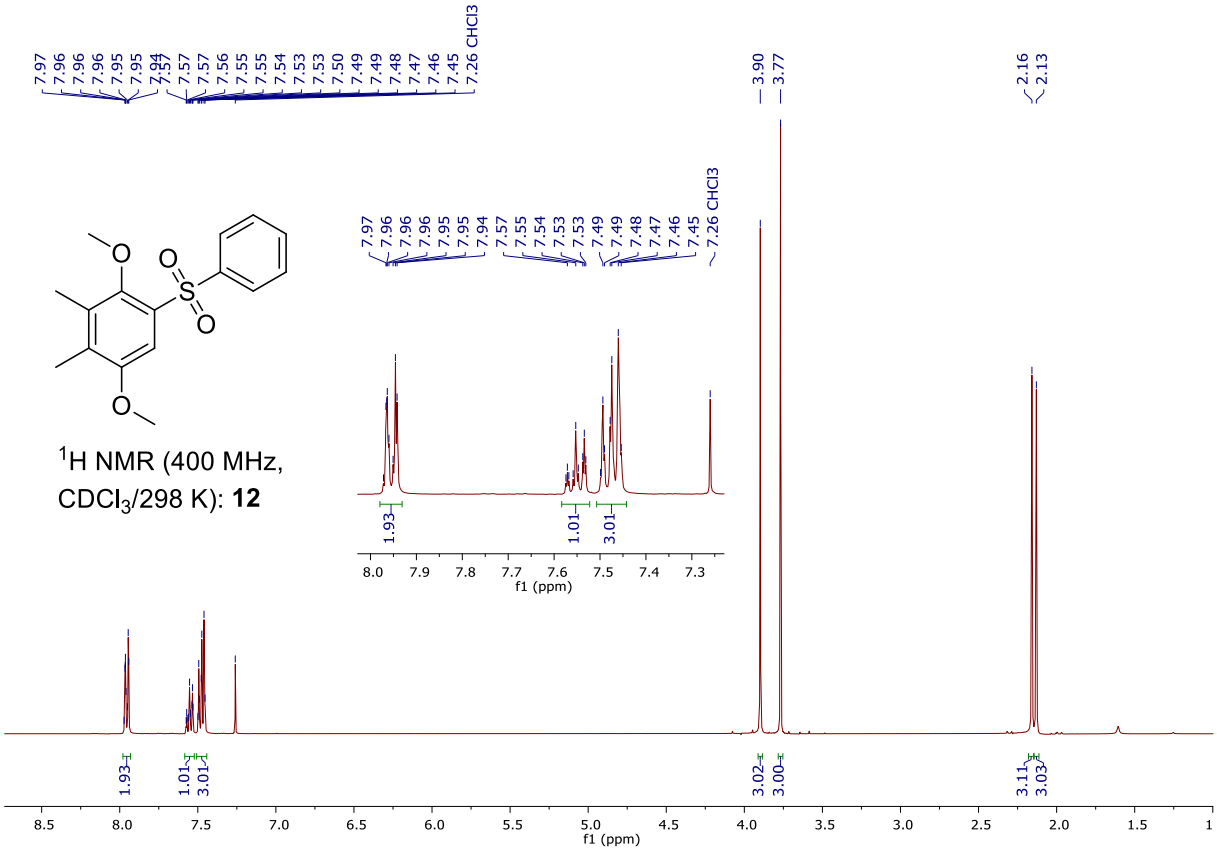

^{1}H NMR (400 MHz, $CDCl_3$/298 K): **12**

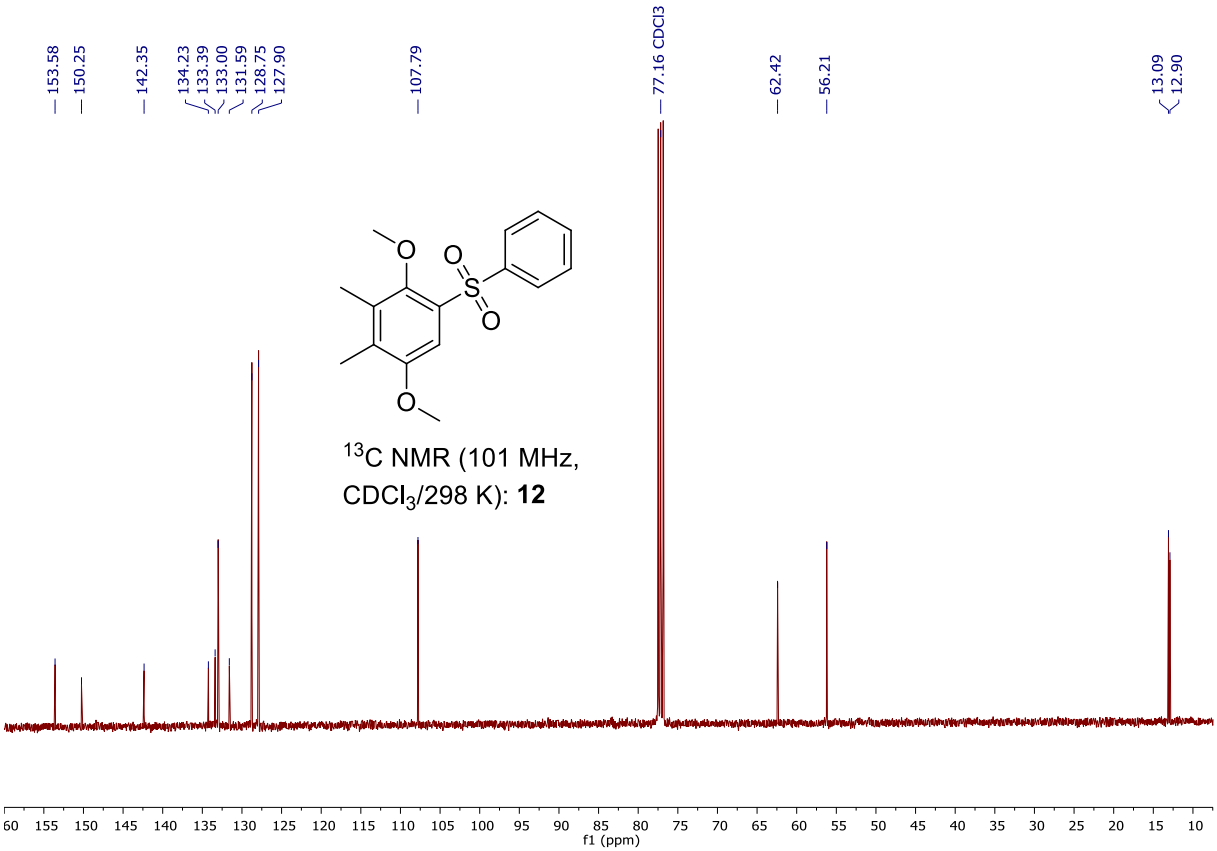

^{13}C NMR (101 MHz, $CDCl_3$/298 K): **12**

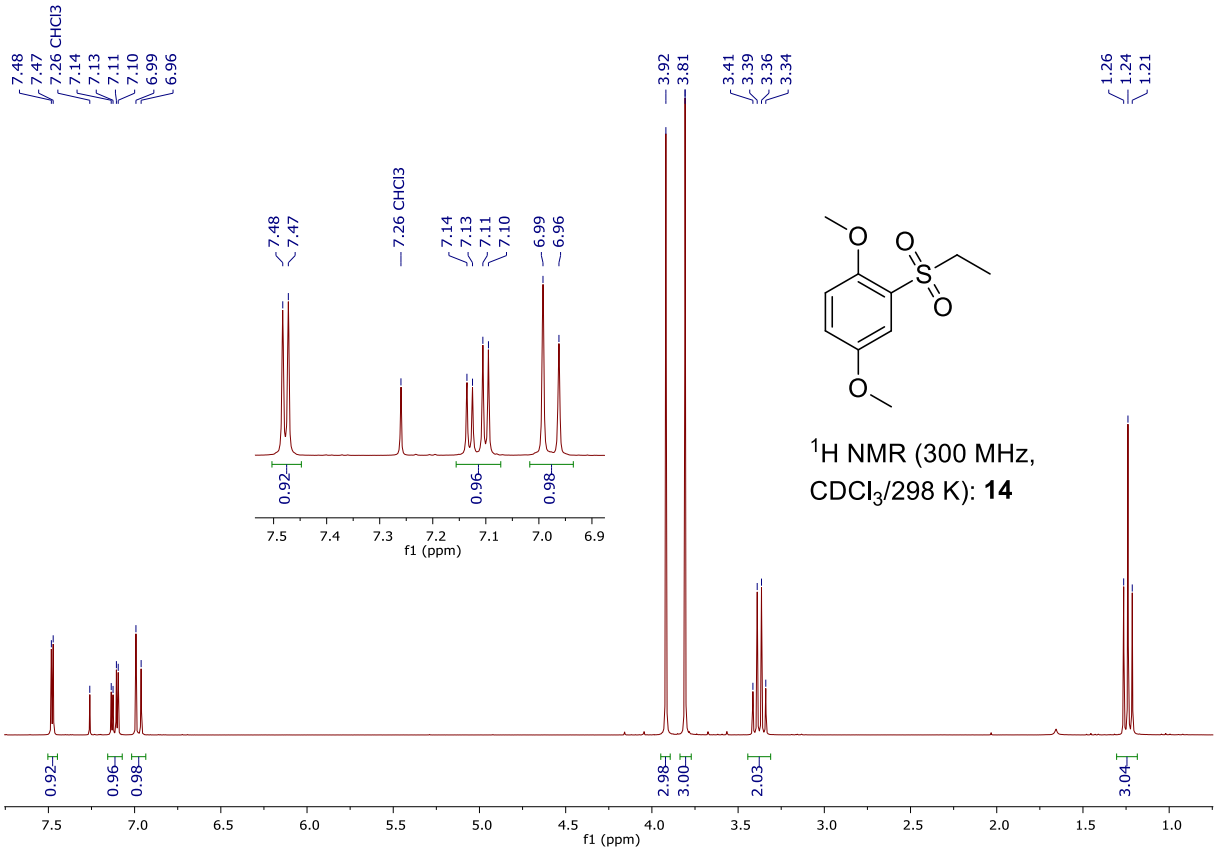

^{1}H NMR (300 MHz, $CDCl_3$/298 K): **14**

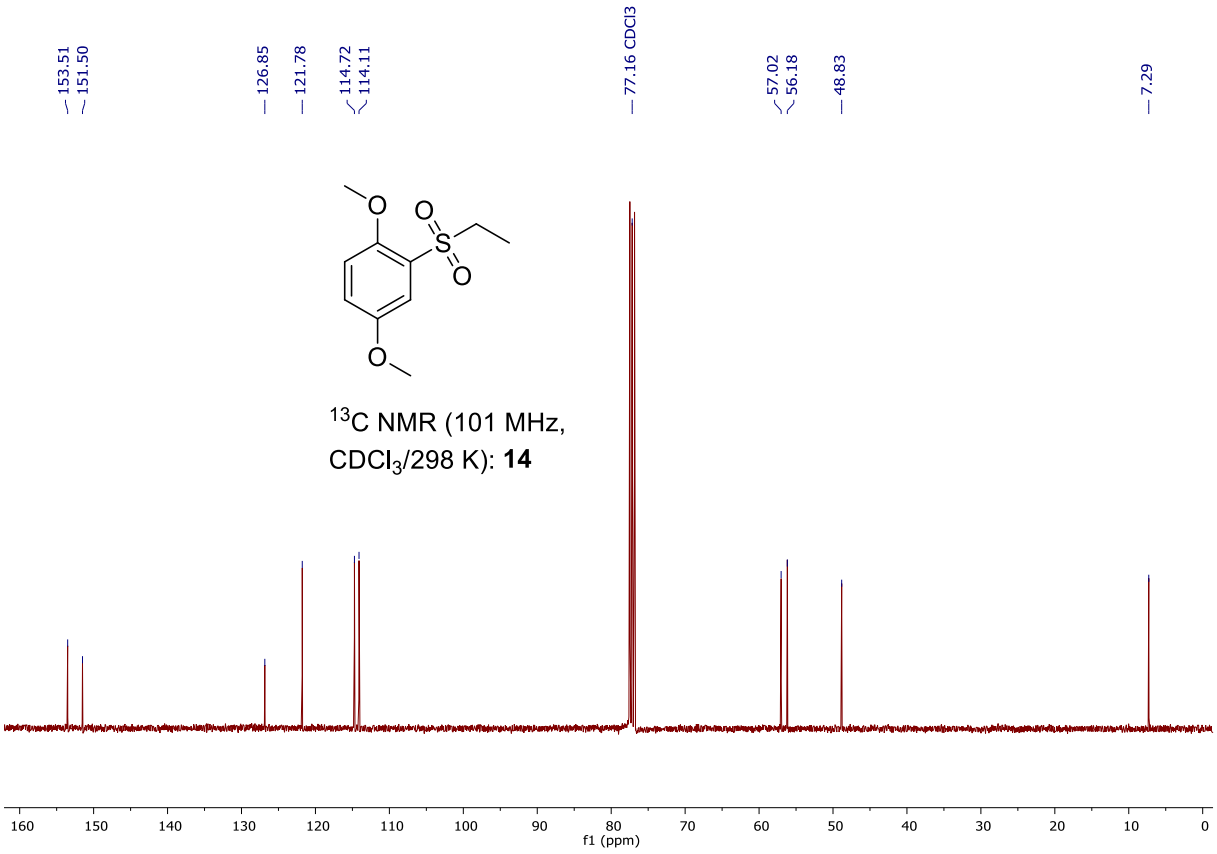

^{13}C NMR (101 MHz, $CDCl_3$/298 K): **14**

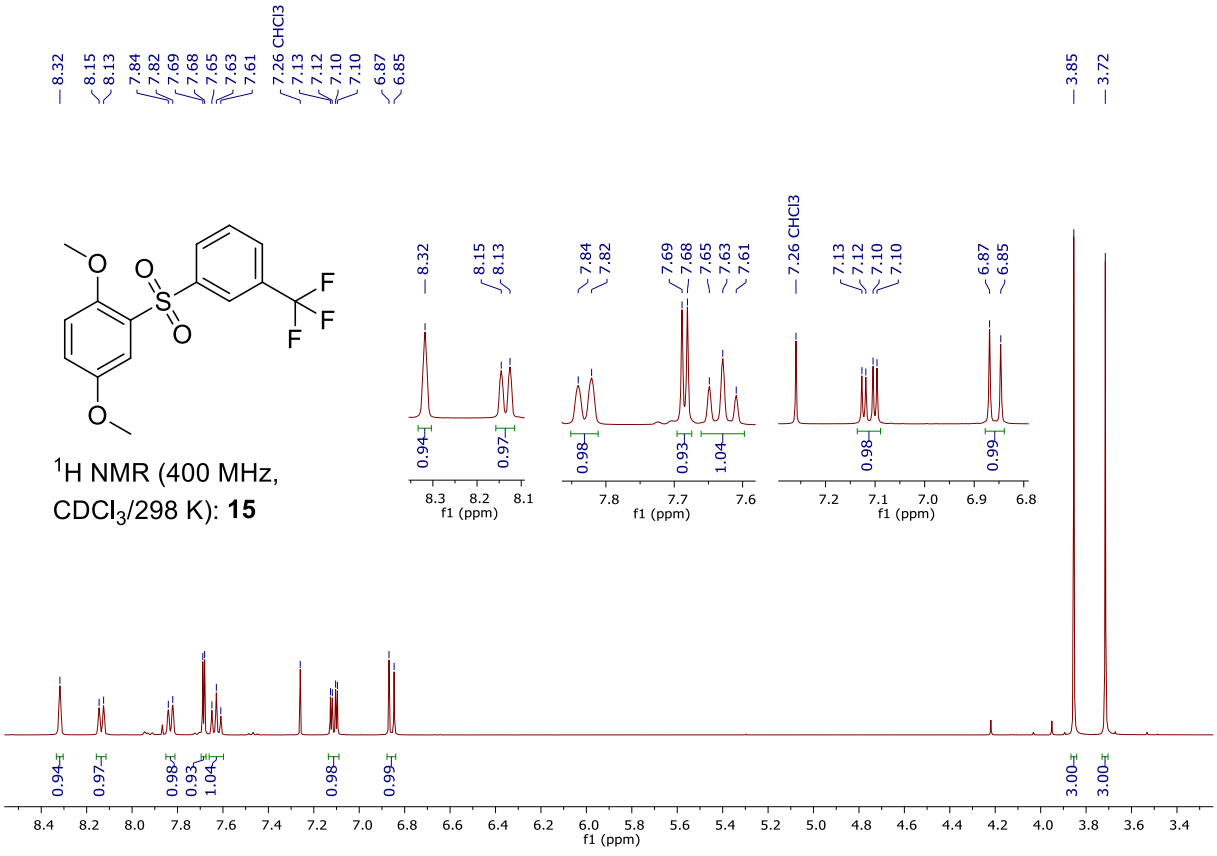

^{1}H NMR (400 MHz, $CDCl_3$/298 K): **15**

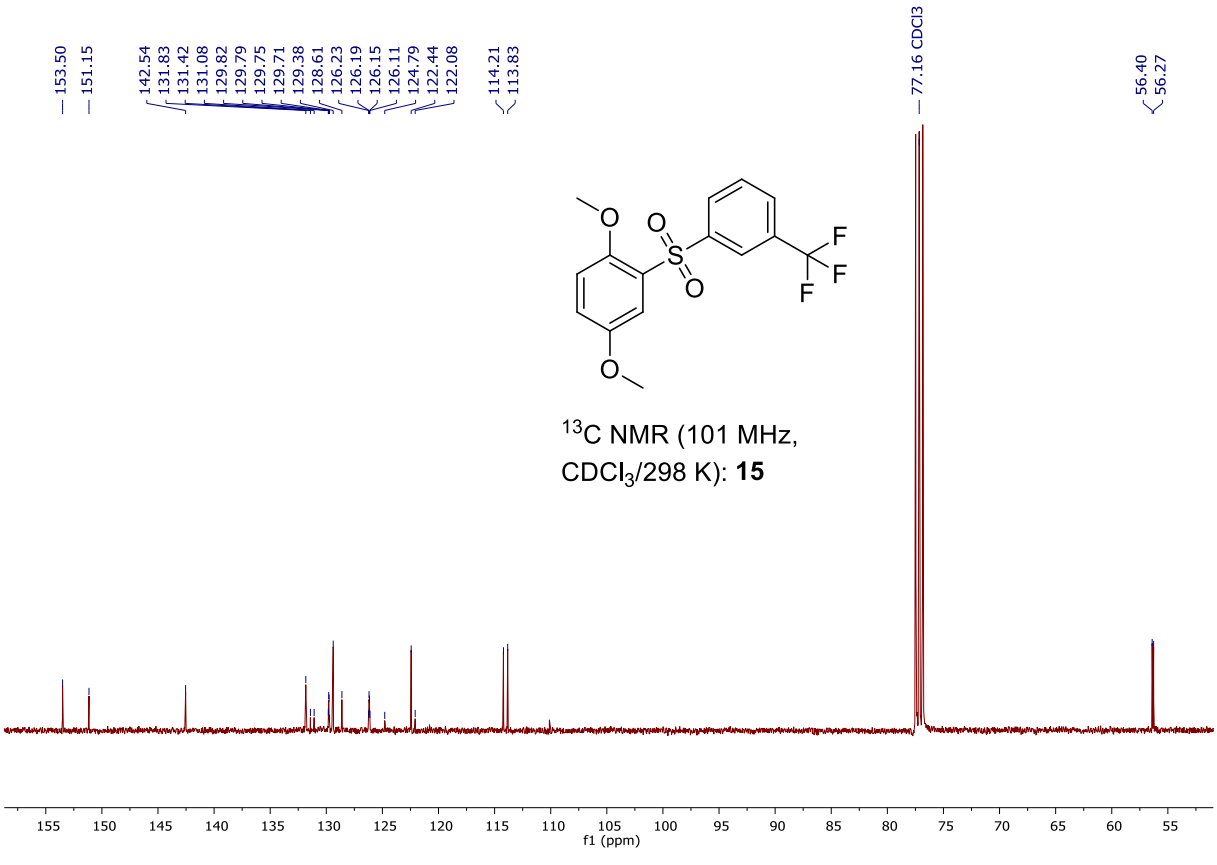

^{13}C NMR (101 MHz, $CDCl_3$/298 K): **15**

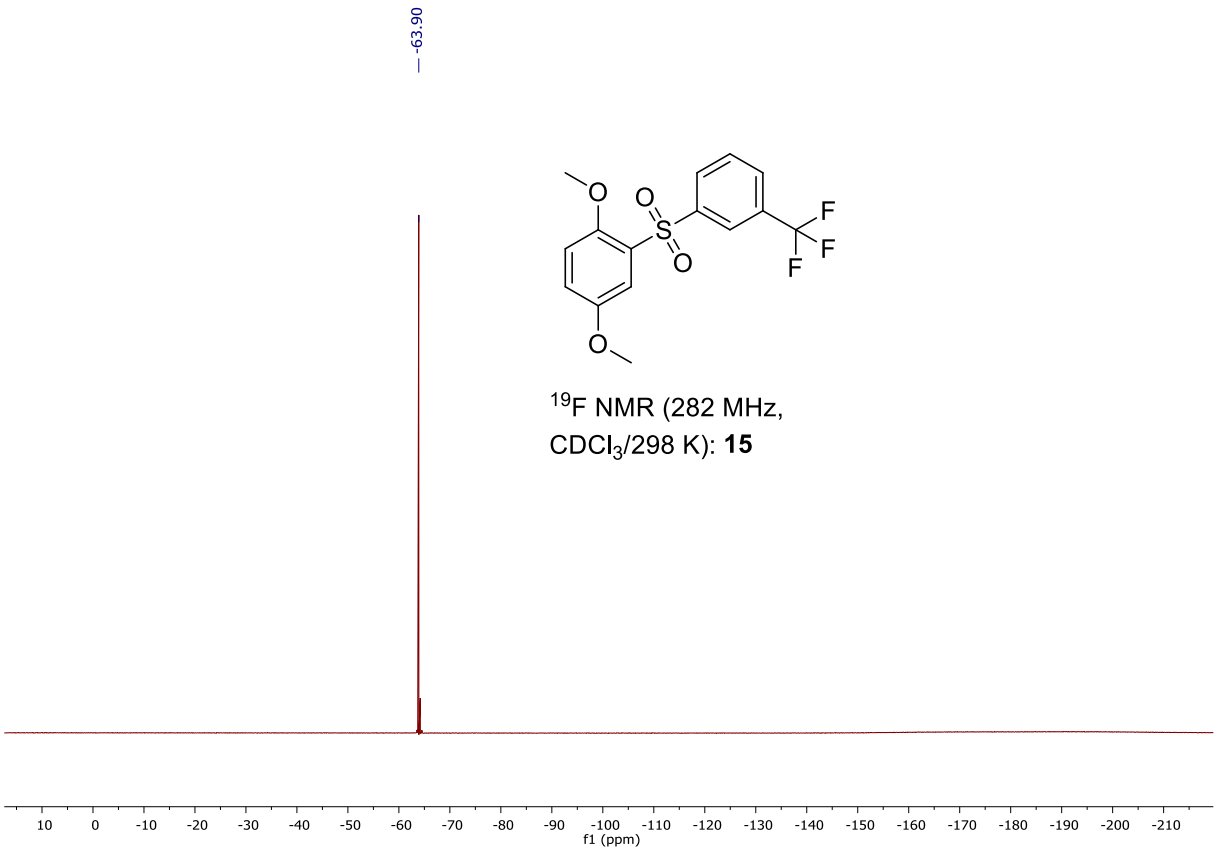

^{19}F NMR (282 MHz, $CDCl_3$/298 K): **15**

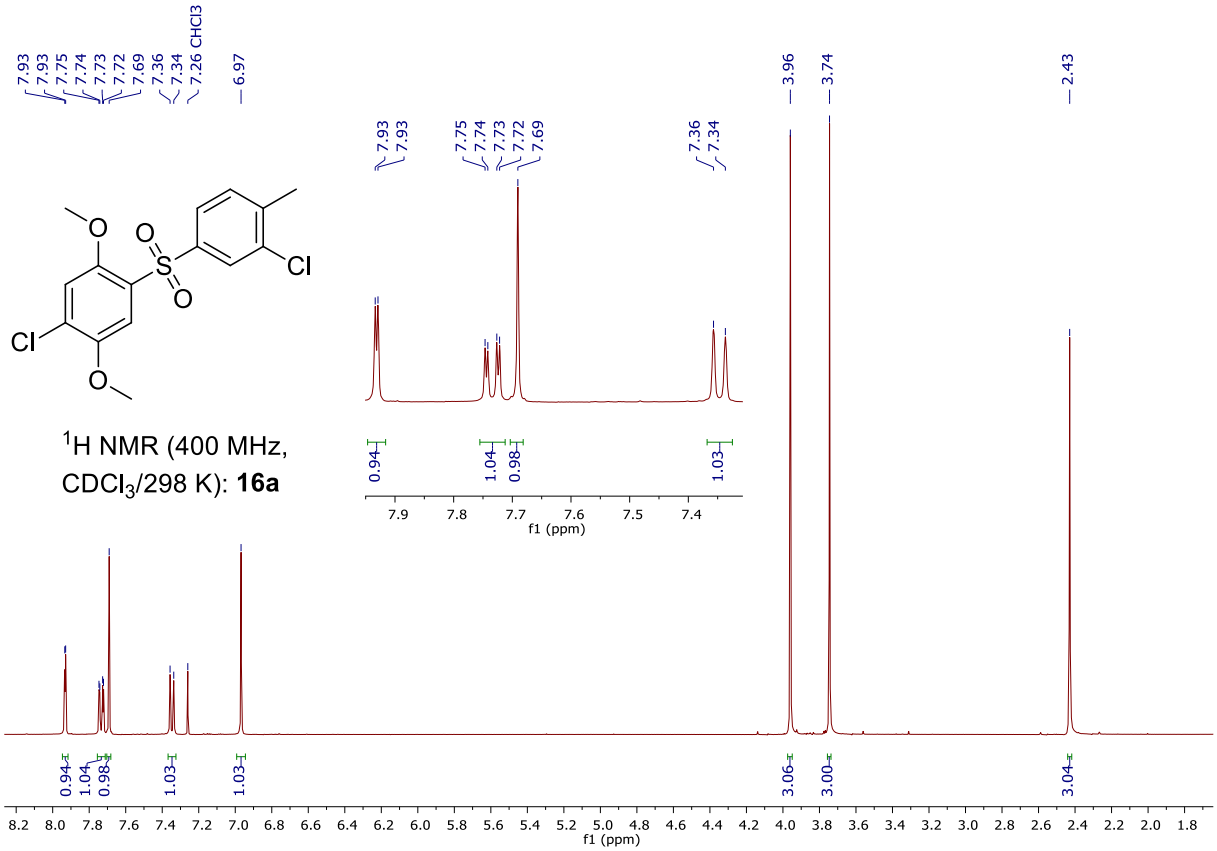

^{1}H NMR (400 MHz, $CDCl_3$/298 K): **16a**

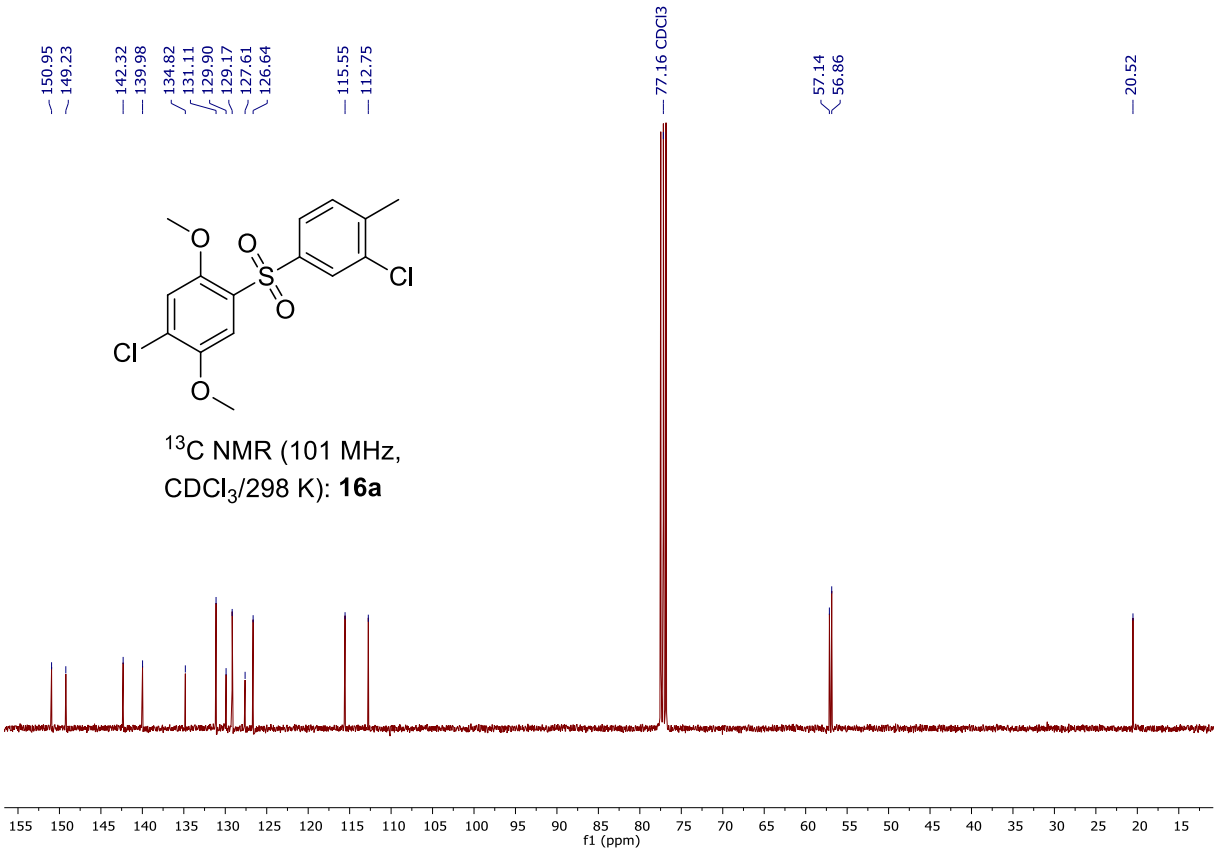

^{13}C NMR (101 MHz, $CDCl_3$/298 K): **16a**

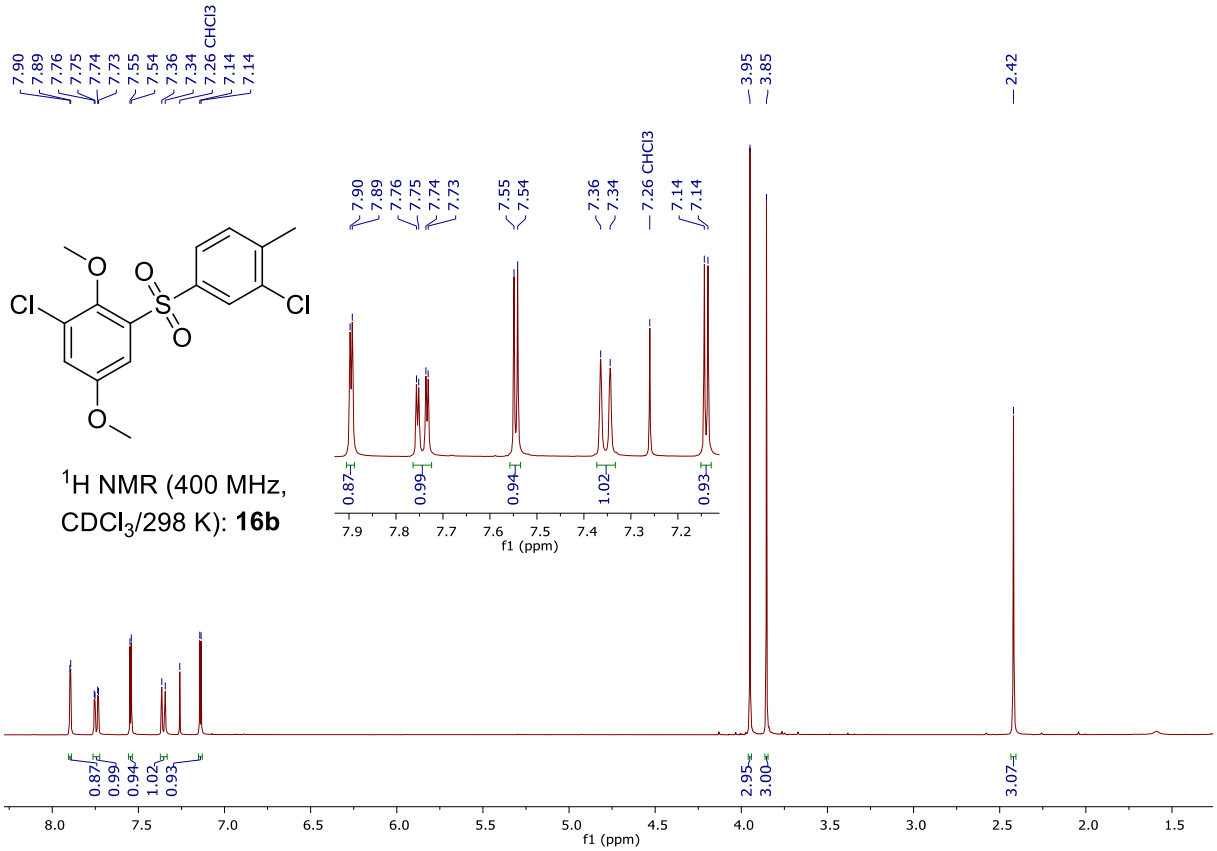

^{1}H NMR (400 MHz, $CDCl_3$/298 K): **16b**

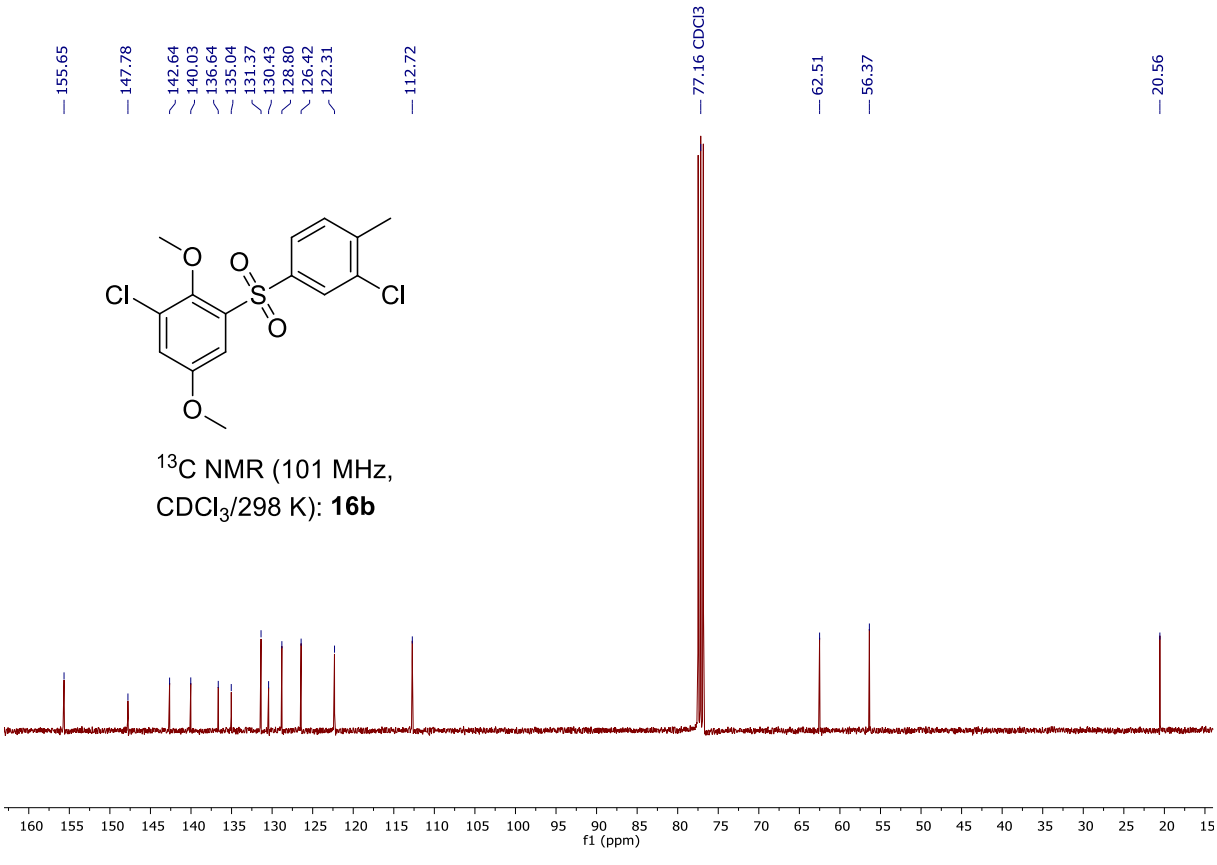

^{13}C NMR (101 MHz, $CDCl_3$/298 K): **16b**

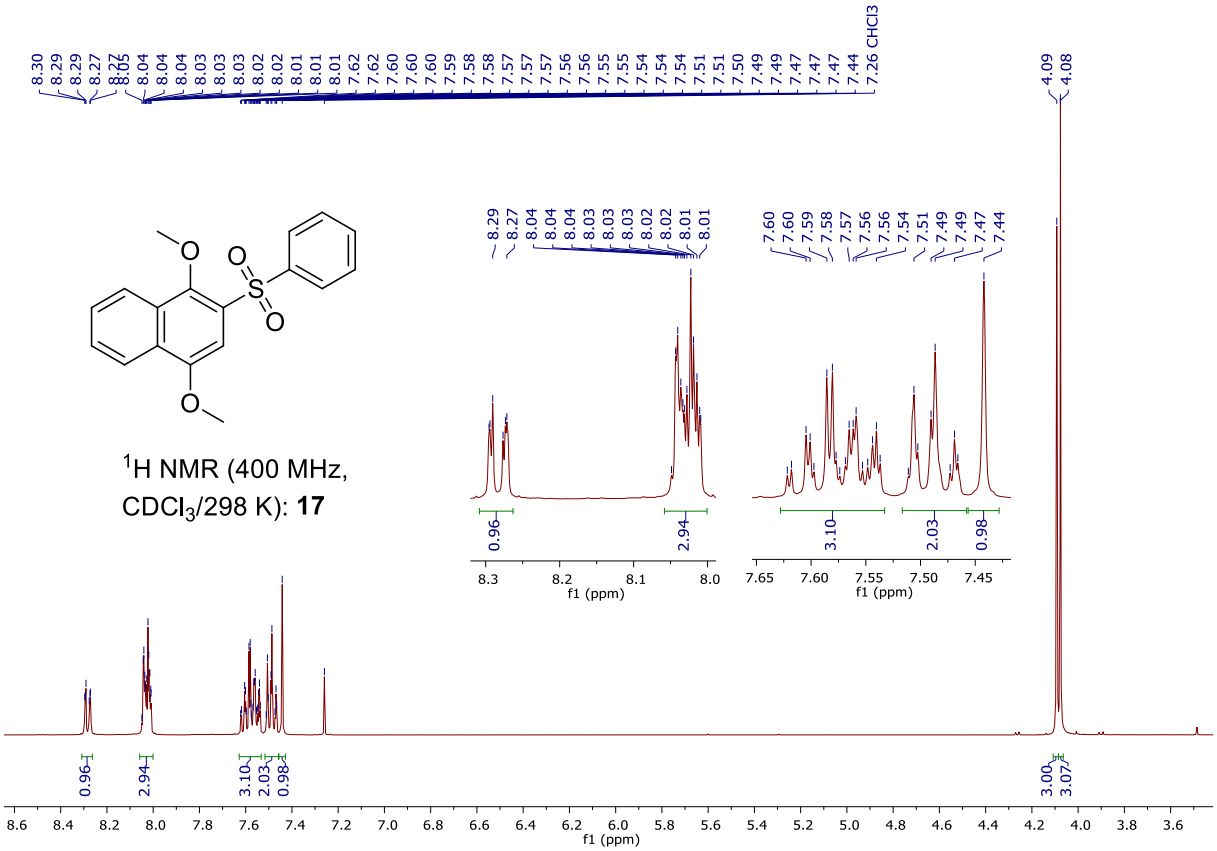

^{1}H NMR (400 MHz, $CDCl_3$/298 K): **17**

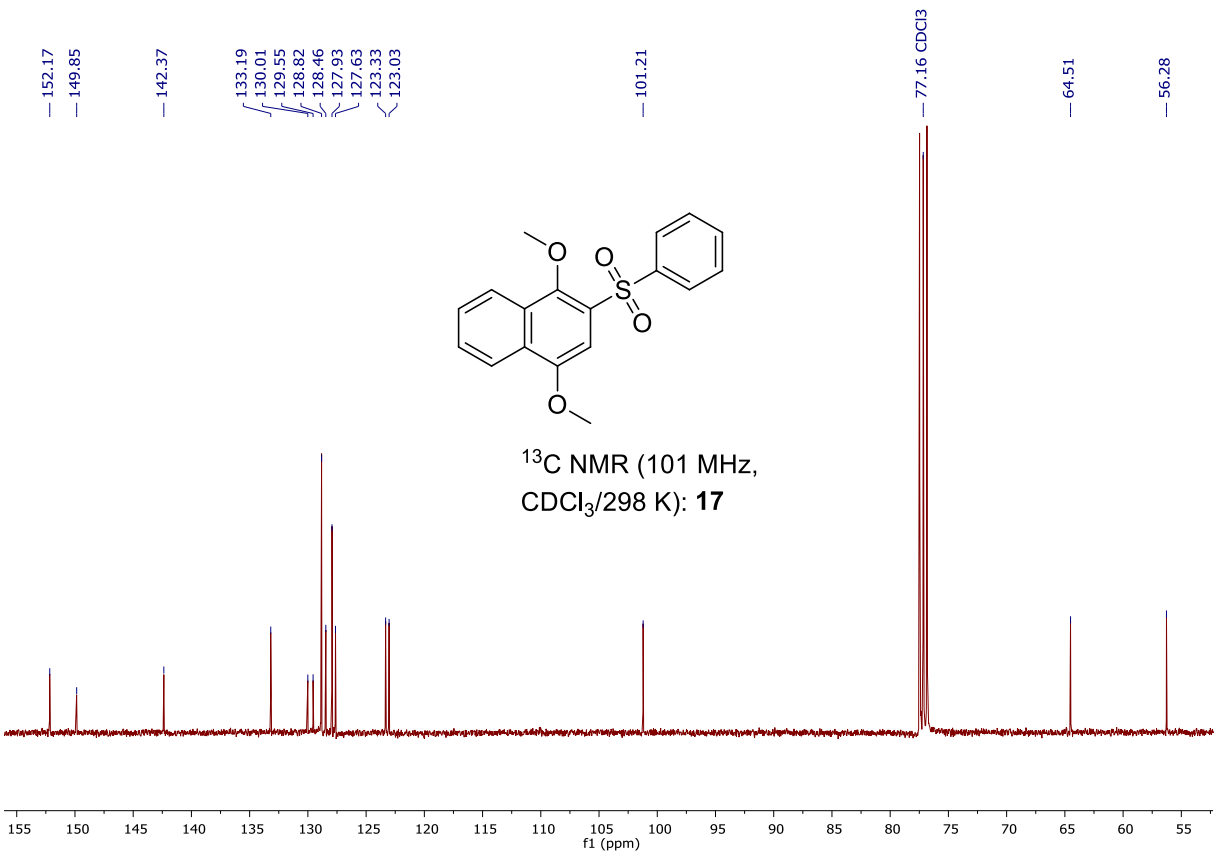

^{13}C NMR (101 MHz, $CDCl_3$/298 K): **17**

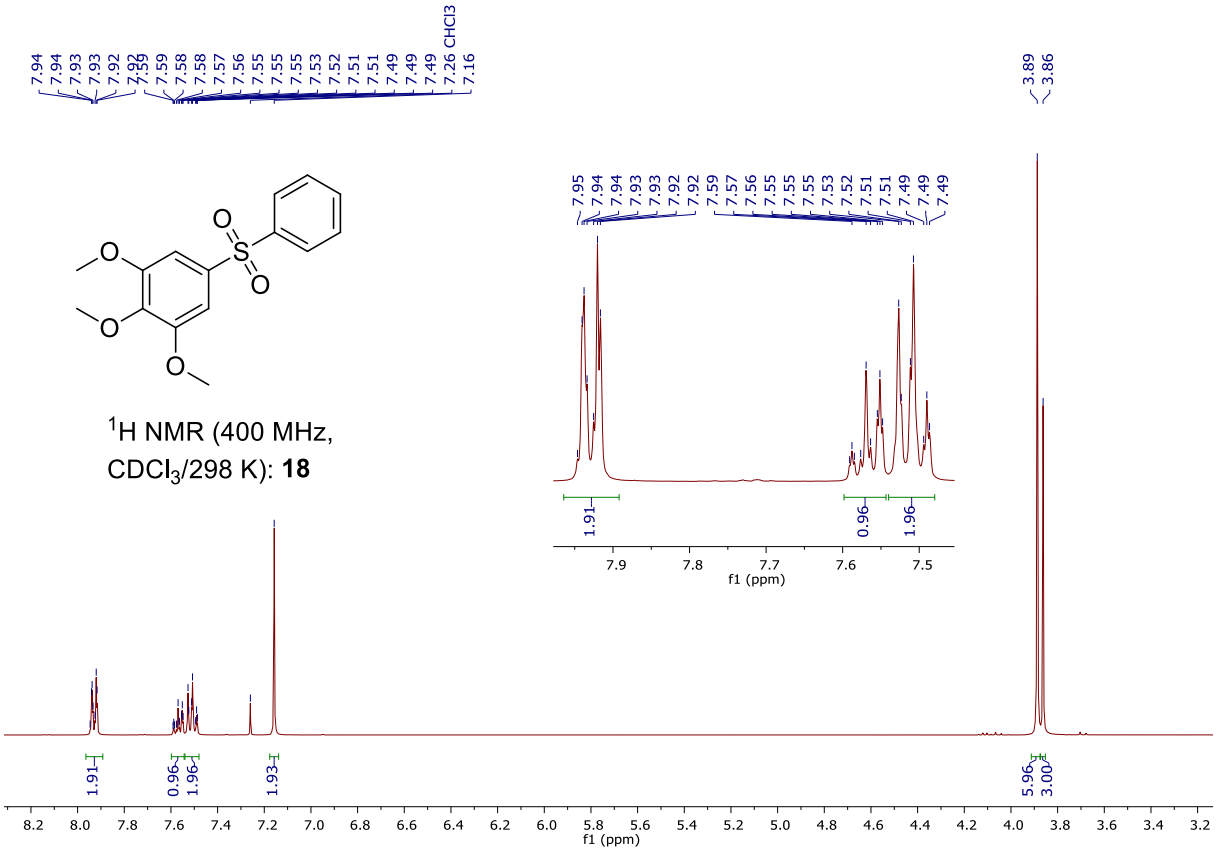
7.94
7.94
7.93
7.93
7.92
7.92
7.59
7.58
7.58
7.57
7.56
7.55
7.55
7.55
7.53
7.52
7.51
7.51
7.49
7.49
7.49
7.26 CHCl3
7.16
3.89
3.86
O
S
O
O
O
O
1H NMR (400 MHz,
CDCl3/298 K): 18
7.95
7.94
7.94
7.93
7.93
7.92
7.92
7.59
7.57
7.56
7.55
7.55
7.55
7.53
7.52
7.51
7.51
7.49
7.49
7.49
1.91
0.96
1.96
7.9
7.8
7.7
7.6
7.5
f1 (ppm)
1.91
0.96
1.96
1.93
5.96
3.00
8.2
8.0
7.8
7.6
7.4
7.2
7.0
6.8
6.6
6.4
6.2
6.0
5.8
5.6
5.4
5.2
5.0
4.8
4.6
4.4
4.2
4.0
3.8
3.6
3.4
3.2
f1 (ppm)

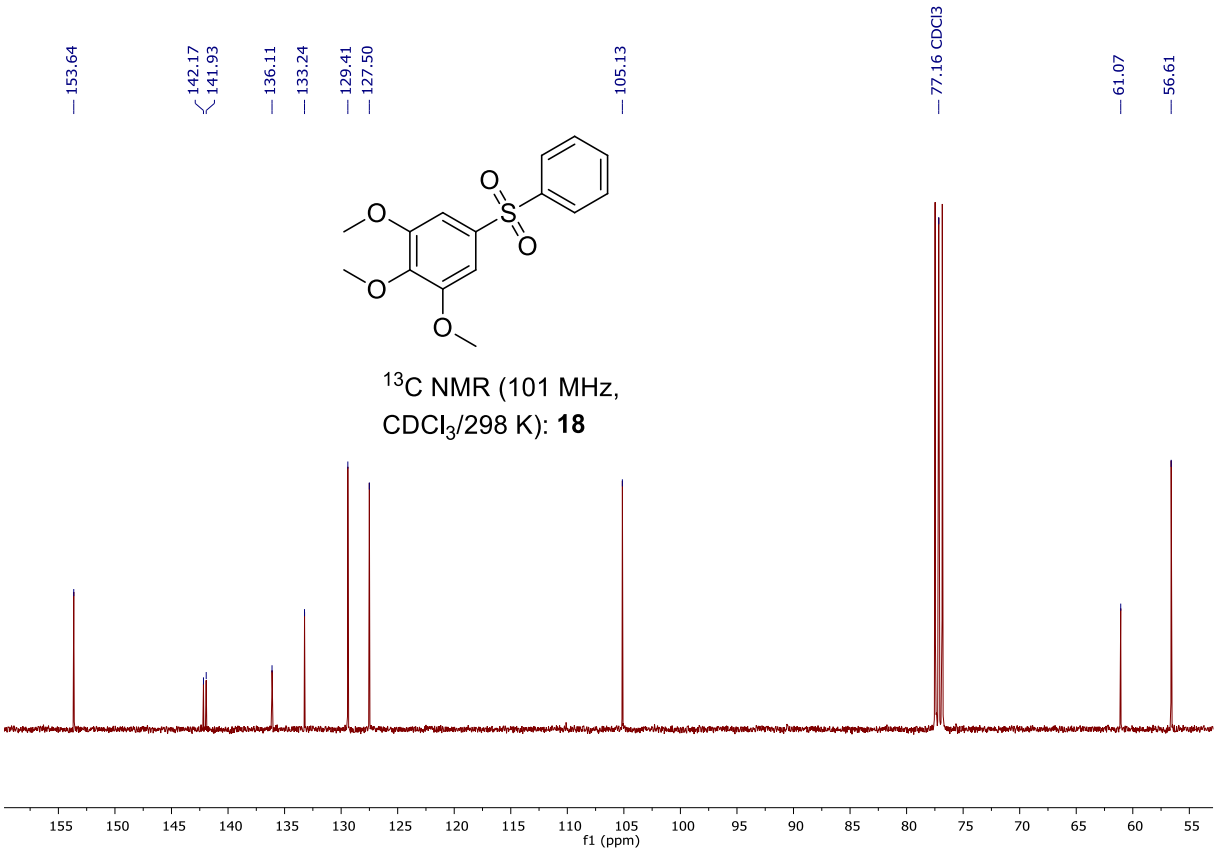
153.64
142.17
141.93
136.11
133.24
129.41
127.50
105.13
77.16 CDCl3
61.07
56.61
O
S
O
O
O
O
13C NMR (101 MHz,
CDCl3/298 K): 18
155
150
145
140
135
130
125
120
115
110
105
100
95
90
85
80
75
70
65
60
55
f1 (ppm)

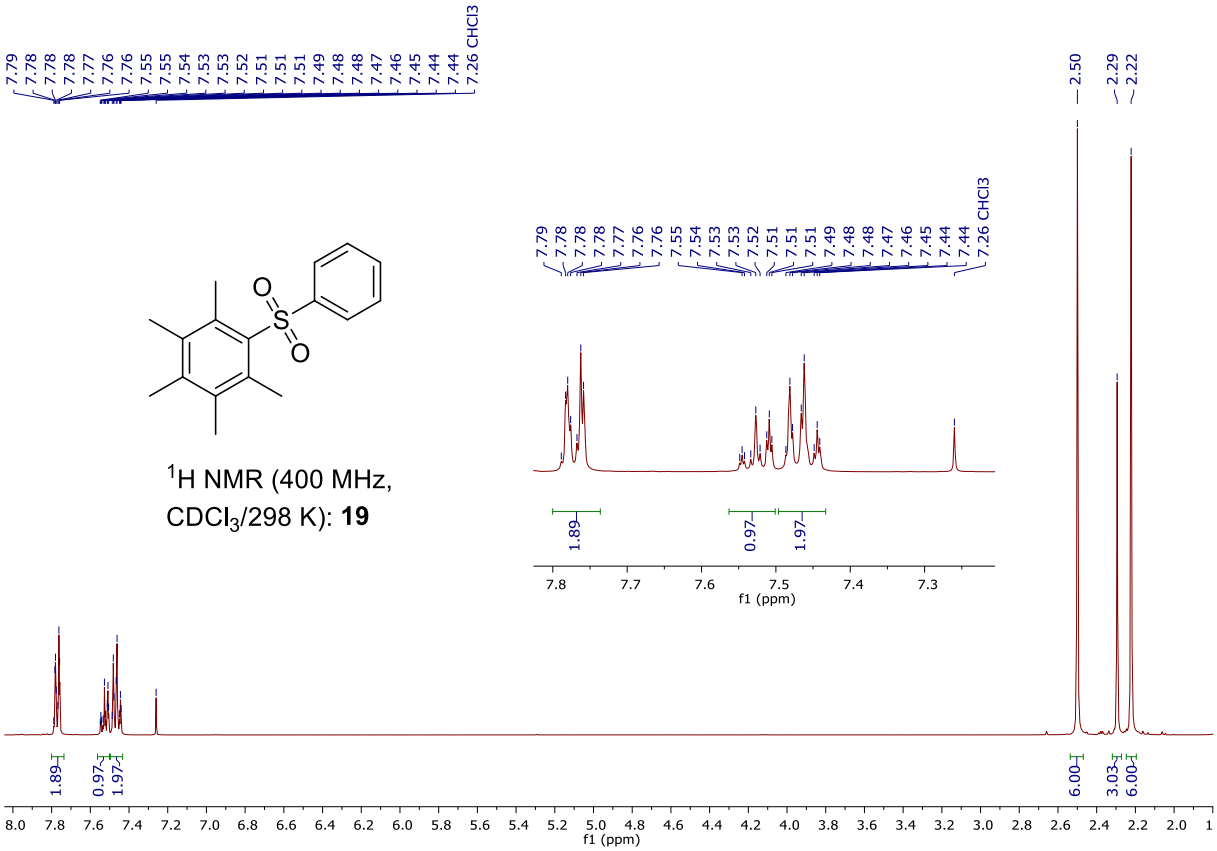

^{1}H NMR (400 MHz, $CDCl_3$/298 K): **19**

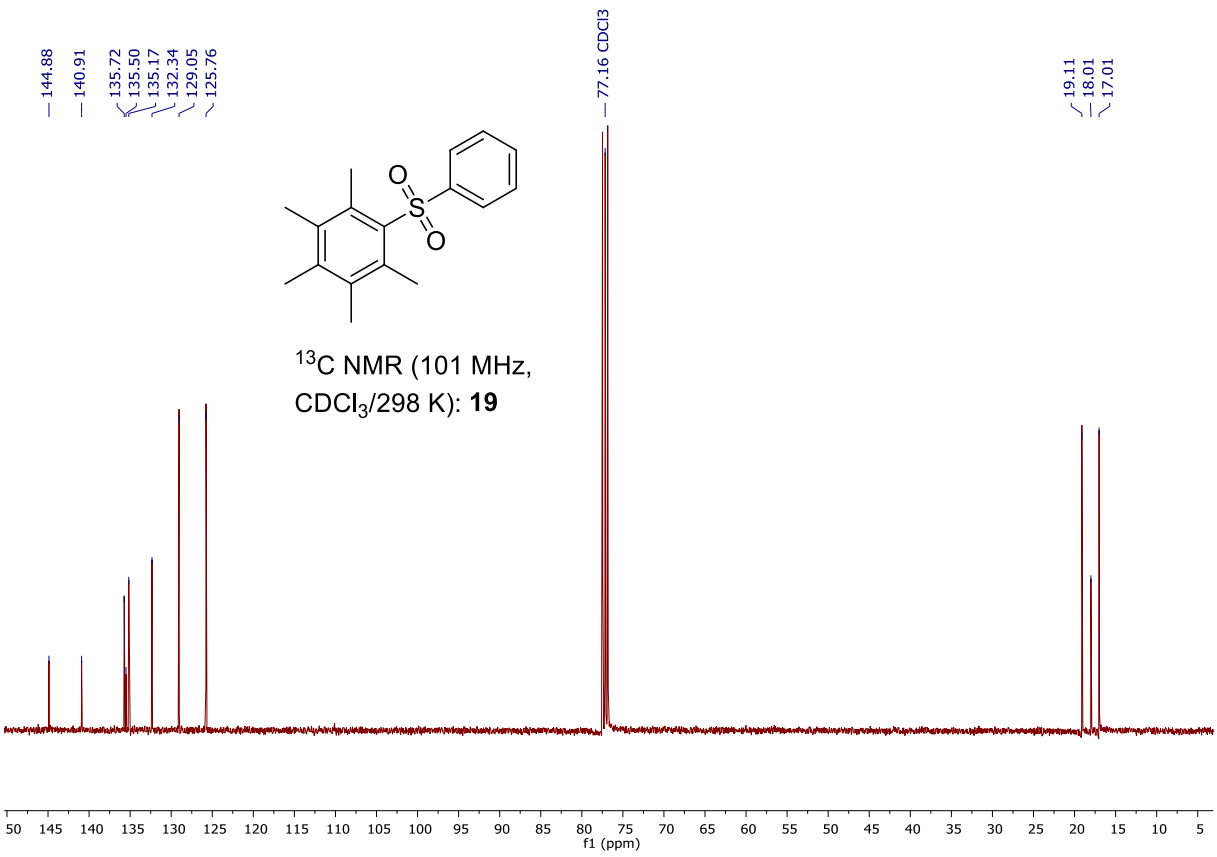

^{13}C NMR (101 MHz, $CDCl_3$/298 K): **19**

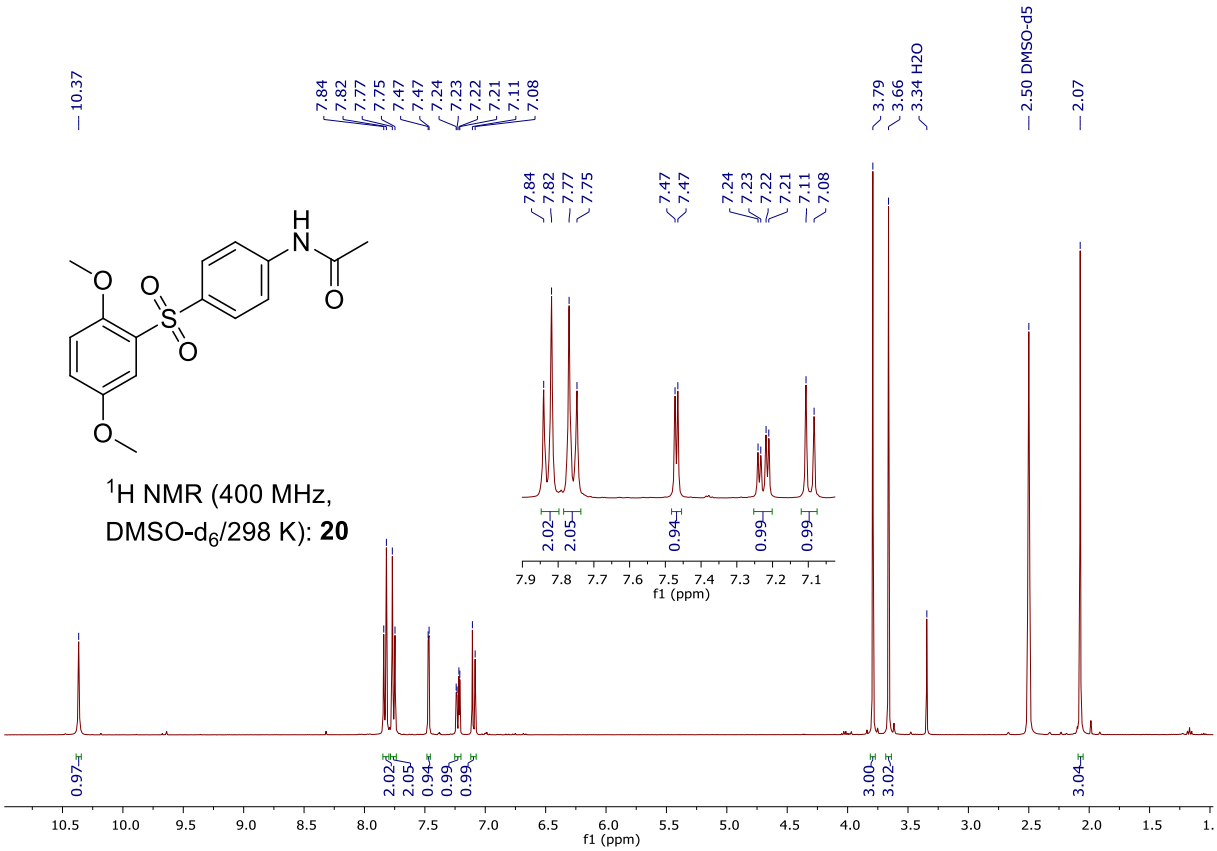

^{1}H NMR (400 MHz, DMSO-d_6/298 K): **20**

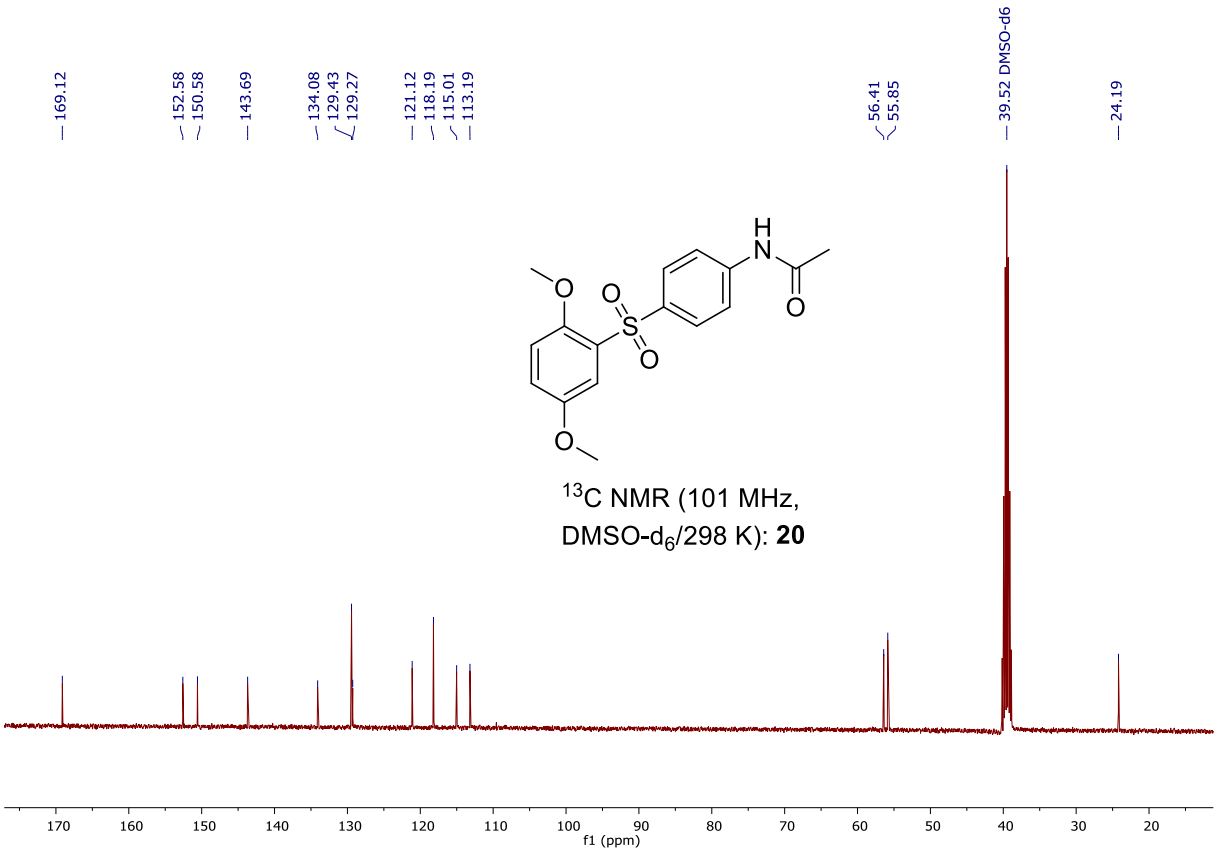

^{13}C NMR (101 MHz, DMSO-d_6/298 K): **20**

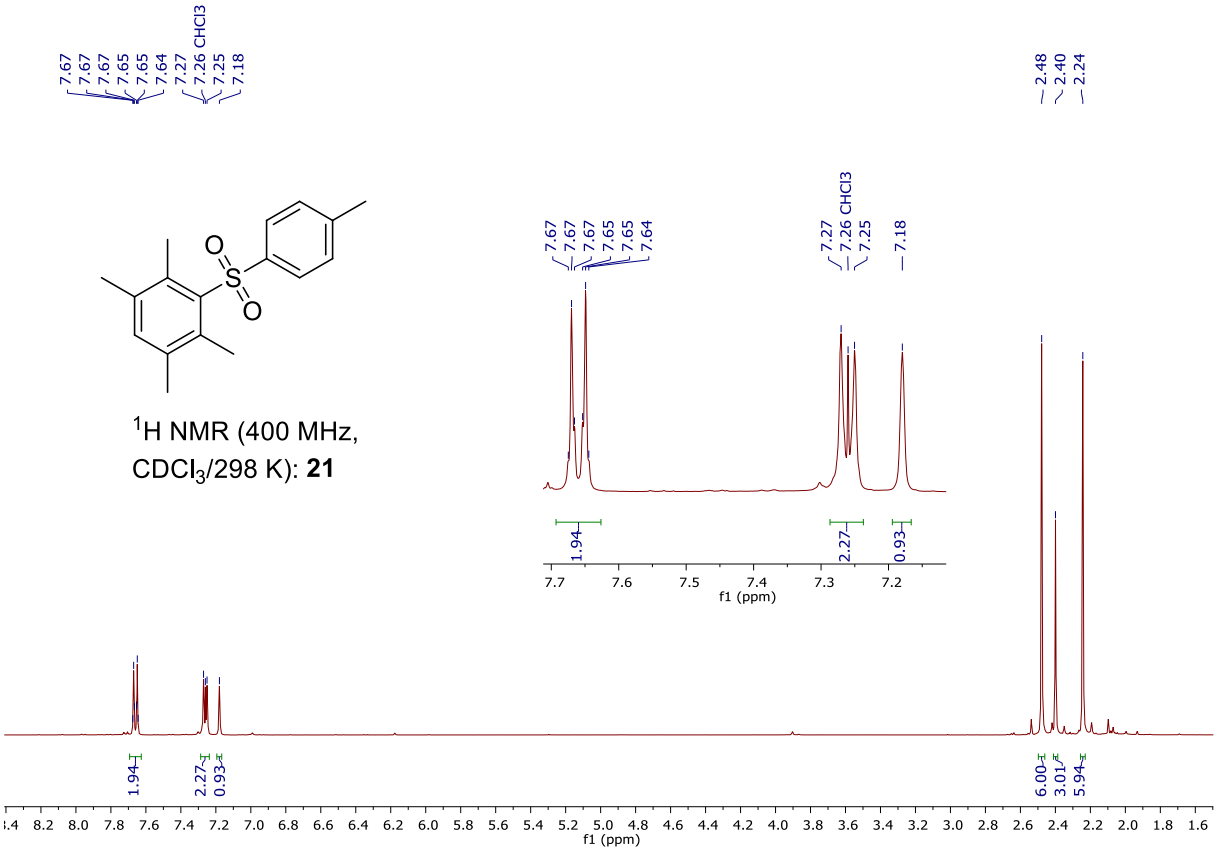

^{1}H NMR (400 MHz, $CDCl_3$/298 K): **21**

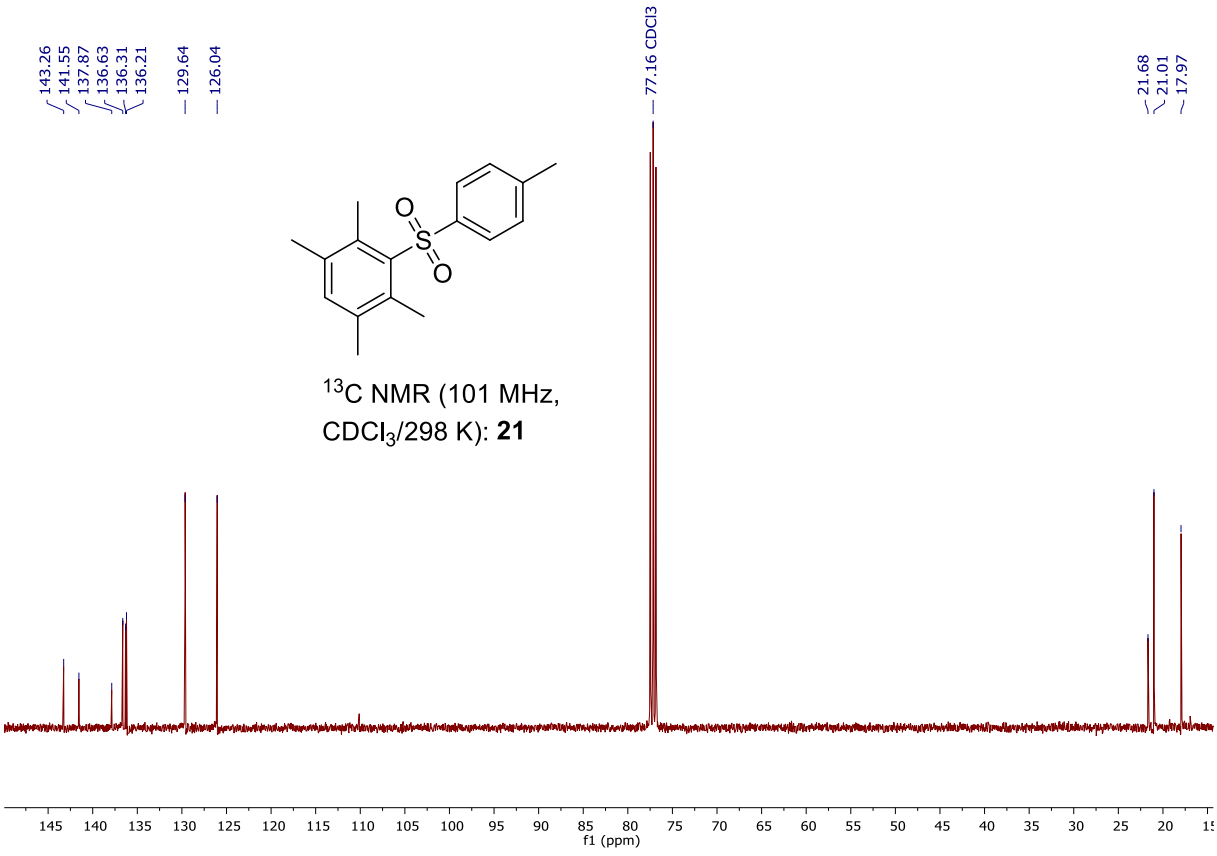

^{13}C NMR (101 MHz, $CDCl_3$/298 K): **21**

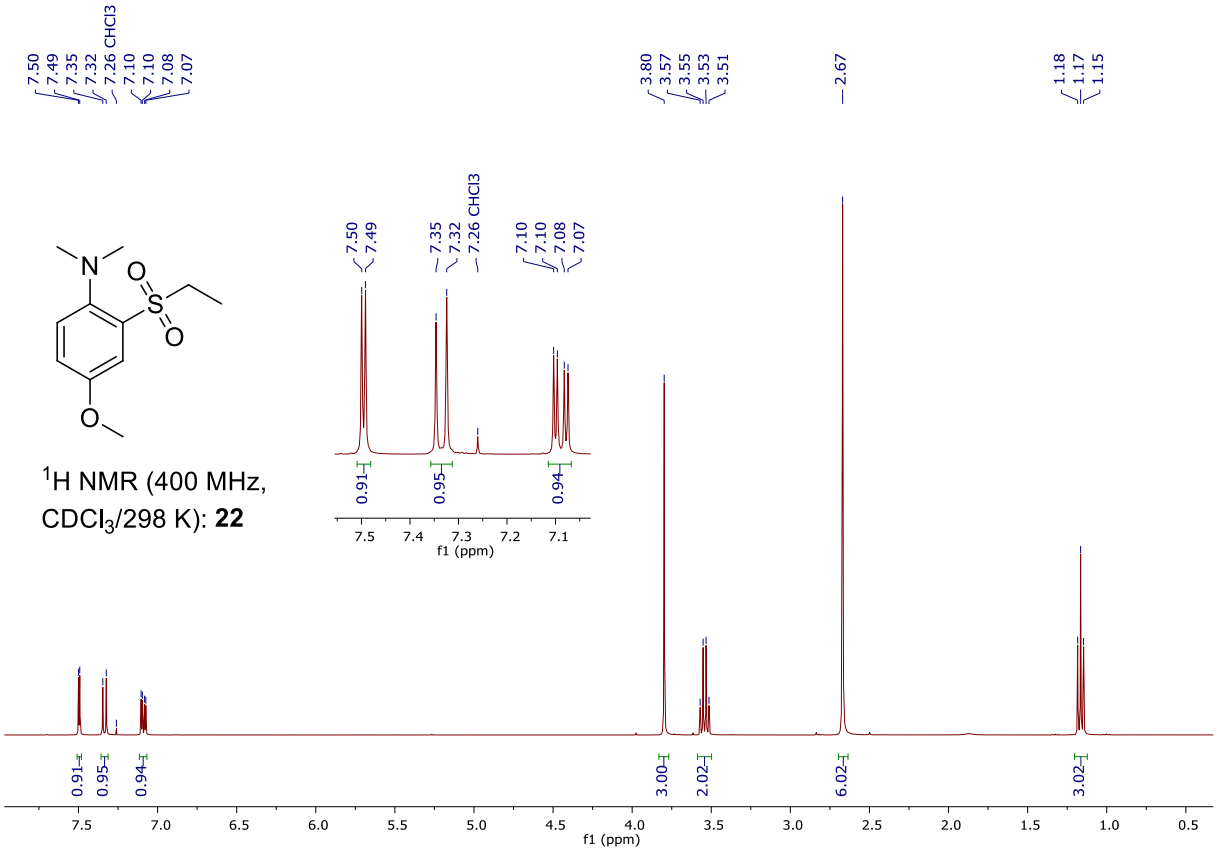

^{1}H NMR (400 MHz, $CDCl_3$/298 K): **22**

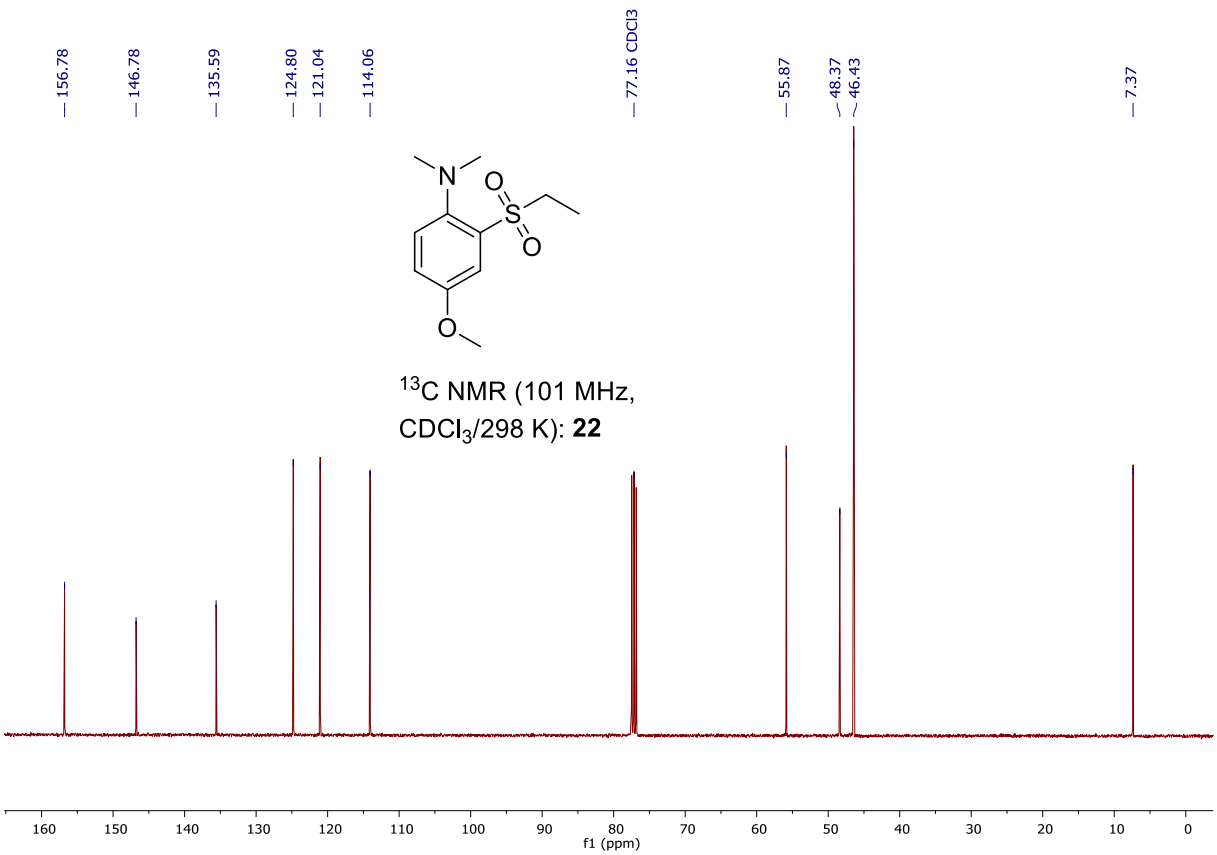

^{13}C NMR (101 MHz, $CDCl_3$/298 K): **22**

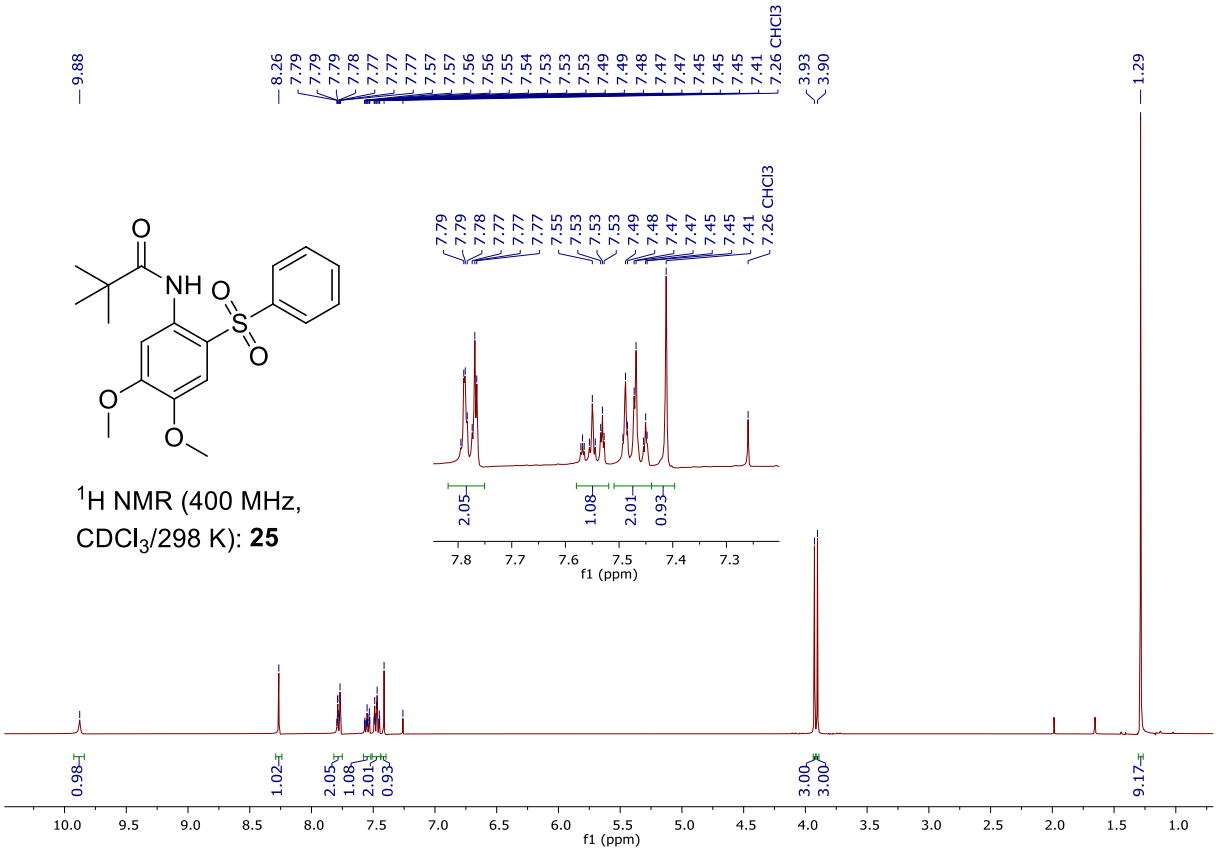

^{1}H NMR (400 MHz, $CDCl_3$/298 K): **25**

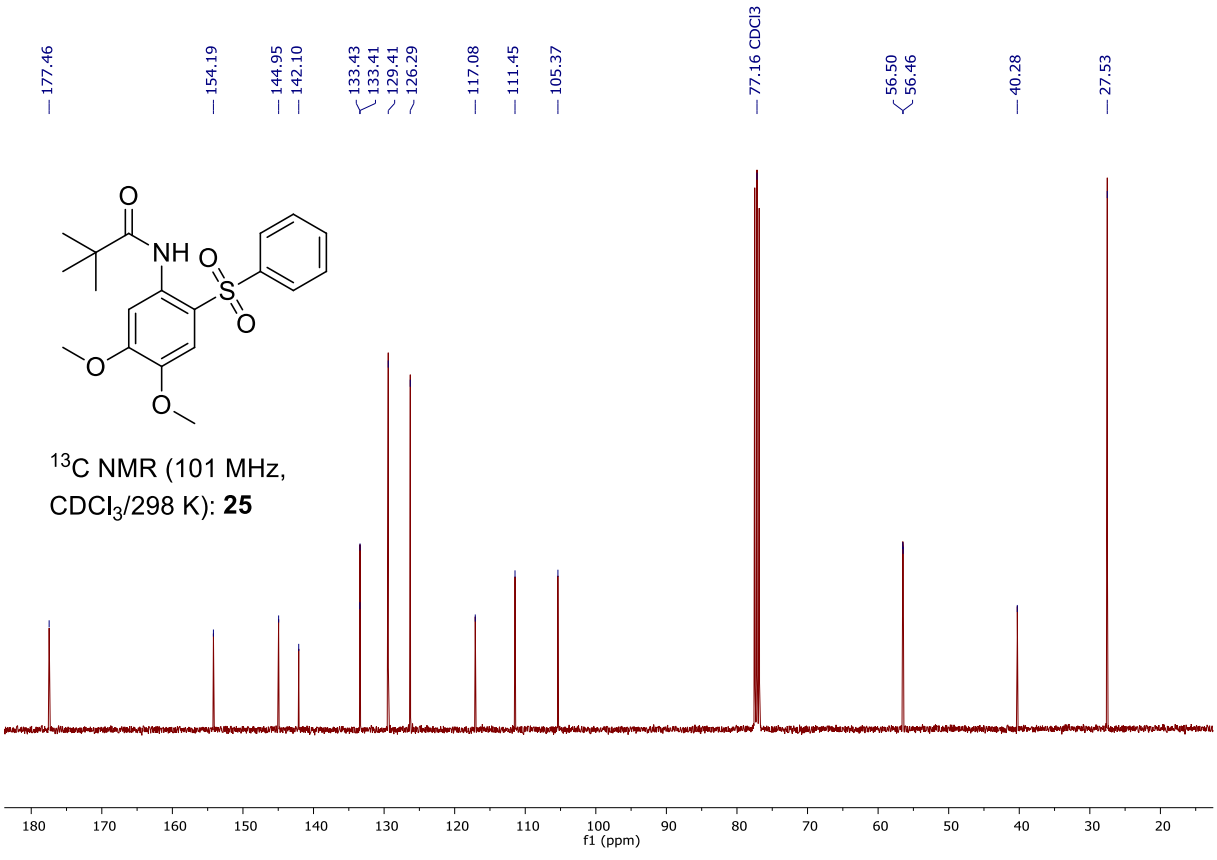

^{13}C NMR (101 MHz, $CDCl_3$/298 K): **25**

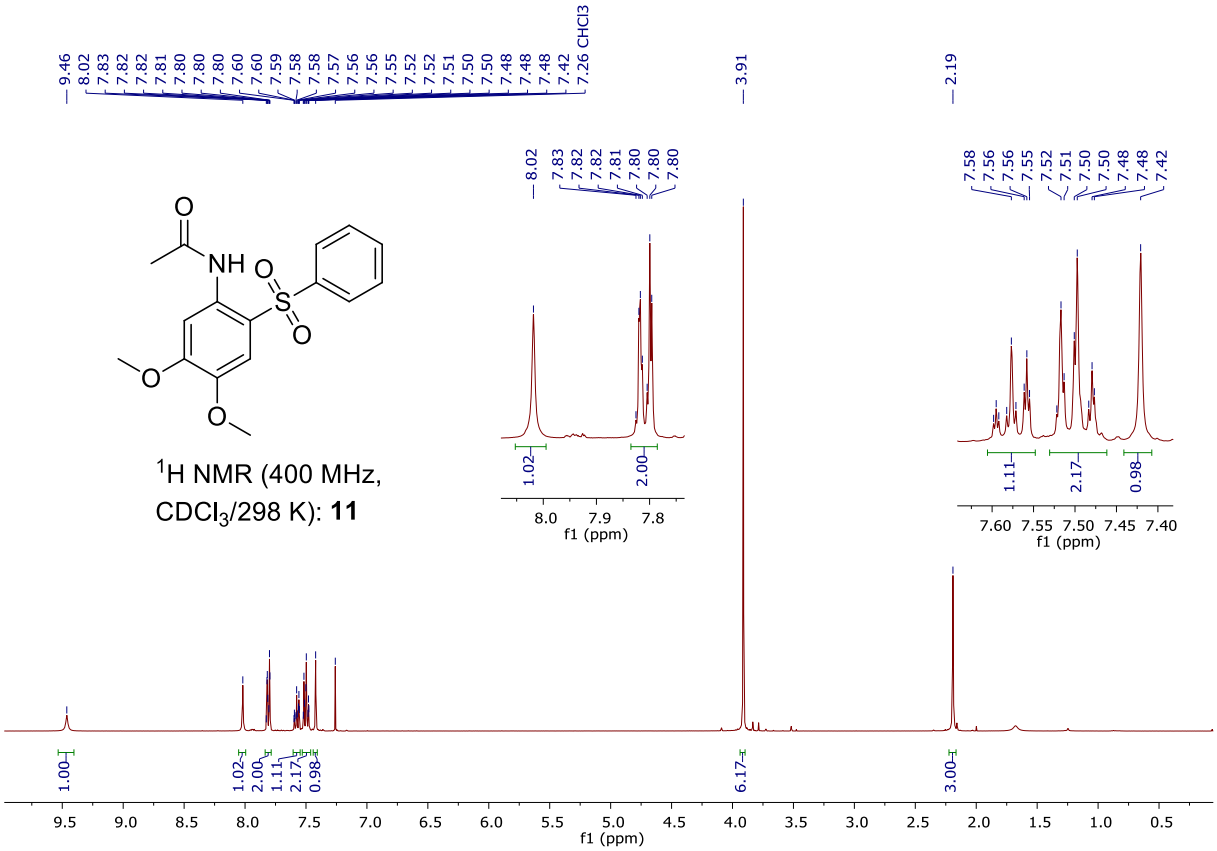

^{1}H NMR (400 MHz, $CDCl_3$/298 K): **11**

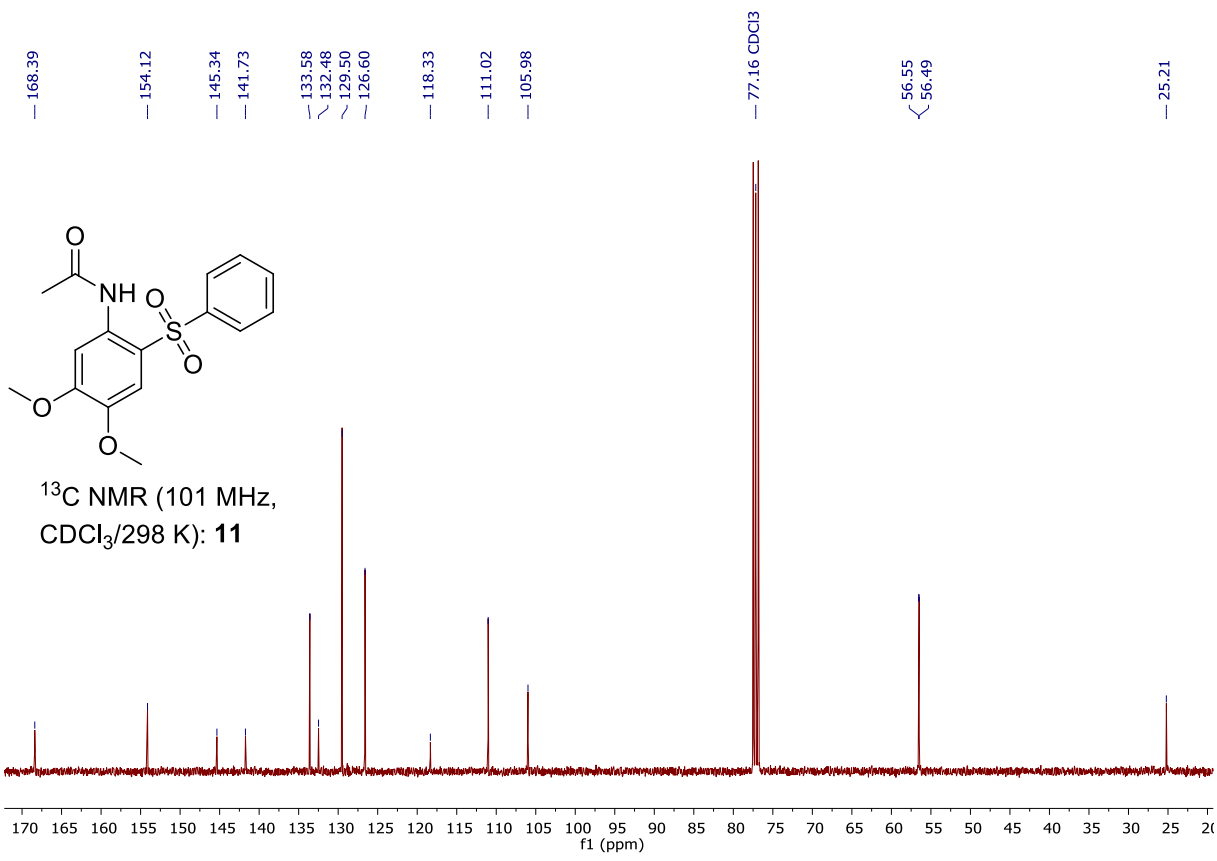

^{13}C NMR (101 MHz, $CDCl_3$/298 K): **11**

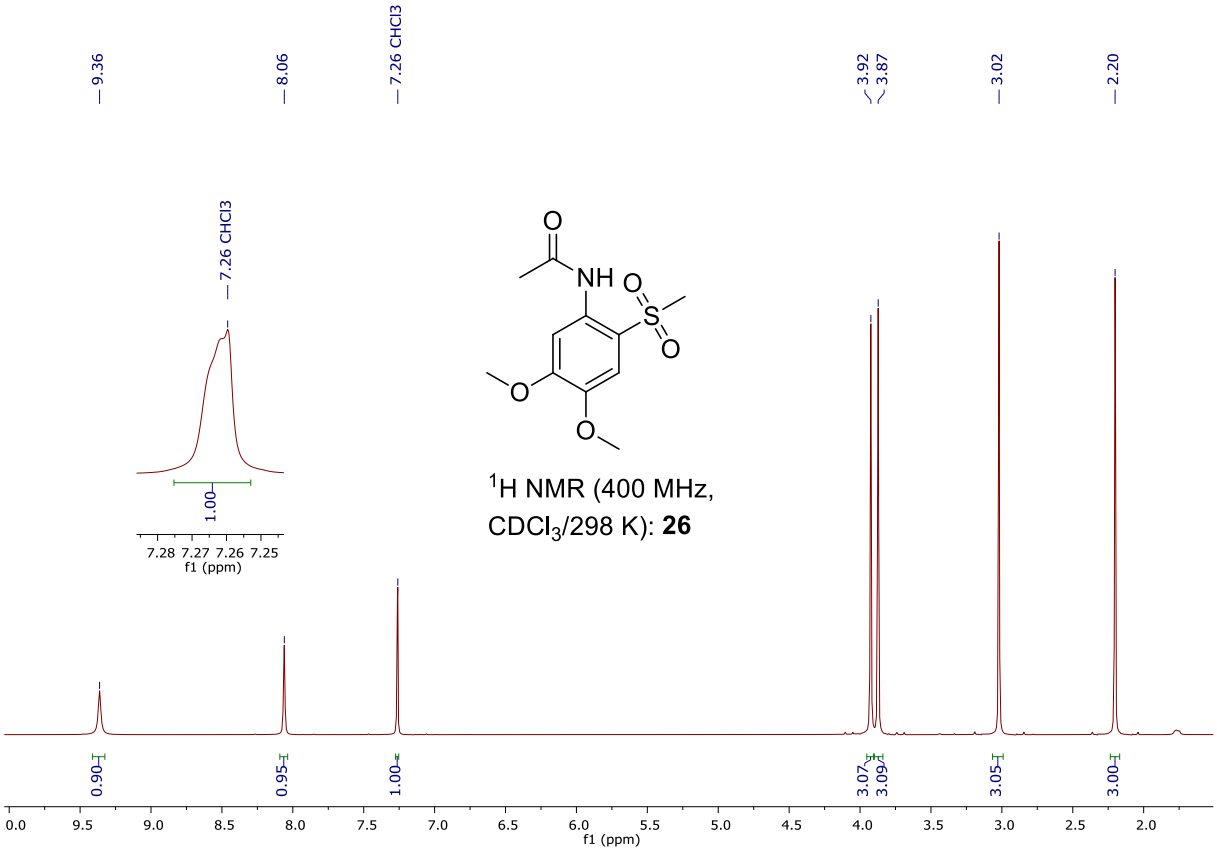
9.36
8.06
7.26 CHCl3
3.92
3.87
3.02
2.20
7.26 CHCl3
1.00
7.28 7.27 7.26 7.25
f1 (ppm)
NH
O
S
O
O
O
^{1}H NMR (400 MHz,
CDCl$_3$/298 K): **26**
0.90
0.95
1.00
3.07
3.09
3.05
3.00
0.0 9.5 9.0 8.5 8.0 7.5 7.0 6.5 6.0 5.5 5.0 4.5 4.0 3.5 3.0 2.5 2.0
f1 (ppm)

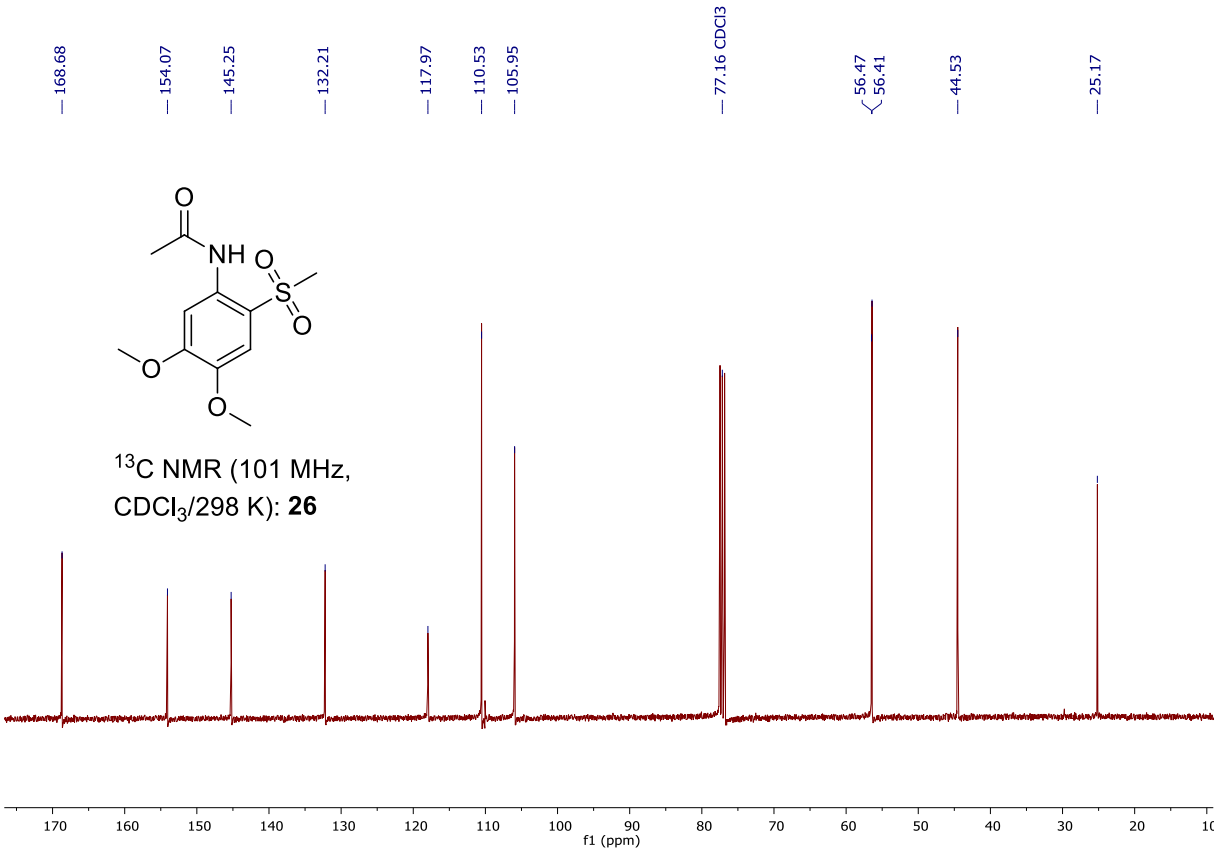
168.68
154.07
145.25
132.21
117.97
110.53
105.95
77.16 CDCl3
56.47
56.41
44.53
25.17
NH
O
S
O
O
O
^{13}C NMR (101 MHz,
CDCl$_3$/298 K): **26**
170 160 150 140 130 120 110 100 90 80 70 60 50 40 30 20
f1 (ppm)

9. References

[1] W. L. F. Armarego, C. L. L. Chai, *Purification of Laboratory Chemicals*, Elsevier Ltd., Oxford, **2012**.

[2] R. K. Harris, E. D. Becker, S. M. Cabral de Menezes, R. Goodfellow, P. Granger, *Pure Appl. Chem.* **2001**, *73*, 1795–1818.

[3] Sheldrick, G.M. SHELXS97 and SHELXL97: Programm for the Refinement of Crystal Structures; Dept. of Structural Chemistry, University of Göttingen: Germany, 1997.

[4] a) C. Gütz, B. Klöckner, S. R. Waldvogel, *Org. Process Res. Dev.* **2016**, *20*, 26–32; b) A. Kirste, G. Schnakenburg, F. Stecker, A. Fischer, S. R. Waldvogel, *Angew. Chem. Int. Ed.* **2010**, *49*, 971-975; *Angew. Chem.* **2010**, *122*, 983-987. (see SI thereof).

[5] a) B. Riehl, K. M. Dyballa, R. Franke, S. R. Waldvogel, *Synthesis* **2017**, *49*, 252–259; b) A. Kirste, G. Schnakenburg, F. Stecker, A. Fischer, S. R. Waldvogel, *Angew. Chem. Int. Ed.* **2010**, *49*, 971–975; *Angew. Chem.* **2010**, *122*, 983–987; c) B. Elsler, A. Wiebe, D. Schollmeyer, K. M. Dyballa, R. Franke, S. R. Waldvogel, *Chem. Eur. J.* **2015**, *21*, 12321–12325; d) J. Nikl, S. Lips, D. Schollmeyer, R. Franke, S. R. Waldvogel, *Chem. Eur. J.* **2019**, *25*, 6891–6895.

[6] N. Umierski, G. Manolikakes, *Org. Lett.* **2013**, *15*, 4972–4975.

[7] S. Liang, Y. Ren, G. Manolikakes, *Eur. J. Org. Chem.* **2017**, 4117–4120.

[8] Y.-C. Wu, S.-S. Jiang, S.-Z. Luo, R.-J. Song, J.-H. Li, *Chem. Commun*. **2019**, *55*, 8995–8998.

[9] K. Zhou, J. Zhang, L. Lai, J. Cheng, J. Sun, J. Wu, *Chem. Commun*. **2018**, *54*, 7459–7462.

4.2 Electrochemical oxo-functionalization of cyclic alkanes and (cyclic-) alkenes with nitrate and oxygen

One manuscript was published for this chapter:

J. Nikl, K. Hofman, S. Mossazghi, I. C. Möller, D. Mondeshki, F. Weinelt, F.-E. Baumann, S. R. Waldvogel, *Electrochemical oxo-functionalization of cyclic alkanes and alkenes using nitrate and oxygen*, *Nat. Commun.* **2023**, *14*, 4565.

DOI: 10.1038/s41467-023-40259-0

Contribution:

F. Weinelt, F.-E. Baumann, S. R. Waldvogel and **I** conceived this work and designed the experiments. K. Hofman, S. Mossazghi, I. C. Möller, D. Mondeshki and **I** conducted the experiments and analyzed the data. S. R. Waldvogel and **I** wrote the manuscript and the supporting information. F. Weinelt and F.-E. Baumann discussed the results and revised the manuscript.

Motivation

The main feature of the novel synthesis method to be investigated is the dual role of the supporting electrolyte as an enhancer of ionic conductivity and electrochemical mediator. The aim behind this approach is to achieve a high atom economy in a material-efficient way and to reduce the generation of reagent waste. Furthermore, a unifying electrochemical method for the conversion of cyclic alkanes and alkenes to oxygenated, value-added products would be desirable from a material-efficient and, thus, sustainable point of view. Such an approach would be advantageous for industrial applications, as cyclic monounsaturated and saturated hydrocarbons are produced in technical mixtures from the polyunsaturated ones in the hydrogenation step (see Chapter 2.5, Figure 12a).

This approach was inspired by literature-known electrochemical protocols, which are based on using nitrate anions as mediators for activating C–H bonds (see Chapter 2.6).[65,179,181]

Summary of the results

The studies used cyclooctane (**35**) and cyclooctene (**57**) as model substrates. Initial studies on the saturated ring **35** showed right at the beginning of the method development that the ketone cyclooctanone (**46**) is formed selectively using tetra-butylammonium nitrate as a supporting electrolyte in acetonitrile.[190] The reactions were first performed on glassy carbon electrodes under ambient conditions. Apart from non-converted starting material **35**, cyclooctanol (**48**) and cyclooctane-1,4-dione were significant by-products.[190] When the electrolysis was carried out under a nitrogen atmosphere (inert gas conditions), no formation of oxidized species was observed, indicating the essential role of molecular oxygen in the atmosphere as the oxygen source. Instead, starting material remained non-converted. Experiments were conducted up to 100 vol.% oxygen subsequently. Changing the supporting electrolyte's anion to commonly used examples like tetrafluoroborate (BF_4^-), hexafluorophosphate (PF_6^-), and perchlorate (ClO_4^-) resulted in all cases to strongly reduced yields of **46**, pointing out the ability of nitrate to serve as an anodic mediator.[190] In comparison, varying the supporting electrolyte's cation to different tetra-alkylammonium or -phosphonium species still resulted in product formation of **46** in comparable yields. In addition to acetonitrile, branched alkyl nitriles like isobutyronitrile, acetone, and nitropropane are also suitable for the reaction. A significant influence on the ketone yield could be assigned to the agitation speed of the stirrer.

A test application of the reaction conditions to cyclooctene **57** as substrate resulted in the formation of octanedioic acid (suberic acid, **43**), observed via HPLC-MS.[190] Also here, the exclusion of oxygen from the atmosphere above the reaction solution did not lead to the formation of the product, indicating molecular oxygen as the oxygen source for the reaction. Scale-up experiments for the cycloalkane oxidation have been performed in a round-bottom flask to ensure a higher gas exchange surface between the electrolyte and the gas-filled compartment inside the cell. The best-achieved reaction conditions using the model substrate **35** are shown in Scheme 14a. Testing cycloalkanes of different ring sizes revealed a product yield distribution comparable with the Prelog strain energy profile (see Chapter 2.5, Figure 12b), indicating a higher reactivity of transannular strained cycloalkanes towards the reaction. Regarding the cycloalkene conversion, dicarboxylic acids of different chain lengths could be synthesized (**41**, **43**, **51**). Other examples are 1,3-cyclopentane diacid **102** from norbornene,

the α,ω-ketocarboxylic acids **103** and **104**, and example **105** derived from the naturally occurring terpene *S*-(−)-limonene (Scheme 14c). Co-electrolysis of both cycloalkane and -alkene of the same ring size (demonstrated on the 8- and 12-membered rings)[190] showed a possibility of simultaneous conversion of both substrate classes, whereby the cycloalkene double bond showed higher reactivity. The adaptability of the reaction conditions was proven by transferring the reaction into a flow electrolyzer, tested on cyclododecene (**56**), where comparable yields were observed for the diacid **51** (batch-type cell: 78%, flow cell: 76%).[190] For industrial purposes, a scale-up (increased amount of substrate), dimethyl carbonate as a non-toxic solvent, and higher current densities (20 mA/cm^2) were applied in flow electrolysis, leading to the formation of **51** in 52% yield.

As a proof of concept for the conversion of biogenic feedstocks, the reaction was applied to linear fatty acids (here: oleic acid (**52**), elaidic acid (**106**) (*E*–*Z* isomers), and methyl oleate (**107**)) which could be converted to pelargonic acid **54**, azelaic acid **53** and monomethyl azelate **108** (Scheme 14e).

Apart from the cyclic substrates and fatty acids, the reaction conditions were tested to convert toluene derivatives to benzaldehydes and benzoic acids. Adjusting the reaction parameters could enable a quite selective conversion either to the aldehyde (isolated via direct derivatization to corresponding semicarbazones) or to the carboxylic acid.[190]

Several additional experiments have been conducted to clarify the reaction mechanism, which is proposed to differ for both substrates, the cycloalkanes and -alkenes (Scheme 14b and 14d). CV studies revealed in both cases the initial oxidation of the supporting electrolyte's anion into a nitrate radical **VI**. Nitrate is, therefore, also the electroactive substance. A Griess test and ion chromatographic measurements show that after electrolysis in an oxygen atmosphere, nitrate is not converted into nitrite during the reaction but acts as a mediator.[190] Reduction of molecular oxygen into superoxide **IX** is the cathodic counter-reaction.[190] Reductive peak potential of oxygen reduction was measured in a range of −1.26 V to −1.02 V (vs. Ag/AgCl), according to literature values.[191] A Karl Fischer titration after electrolysis with cycloalkane being present in the electrolyte showed an increased value of water when the substrate was omitted.[190] A test with titanyl sulfate ($TiOSO_4$) for detecting peroxo compounds showed a characteristic coloring after electrolysis, indicating the formation of hydroperoxide species **X**.[190] An example reaction of cycloalkene **57** in the

absence of oxygen with BDD anode and Ni cathode resulted in signals measured via GC-MS, indicating that the double bond is nitrated, implying the formation of nitrate radicals **IV** during the reaction.[190] HPLC-MS measurements of the reaction solution for the diacid formation indicated aldehyde intermediate **XV** formation.[190]

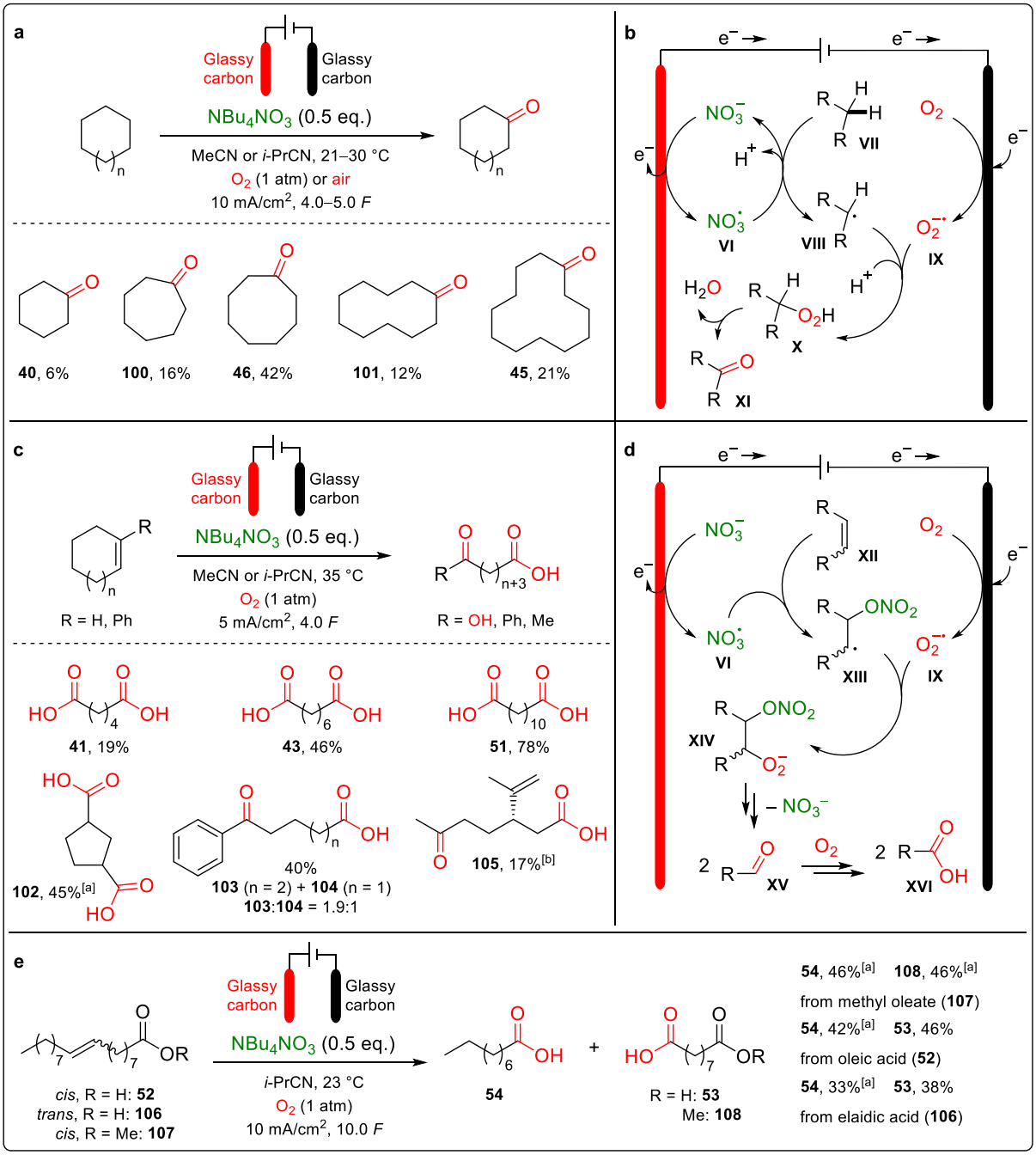

Scheme 14: a General reaction scheme and scope for the oxo-functionalization of cycloalkanes. **b** Proposed reaction mechanism for cycloalkane oxidation based on CV study findings and additional mechanistic studies.[190] **c** General reaction scheme and scope for the C=C double bond cleavage of cycloalkenes to dicarboxylic acids. [a] Reaction at 5 °C. [b] Reaction at 25 °C. **d** Proposed cycloalkene double bond cleavage reaction mechanism based on CV study findings and additional mechanistic studies.[190] **e** Conversion of fatty acid examples to mono and dicarboxylic acids. [a] Yields determined via GC calibration.

Conclusion

A combining method for an oxo-functionalization of cycloalkanes and -alkenes was successfully established. The conditions allow the formation of ketones and dicarboxylic acids in moderate yields without using transition metal catalysts and additional hazardous reagents. Nitrate anions as a component of the supporting electrolyte were used in a dual role as an electrochemical mediator after the model of Figure 9b (Chapter 2.3), which underlines the material efficiency of the method. Molecular oxygen from the atmosphere serves as the oxygen source, which elegantly represents an electroactive species of the cathode reaction. Thus, both electrode reactions are used efficiently for product generation. Furthermore, the conditions can also be applied to the oxidative cleavage of fatty acids to saturated mono- and dicarboxylic acids and for the purpose of benzylic oxidations. The products generated are of great industrial interest, which makes the method an attractive alternative to existing processes.

The results of the electrochemical oxo-functionalization of cyclic alkanes and alkenes have been published in *Nat. Commun*.[190] Detailed information about experimental data can be found in the manuscript (pp. 120–130) and in the supporting information (pp. 131–176), which are included immediately after this section.

nature communications

Article

https://doi.org/10.1038/s41467-023-40259-0

Electrochemical oxo-functionalization of cyclic alkanes and alkenes using nitrate and oxygen

Received: 19 January 2023

Accepted: 14 July 2023

Published online: 28 July 2023

Check for updates

Joachim Nikl[1], Kamil Hofman[1], Samuel Mossazghi[1], Isabel C. Möller[1], Daniel Mondeshki[1], Frank Weinelt[2], Franz-Erich Baumann[2] & Siegfried R. Waldvogel[1]

Direct functionalization of C(sp^3)–H bonds allows rapid access to valuable products, starting from simple petrochemicals. However, the chemical transformation of non-activated methylene groups remains challenging for organic synthesis. Here, we report a general electrochemical method for the oxidation of C(sp^3)–H and C(sp^2)–H bonds, in which cyclic alkanes and (cyclic) olefins are converted into cycloaliphatic ketones as well as aliphatic (di)carboxylic acids. This resource-friendly method is based on nitrate salts in a dual role as anodic mediator and supporting electrolyte, which can be recovered and recycled. Reducing molecular oxygen as a cathodic counter reaction leads to efficient convergent use of both electrode reactions. By avoiding transition metals and chemical oxidizers, this protocol represents a sustainable oxo-functionalization method, leading to a valuable contribution for the sustainable conversion of petrochemical feedstocks into synthetically usable fine chemicals and commodities.

Transforming a chemically inert C(sp^3)–H bond into a functional group is described as a vibrant topic, a great challenge, and even as a holy grail for synthetic organic chemistry[1–3]. Indeed, functionalization and modeling of molecular structures starting from hydrocarbons require the cleavage of carbon–hydrogen or carbon–carbon bonds. Due to the limited preparative application fields, these compounds are commonly used as fuels[4] and organic solvents[5]. Furthermore, alkanes' missing functionalities and lipophilic nature lead to ecological issues since their bioavailability for microorganisms is poor[6]. Naturally occurring monocyclic alkanes were discovered in the 1890s by Markovnikov in Caucasian crude oil called naphtha[7,8]. Cyclohexane, the most prominent example and ubiquitous structural motif in natural and synthetic compounds, is industrially produced via the hydrogenation of benzene[9]. Monocyclic aliphatics with larger ring sizes, especially eight and twelve-membered rings, are formed through cyclooligomerization of butadiene and subsequent hydrogenation[10]. While the fully saturated cyclododecane serves as an essential intermediate for the production of laurolactame via a Bashkirov oxidation to primarily cyclododecanol[11], other saturated cyclic hydrocarbons emerge as by-products and are usually incinerated or discarded. The Bashkirov oxidation mentioned above produces additional reagent waste due to the use of boric acid, which is toxic to reproduction and fertility[12], making it necessary to improve this process towards greater sustainability. Apart from that example, the unsaturated representatives of the same ring size are usually of substantial commercial interest. Cyclohexene, cyclooctene, and cyclododecene serve as important starting materials for synthesizing distinct polymer precursors like dicarboxylic acids, annually produced in several ten thousand tons with strongly increasing demand[13,14]. The incorporation of saturated hydrocarbons back into the value chain provides both economic and also environmental advantages. Therefore, valorization by installing an oxygen-containing group like a carbonyl function leads to synthetic versatility[15].

Over the past decades, different oxo-functionalization methods have been developed (Fig. 1a). Conventional methods for the oxidation of cycloalkanes are predominantly based on transition metal-catalyzed

[1]Department of Chemistry, Johannes Gutenberg University Mainz, Duesbergweg 10–14, 55128 Mainz, Germany. [2]Evonik Operations GmbH, Paul-Baumann-Strasse 1, 45772 Marl, Germany. e-mail: waldvogel@uni-mainz.de

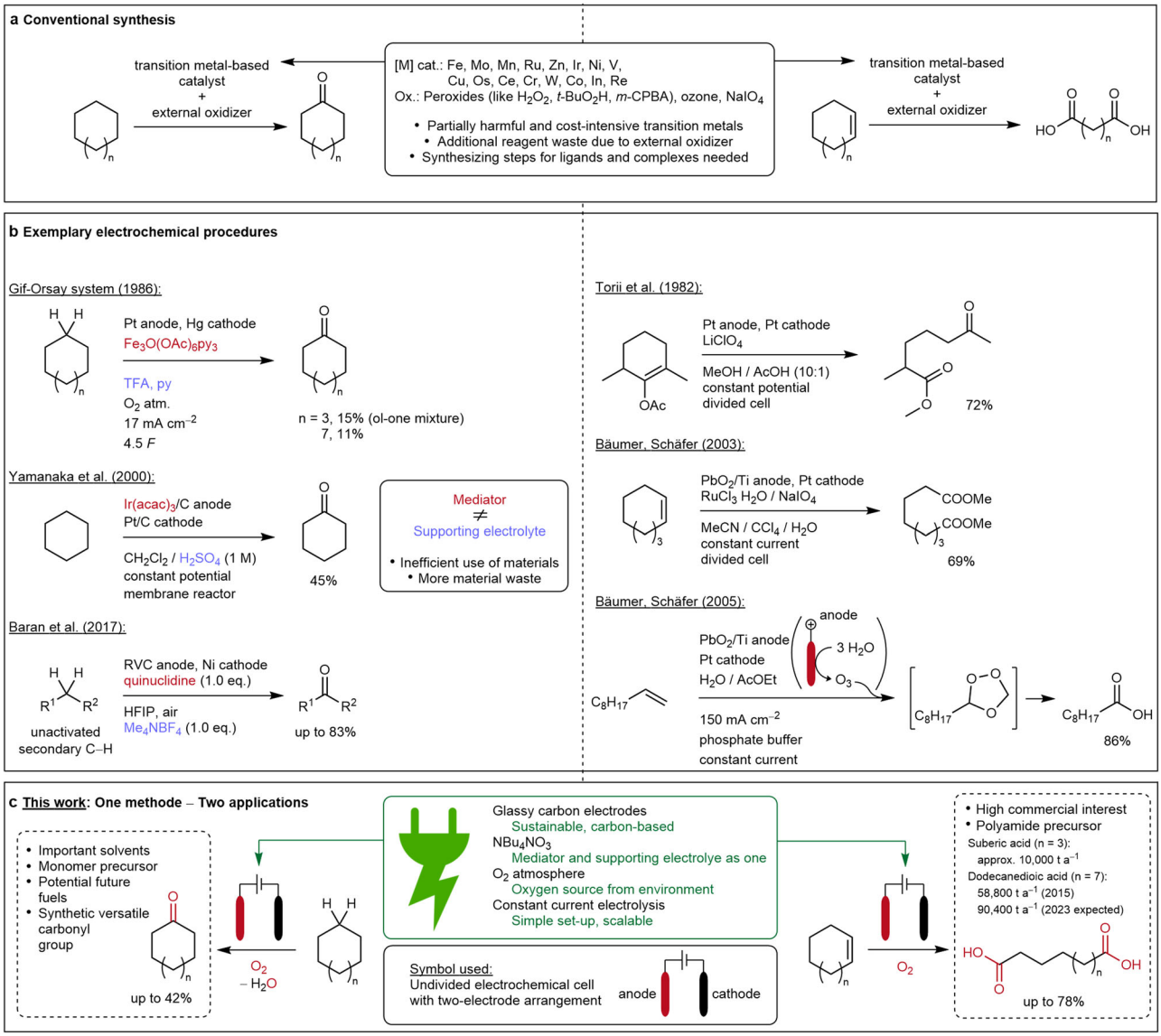

Fig. 1 | Overview of known procedures and the subject of this work. **a** Conventional synthesis protocols for converting cycloaliphatics to ketones and dicarboxylic acids. **b** Known electrochemical procedures for oxo-functionalizing C(sp^3)–H and C=C bonds to ketones and dicarboxylic acids. Mediators labeled in red and supporting electrolytes are labeled in blue. **c** Subject of this work: application of one electrochemical method to valorize saturated and unsaturated cycloaliphatics. Oxygen as O_2 source and oxo-groups are labeled in red.

reactions in combination with chemical oxidizers, mainly peroxides. Frequently, hydrogen peroxide is reported with various catalytically active transition metals such as iron[16], manganese[17], copper, nickel, and vanadium[18]. Ruthenium often serves as a transition metal catalyst in the presence of peracids[19] or *tert*-butyl hydroperoxide[20]. Popular ligand systems are based on porphyrins, including manganese or iron centers, with peroxide species[21] and oxygen[22] as oxidizers. Examples of an iridium catalyst with sodium periodate[23] and an iron(III) nitrate/*N*-hydroxyphthalimide/oxygen system[24] have also been reported.

With regards to C=C double bond cleavage to the corresponding dicarboxylic acids, many conventional methods are already known. Comparable to those previously mentioned, these usually occur in a transition metal-catalyzed manner. Here, osmium[25,26], ruthenium[27,28], and tungsten[29,30] catalysts are most frequently described. Older protocols refer to the use of potassium permanganate[31]. In contrast to these, metal-free processes are also known. For example, via hypervalent iodine species in combination with peracids or oxone[32,33], or classically, via the ozonolysis reaction[34].

Electrochemical protocols for oxidizing C(sp^3)–H bonds to ketones have scarcely been described (Fig. 1b). The Gif-Orsay system, developed in the 1980s, serves as an example[35,36]. Also, using an electrocatalytic MnO_x layer on a titanium anode with oxygen[37] or the oxidation of cyclohexane with water on an iridium-supported carbon anode[38] was reported. The group of Baran published 2017 an electrochemical protocol for C(sp^3)–H oxidation via quinuclidine as a mediator in the presence of oxygen[39]. Adversely, the method is unsuitable for technical scale applications as the solvent, 1,1,1,3,3,3-hexafluoropropan-2-ol (HFIP), has approximately 200 times higher global warming potential (GWP_{100}) than carbon dioxide[40]. Just as with alkanes, only a few electrochemical methods for the double bond cleavage to dicarboxylic acids are known (Fig. 1b), as shown by Schäfer and Bäumer via ruthenium catalysis with electrochemically regenerated periodate[41]. The authors also described electrochemical ozonolysis from water using a lead dioxide anode[42]. Older electrochemical methods use methanol as an oxygen source at a constant potential in a divided cell[43]. The disadvantages of the methods mentioned above

relate to using toxic or, due to their mining, socially and environmentally problematic transition metals[44]. Furthermore, the use of ligands and greater than a stoichiometric amount of oxidizers leads to reagent waste. The known electrochemical processes often use expensive or toxic electrode materials or require a high material input due to the separate roles of electrochemical mediator and supporting electrolyte, devaluing the economic efficiency of these protocols.

With the method presented in this work, both a direct oxo-functionalization of chemically stabile C(sp^3)–H bonds and a cleavage of C=C double bonds to carbonyl and carboxyl compounds can be implemented by using electric current as a clean and safe reagent[45] (Fig. 1c). In terms of sustainability and resource preservation, the use of transition metals and additional oxidizing agents is avoided[46,47]. Furthermore, the method is characterized by the effective use of materials through the dual use of the supporting electrolyte as an electrochemical mediator[48]. Here, the initial anodic oxidation of nitrate anions serves as a radical source, inspired by literature reports[49–51]. Commonly described oxygen reduction to superoxide radicals was found to be the cathodic counter reaction[52,53], completing the electric cycle in a convergent-type electrolysis[54]. Advantageously, the supporting electrolyte can be recovered by extraction and reused for electrolysis, which further supports the sustainability of this electrochemical procedure (see Supplementary Results 2.7). The products are important substrates for organic synthesis and monomer building blocks for polymers and, therefore, highly relevant for industrial applications.

Results

Reaction development

Electrochemical oxidation of saturated hydrocarbons is a very challenging task for several reasons. Direct oxidation of these chemically inert species on the electrode surface is difficult due to their high oxidation potentials[39]. Usually, the electrolyte, consisting of the solvent and the supporting electrolyte salt, is oxidized prior to these substrates. Furthermore, polar solvents with high permittivity are required to avoid high ohmic resistance within the electrochemical cell. Very lipophilic substrates like saturated hydrocarbons frequently display poor solubility in these solvents. Therefore, a suitable strategy is a mediated electrochemical system in which the mediator is transformed into a highly reactive species that allows the target reaction to occur.

As a set-up, a commercially available electrochemical screening system from IKA was used, which was co-developed[55] (see Supplementary Fig. 1). Inspired by literature[51], we focused upon the use of nitrate salts as supporting electrolyte and electrochemical mediator in a dual role since upon oxidation the highly reactive nitrate radicals can split C(sp^3)–H bonds. In initial reactions of converting cyclooctane (**1c**) as a model substrate to cyclooctanone (**2c**), tetra-butylammonium (TBA) nitrate proved itself suitable. Commercially available acetonitrile, a common solvent in electro-organic applications, was used without further purification. Glassy carbon was used as a robust, long-term durable electrode material with excellent electric conductivity properties.

The first experiments were conducted with ambient air in the gas space above the reaction solution. Due to the manufacturing design, the lid used for the electrochemical cell ensures an air exchange with the environment. Cyclooctane (**1c**) was electrolyzed using 10 mA cm^{-2} and a charge of 4 *F*, leading to a 23% yield of **2c** (Table 1, Entry 2). The reaction proved selective, as only cyclooctanol (**3c**) and cyclooctane-1,4-dione (**4c**) were obtained as significant by-products with 2% and 3% yields, respectively. If the reaction was carried out at 100 vol% of N_2, no reaction to oxidized species occurred (Table 1, Entry 3), which underlines the necessity of O_2 in the reaction medium. Increasing the O_2 content in the atmosphere to 100 vol% remarkably led to only 16% of **2c** (Table 1, Entry 1). The decreased yield is assumed to be caused by mutual influences of the atmospheric O_2 amount and the applied current density. However, a maximum yield of 31% was obtained for **2c** under 20 vol% O_2 and 10 mA cm^{-2} (Table 1, Entry 4).

The necessity of nitrate as the anion is demonstrated by comparison with other TBA salts. Tetrafluoroborate (BF_4^-), hexafluorophosphate (PF_6^-), and perchlorate (ClO_4^-) anions only lead to a formation of **2c** in yields of 3–4%. Apart from TBA as the cation, also longer chained tetra-alkylammonium nitrate salts provided product formation in comparable yields of 17–28% (see Supplementary Table 1), and also tetra-butylphosphonium nitrate was suitable with 20% (Table 1, Entry 7). Furthermore, the reaction takes place in different solvents like isobutyronitrile (*i*-PrCN) (24%), acetone (29%), and nitropropane (17%) (see Supplementary Table 1). The stirring rate significantly influences the reaction as a yield drop appears at higher and lower stirring rates than 350 rpm (see Supplementary Table 1). This circumstance is attributed to a disturbed O_2 adsorption on the electrode at higher stirring rates and the reduced reaction partner contact due to lower stirring rates. The reaction also occurs with lower yields at different carbon-based electrodes like boron-doped diamond (BDD) and graphite (see Supplementary Table 1).

Application of the same methodology to cyclic alkenes **5** revealed that they undergo C=C double bond cleavage. Following the observation of a dicarboxylic acid **6** via HPLC-MS, the reaction conditions were varied using cyclooctene (**5b**) as a model substrate. Applying the same standard conditions as for the cyclooctane oxidation led to a 33% yield of suberic acid (**6b**), while lowering the temperature to 5 °C led to 47% (Table 1, Entries 1 and 8). Increasing the charge to 8 *F* caused a yield drop to 28% (Table 1, Entry 9). The exclusion of O_2 showed no formation of a dicarboxylic acid, indicating the necessity for atmospheric oxygen, like for the ketone formation (Table 1, Entry 3). Decreasing the substrate concentration and the current density to 0.05 mol L^{-1} and 5 mA cm^{-2} by varying the applied charge from 4 *F* to 6 *F* and 8 *F* led to similar yields of 39–44% (Table 1, Entries 10, 11, and 12). Using isobutyronitrile as a solvent did not influence the yield (Table 1, Entry 13).

Besides the reaction development trials on **5b**, a further intensified optimization has been carried out with cyclododecene (**5c**) since it results in the highly industry-relevant dodecanedioic acid (**6c**) (see Supplementary Table 2). Due to the poor solubility of **5c** in acetonitrile, the reactions were conducted in isobutyronitrile. Decreasing the substrate concentration and the current density to 0.05 mol L^{-1} and 5 mA cm^{-2} led to the best conditions for forming **6c** with a yield of 78%. As molecular oxygen can act as an oxidizing agent, it is noteworthy that the reaction does not occur if no electricity is applied to the reaction mixture (see Supplementary Table 2).

Scope, batch-type, and flow electrolysis

After varying several reaction parameters with the model substrates for both reaction types, scale-up reactions, and different substrates were tested to investigate the method's applicability. A scale-up experiment regarding the cyclooctane oxidation was performed in a 50 mL round-bottom flask under an air atmosphere providing ketone **2c** in a yield of 35% (see Supplementary Fig. 2a). However, an improved yield of **2c** could be achieved by using a three-necked 100 mL round-bottom flask (see Supplementary Fig. 2b) and pure oxygen atmosphere, to receive **2c** in a yield of 42%. The increased yield can be explained by the different cell set-up allowing a larger contact area between the oxygen-containing atmosphere and the reaction solution. Next, we used this set-up to explore the oxidation of cyclic alkanes containing six to twelve methylene groups (Fig. 2a). In comparison, the yield of cyclooctanone (**2c**) stayed the highest. Smaller and larger ring sizes seem more challenging to convert as mostly starting material remained after electrolysis. Remarkably, compared to the increasing ring sizes, the general trend regarding the ketone yields is approximately following the transannular Prelog strain[56], as cyclohexanone (**2a**, 6% yield) and cyclododecanone (**2e**, 4% yield) gave the lowest

https://doi.org/10.1038/s41467-023-40259-0

Table 1 | Chosen condition examples for the reaction development

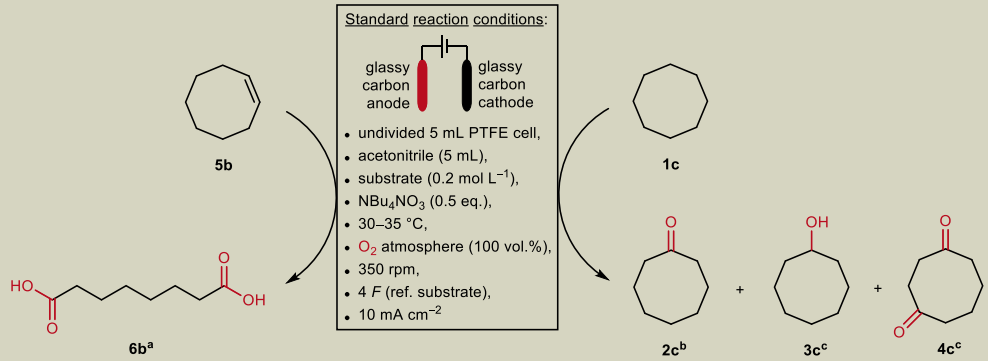

Entry	6b[a]	Deviations from conditions	2c[b]	3c[c]	4c[c]
1	33%	None	16%	1%	1%
2	40%	Air	23%	2%	3%
3	0%	O_2/N_2 = 0/100	0%	0%	0%
4	37%	O_2/N_2 = 20/80	31%	1%	6%
5	Traces	O_2/N_2 = 20/80, NBu_4PF_6	3%	2%	1%
6	Traces	O_2/N_2 = 20/80, acetone	29%	2%	4%
7	21%	PBu_4NO_3	20%[d]	0%	7%
8	47%	5 °C	14%[d]	1%	1%
9	28%	5 °C, 8 *F*	18%[d]	0%	9%
10	41%	substrate (0.05 mol L^{-1}), 5 mA cm^{-1}	12%[d]	1%	1%
11	44%	6 *F*, substrate (0.05 mol L^{-1}), 5 mA cm^{-1}	14%[d]	1%	1%
12	39%	8 *F*, substrate (0.05 mol L^{-1}), 5 mA cm^{-1}	15%[d]	1%	2%
13	46%	*i*-PrCN, substrate (0.05 mol L^{-1}), 5 mA cm^{-1}	15%[d]	1%	2%

Oxygen as O_2 source and oxo-groups are labeled in red. *i*-PrCN: isobutyronitrile. For preparative information, see Methods: "Electrolysis in 5 mL PTFE cells (GP 1)".

[a]Isolated yields.

[b]^{1}H NMR yield (internal standard: 1,3,5-trimethoxybenzene).

[c]GC yields are calculated based on the yield of **2c**.

[d]GC yields (external calibration of **2c**, 1,3,5-trimethoxybenzene as internal standard).

https://doi.org/10.1038/s41467-023-40259-0

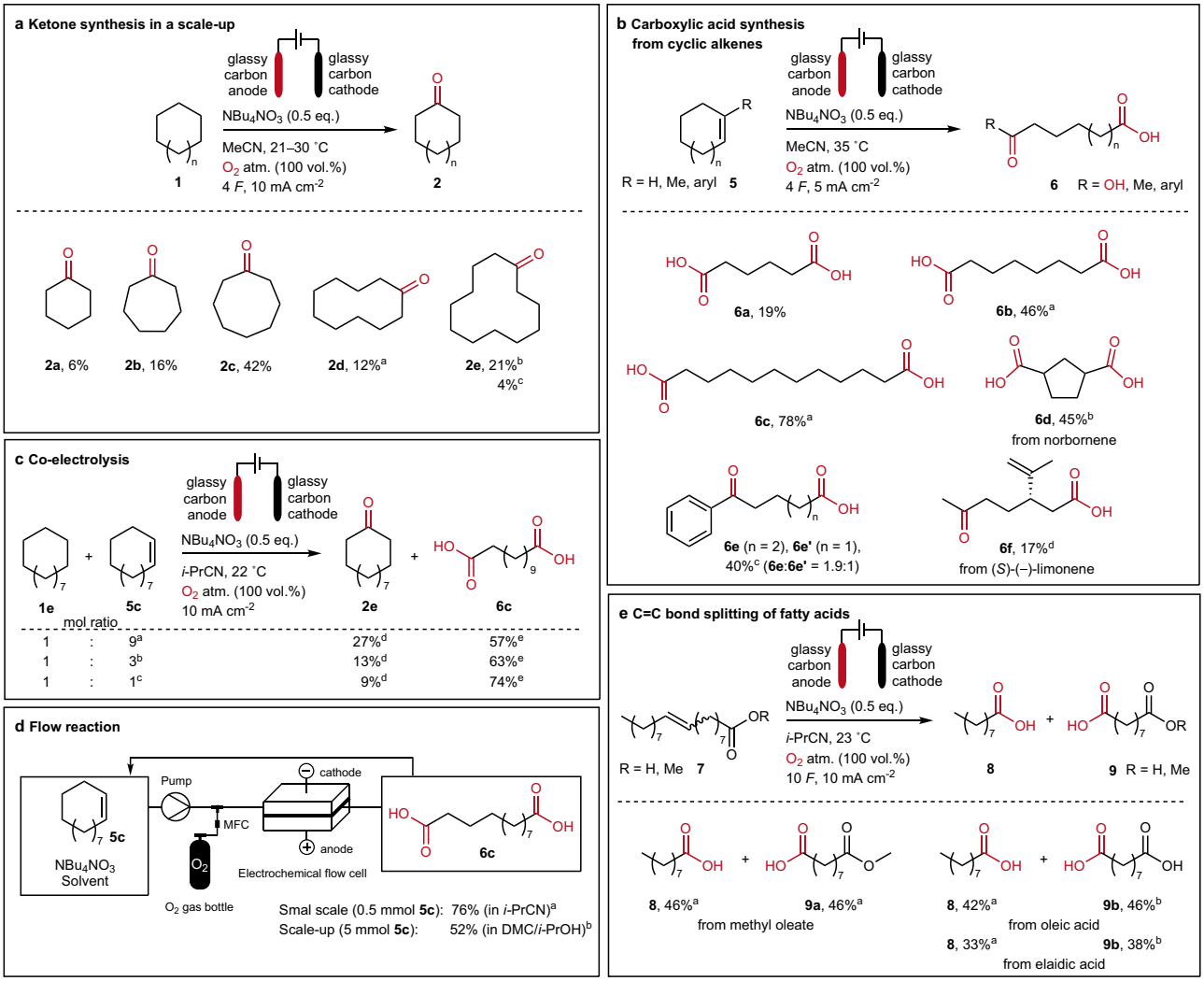

Fig. 2 | Scope of ketones and (di)carboxylic acids, including batch and flow processes. Unless separately indicated, all yields are isolated. Oxygen as O_2 source and oxo-groups are labeled in red. atm.: atmosphere. **a** Conditions: 100 mL round-bottom flask, acetonitrile (MeCN, 25 mL), substrate (0.2 mol L^{-1}), 400 rpm. [a]5 *F*. [b]Isobutyronitrile. [c]50 °C, air atmosphere. **b** Conditions: undivided 5 mL PFTE cell, acetonitrile (MeCN, 5 mL), substrate (0.05 mol L^{-1}), 350 rpm. [a]Isobutyronitrile. [b]5 °C. [c]Combined yield ratio determined via ^{1}H NMR. [d]25 °C. **c** Conditions: undivided 5 mL PFTE cell, isobutyronitrile (*i*-PrCN, 5 mL), NBu_4NO_3 (0.1 mol L^{-1}, 0.5 eq. toward combined mol of **1e** and **5c**), 350 rpm. [a]**1e** 0.02 mol L^{-1}, **5c** 0.18 mol L^{-1}, 7,6 *F*. [b]**1e** 0.05 mol L^{-1}, **5c** 0.15 mol L^{-1}, 7 *F*. [c]**1e** 0.1 mol L^{-1}, **5c** 0.1 mol L^{-1}, 6 *F*. [d]Yields are determined via GC calibration and refer to mol% of **1e**. [e]Isolated yields refer to mol% of **5c**. **d** Flow reactions were carried out using an IKA flow cell with a 2 × 6 cm^2 anode surface. [a]Conditions: glassy carbon anode and cathode, isobutyronitrile (*i*-PrCN, 10 mL), substrate (0.05 mol L^{-1}), NBu_4NO_3 (0.5 eq.), 20 °C, O_2 atmosphere (100 vol%), electrolyte flow: 10 mL min^{-1}, gas flow: 10 mL min^{-1}, 4 *F* (ref. substrate), 5 mA cm^{-2}. [b]Conditions: glassy carbon anode and cathode, dimethyl carbonate (DMC)/isopropanol (*i*-PrOH) 9:1 (9.12 mL), substrate (0.5 mol L^{-1}), NBu_4NO_3 (1 eq.), 50 °C, O_2 atmosphere (100 vol%), electrolyte flow: 18 mL min^{-1}, gas flow: 20 mL min^{-1}, 2 *F* (ref. substrate), 20 mA cm^{-2}. MFC: mass flow controller. **e** Conditions: undivided 5 mL PFTE cell, isobutyronitrile (*i*-PrCN, 5 mL), substrate (0.1 mol L^{-1}), 350 rpm. [a]Yields determined via GC calibration. [b]Isolated yields.

yields compared to cyclooctanone (**2c**, 42% yield). Because of the poor solubility of cyclododecane (**1e**) in acetonitrile, the solvent was replaced by isobutyronitrile, yielding 21% of cyclododecanone (**2e**). Applying the reaction to branched cycloalkanes leads to a mixture of various oxidation products, with general selectivity toward forming ketones rather than alcohols (see Supplementary Results 2.8).

The reactions for cycloalkenes 5a-e, portrayed in Fig. 2b, were carried out in 5 mL PTFE cells under 100 vol% oxygen atmosphere, since here the best result for cyclododecene (**5c**) oxidation was observed (Fig. 2b). Besides of suberic acid (**6b**, 46% yield) and dodecanedioic acid (**6c**, 78% yield) also adipic acid (**6a**) could be synthesized in 19%. As an example of a bicyclic substrate, norbornene led to the formation of 1,3-cyclopentane diacid (**6d**) with a 45% yield. In addition to the formation of α,ω-diacids from disubstituted cycloalkenes, α,ω-ketocarboxylic acids **6e** can be obtained from trisubstituted cycloalkenes. As an example of naturally occurring terpenes, (*S*)-(−)-limonene could also be converted to the corresponding keto-carboxylic acid **6f**, with a yield of 17%, which is comparable to that of adipic acid (**6a**) from cyclohexene (**5a**).

Cycloalkenes of technical grade contain fully saturated analogs as impurities from industrial synthesis steps to specific percentages. Conversion of impure starting materials is beneficial for an industrial application if the impurities do not interfere with the target reaction. To test the applicability of this protocol, a co-electrolysis of **1e** and **5c** has been successfully performed, whereby the yields of ketone **2e** and dicarboxylic acid **6c** depend on the composition of the starting materials (Fig. 2c). For example, the yield of cyclododecanone (**2e**) increases with lower molar amounts of cyclododecane (**1e**) within the substrate composition, and vice versa. The same observation has been made for the unsaturated ring **5c** and the diacid **6c**. Despite that, both substrates can be specifically converted into the ketone or diacid in parallel. A further co-electrolysis example for cyclooctane (**1c**) and

cyclooctene (**5b**) is given in Supplementary Table 3. Here the received products show generally lower yields with 2–4% of cyclooctanone (**2c**) and 40–45% of suberic acid (**6b**).

Besides batch-type electrolysis, flow electrolysis methods are becoming increasingly popular due to the inherent advantages of continuous process control[57,58]. The adaptability of the presented method towards different cell and process designs is presented by conducting the dicarboxylic acid synthesis also in an electrochemical flow set-up (Fig. 2d). These experiments were carried out by pumping the electrolyte through the cell in a cyclic manner until a charge amount of 2–4 *F* was applied[59]. A small-scale trial with cyclododecene (**5c**) in a concentration of 0.05 mol L^{-1} in isobutyronitrile led to a dodecanedioic acid (**6c**) formation of 76%. For larger technical applications, the solvent was exchanged, and a scale-up was pursued. After a few variation trials within the same set-up (see Supplementary Table 4), the reaction could be optimized with a non-toxic dimethyl carbonate/isopropanol (DMC/*i*-PrOH) mixture and a substrate concentration of (0.5 mol L^{-1}) to yield **6c** in 52%.

With the presented method, not only cyclic alkenes **5** but also linear alkenes, here fatty acids **7**, can be converted to their corresponding acids (Fig. 2e). The reaction was performed with elaidic acid and oleic acid, as prominent examples for fatty acids, which only differ from their *E-Z* isomerism. Furthermore, the corresponding methyl oleate, a component of biodiesel, was used to investigate the stability of ester groups under the applied conditions. In all cases, the double bond cleavage successfully led to pelargonic acid (**8**), azelaic acid (**9b**), and mono-methyl azelate (**9a**), respectively, with yields between 33 and 46%.

Mechanistic studies

Instrumental and wet-chemical experiments were carried out to uncover mechanistic detail, which is schematically illustrated in Fig. 3a–c. The initial electrochemical step is assigned to the nitrate oxidation, as shown via cyclic voltammetry experiments (Fig. 3d, e). The formation of nitrate radicals could be proved via a radical quenching experiment conducted on cyclooctene (**5b**) under an argon atmosphere to avoid an oxygen reduction reaction. Among several unidentified materials, the nitrated intermediates **10b** and **11b** were detected via GC-MS; their formation is illustrated by the mechanistic proposal shown in Fig. 3f. Further GC-MS analysis results are given in Supplementary Fig. 17. The conclusion that nitrate serves as a mediator due to its reformation after oxidation to a radical is supported by anion chromatography measurements. After electrolysis and an extraction workup, only nitrate remains in the aqueous layer (Fig. 3g). Furthermore, nitrate is not getting electrochemically reduced to nitrite as shown by an anion chromatography measurement (see Supplementary Fig. 15), and a negative Griess test (Fig. 3h). Instead, the cathodic counter reaction is provided by reduction of dissolved oxygen, that originates from the atmosphere above the reaction solution (Fig. 3i). The resulting superoxide radical anions that are presumably stabilized by lipophilic organic cations like TBA[60] are assumed to react with the hydrocarbon radicals to peroxide intermediates. A peroxide-specific detection test using titanyl sulfate[61,62] showed a positive result for these species directly after electrolysis, as a yellowish coloring of the specific peroxotitanyl ion $(TiO_2)^{2+}$ appears, comparable to the test with other hydroperoxides (Fig. 3j). The dissolved oxygen concentration at a partial pressure of 1 atm has been determined by cyclic voltammetry studies and applying the Randles-Ševčík equation (see Supplementary Note 3.1). At 100 vol% of O_2 in the reaction atmosphere, a concentration of 9.5 ± 0.4 mmol L^{-1} was observed, comparable to literature values[63]. Furthermore, a steady pH value before and after the reaction of 5–6 was observed with standard pH indicator paper, implying no drift into an acidic or alkaline environment (see Supplementary Fig. 16). Carrying out electrolysis with cyclooctane (**1c**) substrate revealed an increased water content compared to the one without a substrate after electrolysis (Fig. 3k). Measurements were conducted using a Karl Fischer titration method (see Supplementary Note 3.2.5). For the C=C double bond cleavage, an addition of the nitrate radical onto the double bond is proposed, according to the findings of the control experiment (Fig. 3f) and to literature descriptions[64]. Further reaction with a superoxide radical lead via an unknown pathway to the formation of aldehydes (Fig. 3b) that are obtained as possible intermediates regarding an HRMS analysis observation of the crude reaction mixture after electrolysis of **5c** to **6c** (see Supplementary Fig. 13). Afterwards, literature described autooxidation like mechanism from aldehydes to carboxylic acids is assumed to occur[65] (Fig. 3c). The oxidation of free carboxylic acids as a competing anodic reaction to nitrate oxidation was not observed (see Supplementary Fig. 18c). The possibility of cathodic hydrogen formation, which is a potential hazard when combined with oxygen, was considered unlikely based on the aprotic conditions applied for the reactions and cyclic voltammetry experiments on the reductive behavior of the electrolyte systems (see Supplementary Note 3.2.7). Dissolved oxygen is preferentially reduced in the applied electrolyte systems over protic solvent additives such as 2-propanol and water. Studies on this method's potential large-scale application are subject of further investigation.

Further method application

To demonstrate the broad applicability of the presented method, the substrate scope was successfully extended to toluene substrates **12**. Benzylic oxidation to either the benzaldehydes **13'**, including subsequent derivatization with semicarbazide hydrochloride **15** to the corresponding semicarbazones **13**, or the benzoic acids **14** could be promoted selectively via tuning the reaction conditions (Fig. 4a). Reaction monitoring via ^{1}H NMR spectra shows the aldehyde as an intermediate, which is further converted to the corresponding carboxylic acid when the toluene substrate is almost entirely converted (Fig. 4b). No intermediates containing an alcohol group were observed. Optimization reactions were carried out in undivided 5 mL PTFE cells (see Supplementary Table 5), while a 25 mL beaker-type glass cell was used for the scale-up reactions. Suitable conditions for the aldehyde formation differ significantly from those for the acid formation by changing the current density, the charge quantity, and the substrate concentration. By applying conditions of 10 mA cm^{-2}, 5 *F*, and 0.02 mol L^{-1} of **12**, the reaction can be stopped after the selective formation of the benzaldehyde **13'**. When these parameters are increased to 30 mA cm^{-2}, 7–12 *F*, and 0.1 mol L^{-1} of **12**, the formation of benzoic acid **14** can be promoted. Mainly methylated toluenes (xylenes) were chosen as substrates, to investigate over-oxidation reactions at the remaining benzylic positions. Only one methyl group is selectively oxidized to the aldehyde and then further into the carboxylic acid. As by-products of the benzoic acid synthesis, *N*-acetylbenzamides **14'** were obtained in a 3–4% yield range. Presumably, acyl radicals are formed as described in Fig. 3c, which react with acetonitrile as a radical scavenger and are further oxidized to **14'** (see Supplementary Fig. 19). Derivatization of the aldehydes to semicarbazones **13** was carried out on the one hand, to prevent further autooxidation of the aldehyde and therefore falsification of the yield determination, and on the other hand to provide a simple protocol for semicarbazone **13** synthesis. Semicarbazones show pharmacological versatility and are known for their anticonvulsant[66,67] and potential anticancer[68] properties.

Discussion

In conclusion, one simple, sustainable approach was developed to facilitate two challenging electrochemical oxidation reactions. With the presented method, cyclic alkanes and (cyclic) alkenes can be oxidized into ketones and (di)carboxylic acids, respectively. The overall moderate yields are balanced by the resource and material saving advantages, like the dual role usage of supporting electrolyte and

https://doi.org/10.1038/s41467-023-40259-0

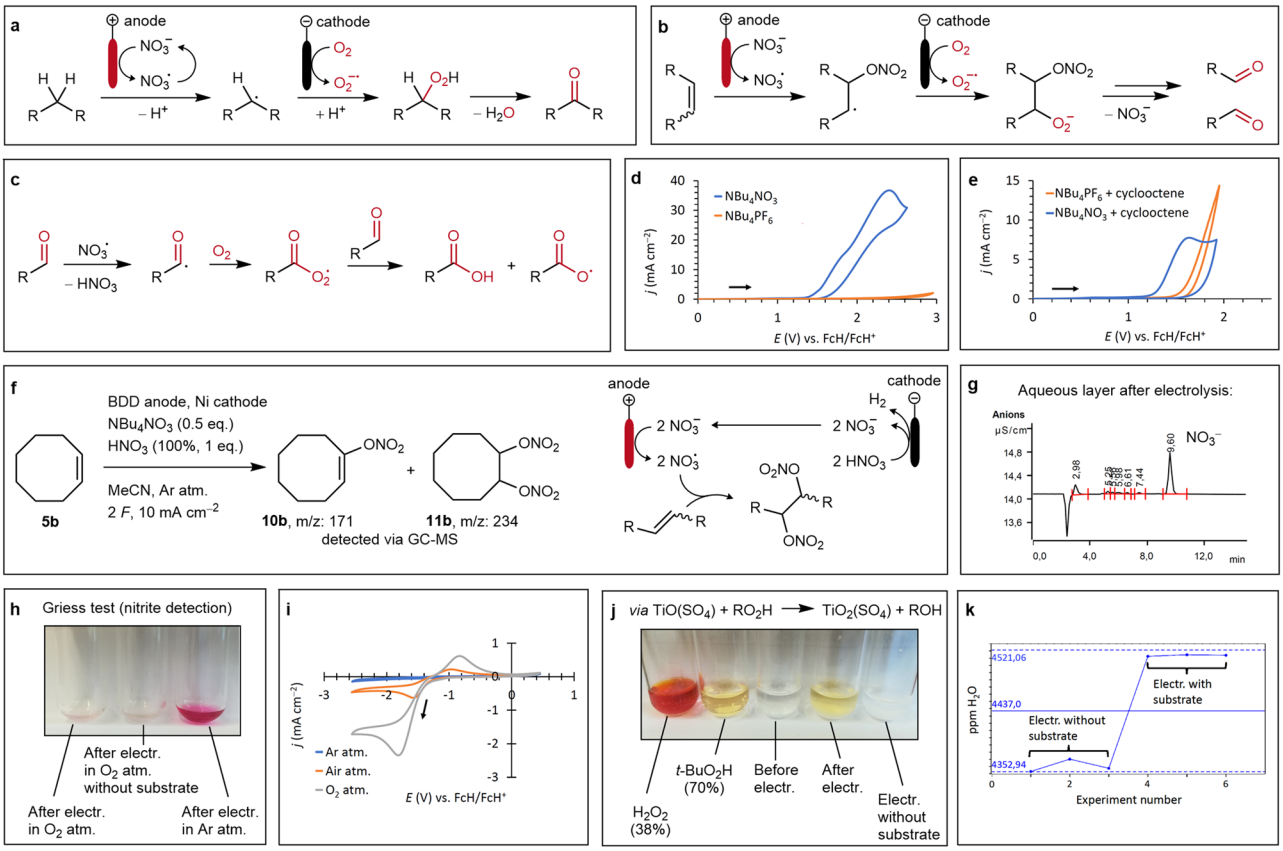

Fig. 3 | Mechanistic studies and proposal. atm.: atmosphere, electr.: electrolysis. Oxygen as O_2 source and oxo-groups are labeled in red. **a** Schematic, mechanistic proposal for cycloalkane oxidation. **b** Schematic, mechanistic proposal for alkene double bond cleavage. **c** Schematic, mechanistic proposal for further oxidation of aldehyde species to carboxylic acids. **d** Cyclic voltammetry of nitrate anion oxidation compared with PF_6^-. Electrolyte: acetonitrile (5 mL), NBu_4NO_3 (0.1 mol L^{-1}), or NBu_4PF_6 (0.1 mol L^{-1}). Conditions: glassy carbon disk (working electrode, 3 mm diameter), glassy carbon rod (counter electrode), Ag/AgCl in saturated LiCl/EtOH (reference electrode), Ferrocene/Ferrocenium (FcH/FcH^+) as internal reference ($E_{1/2}$ = 0.55–0.57 V), 50 mV s^{-1}. **e** Cyclic voltammetry of nitrate anion oxidation compared with PF_6^- in the presence of cyclooctene **5b**. Electrolyte: see Fig. 3d, **5b** (0.2 mol L^{-1}). Conditions: see Fig. 3d, ($E_{1/2}(FcH/FcH^+)$ = 0.55–0.58 V). **f** Quenching experiment in an undivided 5 mL PTFE and schematic mechanism proposal for the formation of nitrated species. MeCN: acetonitrile. For further information, see Supplementary Note 3.2.6. **g** Anion chromatography of the aqueous layer after extractive workup. For preparative information, see Methods: Workup procedure for cyclic ketones and benzaldehydes. **h** Griess test for nitrite detection is negative if the reaction solution is exposed to an O_2 atmosphere (100 vol%) and positive under argon. See Supplementary Note 3.2.1 for detailed protocol. **i** Cyclic voltammetry of oxygen reduction in argon (blue line), air (orange line), and oxygen (gray line) atmosphere above the electrolyte solution. Electrolyte: acetonitrile (5 mL), NBu_4NO_3 (0.1 mol L^{-1}). Conditions: see Fig. 3d, ($E_{1/2}(FcH/FcH^+)$ = 0.55 V). **j** Peroxide test with titanyl sulfate. See Supplementary Note 3.2.4 for detailed protocol. **k** Karl Fischer titration after electrolysis of the reaction solution. See Supplementary Note 3.2.5 for detailed protocol.

electrochemical mediator. Atmospheric oxygen is crucial for the reaction's success, making additional oxidizing agents redundant. No transition metal use is needed for the procedure, as even the electrode material is based on simple glassy carbon. Furthermore, the method shows widely applicable oxo-functionalization properties, as an application for benzylic oxidation successfully led to aldehydes and benzoic acids. This work provides a valuable contribution to sustainable, preparative chemical processes and allows the production of industrially relevant chemicals for large-scale technical plastics production.

Methods

Generated data on experimental procedures can be retrieved from this section and the Supplementary Information.

Electrolysis in 5 mL PTFE cells (GP 1)

The electrolysis set-up is commercially available as IKA Screening System from IKA-Werke GmbH & Co. KG, Staufen, Germany. Gas distributor and associated caps can be purchased separately from IKA. In a 5 mL undivided PFTE cell with a magnetic stirrer, the substrate (0.25–1 mmol) and the supporting electrolyte (NBu_4NO_3, 0.5 eq.) are dissolved in acetonitrile or isobutyronitrile (5 mL). The cell is equipped with a cap, including a gas adapter, where two glassy carbon electrodes (7 cm × 1 cm × 0.3 cm) are fixed at a distance of 0.5 cm from each other. The immersed electrode surface is 1.8 cm^2. The cell is fixed in a stainless-steel set-up, and while stirring, the atmosphere within the cell is filled with oxygen gas (2.5 technical grade, purity ≥99.5%). During electrolysis, a constant flow of oxygen of 20 mL min^{-1} into the cell is ensured. Constant current electrolysis with a current density of 5–10 mA cm^{-2} and an applied charge of 4–8 F is performed. For set-up information, see Supplementary Fig. 1.

Electrolysis in a 100 mL round-bottom flask (GP 2)

In a 100 mL three-necked round-bottom flask with an NS29 Teflon plug incl., electrode holders, magnetic stirrer, and bubble counter, the substrate (5 mmol) and supporting electrolyte (NBu_4NO_3, 0.5 eq.) are dissolved in acetonitrile or isobutyronitrile (25 mL). The cell is equipped with two glassy carbon electrodes (3 cm × 1 cm × 0.3 cm), fixed at a distance of 0.5 cm from each other. The immersed electrode surface is 1.3 cm^2. While stirring, the atmosphere within the cell is filled with oxygen gas (2.5 technical grade, purity ≥99.5%). During electrolysis, a constant flow of oxygen of 20 mL min^{-1} into the cell is ensured.

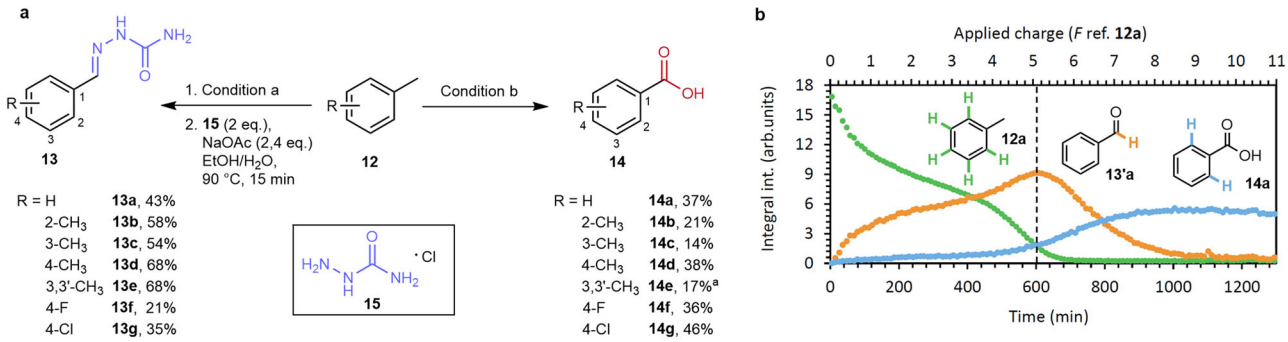

Fig. 4 | Benzylic oxidation as a further application of the method. a Oxidation of toluene substrates to either semicarbazones **13** (semicarbazide moiety in blue) via benzaldehydes or to benzoic acids **14** (carboxyl group in red). Yields are isolated. Condition a: undivided 25 mL beaker-type cell, glassy carbon anode, and cathode, acetonitrile (25 mL), NBu_4NO_3 (1 eq.), substrate (0.02 mol L^{-1}), 33 °C, O_2 atmosphere (100 vol%), 400 rpm, 5 *F*, 10 mA cm^{-2}. Condition b: undivided 25 mL beaker-type cell, glassy carbon anode, and cathode, acetonitrile (25 mL), NBu_4NO_3 (0.5 eq.), substrate (0.1 mol L^{-1}), 27 °C, O_2 atmosphere (100 vol%), 500 rpm, 12 *F*, 30 mA cm^{-2}. [a]7 *F*. **b** Reaction monitoring via a 60 MHz NMR benchtop spectrometer. The ^1H integral intensity was normalized to one proton for better comparison. Recorded tracks of the corresponding protons are assigned by colors (green dots: aromatic protons of **12a**, orange dots: aldehydic proton of **13'a**, blue dots: aromatic protons in the *ortho* position of **14a**).

Constant current electrolysis with a current density of 10 mA cm^{-2} and an applied charge of 4–8 *F* is performed at 20–30 °C. For set-up information, see Supplementary Fig. 2.

Electrolysis in 25 mL beaker-type glass cells (GP 3)

The cells are commercially available as SynLectro™ Electrolysis Platform from Sigma-Aldrich (Merck KGaA, Darmstadt, Germany). In a 25 mL beaker-type glass cell with gas inlet attachment, an NS45/40 Teflon plug incl., electrode holders, and magnetic stirrer, the substrate (0.5–5 mmol) and supporting electrolyte (NBu_4NO_3, 0.5–1 eq.) are dissolved in acetonitrile (25 mL). The cell is equipped with two glassy carbon electrodes (7 cm × 1 cm × 0.3 cm), fixed at a distance of 0.5 cm from each other. The immersed electrode surface is 4.5 cm^2. While stirring, the atmosphere within the cell is filled with oxygen gas (2.5 technical grade, purity ≥99.5%). During electrolysis, a constant flow of oxygen of 20 mL min^{-1} into the cell is ensured. Constant current electrolysis with a current density of 10–30 mA cm^{-2} and an applied charge of 5–13 *F* is performed at 27–33 °C. For set-up information, see Supplementary Fig. 3.

Electrolysis in a flow cell (GP 4)

The electrolysis set-up is made in the university's machine shop[69,70] and is commercially available as IKA ElectraSyn flow. A peristaltic Ismatec Reglo ICC with a TYGON 2765-175 (ID 2.06 mm) hose was used as pumping system. The undivided flow cell was equipped with glassy carbon electrodes (2 × 6 cm^2). In a 20 mL snap cap vial, the substrate (0.5–5 mmol) and supporting electrolyte (NBu_4NO_3, 0.5–1 eq.) are dissolved in isobutyronitrile or a dimethyl carbonate/isopropanol mixture (10 mL). The reaction solution is pumped with 10–18 mL min^{-1} through a t-piece, where oxygen gas is passed through with 10–20 mL min^{-1}. The combined, segmented flow is pumped through the flow cell (electrode gap: 0.05 cm) back into the snap cap vial in a cycling operation mode. Constant current electrolysis with a current density of 5–20 mA cm^{-2} with an applied charge of 2–4 *F* is performed at 20–50 °C, whereby the reservoir is exposed to the heating. During electrolysis, a constant flow of oxygen into the t-piece is ensured. For set-up information, see Supplementary Fig. 4.

Workup protocol for (di)carboxylic acids and benzoic acids

After electrolysis, the solvent is recovered by distillation under reduced pressure. The low-boiling starting material leftover can be recovered by extraction with n-pentane out of the nitrile distillate and monitored via thin-layer chromatography (TLC). The distillation residue is dissolved in ethyl acetate (10 mL) and extracted with HCl aq. (0.1 mol L^{-1}, 10 mL) or HNO_3 aq. (0.1 mol L^{-1}, 10 mL, for recycling of the supporting electrolyte), whereby the supporting electrolyte remains in the aqueous layer and can be recovered quantitatively. The organic fraction is reduced in vacuo to yield the crude product. For purification, the residue is washed with NaOH aq. (1 mol L^{-1}, 10 mL) and extracted with diethyl ether or n-pentane (10 mL), monitored via TLC. After dropwise acidification of the aqueous layer with conc. HCl aq. to pH 1 and extraction with ethyl acetate (2 × 10 mL), the combined organic layers are dried over $MgSO_4$ and reduced in vacuo to yield the desired product.

Workup protocol for cyclic ketones and benzaldehydes

After electrolysis, the solvent is recovered by distillation under reduced pressure. The low-boiling starting material leftover can be recovered by extraction with n-pentane out of the nitrile distillate. The distillation residue is extracted with water (20 mL) and cyclohexane (20 mL) or diethyl ether (20 mL), whereby the supporting electrolyte remains in the aqueous layer and can be recovered quantitatively. The organic layer is dried over $MgSO_4$ and reduced in vacuo to yield the desired product. Special attention has to be paid to the distillations since short-chained cyclic ketones are volatile. Solvent evaporation was carried out to a maximum of 250 mbar at 50 °C for cyclohexane or 970 mbar at 40 °C for diethyl ether.

For derivatization of the benzaldehydes to the semicarbazones: After extraction and evaporation of the solvent from the dried organic layer, the residue is immediately dissolved in 3 mL abs. ethanol and is added dropwise to a 90 °C preheated solution of semicarbazide hydrochloride (2 eq.) and sodium acetate trihydrate (2.4 eq.) in 10 mL water. Heating and stirring are continued for 15 min. Afterward, the solvents are evaporated, and the precipitating semicarbazone is suspended in cold, deionized water, filtrated, washed with cold water, and dried in vacuo.

Workup protocol for the co-electrolysis

After electrolysis, 10 mg of 1,3,5-trimethoxybenze as an internal standard was added to the reaction solution. Three drops were eluted with ethyl acetate through ~330 mg silica 60 M and filled into a vial for quantitative GC-FID analysis. Before the analysis, an external GC calibration of the ketone was performed (see Supplementary Fig. 6). The dicarboxylic acid has been isolated regarding the following workup: The solvent is recovered by distillation under reduced pressure. The low-boiling starting material leftover can be recovered by extraction with n-pentane out of the nitrile distillate and monitored via thin-layer chromatography (TLC). The distillation residue is dissolved in ethyl

acetate (10 mL) and extracted with HCl aq. (0.1 mol L^{-1}, 10 mL), whereby the supporting electrolyte remains in the aqueous layer. The organic fraction is reduced in vacuo. For purification, the residue is washed with NaOH aq. (1 mol L^{-1}, 10 mL) and extracted with diethyl ether or n-pentane (10 mL), monitored via TLC. After dropwise acidification of the aqueous layer with conc. HCl aq. to pH 1 and extraction with ethyl acetate (2 × 10 mL), the combined organic layers are dried over $MgSO_4$ and reduced in vacuo to yield the dicarboxylic acid product.

Workup procedure for carboxylic acids from fatty acids

After electrolysis, 50.5 µL propionic acid was added to the reaction solution as an internal standard. Three drops were eluted with ethyl acetate through ~330 mg silica 60 M and filled into a vial for quantitative GC-FID analysis. Prior to the analysis, an external calibration of the mono-carboxylic acid was performed (see Supplementary Fig. 7). The dicarboxylic acid was isolated via column chromatography using silica 60 M (cyclohexane/ethyl acetate = 1:1 with 1 vol% glacial acetic acid).

Data availability

The authors declare that all data supporting the findings of this study are available within the paper and its Supplementary information. Source data are provided with this paper.

References

1. Parasram, M. & Gevorgyan, V. Silicon-tethered strategies for C–H functionalization reactions. *Acc. Chem. Res.* **50**, 2038–2053 (2017).
2. Zhao, J. & Han, J. in *Alkane Functionalization* 1st edn (eds Pombeiro, A. J. L. & Guedes da Silva, M. F. C.) (John Wiley & Sons Ltd., 2019).
3. Govaerts, S., Nyuchev, A. & Noël, T. Pushing the boundaries of C–H bond functionalization chemistry using flow technology. *J. Flow. Chem.* **10**, 13–71 (2020).
4. Simmie, J. M. Detailed chemical kinetic models for the combustion of hydrocarbon fuels. *Prog. Energ. Combust.* **29**, 599–634 (2003).
5. Sogorb M. Á., Mangas, I., & Vilanova, E. in *Encyclopedia of Toxicology* 3rd edn (Elsevier Inc., 2014).
6. Singh, S. N., Kumari, B. & Mishra, S. in *Microbial Degradation of Xenobiotics. Environmental Science and Engineering* (ed. Singh, S. N.) (Springer, 2012).
7. Markovnikov, V. V. Occurrence of hexanaphthene in caucasian naphtha. *Ber. Dtsch. Chem. Ges.* **28**, 577–578 (1895).
8. Markovnikov, V. V. Some new constituents of caucasian naphtha. *Ber. Dtsch. Chem. Ges.* **30**, 974–977 (1897).
9. Campbell, M. L. in *Ullmann's Encyclopedia of Industrial Chemistry* (Wiley-VCH, 2000).
10. Schiffer, T. & Oenbrink, G. in *Ullmann's Encyclopedia of Industrial Chemistry* (Wiley-VCH, 2000).
11. Bashkirov, A. N. et al. The production of cyclododecanol by the liquid-phase oxidation of cyclododecane. *Neftekhimiya* **1**, 527–534 (1961).
12. ECHA. CLH report for boric acid and borates. https://echa.europa.eu/documents/10162/2842450/clh_rep_boric+acid+and+borates_10344_en.pdf/74c34c0b-2129-abf5-a0f4-2c5b21d7d926 (2018).
13. Lisicki, D. & Orlińska, B. Oxidation of cyclic ketones to dicarboxylic acids. *Pol. J. Chem. Tech.* **20**, 102–107 (2018).
14. Mills, B. M., Talati, M. M. & Winter, G. A. Bio-dodecanedioic acid (DDDA) production. https://repository.upenn.edu/cbe_sdr/100/?utm_source=repository.upenn.edu%2Fcbe_sdr%2F100&utm_medium=PDF&utm_campaign=PDFCoverPages (2018).
15. Shi, F., Wang, H. & Dai, X. *Carbonyl Compounds: Reactants, Catalysts and Products* (Wiley-VCH, 2021).
16. Yu, H. et al. Iron-catalyzed oxidative functionalization of C(sp3)–H bonds under bromide synergized mild conditions. *Chem. Commun.* **55**, 7840–7843 (2019).
17. Wang, W., Xu, D., Sun, Q. & Sun, W. Efficient aliphatic C–H bond oxidation catalyzed by manganese complexes with hydrogen peroxide. *Chem. Asian J.* **13**, 2458–2464 (2018).
18. Silva, T. F. S. et al. V(IV), Fe(II), Ni(II) and Cu(II) complexes bearing 2,2,2-tris(pyrazol-1-yl)ethyl methanesulfonate: application as catalysts for the cyclooctane oxidation. *N. J. Chem.* **40**, 528–537 (2016).
19. Murahashi, S.-I., Oda, Y., Komiya, N. & Naota, T. Ruthenium-catalyzed oxidation of alkanes with peracids. *Tetrahedron Lett.* **35**, 7953–7956 (1994).
20. Denicourt-Nowicki, A., Lebedeva, A., Bellini, C. & Roucoux, A. Highly selective cycloalkane oxidation in water with ruthenium nanoparticles. *ChemCatChem* **8**, 357–362 (2016).
21. Jiang, J., Luo, R., Zhou, X., Wang, F. & Ji, H. Metalloporphyrin-mediated aerobic oxidation of hydrocarbons in cumene: co-substrate specificity and mechanistic consideration. *Mol. Catal.* **440**, 36–42 (2017).
22. Tabor, E., Połtowicz, J., Pamin, K., Basąg, S. & Kubiak, W. Influence of substituents in meso-aryl groups of iron l-oxo porphyrins on their catalytic activity in the oxidation of cycloalkanes. *Polyhedron* **119**, 342–349 (2016).
23. Gupta, S. K. & Choudhury, J. Templating an N-heterocyclic carbene (NHC)-cyclometalated Cp*IrIII-based oxidation precatalyst on a pendant coordination platform: assessment of the oxidative behavior via electrochemical, spectroscopic and catalytic probes. *Dalton Trans.* **44**, 1233–1239 (2015).
24. Miao, C., Zhao, H., Zhao, Q., Xia, C. & Sun, W. NHPI and ferric nitrate: a mild and selective system for aerobic oxidation of benzylic methylenes. *Catal. Sci. Technol.* **6**, 1378–1383 (2016).
25. Travis, B. R., Narayan, R. S. & Borhan, B. Osmium tetroxide-promoted catalytic oxidative cleavage of olefins: an organometallic ozonolysis. *J. Am. Chem. Soc.* **124**, 3824–3825 (2002).
26. Henry, J. R. & Weinreb, S. M. A convenient, mild method for oxidative cleavage of alkenes with Jones reagent/osmium tetraoxide. *J. Org. Chem.* **58**, 4745–4745 (1993).
27. Zimmermann, F., Meux, E., Mieloszynski, J.-L., Lecuire, J.-M. & Oget, N. Ruthenium catalysed oxidation without CCl_4 of oleic acid, other monoenic fatty acids and alkenes. *Tetrahedron Lett.* **46**, 3201–3203 (2005).
28. Che, C.-M., Yip, W.-P. & Yu, W.-Y. Ruthenium-catalyzed oxidation of alkenes, alkynes, and alcohols to organic acids with aqueous hydrogen peroxide. *Chem. Asian J.* **1**, 453–458 (2006).
29. Kadyrov, R. & Hackenberger, D. Oxidative cleavage of long chain olefins to carboxylic acids with hydrogen peroxide. *Top. Catal.* **57**, 1366–1371 (2014).
30. Bhuyan, B., Paul, B., Vadivel, S. & Dhar, S. S. Preparation and characterization of WO_3 bonded imidazolium sulfonic acid chloride as a novel and green ionic liquid catalyst for the synthesis of adipic acid. *RSC Adv.* **6**, 99044–99052 (2016).
31. Choudary, B. M., Valli, V. L. K. & Prasad, A. D. A novel montmorillonite—$KMnO_4$ system for the oxidation of alkenes under triphase conditions. *Synth. Commun.* **21**, 2007–2013 (1991).
32. Miyamoto, K., Sei, Y., Yamaguchi, K. & Ochiai, M. Iodomesitylene-catalyzed oxidative cleavage of carbon–carbon double and triple bonds using *m*-chloroperbenzoic acid as a terminal oxidant. *J. Am. Chem. Soc.* **131**, 1382–1383 (2009).
33. Thottumkara, P. P. & Vinod, T. K. Oxidative cleavage of alkenes using an in situ generated iodonium ion with oxone as a terminal oxidant. *Org. Lett.* **12**, 5640–5643 (2010).
34. Habib, R. M., Chiang, C. Y. & Bailey, P. S. Dicarboxylic acids from ozonolysis of cycloalkenes. *J. Org. Chem.* **49**, 2780–2784 (1984).

35. Balavoine, G. et al. An efficient electrochemical process for the oxidation of saturated hydrocarbons: the Gif-Orsay system. *J. Chem. Soc., Chem. Commun*. **23**, 1727–1729 (1986).
36. Balavoine, G. et al. Selective oxidation of saturated hydrocarbons using an electrochemical modification of the Gif system. *Tetrahedron Lett*. **27**, 2849–2852 (1986).
37. Fang, X. et al. Controllable oxidation of cyclohexane to cyclohexanol and cyclohexanone by a nano-MnO_x/Ti electrocatalytic membrane reactor. *J. Catal*. **329**, 187–194 (2015).
38. Yamanaka, I., Furukawa, T. & Otsuka, K. Oxidation of alkanes with H_2O on $Ir(acac)_3$ supported on a carbon fiber-anode. *Chem. Commun*. **22**, 2209–2210 (2000).
39. Kawamata, Y. et al. Scalable, electrochemical oxidation of unactivated C–H bonds. *J. Am. Chem. Soc*. **139**, 7448–7451 (2017).
40. Godin, P. J., Le Bris, K. & Strong, K. Conformational analysis and global warming potentials of 1,1,1,3,3,3-hexafluoro-2-propanol from absorption spectroscopy. *J. Quant. Spectrosc. Radiat. Transf*. **203**, 522–529 (2017).
41. Bäumer, U.-S. T. & Schäfer, H. J. Cleavage of olefinic double bonds by mediated anodic oxidation. *Electrochim. Acta* **48**, 489–495 (2003).
42. Bäumer, U.-S. T. & Schäfer, H. J. Cleavage of alkenes by anodic oxidation. *J. Appl. Electrochem*. **35**, 1283–1292 (2005).
43. Torii, S., Inokuchi, T. & Oi, R. Electrooxidative cleavage of carbon-carbon linkages. 1. Preparation of acyclic oxoalkanoates from 2-hydroxy- and 2-acetoxy-l-cycloalkanones and cycloalkanone enol acetates. *J. Org. Chem*. **47**, 47–52 (1982).
44. Lèbre, É. et al. The social and environmental complexities of extracting energy transition metals. *Nat. Commun*. **11**, 4823 (2020).
45. Pollok, D. & Waldvogel, S. R. Electro-organic synthesis—a 21st century technique. *Chem. Sci*. **11**, 12386–12400 (2020).
46. Wiebe, A. et al. Electrifying organic synthesis. *Angew. Chem. Int. Ed*. **57**, 5594–5619 (2018).
47. Möhle, S. et al. Modern electrochemical aspects for the synthesis of value-added organic products. *Angew. Chem. Int. Ed*. **57**, 6018–6041 (2018).
48. Francke, R. & Little, R. D. Redox catalysis in organic electrosynthesis: basic principles and recent developments. *Chem. Soc. Rev*. **43**, 2492–2521 (2014).
49. Schmidt, H. & Stange, H. Electrolyses of nitrates in acetonitrile. *Z. Anorg. Allg. Chem*. **293**, 274–285 (1958).
50. Rao, R. R., Milliken, S. B., Robinson, S. L. & Mann, C. K. Anodic oxidation of lithium, cadmium, silver, and tetra-*n*-butylammonium nitrates. *Anal. Chem*. **42**, 1076–1080 (1970).
51. Takahira, Y. et al. Electrochemical C(sp^3)–H fluorination. *Synlett* **30**, 1178–1182 (2019).
52. Li, D., Ma, T.-K., Scott, R. J. & Wilden, J. D. Electrochemical radical reactions of alkyl iodides: a highly efficient, clean, green alternative to tin reagents. *Chem. Sci*. **11**, 5333–5338 (2020).
53. Imada, Y., Okada, Y., Noguchi, K. & Chiba, K. Selective functionalization of styrenes with oxygen using different electrode materials: olefin cleavage and synthesis of tetrahydrofuran derivatives. *Angew. Chem. Int. Ed*. **58**, 125–129 (2019).
54. Klein, M. & Waldvogel, S. R. Counter electrode reactions—important stumbling blocks on the way to a working electro-organic synthesis. *Angew. Chem. Int. Ed*. **61**, e202204140 (2022).
55. Gütz, C., Klöckner, B. & Waldvogel, S. R. Electrochemical screening for electroorganic synthesis. *Org. Process Res. Dev*. **20**, 26–32 (2016).
56. Dunitz, J. D. & Prelog, V. Röntgenographisch bestimmte Konformationen und Reaktivität mittlerer Ringe. *Angew. Chem*. **72**, 896–902 (1960).
57. Atobe, M., Tateno, H. & Matsumura, Y. Applications of flow microreactors in electrosynthetic processes. *Chem. Rev*. **118**, 4541–4572 (2018).
58. Noël, T., Cao, Y. & Laudadio, G. The fundamentals behind the use of flow reactors in electrochemistry. *Acc. Chem. Res*. **52**, 2858–2869 (2019).
59. Gleede, B., Selt, M., Franke, R. & Waldvogel, S. R. Developments in the dehydrogenative electrochemical synthesis of 3,3′,5,5′-tetramethyl-2,2′-biphenol. *Chem. Eur. J*. **27**, 8252–8263 (2021).
60. Zimmermann, M. *Oxygen Reduction Reaction Mechanism on Glassy Carbon in Aprotic Organic Solvents*. Université Grenoble Alpes (2015).
61. Jander, G. & Blasius, E. *Lehrbuch der analytischen und präparativen anorganischen Chemie* 16th edn, 290–291 (S. Hirzel Verlag, 2006).
62. Blaschette, A., Büchel, K.-H., Dahlmann, J., de Meijere, A. & Dankowski, M. in *Houben-Weyl: Methods of Organic Chemistry* 4th edn, Vol. E 13, 1387 (Georg Thieme Verlag, 1989).
63. Achord, J. M. & Hussey, C. L. Determination of dissolved oxygen in nonaqueous electrochemical solvents. *Anal. Chem*. **52**, 601–602 (1980).
64. Berndt, T. & Böge, O. Products and mechanism of the reaction of NO_3 with selected acyclic monoalkenes. *J. Atmos. Chem*. **21**, 275–291 (1995).
65. Sankar, M. et al. The benzaldehyde oxidation paradox explained by the interception of peroxy radical by benzyl alcohol. *Nat. Commun*. **5**, 3332 (2014).
66. Beraldo, H. & Gambino, D. The wide pharmacological versatility of semicarbazones, thiosemicarbazones and their metal complexes. *Mini Rev. Med. Chem*. **4**, 31–39 (2004).
67. Ahsan, M. J. Semicarbazone analogs as anticonvulsant agents: a review. *Cent. Nerv. Syst. Agents Med. Chem*. **13**, 148–158 (2013).
68. Nascimento da Cruz, A. C. et al. Biological evaluation of arylsemicarbazone derivatives as potential anticancer agents. *Pharmaceuticals* **12**, 169 (2019).
69. Gütz, C., Stenglein, A. & Waldvogel, S. R. Highly modular flow cell for electroorganic synthesis. *Org. Process Res. Dev*. **21**, 771–778 (2017).
70. Gleede, B., Selt, M., Gütz, C., Stenglein, A. & Waldvogel, S. R. Large highly modular narrow gap electrolytic flow cell and application in dehydrogenative cross-coupling of phenols. *Org. Process Res. Dev*. **24**, 1916–1926 (2020).

Acknowledgements

S.R.W. gratefully acknowledge the financial support by Forschungsinitiative Rheinland-Pfalz in the frame of SusInnoScience. J.N. thanks J.L. Schröder for preparative support, A.L. Rauen for initial guidance in the subject area and helpful discussions, S. Hofmann for helpful discussions and invention disclosure support, S. Arndt for the introduction in ion chromatography measurements and J. Herszman for introduction into the coulometric titration apparatus.

Author contributions

J.N., F.W., F.-E.B., and S.R.W. conceived this work and designed the experiments. J.N., K.H., S.M., I.C.M., and D.M. conducted the experiments and analyzed the data. F.W. and F.-E.B. discussed the results and commented on the manuscript. J.N. and S.R.W. wrote the manuscript and the Supplementary information.

Funding

Open Access funding enabled and organized by Projekt DEAL.

Competing interests

F.W. is an employee at Evonik and holds shares in the company. F.-E.B. was an employee at Evonik and is retired. S.R.W., F.W., F.-E.B., J.N., and K.H. are inventors in patent applications regarding the manuscript aspects of cyclic alkane oxidation to ketones, cyclic alkene oxidation to dicarboxylic acids, co-electrolysis of cyclic alkanes and alkenes, and oxidative fatty acid cleavage. The patent applications are filed at the European Patent Office and have not yet been published. Searchable application numbers are available upon publication. The remaining authors declare no competing interests.

Additional information

Supplementary information The online version contains supplementary material available at https://doi.org/10.1038/s41467-023-40259-0.

Correspondence and requests for materials should be addressed to Siegfried R. Waldvogel.

Peer review information *Nature Communications* thanks, Irene Bosque, Naoki Shida and the other, anonymous, reviewer for their contribution to the peer review of this work. A peer review file is available.

Supplementary Information

Electrochemical oxo-functionalization of cyclic alkanes and alkenes using nitrate and oxygen

Joachim Nikl[1], Kamil Hofman[1], Samuel Mossazghi[1], Isabel C. Möller[1], Daniel Mondeshki[1], Frank Weinelt[2], Franz-Erich Baumann[2] & Siegfried R. Waldvogel*[1]

[1]Department of Chemistry, Johannes Gutenberg University Mainz, Duesbergweg 10–14, 55128 Mainz, Germany

[2] Evonik Operations GmbH, Paul-Baumann-Straße 1, 45772 Marl, Germany

*Correspondence to: waldvogel@uni-mainz.de

Content

1. Supplementary Methods

1.1 General information

Chemicals were of analytical grade and were obtained from common chemical providers such as TCI, Aldrich, Fluka, and Acros. Oxygen gas was purchased in technical quality of 2.5 from NIPPON GASES Germany GmbH, Düsseldorf, Germany, and used without purification.

As **electrode materials**, SIGRADUR® G glassy carbon, from HTW Hochtemperatur Werkstoffe GmbH, Thierhaupten, Germany, DIACHEM™ boron-doped diamond (BDD, 15 µm diamond layer on silicon support) from CONDIAS GmbH, Itzehoe, Germany and Sigrafin™ V2100 isostatic graphite from SGL Carbon, Bonn, Germany, were used.

As **electronic equipment**, a HMP4040 Programmable Power Supply 384 W, from Rohde & Schwarz GmbH & Co. KG, München, Germany, and a MR Hei-Tec magnetic stirrer, from Heidolph Instruments GmbH & Co.KG, Kelkheim, Germany, were used.

Column chromatography was performed on silica gel 60 M (0.040–0.063 mm, Macherey-Nagel GmbH & Co. KG, Düren, Germany). Therefore, a preparative chromatography system (Büchi, Flawil, Switzerland) was used with a Büchi Control Unit C-620, an UV detector Büchi UV photometer C-635, a Büchi fraction collector C-660 and two Pump Modules C-605 for adjusting the solvent mixtures. As eluent, mixtures of cyclohexane and ethyl acetate (technical grade, purified via distillation prior to use) were used. Optionally, glacial acetic acid was used as an additive. Ratios of the solvent mixture refer to volume ratios.

Thin layer chromatography was performed with silica gel 60 sheets on aluminium (F254, Merck KGaA, Darmstadt, Germany). A potassium permanganate stain (3 g $KMnO_4$, 20 g K_2CO_3, 5 mL NaOH (5%), 300 mL water) and a *p*-anisaldehyde stain (135 mL EtOH, 5 mL conc. H_2SO_4, 1.5 mL of AcOH (100%), 3.7 mL *p*-anisaldehyde) were used for visualization of components.

High performance liquid chromatography was performed on a Shimadzu HPLC-MS with a SIL-20A HT autosampler, a CTO-20AC column oven, two LC-20AD pump modules for adjusting the eluent, a SPD-M20A photodiode array detector, a LCMS-2020 mass spectrometer, a CBM-20A system controller (all: Shimadzu, Japan) and a Eurosphere II 100-5 C18 column (150 x 4 mm, KNAUER Wissenschaftliche Geräte GmbH, Berlin, Germany). Eluent: acetonitrile/water (1:9 → 10:0) + formic acid (1 vol.%).

Gas chromatography for non-acidic compounds was performed on a Shimadzu GC-2025 (Shimadzu, Japan) using a HP-5MS column (Agilent Technologies, Santa Clara, California; length: 30 m, inner diameter: 0.25 mm, film: 0.25 µm, carrier gas: hydrogen). For acidic compounds a Shimadzu GC-2010 (Shimadzu, Japan) equipped with a Zebron ZB-FFAP column (Phenomenex Ltd., Aschaffenburg, Deutschland; length: 30 m, inner diameter: 0.25 mm, film: 0.25 µm, carrier gas: argon) was used. GC-MS measurements were carried out on a Shimadzu GC-2010 (Shimadzu, Japan) using a HP-1 column (Agilent Technologies, Santa Clara, California; length: 30 m, inner diameter: 0.25 mm, film: 0.25 µm, carrier gas: helium). The chromatograph was coupled to a mass spectrometer Shimadzu GC-MS-QP2010. For GC sample preparation a column filtratrion was performed over silica gel 60 M (0.040–0.063 mm, Macherey-Nagel GmbH & Co. KG, Düren, Germany).

Melting ranges (m_R) were determined with a Melting Point Apparatus B-565 (Büchi, Flawil, Switzerland) and are uncorrected. Heating rate: 1 °C min^{-1}.

NMR spectroscopy of ^{1}H, ^{13}C and ^{19}F spectra were recorded at 25 °C, using a Bruker Avance II 400 (400 MHz, 5 mm BBFO-SmartProbe with z gradient and ATM, SampleXPress 60 sample changer, Analytische Messtechnik, Karlsruhe, Germany). Chemical shifts (δ) are reported in parts per million (ppm) relative to traces of $CHCl_3$, DMSO-d_5 or HDO in the corresponding deuterated solvent. For ^{19}F spectra $CFCl_3$, for ^{31}P spectra H_3PO_4 and for ^{13}C NMR spectra Me_4Si are serving as reference compounds if not referenced to the used deuterated solvent[1]. On-line reaction monitoring was performed with a

Spinsolv 60 benchtop NMR spectrometer (60 MHz, resolution: <0.5 Hz (50%) for ^{1}H, Magritek GmbH, Aachen, Germany).

High-resolution mass spectra were obtained by using an Agilent 6545 QTOF-HRAM-MS (Agilent Technologies, Santa Clara, California) apparatus employing $ESI^{+/-}$ and $APCI^{+/-}$.

Cyclic voltammetry was performed in a 10 mL snap-cap vial equipped with an Autolab PGSTAT101 potentiostat (Metrohm AG, Herisau, Switzerland). WE: glassy carbon disk, 3 mm diameter (7.07 mm^2 area); CE: glassy carbon rod; RE: Ag/AgCl in saturated LiCl/EtOH. Solvent: acetonitrile. ν = 0.02–1.5 V s^{-1}, supporting electrolyte: NBu_4PF_6 or NBu_4NO_3 (0.1 mol L^{-1}).

Ion chromatography was performed on an 850 Professional IC (Metrohm AG, Herisau, Switzerland) equipped with a Metrosep A Supp 4 anion exchange column (Metrohm AG, Herisau, Switzerland). Eluent system: Na_2CO_3 (0.9 mmol L^{-1}) and $NaHCO_3$ (0.85 mmol L^{-1}) in H_2O with 5 vol.% acetone.

Coulometric Karl Fischer titration was performed on a Titrando 851 (Metrohm AG, Herisau, Switzerland) equipped with a Stirrer 801 and a Generator electrode with diaphragm (both: Metrohm AG, Herisau, Switzerland). Anolyte: Hydranal™ Coulomat AG (Honeywell, Morristown, USA), Catholyte: Hydranal™ Coulomat CG (Honeywell, Morristown, USA). Analysis program: tiamo™ (Metrohm AG, Herisau, Switzerland).

1.2 Supplementary set-up information for the general protocols (GP)

1.2.1 Set-up to GP 1: 5 mL PTFE cell

The electrolysis set-up is commercially available as IKA Screening System from IKA-Werke GmbH & Co. KG, Staufen, Germany.

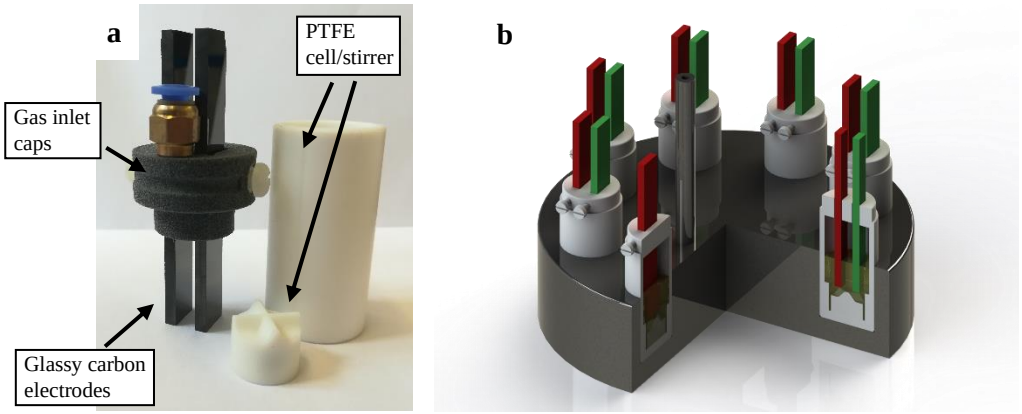

Supplementary Fig. 1: a Single-part 5 mL PTFE cell with glassy carbon electrodes. **b** Schematic representation of an 8-fold screening set-up.

1.2.2 Set-up to GP 2: 100 mL three-necked round-bottom flask

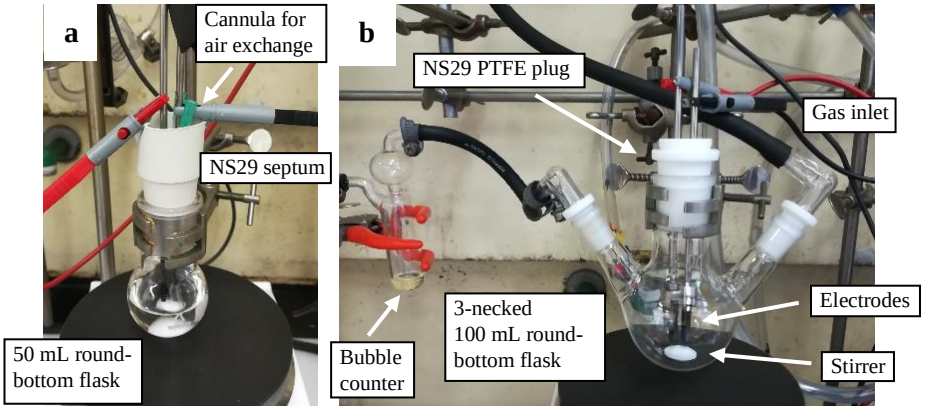

Supplementary Fig. 2: a 50 mL round-bottom flask for electrolysis with a NS29 septum including electrode holders, cannula for air exchange and a magnetic stirrer. **b** 100 mL three-necked round-bottom flask for electrolysis with a NS29 PFTE plug including electrode holders, a magnetic stirrer and a bubble counter.

1.2.3 Set-up to GP 3: 25 mL beaker-type cell

The cells are commercially available as SynLectro™ Electrolysis Platform from Sigma-Aldrich (Merck KGaA, Darmstadt, Germany).

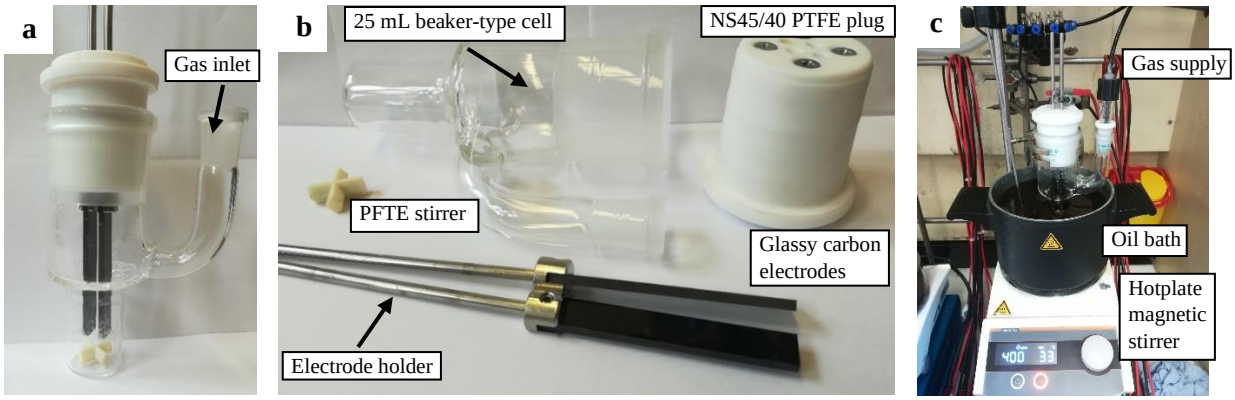

Supplementary Fig. 3: a Assembled 25 mL beaker-type glass cell with gas inlet attachment, manufactured according to specifications from the Waldvogel group by Hans W. Schmidt GmbH & Co. KG, HWS Labortechnik, Mainz, Germany. **b** Disassembled cell. **c** Set-up with gas supply and oil bath.

1.2.4 Set-up to GP 4: Electrochemical flow cell (2 x 6 cm^2)

The electrolysis set-up is commercially available as IKA ElectraSyn flow from IKA-Werke GmbH & Co. KG, Staufen, Germany.

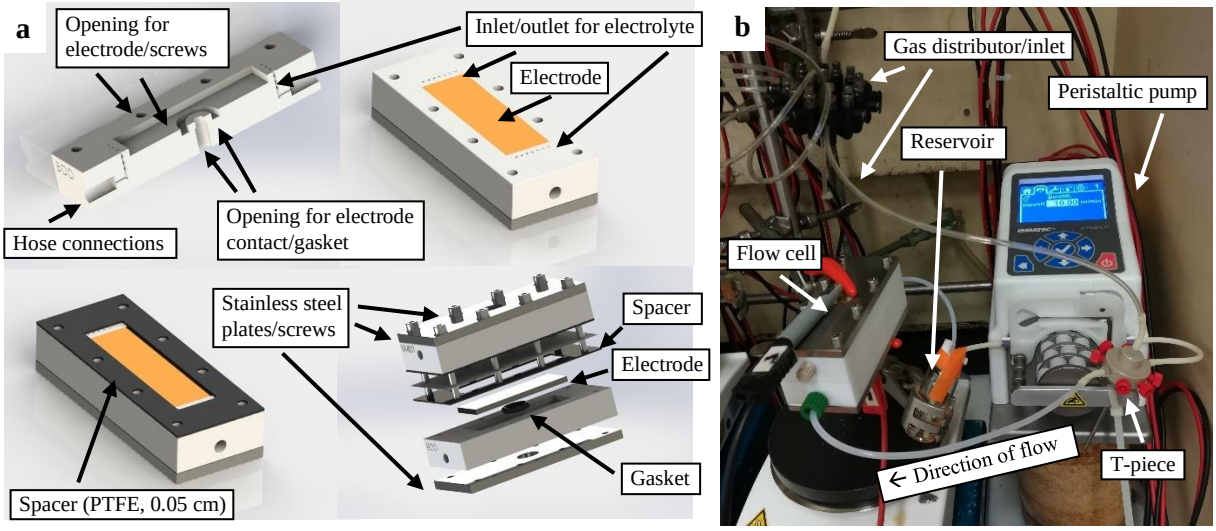

Supplementary Fig. 4: a Schematic disassembled flow cell. **b** Set-up for electrochemical reactions in flow including a peristaltic pump, a gas inlet, the flow cell and a reservoir.

1.2.5 Set-up for oxygen supply

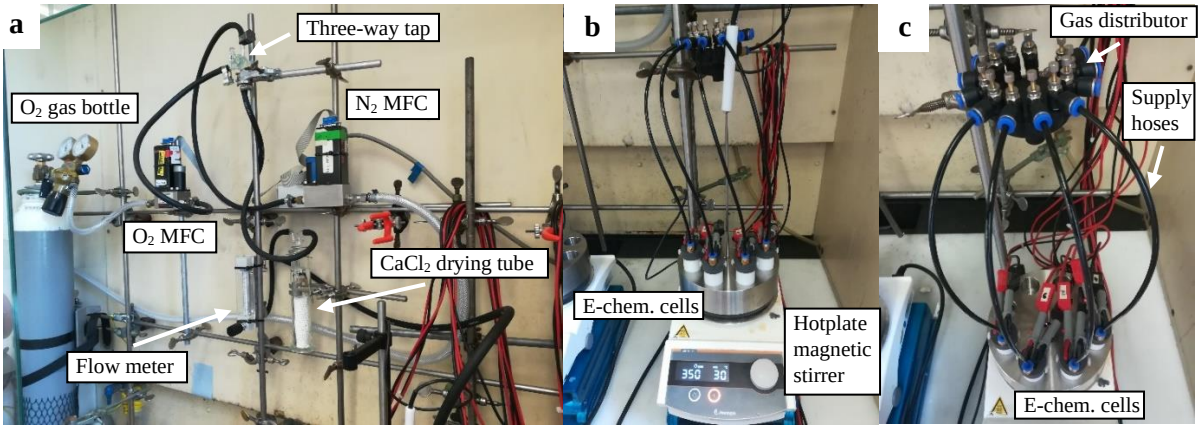

Supplementary Fig. 5: **a** Gas inlet apparatus. **b** Distributor connection to the electrolysis cells. **c** View from above onto the gas distributor.

The gas inlet was controlled via two 5850S mass flow controllers (MFC) from Brooks Instrument B.V., Veenendaal, Netherlands. One controller was used for the oxygen line and one for the nitrogen line. The controllers were operated using Smart DDE software and Matlab R2017b. The volume flow rate was additionally monitored using a DK800 flow meter from KROHNE Messtechnik GmbH, Duisburg, Germany. The total volume flow rate was a constant 20 mL min^{-1} for all tests carried out, which, limited by the MFCs used, also represents the maximum achievable volume flow rate. The percentage volume flows of the two gases were set using the MFCs and their software. The gases used were Oxygen 2.5 from NIPPON GASES Germany GmbH, Düsseldorf, Germany and Nitrogen 5.0 from NIPPON GASES Germany GmbH, Düsseldorf, Germany. The gas distributor as well as the gas inlet lids of the electrolysis cells were purchased from IKA-Werke GmbH & Co. KG, Staufen, Germany[2].

2. Supplementary Results

2.1 External GC calibration with an internal standard for yield determination

For the yield determination via gas chromatography, a calibration was carried out. 1,3,5-trimethoxybenzene (10 mg for each measurement) was used for ketone products and propionic acid (50.5 µL for each measurement) was used for carboxylic acids as internal standard. The molar ratio between the product and the standard *n*(P)/*n*(Std) was related to the measured GC integral ratios between product and standard GC-Int.(P)/GC-Int.(Std). From the resulting linear regression equation, the amount of product substance in an unknown sample can be calculated. The statistical software Origin 7.5 SR6 (OriginLab Corporation, Northampton, Massachusetts) was used for linear regression analysis. Mathematical calculations were performed using Microsoft® Excel® 2019.

Preparation of the calibration solutions: The analyte is dissolved together with the standard in the solvent (acetonitrile or isobutyronitrile, 5 mL) in different concentrations. Three drops form the solution are filtered over silica gel 60 M (approx. 330 mg) into a GC vial (eluent: ethyl acetate).

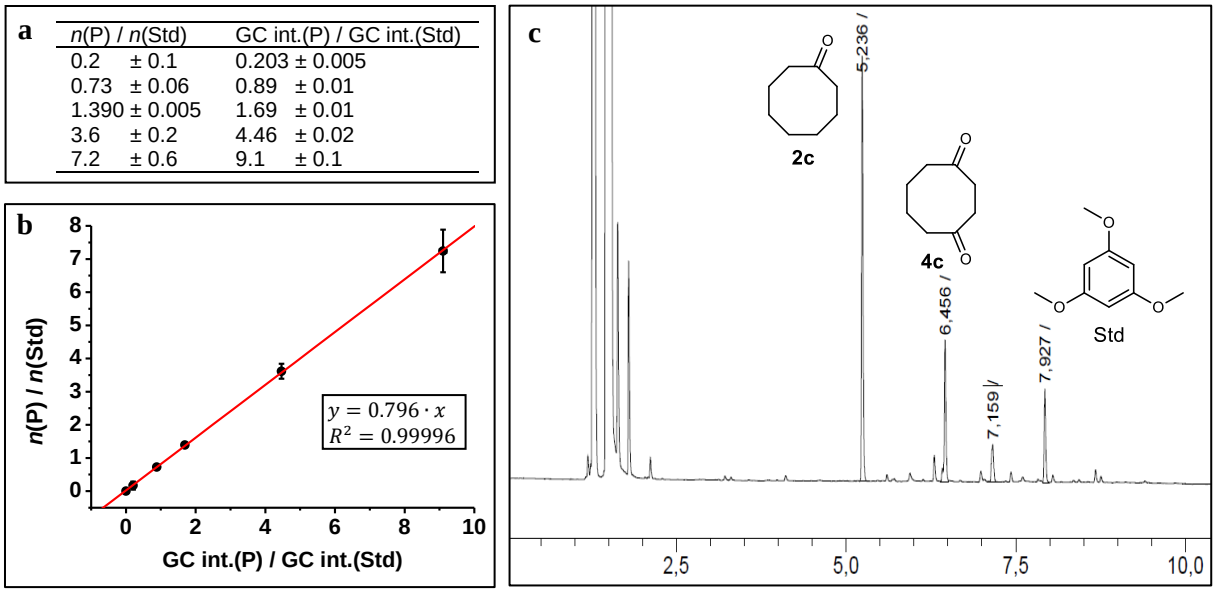

Supplementary Fig. 6: **a** Data of the calibration measurements for cyclooctanone (**2c**). Of each concentration, three samples were prepared and analyzed. **b** External GC calibration of cyclooctanone (**2c**) using 10 mg of 1,3,5-trimethoxybenzene as internal standard for each measurement. Error bars along the *y*-axis are calculated via uncertainty propagation, and error bars along the *x*-axis represent standard deviation with 3 independent replicates. Linear regression straight line is labeled in red. **c** Example GC chromatogram after an electrolysis to visualize the evaluation.

The calibration for the yield determination of cyclododecanone (**2e**) has been carried out analog to cyclododecanone (**2c**).

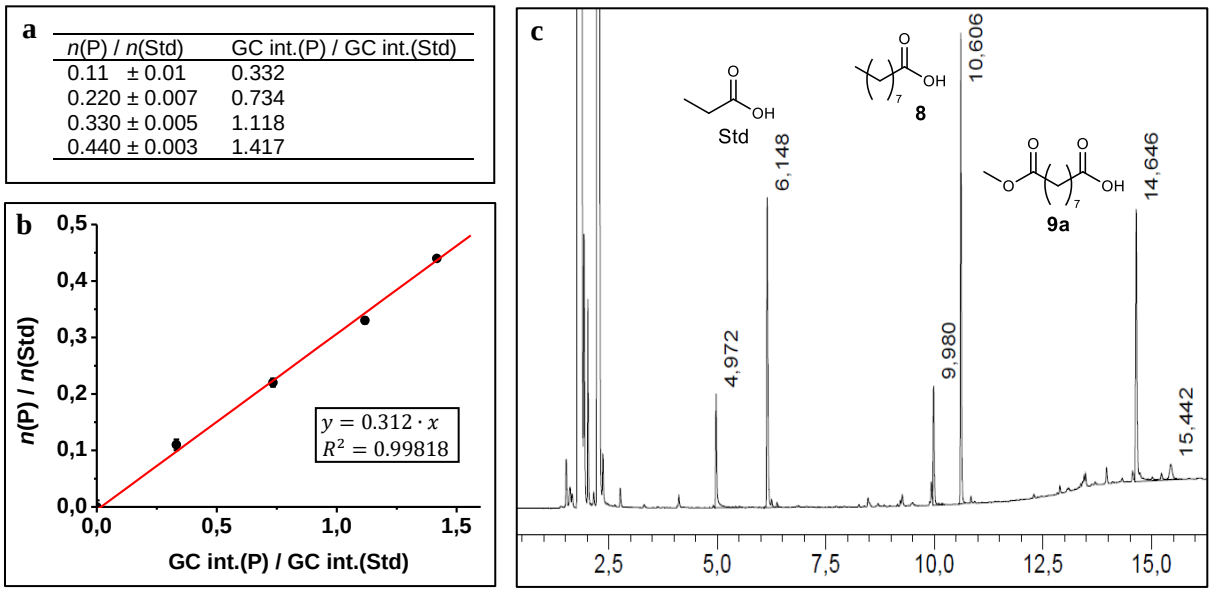

Supplementary Fig. 7: **a** Data of the calibration measurements for azelaic acid monomethyl ester (**9a**). **b** External GC calibration of azelaic acid monomethyl ester (**9a**) using 50.5 µL of propionic acid as internal standard for each measurement. Error bars along the *y*-axis are calculated via uncertainty propagation, and error bars along the *x*-axis represent standard deviation with 3 independent replicates. Linear regression straight line is labeled in red. **c** Example GC chromatogram after an electrolysis to visualize the evaluation.

The calibration for the yield determination of pelargonic acid (**8**) has been carried out analog to azelaic acid monomethyl ester (**9a**).

2.2 Optimization for cycloalkane oxidation

Supplementary Table 1: Optimization reactions for cyclooctane (**1c**) oxidation, according to GP 1.

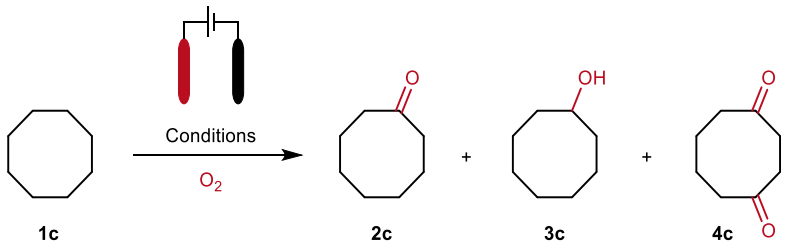

Entry	Deviation from standard conditions[a]	2c[b]	3c[c]	4c[c]
1	None	16%	1%	1%
2	6 *F*	16%	1%	1%
3	8 *F*	15%	1%	1%
4	5 mA cm^{-2}	7%	1%	0%
5	20 mA cm^{-2}	19%	1%	1%
6	30 mA cm^{-2}	18%	2%	1%
7	60 mA cm^{-2}	9%	8%	0%
8	20 mA cm^{-2}, O_2/N_2 = 0/100	0%	0%	0%
9	20 mA cm^{-2}, O_2/N_2 = 20/80	5%	5%	0%
10	O_2/N_2 = 5/95	6%	3%	0%
11	O_2/N_2 = 10/90	7%	3%	0%
12	O_2/N_2 = 20/80	31%	1%	6%
13	Air ($O_2/N_2 \approx 21/78$)	23%	2%	3%
14	O_2/N_2 = 35/65	9%	2%	0%
15	O_2/N_2 = 50/50	15%	1%	1%
16	O_2/N_2 = 20/80, **1c** (0.1 mol L^{-1}), NBu_4NO_3 (0.5 eq.)	30%	2%	4%
17	O_2/N_2 = 20/80, **1c** (0.1 mol L^{-1}), NBu_4NO_3 (1.0 eq.)	30%	1%	6%
18	O_2/N_2 = 20/80, **1c** (0.2 mol L^{-1}), NBu_4NO_3 (0.2 eq.)	26%	2%	4%
19	O_2/N_2 = 20/80, **1c** (0.2 mol L^{-1}), NBu_4NO_3 (1.0 eq.)	27%	1%	4%
20	O_2/N_2 = 20/80, **1c** (0.5 mol L^{-1}), NBu_4NO_3 (0.2 eq.)	23%	1%	4%
21	O_2/N_2 = 20/80, **1c** (0.5 mol L^{-1}), NBu_4NO_3 (0.5 eq.)	22%	1%	4%
22	O_2/N_2 = 20/80, 100 rpm	8%	4%	0%
23	O_2/N_2 = 20/80, 200 rpm	17%	2%	1%
24	O_2/N_2 = 20/80, 500 rpm	8%	2%	0%
25	O_2/N_2 = 20/80, 600 rpm	7%	1%	0%
26	O_2/N_2 = 20/80, 5 °C	27%	1%	4%
27	O_2/N_2 = 20/80, 50 °C	27%	1%	7%
28	O_2/N_2 = 20/80, NBu_4BF_4 (0.5 eq.)	3%	2%	1%
29	O_2/N_2 = 20/80, NBu_4PF_6 (0.5 eq.)	3%	2%	1%
30	O_2/N_2 = 20/80, NBu_4ClO_4 (0.5 eq.)	4%	3%	2%
31	O_2/N_2 = 20/80, MeCN/H_2O (5 mL, 10 vol.% H_2O)	16%[d]	2%	2%
32	O_2/N_2 = 20/80, MeCN/H_2O (5 mL, 20 vol.% H_2O)	12%[d]	3%	1%
33	O_2/N_2 = 20/80, MeCN/H_2O (5 mL, 10 vol.% H_2O), $NaNO_3$ (0,5 eq.)	15%[d]	0%	3%
34	O_2/N_2 = 20/80, MeCN/H_2O (5 mL, 20 vol.% H_2O), $NaNO_3$ (0,5 eq.)	11%[d]	2%	1%
35	O_2/N_2 = 20/80, isobutyronitrile (5 mL)	24%	1%	3%
36	O_2/N_2 = 20/80, acetone (5 mL)	29%	2%	4%
37	Isobutyronitrile (5 mL)	19%	1%	2%
38	1-Nitropropane (5 mL)	17%[d]	2%	2%
39	O_2/N_2 = 20/80, BDD || BDD	20%	2%	3%
40	O_2/N_2 = 20/80, graphite || graphite	15%	1%	2%
41	Hexadecyltrimethylammonium nitrate (0.5 eq.)	21%[d]	1%	3%
42	1-Butyl-3-methylimidazolium nitrate (0.5 eq.)	17%[d]	0%	8%
43	Methyltrioctylammonium nitrate (0.5 eq.)	28%[d]	0%	4%
44	Tetrabutylphosphonium nitrate (0.5 eq.)	20%[d]	0%	7%

[a] Undivided 5 mL PTFE cell, glassy carbon electrodes, acetonitrile (5 mL), **1c** (0.2 mol L^{-1}), NBu_4NO_3 (0.5 eq.), 30 °C, O_2 atm. (100 vol.%), 350 rpm, 4 *F*, 10 mA cm^{-2}. [b] Yield determination via ^1H NMR (1,3,5-trimethoxybenzene as internal standard). [c] Yield determination via GC integrals calculated based on yield of **2c**. [d] Yield determination via GC (external calibration of **2c**, 1,3,5-trimethoxybenzene as internal standard).

2.3 Optimization for cycloalkene oxidation

Supplementary Table 2: Optimization reactions for cyclododecene (**5c**) oxidation, according to GP 1.

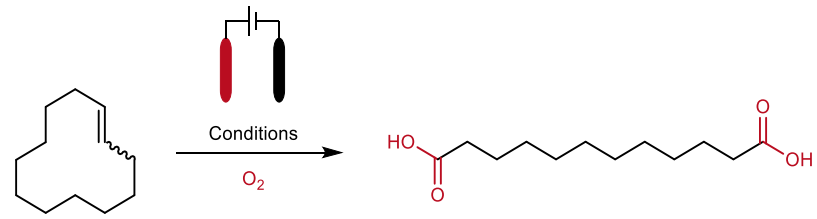

5c, *cis*-/*trans*-mixture

6c

Entry	Deviation from standard conditions[a]	6c[b]
1	None	68%
2	5 °C, 8 *F*	53%
3	22 °C, **5c** (0.1 mol L^{-1}), 8 *F*	69%
4	22 °C, **5c** (0.1 mol L^{-1}), 6 *F*, 5 mA cm^{-2}	70%
5	22 °C, **5c** (0.1 mol L^{-1}), NBu_4NO_3 (1.0 eq.), 8 *F*	61%
6	22 °C, **5c** (0.1 mol L^{-1}), NBu_4NO_3 (2.0 eq.), 8 *F*	71%
7	22 °C, **5c** (0.1 mol L^{-1}), NBu_4NO_3 (1.0 eq.), 8 *F*, 5 mA cm^{-2}	69%
8	22 °C, **5c** (0.1 mol L^{-1}), NBu_4NO_3 (1.0 eq.), 6 *F*, 5 mA cm^{-2}	66%
9	22 °C, **5c** (0.1 mol L^{-1}), NBu_4NO_3 (1.0 eq.), 4 *F*, 5 mA cm^{-2}	68%
10	22 °C, **5c** (0.075 mol L^{-1}), NBu_4NO_3 (1.3 eq.), 8 *F*	73%
11	22 °C, **5c** (0.05 mol L^{-1}), NBu_4NO_3 (2.0 eq.), 8 *F*	76%
12	22 °C, **5c** (0.05 mol L^{-1})	73%
13	22 °C, **5c** (0.05 mol L^{-1}), 2 *F*	63%
14	22 °C, **5c** (0.05 mol L^{-1}), 5 mA cm^{-2}	75%
15	35 °C, **5c** (0.05 mol L^{-1}), 5 mA cm^{-2}	78%
16	5 °C, **5c** (0.05 mol L^{-1}), 5 mA cm^{-2}	71%
17	50 °C, **5c** (0.05 mol L^{-1}), 5 mA cm^{-2}	57%
18	35 °C, **5c** (0.05 mol L^{-1}), 5 mA cm^{-2}, 200 rpm	63%
19	35 °C, **5c** (0.05 mol L^{-1}), 5 mA cm^{-2}, 500 rpm	59%
20	35 °C, **5c** (0.02 mol L^{-1}), 5 mA cm^{-2}	61%
21	22 °C, **5c** (0.05 mol L^{-1}), no electric current	0%

[a]Undivided 5 mL PTFE cell, glassy carbon electrodes, isobutyronitrile (5 mL), **5c** (0.2 mol L^{-1}), NBu_4NO_3 (0.5 eq.), 30 °C, O_2 atm. (100 vol.%), 350 rpm, 4 *F*, 10 mA cm^{-2}. [b]Isolated yields.

2.4 Co-electrolysis reactions for cyclooctane (1c) and cyclooctene (5b)

Supplementary Table 3: Reactions for cyclooctane (**1c**) and cyclooctene (**5b**) co-electrolysis, according to GP 1.

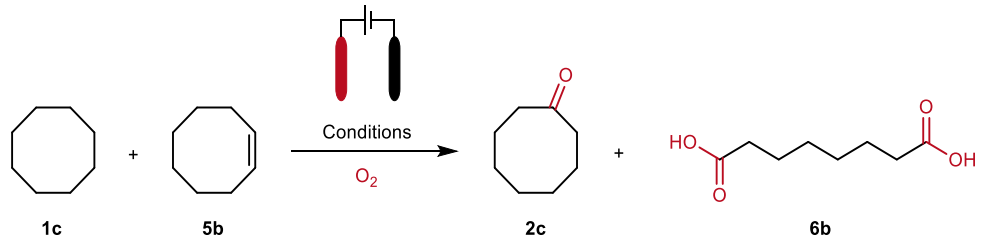

Entry	Mol ratio 1c : 5b	2c[d]	6b[e]
1	1 : 9[a]	4%	40%
2	1 : 3[b]	2%	44%
3	1 : 1[c]	2%	45%

Conditions: Undivided 5 mL PTFE cell, glassy carbon electrodes, acetonitrile (5 mL), NBu_4NO_3 (0.1 mol L^{-1}), 22 °C, O_2 atm. (100 vol.%), 350 rpm, 10 mA cm^{-2}. [a.] **1c** 0.02 mol L^{-1}, **5b** 0.18 mol L^{-1}, 7,6 *F*. [b.] **1c** 0.05 mol L^{-1}, **5b** 0.15 mol L^{-1}, 7 *F*. [c.] **1c** 0.1 mol L^{-1}, **5b** 0.1 mol L^{-1}, 6 *F*. [d.] Yields determined via GC-calibration and refer to mol% of **1c**. [e.] Isolated yields refer to mol% of **5b**.

2.5 Optimization for cycloalkene oxidation in flow

Supplementary Table 4: Optimization reactions for cyclododecene (**5c**) oxidation, according to GP 4.

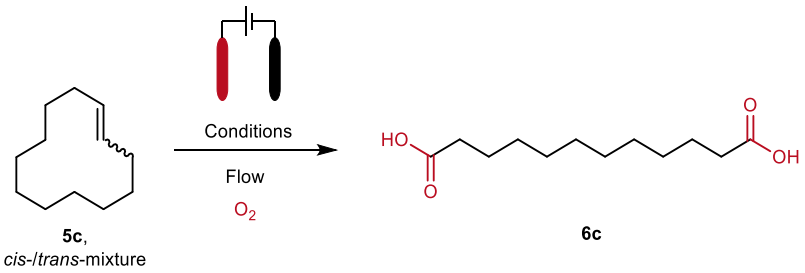

Entry	Deviation from standard conditions[a]	6c[b]
1	None	76%
2	*i*-PrCN (4 mL), **5c** (1.0 mol L^{-1}, 0.96 mL), NBu_4NO_3 (0.25 eq.), 2 *F*, 20 mA cm^{-2}	16%
3	DMC (4 mL), O_2 flow rate: 20 mL min^{-1}, **5c** (1.0 mol L^{-1}, 1 mL), 2 *F*, 20 mA cm^{-2}	10%
4	DMC (4.5 mL), O_2 flow rate: 20 mL min^{-1}, **5c** (0.5 mol L^{-1}, 0.48 mL), 2 *F*, 10 mA cm^{-2}	35%
5	DMC (4.27 mL) + MeOH (0.24 mL), electrolyte flowrate: 5 mL min^{-1}, **5c** (0.5 mol L^{-1}, 0.48 mL), NBu_4NO_3 (0.4 eq.), 2 *F*	33%
6	DMC (4.27 mL) + *i*-PrOH (0.24 mL), O_2 flow rate: 20 mL min^{-1}, electrolyte flowrate: 18 mL min^{-1}, **5c** (0.5 mol L^{-1}, 0.48 mL), NBu_4NO_3 (1.0 eq.), 2 *F*, 20 mA cm^{-2}	38%
7	DMC (8.2 mL) + *i*-PrOH (0.92 mL), 50 °C, O_2 flow rate: 20 mL min^{-1}, electrolyte flowrate: 18 mL min^{-1}, **5c** (0.5 mol L^{-1}, 0.96 mL), NBu_4NO_3 (1.0 eq.), 2 *F*, 20 mA cm^{-2}	52%

[a.] Undivided flow cell, glassy carbon electrodes (2 x 6 cm^2), isobutyronitrile (10 mL), **5c** (0.05 mol L^{-1}), NBu_4NO_3 (0.5 eq.), 20–22 °C, O_2 (100 vol.%) flow rate: 10 mL min^{-1}, electrolyte flowrate: 10 mL min^{-1}, 4 *F*, 5 mA cm^{-2}. [b.] Isolated yields.

2.6 Optimization for benzylic oxidation

Supplementary Table 5: Optimization reactions for the benzylic oxidation, according to GP 1.

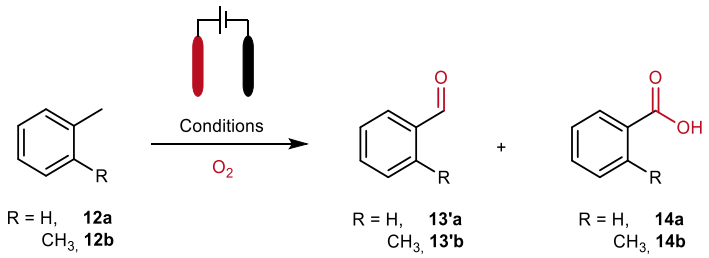

Entry	R	Deviation from standard conditions[a]	13'	14
1	H	None	4%	33%
2	H	5 mA cm^{-2}	15%	3%
3	H	15 mA cm^{-2}	1%	41%
4	H	25 mA cm^{-2}	3%	39%
5	H	30 mA cm^{-2}	3%	37%
6	H	45 mA cm^{-2}	14%	25%
7	H	60 mA cm^{-2}	5%	11%
8	H	5 °C, 15 mA cm^{-2}	1%	35%
9	H	33 °C, **12a** (0.1 mol L^{-1}), NBu_4NO_3 (1.0 eq.), 6 *F*, 30 mA cm^{-2}	6%	42%
10	CH_3	33 °C, **12b** (0.02 mol L^{-1}), NBu_4NO_3 (1.0 eq.), 5 *F*	74%	7%
11	CH_3	33 °C, NBu_4NO_3 (1.0 eq.), 3,2 *F*	27%	0%
12	CH_3	33 °C, NBu_4NO_3 (1.0 eq.), 5 *F*, 20 mA cm^{-2}	45%	1%

[a]Undivided 5 mL PTFE cell, glassy carbon electrodes, acetonitrile (5 mL), **12** (0.2 mol L^{-1}), NBu_4NO_3 (0.5 eq.), 25 °C, O_2 atm. (100 vol.%), 350 rpm, 7 *F*, 10 mA cm^{-2}. Yield determination via ^1H NMR (1,3,5-trimethoxybenzene as internal standard).

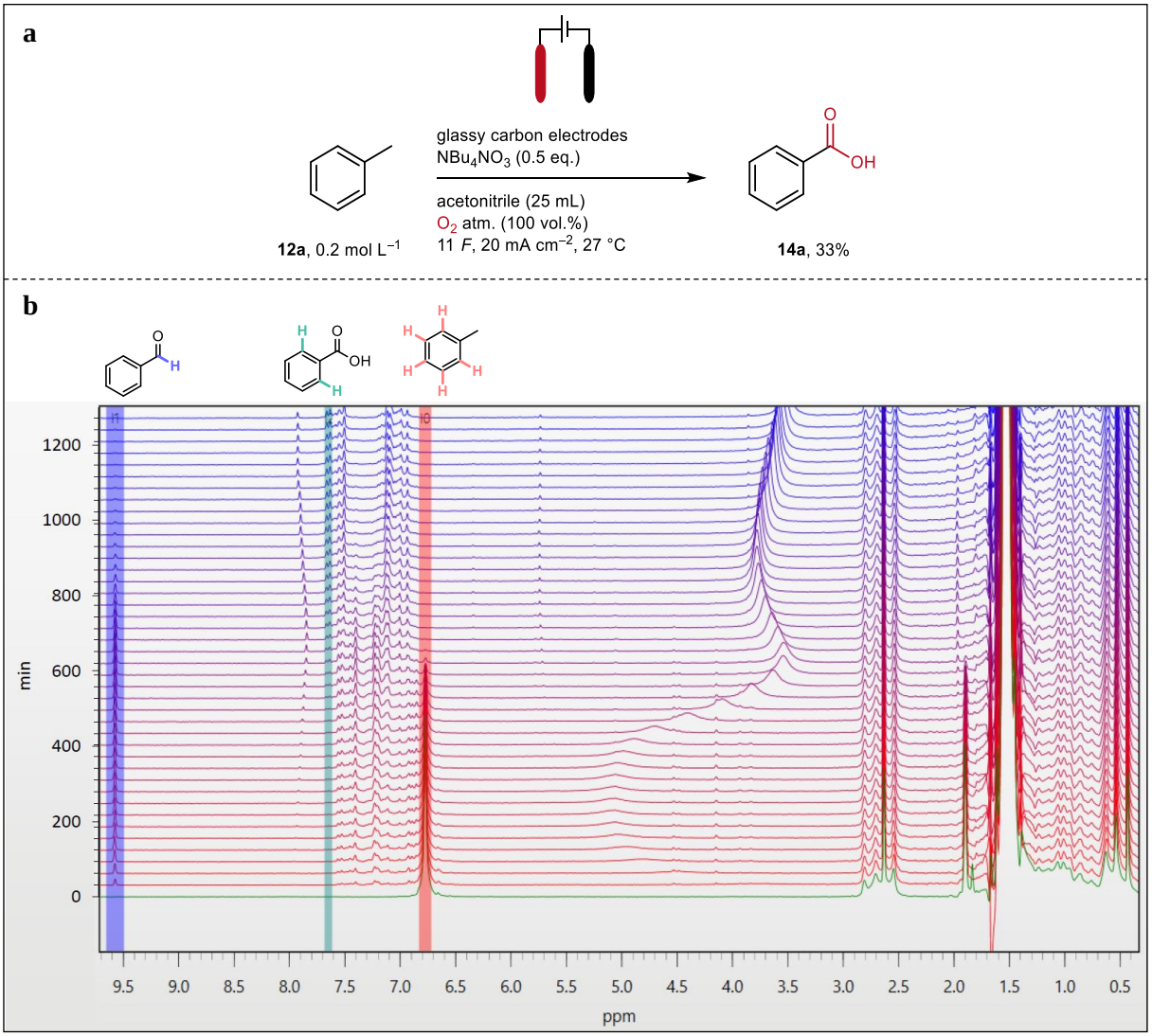

Supplementary Fig. 8: **a** The reaction was performed under the given conditions in a 25 mL beaker-type cell. **b** Stacked ^{1}H NMR spectra for reaction control with a Spinsolv 60 benchtop NMR spectrometer. Signals for integration were chosen in a way that no overlapping occurs. For normalizing the signal intensities to one proton, the toluene (**12a**) proton intensity was divided by 5. The integrated signals for benzaldehyde (**13'a**) and benzoic acid (**14a**) correspond to one proton. Corresponding integration areas are marked as follows: **12a** pink, **13'a** blue, and **14a** green.

2.7 Recovery and reuse of the supporting electrolyte

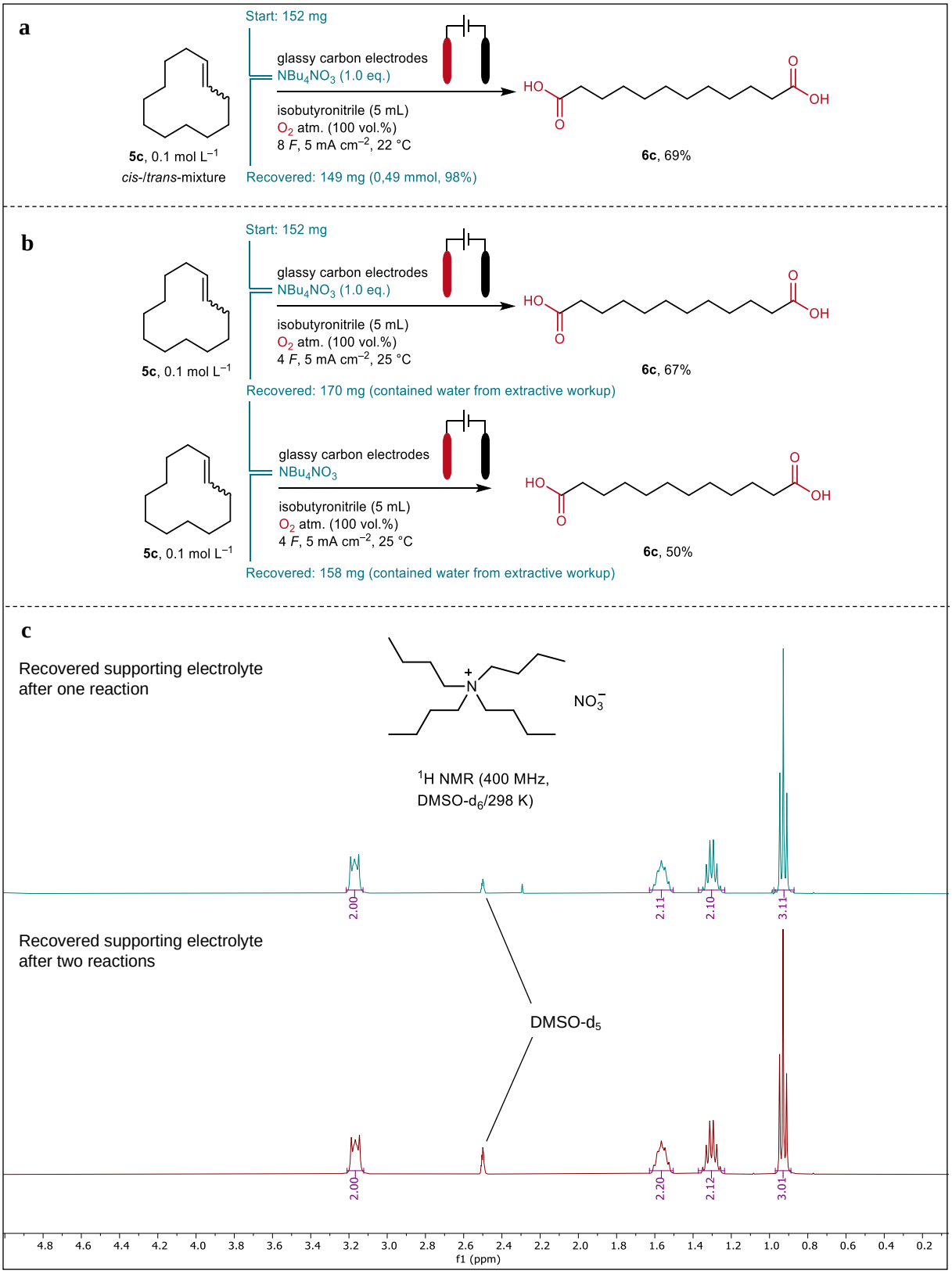

Supplementary Fig. 9: **a** Recovered supporting electrolyte from the aqueous layer of an extractive workup, after one reaction of cyclododecene (**5c**) to dodecanedioic acid (**6c**). **b** Recovery and reuse of supporting electrolyte for a second reaction. **c** Stacked ^{1}H NMR spectra of recovered NBu_4NO_3 supporting electrolyte after one reaction (upper spectrum, blue) and two reactions (lower spectrum, brown).

The supporting electrolyte recovery and recycle was demonstrated in two experiments for synthesizing dodecanedioic acid (**6c**) from cyclododecene (**5c**). During the workup procedure for (di)carboxylic acid and benzoic acid synthesis (see Method section in the manuscript) the supporting electrolyte was recovered from the aqueous layers as a colorless, wax-like solid (149 mg, 0.49 mmol, 98%) (see Supplementary Fig. 9a). The ^{1}H NMR spectrum of the supporting electrolyte is shown in Supplementary Fig. 9c (upper spectrum). In an additional experiment, the supporting electrolyte was recovered after the first electrolysis and reused in a second one to demonstrate recyclability (see Supplementary Fig. 9b). Here, a yield loss of 17% was observed for dodecanedioic acid (**6c**), which could be due to residual water still present in the electrolyte. After reusing the supporting electrolyte, 158 mg was obtained after the second reaction, presumably with residual water after the workup. When comparing the two spectra, it can be seen that no significant organic impurities are present even after the reuse of the supporting electrolyte (see Supplementary Fig. 9c).

2.8 Oxo-functionalization results with branched cycloalkanes

Regioselectivities were investigated on various branched cycloalkanes by GC-FID and GC-MS measurements. The selectivities were determined as GC integral ratios.

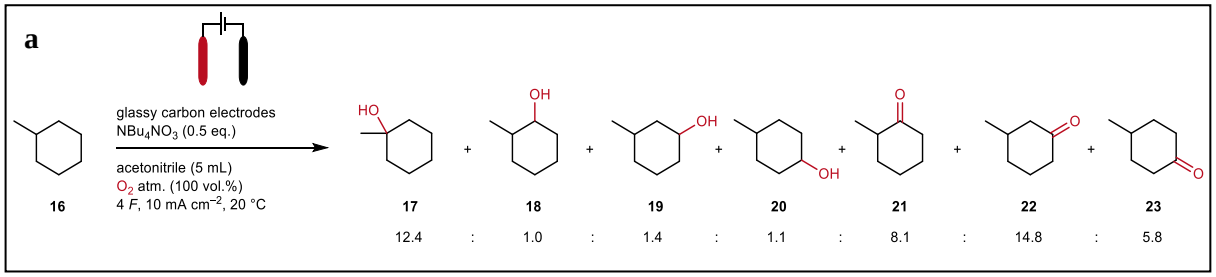

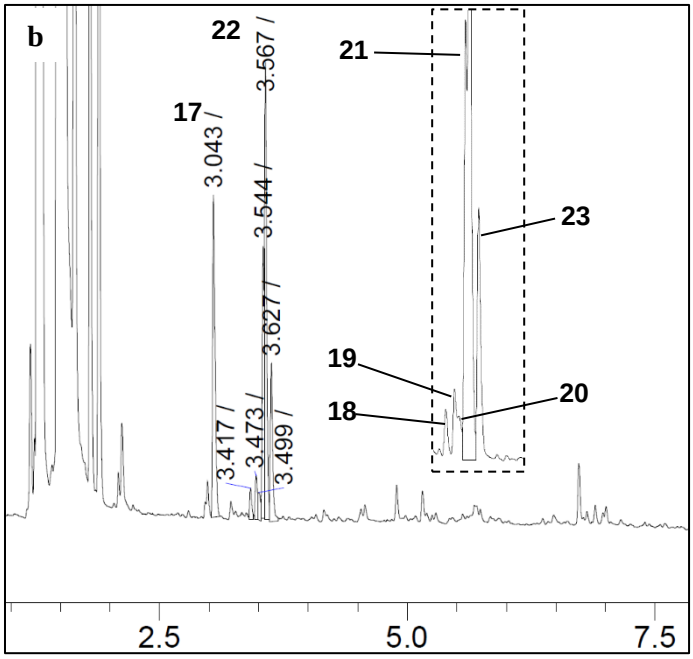

c

Molecule	Ret. time (min)	GC int.	Selectivity ratio
17	3.043	8594	12.4
18	3.417	693	1.0
19	3.473	996	1.4
20	3.499	736	1.1
21	3.544	5624	8.1
22	3.567	10236	14.8
23	3.627	3990	5.8

Supplementary Fig. 10: **a** The reaction of methylcyclohexane (**17**) was performed under the given conditions in a 5 mL PTFE cell. **b** GC-FID chromatogram after the electrolysis. The molecules' assignment has been carried out with GC-MS by comparison of the observed mass spectra with the NIST17 mass spectral library entries. **c** Data of the GC-FID chromatogram to evaluate the selectivity ratios for the assigned products.

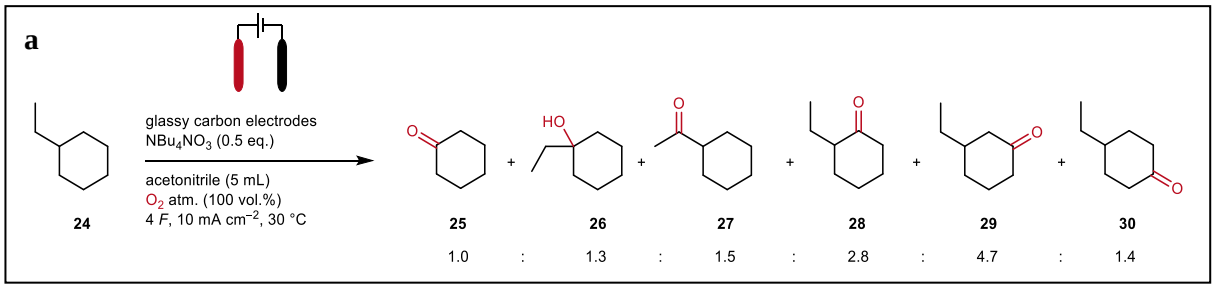

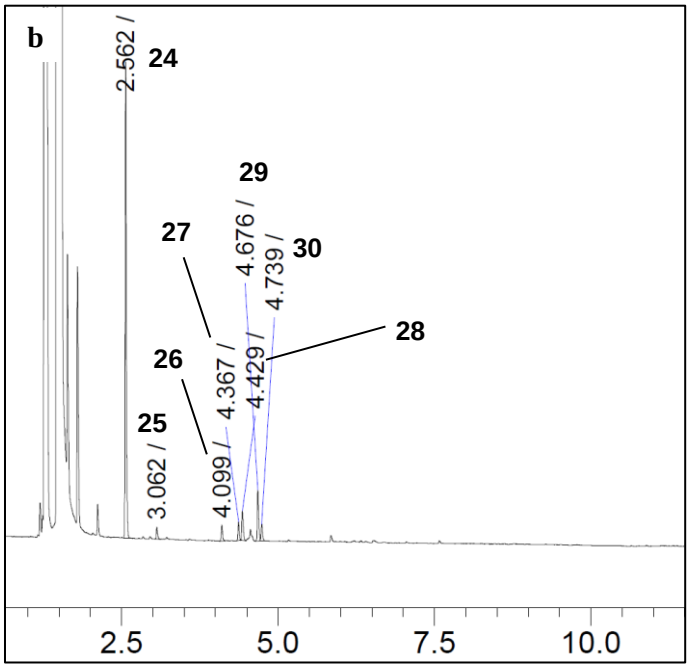

c

Molecule	Ret. time (min)	GC int.	Selectivity ratio
25	3.062	1072	1.0
26	4.099	1447	1.3
27	4.367	1613	1.5
28	4.429	2995	2.8
29	4.676	5036	4.7
30	4.739	1550	1.4

Supplementary Fig. 11: **a** The reaction of ethylcyclohexane (**24**) was performed under the given conditions in a 5 mL PTFE cell. **b** GC-FID chromatogram after the electrolysis. The molecules' assignment has been carried out with GC-MS by comparison of the observed mass spectra with the NIST17 mass spectral library entries. **c** Data of the GC-FID chromatogram to evaluate the selectivity ratios for the assigned products.

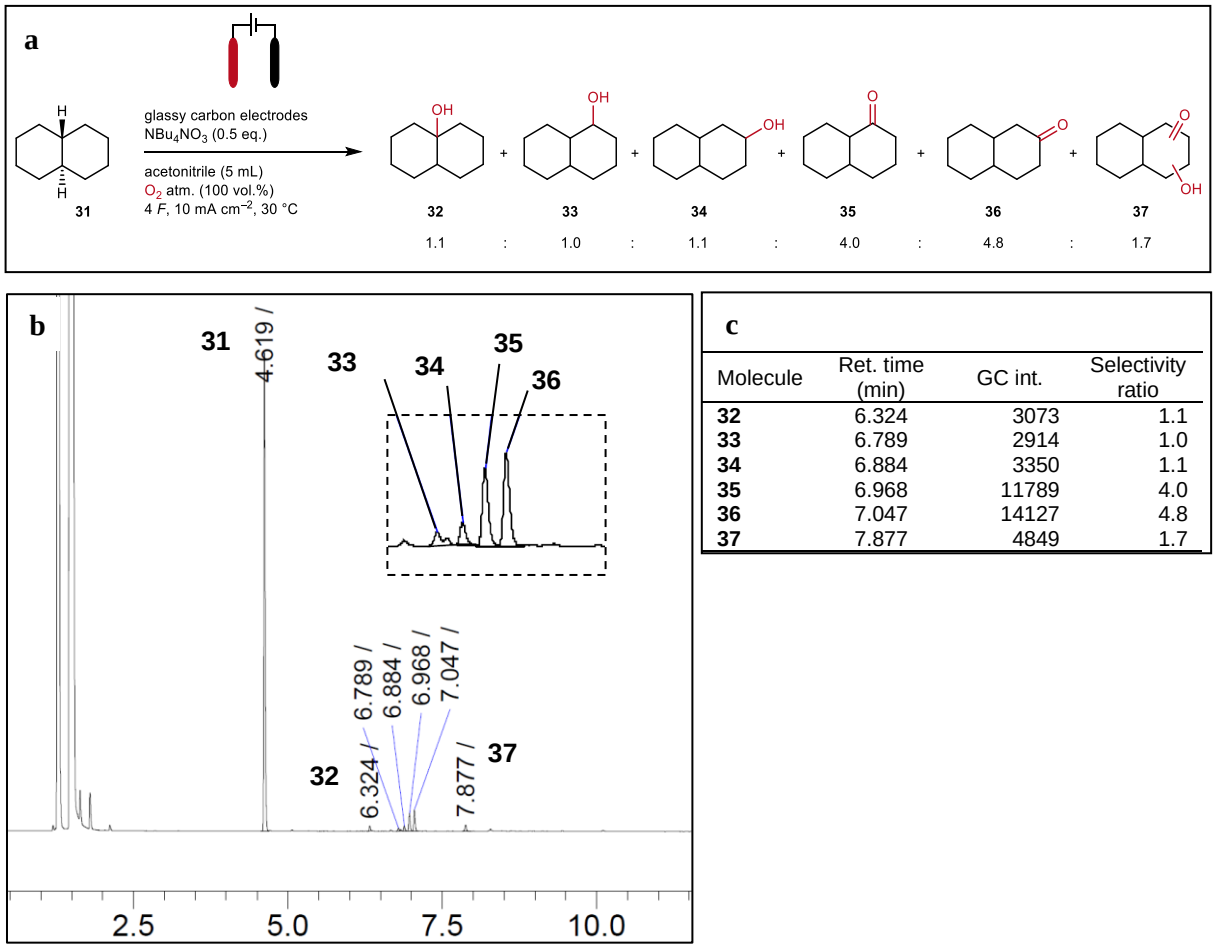

c

Molecule	Ret. time (min)	GC int.	Selectivity ratio
32	6.324	3073	1.1
33	6.789	2914	1.0
34	6.884	3350	1.1
35	6.968	11789	4.0
36	7.047	14127	4.8
37	7.877	4849	1.7

Supplementary Fig. 12: **a** The reaction of *trans*-decalin (**31**) was performed under the given conditions in a 5 mL PTFE cell. **b** GC-FID chromatogram after the electrolysis. The molecules' assignment has been carried out with GC-MS by comparison of the observed mass spectra with the NIST17 mass spectral library entries. **c** Data of the GC-FID chromatogram to evaluate the selectivity ratios for the assigned products.

2.9 Qualitative HRMS analysis of the reaction mixture for diacid synthesis

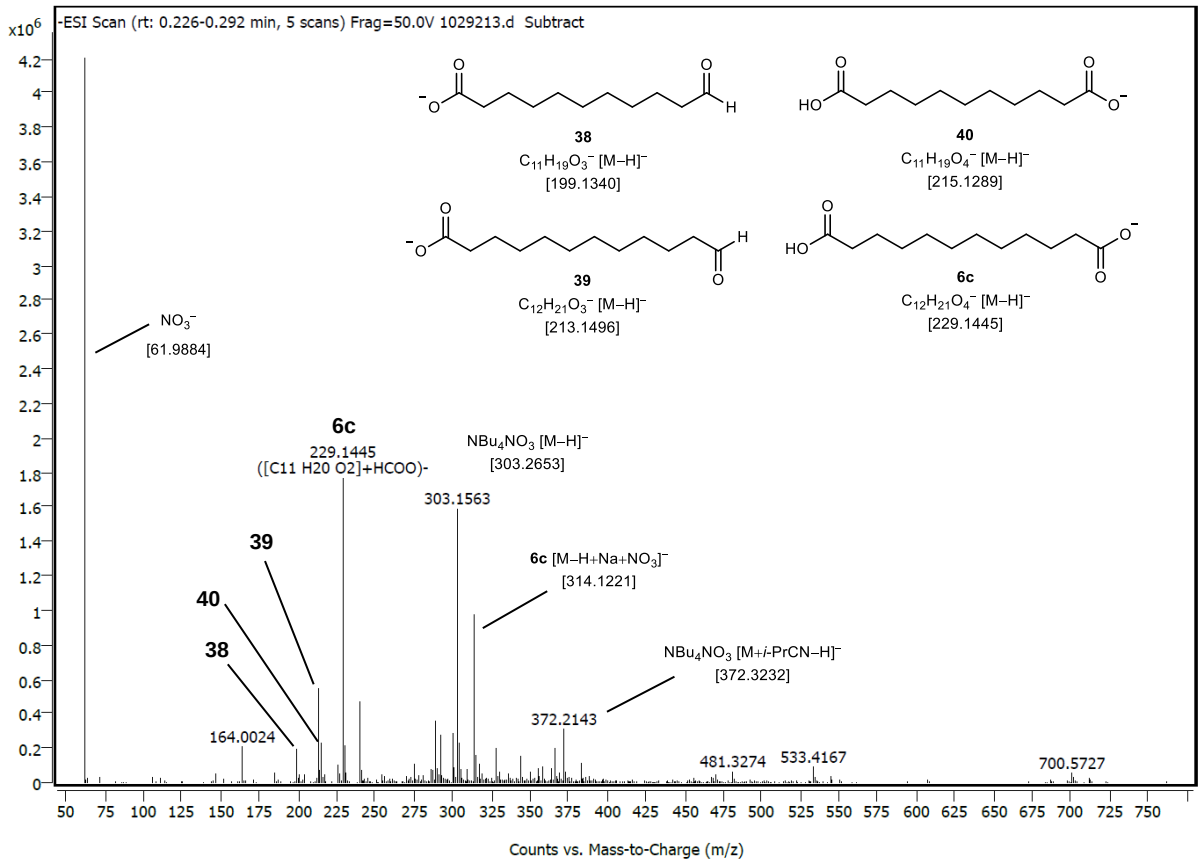

Supplementary Fig. 13: (ESI–)-recorded mass spectra of an HRMS analysis from the reaction solution after electrolysis of cyclododecene (**5c**) to dodecanedioic acid (**6c**) in an isobutyronitrile/NBu_4NO_3 electrolyte.

3. Supplementary Notes

3.1 Determination of dissolved oxygen concentration

Cyclic voltammetry measurements were carried out in a 10 mL snap-cap vial in which the supporting electrolyte (0.1 mol L^{-1}), and optionally the substrate, was dissolved in acetonitrile (5 mL). The composition of the gas space above the electrolyte was adjusted beforehand by using mass flow controllers (5 vol.% O_2 to 100 vol.% O_2 in N_2) and was introduced via a cannula during the entire measurement time. The temperature control of 25 °C was carried out via an oil bath. Between the individual measurements, the electrolyte was stirred at 400 rpm. Before each measurement, the working electrode was polished with BASi® Electrode Polishing Alumina Suspension (Bioanalytical Systems Inc., West Lafayette, Indiana) for approx. 30 seconds.

The statistical software Origin 7.5 SR6 (OriginLab Corporation, Northampton, Massachusetts) was used for linear regression analysis. Mathematical calculations were performed using Microsoft® Excel® 2019. Voltammograms were recorded using NOVA 2.1.3 software (Metrohm AG, Herisau, Switzerland).

To determine the concentration of dissolved oxygen in acetonitrile at different O_2 vol.% values in the atmosphere, a potentiometric method via cyclic voltammetry was used. Given a known diffusion coefficient D of the investigated species, the Randles-Ševčík equation (1) can be used to determine its concentration. The measured peak current I_p is proportional to the concentration c of the species. Using the relationship, $I_p \sim \sqrt{v}$ with v as scan rate, the concentration can be determined from the slope m of a linear fit via the equations (2) and (3). The propagation of uncertainty has been calculated via equations (4) and (5) which derive from the standard error propagation equation[3].

<u>*Randles-Ševčík equation for 25 °C:*</u>

$$j_p = \frac{I_p}{A} = 2.69 \cdot 10^5 c\sqrt{n^3 D v} \qquad (1)$$

$$m = 2.69 \cdot 10^5 c\sqrt{n^3 D} \qquad (2)$$

$$c = \frac{m}{2.69 \cdot 10^5 \sqrt{n^3 D}} \qquad (3)$$

j_p: Maximum of current density [A cm^{-2}]
I_p: Current maximum [A]
A: Electrode area [cm^2]
c: Concentration [mol mL^{-1}]
D: Diffusion coefficient [cm^2 s^{-1}]
v: Scan rate [V s^{-1}]
n: Number of transferred electrons ($n = 1$)
m: Slope of the linear fit of $j_p(\sqrt{v})$

$$\Delta j_p = \Delta \frac{I_p}{A} = \frac{\partial j_p}{\partial I_p}\Delta I_p + \frac{\partial j_p}{\partial A}\Delta A = \frac{\Delta I_p}{A} - \frac{I_p}{A^2}\Delta A \qquad (4)$$

$$\Delta c = \frac{\partial c}{\partial m}\Delta m + \frac{\partial c}{\partial D}\Delta D = \frac{\Delta m}{2.69 \cdot 10^5 \sqrt{n^3 D}} - \frac{m\Delta D}{2 \cdot 2.69 \cdot 10^5 \sqrt{n^3 D^3}} \qquad (5)$$

As diffusion coefficient of dissolved oxygen, a literature known value of $2.1 \cdot 10^{-5}$ cm^2 s^{-1} (in acetonitrile/NBu_4PF_6 (0.1 mol L^{-1})) was used[4]. Cyclic voltammetry has been performed using the conditions in Supplementary Fig. 10d. The values for I_p in Supplementary Table 6 are mean values out of three measurements, each with an associated uncertainty ΔI_p. j_p and Δj_p were calculated using equations (1) and (4). c and Δc were calculated regarding equations (3) and (5). Supplementary Fig. 10 shows furthermore the corresponding plots of j_p vs. $v^{1/2}$ including the linear regressions as well as the dependence of the dissolved oxygen concentration $c(O_2)$ on the atmospheric O_2 content.

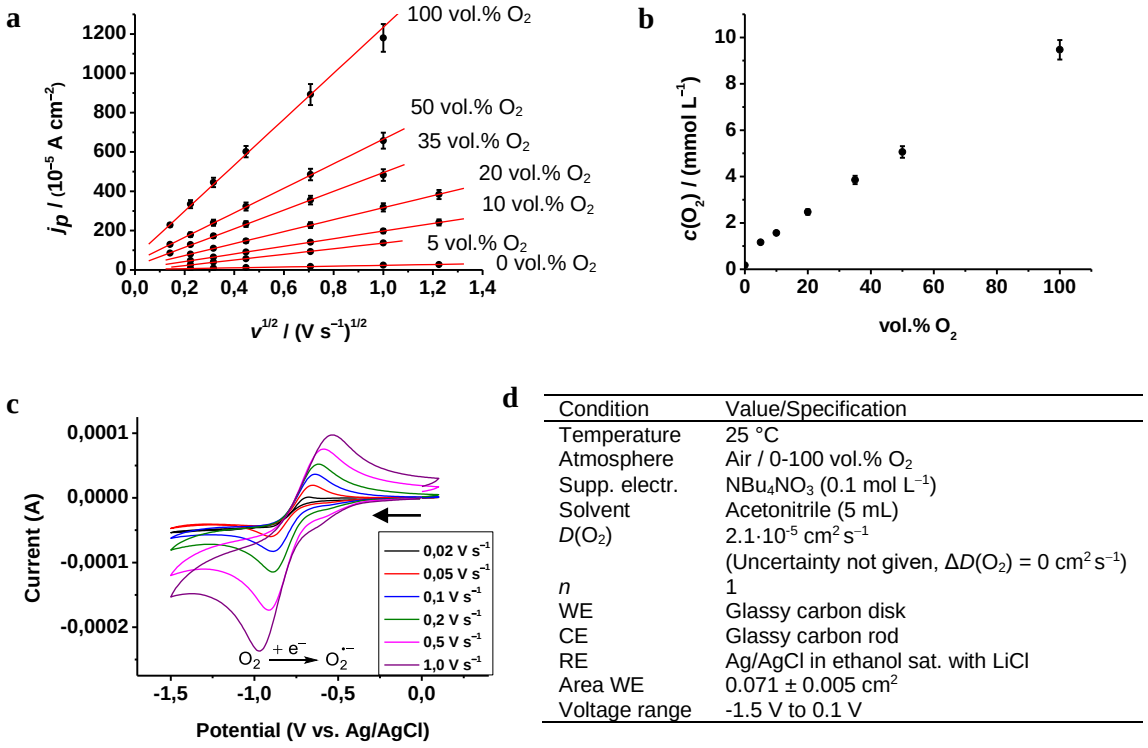

d

Condition	Value/Specification
Temperature	25 °C
Atmosphere	Air / 0-100 vol.% O_2
Supp. electr.	NBu_4NO_3 (0.1 mol L^{-1})
Solvent	Acetonitrile (5 mL)
$D(O_2)$	$2.1 \cdot 10^{-5}$ cm^2 s^{-1}
	(Uncertainty not given, $\Delta D(O_2) = 0$ cm^2 s^{-1})
n	1
WE	Glassy carbon disk
CE	Glassy carbon rod
RE	Ag/AgCl in ethanol sat. with LiCl
Area WE	0.071 ± 0.005 cm^2
Voltage range	-1.5 V to 0.1 V

Supplementary Fig. 14: **a** Plot j_p vs. $v^{1/2}$ for the O_2 measurements in MeCN/NBu_4NO_3 at different atmospheric O_2 contents. Error bars along the *y*-axis are calculated via uncertainty propagation. Linear regression straight lines are labeled in red. **b** Dependence of dissolved oxygen concentration $c(O_2)$ in MeCN on the atmospheric O_2 content. Error bars along the *y*-axis are calculated via uncertainty propagation. **c** Exemplarily cyclic voltammograms for oxygen reduction at different scan rates at air atmosphere. CVs at the remaining atmosphere constitutions were measured and recorded analogously. **d** Cyclic voltammetry conditions for dissolved oxygen concentration determination.

The resulting values for the dissolved oxygen concentrations (at air: (2.4 ± 0.1) mmol L^{-1}; at 100 vol.% O_2: (9.5 ± 0.6) mmol L^{-1}) are comparable to the ones, which are literature described (at air: (2.42 ± 0.14) mmol L^{-1} (photochemical determination)[5], at 100 vol.% O_2: (8.1 ± 0.6) mmol L^{-1} (determination via GC)[6]). In contrast to the latter one, for the determination in this work, O_2 was permanently introduced into the atmosphere above the electrolyte during the measurements.

With regards to the Supplementary Table 1 (entry 10) a minimum dissolved oxygen concentration in the electrolyte of approx. 1 mmol L^{-1} (5 vol.% O_2 in the atmosphere) is necessary for the cycloalkane oxidation to occur.

Supplementary Table 6: Current maximums at different scan rates for O_2 in MeCN/NBu_4NO_3 including the calculated O_2 concentrations.

Atm. (vol.% O_2)	I_p / (10^{-5} A)	v / (V s^{-1})	$\sqrt{v}$ / $\sqrt{\text{V s}^{-1}}$	j_p / (10^{-5} A cm^{-2})	m / $\left(10^{-5}\ \frac{\text{mol}}{\text{mL}}\sqrt{\frac{\text{cm}^2}{\text{s}}}\right)$	**$c(O_2)$ / (mmol L^{-1})**
Air	4.4 ± 0.2	0.02	0.14	62 ± 2	297 ± 14	**2.4 ± 0.1**
	5.57 ± 0.01	0.05	0.22	79 ± 5		
	7.62 ± 0.09	0.10	0.32	108 ± 6		
	10.72 ± 0.07	0.20	0.45	152 ± 9		
	16.9 ± 0.1	0.50	0.71	239 ± 14		
	23.2 ± 0.1	1.00	1.00	328 ± 20		
0	0.50 ± 0.02	0.05	0.22	7.1 ± 0.2	21.0 ± 0.5	**0.171 ± 0.004**
	0.62 ± 0.02	0.10	0.32	8.8 ± 0.4		
	0.87 ± 0.04	0.20	0.45	12.3 ± 0.3		
	1.21 ± 0.07	0.50	0.71	17.2 ± 0.2		
	1.74 ± 0.05	1.00	1.00	24.6 ± 0.9		
	1.95 ± 0.06	1.50	1.22	27.5 ± 1.0		
5	1.8 ± 0.2	0.05	0.22	25.5 ± 0.5	143 ± 6	**1.16 ± 0.05**
	2.84 ± 0.01	0.10	0.32	40 ± 3		
	4.02 ± 0.02	0.20	0.45	57 ± 3		
	6.60 ± 0.02	0.50	0.71	93 ± 6		
	9.7 ± 0.2	1.00	1.00	137 ± 7		
10	3.4 ± 0.1	0.05	0.22	48 ± 2	194 ± 9	**1.57 ± 0.07**
	4.59 ± 0.02	0.10	0.32	65 ± 4		
	6.42 ± 0.04	0.20	0.45	91 ± 5		
	10.0 ± 0.1	0.50	0.71	141 ± 8		
	14.0 ± 0.1	1.00	1.00	198 ± 11		
	17.09 ± 0.03	1.50	1.22	242 ± 16		
20	5.7 ± 0.2	0.05	0.22	81 ± 3	304 ± 15	**2.5 ± 0.1**
	7.76 ± 0.04	0.10	0.32	110 ± 7		
	10.41 ± 0.02	0.20	0.45	147 ± 9		
	16.11 ± 0.04	0.50	0.71	228 ± 15		
	22.51 ± 0.03	1.00	1.00	318 ± 21		
	27.1 ± 0.2	1.50	1.22	383 ± 23		
35	6.1 ± 0.2	0.02	0.14	86 ± 3	475 ± 22	**3.9 ± 0.2**
	9.12 ± 0.06	0.05	0.22	129 ± 8		
	12.2 ± 0.1	0.10	0.32	173 ± 10		
	16.50 ± 0.07	0.20	0.45	233 ± 15		
	25.1 ± 0.1	0.50	0.71	355 ± 22		
	34.1 ± 0.2	1.00	1.00	483 ± 30		
50	9.2 ± 0.3	0.02	0.14	130 ± 4	624 ± 31	**5.1 ± 0.3**
	12.67 ± 0.07	0.05	0.22	179 ± 11		
	16.96 ± 0.04	0.10	0.32	240 ± 15		
	22.80 ± 0.06	0.20	0.45	323 ± 21		
	34.3 ± 0.2	0.50	0.71	486 ± 29		
	46.5 ± 0.2	1.00	1.00	657 ± 41		
100	16.2 ± 0.5	0.02	0.14	229 ± 8	1168 ± 52	**9.5 ± 0.4**
	23.7 ± 0.1	0.05	0.22	335 ± 21		
	31.5 ± 0.4	0.10	0.32	445 ± 24		
	42.5 ± 0.8	0.20	0.45	602 ± 29		
	63.1 ± 0.4	0.50	0.71	892 ± 53		
	83.4 ± 0.6	1.00	1.00	1180 ± 71		

3.2 Mechanism elucidation experiments

3.2.1 Griess test

Griess test for nitrite detection was conducted according to the following procedure:

Solution A and B were freshly prepared before the test. Solution A: in a 10 mL round bottom flask sulfanilic acid (20 mg) is dissolved in aqueous acetic acid (30%, 2,5 mL). Solution B: In a 10 mL round bottom flask 1-naphthylamine (25 mg) is dissolved in aqueous acetic acid (30%, 2,5 mL). Both solutions can be stored at 4 °C. Prior to the test, 1–2 drops out of each solution are combined and mixed in a reagent tube to a colorless liquid. One drop of the sample is added to the reagent tube.

Result: If the solution color turns to red/pink, the test is positive for nitrite, which is present in the sample. Coloring occurs due to the formation of an azo dye compound. Nitrate instead does not lead to a positive result and the reaction solution stays colorless.

3.2.2 Ion chromatography

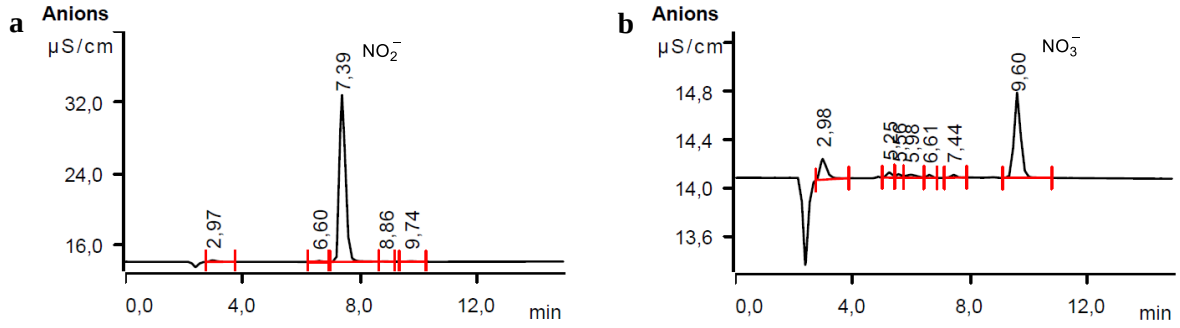

Supplementary Fig. 15: **a** Anion chromatogram of sodium nitrite (0.01 mg mL^{-1} in deionized water) as reference. **b** Anion chromatogram of the aqueous layer after extractive work-up from the reaction solution.

3.2.3 pH test

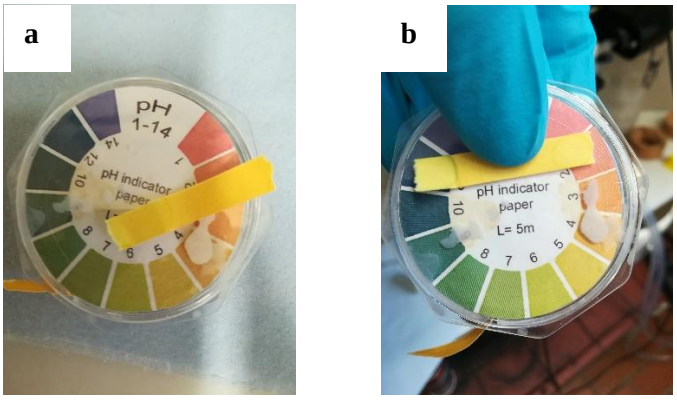

Supplementary Fig. 16: **a** After electrolysis under 100 vol.% oxygen atmosphere: pH 5–6. **b** After electrolysis under 100 vol.% argon atmosphere: pH 8–9.

3.2.4 Peroxide test with titanyl sulfate

Peroxide test for H_2O_2 and organic peroxide detection was conducted after the following procedure:

In a reagent tube titanyl sulfate (10 mg) is suspended in 5 drops of concentrated sulfuric acid. Afterwards, 1 mL of the analysis solution is added into the reagent tube.

Result: if peroxide species are present in the analysis solution the color turns from colorless to yellow/orange, indicating the formation of peroxotitanyl ion $(TiO_2)^{2+}$.

Electrolysis was performed regarding GP 1: the reaction was stopped manually at 50 C and the peroxide test was performed immediately afterwards. Conditions: acetonitrile (5 mL), NBu_4NO_3 (0.1 mol L^{-1}), 10 mA cm^{-2}, under 100 vol.% O_2, once with substrate (cyclooctane (**1c**), 0.2 mol L^{-1}) and once without substrate.

3.2.5 Karl Fischer titration

For the determination of an increased water content after electrolysis, a coulometric Karl Fischer titration was performed after the following procedure:

The titration cell was conditioned until the drift was <10 µg min^{-1}. Prior to the analysis samples 1 mL of a water standard 0.1 solution was measured three times resulting to (0.106 ± 0.002) mg g^{-1} (target: (0.100 ± 0.009) mg g^{-1}). The measurements were conducted following the instruction manual. Approx. 0.5 mL of the analysis sample was drawn into a cannula syringe and tared on a fine balance. Immediately after starting the measurement, the sample was injected within 10 seconds into the titration cell without contacting something of the inner parts. The emptied syringe was weighed and the determined weight entered into the software. The procedure was repeated three times per sample.

Supplementary Table 7: Karl Fischer titration after electrolysis, once with cyclooctane (**1c**) substrate, once without.

Sample	Measurement	*m*(H_2O) / weight of sample taken	ppm H_2O	mg g^{-1} H_2O	
Electrolysis with substrate	1	2222.5 µg / 0.496 g	4513.8	4.4808	4.474 ± 0.006
	2	2147.4 µg / 0.480 g	4514.5	4.4738	
	3	2189.6 µg / 0.490 g	4512.4	4.4686	
Electrolysis without substrate	1	2136.2 µg / 0.495 g	4357.7	4.3156	4.315 ± 0.008
	2	2083.6 µg / 0.482 g	4370.3	4.3228	
	3	2071.7 µg / 0.481 g	4353.3	4.3071	

Electrolysis was performed regarding GP 1: After electrolysis the cell content was transferred into a snap cap vial, weighed and sealed with Parafilm® M. Titration of the samples was performed immediately afterwards. Conditions: acetonitrile (5 mL), NBu_4NO_3 (0.1 mol L^{-1}), 10 mA cm^{-2}, 8 *F*, under 100 vol.% O_2, once with substrate (cyclooctane (**1c**), 0.2 mol L^{-1}) and once without substrate.

3.2.6 Control experiment for nitrate radical observation

The reaction was conducted according to GP 1. As anode boron-doped diamond (BDD) and as cathode nickel were used, since both are stable in an acidic environment and nickel has a relatively low overpotential regarding reductive hydrogen evolution reaction[7]. Instead of oxygen, an argon atmosphere was set within the cell to suppress an oxygen reduction reaction. Cyclooctene (**5b**, 1 mmol) was subjected to 2 *F* and 10 mA cm^{-2}. After electrolysis, three drops were eluted with ethyl acetate through approx. 330 mg silica 60M and filled into a vial for GC-MS analysis.

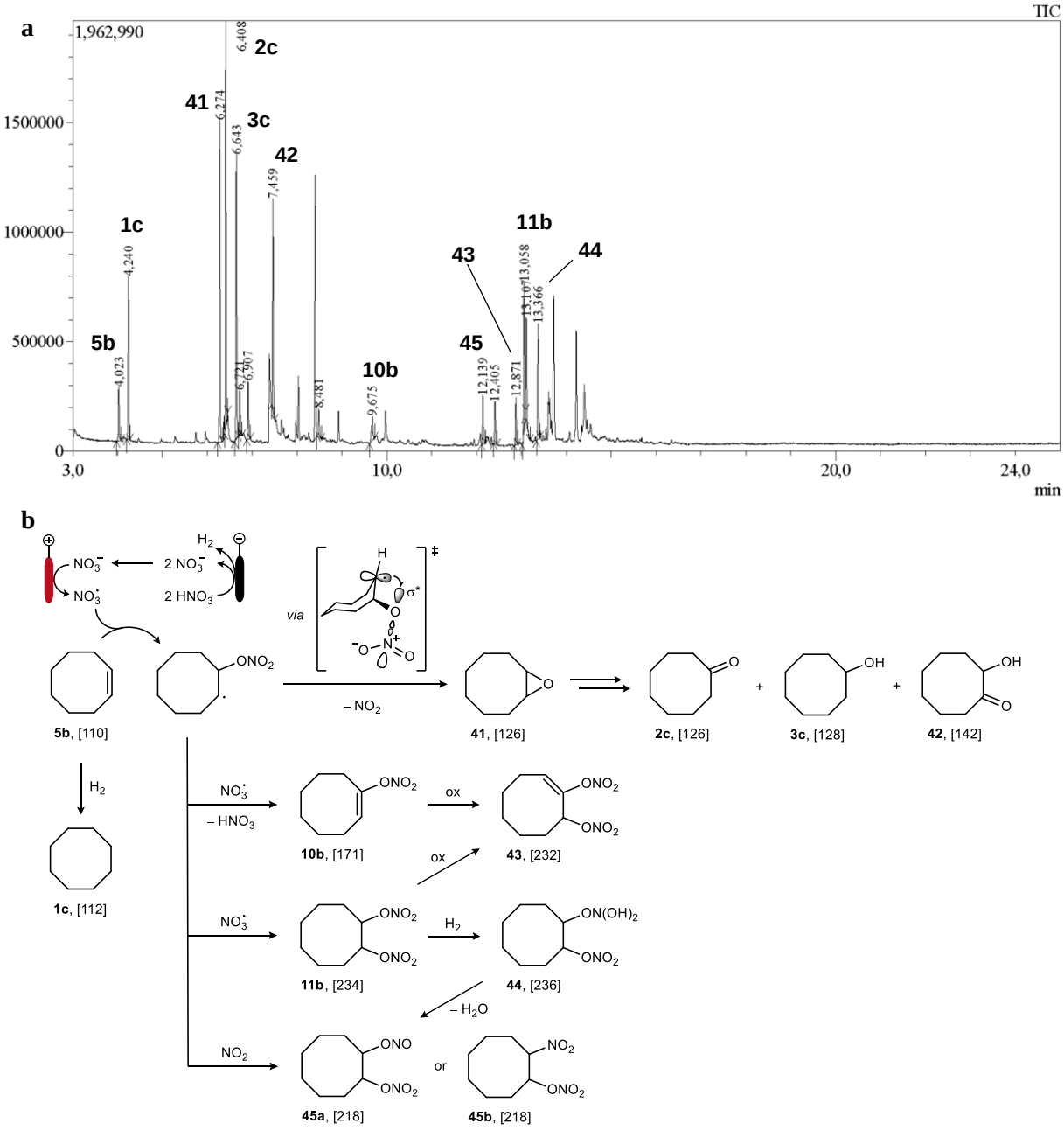

Supplementary Fig. 17: **a** GC-MS of the reaction solution. The molecules' assignment has been carried out by comparison of the observed mass spectra with the NIST17 mass spectral library entries. **b** Mechanistic considerations regarding the observed signals in the GC-MS analysis.

As one of the main products an epoxide **41** was detected. The observation of its formation through the influence of nitrate radicals under argon atmosphere is in accordance to literature reports[8]. The presence of water and the acidic environment due to the use of nitric acid can lead to further oxidized species like **2c**, **3c** and **42**. Nitrate radicals can possibly lead to **10b** via H-abstraction, or **11b** via recombination.

Due to the formation of epoxides, NO_2 radicals are probably present in the reaction solution as well, which could possibly explain the formation of **45** species.

3.2.7 Cyclic voltammetry studies

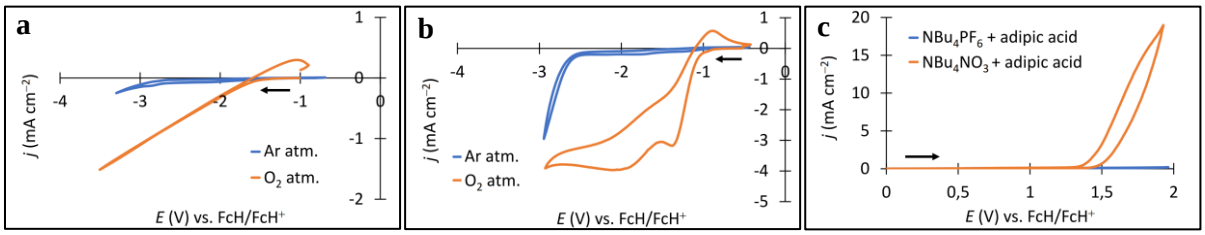

Supplementary Fig. 18: **a** Comparison of the reduction behavior of a dimethyl carbonate/*i*-PrOH (9:1) electrolyte in the presence and absence of oxygen. Electrolyte: dimethyl carbonate (4.5 mL), 2-propanol (0.5 mL), NBu_4NO_3 (0.1 mol L^{-1}). Conditions: glassy carbon disk (working electrode, 3 mm diameter), glassy carbon rod (counter electrode), Ag/AgCl in saturated LiCl/EtOH (reference electrode), Ferrocene/Ferrocenium (FcH/FcH^+) as internal reference ($E_{1/2}$ = 0.79–0.99 V), 50 mV s^{-1}. **b** Comparison of the reduction behavior of an acetonitrile/water (2 vol.%) electrolyte in the presence and absence of oxygen. Electrolyte: acetonitrile (4.9 mL), water (0.9 mL), NBu_4NO_3 (0.1 mol L^{-1}). Conditions: see Supplementary Fig. 18a, ($E_{1/2}(FcH/FcH^+)$ = 0.52–0.54 V). **c** Investigation of an adipic acid oxidation in a NO_3^- and a PF_6^- supported electrolyte system. Electrolyte: acetonitrile (5 mL), NBu_4NO_3 or NBu_4PF_6 (0.1 mol L^{-1}), adipic acid (**6a**, 0.01 mol L^{-1}). Conditions: see Supplementary Fig. 18a, measurements were performed under air atmosphere, ($E_{1/2}(FcH/FcH^+)$ = 0.54–0.58 V).

3.3 *N*-Acetylbenzamide formation

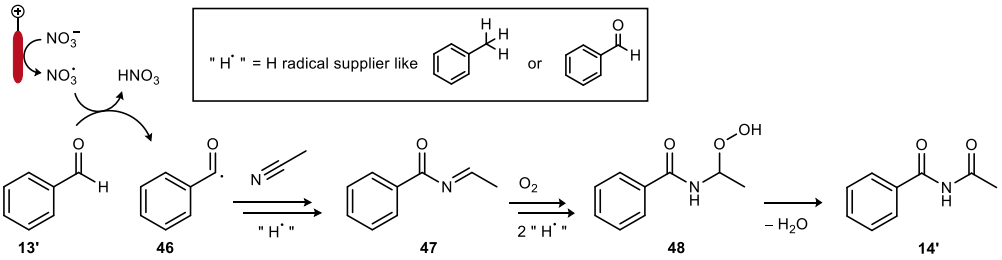

Supplementary Fig. 19: Presumed pathway for *N*-acetylbenzamide formation.

3.4 Syntheses of supporting electrolytes

General procedure: In a 50 mL round-bottom flask silver nitrate (1.1–1.2 eq.) is dissolved in 5 mL deionized water. Alkylammonium (or alkylphosphonium) bromide (1.0 eq.) is dissolved in a water-acetone-mixture and added dropwise to the silver nitrate solution while vigorous stirring. After approx. 10 min, the precipitated silver bromide is filtered and washed with water and acetone. The filtrate is extracted with ethyl acetate, while approx. 300 mg sodium nitrate are added to the aqueous layer for improved phase separation. The organic layer is separated, the solvent is distilled and the remaining product dried under reduced pressure.

Hexadecyltrimethylammonium nitrate

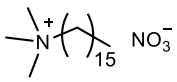

Hexadecyltrimethylammonium bromide (525 mg, 1.44 mmol, 1.0 eq.) is dissolved in 12.5 mL water and 5 mL acetone and is converted according to the general procedure with silver nitrate (294 mg, 1.73 mmol, 1.2 eq.). After workup, the product is obtained as a colorless powder (yield: 53%, 263 mg, 0.76 mmol).

^{1}H NMR (400 MHz, D_2O) δ [ppm] = 3.35–3.31 (m, 2H), 3.13 (s, 9H), 1.80–1.72 (m, 2H), 1.37–1.31 (m, 26H), 0.90–0.87 (m, 3H); ^{13}C NMR (101 MHz, D_2O) δ [ppm] = 66.4, 52.7, 32.1, 30.3, 30.3, 30.3, 30.2, 30.2, 30.1, 30.0, 29.8, 28.7, 29.3, 26.2, 22.8, 22.7, 13.8.

1-Butyl-3-methylimidazolium nitrate

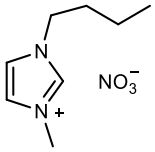

1-Butyl-3-methylimidazolium bromide (543 mg, 2.48 mmol, 1.0 eq.) is dissolved in 2 mL water and 5 mL acetone and is converted according to the general procedure with silver nitrate (463 mg, 2.73 mmol, 1.1 eq.). Due to the product's hydrophily, the aqueous filtrate is distilled directly and the remaining product is dried under reduced pressure. A colorless, highly viscous liquid is obtained (yield: 90%, 446 mg, 2.22 mmol).

^{1}H NMR (400 MHz, D_2O) δ [ppm] = 8.73 (s, 1H), 7.50 (dd, *J* = 2.2 Hz, *J* = 1.8 Hz, 1H), 7.45 (dd, *J* = 2.2 Hz, *J* = 1.8 Hz, 1H), 4.21 (t, *J* = 7.3 Hz, 2H), 3.92 (s, 3H), 1.86 (quint, *J* = 7.4 Hz, 2H), 1.33 (sextet, *J* = 7.4 Hz, 2H), 0.93 (t, *J* = 7.4 Hz, 3H); ^{13}C NMR (101 MHz, D_2O) δ [ppm] = 135.8, 123.4, 122.2, 49.2, 35.5, 31.3, 18.7, 12.6.

Methyltrioctylammonium nitrate

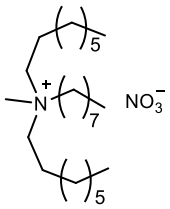

Methyltrioctylammonium bromide (520 mg, 1.16 mmol, 1.0 eq.) is dissolved in 1 mL water and 5 mL acetone and is converted according to the general procedure with silver nitrate (216 mg, 1.28 mmol, 1.1 eq.). After workup, the product is obtained as a highly viscous liquid (yield: 95%, 473 mg, 1.10 mmol).

^{1}H NMR (400 MHz, DMSO-d_6) δ [ppm] = 3.21–3.16 (m, 6H), 2.93 (s, 3H), 1.64–1.56 (m, 6H), 1.32–1.21 (m, 30H), 0.88–0.85 (m, 9H); ^{13}C NMR (101 MHz, DMSO-d_6) δ [ppm] = 60.5, 47.5, 31.2, 28.5, 28.4, 25.8, 22.1, 21.3, 14.0.

Tetrabutylphosphonium nitrate

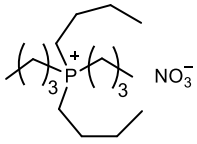

Tetrabutylphosphonium bromide (529 mg, 1.56 mmol, 1.0 eq.) is dissolved in 1 mL water and 5 mL acetone and is converted according to the general procedure with silver nitrate (220 mg, 1.72 mmol, 1.1 eq.). Due to the product's hydrophily, the aqueous filtrate is distilled directly and the remaining product is dried under reduced pressure. A colorless, highly viscous liquid is obtained (yield: 99%, 497 mg, 1.54 mmol).

^{1}H NMR (400 MHz, D_2O) δ [ppm] = 2.19–2.12 (m, 8H), 1.60–1.41 (m, 16H), 0.93 (t, *J* = 7.2 Hz, 12H); ^{13}C NMR (101 MHz, D_2O) δ [ppm] = 23.3 (d, *J* = 15.3 Hz), 22.7 (d, *J* = 4.6 Hz), 17.6 (d, *J* = 48.3 Hz), 12.5; ^{31}P NMR (162 MHz, D_2O) δ [ppm] = 33.20.

3.5 Characterization of oxo-functionalization products

Cyclohexanone (2a)

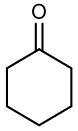

According to the general protocol (GP 2) cyclohexane (0.421 g, 5.00 mmol, 1.0 eq.) and tetrabutylammonium nitrate (0.76 g, 2.50 mmol, 0.5 eq.) are dissolved in acetonitrile (25 mL) and electrolyzed with constant current (10 mA cm^{-2}) at 25 °C, under 100 vol.% oxygen atmosphere and 4 *F*. After with a diethyl ether/water extraction, the product is obtained as colorless liquid (yield: 6%, 30 mg, 0.31 mmol).

R_f (cyclohexane/ethyl acetate = 9:1): 0.40; ^{1}H NMR (400 MHz, $CDCl_3$) δ [ppm] = 2.32–2.29 (m, 4H), 1.86–1.80 (m, 4H), 1.72–1.67 (m, 2H); ^{13}C NMR (101 MHz, $CDCl_3$) δ [ppm] = 212.6, 42.0, 27.1, 25.0; GC-MS (EI): m/z: 98 [M^+], 55 [base peak].

All spectroscopical data match to the reported data[9].

Cycloheptanone (2b)

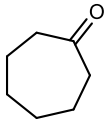

According to the general protocol (GP 2) cycloheptane (0.491 g, 5.00 mmol, 1.0 eq.) and tetrabutylammonium nitrate (0.76 g, 2.50 mmol, 0.5 eq.) are dissolved in acetonitrile (25 mL) and electrolyzed with constant current (10 mA cm^{-2}) at 27 °C, under 100 vol.% oxygen atmosphere and 4 *F*. After work-up with a diethyl ether/water extraction, the product is obtained as a colorless liquid (yield: 16%, 0.090 g, 0.80 mmol).

R_f (cyclohexane/ethyl acetate = 9:1): 0.40; ^{1}H NMR (400 MHz, $CDCl_3$) δ [ppm] = 2.50–2.47 (m, 4H), 1.73–1.64 (m, 8H); ^{13}C NMR (101 MHz, $CDCl_3$) δ [ppm] = 215.9, 44.0, 30.6, 24.5; GC-MS (EI): m/z: 112 [M^+], 55 [base peak].

All spectroscopical data match to the reported data[10].

Cyclooctanone (2c)

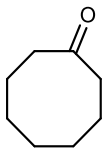

According to the general protocol (GP 2) cyclooctane (0.561 g, 5.00 mmol, 1.0 eq.) and tetrabutylammonium nitrate (0.76 g, 2.50 mmol, 0.5 eq.) are dissolved in acetonitrile (25 mL) and electrolyzed with constant current (10 mA cm^{-2}) at 30 °C, under 100 vol.% oxygen atmosphere and 4 *F*. After work-up with a cyclohexane/water extraction, the product is obtained as colorless liquid (yield: 42%, 0.261 g, 2.07 mmol).

R_f (cyclohexane/ethyl acetate = 7:3): 0.66; ^{1}H NMR (400 MHz, $CDCl_3$) δ [ppm] = 2.39–2.36 (m, 4H), 1.87–1.81 (m, 4H), 1.54–1.48 (m, 4H), 1.36–1.31 (m, 2H); ^{13}C NMR (101 MHz, $CDCl_3$) δ [ppm] = 218.5, 42.0, 27.2, 25.7, 24.8; GC-MS (EI): m/z: 126 [M^+], 55 [base peak].

All spectroscopical data match to the reported data[10].

Cyclodecanone (2d)

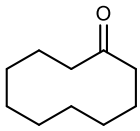

According to the general protocol (GP 2) cyclodecane (0.701 g, 5.00 mmol, 1.0 eq.) and tetrabutylammonium nitrate (0.76 g, 2.50 mmol, 0.5 eq.) are dissolved in acetonitrile (25 mL) and electrolyzed with constant current (10 mA cm^{-2}) at 30 °C, under 100 vol.% oxygen atmosphere and 5 *F*. After removing the solvent in vacuo, the residue was purified by column chromatography (cyclohexane/ethyl acetate = 9:1) to yield the product as a colorless liquid (yield: 12%, 90 mg, 0.59 mmol).

R_f (cyclohexane/ethyl acetate = 9:1): 0.57; ^{1}H NMR (400 MHz, $CDCl_3$) δ [ppm] = 2.51–2.48 (m, 4H), 1.86–1.80 (m, 4H), 1.50–1.44 (m, 4H), 1.36–1.31 (m, 6H); ^{13}C NMR (101 MHz, $CDCl_3$) δ [ppm] = 215.1, 42.1, 25.2, 25.0, 24.9, 23.5; GC-MS (EI): m/z: 154 [M^+], 55 [base peak].

Cyclododecanone (2e)

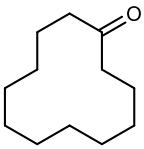

According to the general protocol (GP 2) cyclododecane (0.842 g, 5.00 mmol, 1.0 eq.) and tetrabutylammonium nitrate (0.76 g, 2.50 mmol, 0.5 eq.) are dissolved in isobutyronitrile (25 mL) and electrolyzed with constant current (10 mA cm^{-2}) at 27 °C, under 100 vol.% oxygen atmosphere and 4 *F*. After removing the solvent in vacuo, the residue was purified by column chromatography (cyclohexane/ethyl acetate = 10:0 → 9:1) to yield the product as a colorless solid (yield: 21%, 0.194 g, 1.06 mmol).

R_f (cyclohexane/ethyl acetate = 9:1): 0.48; ^{1}H NMR (400 MHz, $CDCl_3$) δ [ppm] = 2.47–2.44 (m, 4H), 1.74–1.68 (m, 4H), 1.33–1.24 (m, 14H); ^{13}C NMR (101 MHz, $CDCl_3$) δ [ppm] = 213.1, 40.5, 24.9, 24.7, 24.4, 22.7, 22.5; GC-MS (EI): m/z: 182 [M^+], 41 [base peak].

All spectroscopical data match to the reported data[10].

Hexane-1,6-dioic acid (6a)

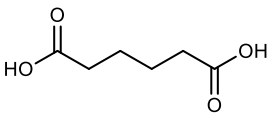

According to the general protocol (GP 1) cyclohexene (21 mg, 0.25 mmol, 1.0 eq.) and tetrabutylammonium nitrate (38 mg, 0.125 mmol, 0.5 eq.) are dissolved in acetonitrile (5 mL) and electrolyzed with constant current (5 mA cm^{-2}) at 35 °C, under 100 vol.% oxygen atmosphere and 4 *F*. After workup, the product is obtained as colorless solid (yield: 19%, 7 mg, 0.05 mmol).

R_f (cyclohexane/ethyl acetate = 1:1 + 1 vol.% glacial acetic acid): 0.40; ^{1}H NMR (400 MHz, DMSO-d_6) δ [ppm] = 12.03 (s, 2H) 2.23–2.18 (m, 4H), 1.54–1.45 (m, 4H); ^{13}C NMR (101 MHz, DMSO-d_6) δ [ppm] = 174.4, 33.4, 24.1; HRMS for $C_6H_9O_4^-$ (ESI–) [M–H]$^-$: calc.: 145.0506, found: 145.0501.

All spectroscopical data match to the reported data[11].

Octane-1,8-dioic acid (6b)

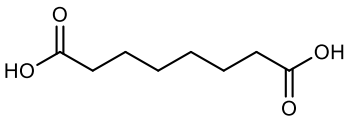

According to the general protocol (GP 1) cyclooctene (28 mg, 0.25 mmol, 1.0 eq.) and tetrabutylammonium nitrate (38 mg, 0.125 mmol, 0.5 eq.) are dissolved in isobutyronitrile (5 mL) and electrolyzed with constant current (5 mA cm^{-2}) at 35 °C, under 100 vol.% oxygen atmosphere and 4 *F*. After workup, the product is obtained as colorless solid (yield: 46%, 20 mg, 0.12 mmol).

R_f (cyclohexane/ethyl acetate = 1:1 + 1 vol.% glacial acetic acid): 0.43; ^{1}H NMR (400 MHz, DMSO-d_6) δ [ppm] = 11.98 (s, 2H), 2.18 (t, *J* = 7.4 Hz, 4H), 1.51–1.44 (m, 4H), 1.27–1.23 (m, 4H); ^{13}C NMR (101 MHz, DMSO-d_6) δ [ppm] = 174.5, 33.6, 28.3, 24.4; HRMS for $C_8H_{13}O_4^-$ (ESI–) [M–H]$^-$: calc.: 173.0819, found: 173.0815.

All spectroscopical data match to the reported data[12].

Dodecane-1,12-dioic acid (6c)

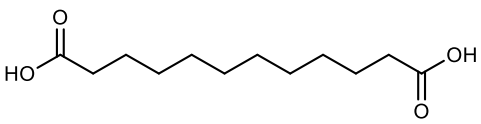

According to the general protocol (GP 1) cyclododecene (42 mg, 0.25 mmol, 1.0 eq.) and tetrabutylammonium nitrate (38 mg, 0.125 mmol, 0.5 eq.) are dissolved in isobutyronitrile (5 mL) and electrolyzed with constant current (5 mA cm^{-2}) at 35 °C, under 100 vol.% oxygen atmosphere and 4 *F*. After workup, the product is obtained as colorless solid (yield: 78%, 45 mg, 0.20 mmol).

R_f (cyclohexane/ethyl acetate = 1:1 + 1 vol.% glacial acetic acid): 0.56; ^{1}H NMR (400 MHz, DMSO-d_6) δ [ppm] = 11.97 (s, 2H), 2.18 (t, *J* = 7.4 Hz, 4H), 1.51–1.44 (m, 4H), 1.24 (bs, 12H); ^{13}C NMR (101 MHz, DMSO-d_6) δ [ppm] = 174.5, 33.7, 28.9, 28.8, 28.6, 24.5; HRMS for $C_{12}H_{21}O_4^-$ (ESI–) [M–H]$^-$: calc.: 229.1445, found: 229.1439.

All spectroscopical data match to the reported data[11].

Cyclopentane-1,3-dicarboxylic acid (6d)

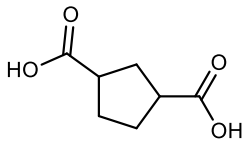

According to the general protocol (GP 1) norbornene (24 mg, 0.25 mmol, 1.0 eq.) and tetrabutylammonium nitrate (38 mg, 0.125 mmol, 0.5 eq.) are dissolved in acetonitrile (5 mL) and electrolyzed with constant current (5 mA cm^{-2}) at 5 °C, under 100 vol.% oxygen atmosphere and 4 *F*. After workup, the product is obtained as off-white highly viscous liquid (yield: 45%, 18 mg, 0.11 mmol).

^{1}H NMR (400 MHz, DMSO-d_6) δ [ppm] = 12.14 (s, 2H), 2.78–2.62 (m, 2H), 2.13–2.06 (m, 1H), 1.88–1.72 (m, 5H); ^{13}C NMR (101 MHz, DMSO-d_6) δ [ppm] = 176.4, 43.3, 32.8, 28.9; HRMS for $C_7H_9O_4^-$ (ESI–) $[M–H]^-$: calc.: 157.0506, found: 157.0507.

All spectroscopical data match to the reported data[13].

6-Oxo-6-phenylhexanoic acid (6e)

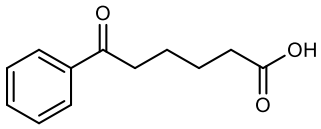

According to the general protocol (GP 1) 1-phenyl-1-cyclohexene (40 mg, 0.25 mmol, 1.0 eq.) and tetrabutylammonium nitrate (38 mg, 0.125 mmol, 0.5 eq.) are dissolved in isobutyronitrile (5 mL) and electrolyzed with constant current (5 mA cm^{-2}) at 20 °C, under 100 vol.% oxygen atmosphere and 4 *F*. After workup, the product is obtained as colorless solid (yield: 26%, 13 mg, 0.07 mmol).

R_f (cyclohexane/ethyl acetate = 1:1 + 1 vol.% glacial acetic acid): 0.60; ^{1}H NMR (400 MHz, DMSO-d_6) δ [ppm] = 12.16 (s, 1H), 7.98–7.94 (m, 2H), 7.65–7.60 (m, 1H), 7.55–7.49 (m, 2H), 3.03 (t, *J* = 7.4 Hz, 2H), 2.25 (t, *J* = 7.4 Hz, 2H), 1.66–1.54 (m, 4H); ^{13}C NMR (101 MHz, DMSO-d_6) δ [ppm] = 199.9, 174.4, 136.7, 133.1, 128.7, 127.9, 37.6, 33.6, 24.1, 23.3; HRMS for $C_{12}H_{13}O_3^-$ (ESI–) $[M–H]^-$: calc.: 205.0870, found: 205.0861.

All spectroscopical data match to the reported data[14].

By-product: 5-Oxo-5-phenylpentanoic acid (**6e'**)

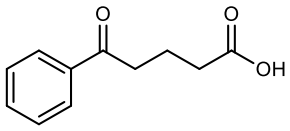

Mol ratio to **6e**: 1:1,9 (yield: 14%, 7 mg, 0.04 mmol).

R_f (cyclohexane/ethyl acetate = 1:1 + 1 vol.% glacial acetic acid): 0.60; ^{1}H NMR (400 MHz, DMSO-d_6) δ [ppm] = 12.16 (s, 1H), 7.98–7.94 (m, 2H), 7.65–7.60 (m, 1H), 7.55–7.49 (m, 2H), 3.06 (t, *J* = 7.4 Hz, 2H), 2.30 (t, *J* = 7.4 Hz, 2H), 1.83 (p, *J* = 7.4 Hz, 2H); ^{13}C NMR (101 MHz, DMSO-d_6) δ [ppm] = 199.6, 174.3, 136.6, 133.1, 128.7, 127.9, 37.2, 32.8, 19.2; HRMS for $C_{11}H_{11}O_3^-$ (ESI–) $[M–H]^-$: calc.: 191.0714, found: 191.0708.

All spectroscopical data match to the reported data[15].

(3*S*)-4-Methyl-3-(3-oxobutyl)pent-4-enoic acid (6f)

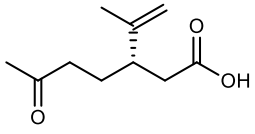

According to the general protocol (GP 1) *S*-(–)-limonene (34 mg, 0.25 mmol, 1.0 eq.) and tetrabutylammonium nitrate (38 mg, 0.125 mmol, 0.5 eq.) are dissolved in acetonitrile (5 mL) and electrolyzed with constant current (5 mA cm^{-2}) at 25 °C, under 100 vol.% oxygen atmosphere and 4 *F*. After workup and column chromatographic purification (cyclohexane/ethyl acetate = 1:1 + 1 vol.% glacial acetic acid), the product is obtained as colorless highly viscous liquid (yield: 17%, 8 mg, 0.04 mmol).

R_f (cyclohexane/ethyl acetate = 1:1 + 1 vol.% glacial acetic acid): 0.53; ^{1}H NMR (400 MHz, DMSO-d_6) δ [ppm] = 12.04 (s, 1H), 4.75–4.69 (m, 2H), 2.44–2.37 (m, 1H), 2.33 (t, *J* = 7.7 Hz, 2H), 2.26 (dd, *J* = 14.9 Hz, *J* = 8.3 Hz, 1H), 2.24 (dd, *J* = 14.9 Hz, *J* = 6.6 Hz, 1H), 2.05 (s, 3H), 1.60 (s, 3H), 1.59–1.45 (m, 2H); ^{13}C NMR (101 MHz, DMSO-d_6) δ [ppm] = 208.1, 173.3, 146.1, 112.0, 42.4, 40.4, 38.6, 29.8, 26.1, 18.6; HRMS for $C_{10}H_{15}O_3^-$ (ESI–) $[M–H]^-$: calc.: 183.1027, found: 183.1029.

Nonane-1,9-dioic acid (9b)

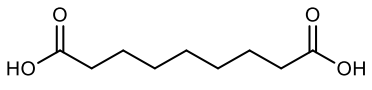

According to the general protocol (GP 1) oleic acid (141 mg, 0.5 mmol, 1.0 eq.) or elaidic acid (141 mg, 0.5 mmol, 1.0 eq.) and tetrabutylammonium nitrate (76 mg, 0.25 mmol, 0.5 eq.) are dissolved in isobutyronitrile (5 mL) and electrolyzed with constant current (10 mA cm^{-2}) at 30 °C, under 100 vol.% oxygen atmosphere and 10 *F*. After workup, and column chromatographic purification (cyclohexane/ethyl acetate = 1:1 + 1 vol.% glacial acetic acid), the product is obtained as colorless solid (from oleic acid: yield: 46%, 44 mg, 0.23 mmol; from elaidic acid: yield: 38%, 36 mg, 0.19 mmol).

R_f (cyclohexane/ethyl acetate = 1:1 + 1 vol.% glacial acetic acid): 0.47; ^{1}H NMR (400 MHz, DMSO-d_6) δ [ppm] = 11.98 (s, 2H), 2.18 (t, *J* = 7.4 Hz, 4H), 1.51–1.43 (m, 4H), 1.25 (bs, 6H); ^{13}C NMR (101 MHz, DMSO-d_6) δ [ppm] = 174.5, 33.7, 28.5, 28.4, 24.5; HRMS for $C_9H_{15}O_4$ (ESI–) $[M–H]^–$: calc.: 187.0976, found: 187.0987.

All spectroscopical data match to the reported data[11].

Benzaldehyde semicarbazone (13a)

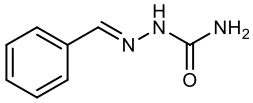

According to the general protocol (GP 3) toluene (46 mg, 0.5 mmol, 1.0 eq.) and tetrabutylammonium nitrate (152 mg, 0.5 mmol, 1.0 eq.) are dissolved in acetonitrile (5 mL) and electrolyzed with constant current (10 mA cm^{-2}) at 33 °C, under 100 vol.% oxygen atmosphere and 5 *F*. After workup and derivatization, the product is obtained as colorless solid (yield: 43%, 35 mg, 0.21 mmol).

m_R: 205–207 °C; R_f (ethyl acetate): 0.44; ^{1}H NMR (400 MHz, DMSO-d_6) δ [ppm] = 10.29 (s, 1H), 7.84 (s, 1H), 7.72–7.69 (m, 2H), 7.40–7.31 (m, 3H), 6.50 (bs, 2H); ^{13}C NMR (101 MHz, DMSO-d_6) δ [ppm] = 156.8, 139.3, 134.8, 129.0, 128.6, 126.6; HRMS for $C_8H_{10}N_3O^+$ (ESI+) $[M+H]^+$: calc.: 164.0818, found: 164.0820.

***o*-Tolualdehyde semicarbazone (13b)**

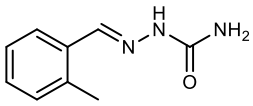

According to the general protocol (GP 3) 1,2-dimethylbenzene (53 mg, 0.5 mmol, 1.0 eq.) and tetrabutylammonium nitrate (152 mg, 0.5 mmol, 1.0 eq.) are dissolved in acetonitrile (5 mL) and electrolyzed with constant current (10 mA cm^{-2}) at 33 °C, under 100 vol.% oxygen atmosphere and 5 *F*. After workup and derivatization, the product is obtained as colorless solid (yield: 58%, 51 mg, 0.29 mmol).

m_R: 199–202 °C; R_f (ethyl acetate): 0.46; ^{1}H NMR (400 MHz, DMSO-d_6) δ [ppm] = 10.21 (s, 1H), 8.14 (s, 1H), 7.93–7.91 (m, 1H), 7.25–7.17 (m, 3H), 6.46 (bs, 2H), 2.36 (s, 3H); ^{13}C NMR (101 MHz, DMSO-d_6) δ [ppm] = 156.7, 137.9, 135.8, 132.6, 130.6, 128.8, 126.0, 125.6, 19.0; HRMS for $C_9H_{12}N_3O^+$ (ESI+) $[M+H]^+$: calc.: 178.0975, found: 178.0978.

All spectroscopical data match to the reported data[16].

***m*-Tolualdehyde semicarbazone (13c)**

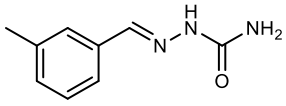

According to the general protocol (GP 3) 1,3-dimethylbenzene (53 mg, 0.5 mmol, 1.0 eq.) and tetrabutylammonium nitrate (152 mg, 0.5 mmol, 1.0 eq.) are dissolved in acetonitrile (5 mL) and electrolyzed with constant current (10 mA cm^{-2}) at 33 °C, under 100 vol.% oxygen atmosphere and 5 *F*. After workup and derivatization, the product is obtained as colorless solid (yield: 54%, 48 mg, 0.27 mmol).

m_R: 206–208 °C; R_f (ethyl acetate): 0.46; ^{1}H NMR (400 MHz, DMSO-d_6) δ [ppm] = 10.24 (s, 1H), 7.80 (s, 1H), 7.56 (s, 1H), 7.47 (d, *J* = 7.6 Hz, 1H), 7.26 (t, *J* = 7.6 Hz, 1H), 7.15 (d, *J* = 7.6 Hz, 1H), 6.50 (bs, 2H), 2.31 (s, 3H); ^{13}C NMR (101 MHz, DMSO-d_6) δ [ppm] = 156.8, 139.4, 137.8, 134.7, 129.7, 128.5, 126.9, 124.0, 20.9; HRMS for $C_9H_{12}N_3O^+$ (ESI+) $[M+H]^+$: calc.: 178.0975, found: 178.0975.

***p*-Tolualdehyde semicarbazone (13d)**

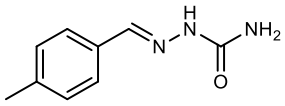

According to the general protocol (GP 3) 1,4-dimethylbenzene (53 mg, 0.5 mmol, 1.0 eq.) and tetrabutylammonium nitrate (152 mg, 0.5 mmol, 1.0 eq.) are dissolved in acetonitrile (5 mL) and electrolyzed with constant current (10 mA cm^{-2}) at 33 °C, under 100 vol.% oxygen atmosphere and 5 *F*. After workup and derivatization, the product is obtained as colorless solid (yield: 68%, 60 mg, 0.34 mmol).

m_R: 203–206 °C; R_f (ethyl acetate): 0.44; ^{1}H NMR (400 MHz, DMSO-d_6) δ [ppm] = 10.19 (s, 1H), 7.80 (s, 1H), 7.60 (d, *J* = 8.0 Hz, 2H), 7.19 (d, *J* = 8.0 Hz, 2H), 6.46 (bs, 2H), 2.31 (s, 3H); ^{13}C NMR (101 MHz, DMSO-d_6) δ [ppm] = 156.8, 139.3, 138.6, 132.1, 129.2, 126.5, 21.0; HRMS for $C_9H_{12}N_3O^+$ (ESI+) $[M+H]^+$: calc.: 178.0975, found: 178.0975.

All spectroscopical data match to the reported data[17].

3,5-Dimethylbenzaldehyde semicarbazone (13e)

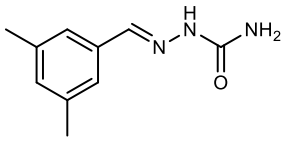

According to the general protocol (GP 3) 1,3,5-trimethylbenzene (60 mg, 0.5 mmol, 1.0 eq.) and tetrabutylammonium nitrate (152 mg, 0.5 mmol, 1.0 eq.) are dissolved in acetonitrile (5 mL) and electrolyzed with constant current (10 mA cm^{-2}) at 33 °C, under 100 vol.% oxygen atmosphere and 5 *F*. After workup and derivatization, the product is obtained as colorless solid (yield: 68%, 65 mg, 0.34 mmol).

m_R: 200–202 °C; R_f (ethyl acetate): 0.41; ^{1}H NMR (400 MHz, DMSO-d_6) δ [ppm] = 10.20 (s, 1H), 7.76 (s, 1H), 7.32 (s, 2H), 6.96 (s, 1H), 6.48 (bs, 2H), 2.27 (s, 6H); ^{13}C NMR (101 MHz, DMSO-d_6) δ [ppm] = 156.8, 139.5, 137.6, 134.7, 130.6, 124.4, 20.8; HRMS for $C_{10}H_{14}N_3O^+$ (ESI+) $[M+H]^+$: calc.: 192.1131, found: 192.1132.

4-Fluorobenzaldehyde semicarbazone (13f)

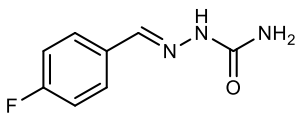

According to the general protocol (GP 3) 4-fluorotoluene (55 mg, 0.5 mmol, 1.0 eq.) and tetrabutylammonium nitrate (152 mg, 0.5 mmol, 1.0 eq.) are dissolved in acetonitrile (5 mL) and electrolyzed with constant current (10 mA cm^{-2}) at 33 °C, under 100 vol.% oxygen atmosphere and 5 *F*. After workup and derivatization, the product is obtained as colorless solid (yield: 21%, 19 mg, 0.10 mmol).

m_R: 204–207 °C; R_f (ethyl acetate): 0.39; ^{1}H NMR (400 MHz, DMSO-d_6) δ [ppm] = 10.26 (s, 1H), 7.82 (s, 1H), 7.81–7.76 (m, 2H), 7.24–7.18 (m, 2H), 6.51 (bs, 2H); ^{13}C NMR (101 MHz, DMSO-d_6) δ [ppm] = 162.5 (d, *J* = 246.4 Hz), 156.8, 138.0, 131.5 (d, *J* = 3.0 Hz), 128.6 (d, *J* = 8.3 Hz), 115.6 (d, *J* = 21.7 Hz); ^{19}F NMR (282 MHz, DMSO-d_6) δ [ppm] = −112.23; HRMS for $C_8H_9FN_3O^+$ (ESI+) $[M+H]^+$: calc.: 182.0724, found: 182.0728.

4-Chlorobenzaldehyde semicarbazone (13g)

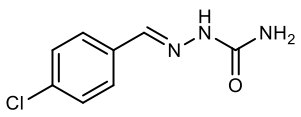

According to the general protocol (GP 3) 4-chlorotoluene (63 mg, 0.5 mmol, 1.0 eq.) and tetrabutylammonium nitrate (152 mg, 0.5 mmol, 1.0 eq.) are dissolved in acetonitrile (5 mL) and electrolyzed with constant current (10 mA cm^{-2}) at 33 °C, under 100 vol.% oxygen atmosphere and 5 *F*. After workup and derivatization, the product is obtained as colorless solid (yield: 35%, 35 mg, 0.18 mmol).

m_R: 208–212 °C; R_f (ethyl acetate): 0.39; ^{1}H NMR (400 MHz, DMSO-d_6) δ [ppm] = 10.33 (s, 1H), 7.81 (s, 1H), 7.77–7.74 (m, 2H), 7.44–7.41 (m, 2H), 6.55 (bs, 2H); ^{13}C NMR (101 MHz, DMSO-d_6) δ [ppm] = 156.7, 137.9, 133.8, 133.4, 128.6, 128.2; HRMS for $C_8H_9{}^{35}ClN_3O^+$ (ESI+) $[M+H]^+$: calc.: 198.0429, found: 198.0430.

All spectroscopical data match to the reported data[17].

Benzoic acid (14a)

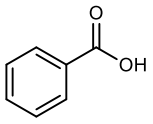

According to the general protocol (GP 3) toluene (230 mg, 2.5 mmol, 1.0 eq.) and tetrabutylammonium nitrate (381 mg, 1.25 mmol, 0.5 eq.) are dissolved in acetonitrile (25 mL) and electrolyzed with constant current (30 mA cm^{-2}) at 27 °C, under 100 vol.% oxygen atmosphere and 12 *F*. After workup and column chromatographic purification (cyclohexane/ethyl acetate = 1:1 + 1 vol.% glacial acetic acid), the product is obtained as colorless solid (yield: 37%, 112 mg, 0.92 mmol).

m_R: 117–120 °C; R_f (cyclohexane/ethyl acetate = 1:1 + 1 vol.% glacial acetic acid): 0.67; ^{1}H NMR (400 MHz, DMSO-d_6) δ [ppm] = 12.95 (s, 1H), 7.97–7.94 (m, 2H), 7.64–7.59 (m, 1H), 7.52–7.47 (m, 2H); ^{13}C NMR (101 MHz, DMSO-d_6) δ [ppm] = 167.4, 132.9, 130.8, 129.3, 128.6; HRMS for $C_7H_5O_2^-$ (ESI–) $[M–H]^-$: calc.: 121.0295, found: 121.0292.

All spectroscopical data match to the reported data[18].

2-Methylbenzoic acid (14b)

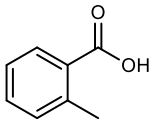

According to the general protocol (GP 3) 1,2-dimethylbenzene (265 mg, 2.5 mmol, 1.0 eq.) and tetrabutylammonium nitrate (381 mg, 1.25 mmol, 0.5 eq.) are dissolved in acetonitrile (25 mL) and electrolyzed with constant current (30 mA cm^{-2}) at 27 °C, under 100 vol.% oxygen atmosphere and 12 *F*. After workup and column chromatographic purification (cyclohexane/ethyl acetate = 1:1 + 1 vol.% glacial acetic acid), the product is obtained as colorless solid (yield: 21%, 72 mg, 0.53 mmol).

m_R: 99–101 °C; R_f (cyclohexane/ethyl acetate = 1:1 + 1 vol.% glacial acetic acid): 0.66; ^{1}H NMR (400 MHz, DMSO-d_6) δ [ppm] = 12.81 (s, 1H), 7.82–7.80 (m, 1H), 7.46–7.42 (m, 1H), 7.30–7.25 (m, 2H), 2.51 (s, 3H); ^{13}C NMR (101 MHz, DMSO-d_6) δ [ppm] = 168.7, 139.0, 131.8, 131.5, 130.4, 130.2, 125.9, 21.3; HRMS for $C_8H_7O_2^-$ (ESI–) $[M–H]^-$: calc.: 135.0452, found: 135.0447.

All spectroscopical data match to the reported data[18].

3-Methylbenzoic acid (14c)

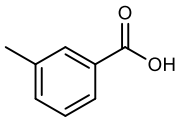

According to the general protocol (GP 3) 1,3-dimethylbenzene (265 mg, 2.5 mmol, 1.0 eq.) and tetrabutylammonium nitrate (381 mg, 1.25 mmol, 0.5 eq.) are dissolved in acetonitrile (25 mL) and electrolyzed with constant current (30 mA cm^{-2}) at 27 °C, under 100 vol.% oxygen atmosphere and 12 *F*. After workup and column chromatographic purification (cyclohexane/ethyl acetate = 1:1 + 1 vol.% glacial acetic acid), the product is obtained as colorless solid (yield: 14%, 48 mg, 0.35 mmol).

m_R: 96–100 °C; R_f (cyclohexane/ethyl acetate = 1:1 + 1 vol.% glacial acetic acid): 0.67; ^{1}H NMR (400 MHz, DMSO-d_6) δ [ppm] = 12.89 (s, 1H), 7.77–7.72 (m, 2H), 7.44–7.41 (m, 1H), 7.39–7.35 (m, 1H), 2.35 (s, 3H); ^{13}C NMR (101 MHz, DMSO-d_6) δ [ppm] = 167.4, 137.9, 133.5, 130.7, 129.8, 128.5, 126.5, 20.8; HRMS for $C_8H_7O_2^-$ (ESI–) $[M–H]^-$: calc.: 135.0452, found: 135.0449.

All spectroscopical data match to the reported data[18].

4-Methylbenzoic acid (14d)

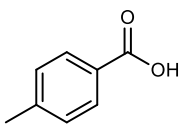

According to the general protocol (GP 3) 1,4-dimethylbenzene (265 mg, 2.5 mmol, 1.0 eq.) and tetrabutylammonium nitrate (381 mg, 1.25 mmol, 0.5 eq.) are dissolved in acetonitrile (25 mL) and electrolyzed with constant current (30 mA cm^{-2}) at 27 °C, under 100 vol.% oxygen atmosphere and 12 *F*. After workup and column chromatographic purification (cyclohexane/ethyl acetate = 1:1 + 1 vol.% glacial acetic acid), the product is obtained as colorless solid (yield: 38%, 128 mg, 0.94 mmol).

m_R: 174–178 °C; R_f (cyclohexane/ethyl acetate = 1:1 + 1 vol.% glacial acetic acid): 0.67; ^{1}H NMR (400 MHz, DMSO-d_6) δ [ppm] = 12.79 (s, 1H), 7.83 (d, *J* = 8.1 Hz, 2H), 7.29 (d, *J* = 8.1 Hz, 2H), 2.36 (s, 3H); ^{13}C NMR (101 MHz, DMSO-d_6) δ [ppm] = 167.4, 143.1, 129.4, 129.2, 128.1, 21.2; HRMS for $C_8H_7O_2^-$ (ESI–) [M–H]$^-$: calc.: 135.0452, found: 135.0449.

All spectroscopical data match to the reported data[18].

3,5-Dimethylbenzoic acid (14e)

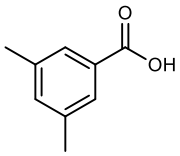

According to the general protocol (GP 3) 1,3,5-trimethylbenzene (301 mg, 2.5 mmol, 1.0 eq.) and tetrabutylammonium nitrate (381 mg, 1.25 mmol, 0.5 eq.) are dissolved in acetonitrile (25 mL) and electrolyzed with constant current (30 mA cm^{-2}) at 27 °C, under 100 vol.% oxygen atmosphere and 7 *F*. After workup and column chromatographic purification (cyclohexane/ethyl acetate = 1:1 + 1 vol.% glacial acetic acid), the product is obtained as colorless solid (yield: 17%, 62 mg, 0.41 mmol).

m_R: 154–157 °C; R_f (cyclohexane/ethyl acetate = 1:1 + 1 vol.% glacial acetic acid): 0.68; ^{1}H NMR (400 MHz, DMSO-d_6) δ [ppm] = 12.78 (s, 1H), 7.55 (s, 2H), 7.22 (s, 1H), 2.31 (s, 3H); ^{13}C NMR (101 MHz, DMSO-d_6) δ [ppm] = 167.5, 137.7, 134.2, 130.7, 127.0, 20.7; HRMS for $C_9H_9O_2^-$ (ESI–) [M–H]$^-$: calc.: 149.0608, found: 149.0618.

All spectroscopical data match to the reported data[18].

4-Fluorobenzoic acid (14f)

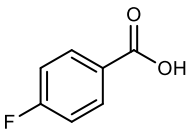

According to the general protocol (GP 3) 4-fluorotoluene (275 mg, 2.5 mmol, 1.0 eq.) and tetrabutylammonium nitrate (381 mg, 1.25 mmol, 0.5 eq.) are dissolved in acetonitrile (25 mL) and electrolyzed with constant current (30 mA cm^{-2}) at 27 °C, under 100 vol.% oxygen atmosphere and 12 *F*. After workup and column chromatographic purification (cyclohexane/ethyl acetate = 1:1 + 1 vol.% glacial acetic acid), the product is obtained as colorless solid (yield: 36%, 127 mg, 0.91 mmol).

m_R: 182–184 °C; R_f (cyclohexane/ethyl acetate = 1:1 + 1 vol.% glacial acetic acid): 0.62; ^{1}H NMR (400 MHz, DMSO-d_6) δ [ppm] = 13.05 (s, 1H), 8.02–7.97 (m, 2H), 7.34–7.28 (m, 2H); ^{13}C NMR (101 MHz, DMSO-d_6) δ [ppm] = 166.4, 164.9 (d, *J* = 250.6 Hz), 132.1 (d, *J* = 9.6 Hz), 127.4 (d, *J* = 2.8 Hz), 115.6 (d, *J* = 22.1 Hz); ^{19}F NMR (376 MHz, DMSO-d_6) δ [ppm] = –108.08; HRMS for $C_7H_4FO_2^-$ (ESI–) [M–H]$^-$: calc.: 139.0201, found: 139.0199.

All spectroscopical data match to the reported data[18].

4-Chlorobenzoic acid (14g)

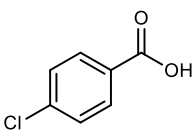

According to the general protocol (GP 3) 4-chlorotoluene (316 mg, 2.5 mmol, 1.0 eq.) and tetrabutylammonium nitrate (381 mg, 1.25 mmol, 0.5 eq.) are dissolved in acetonitrile (25 mL) and electrolyzed with constant current (30 mA cm^{-2}) at 27 °C, under 100 vol.% oxygen atmosphere and 12 *F*. After workup and column chromatographic purification (cyclohexane/ethyl acetate = 1:1 + 1 vol.% glacial acetic acid), the product is obtained as colorless solid (yield: 46%, 180 mg, 1.15 mmol).

m_R: 229–234 °C; R_f (cyclohexane/ethyl acetate = 1:1 + 1 vol.% glacial acetic acid): 0.57; ^{1}H NMR (400 MHz, DMSO-d_6) δ [ppm] = 13.18 (s, 1H), 7.95–7.92 (m, 2H), 7.58–7.54 (m, 2H); ^{13}C NMR (101 MHz, DMSO-d_6) δ [ppm] = 166.5, 137.8, 131.2, 129.7, 128.8; HRMS for $C_7H_4ClO_2^-$ (ESI–) [M–H]$^-$: calc.: 154.9905, found: 154.9905.

All spectroscopical data match to the reported data[18].

4. Supplementary Spectra (literature unreported)

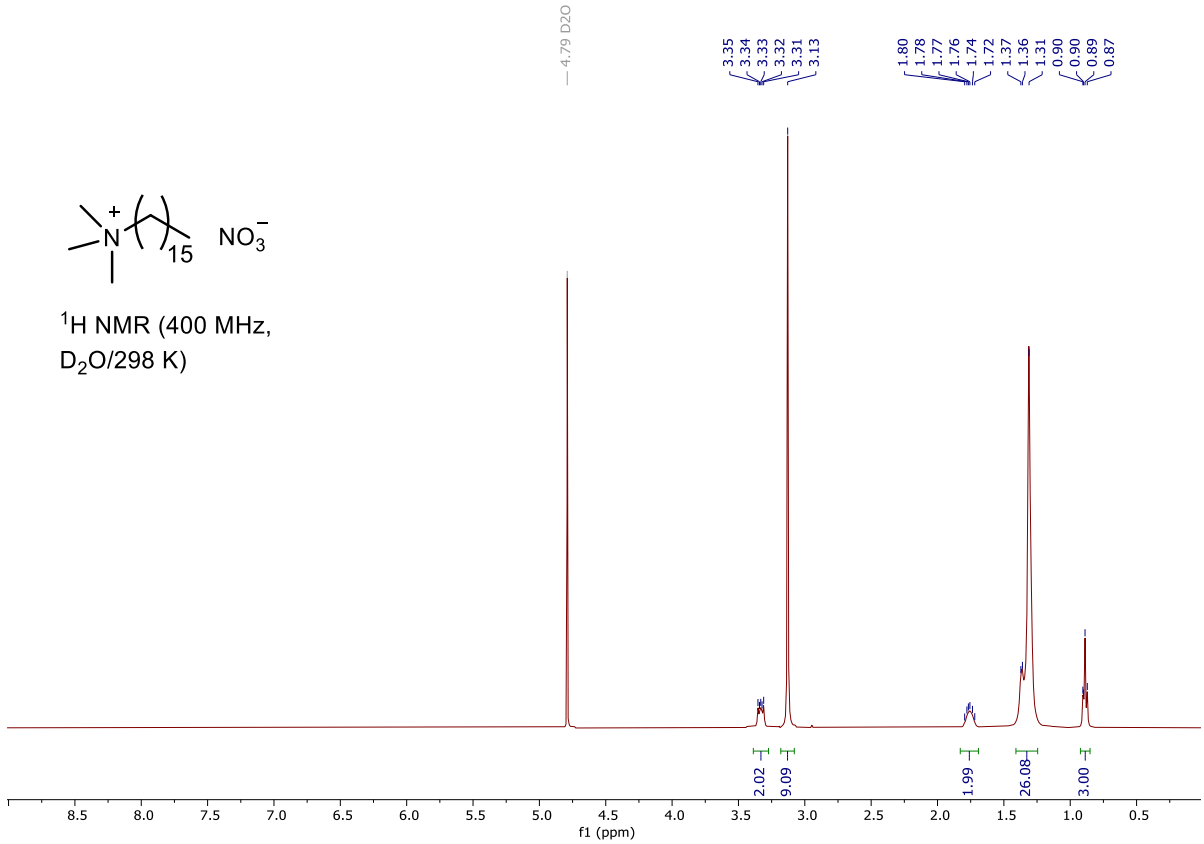

Supplementary Fig. 20: ^{1}H NMR (400 MHz, D_2O, 298 K) of hexadecyltrimethylammonium nitrate.

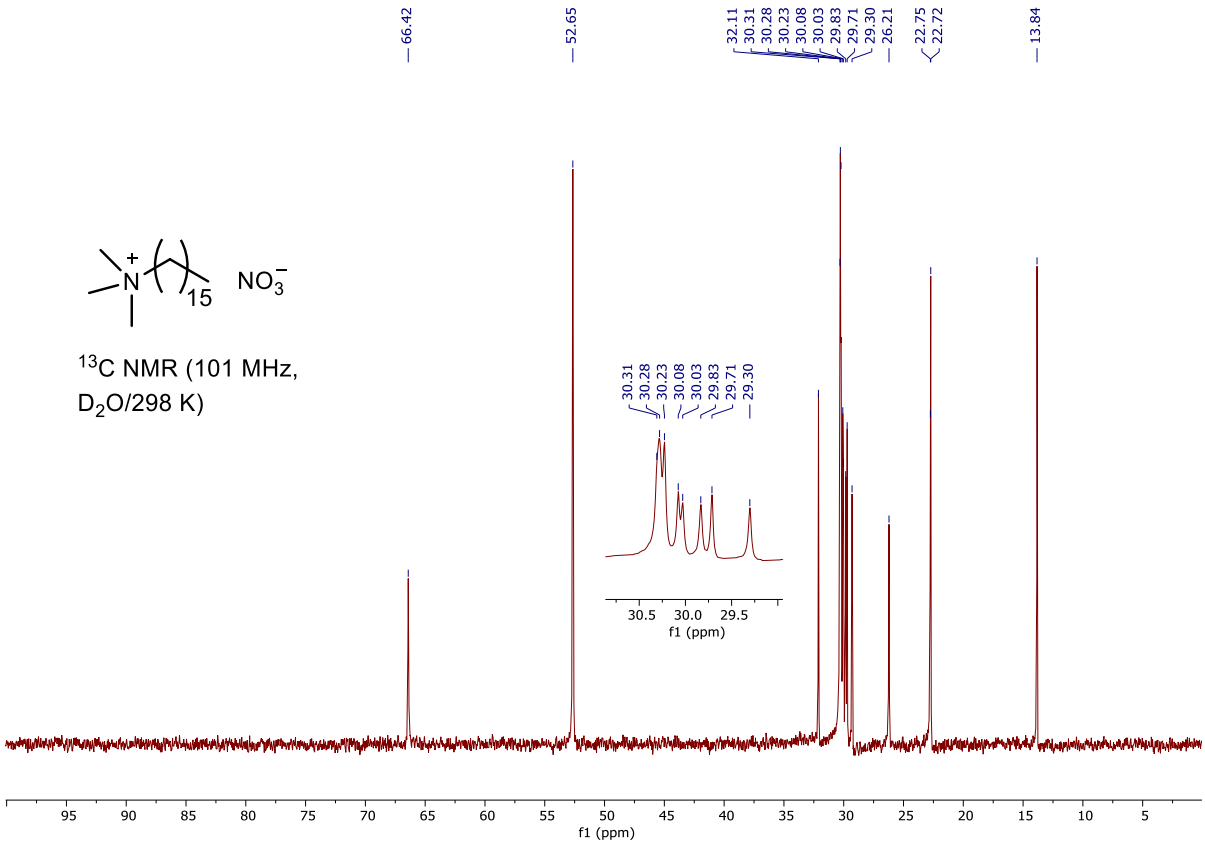

Supplementary Fig. 21: ^{13}C NMR (101 MHz, D_2O, 298 K) of hexadecyltrimethylammonium nitrate.

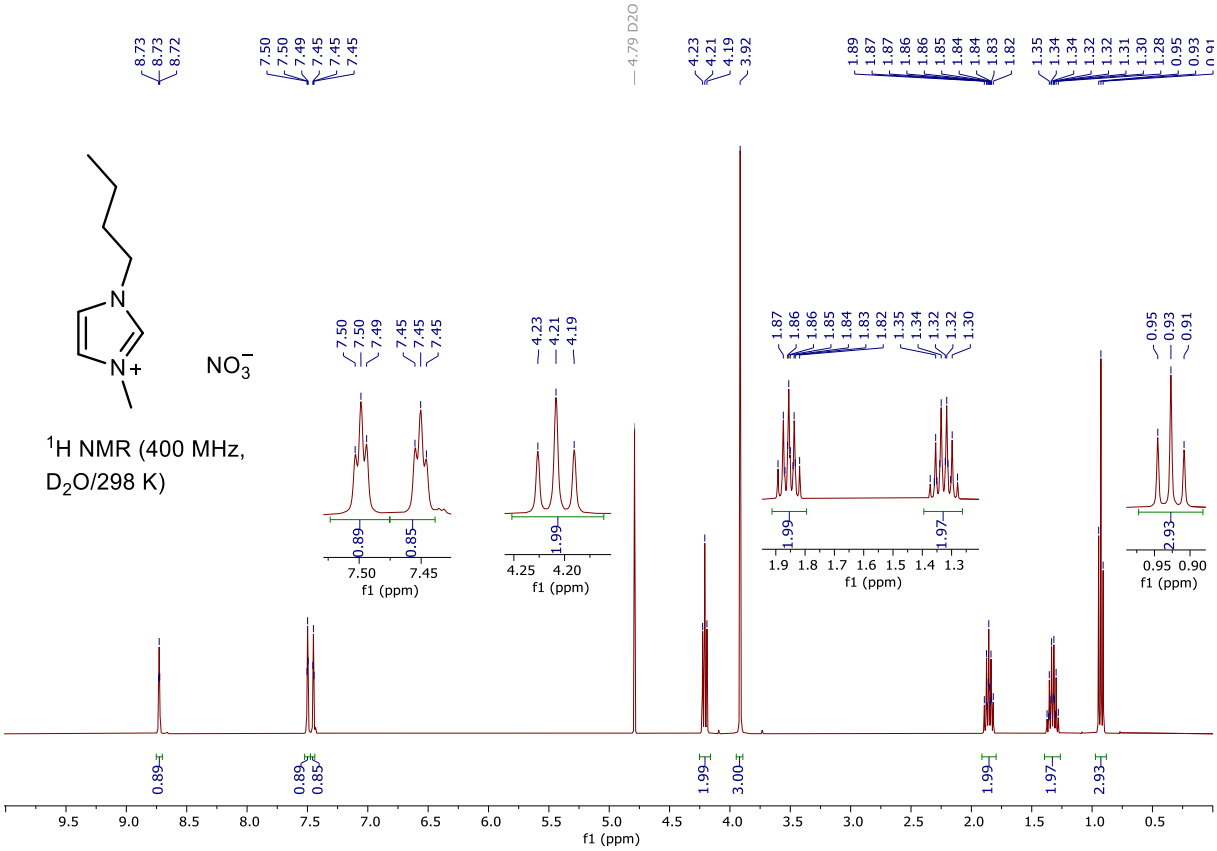

Supplementary Fig. 22: ^{1}H NMR (400 MHz, D_2O, 298 K) of 1-butyl-3-methylimidazolium nitrate.

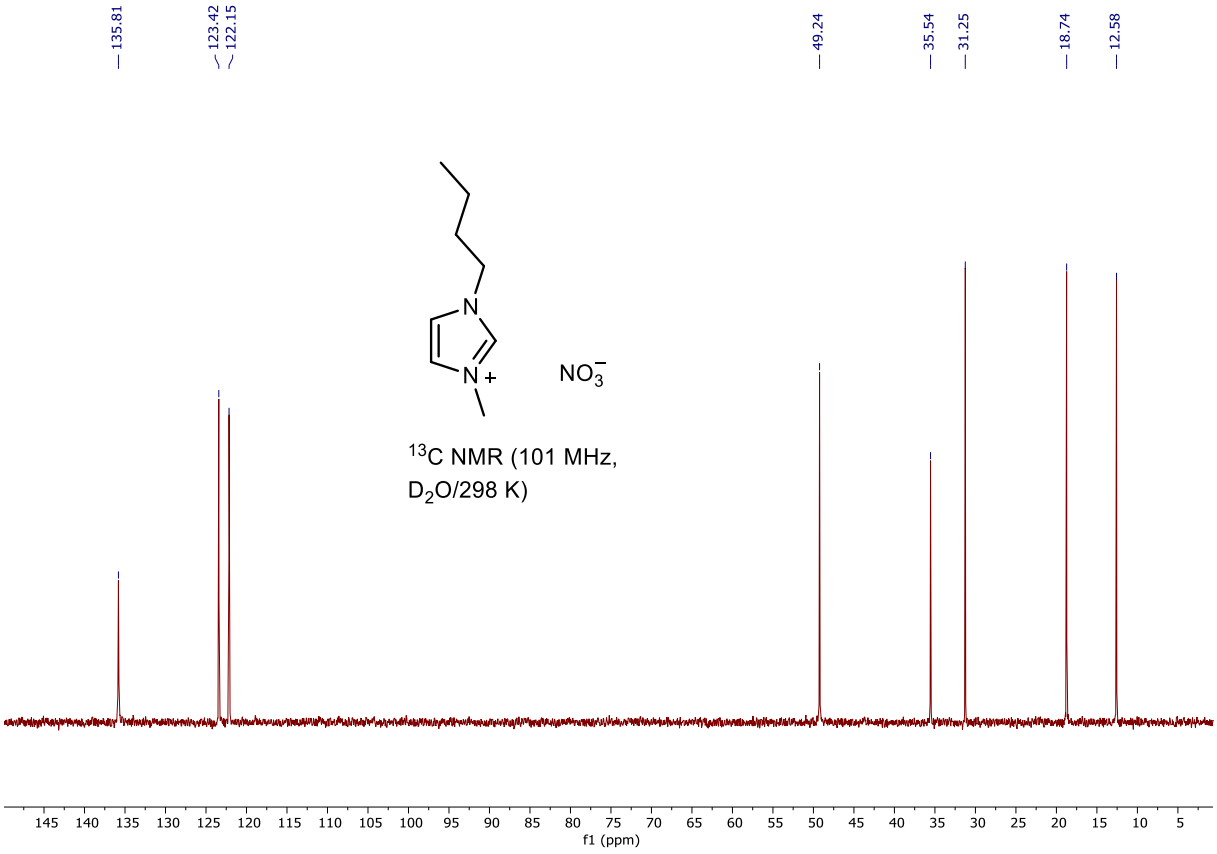

Supplementary Fig. 23: ^{13}C NMR (101 MHz, D_2O, 298 K) of 1-butyl-3-methylimidazolium nitrate.

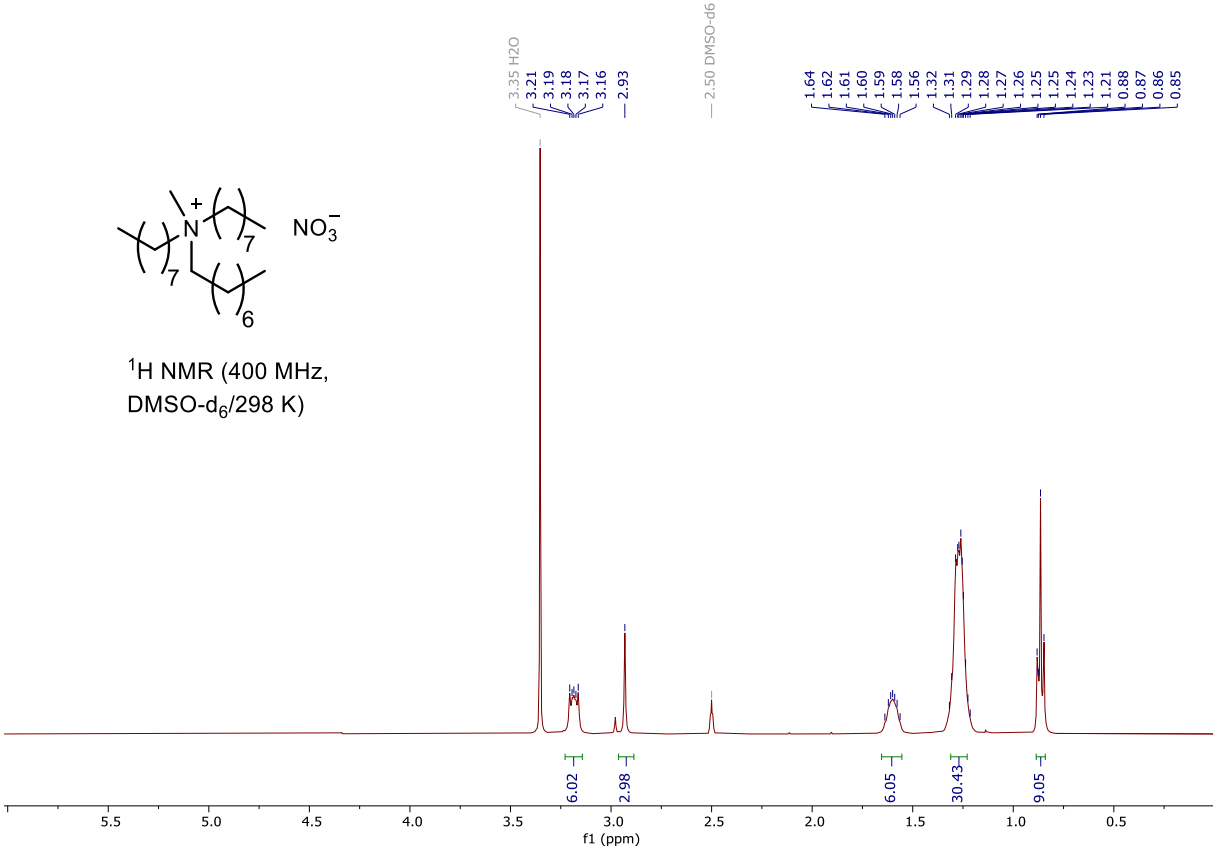

Supplementary Fig. 24: ^{1}H NMR (400 MHz, DMSO-d_6, 298 K) of methyltrioctylammonium nitrate.

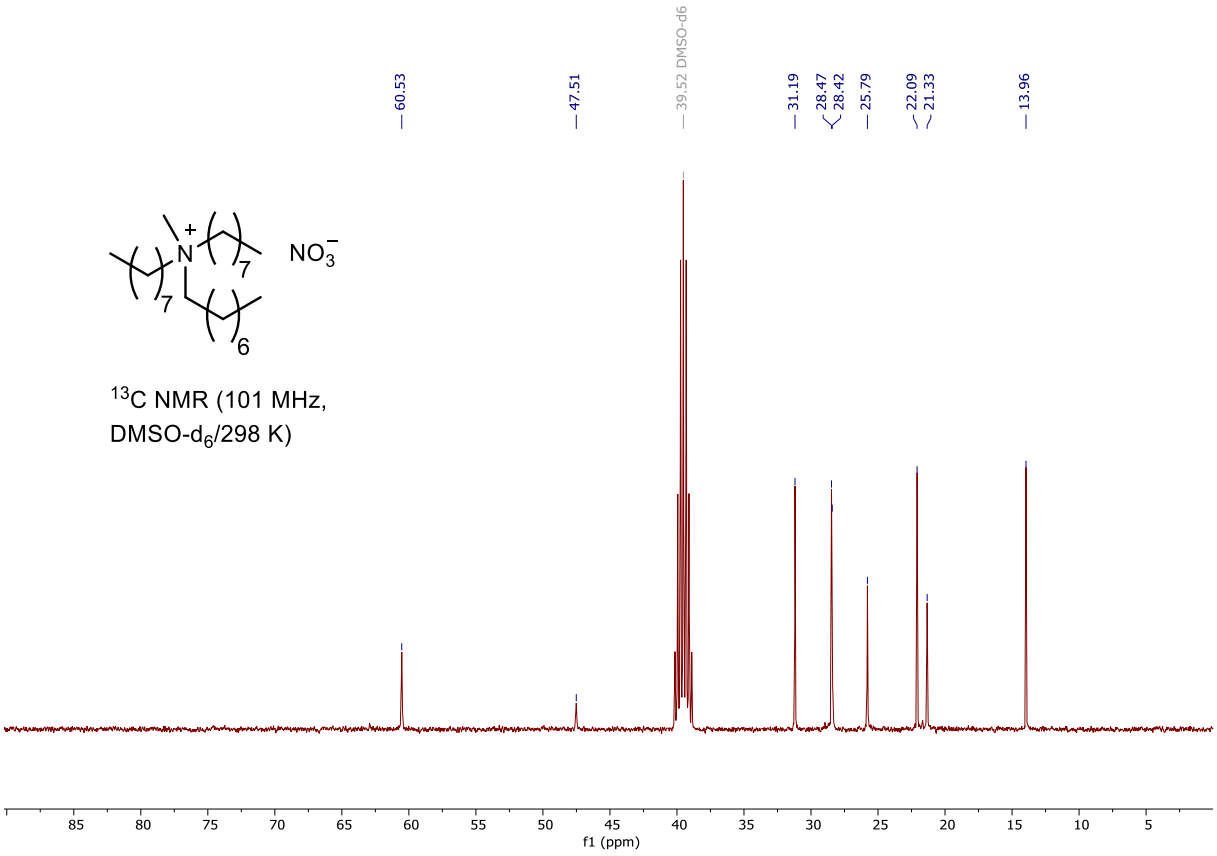

Supplementary Fig. 25: ^{13}C NMR (101 MHz, DMSO-d_6, 298 K) of methyltrioctylammonium nitrate.

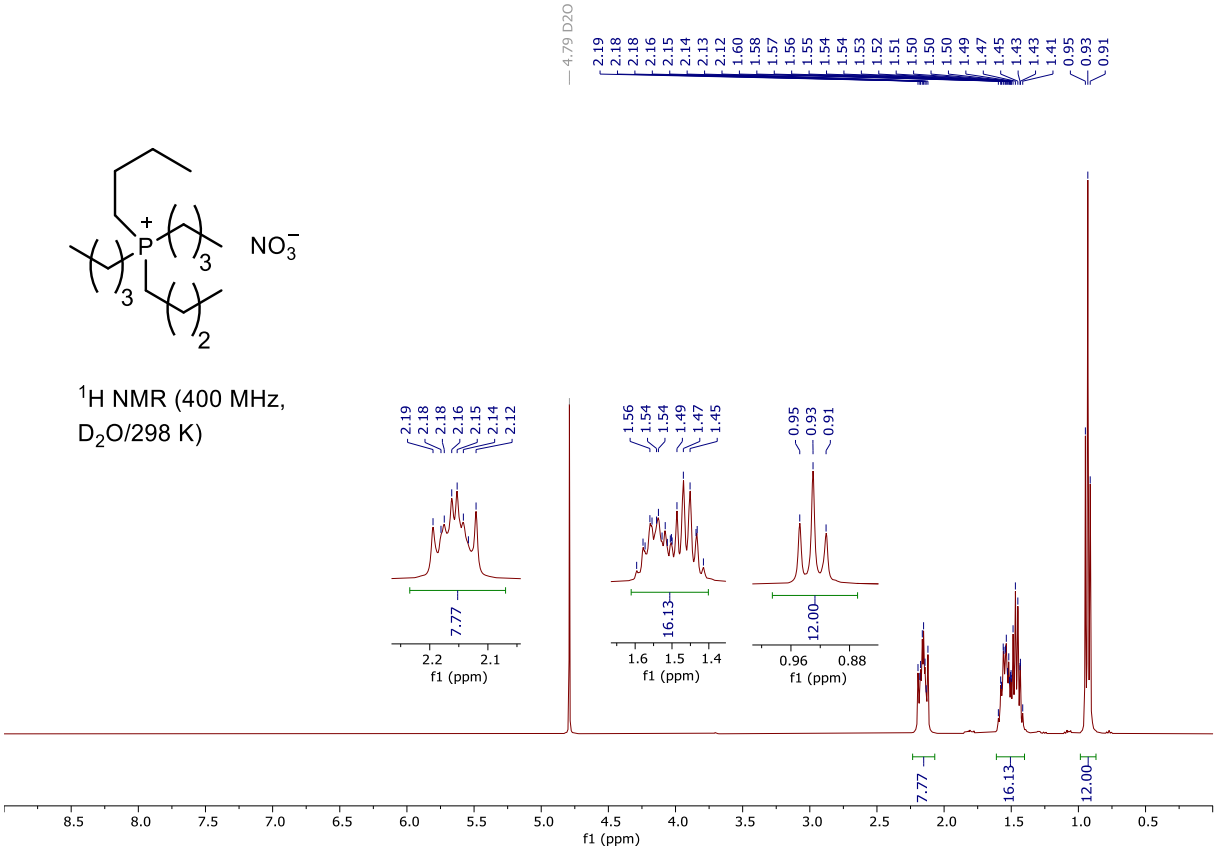

Supplementary Fig. 26: ^{1}H NMR (400 MHz, D_2O, 298 K) of tetrabutylphosphonium nitrate.

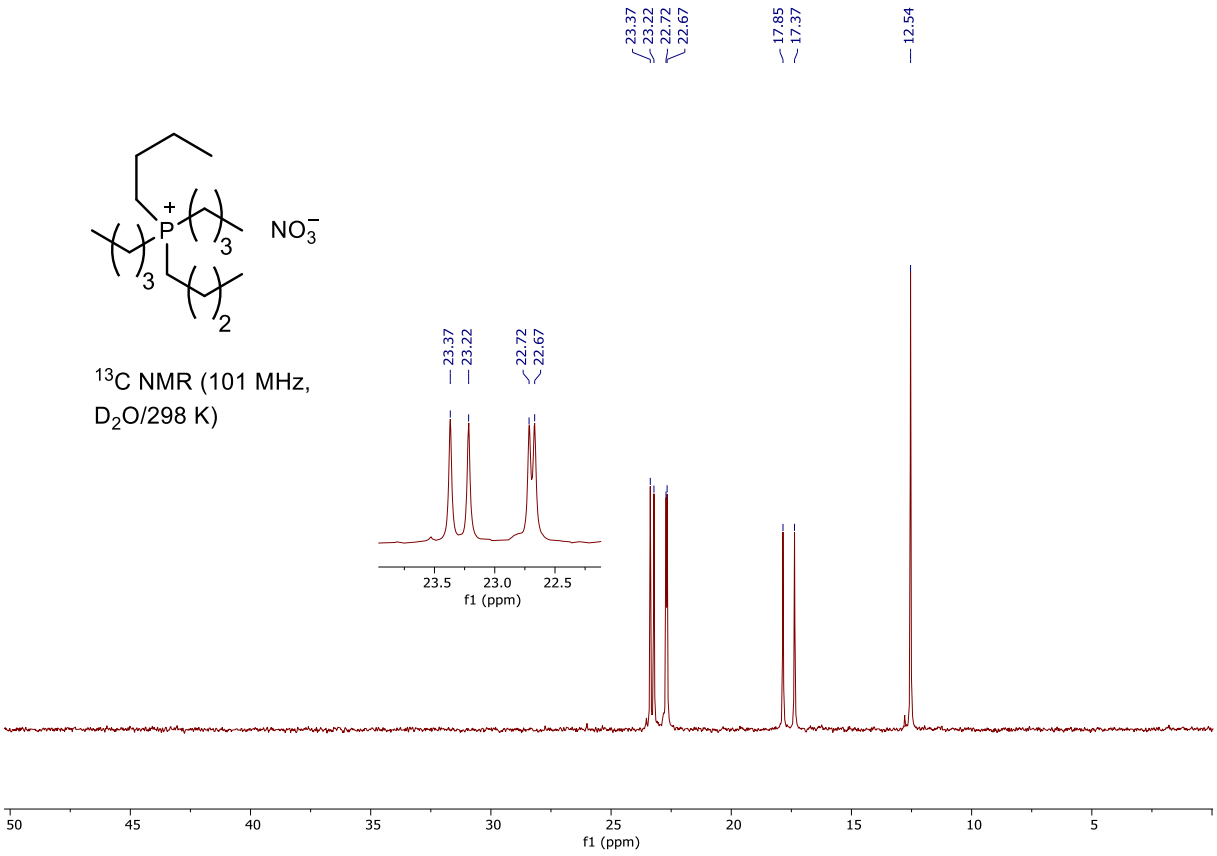

Supplementary Fig. 27: ^{13}C NMR (101 MHz, D_2O, 298 K) of tetrabutylphosphonium nitrate.

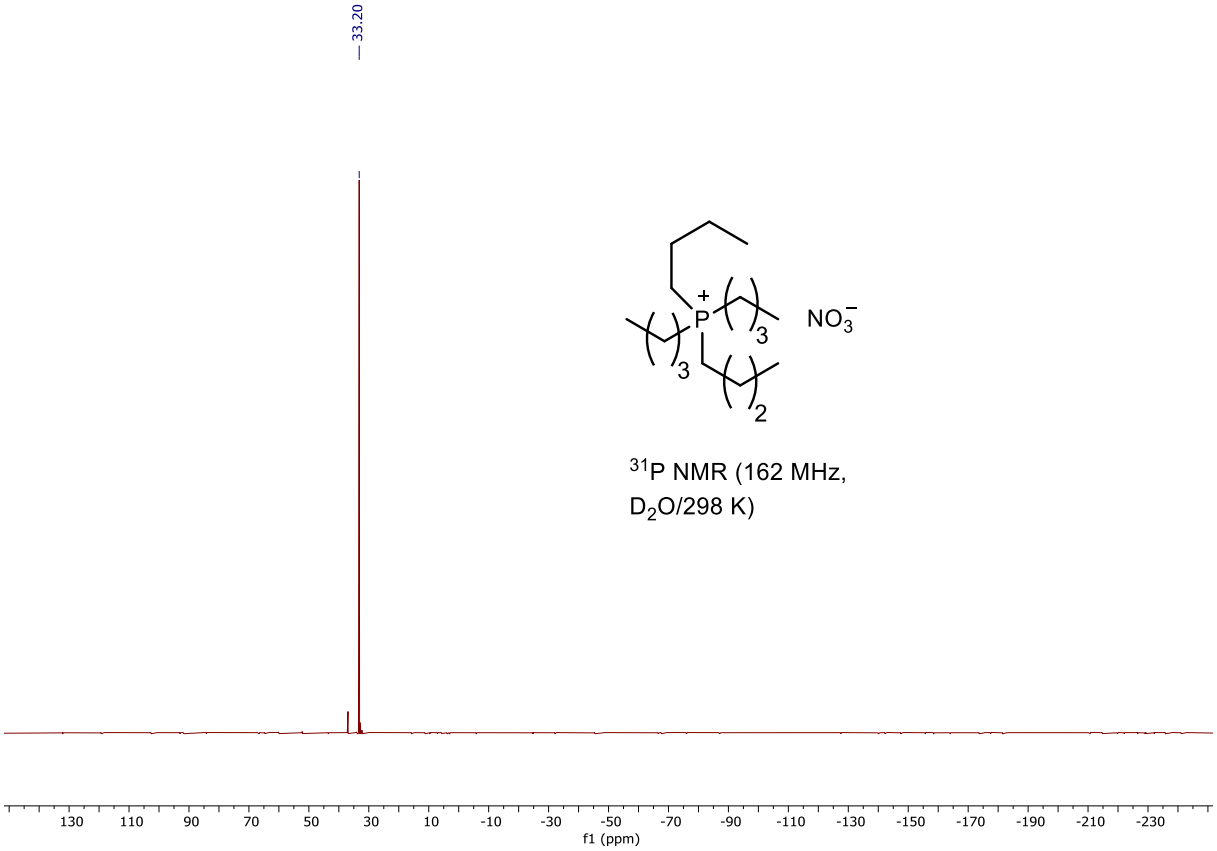

Supplementary Fig. 28: ^{31}P NMR (162 MHz, D_2O, 298 K) of tetrabutylphosphonium nitrate.

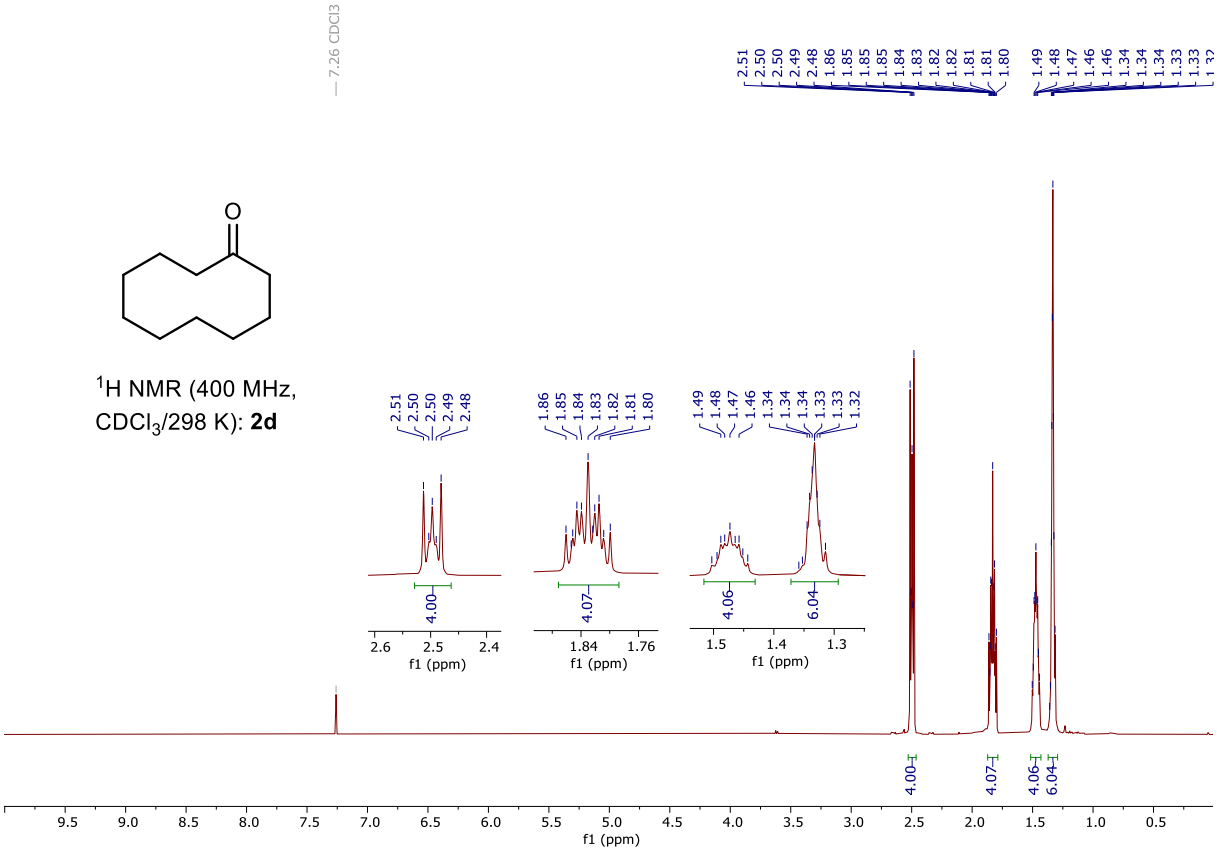

Supplementary Fig. 29: ^{1}H NMR (400 MHz, $CDCl_3$, 298 K) of compound **2d**.

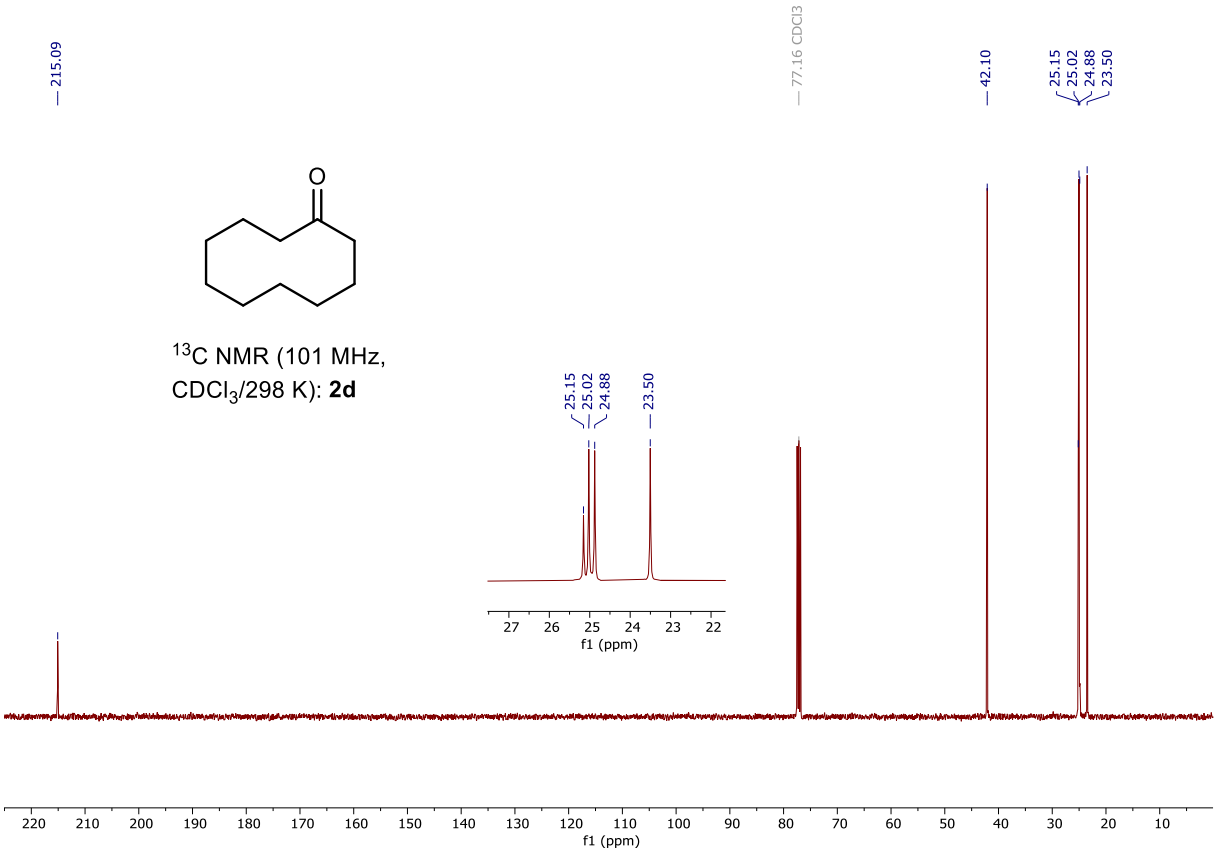

Supplementary Fig. 30: ^{13}C NMR (101 MHz, $CDCl_3$, 298 K) of compound **2d**.

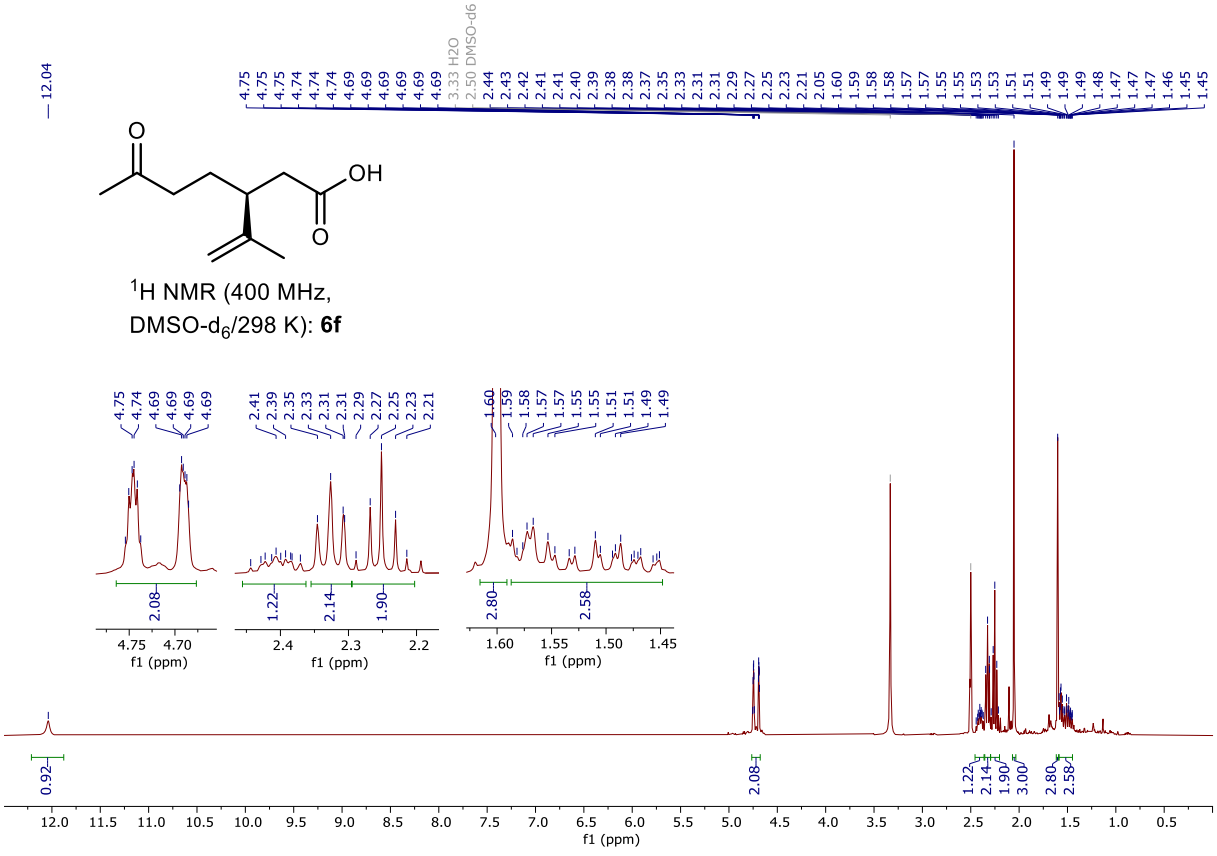

Supplementary Fig. 31: ^{1}H NMR (400 MHz, DMSO-d_6, 298 K) of compound **6f**.

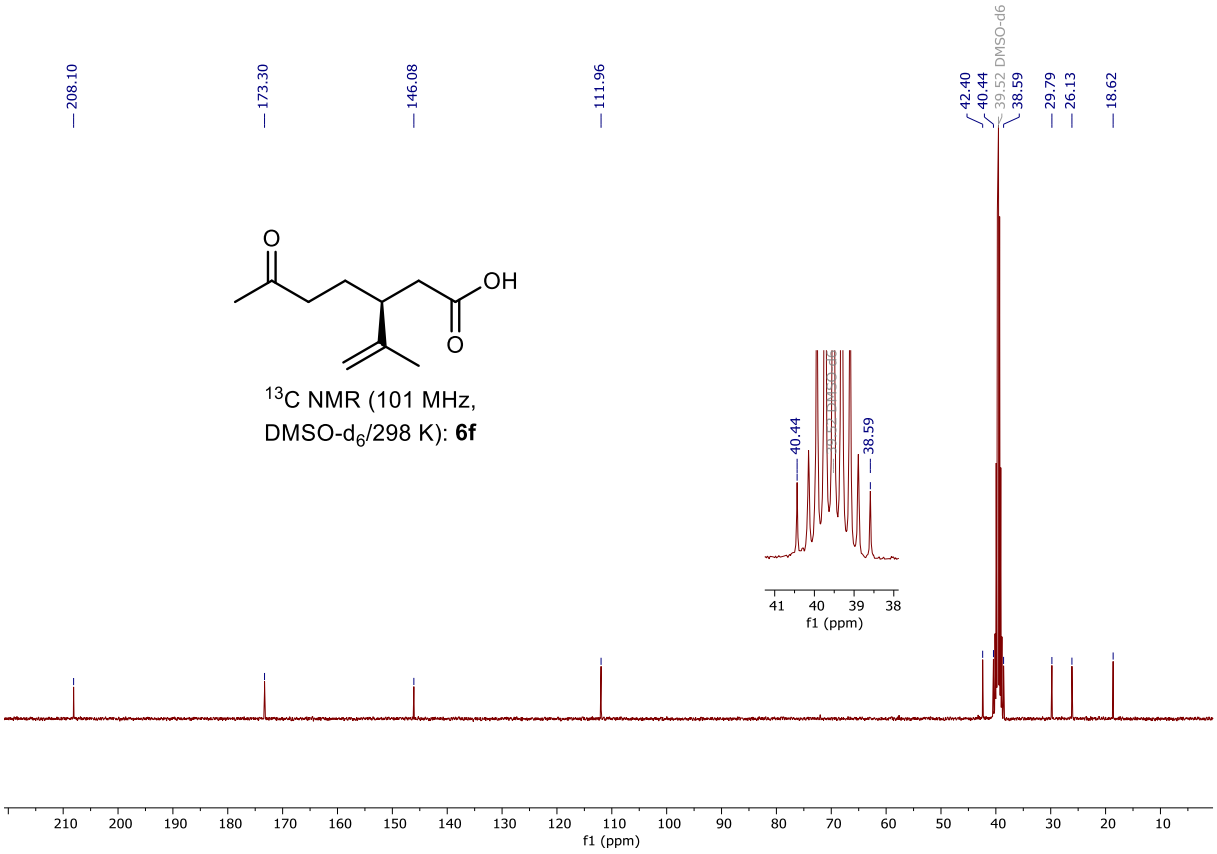

Supplementary Fig. 32: ^{13}C NMR (101 MHz, DMSO-d_6, 298 K) of compound **6f**.

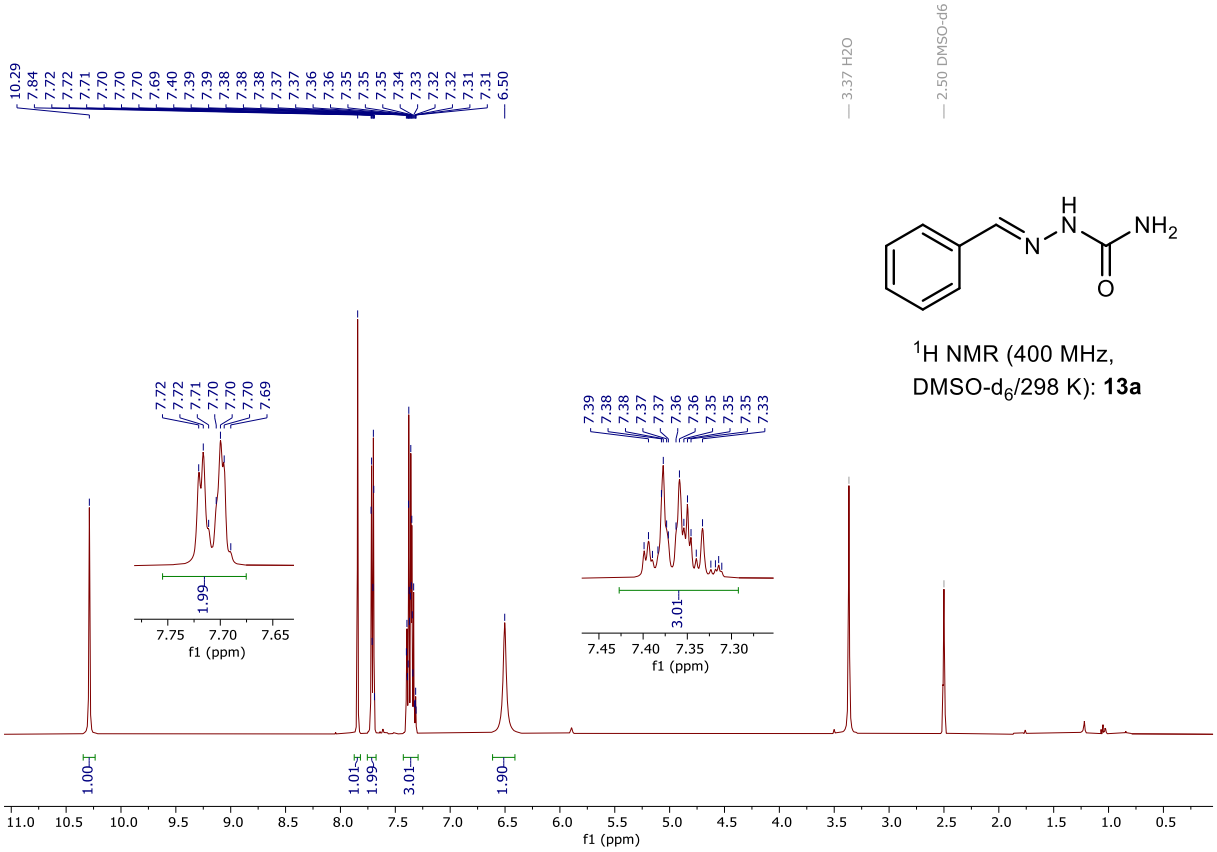

Supplementary Fig. 33: ^{1}H NMR (400 MHz, DMSO-d_6, 298 K) of compound **13a**.

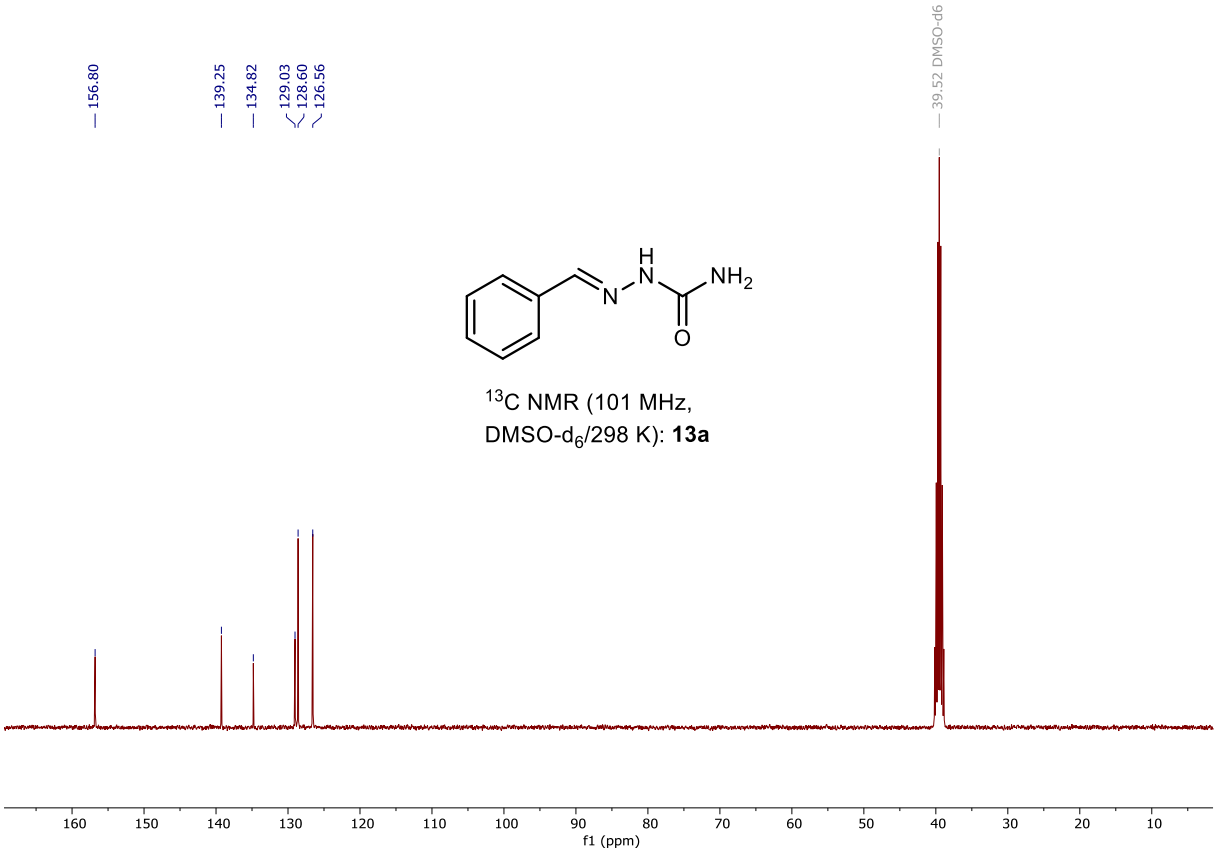

Supplementary Fig. 34: ^{13}C NMR (101 MHz, DMSO-d_6, 298 K) of compound **13a**.

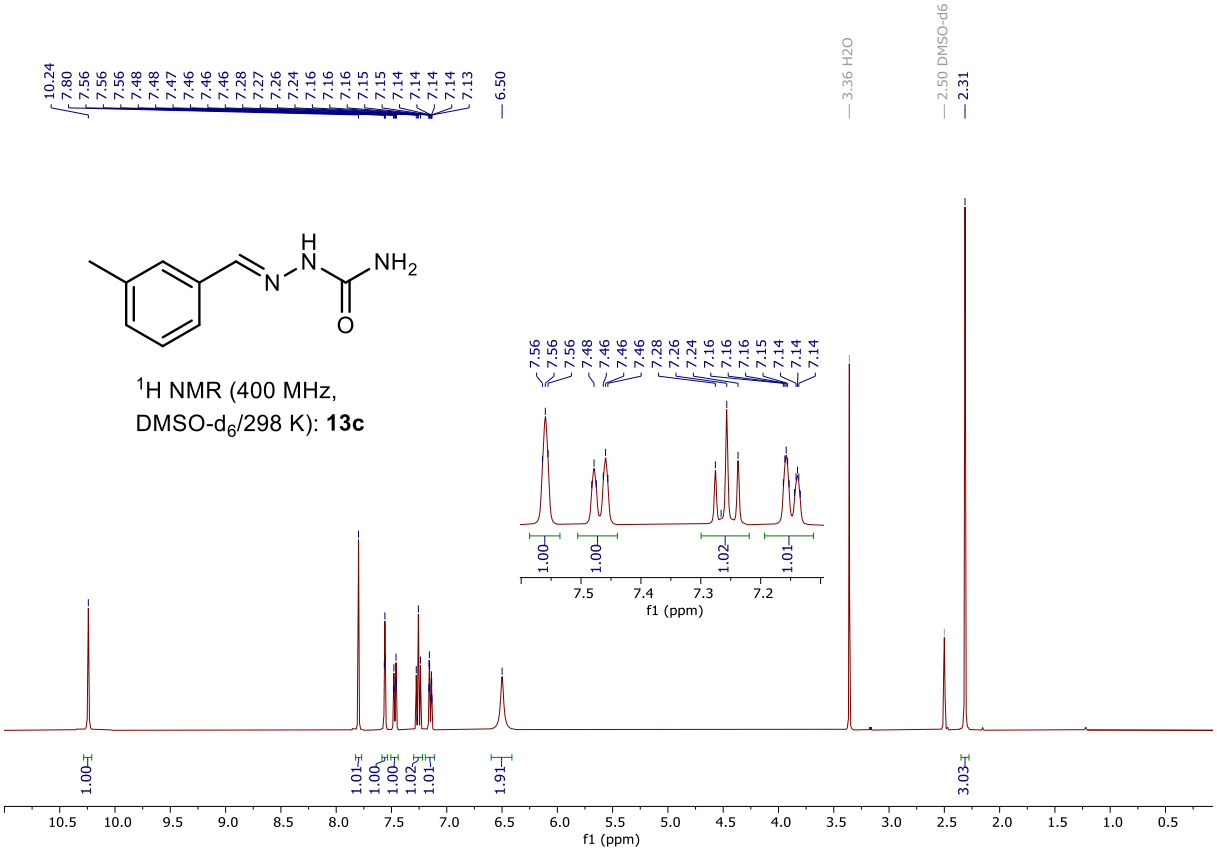

Supplementary Fig. 35: ^{1}H NMR (400 MHz, DMSO-d_6, 298 K) of compound **13c**.

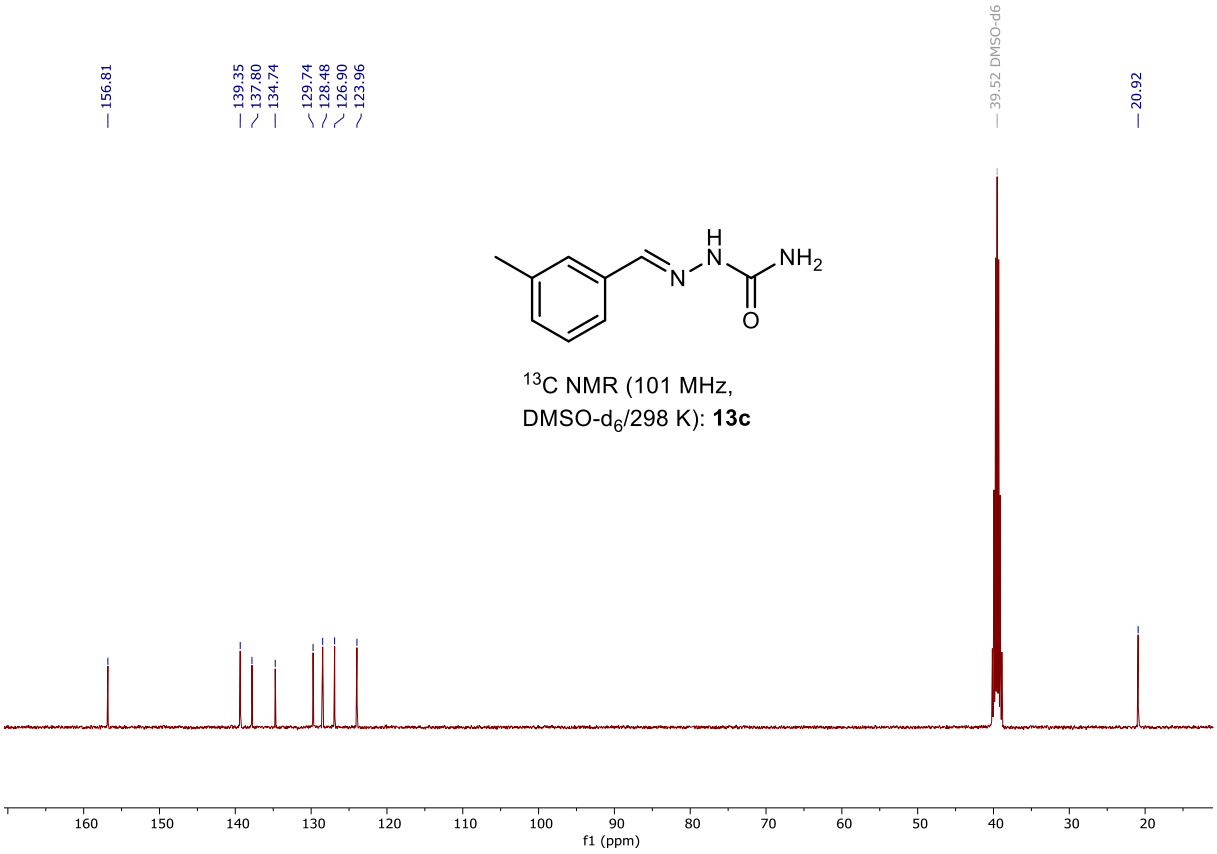

Supplementary Fig. 36: ^{13}C NMR (101 MHz, DMSO-d_6, 298 K) of compound **13c**.

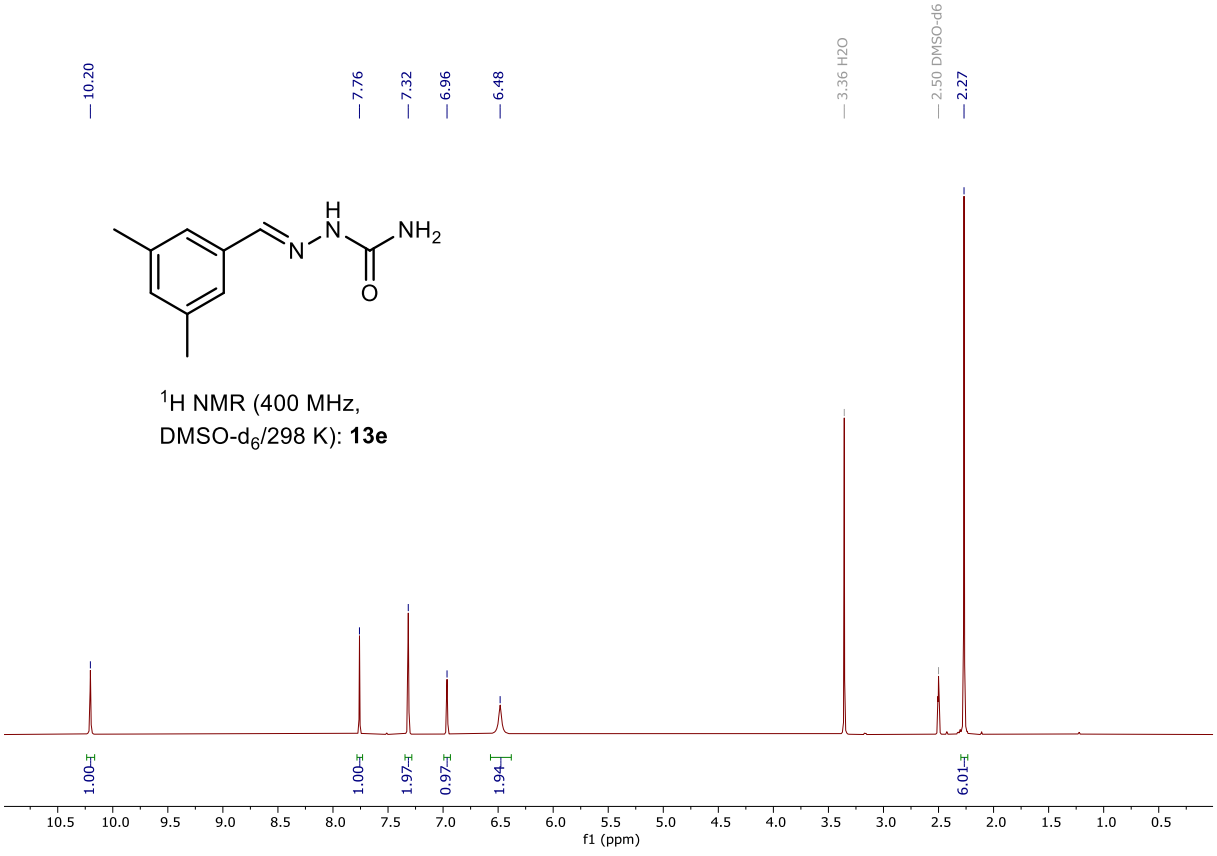

Supplementary Fig. 37: ^{1}H NMR (400 MHz, DMSO-d_6, 298 K) of compound **13e**.

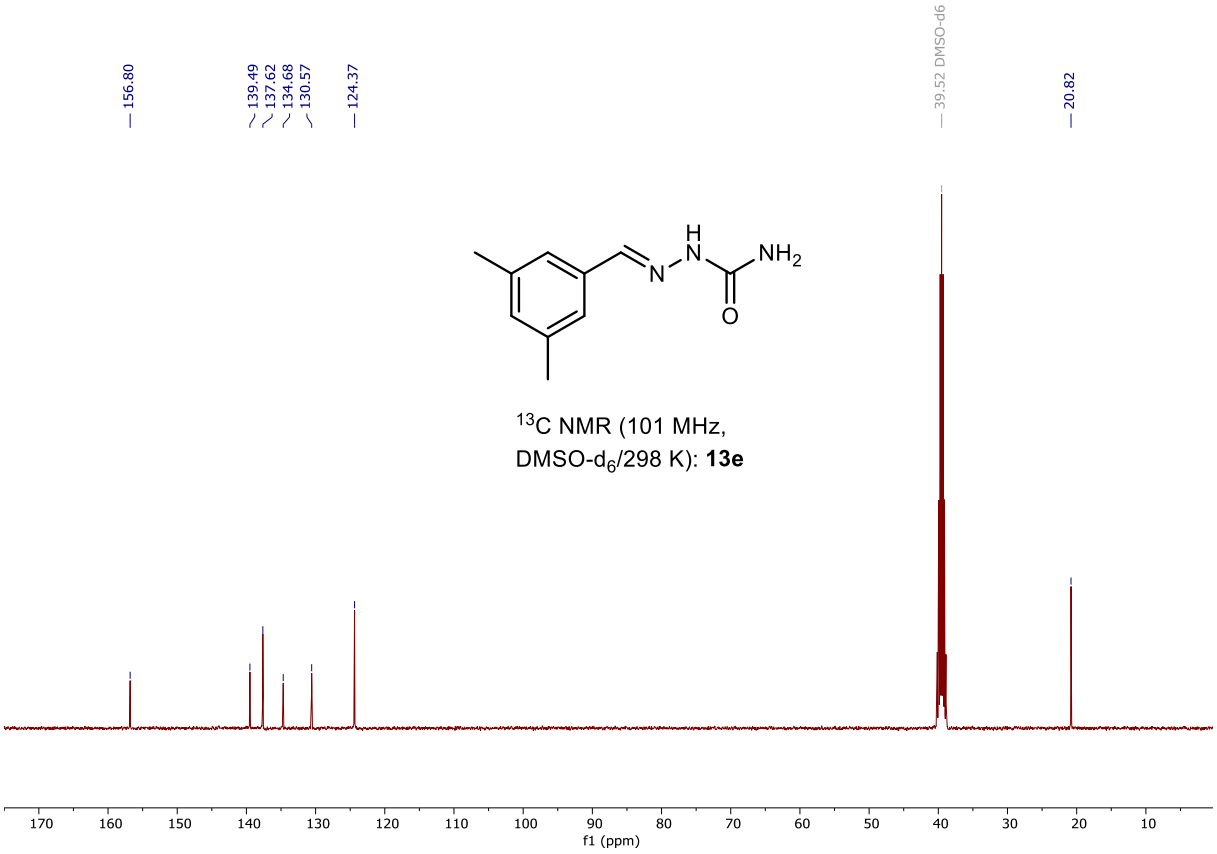

Supplementary Fig. 38: ^{13}C NMR (101 MHz, DMSO-d_6, 298 K) of compound **13e**.

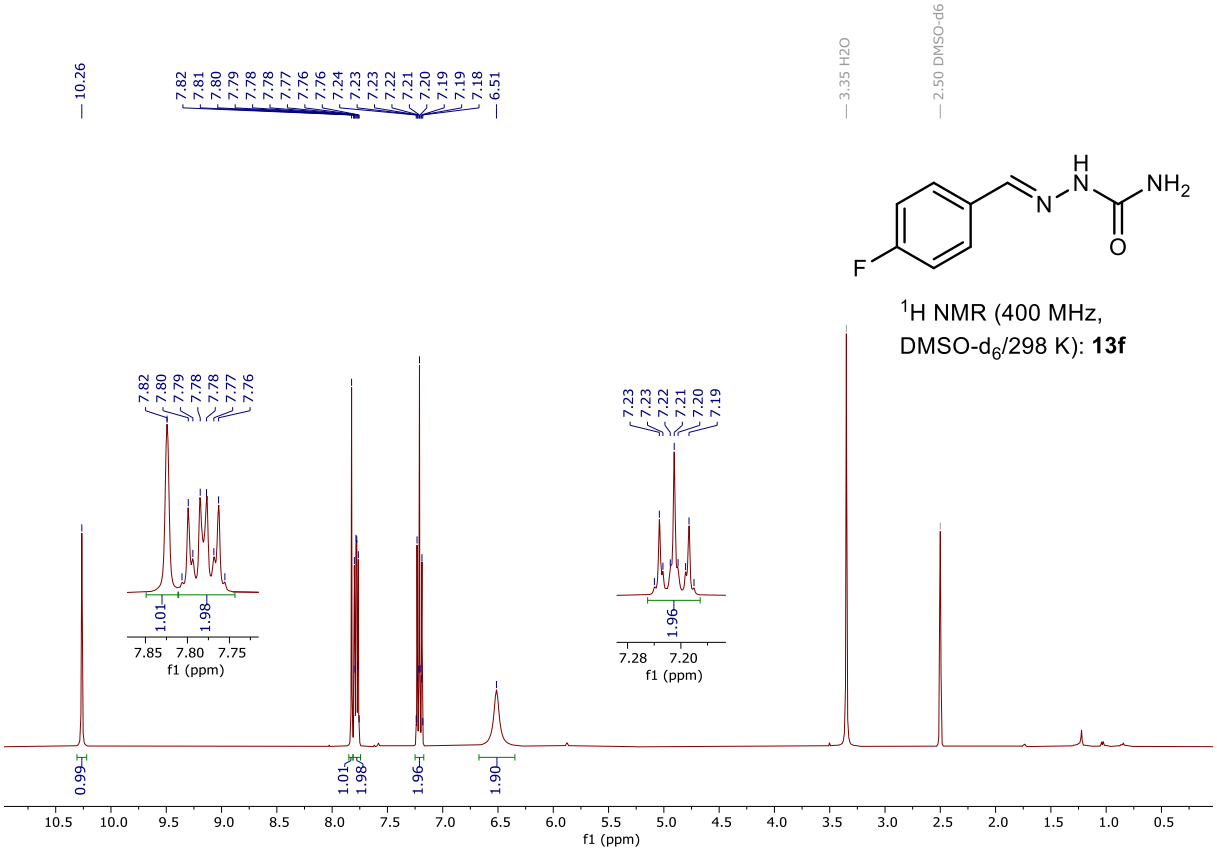

Supplementary Fig. 39: ^{1}H NMR (400 MHz, DMSO-d_6, 298 K) of compound **13f**.

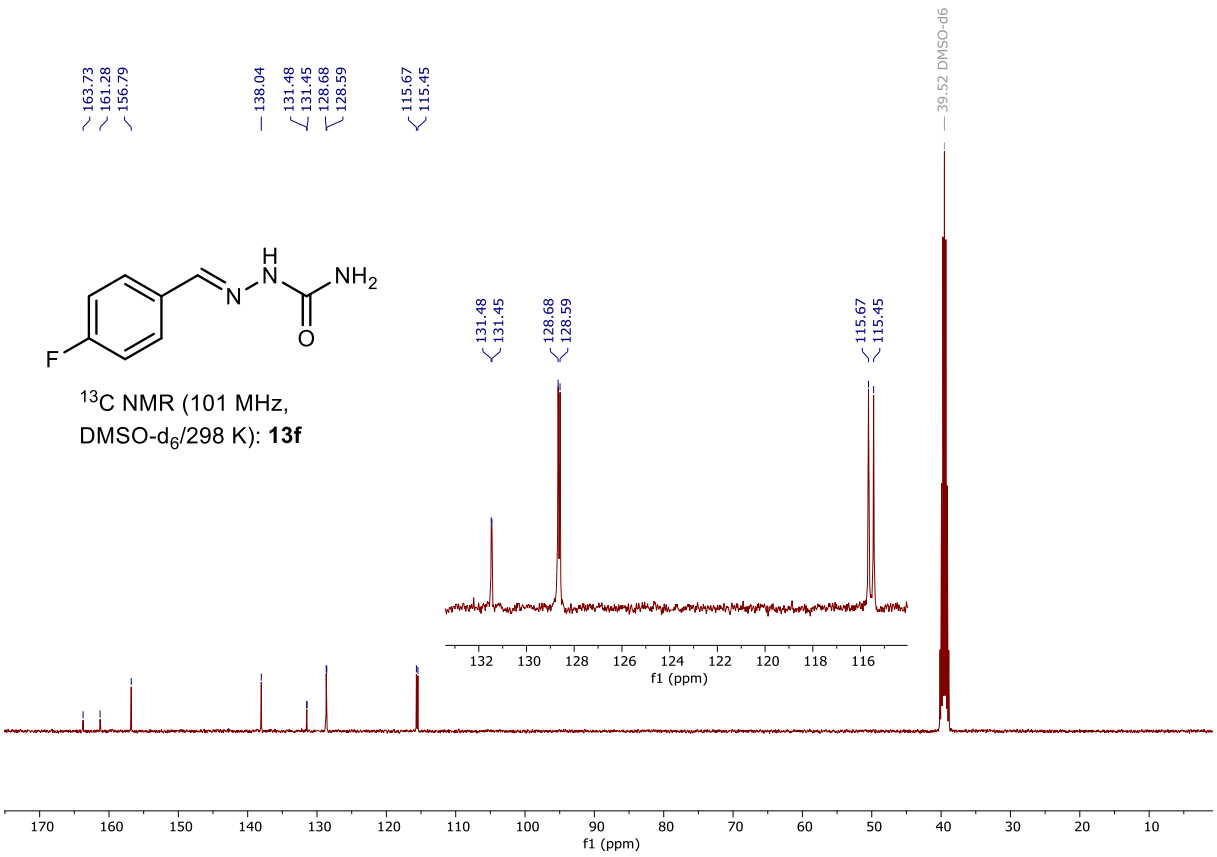

Supplementary Fig. 40: ^{13}C NMR (101 MHz, DMSO-d_6, 298 K) of compound **13f**.

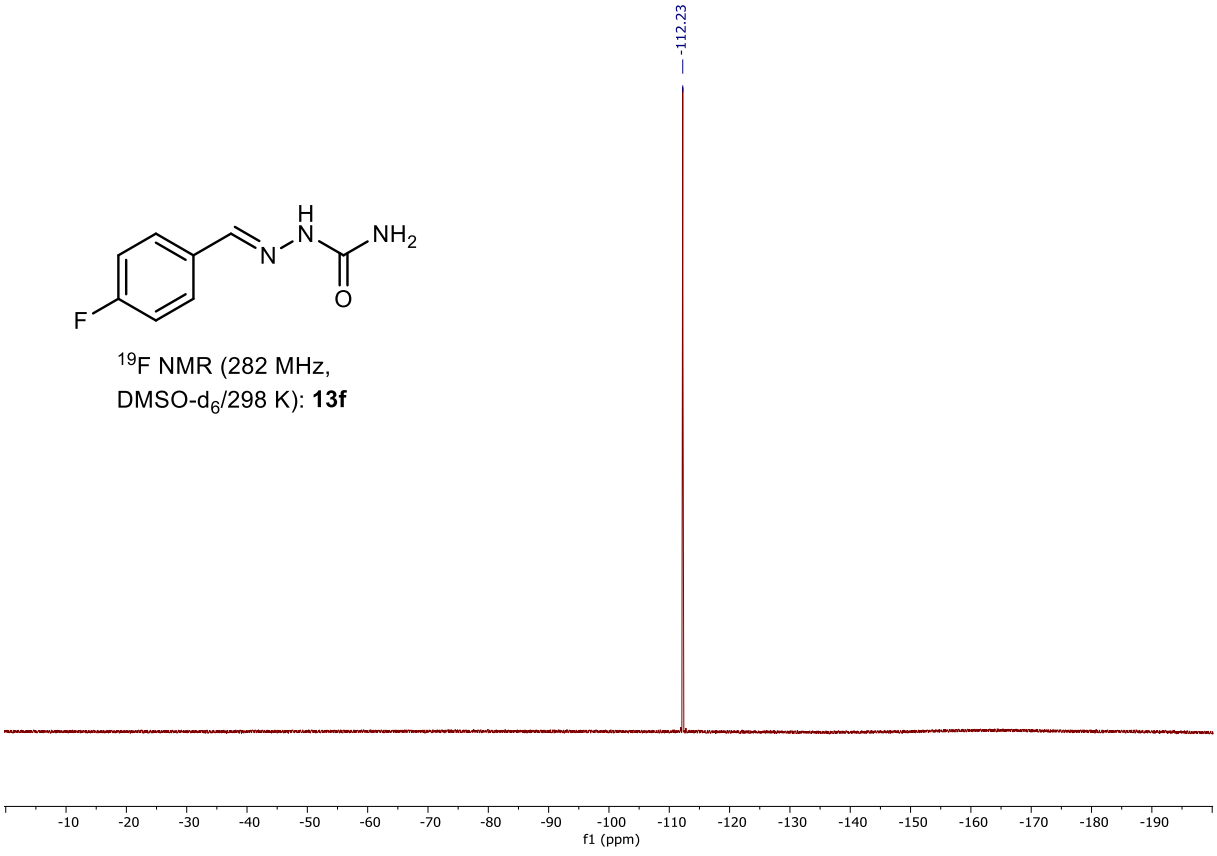

Supplementary Fig. 41: ^{19}F NMR (282 MHz, DMSO-d_6, 298 K) of compound **13f**.

5. Supplementary References

1. Harris, R. K., Becker, E. D., Cabral de Menezes, S. M., Goodfellow, R. & Granger, P. NMR nomenclature. Nuclear spin properties and conventions for chemical shifts. *Pure Appl. Chem*. **73**, 1795–1818 (2001).

2. Dörr, M., Waldmann, D. & Waldvogel, S. R. Screening in der Elektrosynthese – Schnelle und nachhaltige Entwicklung der innovativen Chemie von morgen. *GIT Labor-Fachz.* **7–8**, 26–28 (2021).

3. Tellinghuisen, J. Statistical Error Propagation. *J. Phys. Chem. A* **105**, 3917−3921 (2001).

4. Ó'Laoire, C. M. Investigations of oxygen reduction reactions in nonaqueous electrolytes and the lithium-air battery. (Northeastern University, Boston, Massachusetts, 2010, p. 84).

5. Franco, C. & Olmsted III, J. Photochemical determination of the solubility of oxygen in various media. *Talanta* **37**, 905–909 (1990).

6. Achord, J. M. & Hussey, C. L. Determination of dissolved oxygen in nonaqueous electrochemical solvents. *Anal. Chem.* **52**, 601−602 (1980).

7. Heard, D. M. & Lennox, A. J. J. Electrode materials in modern organic electrochemistry. *Angew. Chem. Int. Ed.* **59**, 18866−18884 (2020).

8. Skov, H., Benter, T., Schindler, R. N., Hjorth, J. & Restelli, G. Epoxide formation in the reactions of the nitrate radical with 2,3-dimethyl-2-butene, *cis*- and *trans*-2-butene and isoprene. *Atmos. Environ.* **28**, 1583−1592 (1994).

9. Guo, T., Gao, Y., Li, Z., Liu, J. & Guo, K. Cyclopropenium-activated DMSO for swern-type oxidation. *Synlett* **30**, 329−332 (2019).

10. He, C., Ma, F., Zhang, W. & Tong, R. Reinvestigating $FeBr_3$-catalyzed alcohol oxidation with H_2O_2: Is high-valent iron species (HIS) or reactive brominating species (RBS) responsible for alcohol oxidation? *Org. Lett.* **24**, 3499–3503 (2022).

11. Yang, J., Liu, J., Ge, Y., Huang, W., Neumann, H., Jackstell, R. & Beller, M. Direct and selective synthesis of adipic and other dicarboxylic acids by palladium-catalyzed carbonylation of allylic alcohols. *Angew. Chem. Int. Ed*. **59**, 20394–20398 (2020).

12. Jiang, X., Zhang, J. & Ma, S. Iron catalysis for room-temperature aerobic oxidation of alcohols to carboxylic acids. *J. Am. Chem. Soc*. **138**, 8344–8347 (2016).

13. Hoeschele, J. D., Kasparkova, J., Kostrhunova, H. Novakova, O., Pracharova, J., Pineau, P. & Brabec, V. Synthesis, antiproliferative activity in cancer cells and DNA interaction studies of [Pt(*cis*-1,3-diaminocycloalkane)Cl_2] analogs. *J. Biol. Inorg. Chem.* **25**, 913–924 (2020).

14. Xin, H., Duan, X.-H., Liu, L. & Guo, L.-N. Metal-free, visible-light-induced selective C−C bond cleavage of cycloalkanones with molecular oxygen. *Chem. Eur. J*. **26**, 11690–11694 (2020).

15. Xin, H., Duan, X.-H., Yang, M., Zhang, Y. & Guo, L.-N. Visible light-driven, copper-catalyzed aerobic oxidative cleavage of cycloalkanones. *J. Org. Chem.* **86**, 8263–8273 (2021).

16. Wen, F. & Li., Z. Semicarbazide: A transient directing group for C(sp3)−H arylation of 2-methylbenzaldehydes. *Adv. Synth.Catal.* **362**, 133–138 (2020).

17. Nascimento da Cruz, A. C. et al. Biological evaluation of arylsemicarbazone derivatives as potential anticancer agents. *Pharmaceuticals* **12**, 169 (2019).

18. Wang, Y., Jiang, X. & Wang, B. Cobalt-catalyzed carboxylation of aryl and vinyl chlorides with CO_2. *Chem. Commun*. **56**, 14416–14419 (2020).

5 Conclusion

The overarching context of this dissertation is the development of electrochemical methods with a material-efficient dual role of supporting electrolytes. This dual role was demonstrated by two different applications: electrolyte constituents as a reaction partner (reagent) and as a mediator (electrocatalyst). The methods developed within the framework of this dissertation, thus, fulfill the set objectives. A method for the sulfonylation of electron-rich aromatics was successfully established, using sodium sulfinate salts as an ion conductor and reagent. Two first-author publications were published as part of this research. The method allows the sulfonylation of phenols, arenes, and aniline derivatives using only an HFIP/water mixture and the sulfinates on BDD electrodes in an undivided cell under simple constant current conditions (Scheme 15a). In the second part of this work, a method was developed for the oxo-functionalization of cycloalkanes and cycloalkenes to ketones and dicarboxylic acids, using nitrate anions in a dual role as an electrolyte component and an anodic mediator. Applying molecular oxygen as the oxygen source allows both electrode reactions to be used efficiently for product generation. Besides the oxygen, only nitriles as solvents and nitrate salts as mediators are required in the undivided cell under constant current conditions on glassy carbon electrodes (Scheme 15b). One first-author publication was published as part of this research. The procedures demonstrated in this dissertation for the dual roles of supporting electrolytes can help to guide the general electrochemical method development towards material- and resource-saving requirements.

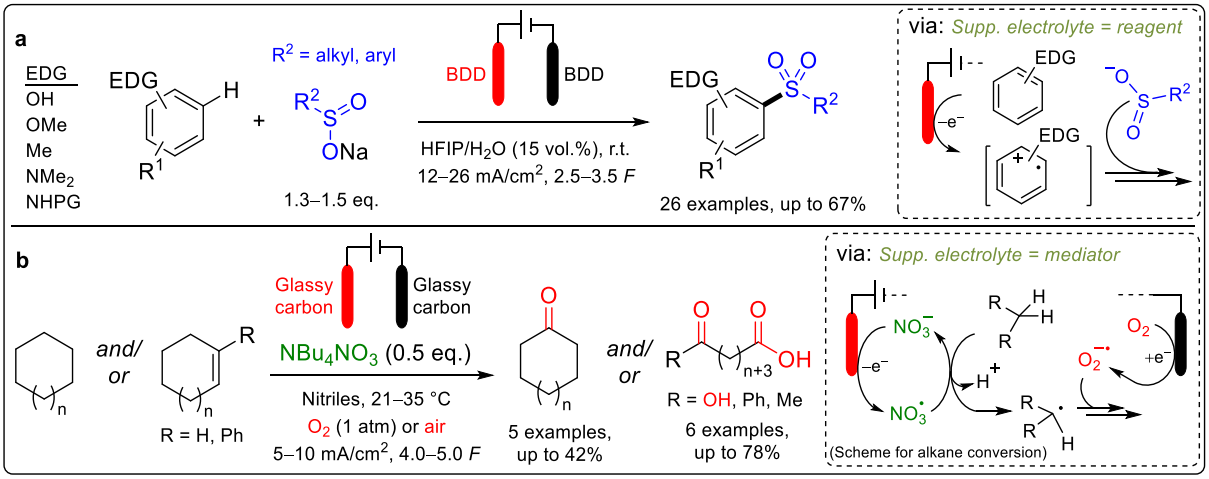

Scheme 15: a Electrochemical sulfonylation of electron-rich aromatics using sulfinate supporting electrolytes as reagents. **b** Electrochemical oxo-functionalization of cycloalkanes and -alkenes using nitrate supporting electrolytes as mediator.

6 Outlook

The lack of material efficiency of electro-organic reactions is often due to the conventional electrolyte composition of organic solvent and supporting electrolyte, with the latter one only providing the role of ionic conductivity. Another approach, therefore, deals with using so-called solid polymer electrolytes (SPE), a technique well known from fuel cells.[192] The ionic conductor role of the SPE allows the exclusion of supporting electrolytes. A theoretical application within the scope of the topics covered in this dissertation could be to replace nitrate salt with an anion exchange membrane (AEM). Solid-phase tethered quaternary ammonium or imidazolium groups and nitrate counterions could serve as an ion-conducting membrane. For this purpose, a possible application of so-called zero-gap electrolyzers could also be tested, which are being investigated by the Apfel group (Ruhr-Universität Bochum/Fraunhofer UMSICHT) to reduce gases such as CO_2.[193] A theoretical mass transfer, adapted from literature descriptions[194] and mechanistic considerations, is shown in Figure 14.

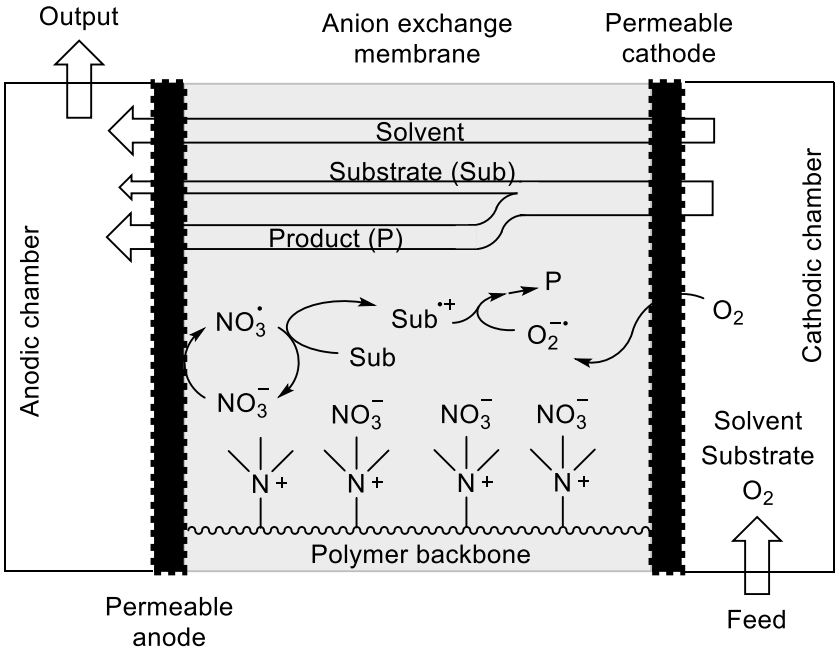

Figure 14: Schematic representation of an anion (nitrate) exchange membrane SPE cell regarding the nitrate-mediated electrochemical oxidation methodology from this dissertation. Adapted and modified from ref [194].

The utilization of supporting electrolytes based on nitrates is a good strategic choice. An increasing global population, estimated to be nearly 10 billion inhabitants in 2050,[195] will require a higher supply of agricultural food and, thus, fertilizer. Ammonium nitrate (NH_4NO_3)

is an important nitrogen fertilizer in agriculture, with a worldwide production capacity of 63 million tonnes annually.[196] However, it has often been misused as an explosive and has a long record of fatal accidents.[196b,197] Hence, there are increasing restrictions on its use and purchase.[198] Structural analog anions like orthoborate (BO_3^{3-}) or carbonate (CO_3^{2-}) could be an alternative to nitrate. Here, of particular interest might be the corresponding tetrabutylammonium salts: tris(tetrabutylammonium) orthoborate ($(NBu_4)_3BO_3$) and bis(tetrabutylammonium) carbonate ($(NBu_4)_2CO_3$), which could be obtained presumably as ionic liquids via acid-base reaction (Scheme 16). Just for the carbonate salt, an experimental procedure is already described.[199] An interesting feature is the higher lipophilicity of these salts due to the higher number of long-chained alkyl cations, which could facilitate the dissolution of very lipophilic substrates. Therefore, polar solvents with a higher permittivity could also be used for these substrates, lowering the electrolyte resistance and cell voltage and, thus, the energy consumption of the electrochemical conversion.

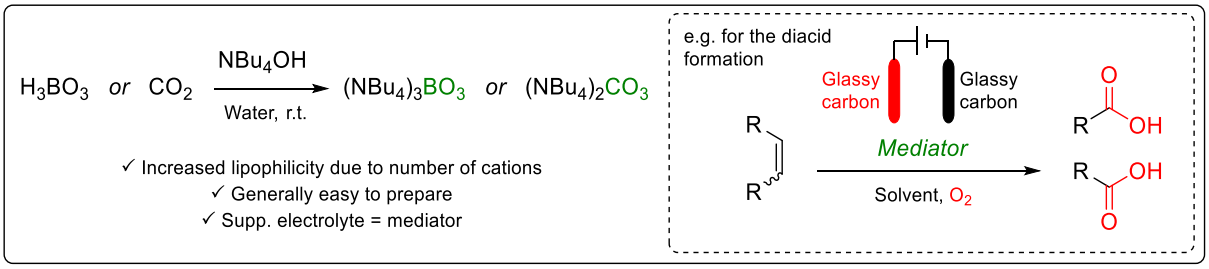

Scheme 16: Possible synthesis of $(NBu_4)_3BO_3$ and $(NBu_4)_2CO_3$ and usage as supporting electrolyte and mediator in electrosynthesis.

In the context of alkene cleavage to diacids, it was shown that fatty acids can also be converted to mono- and dicarboxylic acids using the developed method. Based on this, the method could convert biogenic fatty acids, such as tall oil fatty acids (TOFA), obtained by distillation from the natural product tall oil, a waste stream from the paper pulp industry. The resulting dicarboxylic acids could serve, for example, as polymer building blocks and the monocarboxylic acids as flavorings[200] or herbicides[201] (Scheme 17). Thus, this method can create an opportunity to exploit the potential of TOFA as a sustainable resource for industrial commodities.

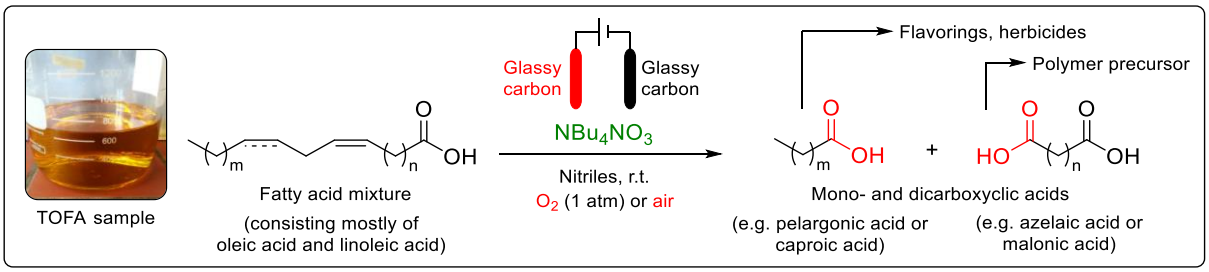

Scheme 17: Electrochemical conversion of TOFA to mono- and dicarboxylic acids.

On the small mmol scale, an oxygen atmosphere in the gas space above the reaction mixture was sufficient for an oxygenation reaction. Regarding a scale-up considering production rates in g/h, it is necessary to saturate the electrolyte with oxygen as efficiently as possible before electrolysis. For this purpose, so-called bubble column reactors, e.g., known from fermentation processes, can be used (Figure 15).[202] Efficient oxygen transfer into the liquid phase depends on a small initial bubble size and, therefore, on the orifice size of the diffusers used. In contrast, energetic considerations lead to an optimum bubble size.[203]

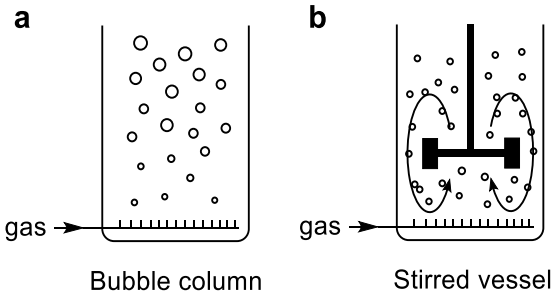

Figure 15: Typical aeration devices: **a** Bubble column reactor and **b** stirred gas-liquid dispersion with a higher degree of back mixing. The figure is adapted from ref [202].

7 List of abbreviations

[M]	Transition metal catalyst
°C	Degree Celsius
A	Active electrode surface [cm^2]
A	Ampere
A^-	Anion
Å	Angstrom
Ac	Acetyl
acac	Acetylacetone
AEM	Anion exchange membrane
AIBN	Azobisisobutyronitrile
aq.	Aqueous
Ar	Aryl
atm	Atmospheric pressure (1 atm ≈ 1 bar)
BDD	Boron-doped diamond
c	Concentration [mol/L]
C	Coulomb (1 C = 1 As)
c	Centi (10^{-1}) (prefix)
C^+	Cation
cal	Calorie (1 cal ≈ 4.18 J)
CCE	Constant current electrolysis
CE	Counter electrode
CPE	Constant potential electrolysis
CV	Cyclic voltammetry
DDQ	2,3-Dichloro-5,6-dicyano-1,4-benzoquinone
DIPEA	*N*,*N*-Diisopropylethylamine
DL	Diffuse layer
DMC	Dimethyl carbonate
DMF	*N*,*N*-Dimethylformamide
DMSO	Dimethyl sulfoxide
E	Electric potential [V]
E	Electrophile
EDC	1,2-Dichloroethane (ethylene dichloride)
EDG	Electron-donating group
E_{ox}	Oxidation potential
eq.	Equivalents (commonly mol-eq.)
eV	Electron Volt (1 eV = $1.6 \cdot 10^{-19}$ J)
EWG	Electron-withdrawing group
F	Faraday constant (96485 C/mol)
g	Gram
GC	Gas chromatography
h	Hours
HAT	Hydrogen atom transfer
HER	Hydrogen evolution reaction
HFIP	1,1,1,3,3,3-Hexafluoro-2-propanol
HOMO	Highest occupied molecular orbital
HPLC	High-performance liquid chromatography
hv	Denotation for photon energy
I	Electric current [A]
i	*iso* (prefix)
IEC	International Electrotechnical Commission
IHP	Inner Helmholtz plane
IUPAC	International Union of Pure and Applied Chemistry
j	Current density [mA/cm^2]
J	Joule
k	Kilo (10^3) (prefix)
KA	Ketone/Alcohol
L	Liter
LUMO	Lowest unoccupied molecular orbital
m	Milli (10^{-3}) (prefix)
M	molar (1 M = 1 mol/L)
M	Mediator
m	*meta* (prefix)
M	Multiplicity
m	Meter
m-CPBA	*meta*-Chloroperoxybenzoic acid
min	Minutes
MO	Molecular Orbital
mol	Mole (amount of substance)

MS	Molecular sieve
MS	Mass spectrometry (with HPLC or GC)
MTBS	Methyltributylammonium methylsulfate
n	Amount of substance [mol]
n	straight-chain (prefix)
N	Nitrogen bonded substituent
NADPH	Reduced form of nicotinamide adenine dinucleotide phosphate
NHPI	*N*-Hydroxyphthalimide
NSCLC	Non-small cell lung carcinoma
Nu	Nucleophile
o	*ortho* (prefix)
OHP	Outer Helmholtz plane
OTf	Triflate
OTs	Tosylate
Ox	Oxidizing agent
p	*para* (prefix)
p	Pico (10^{-12}) (prefix)
P or P'	Product
PC	Propylene carbonate
pH	Potential of hydrogen (lat. potentia hydrogenii)
PIDA	Phenyliodine(III) diacetate
pK_a	Negative decadic logarithm of the acid dissociation constant K_a
PTFE	Poly(1,1,2,2-tetrafluoroethylene)
py	Pyridine
Q	Charge [C]
R	Rest (commonly known as organic group)
r.t.	Room temperature
RE	Reference electrode
rpm	Revolutions per minute (sirring speed)
RVC	Reticulated vitreous carbon
s	Seconds
S	Electron Spin
S or S'	Substrate
salen	*N*,*N'*-Ethylenebis(salicylimine)
SCE	Saturated calomel electrode
SET	Single electron transfer
SPE	Solid polymer electrolytes
t	Time [s]
T	Temperature [°C]
TBHP	*tert*-Butyl hydroperoxide
TCHQ	Tetrachlorohydroquinone
TCQ	2,3,5,6-Tetrachloro-1,4-benzoquinone
TEMPO	(2,2,6,6-Tetramethylpiperidin-1-yl)oxyl
TFA	Trifluoroacetic acid
TOFA	Tall oil fatty acids
Ts	Tosyl
UNEP	United Nations Environment Program
V	Volt
vol.	Volume
WE	Working electrode
X^-	Halide anion
z	Amount of transfered electrons
ε	Permittivity/dielectric constant

8 References

[1] UNEP, *21 Issues for the 21st Century*: Results of the UNEP Foresight Process on Emerging Environmental Issues, Nairobi, Kenya, **2012**.

[2] J. Krane, *MRS Energy & Sustainability* **2017**, *4*, 2.

[3] M. Wei, C. A. McMillan, S. de La Rue Can, *Curr. Sustainable Renewable Energy Rep.* **2019**, *6*, 140–148.

[4] a) J. Burre, D. Bongartz, L. Brée, K. Roh, A. Mitsos, *Chem. Ing. Tech.* **2020**, *92*, 74–84; b) E. Erdem, *Environ. Prog. Sustainable Energy* **2021**, *40*, e13545.

[5] A. Sternberg, A. Bardow, *ACS Sustainable Chem. Eng.* **2016**, *4*, 4156–4165.

[6] S. R. Foit, I. C. Vinke, L. G. J. de Haart, R.-A. Eichel, *Angew. Chem. Int. Ed.* **2017**, *56*, 5402–5411; *Angew. Chem.* **2017**, *129*, 5488–5498.

[7] a) M. D. Kärkäs, *Chem. Soc. Rev.* **2018**, *47*, 5786–5865; b) E. J. Horn, B. R. Rosen, P. S. Baran, *ACS Cent. Sci.* **2016**, *2*, 302–308.

[8] D. Pollok, S. R. Waldvogel, *Chem. Sci.* **2020**, *11*, 12386–12400.

[9] a) D. Pollok, Electro-organic Key Transformations in the Syntheses of Natural Products and Active Pharmaceutical Ingredients, Dissertation, Johannes Gutenberg University Mainz, **2022**; b) H. Braxmeier, S. Steinberger, "Stunning free images & royalty free stock", to be found under https://pixabay.com/ (accessed: October 2022).

[10] a) S. R. Waldvogel, B. Janza, *Angew. Chem. Int. Ed.* **2014**, *53*, 7122–7123; *Angew. Chem.* **2014**, *126*, 7248–7249; b) M. Yan, Y. Kawamata, P. S. Baran, *Chem. Rev.* **2017**, *117*, 13230–13319.

[11] C. A. C. Sequeira, D. M. F. Santos, *J. Braz. Chem. Soc.* **2009**, *20*, 387–406.

[12] B. A. Frontana-Uribe, R. D. Little, J. G. Ibanez, A. Palma, R. Vasquez-Medrano, *Green Chem.* **2010**, *12*, 2099–2119.

[13] H. J. Schäfer, *C.R. Chim.* **2011**, *14*, 745–765.

[14] D. Pollok, L. M. Großmann, T. Behrendt, T. Opatz, S. R. Waldvogel, *Chem. Eur. J.* **2022**, *28*, e202201523.

[15] C. Zhu, N. W. J. Ang, T. H. Meyer, Y. Qiu, L. Ackermann, *ACS Cent. Sci.* **2021**, *7*, 415–431.

[16] a) J. L. Röckl, D. Pollok, R. Franke, S. R. Waldvogel, *Acc. Chem. Res.* **2020**, *53*, 45–61; b) L. Eberson, M. P. Hartshorn, O. Persson, F. Radner, *Chem. Commun.* **1996**, 2105–2112; c)

D. E. Blanco, R. Atwi, S. Sethuraman, A. Lasri, J. Morales, N. N. Rajput, M. A. Modestino, *J. Electrochem. Soc.* **2020**, *167*, 155526.

[17] T. Fuchigami, M. Atobe, S. Inagi, *Fundamentals and Applications of Organic Electrochemistry*: Synthesis, Materials, Devices; John Wiley & Sons, Ltd, Chichester, UK, **2015**.

[18] IEC, "IEV ref: 482-02-27, anode", to be found under https://www.electropedia.org/iev/iev.nsf/display?openform&ievref=482-02-27 (accessed: 28.02.2023).

[19] IEC, "IEV ref: 482-02-28, cathode", to be found under https://www.electropedia.org/iev/iev.nsf/display?openform&ievref=482-02-28 (accessed: 28.02.2023).

[20] a) M. Selt, B. Gleede, R. Franke, A. Stenglein, S. R. Waldvogel, *J. Flow Chem.* **2021**, *11*, 143–162; b) C. Gütz, A. Stenglein, S. R. Waldvogel, *Org. Process Res. Dev.* **2017**, *21*, 771–778; c) M. Linden, M. M. Hielscher, B. Endrődi, C. Janáky, S. R. Waldvogel in *Volume 2 Flow Chemistry – Applications*; (Eds. F. Darvas, G. Dormán, V. Hessel, S. V. Ley), De Gruyter, Berlin, Boston, **2021**, pp. 31–68.

[21] F. C. Strong, *J. Chem. Educ.* **1961**, *38*, 98.

[22] a) C. Schotten, T. P. Nicholls, R. A. Bourne, N. Kapur, B. N. Nguyen, C. E. Willans, *Green Chem.* **2020**, *22*, 3358–3375; b) H. Lund in *Organic Electrochemistry*. *Fourth Edition, Revised and Expanded*; (Eds. H. Lund, O. Hammerich), Marcel Dekker Inc, New York, **2001**, pp. 223–292.

[23] D. M. Heard, A. J. J. Lennox, *Angew. Chem. Int. Ed.* **2020**, *59*, 18866–18884.

[24] M. Ingelsson, N. Yasri, E. P. L. Roberts, *Water Res.* **2020**, *187*, 116433.

[25] a) R. A. Bernhoft, *J. Environ. Public Health* **2012**, *2012*, 460508; b) A. L. Wani, A. Ara, J. A. Usmani, *Interdiscip. Toxicol.* **2015**, *8*, 55–64.

[26] H. U. Sverdrup, K. V. Ragnarsdottir, *Resour. Conserv. Recycl.* **2016**, *114*, 130–152.

[27] R. L. McCreery, *Chem. Rev.* **2008**, *108*, 2646–2687.

[28] S. Lips, S. R. Waldvogel, *ChemElectroChem* **2019**, *6*, 1649–1660.

[29] a) R. Sengupta, M. Bhattacharya, S. Bandyopadhyay, A. K. Bhowmick, *Prog. Polym. Sci.* **2011**, *36*, 638–670; b) R. R. Saxena, R. H. Bragg, *J. Non-Cryst. Solids* **1978**, *28*, 45–60.

[30] a) IKA®-Werke GmbH & CO. KG, "Accessories - Electrochemistry Kit", to be found under https://www.ika.com/en/Products-Lab-Eq/Electrochemistry-Kit-Accessories-cspacc-516/ (accessed: 30.03.2023); b) P. J. F. Harris, *Philosophical Magazine* **2004**, *84*, 3159–3167.

[31] Creative Commons, "Attribution 4.0 International (CC BY 4.0)", to be found under https://creativecommons.org/licenses/by/4.0/ (accessed: 14.12.2022).

[32] J. Masa, S. Barwe, C. Andronescu, W. Schuhmann, *Chem. Eur. J.* **2019**, *25*, 158–166.

[33] L. Meites, P. Zuman, H. W. Nurnberg, *Pure & Appl. Chem.* **1985**, *57*, 1491–1505.

[34] P. Westbroek, G. Priniotakis, P. Kiekens, *Analytical electrochemistry in textiles*: 1 - Fundamentals of electrochemistry; Woodhead Publishing, Sawston, UK, **2005**.

[35] G. Hilt, *ChemElectroChem* **2020**, *7*, 395–405.

[36] I. Colomer, A. E. R. Chamberlain, M. B. Haughey, T. J. Donohoe, *Nat. Rev. Chem.* **2017**, *1*, 88.

[37] L. Schulz, S. Waldvogel, *Synlett* **2019**, *30*, 275–286.

[38] C. Wohlfarth in *CRC Handbook of Chemistry and Physics*; (Eds. W. M. Haynes, D. R. Lide, T. J. Bruno), CRC Press, Boca Raton, FL, **2016–2017**, 6-199–6-220.

[39] a) M. König, J. Vaes, E. Klemm, D. Pant, *iScience* **2019**, *19*, 135–160; b) M. Kathiresan, D. Velayutham, *Chem. Commun.* **2015**, *51*, 17499–17516; c) J. Yoshida, K. Kataoka, R. Horcajada, A. Nagaki, *Chem. Rev.* **2008**, *108*, 2265–2299.

[40] H. Helmholtz, *Ann. Phys. Chem.* **1853**, *165*, 211–233.

[41] D. C. Grahame, *Chem. Rev.* **1947**, *41*, 441–501.

[42] M. Dunwell, Y. Yan, B. Xu, *Curr. Opin. Chem. Eng.* **2018**, *20*, 151–158.

[43] R. Parsons, *Chem. Rev.* **1990**, *90*, 813–826.

[44] C. Amatore in *Organic Electrochemistry*. *Fourth Edition, Revised and Expanded*; (Eds. H. Lund, O. Hammerich), Marcel Dekker Inc, New York, **2001**, pp. 1–94.

[45] R. Francke, R. D. Little, *Chem. Soc. Rev.* **2014**, *43*, 2492–2521.

[46] a) H. Roth, N. Romero, D. Nicewicz, *Synlett* **2016**, *27*, 714–723; b) Y. Kawamata, M. Yan, Z. Liu, D.-H. Bao, J. Chen, J. T. Starr, P. S. Baran, *J. Am. Chem. Soc.* **2017**, *139*, 7448–7451; c) L. M. Reid, T. Li, Y. Cao, C. P. Berlinguette, *Sustainable Energy Fuels* **2018**, *2*, 1905–1927.

[47] D. Vanmaekelbergh in *Electron Transfer in Chemistry*; (Ed. V. Balzani), WILEY-VCH Verlag GmbH, Weinheim, **2001**, pp. 126–188.

[48] R. A. Marcus, *Angew. Chem. Int. Ed. Engl.* **1993**, *32*, 1111–1121.

[49] K. J. Laidler, *Pure & Appl. Chem.* **1996**, *68*, 149–192.

[50] S. P. Blum, T. Karakaya, D. Schollmeyer, A. Klapars, S. R. Waldvogel, *Angew. Chem. Int. Ed.* **2021**, *60*, 5056–5062; *Angew. Chem.* **2021**, *133*, 5114–5120.

[51] S. P. Blum, D. Schollmeyer, M. Turks, S. R. Waldvogel, *Chem. Eur. J.* **2020**, *26*, 8358–8362.

[52] J. L. Röckl, M. Dörr, S. R. Waldvogel, *ChemElectroChem* **2020**, *7*, 3686–3694.

[53] J. L. Röckl, Y. Imada, K. Chiba, R. Franke, S. R. Waldvogel, *ChemElectroChem* **2019**, *6*, 4184–4187.

[54] Y. Imada, J. L. Röckl, A. Wiebe, T. Gieshoff, D. Schollmeyer, K. Chiba, R. Franke, S. R. Waldvogel, *Angew. Chem. Int. Ed.* **2018**, *57*, 12136–12140; *Angew. Chem.* **2018**, *130*, 12312–12317.

[55] S. P. Blum, C. Nickel, L. Schäffer, T. Karakaya, S. R. Waldvogel, *ChemSusChem* **2021**, *14*, 4936–4940.

[56] M. R. Scheide, C. R. Nicoleti, G. M. Martins, A. L. Braga, *Org. Biomol. Chem.* **2021**, *19*, 2578–2602.

[57] L. G. Gombos, S. R. Waldvogel, *Sustain. Chem.* **2022**, *3*, 430–454.

[58] L. G. Gombos, L. Werner, D. Schollmeyer, C. A. Martínez-Huitle, S. R. Waldvogel, *Eur. J. Org. Chem.* **2022**, *47*, e202200857.

[59] J. Strehl, M. L. Abraham, G. Hilt, *Angew. Chem. Int. Ed.* **2021**, *60*, 9996–10000; *Angew. Chem.* **2021**, *133*, 10084–10088.

[60] a) J. N. Brönsted, *Recl. Trav. Chim. Pays-Bas* **1923**, *42*, 718–728; b) T. M. Lowry, *J. Chem. Technol. Biotechnol.* **1923**, *42*, 43–47.

[61] E. Estrada, A. Rieker, *Z. Naturforsch.* **1994**, *49 b*, 1566–1568.

[62] A. A. Sokolov, M. A. Syroeshkin, V. N. Solkan, T. V. Shebunina, R. S. Begunov, L. V. Mikhal'chenko, M. Y. Leonova, V. P. Gultyai, *Russ. Chem. Bull.* **2014**, *63*, 372–380.

[63] Y. Li, C.-C. Sun, C.-C. Zeng, *J. Electroanal. Chem.* **2020**, *861*, 113941.

[64] F. Lian, K. Xu, C. Zeng, *Chem. Rec.* **2021**, *21*, 2290–2305.

[65] Y. Takahira, M. Chen, Y. Kawamata, P. Mykhailiuk, H. Nakamura, B. K. Peters, S. H. Reisberg, C. Li, L. Chen, T. Hoshikawa, T. Shibuguchi, P. S. Baran, *Synlett* **2019**, *30*, 1178–1182.

[66] E. Steckhan, *Angew. Chem. Int. Ed. Engl.* **1986**, *25*, 683–701; *Angew. Chem.* **1986**, *98*, 681–699.

[67] S. Torii, H. Tanaka, S. Hamano, N. Tada, J. Nokami, M. Sasaoka, *Chem. Lett.* **1984**, *13*, 1823–1826.

[68] S. P. Blum, L. Schäffer, D. Schollmeyer, S. R. Waldvogel, *Chem. Commun.* **2021**, *57*, 4775–4778.

[69] H. Letheby, *J. Chem. Soc.* **1862**, *15*, 161–163.

[70] M. Zhang, Q. Shi, X. Song, H. Wang, Z. Bian, *Environ. Sci. Pollut. Res.* **2019**, *26*, 10457–10486.

[71] D. Pletcher, M. Razaq, G. D. Smilgin, *J. Appl. Electrochem.* **1981**, *11*, 601–603.

[72] a) R. Tomat, A. Rigo, *J. Appl. Electrochem.* **1980**, *10*, 549–552; b) R. Tomat, A. Rigo, *J. Appl. Electrochem.* **1985**, *15*, 167–173; c) R. Tomat, A. Rigo, *J. Appl. Electrochem.* **1976**, *6*, 257–261.

[73] C. Walling, *Acc. Chem. Res.* **1975**, *8*, 125–131.

[74] B. S. Jayashree, P. S. Nikhil, S. Paul, *Med. Chem.* **2022**, *18*, 915–925.

[75] J. Clayden, N. Greeves, S. Warren, *Organic Chemistry;* Oxford University Press, Oxford, **2012**.

[76] W. N. Haworth, C. K. Ingold, T. A. Henry, *Annu. Rep. Prog. Chem.* **1926**, *23*, 74–185.

[77] a) M. Feng, B. Tang, S. H. Liang, X. Jiang, *Curr. Top. Med. Chem.* **2016**, *16*, 1200–1216; b) K. Hofman, N.-W. Liu, G. Manolikakes, *Chem. Eur. J.* **2018**, *24*, 11852–11863.

[78] G. L. Patrick, *An Introduction to Medicinal Chemistry;* Oxford University Press, Oxford, **2013**.

[79] A. C. McDougall, *Clin. Exp. Dermatol.* **1979**, *4*, 139–142.

[80] J. T. Lear, *N. Engl. J. Med.* **2012**, *366*, 2225–2226.

[81] I. D. Cockshott, *Clin. Pharmacokinet.* **2004**, *43*, 855–878.

[82] S. Khozin, G. M. Blumenthal, L. Zhang, S. Tang, M. Brower, E. Fox, W. Helms, R. Leong, P. Song, Y. Pan, Q. Liu, P. Zhao, H. Zhao, D. Lu, Z. Tang, A. Al Hakim, K. Boyd, P. Keegan, R. Justice, R. Pazdur, *Clin. Cancer Res.* **2015**, *21*, 2436–2439.

[83] P. J. Goadsby, M. D. Ferrari, J. Olesen, L. J. Stovner, J. M. Senard, N. C. Jackson, P. H. Poole, *Neurology* **2000**, *54*, 156–163.

[84] R. Beaudegnies, A. J. F. Edmunds, T. E. M. Fraser, R. G. Hall, T. R. Hawkes, G. Mitchell, J. Schaetzer, S. Wendeborn, J. Wibley, *Bioorg. Med. Chem.* **2009**, *17*, 4134–4152.

[85] S. Ida in *Encyclopedia of Polymeric Nanomaterials*; (Eds. S. Kobayashi, K. Müllen), Springer, Berlin, Heidelberg, **2020**.

[86] a) H.-S. Lee, A. Roy, O. Lane, J. E. McGrath, *Polymer* **2008**, *49*, 5387–5396; b) R. Nolte, K. Ledjeff, M. Bauer, R. Mülhaupt, *J. Membr. Sci.* **1993**, *83*, 211–220.

[87] a) B. M. Trost, *Bull. Chem. Soc. Jpn.* **1988**, *61*, 107–124; b) M. Nielsen, C. B. Jacobsen, N. Holub, M. W. Paixão, K. A. Jørgensen, *Angew. Chem. Int. Ed.* **2010**, *49*, 2668–2679; c) B. M. Trost, C. A. Kalnmals, *Chem. Eur. J.* **2019**, *25*, 11193–11213.

[88] M. Julia, J.-M. Paris, *Tetrahedron Lett.* **1973**, *14*, 4833–4836.

[89] P. R. Blakemore, *J. Chem. Soc, Perkin Trans. 1* **2002**, 2563–2585.

[90] N.-W. Liu, S. Liang, G. Manolikakes, *Synthesis* **2016**, *48*, 1939–1973.

[91] a) E. Voutyritsa, I. Triandafillidi, C. Kokotos **2017**, *49*, 917–924; b) Z. Cheng, P. Sun, A. Tang, W. Jin, C. Liu, *Org. Lett.* **2019**, *21*, 8925–8929; c) N. K. Jana, J. G. Verkade, *Org. Lett.* **2003**, *5*, 3787–3790; d) A. Shaabani, P. Mirzaei, S. Naderi, D. G. Lee, *Tetrahedron* **2004**, *60*, 11415–11420.

[92] a) G. A. Olah, S. Kobayashi, J. Nishimura, *J. Am. Chem. Soc.* **1973**, *95*, 564–569; b) J. A. Hyatt, A. W. White, *Synthesis* **1984**, 214–217; c) F. Effenberger, K. Huthmacher, *Angew. Chem. Int. Ed.* **1974**, *13*, 409–410; d) B. M. Graybill, *J. Org. Chem.* **1967**, *32*, 2931–2933; e) M. Ono, Y. Nakamura, S. Sato, I. Itoh, *Chem. Lett.* **1988**, *17*, 395–398.

[93] a) J. S. Meek, J. S. Fowler, *J. Org. Chem.* **1968**, *33*, 3422–3424; b) S. Liang, R.-Y. Zhang, L.-Y. Xi, S.-Y. Chen, X.-Q. Yu, *J. Org. Chem.* **2013**, *78*, 11874–11880; c) K. M. Maloney, J. T. Kuethe, K. Linn, *Org. Lett.* **2011**, *13*, 102–105; d) S. Liang, R.-Y. Zhang, G. Wang, S.-Y. Chen, X.-Q. Yu, *Eur. J. Org. Chem.* **2013**, 7050–7053.

[94] a) S. K. Kang, B. S. Ko, Y. H. Ha, *J. Org. Chem.* **2001**, *66*, 3630–3633; b) S.-K. Kang, H.-W. Seo, Y.-H. Ha, *Synthesis* **2001**, 1321–1326; c) N. Mantrand, P. Renaud, *Tetrahedron* **2008**, *64*, 11860–11864; d) I. V. Alabugin, V. I. Timokhin, J. N. Abrams, M. Manoharan, R. Abrams, I. Ghiviriga, *J. Am. Chem. Soc.* **2008**, *130*, 10984–10995.

[95] R. J. Reddy, A. H. Kumari, *RSC Adv.* **2021**, *11*, 9130–9221.

[96] a) C. Wang, H. Zhang, Z. Li, Z. Wang, *J. Chem. Res.* **2014**, *38*, 639–642; b) W. Zhang, K. Li, B. Zhao, *J. Chem. Res.* **2014**, *38*, 269–271; c) Y. Yuan, S. Guo, *Synlett* **2011**, 2750–2756; d) S. H. Gund, R. S. Shelkar, J. M. Nagarkar, *RSC Adv.* **2015**, *5*, 62926–62930.

[97] S. Cacchi, G. Fabrizi, A. Goggiamani, L. M. Parisi, R. Bernini, *J. Org. Chem.* **2004**, *69*, 5608–5614.

[98] L. S. Teseletso, T. Adachi, *Miner. Econ.* **2021**, https://doi.org/10.1007/s13563-021-00283-2.

[99] É. Lèbre, M. Stringer, K. Svobodova, J. R. Owen, D. Kemp, C. Côte, A. Arratia-Solar, R. K. Valenta, *Nat. Commun.* **2020**, *11*, 4823.

[100] S. Liang, Y. Ren, G. Manolikakes, *Eur. J. Org. Chem.* **2017**, 4117–4120.

[101] J. Liu, L. Yu, S. Zhuang, Q. Gui, X. Chen, W. Wang, Z. Tan, *Chem. Commun.* **2015**, *51*, 6418–6421.

[102] a) Y. Zhou, W.-B. Cao, L.-L. Zhang, X.-P. Xu, S.-J. Ji, *J. Org. Chem.* **2018**, *83*, 6056–6065; b) U. Karmakar, R. Samanta, *J. Org. Chem.* **2019**, *84*, 2850–2861; c) W.-H. Rao, B.-F. Shi, *Org. Lett.* **2015**, *17*, 2784–2787.

[103] P. Halder, V. T. Humne, S. B. Mhaske, *J. Org. Chem.* **2019**, *84*, 1372–1378.

[104] a) P. Katrun, C. Mueangkaew, M. Pohmakotr, V. Reutrakul, T. Jaipetch, D. Soorukram, C. Kuhakarn, *J. Org. Chem.* **2014**, *79*, 1778–1785; b) F. Xiao, S. Chen, J. Tian, H. Huang, Y. Liu, G.-J. Deng, *Green Chem.* **2016**, *18*, 1538–1546.

[105] C. Xia, K. Wang, J. Xu, Z. Wei, C. Shen, G. Duan, Q. Zhu, P. Zhang, *RSC Adv.* **2016**, *6*, 37173–37179.

[106] H. Mei, R. Pajkert, L. Wang, Z. Li, G.-V. Röschenthaler, J. Han, *Green Chem.* **2020**, *22*, 3028–3059.

[107] P. Qian, M. Bi, J. Su, Z. Zha, Z. Wang, *J. Org. Chem.* **2016**, *81*, 4876–4882.

[108] Q. Zhong, Y. Zhao, S. Sheng, J. Chen, *Synthetic Commun.* **2020**, *50*, 161–167.

[109] Y.-C. Luo, X.-J. Pan, G.-Q. Yuan, *Tetrahedron* **2015**, *71*, 2119–2123.

[110] C.-K. Chan, N.-C. Lo, P.-Y. Chen, M.-Y. Chang, *Synthesis* **2017**, *49*, 4469–4477.

[111] M.-J. Luo, B. Liu, Y. Li, M. Hu, J.-H. Li, *Adv. Synth. Catal.* **2019**, *361*, 1538–1542.

[112] M. Jiang, Y. Yuan, T. Wang, Y. Xiong, J. Li, H. Guo, A. Lei, *Chem. Commun.* **2019**, *55*, 13852–13855.

[113] M.-L. Feng, L.-Y. Xi, S.-Y. Chen, X.-Q. Yu, *Eur. J. Org. Chem.* **2017**, 2746–2750.

[114] Y.-C. Wu, S.-S. Jiang, S.-Z. Luo, R.-J. Song, J.-H. Li, *Chem. Commun.* **2019**, *55*, 8995–8998.

[115] F. Lu, J. Li, T. Wang, Z. Li, M. Jiang, X. Hu, H. Pei, F. Yuan, L. Lu, A. Lei, *Asian J. Org. Chem.* **2019**, *8*, 1838–1841.

[116] H.-L. Xiao, C.-W. Yang, N.-T. Zhang, C.-C. Zeng, L.-M. Hu, H.-Y. Tian, R. D. Little, *Tetrahedron* **2013**, *69*, 658–663.

[117] A. Alizadeh, M. M. Khodaei, M. Fakhari, M. Shamsuddin, *RSC Adv.* **2014**, *4*, 20781–20788.

[118] Y.-Y. Jiang, S. Liang, C.-C. Zeng, L.-M. Hu, B.-G. Sun, *Green Chem.* **2016**, *18*, 6311–6319.

[119] I. Yavari, S. Shaabanzadeh, *Org. Lett.* **2020**, *22*, 464–467.

[120] Y. Gao, H. Mei, J. Han, Y. Pan, *Chem. Eur. J.* **2018**, *24*, 17205–17209.

[121] H. Mei, J. Liu, Y. Guo, J. Han, *ACS omega* **2019**, *4*, 14353–14359.

[122] J. Zhao, J. Han in *Alkane Functionalization*; (Eds. A. J. L. Pombeiro, M. F. C. Guedes da Silva), John Wiley & Sons Ltd, Hoboken, NJ, **2019**, pp. 503–521.

[123] S. J. Blanksby, G. B. Ellison, *Acc. Chem. Res.* **2003**, *36*, 255–263.

[124] Z. Tian, A. Fattahi, L. Lis, S. R. Kass, *J. Am. Chem. Soc.* **2006**, *128*, 17087–17092.

[125] K. Krumova, G. Cosa in *Singlet Oxygen: Applications in Biosciences and Nanosciences*; (Eds. S. Nonell, C. Flors), Royal Society of Chemistry, Cambridge, UK, **2016**, pp. 3–21.

[126] C. E. Housecroft, A. G. Sharpe, *Inorganic Chemistry;* Pearson, Harlow, England, **2005**.

[127] R. D. Harcourt in *Pauling's Legacy*. *Modern Modelling of the Chemical Bond*; (Eds. Z. B. Maksić, W. J. Orville-Thomas), Elsevier Science Ltd, Amsterdam, **1999**, pp. 449–480.

[128] a) G. Chen, Y. Sun, R. R. Chen, C. Biz, A. C. Fisher, M. P. Sherburne, J. W. Ager III, J. Gracia, Z. J. Xu, *J. Phys. Energy* **2021**, *3*, 31004; b) J. Al-Nu'airat, I. Oluwoye, N. Zeinali, M. Altarawneh, B. Z. Dlugogorski, *Chem. Rec.* **2021**, *21*, 315–342.

[129] C. Schweitzer, R. Schmidt, *Chem. Rev.* **2003**, *103*, 1685–1757.

[130] R. Y. N. Ho, J. F. Liebman, J. S. Valentine in *Active Oxygen in Chemistry*. *Structure Energetics and Reactivity in Chemistry Series (SEARCH Series)*; (Eds. C. S. Foote, J. S. Valentine, A. Greenberg, J. F. Liebman), Springer, Dordrecht, **1995**, pp. 1–23.

[131] E. L. Clennan in *Singlet Oxygen: Applications in Biosciences and Nanosciences*; (Eds. S. Nonell, C. Flors), Royal Society of Chemistry, Cambridge, UK, **2016**, pp. 353–367.

[132] W. T. Borden, R. Hoffmann, T. Stuyver, B. Chen, *J. Am. Chem. Soc.* **2017**, *139*, 9010–9018.

[133] I. M. Aldous, L. J. Hardwick, *J. Phys. Chem. Lett.* **2014**, *5*, 3924–3930.

[134] D. T. Sawyer, J. S. Valentine, *Acc. Chem. Res.* **1981**, *14*, 393–400.

[135] M. Hayyan, M. A. Hashim, I. M. AlNashef, *Chem. Rev.* **2016**, *116*, 3029–3085.

[136] F. A. Carey, R. J. Sundberg, *Advanced Organic Chemistry*: Part B: Reactions and Synthesis; Springer, Boston, **2007**.

[137] K. Weissermel, H.-J. Arpe, *Industrial Organic Chemistry;* WILEY-VCH GmbH & Co. KGaA, Weinheim, **2003**.

[138] K. Marchildon, *Macromol. React. Eng.* **2011**, *5*, 22–54.

[139] D. Veit, *Fibers*: History, Production, Properties, Market; Springer, Cham, Switzerland, **2022**.

[140] B. Schmidt, J. Hermanns in *Grundlagen der Organischen Chemie*; (Ed. J. Buddrus), De Gruyter, Berlin, Boston, **2022**, pp. 54–66.

[141] a) A. de Meijere, *Angew. Chem. Int. Ed.* **2005**, *44*, 7836–7840; *Angew. Chem.* **2005**, *117*, 8046–8050; b) R. Huisgen, *Angew. Chem. Int. Ed.* **1986**, *25*, 297–311.

[142] R. F. Curl, W. D. Gwinn, *J. Phys. Chem.* **1990**, *94*, 7743–7753.

[143] V. Prelog, *Pure & Appl. Chem.* **1963**, *6*, 545–560.

[144] V. Dragojlovic, *ChemTexts* **2015**, *1*, 14.

[145] Q. Cheng, S. M. Thomas, P. Rouvière, *Appl. Microbiol. Biotechnol.* **2002**, *58*, 704–711.

[146] M. K. Trower, R. M. Buckland, R. Higgins, M. Griffin, *Appl. Environ. Microbiol.* **1985**, *49*, 1282–1289.

[147] J. D. Schumacher, R. M. Fakoussa, *Appl. Microbiol. Biotechnol.* **1999**, *52*, 85–90.

[148] R. Mello, M. Fiorentino, C. Fusco, R. Curci, *J. Am. Chem. Soc.* **1989**, *111*, 6749–6757.

[149] Y. Matsumoto, M. Kuriyama, K. Yamamoto, K. Nishida, O. Onomura, *Org. Process Res. Dev.* **2018**, *22*, 1312–1317.

[150] A. R. Ravishankara, J. S. Daniel, R. W. Portmann, *Science* **2009**, *326*, 123–125.

[151] S. Rana, J. P. Biswas, S. Paul, A. Paik, D. Maiti, *Chem. Soc. Rev.* **2021**, *50*, 243–472.

[152] F. Gozzo, *J. Mol. Catal. A: Chem.* **2001**, *171*, 1–22.

[153] D. H. R. Barton, D. Doller, *Acc. Chem. Res.* **1992**, *25*, 504–512.

[154] D. H. R. Barton, J. Boivin, M. Gastiger, J. Morzycki, R. S. Hay-Motherwell, W. B. Motherwell, N. Ozbalik, K. M. Schwartzentruber, *J. Chem. Soc, Perkin Trans. 1* **1986**, 947–955.

[155] C. Pavan, J. Legros, C. Bolm, *Adv. Synth. Catal.* **2005**, *347*, 703–705.

[156] S. Lee, P. L. Fuchs, *J. Am. Chem. Soc.* **2002**, *124*, 13978–13979.

[157] P. A. Ganeshpure, G. L. Tembe, S. Satish, *J. Mol. Catal. A: Chem.* **1996**, *113*, L423-L425.

[158] N. Nakayama, S. Tsuchiya, S. Ogawa, *J. Mol. Catal. A: Chem.* **2007**, *277*, 61–71.

[159] Y. Ishii, T. Iwahama, S. Sakaguchi, K. Nakayama, Y. Nishiyama, *J. Org. Chem.* **1996**, *61*, 4520–4526.

[160] P. H. J. Carlsen, *Synthetic Commun.* **1987**, *17*, 19–23.

[161] C. S. Yi, K.-H. Kwon, D. W. Lee, *Org. Lett.* **2009**, *11*, 1567–1569.

[162] G. Balavoine, D. H. Barton, J. Boivin, A. Gref, N. Ozbalik, H. Rivière, *Tetrahedron Lett.* **1986**, *27*, 2849–2852.

[163] G. Balavoine, D. H. R. Barton, J. Boivin, A. Gref, N. Ozbalik, H. Rivière, *J. Chem. Soc, Chem. Commun.* **1986**, 1727–1729.

[164] I. Yamanaka, T. Furukawa, K. Otsuka, *Chem. Commun.* **2000**, 2209–2210.

[165] Y. Kawamata, M. Yan, Z. Liu, D.-H. Bao, J. Chen, J. T. Starr, P. S. Baran, *J. Am. Chem. Soc.* **2017**, *139*, 7448–7451.

[166] P. Spannring, P. C. A. Bruijnincx, B. M. Weckhuysen, R. J. M. Klein Gebbink, *RSC Adv.* **2013**, *3*, 6606–6613.

[167] P. P. Thottumkara, T. K. Vinod, *Org. Lett.* **2010**, *12*, 5640–5643.

[168] P. Spannring, P. C. A. Bruijnincx, B. M. Weckhuysen, R. J. M. Klein Gebbink, *Catal. Sci. Technol.* **2014**, *4*, 2182–2209.

[169] P. H. J. Carlsen, T. Katsuki, V. S. Martin, K. B. Sharpless, *J. Org. Chem.* **1981**, *46*, 3936–3938.

[170] T. Oguchi, T. Ura, Y. Ishii, M. Ogawa, *Chem. Lett.* **1989**, *18*, 857–860.

[171] B. R. Travis, R. S. Narayan, B. Borhan, *J. Am. Chem. Soc.* **2002**, *124*, 3824–3825.

[172] B. C. Ranu, S. Bhadra, L. Adak, *Tetrahedron Lett.* **2008**, *49*, 2588–2591.

[173] E. Antonelli, R. D'Aloisio, M. Gambaro, T. Fiorani, C. Venturello, *J. Org. Chem.* **1998**, *63*, 7190–7206.

[174] S.-H. Shi, Y. Liang, N. Jiao, *Chem. Rev.* **2021**, *121*, 485–505.

[175] U.-S. Bäumer, H. J. Schäfer, *Electrochim. Acta* **2003**, *48*, 489–495.

[176] U.-S. Bäumer, H. J. Schäfer, *J. Appl. Electrochem.* **2005**, *35*, 1283–1292.

[177] H. Schmidt, H. Stange, *Z. Anorg. Allg. Chem.* **1958**, *293*, 274–285.

[178] R. R. Rao, S. B. Milliken, S. L. Robinson, C. K. Mann, *Anal. Chem.* **1970**, *42*, 1076–1080.

[179] J. E. Leonard, P. C. Scholl, T. P. Steckel, S. E. Lentsch, M. R. van de Mark, *Tetrahedron Lett.* **1980**, *21*, 4695–4698.

[180] C. Christopher, S. Lawrence, A. J. Bosco, N. Xavier, S. Raja, *Catal. Sci. Technol.* **2012**, *2*, 824–827.

[181] T. Shono, T. Soejima, K. Takigawa, Y. Yamaguchi, H. Maekawa, S. Kashimura, *Tetrahedron Lett.* **1994**, *35*, 4161–4164.

[182] a) B. Mokhtari, D. Nematollahi, H. Salehzadeh, *Green Chem.* **2018**, *20*, 1499–1505; b) D. Nematollahi, M. Malakzadeh, *J. Electroanal. Chem.* **2003**, *547*, 191–195; c) D. Nematollahi, R. Rahchamani, *J. Electroanal. Chem.* **2002**, *520*, 145–149; d) D. Nematollahi, F. Varmaghani, *Electrochim. Acta* **2008**, *53*, 3350–3355; e) D. Nematollahi, M. Baniardalan, S. Khazalpour, M. R. Pajohi-Alamoti, *Electrochim. Acta* **2016**, *191*, 98–105; f) D. Nematollahi, S. Hosseinzadeh, B. Dadpou, *J. Electroanal. Chem.* **2015**, *759*, 144–152; g) D. Nematollahi, S. Momeni, S. Khazalpour, *Electrochim. Acta* **2014**, *147*, 310–318; h) D. Nematollahi, A. Sayadi, F. Varmaghani, *J. Electroanal. Chem.* **2012**, *671*, 44–50; i) M. Sharafi-Kolkeshvandi, D. Nematollahi, F. Nikpour, *Synthesis* **2017**, *49*, 1555–1560.

[183] S. Lips, Metall- und reagensfreie anodische Kreuzkupplung von Phenolen mit aromatischen Substraten, Dissertation, Johannes Gutenberg University Mainz, **2018**.

[184] J. Nikl, S. Lips, D. Schollmeyer, R. Franke, S. R. Waldvogel, *Chem. Eur. J.* **2019**, *25*, 6891–6895.

[185] X. Yang, J. Kirsch, J. Fergus, A. Simonian, *Electrochim. Acta* **2013**, *94*, 259–268.

[186] O. Hollóczki, A. Berkessel, J. Mars, M. Mezger, A. Wiebe, S. R. Waldvogel, B. Kirchner, *ACS Catal.* **2017**, *7*, 1846–1852.

[187] J. Simonet, *Phosphorus Sulfur Silicon Relat. Elem.* **1993**, *74*, 93–112.

[188] J. Nikl, D. Ravelli, D. Schollmeyer, S. R. Waldvogel, *ChemElectroChem* **2019**, *6*, 4450–4455.

[189] N. Gospodinova, L. Terlemezyan, *Prog. Polym. Sci.* **1998**, *23*, 1443–1484.

[190] J. Nikl, K. Hofman, S. Mossazghi, I. C. Möller, D. Mondeshki, F. Weinelt, F.-E. Baumann, S. R. Waldvogel, *Nat. Commun.* **2023**, *14*, 4565.

[191] M. Zimmermann, Oxygen reduction reaction mechanism on glassy carbon in aprotic organic solvents, Dissertation, Université Grenoble Alpes, **2015**.

[192] J. Jörissen, *J. Appl. Electrochem.* **2003**, *33*, 969–977.

[193] L. Hoof, N. Thissen, K. Pellumbi, K. junge Puring, D. Siegmund, A. K. Mechler, U.-P. Apfel, *Cell Reports Physical Science* **2022**, *3*, 100825.

[194] J. Jörissen, *Electrochim. Acta* **1996**, *41*, 553–562.

[195] United Nations, Department of Economic and Social Affairs, Population Division, *World Population Prospects: The 2017 Revision*: Key Findings and Advance Tables, Working Paper No. ESA/P/WP/248, **2017**.

[196] a) J. Oxley, *Proc. Safety Prog.* **2020**, *39*, e12204; b) T. M. Klapötke, *Chem. Unserer Zeit* **2021**, *55*, 256–263.

[197] a) H. J. Pasman, C. Fouchier, S. Park, N. Quddus, D. Laboureur, *Proc. Safety Prog.* **2020**, *39*, e12203; b) W. Pittman, Z. Han, B. Harding, C. Rosas, J. Jiang, A. Pineda, M. S. Mannan, *J. Hazard. Mater.* **2014**, *280*, 472–477.

[198] *Regulation (EU) 2019/1148 of the European Parliament and of the Council of 20 June 2019 on the marketing and use of explosives precursors, amending Regulation (EC) No 1907/2006 and repealing Regulation (EU) No 98/2013 (Text with EEA relevance)*, **2019**.

[199] C.-T. Yang, Y. Fu, Y.-B. Huang, J. Yi, Q.-X. Guo, L. Liu, *Angew. Chem. Int. Ed.* **2009**, *48*, 7398–7401.

[200] European Food Safety Authority (EFSA), Parma, Italy, *EFSA Journal* **2013**, *11*, 3169.

[201] R. A. Smiley. Method of using ammonium fatty acid salts as non-selective herbicides (US6323156B1), November 27, 2001.

[202] R. Krishna, J. Ellenberger, M. I. Urseanu, F. J. Keil, *Naturwissenschaften* **2000**, *87*, 455–459.

[203] N. Palya, D. W. MacPhee, *Energy Efficiency* **2023**, *16*, 3.

9 Publications, patents, conference contributions & student mentoring

Publications

J. Nikl, K. Hofman, S. Mossazghi, I. C. Möller, D. Mondeshki, F. Weinelt, F.-E. Baumann, S. R. Waldvogel, *Electrochemical oxo-functionalization of cyclic alkanes and alkenes using nitrate and oxygen*, *Nat. Commun*. **2023**, *14*, 4565.

J. Nikl, D. Ravelli, D. Schollmeyer, S. R. Waldvogel, *Straightforward Electrochemical Sulfonylation of Arenes and Aniline Derivatives using Sodium Sulfinates, ChemElectroChem* **2019**, *6*, 4450–4455.

J. Nikl, S. Lips, D. Schollmeyer, R. Franke, S. R. Waldvogel, *Direct Metal- and Reagent-Free Sulfonylation of Phenols with Sodium Sulfinates by Electrosynthesis, Chem. Eur. J.* **2019**, *25*, 6891–6895.

Patents

S. R. Waldvogel, K. Hofman, **J. Nikl**, F. Weinelt, F.-E. Baumann, *Elektrochemische Oxidation von Fettsäuren und Fettsäureestern zu Monocarbonsäuren und α,ω-Dicarbonsäuren*, filed at the European Patent Office, not yet published.

S. R. Waldvogel, **J. Nikl**, F. Weinelt, F.-E. Baumann, *Elektrochemische Oxidation von Cycloalkenen und Cycloalkanen zu α,ω-Dicarbonsäuren oder Ketocarbonsäuren und Cycloalkanon-Verbindungen*, filed at the European Patent Office, not yet published.

S. R. Waldvogel, **J. Nikl**, S. Hofmann, F. Weinelt, F.-E. Baumann, *Elektrochemische Oxidation von Cycloalkanen zu α,ω-Dicarbonsäuren und Ketocarbonsäuren*, filed at the European Patent Office, not yet published.

S. R. Waldvogel, **J. Nikl**, A. L. Rauen, F. Weinelt, F.-E. Baumann, *Elektrochemische Oxidation von Cycloalkanen zu Cycloalkanon-Verbindungen*, filed at the European Patent Office, not yet published.

Conference contributions

Oral Presentation at the 14th Manuel M. Baizer Memorial Symposium on Organic Electrochemistry (Montreal, Canada, 2020) (cancelled due to COVID-19 pandemia).
Title: *Electrochemical Sulfonylation of Electron-Rich Aromatic Substrates with Sodium Sulfinates.*
ECS Meeting Abstract: Joachim Nikl *et al* 2020 *Meet. Abstr*. **MA2020-01** 2506.

Supervision of undergraduate research work

2021, Isabel Clementine Möller, Bachelor thesis.
Thesis title: *Selektive Benzylische Oxidation von Toluol- zu Benzoesäurederivaten unter Nitrat- und Sauerstoffeinfluss.*

2021, Jens Linus Schröder, Internship from Hochschule Bonn-Rhein-Sieg.
Report titel: *Electrochemical Oxidation of β-Isophorone to 4-Oxoisophorone and oxidative C=C Double Bond Cleavage of Cyclic Alkenes to Aldehydes/Carboxylic Acids.*

2021, Daniel Mondeshki, Undergraduate research assistant.

2020, Samuel Mossazghi, Bachelor thesis.
Thesis title: *Elektrochemische, Nitrat-mediierte Oxidation von Xylol- zu Methylbenzaldehyd-Derivaten unter Sauerstoffeinfluss.*